UC Berkeley
UC Berkeley Electronic Theses and Dissertations

Title

Total Synthesis of Resiniferatoxin

Permalink

https://escholarship.org/uc/item/71q0s0n6

Author

Vasilev, Vasil Hristov

Publication Date

2022

Peer reviewed|Thesis/dissertation

eScholarship.org Powered by the California Digital Library
University of California

Total Synthesis of Resiniferatoxin

By

Vasil H Vasilev

A dissertation submitted in partial satisfaction of the

requirements for the degree of

Doctor of Philosophy

in

Chemistry

in

the Graduate Division

of the

University of California, Berkeley

Committee in Charge:

Professor Thomas Maimone, Chair
Professor Richmond Sarpong
Professor Wenjun Zhang

Fall 2022

Abstract

Total Synthesis of Resiniferatoxin

by

Vasil H Vasilev

Doctor of Philosophy in Chemistry

University of California, Berkeley

Professor Thomas Maimone, Chair

Resiniferatoxin (RTX) is the flagship member of the daphnane diterpenoid orthoesters (DDOs), a class of natural products with highly complex structures and pharmaceutically relevant biological properties such as anti-HIV and antitumor bioactivities. RTX itself is a potent analgesic that has been granted Orphan Drug Status by the FDA. Despite their biochemical potential, no general synthetic route to the DDOs exists owing to the topological and stereochemical complexity of these molecules. Herein we disclose a new retrosynthetic logic, orthogonal to exiting efforts toward these natural products, to rapidly access the daphnane diterpene core in a convergent and stereoselective manner. These efforts culminated in the successful 15-step total synthesis of resiniferatoxin.

The synthetic route disclosed herein centers on the late-stage assembly of the stereochemically dense 6-membered ring of the daphnanes in stark contrast to previous syntheses of RTX and related natural products, wherein this part of the molecule is constructed early on. Forging the 6-membered ring last allows for a more convergent and hence more rapid synthetic route, via which the daphnane diterpenoid orthoester core can be accessed in only 12 steps from commercially available materials. Key synthetic sequences are an allylation/Pd-catalyzed 7-*exo*-trig cyclization to construct the 7-membered ring of the diterpene scaffold as well as a series of a highly diastereoselective aldol reaction followed by SmI_2-mediated 6-*exo*-trig cyclization. Using these two reactions the complex 6-membered ring of the natural product, which is decorated with 5 contiguous stereocenters, can be quickly and stereoselectively constructed. In the latter of the two steps a halide atom at the cyclization terminus was successfully used to modulate the inherent stereochemical preference in order to access the desired diastereomer of the tricyclic product. Given the rapid assembly of the DDO scaffold and the modular nature of the route, this new retrosynthetic logic has a lot of future potential for synthesizing previously inaccessible daphnane natural products.

Table of Contents

Acknowledgements ii
List of Abbreviations vi

Chapter 1. Daphnane Diterpenoid Orthoesters 1
Chapter 1.1. Resiniferatoxin, Related Natural Products, and Biosynthesis 2
Chapter 1.2. Bioactivity of Resiniferatoxin 5
Chapter 1.3. Bioactivity of the Daphnane Diterpenoid Orthoesters 6
Chapter 1.4. Prior Art in the Total Synthesis of Daphnane Diterpenoid Orthoesters 7
Chapter 1.5. Retrosynthetic Analysis of Resiniferatoxin 13
Chapter 1.6. References 15
Chapter 1.7. Structures of the Daphnane Diterpenoid Orthoesters 22

Chapter 2. Total Synthesis of Resiniferatoxin 30
Chapter 2.1. Synthesis of Trans-Fused Hydroazulenol **2.1.10** 31
Chapter 2.2. Oxidative Manipulations of the Hydroazulene Fragment and Forays into Formation of the C8-C14 Bond 33
Chapter 2.3. Initial Exploration of Linear Fragments and C Ring Formation 34
Chapter 2.4. SmI_2-Mediated Construction of the Daphnane Core Based on a Thiophenol-Bearing Cyclization Precursor 43
Chapter 2.5. Identification of Stereoselective Conditions for the Formation of the C8-C14 Bond 48
Chapter 2.6. Harnessing the Adventitious 1,5-HAT Event toward a Substrate with a More Suitably Functionalized Five-Membered Ring 52
Chapter 2.7. Forging the Orthoester and Completion of the Total Synthesis of Resiniferatoxin 54
Chapter 2.8. Optimized 12-step Synthetic Route to the Daphnane Diterpene Orthoesters. A 15-Step Total Synthesis of Resiniferatoxin 57
Chapter 2.9. Conclusion 60
Chapter 2.10. Distribution of Credit 61
Chapter 2.11. References 61
Chapter 2.12. Experimental Procedures and Crystallographic Data 65

Appendix – NMR Spectra 139

Acknowledgements:

Firstly, my boss – the one and only
Prof. Thomas Maimone: Dear Tom, thank you very much for allowing me to be a graduate student in your lab! I knew from the moment we met that something special would happen if I joined your lab and I am immensely grateful for all your help and support throughout the years. I came to Berkeley to learn your unique way of thinking about molecules and retrosynthesis, but I could scarcely anticipate the amount of knowledge and skills I would gain under your mentorship. Thank you for being there during my slow and difficult start, thank you for being patient and for encouraging me to grow and gain independence as a chemist. Being able to work on such an exciting project like RTX with so much freedom to explore new ideas has been a once in a lifetime experience that I will never forget. You have helped me along every step of the way and, looking back, I see how much I've grown as a scientist. I hope I've made you proud. I am confident that the future is very bright indeed – *fiat lux!*

Then, my esteemed qualifying exam/PhD dissertation committee:
Prof. Richmond Sarpong and **Prof. Wenjun Zhang**, I thank both of you for serving on my qualifying exam committee and my PhD thesis committee. You have made my journey through graduate school both smooth and instructive.

My fellow teammates on the RTX project:
Lukas: Oh Lukas, what a journey it has been. I never thought that I would get such a motivated and hard-working visiting scholar such as yourself and yet you showed up, ready to put grams upon grams of carvone into the γ-oxidation. What came next – COVID, you coming back as a fully-fledged graduate student, and the completion of the RTX synthesis – was so unexpected that it still feels only half-real. I thank you for working with me on RTX and for putting up with me. Over the past two years you've shown that you can be highly productive, but now is the time to show that you are also an independent thinker, that you can work both hard and smart. As both your mentor and your friend I am truly looking forward to you completing the synthesis of gnidimacrin! It would make me very happy to see you grow not only in terms of muscle mass but also in terms of high-level chemistry skills – it is time for you to realize your true potential!

Kuan: During our brief time working together on RTX I learned a lot from you, for which I am thankful. You're always in lab so I'm sure you have what it takes to become a professor – good luck!

Past Maimone lab members – Tempus fugit!
Danny T.: Oh Danny. You were instrumental in getting me to join the Maimone lab not only by applying superstoichiometric amounts of Grey Goose vodka during visiting weekend but by virtue of your intellect (you're a mastermind when it comes to science and disinformation campaigns), work ethic, and immense passion for chemistry. You were the ideal labmate I envisioned (minus your habits of rarely cleaning glassware) and I am very glad we grew to be friends as well. I am thankful that you were always there for me – my lazy year(s), my angry year(s) and my spicy year and I truly appreciate all your advice and support. You motivated me to be a better chemist (and to quit vaping) and more importantly, a Cowboys fan. You should know that I truly value your friendship, even if I don't always show it, and that I remain infinitely impressed by your chemistry

skills and the zeal with which you tackle scientific problems. I can only dream of matching your productivity. You are a personification of the motto *Per aspera ad astra* - you've worked so hard, come very far, and the best is yet to come. I know you'll become a great chemistry professor and you'll reach the stars (where you'll wisely steer clear of the Protoss). I wish you and Rachel all the best and I'm looking forward to reading your papers.

Karl: Dr. Haelsig, you'll be the first person I invite to my secret volcano island hideout once I build it (rest assured, there will be a landing strip for your F-14). I look up to you as a chemist and I'm grateful to have you as a friend. Your perseverance has been an inspiration to me throughout the years and I'll always fondly remember your sense of humor. Many thanks for your support on my scientific journey and I hope that one day we'll be working in the same pharma company.

Rachel: I still have the paper snowflake you made as Christmas decoration during my first year – thank you so much for keeping everyone's spirits up! It's amazing how you remained kind, friendly and hard-working in the face of great chemical challenges. You are a wonderful chemist with real passion for knowledge and you have a commendable desire to do things right and by the numbers – a rare quality these days, which makes it all the more important. Thank you for being my friend, for ordering disposables and cucumber-flavored Juul pods, and I wish you and Danny all the best!

Bingqi: Bingqi, you're just awesome. No doubt about it – so very hard-working and so very nice and friendly. I'm amazed how after 5 years of grad school your remain so kind and helpful. I'm glad to hear you're enjoying your postdoc and I know that given your impressive chemistry skills and unparalleled work ethic will lead to you achieving great things!

Xirui: You were one hell of an upperclassman to look up to! Thank you for gifting me your red OChem textbook, for your sage advice and for helping me with BMS.

Claire: I cannot find the words to describe how impressive your achievements are. It must take superhuman strength and willpower to finish a molecule on your own while pregnant/nursing little Julien with COVID raging all around. I have nothing but respect for your and I know that you will have great achievements in all aspects of your life, both career and family. I wish you and your family all the best!

Kevin: You continue to inspire me with your unique outlook on life and I'm grateful that even though we didn't overlap for long you're there to exchange advice for Angeline's (or even offer it for free!). I know you won't lose your style in the future either.

Mikiko: I'm glad we got to spend some time together in the Maimone lab – you're a brilliant chemist and I know you have a bright future at Genentech! Thank you for your help and support and for bringing some level of class to 909.

Drew: Oh Drew, you're one-of-a-kind chemist and character and I count myself very fortunate to have met you! I remember you having a lot of fun during my visiting weekend (and on subsequent occasions as well) and how professional and detailed your subgroups were – you're truly an exemplification of the work hard, play hard mentality. I've looked up to you all these years and I am truly thankful for your help and support during my early years and my journey towards employment. I know you're having a great time on the East coast and that you're crushing it at Merck. I wish you and Patti all the best!

SMartin: I'm glad you brought some much-needed European urbanity to 909 and for filling up the empty hood next to mine. I hope you enjoyed your time at Berkeley and I wish you all the best! BI is lucky to have you and your nice personality certainly makes you a great co-worker.

Naifeng: It was great making some molecular glues with you – I learned a lot. Your patience and perseverance were impressive and I know that a bright future awaits you.

Jun: I miss your presence in 908 – you've certainly left your mark on the lab culture and publication record. I wish you all the best!
Matt Condakes: I wish we could've overlapped for a long period of time so I could've learned more from you. Your vast knowledge and chemistry skills truly impressed me. Thank you for hosting me and helping with my qual! One day we may work at the same BMS site – that would be great.
Linus, CEO: You have a PhD and a start-up and a BMW. Is there more to life? Although two of these three things can crash… I wish you good luck and abundant funding.
Malte: Though our time together was brief I think it was quite fun. You faced the hardships of Nimbolide as I faced the hardships of gradschool and I am very glad that we're still friends. It's impressive what you can do with a balloon and a solvent drum and I know this creativity will serve you well at BASF.
Fernando: Chemistry is metal, bro! What you did is not easy but looking out for #1 (you) is certainly the right thing to do.
Jordan: Undergrad extraordinaire, exemplar for the rest of 'em – it's been wonderful to watch you grow as a scientist and to witness you give people the business on the ice. I'm amazed at how you can balance being a great chemist, playing hockey, and being such a nice person and I know you'll do super well in the future.

Current Maimone lab members (for optimal productivity, the following is to be read while you're waiting for your TLC to develop):
Danny H.: Oh Danny, thank you for bringing some much-needed Harvard pedigree to my side of the lab and thank you even more for being such a great friend and awesome chemist. Seven-membered rings are never easy but I know you'll figure yours out and with a precise slice at its cycloheptane-shaped neck your titan of a natural product will fall. Remember that when things seem grim it's time to go on the attack – after all, the night is always darkest before the dawn. I never believed that myself until I saw the light at the end of the tunnel, but now I get to say it. I'm truly grateful that you were there for such a big part of my journey – you uphold the necessary sharpness levels very well and are unmatched with a metal file. You are a very talented scientist with a great career ahead of you and the way your mentee Anna is growing as a chemist is proof that you'll be a great professor. Keep your blade sharp (no matter what skin you have on it) and your wits sharper!
Paulo: Oh man, how I wish we had started hiking sooner. Being in nature (or drinking beer) with you does wonders for my grumpiness. I'm so grateful that you were there for me with kind words and tasty beverages and you should know I'm happy to help whenever you need it. Chemistry is a harsh mistress so never giving up is part of the experience. You've stood tall in the face of the challenges in your PhD and you continue to grow as a chemist – Gilead will be thrilled to have you working for them again. Best of luck making the stickiest acrylamides!
Beth: There was a time when you worked in 909 and your light-up shoes always brightened my day. I am so happy to see how you've grown as a chemist and that you finished your natural product! You are very hard-working and a logical thinker, not to mention that you have the heart of a lion. You'll do great whatever you do in the future – maybe you should start a company to rival Linus' start-up. Best of luck and make sure Yi does what you say!
Yi: Between you being there as an undergrad and then grad student, I feel like we've spent about the same amount of time in the Maimone lab. I only wish we spent more time talking about anime and/or chemistry – I'm sure you have a thing or two to teach me in either field. You're very brave

tackling such a tough natural product but I'm confident you'll get an NMR of those complex myrmicarins before they decompose. I'm excited to see where your scientific career takes you. Remember to obey Beth.
Kincade: Bro, during your short time in lab you've managed to impress me with your excitement for chemistry and your work ethic. Keep working until 2 am and great things will come – you've already made impressive progress on your scaffold and I'm looking forward to seeing how and when you'll wrap up the molecule. You are the future leader of the lab and the task of picking up the banner and being someone younger students look up to will fall to you. Make us older students proud!
Kelvin: You have great potential to become a wonderful scientist. I regret not talking to you more but hit me up if you need any help. Keep working hard at the things that make you happy!
Shang: Motorcycle – check. Adidas track pants – check. Lots of reactions in your hood – check. You're on the right track and I know you'll weather any challenge your PhD throws at you. Follow the three white stripes ever onwards.
Vanessa: You have a heart as big as Texas and the motivation to become a great synthetic chemist – keep at it!
Tanner: Starting out can be very hard – I know it was for me and what got me through was talking to Tom and persevering. Hang in there, you have a tough molecule to make.
Stanford chemists, both mentors and peers:
Noah: Thank you so much for mentoring me as an undergraduate! Working in your lab truly sparked my excitement for total synthesis and inspired me to become a synthetic organic chemist. I will always fondly remember my time at Stanford, especially the summers when I could work in lab full time.
Alex: Thanks to you I've learned so much, but most importantly – to try and answer my own questions. You taught me how to think as a chemist and how to write as a chemist for which I will always be grateful. I hope we have the chance to work together in industry at some point!
Dennis: Thank you for being my first mentor! You showed me a glimpse of how awesome science is (and more than a glimpse of how awesome you are).
Matt: I truly appreciate that we overlapped for some time in the Burns lab! I loved how excited you were about chemistry and I'm glad to see you transferred your excitement to Genentech. Thank you for all your help throughout the years!
Joy: Thank you for being such a good friend! We braved the perils of a Berkeley PhD together and made it. I wish you and Lewis all the best!
Alastair: Thank you for being my big in AXE and my friend! I'm excited to see where our chemical journey takes us and I know the process chem department at Gilead is lucky to have you.
Jovan: Ah Jovan, thanks for all the stir bars! I'm glad to know you'll be my doctor one day.
My parents, friends, and mentors in Bulgaria:
С огромна благодарност най-вече за милата ми майка и нейната константна, макар и дистанционна, подкрепа. С благодарност и за баща ми, който ме вдъхнови да изследвам света около мен. Разбира се дължа много на доц. Донка Ташева, доц. Христо Чанев и останалите членове на олимпийския комитет - благодаря ви за шанса да се занимавам с химия. Ице, благодаря ти за мъдростта и помощта и да дойдеш пак на гости. Силви, макар и от далеч ние оставаме все така добри приятели, което истински ме радва. Твоята доброта и работливост нямат граници. И с благодарност към други любими хора, включително и тези които вече не са сред нас - всички ми помогнахте много. Време е да продължа пътя си - с Бог все напред и нагоре.

List of Abbreviations

Ac	acetate
AIBN	azobisisobutyronitrile
AZADO	2-azaadamantane, N-Oxyl
AZADOL	N-hydroxy 2-azaadamantane
Brsm	based on recovered starting material
Bn	benzyl
Bz	benzoyl
CAN	cerium ammonium nitrate
CSA	camphorsulfonic acid
DABCO	1,4-diazabicyclo[2.2.2]octane
DBAD	di-*tert*-butyl azodicarboxylate
DCC	*N,N'*-dicyclohexylcarbodiimide
DCE	1,2-dichloroethane
DCM	dichloromethane
DDQ	2,3-Dichloro-5,6-dicyano-1,4-benzoquinone
DIBAL	diisobutylaluminum hydride
DIPT	Diisopropyl tartrate
DMAP	dimethylamino pyridine
DMF	N,N-dimethylformamide
DMP	Dess-Martin periodinane
DMS	dimethyl sulfide
DMSO	dimethyl sulfoxide
EDC•HCl	N-(3-dimethylaminopropyl)-N'-ethylcarbodiimide hydrochloride
Fur	Furyl
Fod	6,6,7,7,8,8,8-heptafluoro-2,2-dimethyl-3,5-octanedionato
hfacac	hexafluoroacetylacetonate
HG	Hoveyda-Grubbs
HMPA	bis(trimethylsilyl)amide
HRMS	high-resolution mass spectrometry
IBX	2-iodoxybenzoic acid
Imid.	imidazole
KHMDS	potassium bis(trimethylsilyl)amide
LAH	Lithium aluminum hydride
LDA	lithium diisopropylamine
LHMDS	lithium bis(trimethylsilyl)amide
m-CPBA	*meta*-chloroperoxybenzoic acid
MeCN	acetonitrile
MsCl	Methanesulfonyl chloride
TsCl	4-Toluenesulfonyl chloride
Naph	Naphthalenide
NaHMDS	sodium bis(trimethylsilyl)amide
NBS	*N*-bromosuccinimide
NIS	*N*-iodosuccinimide
NMO	N-methylmorpholine N-oxide

PhMe	toluene
PIDA	(diacetoxyiodo)benzene
PIFA	(Bis(trifluoroacetoxy)iodo)benzene
PKC	Protein kinase C
PPTS	pyridinium p-toluenesulfonate
pyr	pyridine
RCM	ring closing metathesis
TBAF	tetrabutylammonium fluoride
TBAI	tetrabutylammonium iodide
TBHP	*tert*-butyl hydroperoxide
TBS	*tert*-butyldimethylsilyl
TBSCl	*tert*-butyldimethylsilyl chloride
TEMPO	(2,2,6,6-Tetramethylpiperidin-1-yl)oxyl
Tf	Triflate or trifluoromethanesulfonate
THF	Tetrahydrofuran
TIPS	Triisopropylsilyl
TIPSCl	Triisopropylsilyl chloride
TIPSOTf	Triisopropylsilyl triflate
TLC	thin layer chromatography
TMP	2,2,6,6-Tetramethylpiperidine
TMS	Trimethylsilyl
TMSCl	Trimethylsilyl chloride
TMSOTf	Trimethylsilyl triflate
TPAP	Tetrapropylammonium perruthenate
TsOH	*p*-Toluenesulfonic acid
V-40	1,1'-azobis(cyclohexanecarbonitrile)

Chapter 1.

Daphnane Diterpenoid Orthoesters

Background and Significance; Retrosynthetic Analysis

1.1 *Resiniferatoxin, Related Natural Products, and Biosynthesis*

Resiniferatoxin (RTX, **1.1.1**, Figure 1.1.1) is a complex natural product with fascinating bioactivity at sub-nanomolar concentrations.[1] Structurally, resiniferatoxin is comprised of three subunits – a homovanillic acid ester (highlighted in red) and a phenylacetic acid orthoester (highlighted in green) bound to a 5,7,6-fused tricyclic core bearing seven contiguous stereocenters, most of which are centered around the 6-membered ring.[2] This tricycle is the key structural feature of the daphnane diterpenoid orthoesters (DDOs), a class of more than 200 natural products found in various plants of the *Thymelaeaceae* and *Euphorbiaceae* families.[3,4] Similarly to resiniferatoxin, most of these natural compounds contain an orthoester bound to the stereochemically dense six-membered ring of the tricyclic motif known as the daphnane diterpene core.[5] Because they contain twenty carbons in their 5,7,6-fused tricycles but more than twenty carbon atoms if the orthoester sidechains are accounted for, the DDOs are also interchangeably referred to as daphnane diterpenes, daphnane diterpenoids, and daphnane-type diterpenoids in literature.[3,4,5] The exact C ring carbons connected to the orthoester moiety differ between family members, which, combined with the possibility for additional oxidation to be present around the 5,7,6-fused tricycle accounts for the staggering diversity of isolated structures. In terms of overall oxidation level, RTX is at the lower end of the spectrum despite containing five oxygen atoms bound to its daphnane core, with the majority of DDOs containing additional oxygen atoms, most commonly at C5, C6, and C7 as evidenced by all of the structures depicted in Figure 1.1.1 except RTX itself. The presence of additional oxygen atoms at C12, C15, and C18 is also noted in certain members. Due to their sheer number, DDOs containing an epoxide at C6 and C7 such as daphnetoxin (**1.1.2**),[6] synaptolepisfactor K_7 (**1.1.3**),[7] yuanhuapine (**1.1.5**),[8] yuanhuacine (**1.1.7**),[9] thymeleatoxin (**1.1.8**)[10] and genkwadaphnin-20-palmitate (**1.1.9**)[11] are grouped together and referred to as the 6-epoxydaphnanes in the existing literature. Other functional groups at C6 and C7 are also possible, such as the hydroxyl groups found in genkwanine A (**1.1.4**)[12] and yuanhuaoate B (**1.1.6**).[13] Further examples of the structural diversity of the daphnane diterpenoid orthoesters, made even more vast by virtue of different permutations of relative stereochemistry or ester sidechain substitution (compare **1.1.7** and **1.1.8** for instance) can be found in Section 1.7 of the thesis.

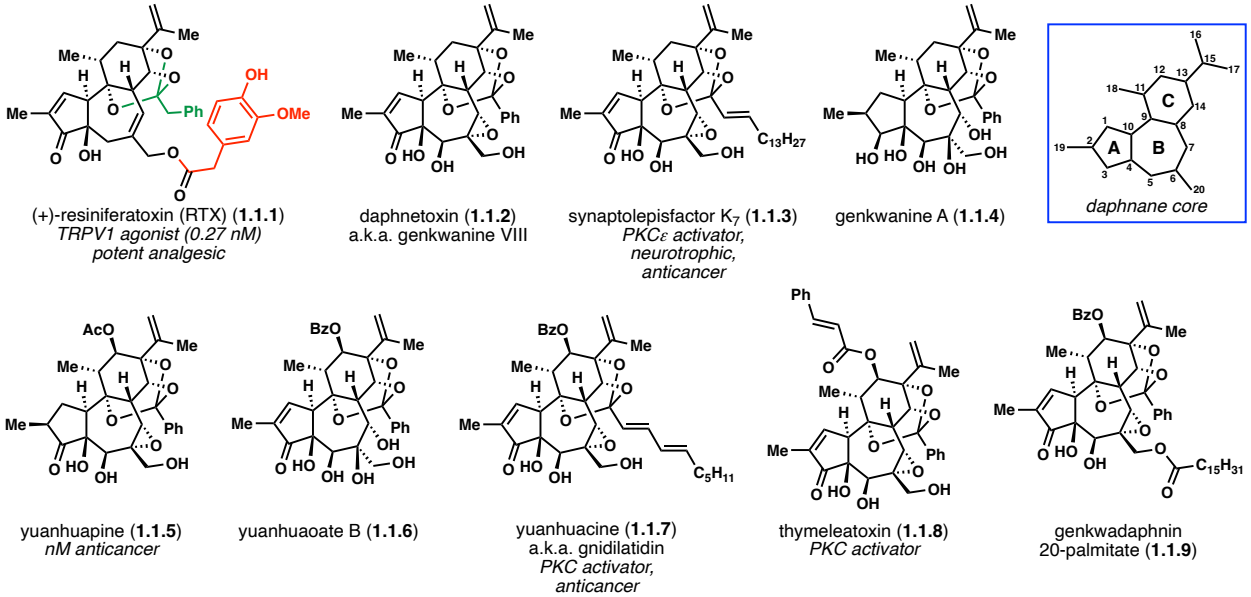
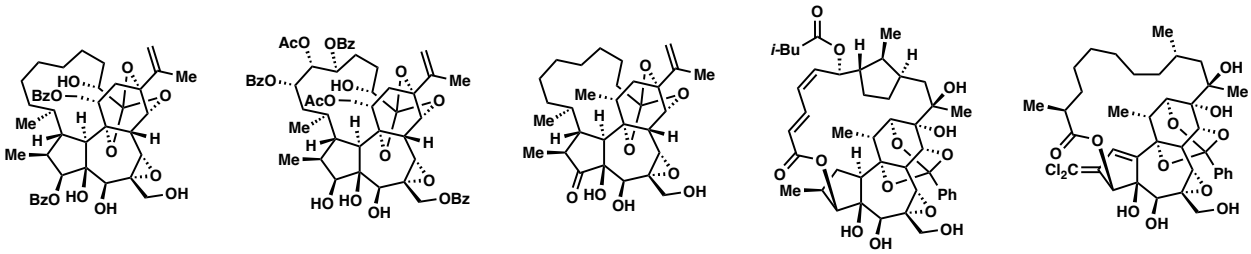


Figure 1.1.1. Structures of resiniferatoxin and other daphnane diterpenoid orthoesters as well as general structure of the daphnane diterpene core. Selected bioactivity profiles are also reported.

Another way in which DDO structural diversity is altered is by the attachment of an additional carbon chain tethered to the 5,7,6-fused tricycle, resulting in a macrocyclic ring (Figure 1.1.2). This increase in complexity results in the fascinating structures of the 1-alkyldaphnanes and the rediocides.[7,14] In the former, the carbon chain of the C ring orthoester is also tethered to the α-face of the A ring at C1, with different substitution patterns on the sidechain being possible in addition to a methyl-bound stereocenter featured in all members of this subfamily. Examples include gnidimacrin (**1.1.10**),[15] daphneodorin C (**1.1.11**),[16] and wikstroelide E (**1.1.12**).[17,18] In contrast to the 1-alkyldaphnanes, the C–C bond in the macrocycle of the rediocides such as rediocide A (**1.1.13**)[14] is found at C16 of the daphnane diterpene core, with the other end of the additional carbon chain being attached via an ester linkage to a β-face hydroxy group at C3. In most rediocides, an extra 3-, 5-, or 6-membered ring is present in the macrocycle backbone, drastically increasing the topological complexity of these already remarkable structures. Other natural products such as trigocherriolide E (**1.1.14**)[19] also contain a similar macrocyclic lactone. Finally, a further degree of structural diversity is found when the different possible substituents at C20 of the daphnane core are taken into consideration, as some DDOs contain various C20 ester groups such as genkwadaphnin-20-palmitate (**1.1.9**) and RTX itself, with the nature of the ester sidechain being potentially very impactful for the bioactivity of the corresponding natural product, as will be discussed below in the case of resiniferatoxin.



(–)-gnidimacrin (**1.1.10**)
PKC activator
pM anti-HIV
pM anticancer

daphneodorin C (**1.1.11**)

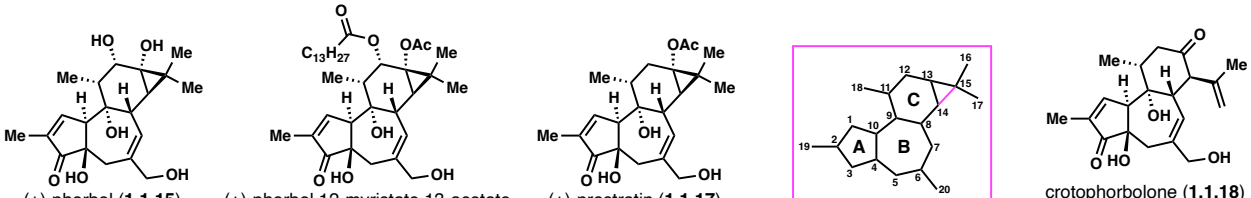
wikstroelide E (**1.1.12**)
a.k.a. Pimelea factor S_6
PKC activator
anti-HIV

rediocide A (**1.1.13**)
insecticide
downregulates CD155

trigocherriolide E (**1.1.14**)
PKC activator
anti-viral

Figure 1.1.2. Examples of the 1-alkyldaphnanes and rediocides-type macrocyclic scaffolds.

While not technically daphnanes, the tigliane and rhamnofolane diterpenes are also worth discussing as they also possess complex 5,7,6-fused tricycles (see Figure 1.1.3 on the next page).[20] In fact, the oxidation pattern and stereochemistry around the tricyclic cores of these related natural product families closely match the daphnane diterpene moiety of the DDOs as all three classes of compounds share a common biosynthetic precursor. The only difference in connectivity is the extra C14-C15 bond in the tiglianes, resulting in an additional cyclopropane ring fused to the common tricyclic motif. The most studied tiglianes are phorbol (**1.1.15**)[21,22] and its diesters at C12 and C13, exemplified by phorbol 12-myristate 13-acetate (PMA, **1.1.16**)[23] as well as prostratin (**1.1.17**),[24] which lacks the C12 oxidation. The rhamnofolanes, represented here by the scaffold of



(+)-phorbol (**1.1.15**)
PKC activator
tumor promoter

(+)-phorbol 12-myristate 13-acetate (PMA) (**1.1.16**)
PKC activator
tumor promoter

(+)-prostratin (**1.1.17**)
PKC activator
anti-HIV
anticancer

tigliane core

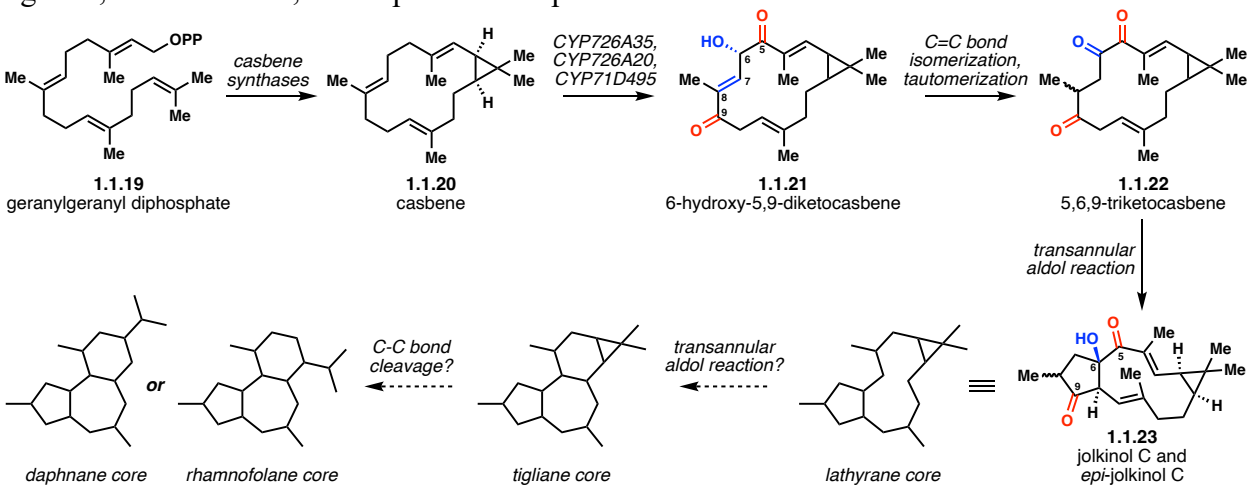
crotophorbolone (**1.1.18**)
rhamnofolane diterpene

Figure 1.1.3. Structures of the biosynthetically related tigliane and rhamnofolane diterpenes.

crotophorbolone (**1.1.18**),[21] feature a C14-C15 bond but no bond between C13 and C15. The number of compounds featuring a highly decorated 5,7,6-fused tricycle thus extends beyond the daphnane diterpenoid orthoesters and includes members of biosynthetically related families of natural products.

A brief overview of the proposed biosynthesis of the daphnanes, tiglianes, and rhamnofolanes is included herein to both highlight the common origin of these compounds as well contrast the way in which such complex structures are made in Nature versus in the synthetic laboratory (discussed in Sections 1.4 and Chapter 2). According to our current biosynthetic understanding, the carbon scaffold of the daphnanes and tiglianes originates from casbene (**1.1.20**, Scheme 1.1.1), itself the result of an enzyme-mediated macrocyclization of geranylgeranyl diphosphate (GGDP, **1.1.19**).[25] Site-selective oxidation of casbene by cytochrome enzymes results in more oxidized congeners capable of undergoing intramolecular aldol reactions to forge C-C bonds across the macrocycle. The first such event likely connects C6 and C10 (casbene numbering), resulting in the lathyrane scaffold, since lathyrane diterpenes can be isolated alongside tiglianes and daphnanes from a variety of plants.[26] In fact, the monooxygenase CYP enzymes responsible for the oxidation of casbene to ultimately provide the lathyrane jolkinol C (**1.1.23**) have been experimentally determined in *Jatropha curcas*.[26] Diketone **1.1.21** was proposed to be a key intermediate, resulting from multiple enzyme-mediated oxidation reactions, which then undergoes non-enzymatic transposition of the C7-C8 olefin followed by tautomerization, resulting in transient formation of triketone **1.1.22**. This intermediate in turn is proposed to rapidly react via a transannular aldol process to construct the lathyrane diterpene jolkinol C (**1.1.23**) alongside its C8 epimer. Similar intermediates have also been identified in a biosynthesis study involving *Euphorbia lathyris* L. and were observed to also ultimately provide jolkinol C.[27] Based on these results the conversion of the lathyrane core to the tigliane core via a similar series of oxidations and another intramolecular aldol reaction can be proposed, although the nature of all enzymes responsible for the oxidase phase of the sequence have yet to be determined. From the tigliane core a bond cleavage, most likely oxidative, between either C13 and C15 or C14 and C15 would result in formation of the rhamnofolane and daphnane cores respectively. Thus, from the simple linear substrate GGDP a treasure-trove of structural complexity and fascinating bioactivities in the form of the DDOs and related natural products can arise.

Scheme 1.1.1. Biosynthesis of lathyrane diterpene jolkinol C and proposed biosynthesis of the tigliane, rhamnofolane, and daphnane diterpenes.



1.2 *Bioactivity of Resiniferatoxin*

The bioactivity of RTX is dictated by the presence of the homovanillic acid ester at C20 (Figure 1.2.1). A very similar moiety to the latter structural motif is also found in capsaicin (**1.2.1**), the active ingredient of chili peppers which is responsible for their pungency/spiciness. It is therefore not surprising that RTX and capsaicin bind to the same protein – TRPV1, a cation channel also known as vanilloid receptor 1.[28,29] This protein exists as a tetramer spanning the cellular membrane of various neurons and is responsible for the detection of different noxious stimuli such as high temperature and pain.[30] Both resiniferatoxin and capsaicin bind to the vanilloid binding pocket, a space between the S3 and S4 α-helical subunits and S4-S5 subunit linker of TRPV1.[31] Hydrogen bonding interactions between serine, threonine, tyrosine, and glutamic acid residues and the homovanillic moieties of RTX and **1.2.1** are partially responsible for binding, but hydrophobic interactions of the lipophilic residues on the S3 and S4 α-helices with the daphnane core and phenylacetic acid orthoester (respectively with the hydrocarbon sidechain of capsaicin) also play a major role.[32] In fact, a crystal structure of **1.2.1** bound to TRPV1 suggests that the linear chain of capsaicin can only partially occupy a large cavity between the S3 and S4 subunits,[33] from which can be inferred that the much bulkier and largely hydrophobic DDO component of RTX is a much better fit and therefore responsible for the much better binding of resiniferatoxin to TRPV1. Indeed, **1.1.1** exhibits its agonist activity with an EC_{50} of 0.27 nM for inducing Ca^{2+} influx through TRPV1 channels heterologously expressed in Chinese hamster ovary (CHO) cells.[34] In the same system capsaicin was recorded to have an EC_{50} of 44.8 nM, a difference in two orders of magnitude. In other experimental comparisons such as pain induction in mouse models,[28] resiniferatoxin was shown to be 1,000 times more potent than capsaicin and can therefore be considered the spiciest compound in the world.

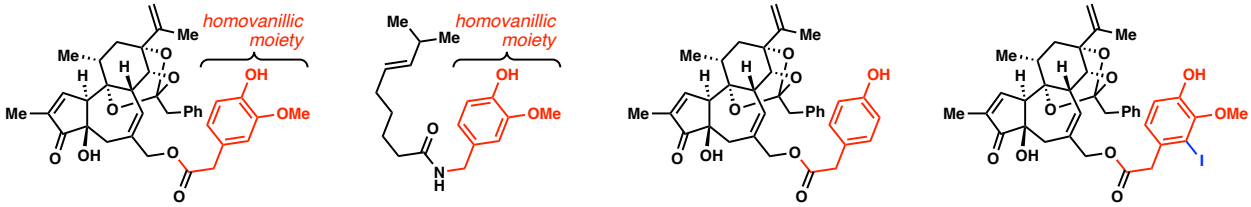


Figure 1.2.1. Structures of RTX and related compounds in terms of bioactivity.

Structure-activity relationship (SAR) studies have shed some light on the key moieties in RTX responsible for its incredibly high activity and have proven that the presence of the daphnane diterpene core and pendant orthoester are crucial for high potency.[35–38] The exact nature of the orthoester sidechain does not seem to have a huge impact on agonist activity, with benzoic and acetic acid orthoesters behaving similarly to RTX. However, the presence of an orthoester, irrespective of its sidechain, is crucial, since a tigliane bearing a homovanillic acid ester at C20 did not approach the potency levels of RTX. The oxidation at C3 was also relevant, possibly as another hydrogen bond acceptor, since compounds containing a 5,7,6-fused tricycle without a ketone or hydroxy group at C3 were not potent binders of TRPV1. Also worth mentioning as examples of SAR on the homovanillic acid ester are tinyatoxin (**1.2.2**),[39] a daphnane diterpenoid orthoester with a slightly different sidechain at C20, and iodo-resiniferatoxin (**1.2.3**)[40] which acts as an antagonist of TRPV1. The latter is proposed to have a different binding site and to act via allosteric modulation of the agonist binding site. Based on these SAR studies, attempts have been made to mimic the bioactivity of resiniferatoxin by a simpler structure containing a homovanillic

acid ester, a ketone corresponding to the C3 ketone of RTX, and a phenylacetic acid orthoester linked by a flexible carbon chain instead of the complex 5,7,6-fused tricycle. While these efforts did result in two test compounds that had bioactivity on the same order of magnitude as RTX, the latter remains the most active agonist and the preferred binder of TRPV1 in many biological assays.

In terms of downstream bioactivity, binding of RTX to TRPV1 results in a repositioning and rotation of the S4-S5 linker and S6 helical subunit, which movements in turn open the pore of the tetrameric ion channel to cation influx.[1,41,42] This influx, predominantly consisting of Ca^{2+} ions, initially triggers depolarization of the neuronal membrane and the resulting impulse is interpreted as pain. However, resiniferatoxin is such a potent binder of the vanilloid receptor that the ion channel stays open for prolonged periods of time, resulting in necrosis of the neurons expressing TRPV1. The overall systemic effect of RTX is thus actually analgesic and is very long-lasting as the regrowth of new neurons that contain TRPV1 in their cellular membrane requires several weeks. Since resiniferatoxin thus selectively targets the neurons of pain receptors, other nerve-driven functions such as motor control or pressure sensing/touch are not impaired when this DDO is administered. While heat sensing is also lost upon treatment with compound **1** since TRPV1 is involved in heat detection, the long-lasting analgesic effects and selectivity of resiniferatoxin have prompted the study of this natural product as an alternative to opioids for the treatment of chronic pain. Indeed, RTX is currently investigated in Phase II clinical trials for the management of pain in patients with advanced forms of cancer and knee arthritis and has been granted Orphan Drug Status by the FDA for treatment of intractable cancer pain – a testament to the highly potent bioactivity of this daphnane diterpenoid orthoester.

1.3 *Bioactivity of the Daphnane Diterpenoid Orthoesters*

As the majority of the DDOs do not possess a homovanillic acid ester at C20, they do not exhibit particularly high binding affinities for TRPV1, the protein target of resiniferatoxin. While some daphnane diterpenoids can technically bind to the vanilloid receptor at μM concentrations, most members of this natural product family bind to different classes of proteins and thereby elicit a wide variety of biological functions. Of particular interest are the interactions of the DDOs with different protein kinase C (PKC) isoforms, as these have been implicated in pharmacologically relevant anti-viral, neuroprotective, and anticancer properties among others.[43,44] RTX itself has been reported to interact with PKC,[45] which is perhaps surprising as most daphnane diterpenoids confirmed to be PKC activators have a free hydroxy group as C20. One possible explanation for this phenomenon is that the homovanillic acid ester of RTX is slowly hydrolyzed under physiological conditions, releasing a free alcohol which can interact with PKC. The reason for this is that the daphnanes and tiglianes are proposed to mimic diacyl glycerols (DAGs), exogenous co-factors for PKC activation, in terms of binding, with the hydroxyl group at C20 corresponding to the free OH of the DAGs, and the ester/orthoester sidechains bound to the tigliane/daphnane C ring mapping onto the two lipid tails of the DAGs.[46,47] The former functional groups are proposed to bind to PKC C1 subunits via hydrogen bonding interactions, while the latter hydrophobic moieties reside in the cellular membrane, thereby anchoring the C1 subunits of PKC to the cell membrane. This positioning in turn exposes the catalytic domain of PKC, leading to overall activation of the enzyme, with small differences in the structures of the tiglianes and DDOs being proposed to account for potential selectivity for different PKC isoforms and perhaps differing hydrophobic interactions with the membrane.

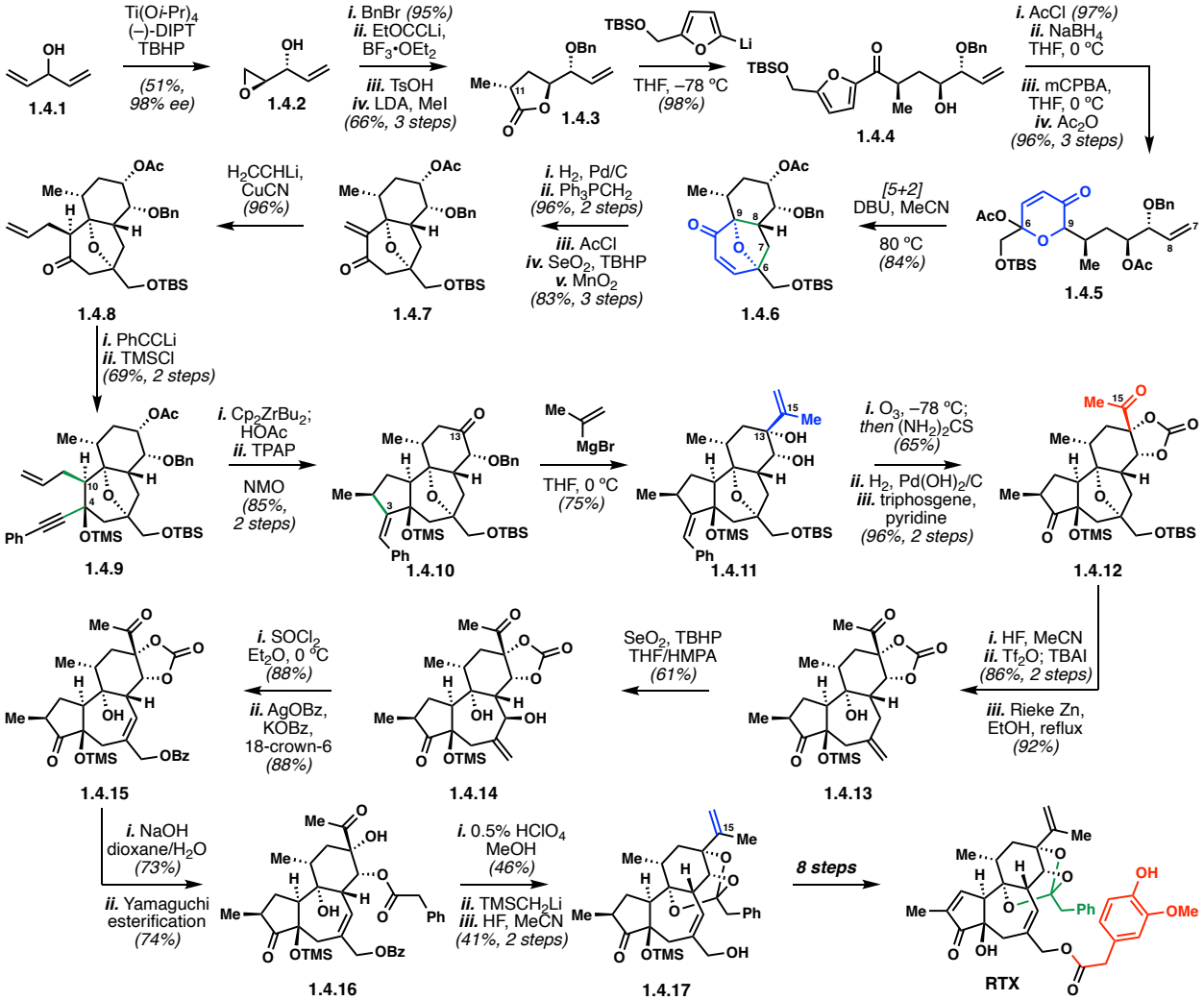
It is then no surprise that several daphnane diterpenoid orthoesters containing free hydroxy groups at C20 as well as long lipophilic orthoester sidechains, in some cases forming a macrocycle, have been experimentally confirmed as PKC activators. For instance, gnidimacrin (**1.1.10**)[15,48–50] was found to inhibit the growth of leukemia K562 cells by acting as PKC activator and thereby inhibiting the cdk2 pathway.[51] Later studies that the βII isoform of PKC is crucial for the antitumor activity of gnidimacrin.[52] Yuanhuacine (**1.1.7**) was also observed to possess anticancer properties, in this case against the basal-like 2 (BL2) subtype of triple negative breast cancer (TNBC) via activation of protein kinase C.[53] This natural product also exhibits activity against non-small cell lung cancer (NSCLC) cells by interacting with the mTOR pathway.[54] In this case downstream deactivation of PKCα is implicated, clearly showing the complexity of PKC-related pathways. Another example of a DDO acting as PKC activator is synaptolepisfactor K_7 which was found to exhibit antitumor and neurotrophic properties by activating PKCε.[55] In terms of antiviral activities, wikstroelide E (**1.1.12**) was shown to reverse latent HIV infection by activating PKC, which in turn modulates downstream NFκB signaling.[56,57] The ability of trigocherriolide E to inhibit the replication of chikungunya virus (CHIKV) is also suggested to arise from PKC activation.[44] Thus, ample evidence exists that the bioactivities of some DDOs are closely tied to the fact that these natural products are PKC activators. However, the complex nature of PKC-based signaling cascades and the presence of multiple PKC isoforms means that the specifics behind the exhibited bioactivities of the majority of DDOs remain largely unexplored as even in some of the examples cited above the exact protein targets have not been determined yet. A lot of work remains to be done to deconvolute the exact mode of action of the DDOs, not to mention the possibility of using these natural products as probes in other PKC-related chemical biology studies.

1.4 *Prior Art in the Total Synthesis of Daphnane Diterpenoid Orthoesters and Related Diterpenes*

With their intricate structures and promising bioactivities, the daphnane diterpenoid orthoesters and related diterpenes from the tigliane and rhamnofolane families have become prime targets for synthetic organic chemists. Despite much effort, the only DDO to be synthesized to date is RTX itself. The impressive syntheses of this molecule by the groups of Paul Wender at Stanford in 1997[58] and Masayuki Inoue at the University of Tokyo in 2017[59] will be discussed here in detail, followed by an overview of some synthetic studies aimed at the daphnanes. Finally, the retrosynthetic logic of some total syntheses of the tiglianes phorbol and prostratin and the rhamnofolane crotophorbolone will also be shown. This overview of prior synthetic efforts is intended to provide context for subsequent chapters and frame the current synthetic efforts disclosed in Chapter 2.

Pioneering efforts by the Wender group resulted initially in the total syntheses of the tigliane phorbol and later culminated with the first total synthesis of RTX via a similar retrosynthetic strategy involving a key [5+2] cycloaddition reaction to forge the B and C rings of the 5,7,6-fused tricyclic system found in the tiglianes and daphnanes (Scheme 1.4.1).[60–64] Beginning with meso-alcohol **1.4.1**, a desymmetrizing Sharpless asymmetric epoxidation reaction resulted in epoxide **1.4.2**. The latter alcohol was converted to lactone **1.4.3** over 4 steps, including a stereoselective methylation to install the C11 methyl group of a natural product. Addition of a lithiated furan further extended the carbon chain of the cyclization precursor, resulting in ketone **1.4.4**. A few functional group manipulations and an Achmatowicz rearrangement were required to arrive at dihydropyran **1.4.5** which was poised to undergo the key [5+2] cycloaddition event.

Scheme 1.4.1. Total synthesis of RTX by the Wender group.

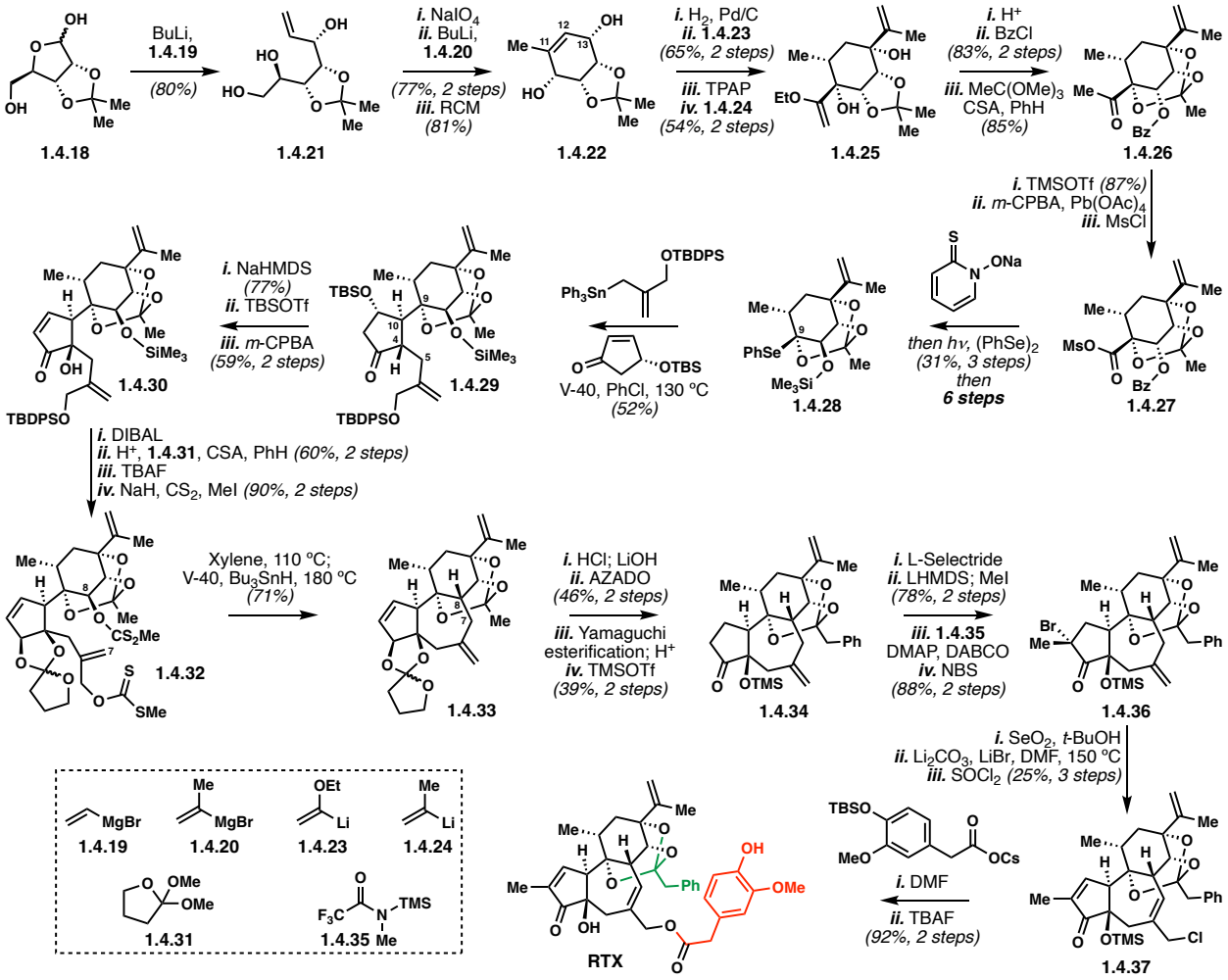


In order to generate the key oxidopyrylium intermediate required for the [5+2] cycloaddition, compound **1.4.5** was deprotonated with DBU. This event was followed by spontaneous loss of acetate to generate an oxidopyrylium ylide with concomitant cyclization with the pendant olefin to provide complex intermediate **1.4.6** containing both the 6- and 7-membered rings of the natural product with several important stereocenters correctly set. Construction of the 5-membered ring of the daphnane core followed via enone **1.4.7**, generated in 5 steps, which was subjected to a Michael addition to install two carbon atoms and set the C10 stereocenter. A 1,2-addition on the opposite face of the allyl chain followed, thereby preparing the *trans* junction between the future 5-membered ring and the 7-membered ring. After TMS protection of the C4 alcohol, closure of the A-ring via a hydrozirconation-initiated pathway followed by oxidation at C13 resulted in tricyclic ketone **1.4.10**. Vinylation of this intermediate was observed to proceed from the desired *β*-face, thereby setting the C13 stereocenter and adding the C15, C16, and C17 carbons onto intermediate **1.4.11**. However, one of these carbon atoms would have to be excised in a subsequent ozonolysis reaction necessary to cleave the unwanted styrenyl olefin appended to the A ring, providing diketone **1.4.12** after some functional group manipulations. Deprotection of the C20 silanol in **1.4.12** followed by triflation of the resulting tertiary alcohol and elimination

under reductive conditions with concomitant cleavage of the tetrahydrofuran ring gave rise to 1,1-disubstituted alkene **1.4.13**. Allylic oxidation at C7 provided secondary alcohol **1.4.14**, which was transposed to primary allylic alcohol **1.4.15** via a two-step sequence. The orthoester moiety was installed next – after deprotection of the carbonate and Yamaguchi esterification with phenylacetic acid to obtain ester **1.4.16**, dilute perchloric acid brought about formation of an orthoester pendant from the oxygen atoms at C9, C13, and C14. A two-step olefination at C15 to restore the missing carbon atom lost in the ozonolysis step gave rise to in compound **1.4.17** representing a completed DDO core. From there another 8 steps were necessary to increase the oxidation state in the A ring and install the homovanillic acid sidechain, resulting in a 44-step total synthesis of resiniferatoxin.

These impressive synthetic efforts were not superseded for the next two decades until the Inoue group disclosed their route to RTX in 2017 featuring key radical cyclization cascades to construct several C-C bonds around the 7-membered rings (Scheme 1.4.2).[59,65,66] In this route the 6-membered ring was constructed first using a (D)-ribose-derived chiral pool starting material **1.4.18**. The carbon chain thereof was elongated with vinyl Grignard (**1.4.19**) and shortened via a Malaprade reaction of free diol **1.4.21**. The newly unveiled carbonyl group was reacted with Grignard reagent **1.4.20** and the resulting addition product was subjected to ring-closing metathesis conditions to generate cyclohexene **1.4.22** containing the 6-membered ring of the natural product.

Scheme 1.4.2. Total synthesis of resiniferatoxin by the Inoue group.

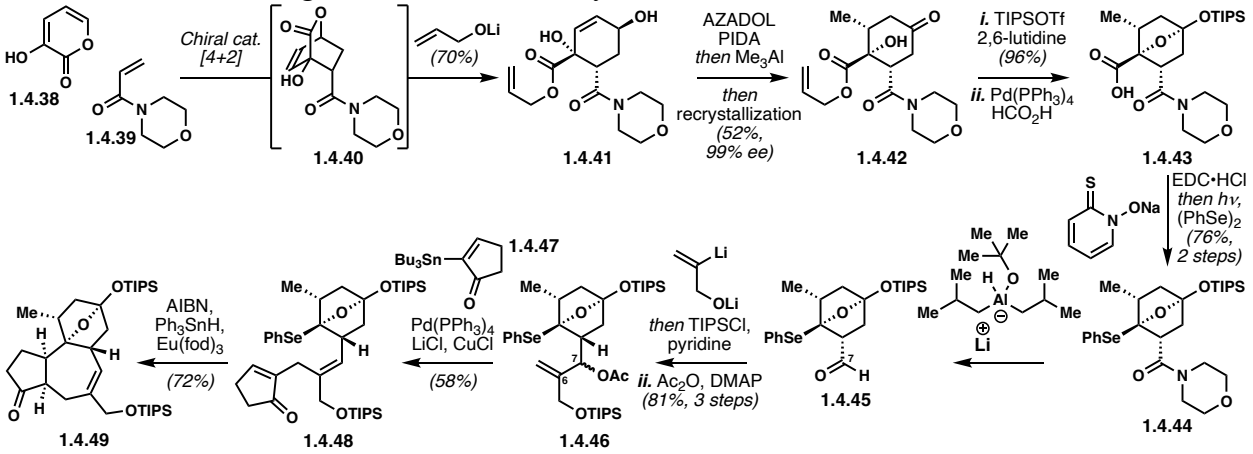


Having forged the C ring of the daphnane diterpenes early on, the Inoue group proceeded to increase the complexity of this intermediate via diol **1.4.25** to arrive at orthoester **1.4.26**. The presence of an orthoester bound to the cyclohexane was required to prevent changes in conformation of subsequent radical intermediates generated at C9. However, in order to access the precursor for such intermediates the two-carbon chain bound to C9 in **1.4.26** had to be removed. An oxidative sequence involving the silyl enol ether of **1.4.26** resulted via extrusion of one carbon atom in mesylate **1.4.27**. The mesylate in this intermediate was converted to a Barton ester, which in turn was transformed into the desired C9 phenylselenide which would act as radical precursor. A further sequence of 6 steps was necessary to arrive at phenylselenide **1.4.28** poised to undergo the first radical cascade and thereby forge two C-C bonds.

In this reaction the C9 radical generated from **1.4.28**, unable to planarize or undergo stereochemical inversion due to the caged nature of the intermediate, was observed to undergo Giese addition with a functionalized cyclopentenone and the resulting α-keto radical was trapped by an allyltin species to provide complex intermediate **1.4.29** bearing the A ring of the daphnane core as well as the carbon atoms necessary for closure of the 7-membered ring. Some oxidative manipulations and installation of the two methyl xanthates needed for formation of the last C-C bond provided **1.4.32** via enone **1.4.30**. A radical 7-*exo*-trig cyclization of this intermediate, followed by formation of an exocyclic olefin at C6 generated tricycle **1.4.33** containing all but one carbons and all stereocenters of the daphnane diterpenoid core. The acetic acid orthoester employed thus far was replaced at this stage with the desired orthoester of phenylacetic acid using a two-step procedure involving Yamaguchi esterification at the C14 alcohol followed by acid-mediated orthoester closure similar to the sequence used by the Wender group. Intermediate **1.4.34** was subjected to functional group manipulations around the A ring, resulting in tricyclic compound **1.4.36**. Using logic similar to that of Wender, the 1,1-disubstituted olefin in **1.4.36** was subjected to allylic oxidation conditions and eventually converted to primary allylic chloride **1.4.37**. From there a two-step sequence provided synthetic RTX in a total of 43 steps.

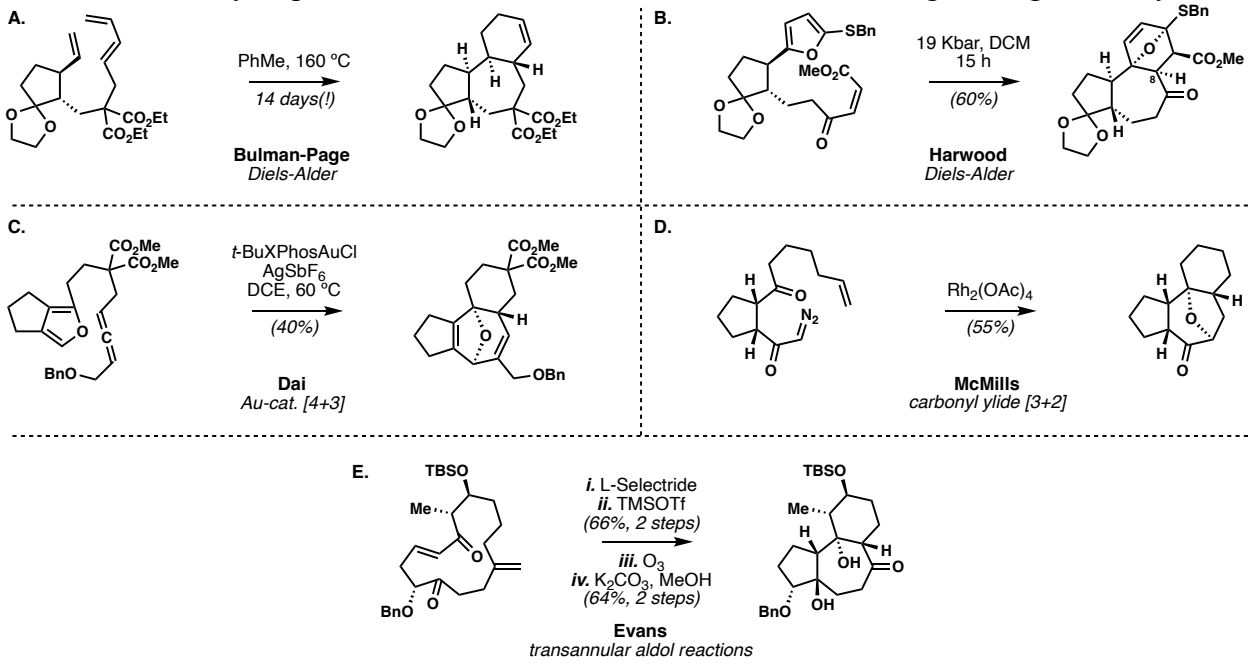
The Inoue group also disclosed a shorter second-generation synthetic route centered on similar disconnections but more rapid construction of an intermediate containing the C ring of the natural product (Scheme 1.4.3).[67] In the first step of this sequence hydroxypyran **1.4.38** and acrylamide **1.4.39** are united in a Diels-Alder reaction mediated by a chiral catalyst, resulting in bicyclic lactone **1.4.40** which is then cleaved to ester **1.4.41**. Since the enantioinduction observed in the [4+2] cycloaddition is modest, ketone **1.4.42** resulting from oxidation of allylic alcohol **1.4.41** was recrystallized to increase the enantiopurity of the material. Ketalization followed by conversion of the allyl ester to the free carboxylic acid **1.4.43** set the stage for a decarboxylative installation of a phenylselenide at C9 via a Barton ester intermediate – a sequence similar to the one used in the first-generation route. The resulting phenylselenide **1.4.44** was converted to aldehyde **1.4.45** via careful reduction of the morpholine amide. In a departure from the previous route, a 1,2-reduction into the carbonyl group of **1.4.45** forged the first C-C bond of the 7-membered ring, providing silanol **1.4.46** after acetylation. The allyl acetate moiety in this compound was harnessed in the second C-C bond forming event, a Pd-mediated allylation with vinyl stannane **1.4.47**. An intramolecular Giese addition of the C9 radical generated from phenylselenide **1.4.48** resulted in tricycle **1.4.49** in only 9 steps. From this intermediate RTX was accessed in another 12 steps. Furthermore, 1.4.49 could be converted to tigliane and rhamnofolane diterpenes as well.

Scheme 1.4.3. Second-generation route to tricyclic intermediate *en route* to RTX.



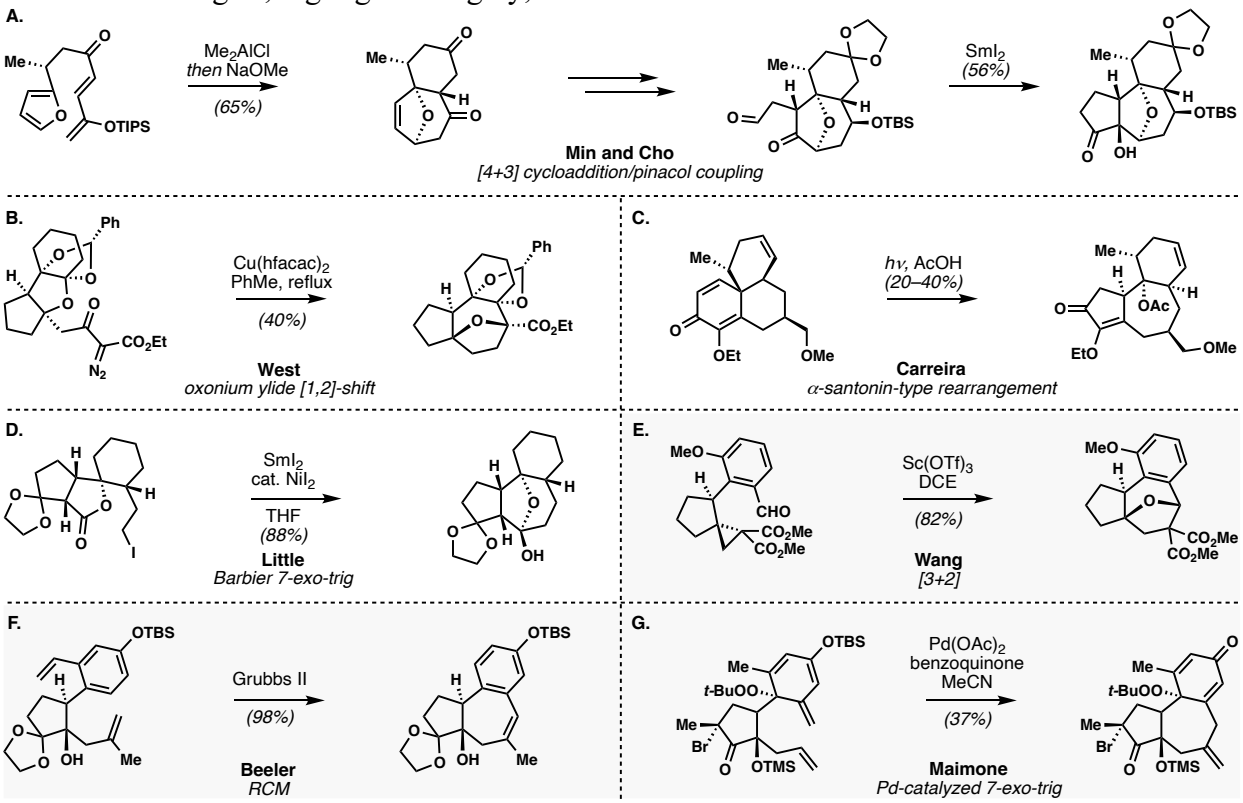
In terms of strategy, the syntheses discussed above relied on early-stage construction of the stereochemically dense C ring followed by further elaboration to a 5,7,6-fused tricycle, with the phenylacetic acid orthoester being installed at a late stage and the homovanillic acid ester being added in the final few steps of each route. This approach appeared logical given the complexity of the 6-membered ring and stood in partial contrast with the routes disclosed in several synthetic studies to the DDOs wherein this ring is assembled at a late stage (Scheme 1.4.4). For instance, the groups of Bulman-Page and Harwood (Scheme 1.4.4A and 1.4.4B) envisioned that the C ring could be forged late-stage, with concomitant formation of the B ring, via a Diels-Alder reaction leading to 5,7,6-fused tricyclic intermediates.[68–71] Similar approaches centered around simultaneous formation of the 6- and 7-membered rings via cyclization of substrates already containing the A ring were exemplified by Dai's gold-catalyzed [4+3] reaction[72] or McMills' carbonyl ylide [3+2] cyclization.[73] Finally, a series of biosynthesis-inspired transannular aldol reactions reported by the Evans group also involved late-stage formation of the C ring (Scheme 1.4.4E).[74]

Scheme 1.4.4. Key steps used in studies toward DDOs based on late-stage C ring assembly.



In the remainder of the synthetic studies however (Scheme 1.4.5), the 6-membered ring was included in the structure of the synthetic intermediates early on, and the 7-membered ring was forged last. The approach by Min and Cho (Scheme 1.4.5A) conceptually follows the logic used in Wender's route to RTX but includes a different kind cycloaddition event.[75] Other methods of closing the B ring include a *1,2*-shift of an oxonium ylide intermediate (West, Scheme 1.4.5B),[76] a photochemical α-santonin-type rearrangement carried out on a complex decalin scaffold (Carreira, Scheme 1.4.5C),[77] or a Barbier reaction (Little, Scheme 1.4.5D).[78] A specific subset of the routes centered on early C ring installation and later B ring formation involved a dearomative strategy (Scheme 1.4.5E, 1.4.5F, 1.4.5G) wherein the 6-membered ring is introduced as an arene, showcased here by the approaches by Wang[79] and Beeler[80] as well as prior studies in the Maimone lab[81] that involved a dearomatization of the C ring prior to Pd-mediated 7-*exo*-trig cyclization to arrive at a highly functionalized 5,7,6-fused tricycle. Such a dearomative approach was also used in the total syntheses of prostratin discussed below.

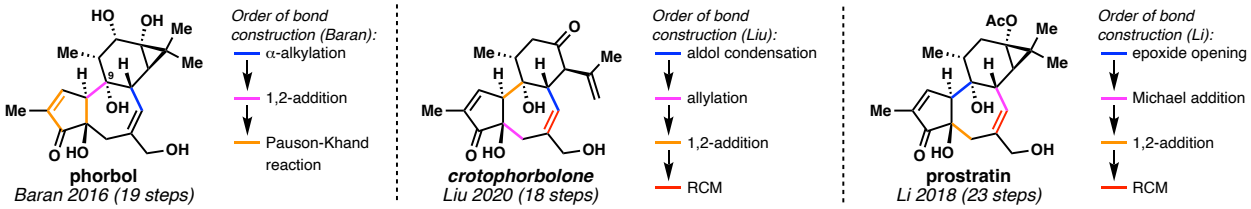
Scheme 1.4.5. Key steps in synthetic studies based on early incorporation of the C ring by Min and Cho (**A**), West (**B**), Carreira (**C**), Little (**D**), Wang (**E**), Beeler (**F**), and Maimone (**G**). The latter three strategies, highlighted in grey, are dearomative.



Indeed, an overview of the total syntheses of tiglianes phorbol and prostratin as well as the rhamnofolane crotophorbolone revealed that the same strategy of forging and/or decorating the C ring at an early stage was successfully used in each case (Scheme 1.4.6). In the Baran synthesis of phorbol,[82] the 6-membered ring was sourced from the chiral pool starting material 3-carene, decorated via α-alkylation of a ketone followed by 1,2-addition and subsequent closure of the 5- and 7-membered rings via a Pauson-Khand reaction. The other two routes followed a similar logic, with the C ring originating from carvone and an anisole derivative in the syntheses of

crotophorbolone and prostratin respectively.[83,84] In both cases the B ring was formed last via a ring-closing metathesis reaction. It hence appeared that the successful strategies utilized to access RTX, phorbol, prostratin, and crotophorbolone all relied on early-stage construction of the 6-membered ring of these natural products.

Scheme 1.4.6. Overview of the retrosynthetic logic used toward phorbol, crotophorbolone, and prostratin.



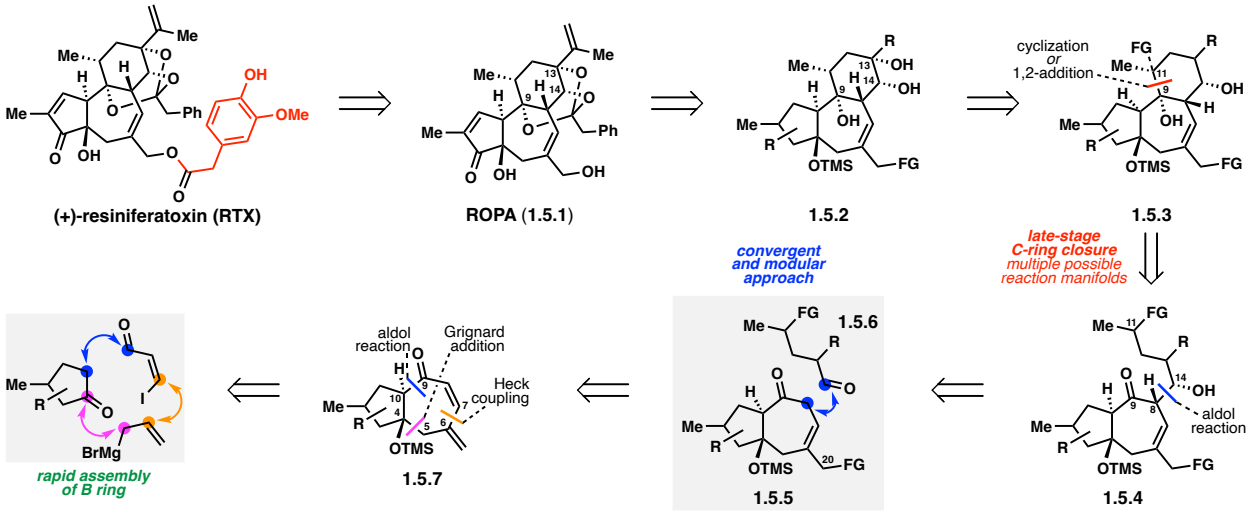
1.5 *Retrosynthetic Analysis of Resiniferatoxin*

Resiniferatoxin and the daphnane diterpenoid orthoesters are highly attractive synthetic targets, firstly by virtue of their compellingly complex structures. With the exception of RTX, these natural products have loomed over the synthetic community as a yet insurmountable challenge,[85] and as already mentioned, despite many synthetic studies diterpenoid **1** itself has only succumbed to total syntheses by two groups even though it has been known for nearly half a century. Clearly there is ample synthetic space yet to be explored *en route* to the DDOs and resiniferatoxin, especially since prior efforts to this molecule and related tiglianes and rhamnofolanes all focus on the same logic of early construction and decoration of the C ring. A different strategy orthogonal to the prior art could prove more rapid, reveal new insights into the complex chemistry of the 5,7,6-tricyclic scaffold, and most importantly, serve as a steppingstone to access more complex DDOs – something which existing routes to RTX have not done to date in published literature. Secondly, while several SAR studies related to RTX exist, comparatively little is known about the bioactivities of daphnane diterpenoids that interact with PKC and how there binding effects downstream PKC signaling. A route that allows for the total synthesis of RTX and more highly oxidized DDOs would be a valuable tool for the detailed study of the biological properties of less explored members of the daphnane family. Thus, the development of a new general synthetic route to these natural products would serve the dual purpose of advancing the field of total synthesis and providing chemical biologists with tools for further elucidation of the biological properties of complex daphnane diterpenoid orthoesters. For these reasons we sought to enter the synthetic discourse on this family of natural products and selected resiniferatoxin as the initial synthetic target, in order to serve as proof of concept for the envisioned general route to the DDOs.

The stereochemically complex C ring of RTX and related diterpenes is undoubtedly the most challenging part of these structures and the selective assembly of this motif at any stage of the synthesis can be a daunting task. It is not surprising that in successful syntheses of resiniferatoxin and the tiglianes this part of the molecule is constructed at an early stage prior to the assembly of the 7-membered ring or the full tricyclic core. Our initial studies, discussed elsewhere, also tried to employ this logic but the routes were invariably hampered by low functional group tolerance or lack of stereoselectivity and culminated in substrates either lacking one C-C bond of the desired 5,7,6-fused tricyclic core or sufficient functionality for further elaboration. These problems could ultimately be traced back to the use of carvone as a chiral pool starting material containing a 6-membered ring.

To avoid such issues, a radically new retrosynthetic route was envisioned, in which, contrary to existing precedent, the C ring would be assembled late-stage via a two-step union of a 5,7-fused bicycle **1.5.5** and a linear fragment **1.5.6** (Scheme 1.5.1). Importantly, this type of disconnection is not reported in prior syntheses or synthetic studies and is orthogonal to the logic of early 6-membered ring construction utilized in prior syntheses. Such a novel approach however would allow for a highly modular and convergent route that could be ideally suited to arrive not only RTX but also previously inaccessible DDOs.

Scheme 1.5.1. Novel retrosynthetic approach involving late-stage assembly of the C ring of the daphnane diterpenoid orthoesters.



Specifically, RTX was simplified to triol **1.5.2** via late stage orthoesterification to resiniferonol 13,14,15-orthophenylacetate (ROPA, **1.5.1**) and installation of the homovanillic acid ester as the final step. The introduction of these two sidechains was postponed to the last part of the synthesis in order to avoid undesired chemo- and regioselectivity issues involving the potentially acid-labile orthoester and very electron-rich arene in the ester sidechain. Tricycle **1.5.2** was further simplified to less functionalized congener **1.5.3**, envisioned to arise from an intramolecular cyclization reaction connecting carbons C9 and C11. The exact mechanism for such a transformation was unclear at this stage but an intramolecular mode of closing the 6-membered ring was preferred from the outset due to the hindered nature of the C9 ketone. Indeed, attempts at intermolecular functionalization of this moiety, discussed in Chapter 2.3, were futile. The cyclization precursor for the envisioned C ring closure, ketone **1.5.4**, was further simplified via an aldol reaction to hydroazulene **1.5.5** and aldehyde **1.5.6**. We envisioned that the exact structure of these building blocks could be varied to accommodate the different oxidation patterns found across the daphnane diterpenoid orthoesters and were optimistic that the venerable aldol reaction would forge the C8 and C14 bond without issues. Furthermore, given the ample precedent for stereocontrol observed in aldol reactions we hypothesized that fragments **1.5.5** and **1.5.6** could be united in a stereoselective way, thereby making the daunting task of constructing the 5 contiguous stereocenters decorating the C ring of the daphnanes somewhat simpler. While we were less sure of the degree of stereocontrol with which the C9-C11 bond formation would proceed, the ability to harness different reagents and reaction mechanisms for this transformation meant that a substrate and/or conditions leading to stereoselective closure of the 6-membered ring could be

found. This flexibility in terms of reaction manifold for the union of C9 and C11 was also expected to circumvent chemo- and regioselectivity issues. Given these considerations we hypothesized that the envisioned synthetic route was feasible, and the challenge of late-stage C ring assembly could be solved.

Trans-fused hydroazulene **1.5.5** was further simplified to less oxidized congener **1.5.7**. Notably, the C20 functional group envisioned as a handle for subsequent installation of the requisite hydroxyl group could be installed by conjugate 1,6-addition into vinylogous enone **1.5.7** and we entertained the idea of carrying out such an addition and trapping the resulting enolate with aldehyde **1.5.6**, thereby arriving at cyclization precursor **1.5.4** in a single step from enone **1.5.7**. In the event that such a cascade was not feasible, a discrete intermediate **1.5.5** containing suitable functionality would be used instead. The 7-membered ring of **1.5.6** was disconnected at three C-C bonds taking inspiration from the previously disclosed synthetic studies carried out in the Maimone lab. A similar Pd-mediated 7-*exo*-trig reaction was planned to close the B ring by connecting C6 and C7. The carbons needed for construction of the 7-membered ring would be tethered to a functionalized cyclopentanone via an aldol reaction between C9 and C10 and a 1,2-addition to construct the C4-C5 bond. In this way 5,7-fused bicycle **1.5.7** was simplified to three bifunctional intermediates, each containing two orthogonal functional handles for the formation of two C-C bonds. The reaction mechanisms for these disconnections were specifically chosen to allow for functional group compatibility and rapid formation of the B ring. While the exact substitution at the A ring was unclear at the outset, we hypothesized that the oxidation of that ring could be gradually built up along the course of the synthesis, with the aim of minimizing potential chemo- and regioselectivity issues stemming from a highly functionalized A ring being present during C-C bond construction. Thus, the hypothetic retrosynthetic approach disclosed herein would be rapid, convergent, chemo-, regio-, and hopefully stereoselective and would hence result in facile construction of RTX with the potential to be adapted for the synthesis of other daphnane diterpenoid orthoester natural products.

1.6 *References*

(1) Brown, D. C. Resiniferatoxin: The Evolution of the “Molecular Scalpel” for Chronic Pain Relief. *Pharmaceuticals* **2016**, *9* (3), 47.

(2) Hergenhahn, M.; Adolf, W.; Hecker, E. Resiniferatoxin and Other Esters of Novel Polyfunctionacl Diterpenes from Euphorbia Resinifera and Unispina. *Tetrahedron Lett.* **1975**, *16* (19), 1595–1598.

(3) Liao, S.-G.; Chen, H.-D.; Yue, J.-M. Plant Orthoesters. *Chem. Rev.* **2009**, *109* (3), 1092–1140.

(4) Nie, Y.-W.; Li, Y.; Luo, L.; Zhang, C.-Y.; Fan, W.; Gu, W.-Y.; Shi, K.-R.; Zhai, X.-X.; Zhu, J.-Y. Phytochemistry and Pharmacological Activities of the Diterpenoids from the Genus Daphne. *Molecules* **2021**, *26* (21), 6598.

(5) Jin, Y.-X.; Shi, L.-L.; Zhang, D.-P.; Wei, H.-Y.; Si, Y.; Ma, G.-X.; Zhang, J. A Review on Daphnane-Type Diterpenoids and Their Bioactive Studies. *Molecules* **2019**, *24* (9), 1842.

(6) Dagang, W.; Sorg, B.; Adolf, W.; Seip, E. H.; Hecker, E. Oligo- and Macrocyclic Diterpenes in Thymelaeaceae and Euphorbiaceae Occurring and Utilized in Yunnan (Southwest China) 1. Daphnane Type Diterpene Esters from Daphne Feddei. *Phytother. Res.* **1991**, *5* (4), 163–168.

(7) Adolf, W.; Seip, E. H.; Hecker, E.; Dossaji, S. F. Irritant Principles of the Mezereon Family (Thymelaeaceae), V. New Skin Irritants and Tumor Promoters of the Daphnane and 1α-

Alkyldaphnane Type from Synaptolepis Kirkii and Synaptolepis Retusa. *J. Nat. Prod.* **1988**, *51* (4), 662–674.
(8) Chen, Y.; Guo, J.; Tang, Y.; Wu, L.; Tao, W.; Qian, Y.; Duan, J. Pharmacokinetic Profile and Metabolite Identification of Yuanhuapine, a Bioactive Component in Daphne Genkwa by Ultra-High Performance Liquid Chromatography Coupled with Tandem Mass Spectrometry. *J. Pharm. Biomed. Anal.* **2015**, *112*, 60–69.
(9) Karalai, C.; Wiriyachitra, P.; Sorg, B.; Hecker, E. Medicinal Plants of Euphorbiaceae Occurring and Utilized in Thailand. V. Skin Irritants of the Daphnane and Tigliane Type in Latex of Excoecaria Bicolor and the Uterotonic Activity of the Leaves of the Tree. *Phytother. Res.* **1995**, *9* (7), 482–488.
(10) Rizk, A. M.; Hammouda, F. M.; Ismail, S. E.; El-Missiry, M. M.; Evans, F. J. Irritant Resiniferonol Derivatives from EgyptianThymelaea Hirsuta L. *Experientia* **1984**, *40* (8), 808–809.
(11) Taninaka, H.; Takaishi, Y.; Honda, G.; Imakura, Y.; Sezik, E.; Yesilada, E. Terpenoids and Aromatic Compounds from Daphne Oleoides Ssp. Oleoides. *Phytochemistry* **1999**, *52* (8), 1525–1529.
(12) Zhan, Z.-J.; Fan, C.-Q.; Ding, J.; Yue, J.-M. Novel Diterpenoids with Potent Inhibitory Activity against Endothelium Cell HMEC and Cytotoxic Activities from a Well-Known TCM Plant Daphne Genkwa. *Bioorg. Med. Chem.* **2005**, *13* (3), 645–655.
(13) Zeng, Y.-M.; Zuo, W.-J.; Sun, M.-G.; Meng, H.; Wang, Q.-H.; Wang, J.-H.; Li, X. Three New Daphne Diterpenes from the Buds of Daphne genkwa Sieb. et Zucc. Processed by Rice Vinegar. *Helv. Chim. Acta* **2009**, *92* (7), 1273–1281.
(14) Jayasuriya, H.; Zink, D. L.; Singh, S. B.; Borris, R. P.; Nanakorn, W.; Beck, H. T.; Balick, M. J.; Goetz, M. A.; Slayton, L.; Gregory, L.; Zakson-Aiken, M.; Shoop, W.; Singh, S. B. Structure and Stereochemistry of Rediocide A, A Highly Modified Daphnane from Trigonostemon Reidioides Exhibiting Potent Insecticidal Activity. *J. Am. Chem. Soc.* **2000**, *122* (20), 4998–4999.
(15) Yoshida, M.; Feng, W.; Saijo, N.; Ikekawa, T. Antitumor Activity of Daphnane-Type Diterpene Gnidimacrin Isolated from Stellera Chamaejasme L. *Int. J. Cancer* **1996**, *66* (2), 268–273.
(16) Otsuki, K.; Li, W.; Asada, Y.; Chen, C.-H.; Lee, K.-H.; Koike, K. Daphneodorins A–C, Anti-HIV Gnidimacrin Related Macrocyclic Daphnane Orthoesters from Daphne Odora. *Org. Lett.* **2020**, *22* (1), 11–15.
(17) Abe, F.; Iwase, Y.; Yamauchi, T.; Kinjo, K.; Yaga, S. Daphnane Diterpenoids from the Bark of Wikstroemia Retusa. *Phytochemistry* **1997**, *44* (4), 643–647.
(18) Abe, F.; Iwase, Y.; Yamauchi, T.; Kinjo, K.; Yaga, S.; Ishii, M.; Iwahana, M. Minor Daphnane-Type Diterpenoids from Wikstroemia Retusa. *Phytochemistry* **1998**, *47* (5), 833–837.
(19) Bourjot, M.; Leyssen, P.; Neyts, J.; Dumontet, V.; Litaudon, M. Trigocherrierin A, a Potent Inhibitor of Chikungunya Virus Replication. *Molecules* **2014**, *19* (3), 3617–3627.
(20) Wang, H.-B.; Wang, X.-Y.; Liu, L.-P.; Qin, G.-W.; Kang, T.-G. Tigliane Diterpenoids from the Euphorbiaceae and Thymelaeaceae Families. *Chem. Rev.* **2015**, *115* (9), 2975–3011.
(21) Flaschenträger, B.; von Falkenhausen, F. Frhr. Über Den Giftstoff Im Krotonöl. II. Zur Konstitution von Krotophorbolon. *Justus Liebigs Ann. Chem.* **1934**, *514* (1), 252–260.

(22) Hecker, E.; Kubinyi, H.; Szczepanski, Ch. v.; Härle, E.; Bresch, H. Phorbol - ein neues tetracyclisches diterpen aus crotonöl. *Tetrahedron Lett.* **1965**, *6* (23), 1837–1842.
(23) Damascena, H. L.; Silveira, W. A. A.; Castro, M. S.; Fontes, W. Neutrophil Activated by the Famous and Potent PMA (Phorbol Myristate Acetate). *Cells* **2022**, *11* (18), 2889.
(24) Cashmore, A. R.; Seelye, R. N.; Cain, B. F.; Mack, H.; Schmidt, R.; Hecker, E. The Structure of Prostratin : A Toxic Tetracyclic Diterpene Ester from Pimelea Prostrata. *Tetrahedron Lett.* **1976**, *17* (20), 1737–1738.
(25) Kirby, J.; Nishimoto, M.; Park, J. G.; Withers, S. T.; Nowroozi, F.; Behrendt, D.; Rutledge, E. J. G.; Fortman, J. L.; Johnson, H. E.; Anderson, J. V.; Keasling, J. D. Cloning of Casbene and Neocembrene Synthases from Euphorbiaceae Plants and Expression in Saccharomyces Cerevisiae. *Phytochemistry* **2010**, *71* (13), 1466–1473.
(26) King, A. J.; Brown, G. D.; Gilday, A. D.; Forestier, E.; Larson, T. R.; Graham, I. A. A Cytochrome P450-Mediated Intramolecular Carbon–Carbon Ring Closure in the Biosynthesis of Multidrug-Resistance-Reversing Lathyrane Diterpenoids. *ChemBioChem* **2016**, *17* (17), 1593–1597.
(27) Luo, D.; Callari, R.; Hamberger, B.; Wubshet, S. G.; Nielsen, M. T.; Andersen-Ranberg, J.; Hallström, B. M.; Cozzi, F.; Heider, H.; Møller, B. L.; Staerk, D.; Hamberger, B. Oxidation and Cyclization of Casbene in the Biosynthesis of Euphorbia Factors from Mature Seeds of Euphorbia Lathyris L. *Proc. Natl. Acad. Sci.* **2016**, *113* (34), E5082–E5089.
(28) Szallasi, A.; Blumberg, P. M. Resiniferatoxin, a Phorbol-Related Diterpene, Acts as an Ultrapotent Analog of Capsaicin, the Irritant Constituent in Red Pepper. *Neuroscience* **1989**, *30* (2), 515–520.
(29) Szallasi, A.; Blumberg, P. M. Specific Binding of Resiniferatoxin, an Ultrapotent Capsaicin Analog, by Dorsal Root Anglion Membranes. *Brain Res.* **1990**, *524* (1), 106–111.
(30) Cao, E.; Liao, M.; Cheng, Y.; Julius, D. TRPV1 Structures in Distinct Conformations Reveal Activation Mechanisms. *Nature* **2013**, *504* (7478), 113–118.
(31) Zhang, K.; Julius, D.; Cheng, Y. Structural Snapshots of TRPV1 Reveal Mechanism of Polymodal Functionality. *Cell* **2021**, *184* (20), 5138-5150.e12.
(32) Zhang, F.; Hanson, S. M.; Jara-Oseguera, A.; Krepkiy, D.; Bae, C.; Pearce, L. V.; Blumberg, P. M.; Newstead, S.; Swartz, K. J. Engineering Vanilloid-Sensitivity into the Rat TRPV2 Channel. *eLife* **2016**, *5*, e16409.
(33) Yang, F.; Zheng, J. Understand Spiciness: Mechanism of TRPV1 Channel Activation by Capsaicin. *Protein Cell* **2017**, *8* (3), 169–177.
(34) Lee, J.; Kim, S. Y.; Park, S.; Lim, J.-O.; Kim, J.-M.; Kang, M.; Lee, J.; Kang, S.-U.; Choi, H.-K.; Jin, M.-K.; Welter, J. D.; Szabo, T.; Tran, R.; Pearce, L. V.; Toth, A.; Blumberg, P. M. Structure–Activity Relationships of Simplified Resiniferatoxin Analogues with Potent VR1 Agonism Elucidates an Active Conformation of RTX for VR1 Binding. *Bioorg. Med. Chem.* **2004**, *12* (5), 1055–1069.
(35) Appendino, G.; Bertolino, A.; Minassi, A.; Annunziata, R.; Szallasi, A.; de Petrocellis, L.; Di Marzo, V. Synthesis and Biological Evaluation of Phorbol-Resiniferatoxin (RTX) Hybrids. *Eur. J. Org. Chem.* **2004**, *2004* (16), 3413–3421.
(36) Appendino, G.; Ech-Chahad, A.; Minassi, A.; Bacchiega, S.; Petrocellis, L. D.; Marzo, V. D. Structure–Activity Relationships of the Ultrapotent Vanilloid Resiniferatoxin (RTX): The Homovanillyl Moiety. *Bioorg. Med. Chem. Lett.* **2007**, *17* (1), 132–135.

(37) Appendino, G.; Ech-Chahad, A.; Minassi, A.; De Petrocellis, L.; Marzo, V. D. Structure–Activity Relationships of the Ultrapotent Vanilloid Resiniferatoxin (RTX): The Side Chain Benzylic Methylene. *Bioorg. Med. Chem. Lett.* **2010**, *20* (1), 97–99.
(38) Appendino, G.; Cravotto, G.; Palmisano, G.; Annunziata, R.; Szallasi, A. Synthesis and Evaluation of Phorboid 20-Homovanillates: Discovery of a Class of Ligands Binding to the Vanilloid (Capsaicin) Receptor with Different Degrees of Cooperativity. *J. Med. Chem.* **1996**, *39* (16), 3123–3131.
(39) Williamson, E. M.; Westwick, J.; Evans, F. J. The Effect of Daphnane Esters on Platelet Aggregation and Erythema of the Mouse Ear. *J. Pharm. Pharmacol.* **1980**, *32* (1), 373–374.
(40) Wahl, P.; Foged, C.; Tullin, S.; Thomsen, C. Iodo-Resiniferatoxin, a New Potent Vanilloid Receptor Antagonist. *Mol. Pharmacol.* **2001**, *59* (1), 9–15.
(41) Caterina, M. J.; Schumacher, M. A.; Tominaga, M.; Rosen, T. A.; Levine, J. D.; Julius, D. The Capsaicin Receptor: A Heat-Activated Ion Channel in the Pain Pathway. *Nature* **1997**, *389* (6653), 816–824.
(42) Moran, M. M.; McAlexander, M. A.; Bíró, T.; Szallasi, A. Transient Receptor Potential Channels as Therapeutic Targets. *Nat. Rev. Drug Discov.* **2011**, *10* (8), 601–620.
(43) He, S.; Li, Q.; Huang, Q.; Cheng, J. Targeting Protein Kinase C for Cancer Therapy. *Cancers* **2022**, *14* (5), 1104.
(44) Remy, S.; Litaudon, M. Macrocyclic Diterpenoids from Euphorbiaceae as A Source of Potent and Selective Inhibitors of Chikungunya Virus Replication. *Molecules* **2019**, *24* (12), 2336.
(45) Ryves, W. j; Garland, L. g.; Evans, A. t.; Evans, F. j. A Phorbol Ester and a Daphnane Ester Stimulate a Calcium-Independent Kinase Activity from Human Mononuclear Cells. *FEBS Lett.* **1989**, *245* (1–2), 159–163.
(46) Irie, K.; Oie, K.; Nakahara, A.; Yanai, Y.; Ohigashi, H.; Wender, P. A.; Fukuda, H.; Konishi, H.; Kikkawa, U. Molecular Basis for Protein Kinase C Isozyme-Selective Binding: The Synthesis, Folding, and Phorbol Ester Binding of the Cysteine-Rich Domains of All Protein Kinase C Isozymes. *J. Am. Chem. Soc.* **1998**, *120* (36), 9159–9167.
(47) Newton, A. C. Protein Kinase C: Structure, Function, and Regulation (*). *J. Biol. Chem.* **1995**, *270* (48), 28495–28498.
(48) Huang, L.; Ho, P.; Yu, J.; Zhu, L.; Lee, K.-H.; Chen, C.-H. Picomolar Dichotomous Activity of Gnidimacrin Against HIV-1. *PLOS ONE* **2011**, *6* (10), e26677.
(49) Liu, Q.; Cheng, Y.-Y.; Li, W.; Huang, L.; Asada, Y.; Hsieh, M.-T.; Morris-Natschke, S. L.; Chen, C.-H.; Koike, K.; Lee, K.-H. Synthesis and Structure–Activity Relationship Correlations of Gnidimacrin Derivatives as Potent HIV-1 Inhibitors and HIV Latency Reversing Agents. *J. Med. Chem.* **2019**, *62* (15), 6958–6971.
(50) Yoshida, M.; Yokokura, H.; Hidaka, H.; Ikekawa, T.; Saijo, N. Mechanism of Antitumor Action of PKC Activator, Gnidimacrin. *Int. J. Cancer* **1998**, *77* (2), 243–250.
(51) Yoshida, M.; Feng, W.; Nishio, K.; Takahashi, M.; Heike, Y.; Saijo, N.; Wakasugi, H.; Ikekawa, T. Antitumor Action of the PKC Activator Gnidimacrin through Cdk2 Inhibition. *Int. J. Cancer* **2001**, *94* (3), 348–352.
(52) Yoshida, M.; Heike, Y.; Ohno, S.; Ikekawa, T.; Wakasugi, H. Involvement of PKC BII in Anti-Proliferating Action of a New Antitumor Compound Gnidimacrin. *Int. J. Cancer* **2003**, *105* (5), 601–606.

(53) Fermaintt, C. S.; Peramuna, T.; Cai, S.; Takahashi-Ruiz, L.; Essif, J. N.; Grant, C. V.; O'Keefe, B. R.; Mooberry, S. L.; Cichewicz, R. H.; Risinger, A. L. Yuanhuacine Is a Potent and Selective Inhibitor of the Basal-Like 2 Subtype of Triple Negative Breast Cancer with Immunogenic Potential. *Cancers* **2021**, *13* (11), 2834.

(54) Kang, J. I.; Hong, J.-Y.; Lee, H.-J.; Bae, S. Y.; Jung, C.; Park, H. J.; Lee, S. K. Anti-Tumor Activity of Yuanhuacine by Regulating AMPK/MTOR Signaling Pathway and Actin Cytoskeleton Organization in Non-Small Cell Lung Cancer Cells. *PLOS ONE* **2015**, *10* (12), e0144368.

(55) Van Kolen, K.; Bruinzeel, W.; He, W.; De Kimpe, N.; Van Puyvelde, L.; Cik, M.; Pullan, S. Investigation of Signalling Cascades Induced by Neurotrophic Synaptolepis Factor K7 Reveals a Critical Role for Novel PKCε. *Eur. J. Pharmacol.* **2013**, *701* (1), 73–81.

(56) Li, S.-F.; Liang, X.; Wu, X.-K.; Gao, X.; Zhang, L.-W. Discovering the Mechanisms of Wikstroelide E as a Potential HIV-Latency-Reversing Agent by Transcriptome Profiling. *J. Nat. Prod.* **2021**, *84* (4), 1022–1033.

(57) Zhang, X.; Huang, S.-Z.; Gu, W.-G.; Yang, L.-M.; Chen, H.; Zheng, C.-B.; Zhao, Y.-X.; Wan, D. C.-C.; Zheng, Y.-T. Wikstroelide M Potently Inhibits HIV Replication by Targeting Reverse Transcriptase and Integrase Nuclear Translocation. *Chin. J. Nat. Med.* **2014**, *12* (3), 186–193.

(58) Wender, P. A.; Jesudason, C. D.; Nakahira, H.; Tamura, N.; Tebbe, A. L.; Ueno, Y. The First Synthesis of a Daphnane Diterpene: The Enantiocontrolled Total Synthesis of (+)-Resiniferatoxin. *J. Am. Chem. Soc.* **1997**, *119* (52), 12976–12977.

(59) Hashimoto, S.; Katoh, S.; Kato, T.; Urabe, D.; Inoue, M. Total Synthesis of Resiniferatoxin Enabled by Radical-Mediated Three-Component Coupling and 7-Endo Cyclization. *J. Am. Chem. Soc.* **2017**, *139* (45), 16420–16429.

(60) Wender, P. A.; Mascarenas, J. L. Studies on Tumor Promoters. 11. A New [5+2] Cycloaddition Method and Its Application to the Synthesis of BC Ring Precursors of Phorboids. *J. Org. Chem.* **1991**, *56* (22), 6267–6269.

(61) Wender, P. A.; McDonald, F. E. Studies on Tumor Promoters. 10. Synthesis of the Abc Ring System of the Tiglianes and Daphnanes by a Zirconium-Mediated Intramolecular Enyne Carbocyclization. *Tetrahedron Lett.* **1990**, *31* (26), 3691–3694.

(62) Wender, P. A.; Lee, H. Y.; Wilhelm, R. S.; Williams, P. D. Studies on Tumor Promoters. 7. The Synthesis of a Potentially General Precursor of the Tiglianes, Daphnanes, and Ingenanes. *J. Am. Chem. Soc.* **1989**, *111* (24), 8954–8957.

(63) Wender, P. A.; Rice, K. D.; Schnute, M. E. The First Formal Asymmetric Synthesis of Phorbol. *J. Am. Chem. Soc.* **1997**, *119* (33), 7897–7898.

(64) Wender, P. A.; Kogen, H.; Lee, H. Y.; Munger, J. D. Jr.; Wilhelm, R. S.; Williams, P. D. Studies on Tumor Promoters. 8. The Synthesis of Phorbol. *J. Am. Chem. Soc.* **1989**, *111* (24), 8957–8958.

(65) Asaba, T.; Katoh, Y.; Urabe, D.; Inoue, M. Total Synthesis of Crotophorbolone. *Angew. Chem. Int. Ed.* **2015**, *54* (48), 14457–14461.

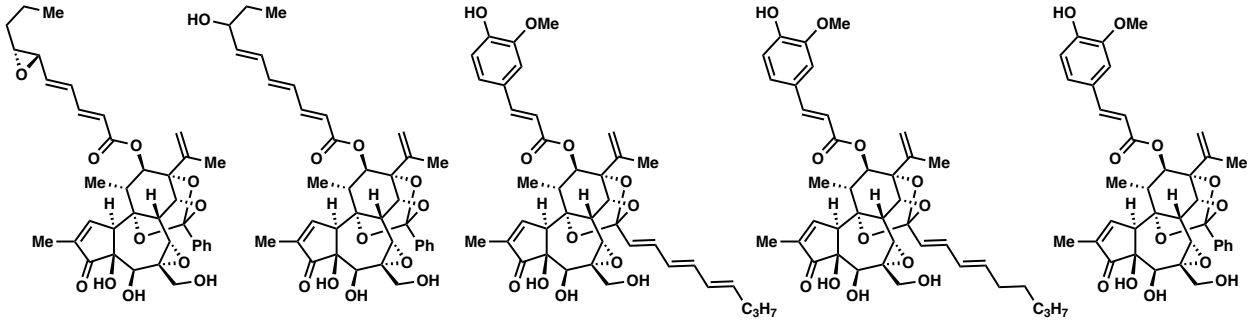
(66) Murai, K.; Katoh, S.; Urabe, D.; Inoue, M. A Radical-Based Approach for the Construction of the Tetracyclic Structure of Resiniferatoxin. *Chem. Sci.* **2013**, *4* (6), 2364–2368.

(67) Hirose, A.; Watanabe, A.; Ogino, K.; Nagatomo, M.; Inoue, M. Unified Total Syntheses of Rhamnofolane, Tigliane, and Daphnane Diterpenoids. *J. Am. Chem. Soc.* **2021**, *143* (31), 12387–12396.

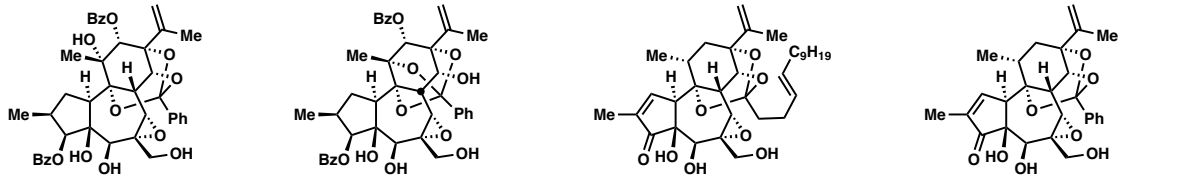
(68) Page, P. C. B.; Hayman, C. M.; McFarland, H. L.; Willock, D. J.; Galea, N. M. An IMDA Approach to Tigliane and Daphnane Diterpenoids: Generation of Rings A, B and C Incorporating C-18. *Synlett* **2002**, *2002* (04), 0583–0587.
(69) Bulman Page, P. C.; Jennens, D. C.; McFarland, H. An IMDA Approach to Tigliane and Daphnane Diterpenoids: Generation of the Tetracyclic Ring System of the Tiglianes. *Tetrahedron Lett.* **1997**, *38* (39), 6913–6916.
(70) Page, P. C. B.; Jennens, D. C.; Porter, R. A.; Baldock, A. N. A Model for the Synthesis of the Tigliane and Daphnane Diterpenes Using an Intramolecular Diels-Alder Reaction. *Synlett* **1991**, *1991* (07), 472–474.
(71) Brickwood, A. C.; Drew, M. G. B.; Harwood, L. M.; Ishikawa, T.; Marais, P.; Morisson, V. Synthetic Approaches towards Phorbols via the Ultra-High-Pressure Mediated Intramolecular Diels–Alder Reaction of Furans (IMDAF): Effect of Furan Substitution. *J. Chem. Soc. Perkin 1* **1999**, No. 8, 913–922.
(72) Li, Y.; Wei, M.; Dai, M. Gold Catalysis-Facilitated Rapid Synthesis of the Daphnane/Tigliane Tricyclic Core. *Tetrahedron* **2017**, *73* (29), 4172–4177.
(73) McMills, M. C.; Zhuang, L.; Wright, D. L.; Watt, W. A Carbonyl-Ylide Approach to the Tigliane Diterpenes. *Tetrahedron Lett.* **1994**, *35* (45), 8311–8314.
(74) Catino, A. J.; Sherlock, A.; Shieh, P.; Wzorek, J. S.; Evans, D. A. Approach to the Tricyclic Core of the Tigliane–Daphnane Diterpenes. Concerning the Utility of Transannular Aldol Additions. *Org. Lett.* **2013**, *15* (13), 3330–3333.
(75) Hassan, A. H. E.; Lee, J. K.; Pae, A. N.; Min, S.-J.; Cho, Y. S. Synthesis of the Tricyclic Ring Structure of Daphnanes via Intramolecular [4 + 3] Cycloaddition/SmI2-Pinacol Coupling. *Org. Lett.* **2015**, *17* (11), 2672–2675.
(76) Stewart, C.; McDonald, R.; West, F. G. Expedient Route to the Tigliane-Daphnane Skeleton via Oxonium Ylide [1,2]-Shift. *Org. Lett.* **2011**, *13* (4), 720–723.
(77) Jackson, S. R.; Johnson, M. G.; Mikami, M.; Shiokawa, S.; Carreira, E. M. Rearrangement of a Tricyclic 2,5-Cyclohexadienone: Towards a General Synthetic Route to the Daphnanes and (+)-Resiniferatoxin. *Angew. Chem. Int. Ed.* **2001**, *40* (14), 2694–2697.
(78) Carroll, G. L.; Little, R. D. Inter- and Intramolecular Reductive Coupling Reactions: An Approach to the Phorbol Skeleton. *Org. Lett.* **2000**, *2* (18), 2873–2876.
(79) Cui, Y.; Lv, J.; Song, T.; Ren, J.; Wang, Z. Highly Efficient Construction of an Oxa-[3.2.1]Octane-Embedded 5–7–6 Tricyclic Carbon Skeleton and Ring-Opening of the Bridged Ring via C–O Bond Cleavage. *RSC Adv.* **2022**, *12* (16), 9519–9523.
(80) Nguyen, L. V.; Beeler, A. B. Synthesis of Complex Stereoheptads En Route to Daphnane Diterpene Orthoesters. *Org. Lett.* **2018**, *20* (17), 5177–5180.
(81) Brill, Z. G.; Zhao, Y.-M.; Vasilev, V. H.; Maimone, T. J. Synthetic Approaches to the Daphnane and Tigliane Diterpenes from Aromatic Precursors. *Tetrahedron* **2019**, *75* (32), 4212–4221.
(82) Kawamura, S.; Chu, H.; Felding, J.; Baran, P. S. Nineteen-Step Total Synthesis of (+)-Phorbol. *Nature* **2016**, *532* (7597), 90–93.
(83) Yu, T.; Sun, Y.; Tu, C.; Chen, T.; Fu, S.; Liu, B. Total Synthesis of Crotophorbolone. *Chem. Sci.* **2020**, *11* (27), 7177–7181.
(84) Tong, G.; Liu, Z.; Li, P. Total Synthesis of (±)-Prostratin. *Chem* **2018**, *4* (12), 2944–2954.

(85) Liu, Z.; Ding†, Z.; Chen, K.; Xu, M.; Yu, T.; Tong, G.; Zhang, H.; Li, P. Balancing Skeleton and Functional Groups in Total Syntheses of Complex Natural Products: A Case Study of Tigliane, Daphnane and Ingenane Diterpenoids. *Nat. Prod. Rep.* **2021**, *38* (9), 1589–1617.
(86) El-Desoky, A. H. H.; Eguchi, K.; Kishimoto, N.; Asano, T.; Kato, H.; Hitora, Y.; Kotani, S.; Nakamura, T.; Tsuchiya, S.; Kawahara, T.; Watanabe, M.; Wada, M.; Nakajima, M.; Watanabe, T.; Misumi, S.; Tsukamoto, S. Isolation, Synthesis, and Structure–Activity Relationship Study on Daphnane and Tigliane Diterpenes as HIV Latency-Reversing Agents. *J. Med. Chem.* **2022**.
(87) Xie, R.; Xia, G.; Zhu, J.; Lin, P.; Fan, X.; Zi, J. Daphnane-Type Diterpenoids from Euphorbia Fischeriana Steud and Their Cytotoxic Activities. *Fitoterapia* **2021**, *149*, 104810.
(88) Otsuki, K.; Zhang, M.; Kikuchi, T.; Tsuji, M.; Tejima, M.; Bai, Z.-S.; Zhou, D.; Huang, L.; Chen, C.-H.; Lee, K.-H.; Li, N.; Koike, K.; Li, W. Identification of Anti-HIV Macrocyclic Daphnane Orthoesters from Wikstroemia Ligustrina by LC–MS Analysis and Phytochemical Investigation. *J. Nat. Med.* **2021**, *75* (4), 1058–1066.
(89) Zhao, H.-D.; Lu, Y.; Yan, M.; Chen, C.-H.; Morris-Natschke, S. L.; Lee, K.-H.; Chen, D.-F. Rapid Recognition and Targeted Isolation of Anti-HIV Daphnane Diterpenes from Daphne Genkwa Guided by UPLC-MSn. *J. Nat. Prod.* **2020**, *83* (1), 134–141.
(90) Trinel, M.; Le Lamer, A.-C.; Jullian, V.; Jacquemin, D.; Graton, J.; Cristofoli, V.; Crossay, E.; Yassine, M.; Rolland, C.; Vergnolle, N.; Mejia, K.; Joel Cabanillas, B.; Racaud-Sultan, C.; Fabre, N. Daphnanes Diterpenes from the Latex of Hura Crepitans L. And Activity against Human Colorectal Cancer Cells Caco-2. *Bioorganic Chem.* **2020**, *103*, 104132.
(91) Allard, P.-M.; Martin, M.-T.; Tran Huu Dau, M.-E.; Leyssen, P.; Guéritte, F.; Litaudon, M. Trigocherrin A, the First Natural Chlorinated Daphnane Diterpene Orthoester from Trigonostemon Cherrieri. *Org. Lett.* **2012**, *14* (1), 342–345.
(92) Hou, X.; Chen, J.; Hou, X.; Gao, P.; Wang, J.; Song, S.; Li, L. Genkwadane F—I, New Daphnane-Type Diterpenes from the Flower Buds of Daphne Genkwa Sieb.et Zucc. Exhibit Anti-Tumor Activities via Inducing Apoptosis. *Chin. J. Chem.* **2020**, *38* (12), 1600–1606.
(93) Hou, X.-W.; Han, S.; Zhang, Y.-Y.; Su, H.-B.; Gao, P.-Y.; Li, L.-Z.; Song, S.-J. Neogenkwanine I from the Flower Buds of Daphne Genkwa with Its Stereostructure Confirmation Using Quantum Calculation Profiles and Antitumor Evaluation. *Nat. Prod. Res.* **2020**, *34* (3), 405–412.
(94) Liu, Y.-Y.; Liu, Y.-P.; Wang, X.-P.; Qiao, Z.-H.; Yu, X.-M.; Zhu, Y.-Z.; Xie, L.; Qiang, L.; Fu, Y.-H. Bioactive Daphnane Diterpenes from Wikstroemia Chuii with Their Potential Anti-Inflammatory Effects and Anti-HIV Activities. *Bioorganic Chem.* **2020**, *105*, 104388.

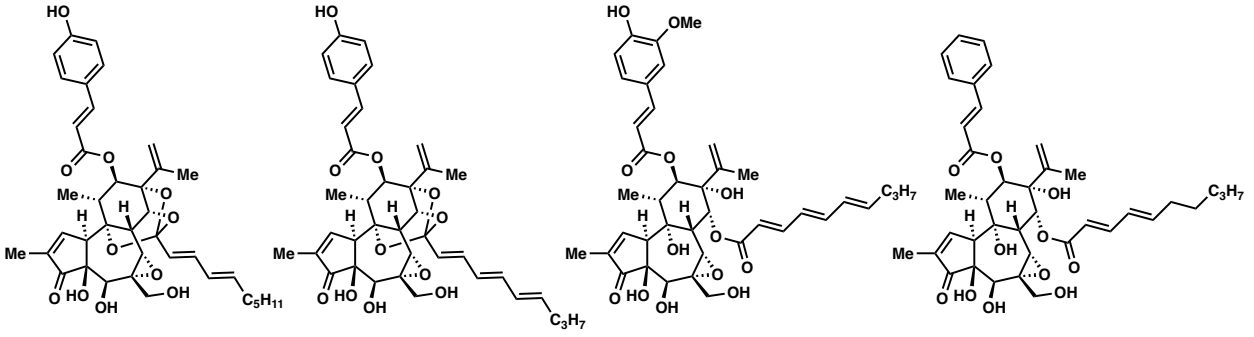
1.7. *Structures of daphnane diterpenoid orthoesters*[4,86-94]



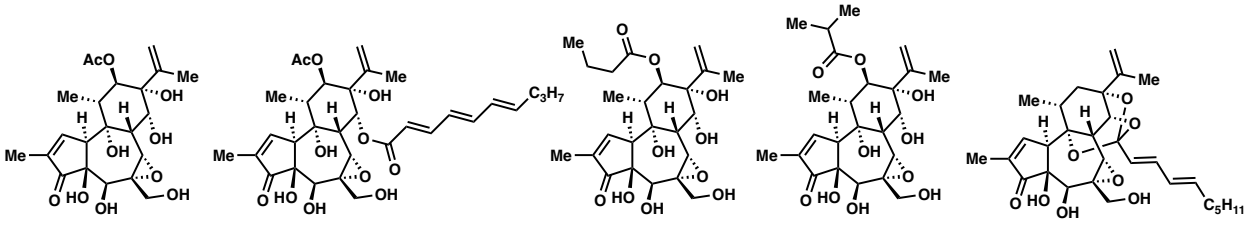
acutilobin A **acutilobin B** **acutilobin C** **acutilobin D** **acutilobin E**



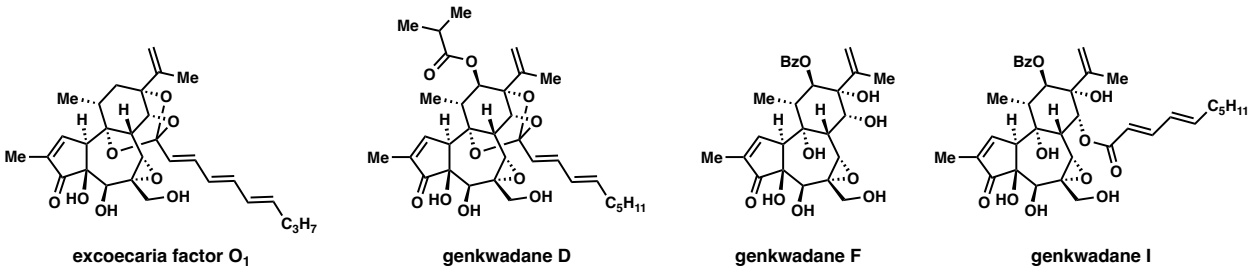
codiapeltine A **codiapeltine B** **2',3'-dihydrohuratoxin** **daphnetoxin** also **genkwanine VIII**



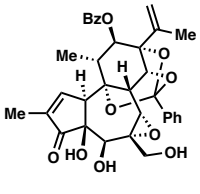
daphneodorin D **daphneodorin E** **daphneodorin F** **daphneodorin G**



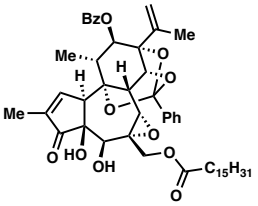
daphgenkin D **daphgenkin E** **daphgenkin F** **daphgenkin G** **excoecaria toxin**



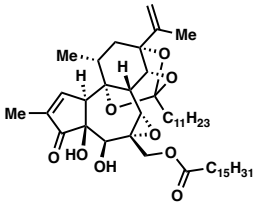
excoecaria factor O_1 **genkwadane D** **genkwadane F** **genkwadane I**



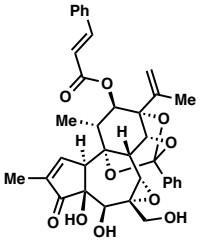
genkwadaphnine



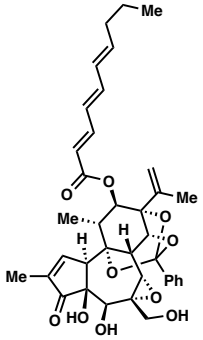
genkwadaphnin-20-palmitate



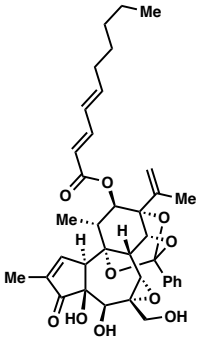
glabrescin



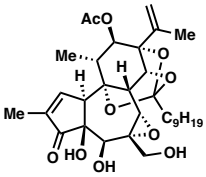
gnidicin



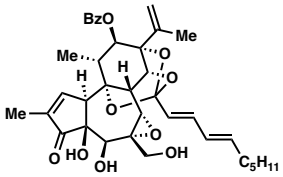
gniditrin



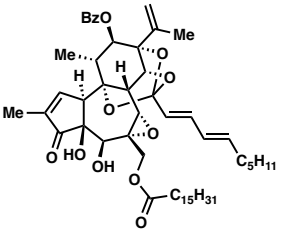
gnididin



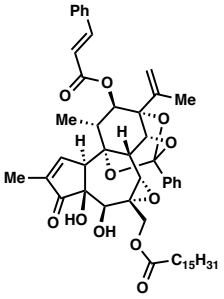
gnidiglaucin



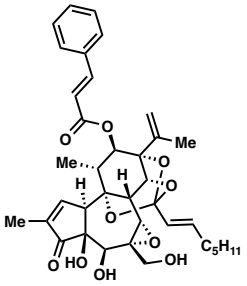
gnidilatidin
also **yuanhuacine**



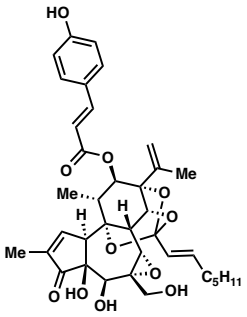
gnidilatidin-20-palmitate



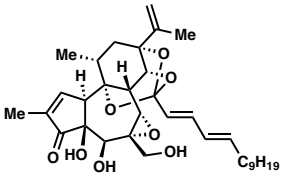
gnidicin-20-palmitate



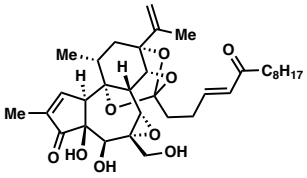
hirsein A



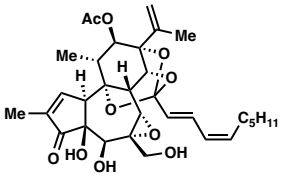
hirsein B



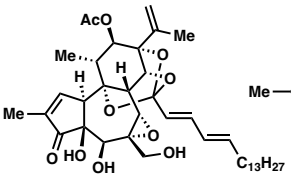
huratoxin



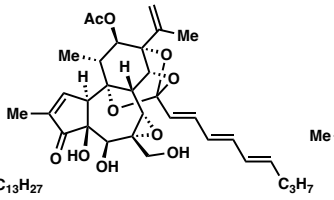
6'-oxohuratoxin



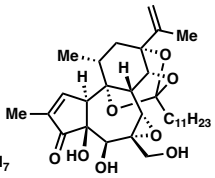
isoyuanhuadine



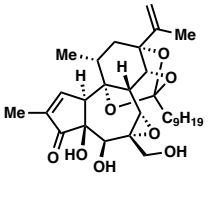
kirkinine



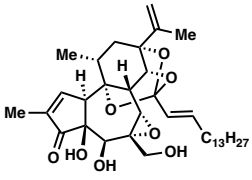
kirkinine D
also **yuanhuagine**



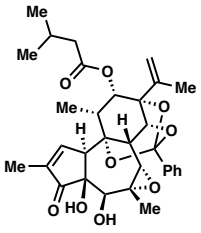
montanin



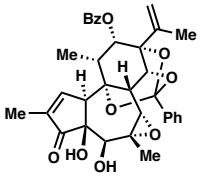
simplexin
(wikstrotoxin D)



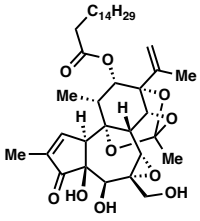
synaptolepisfactor K_7



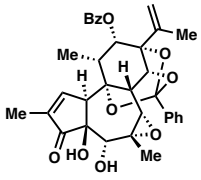
trigochinin G



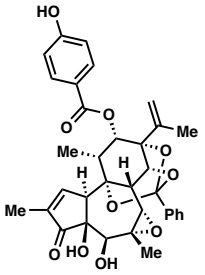
trigoxyphin A



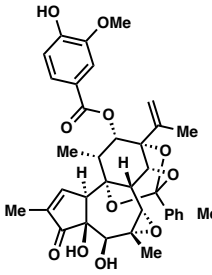
trigoxyphin J



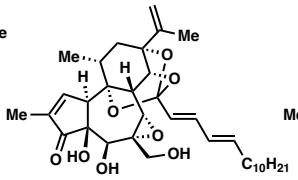
trigoxyphin K



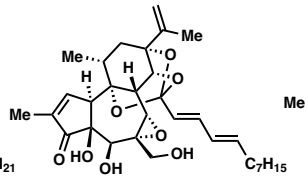
trigochinin H



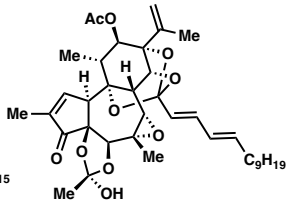
trigochinin I



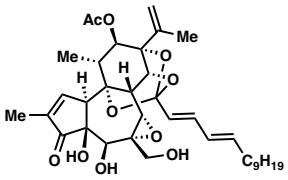
wikstrotoxin A



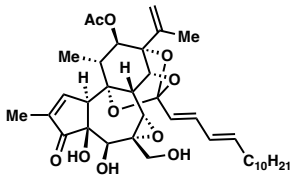
wikstrotoxin B



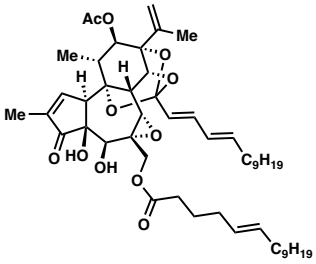
wikstrotoxin C



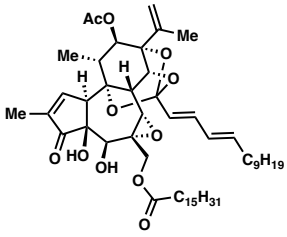
wikstroelide A



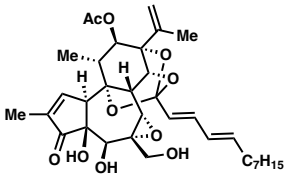
wikstroelide B



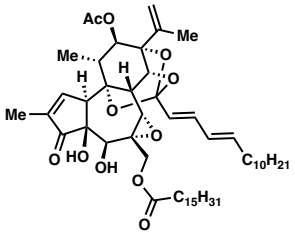
wikstroelide C



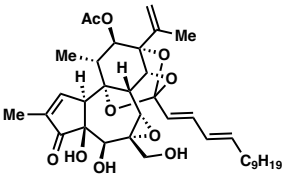
wikstroelide D



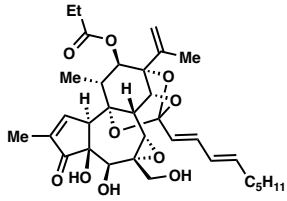
wikstroelide H



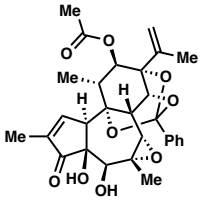
wikstroelide I



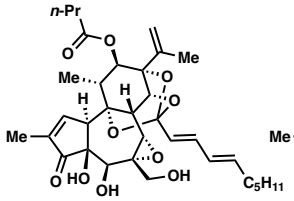
wikstroelide L



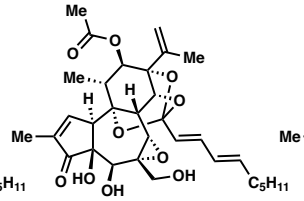
yuanhuahine



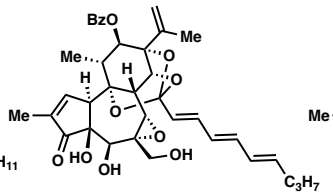
yuanhuafine



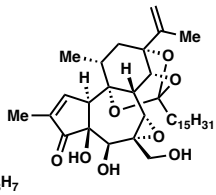
yuanhualine



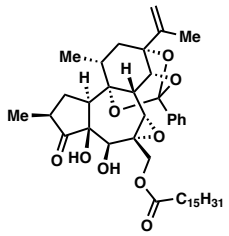
yuanhuadine



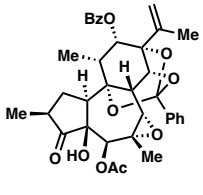
yuanhuajine



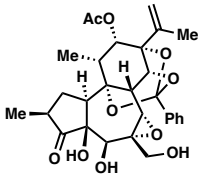
14'-ethyl tetrahydrohuratoxin



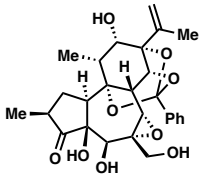
1,2-dihydrodaphnegiraldifin
also 2α-dihydro-20-palimoyldaphnetoxin



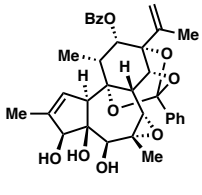
trigoxyphin C



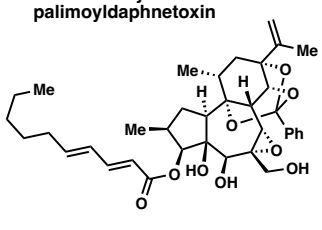
yuanhuapine



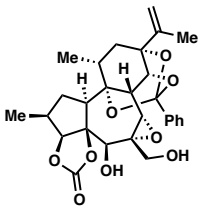
1,2-dihydrodaphnetoxin



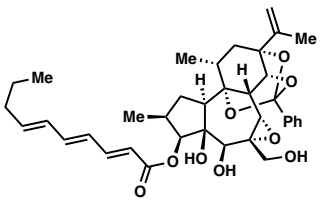
trigothysoid M



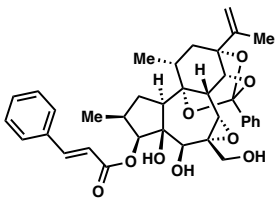
wikstroemia factor M_1



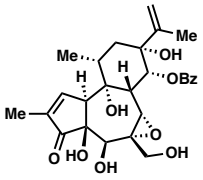
genkwanin I



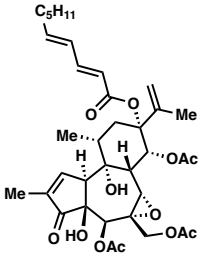
acutilobin F



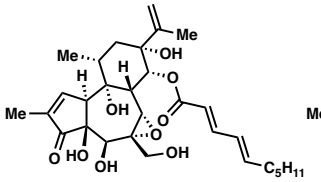
acutilobin G



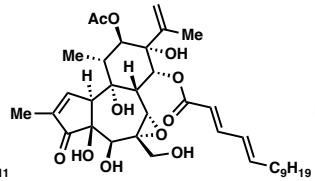
daphnegiraldigin



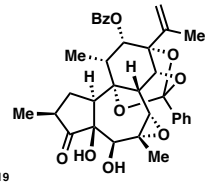
isovesiculosin



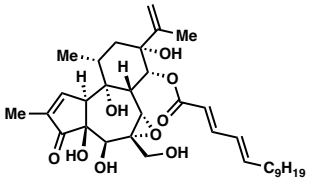
vesiculosin



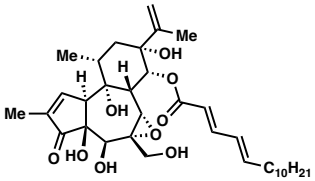
wikstroelide J



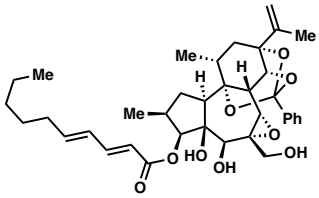
trigoxyphin B



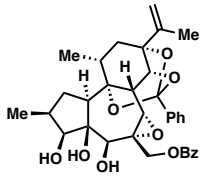
wikstroelide M



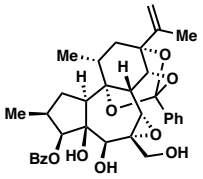
wikstroelide N



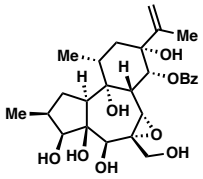
wikstroemia factor M_1



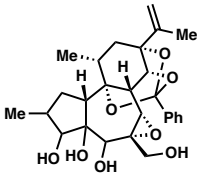
genkwanine M



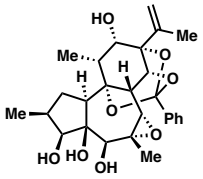
genkwanine N



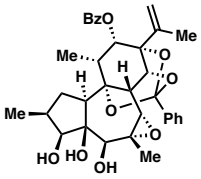
genkwanine O



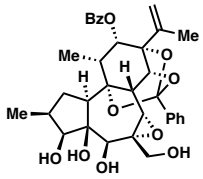
"orthobenzoate 2"



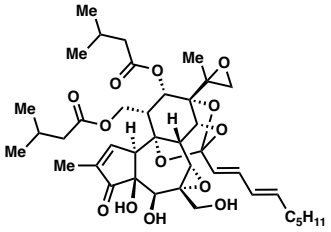
trigonostempene C



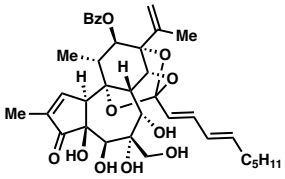
trigonosin A



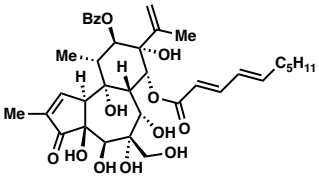
trigonosin B



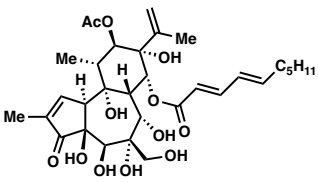
maprouneacin



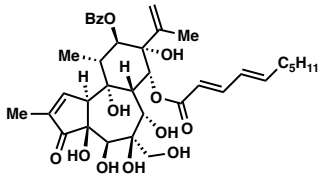
daphgenkin A



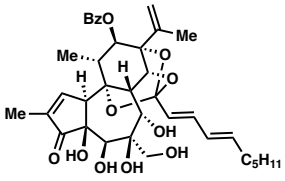
daphgenkin B



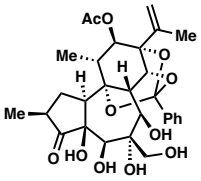
daphgenkin C



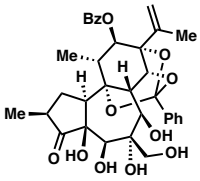
genkwadane G



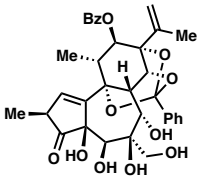
genkwadane H



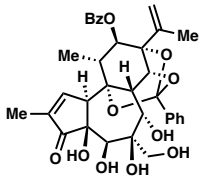
genkwanine L



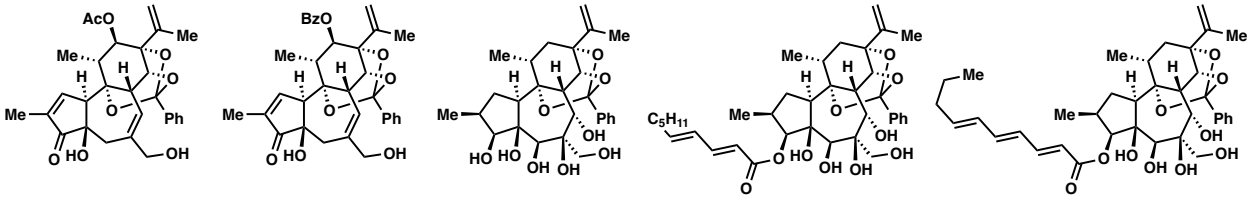
yuanhuatine



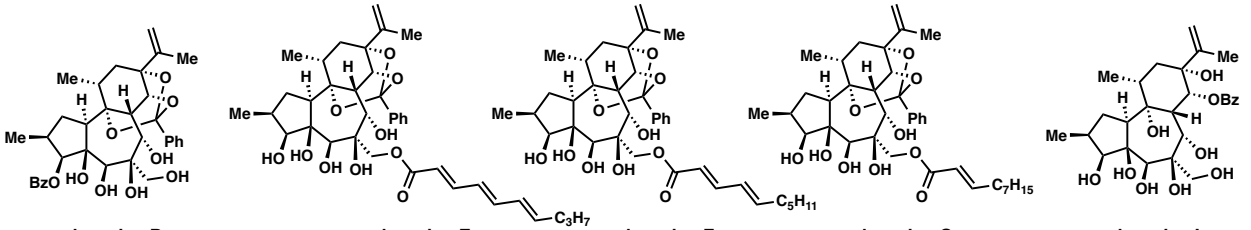
genkwadane A



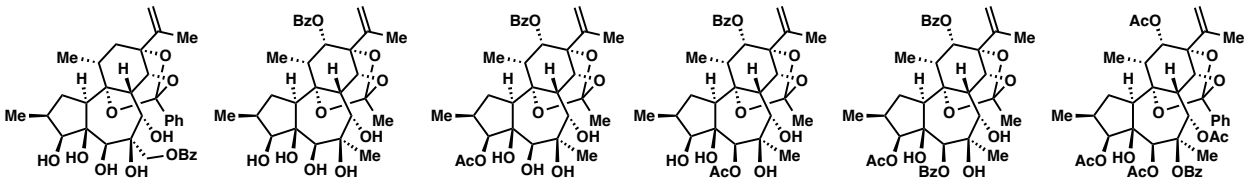
yuanhuaoate B



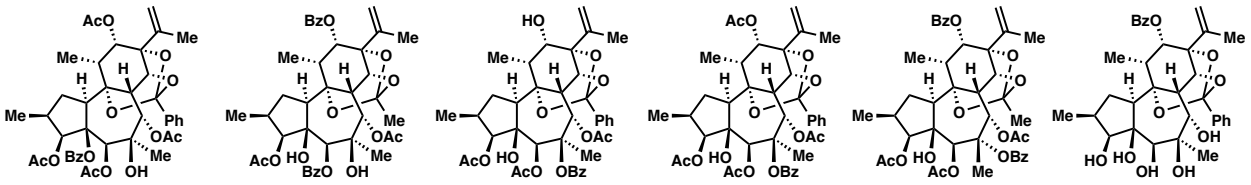
daphneresiniferin A | daphneresiniferin B | genkwanine A | genkwanine B | genkwanine C



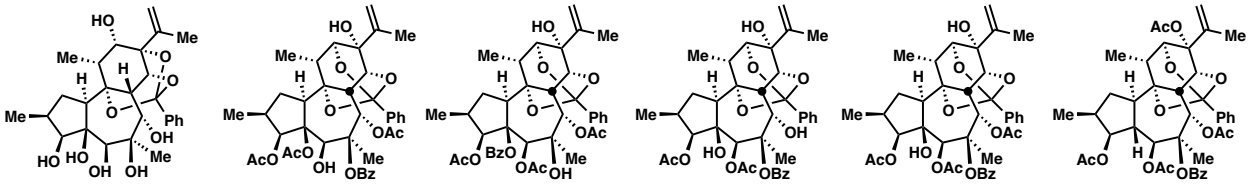
genkwanine D | genkwanine E | genkwanine F | genkwanine G | genkwanine I (different from genkwanin)



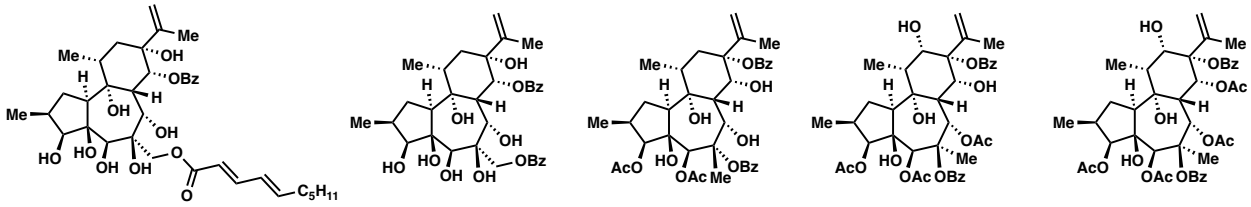
genkwanine H | trigothysoid D | trigothysoid E | trigothysoid F | trigothysoid G | trigothysoid H



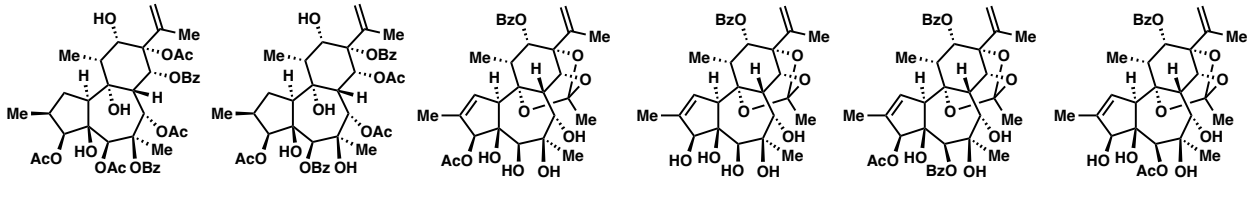
trigohownin D | trigohownin E | trigoxyphin F | trigoxyphin I | trigoxyphin U | trigonosin C



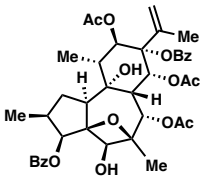
trigonothyrin F | trigohownin A | trigohownin B | trigohownin C | trigoxyphin D | trigoxyphin E



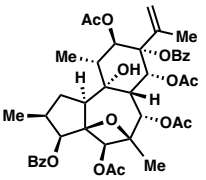
genkwanine J | genkwanine K | trigoxyphin W | trigohownin F | trigohownin G



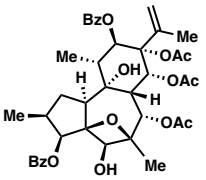
trigohownin H | trigohownin I | trigonothyrin G | trigothysoid A | trigothysoid B | trigothysoid C



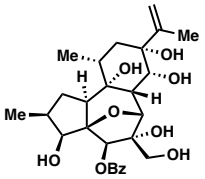
wikstroechuin A



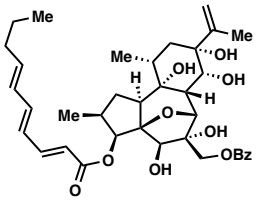
wikstroechuin B



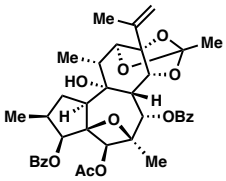
wikstroechuin C



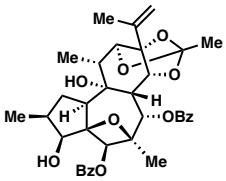
neogenkwanine I



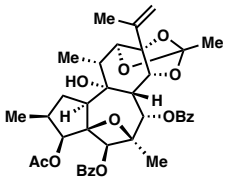
daphneodorin H



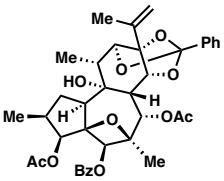
trigonothyrin A



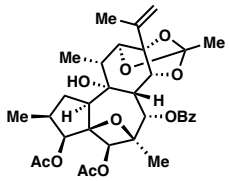
trigonothyrin B



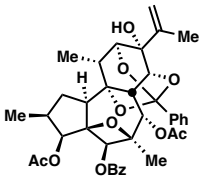
trigonothyrin C



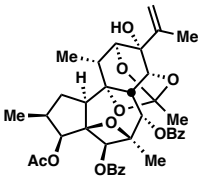
trigothysoid L



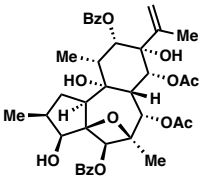
trigonostempene B



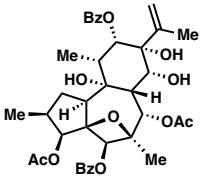
trigochinin C



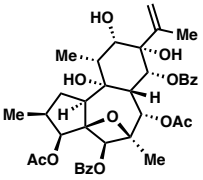
trigothysoid K



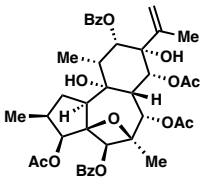
trigolins A



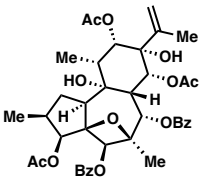
trigolins B



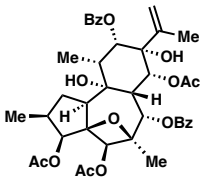
trigolins C



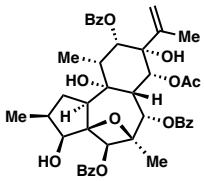
trigolins D



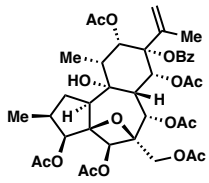
trigolins E



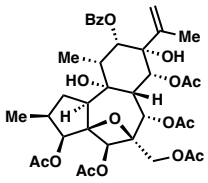
trigolins F



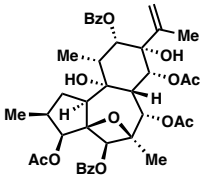
trigolins G



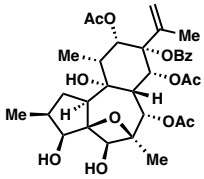
trigothysoid H



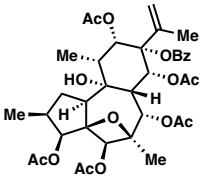
trigothysoid I



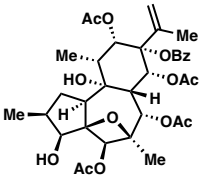
trigothysoid J



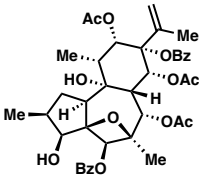
trigonosin D



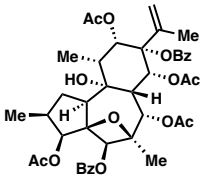
trigonothyrin D



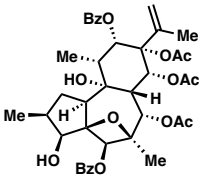
trigonothyrin E



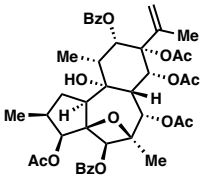
trigochinin A



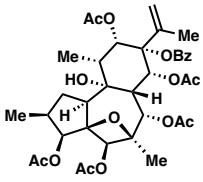
trigochinin B



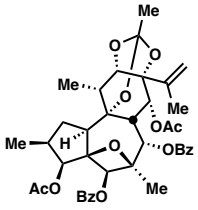
trigochinin D



trigochinin E

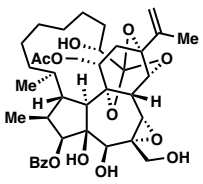


trigochinin F

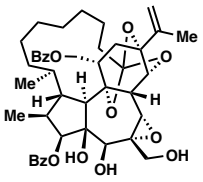


trigonostempene A

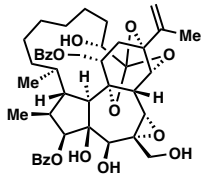
1-alkyldaphnanes:



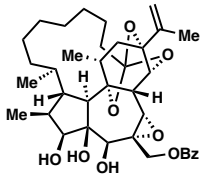
stellaralide A



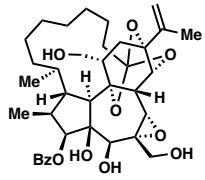
stellaralide B



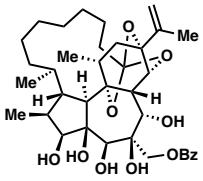
gnidimacrin



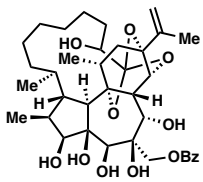
genkwadane B



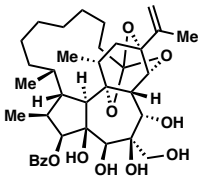
pimela factor P_2



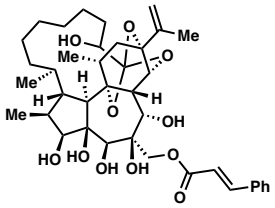
genkwadane C



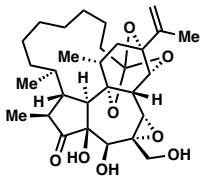
wikstroelide R



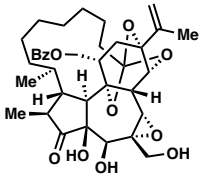
wikstroelide S



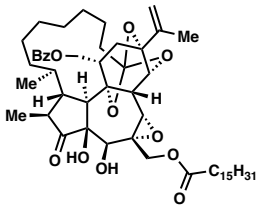
wikstroelide T



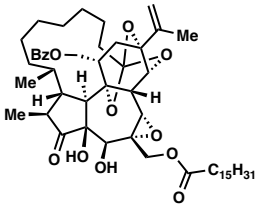
wikstroelide E
aka Pimelea factor S_6



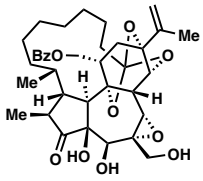
wikstroelide F



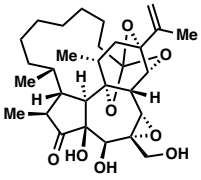
wikstroelide G



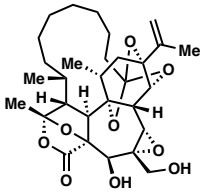
wikstroelide K



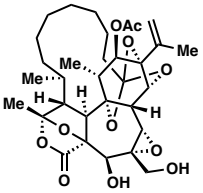
wikstroelide O



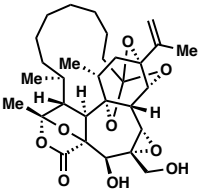
Pimelea factor S_7



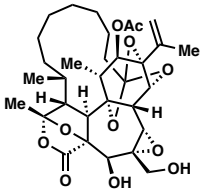
Pimelotide A



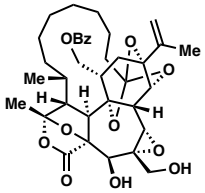
Pimelotide B



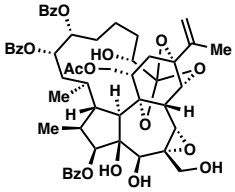
Pimelotide C



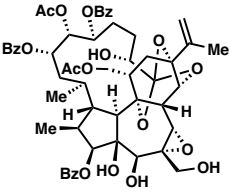
Pimelotide D



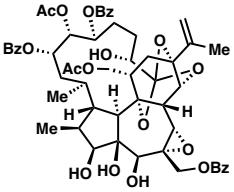
Stellaralide C



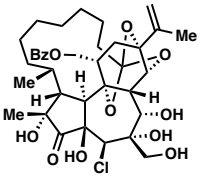
daphneodorin A



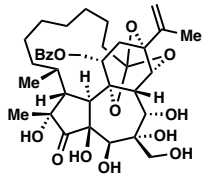
daphneodorin B



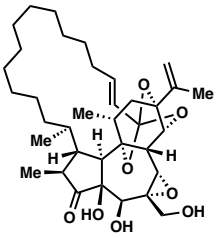
daphneodorin C



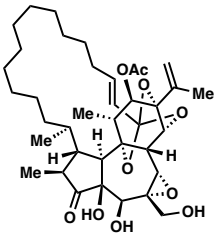
stellejasmin A



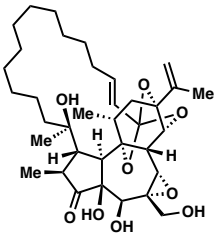
stellejasmin B



kirkinine B

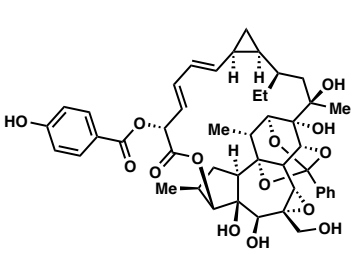


kirkinine C

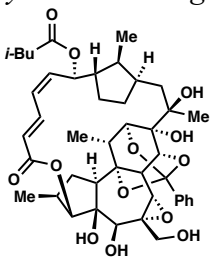


kirkinine E

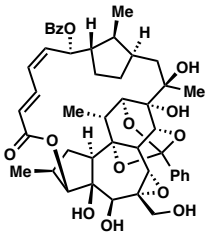
Other macrocycle-containing DDOs; chlorinated DDOs:



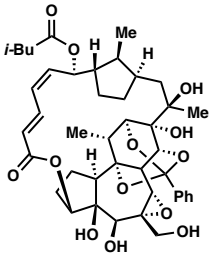
trigochilide A



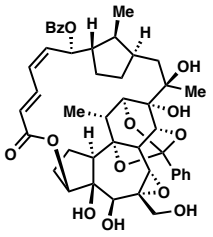
rediocide A



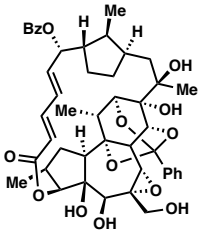
rediocide C



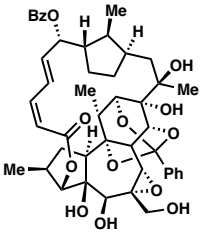
rediocide E



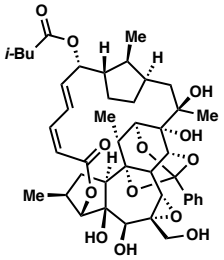
rediocide F



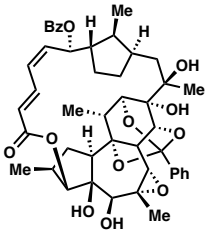
trigonosin E



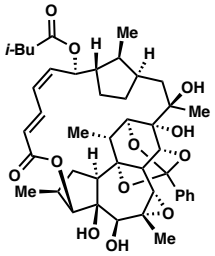
trigonosin F



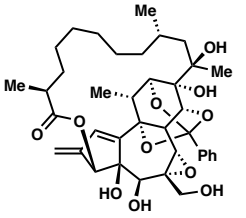
trigothysoid N



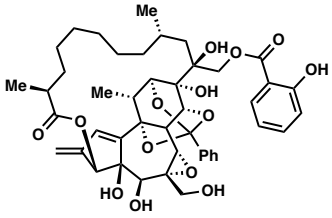
trigothysoid O



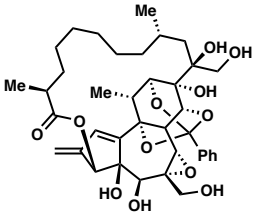
trigothysoid P



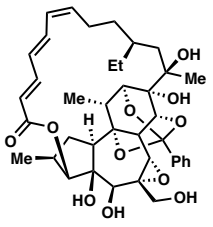
trigonolactone B



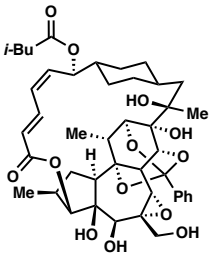
trigonolactone D



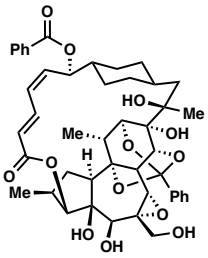
trigonolactone E



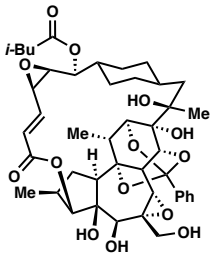
trigochilide B



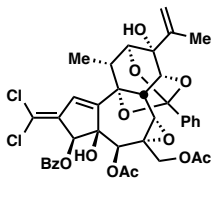
rediocide B



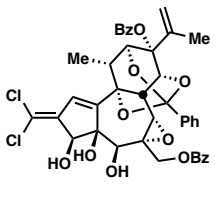
rediocide G



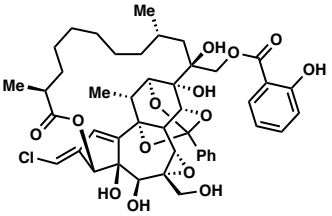
rediocide D



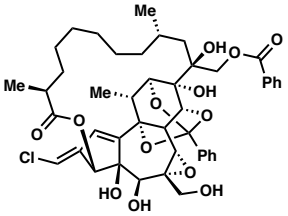
trigocherrin A



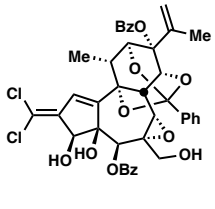
trigocherrin B



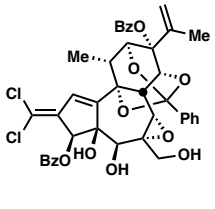
trigocherriolide A



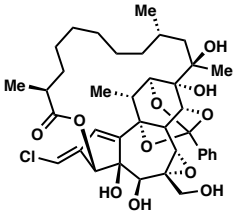
trigocherriolide C



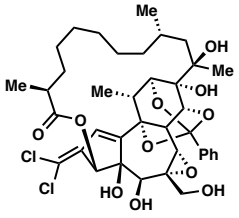
trigocherrin D



trigocherrin F



trigocherriolide B



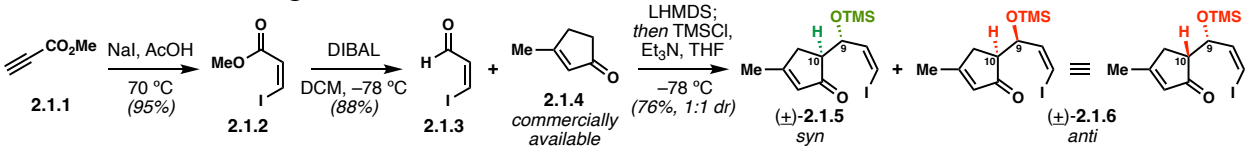
trigocherriolide D

Chapter 2.
Total Synthesis of Resiniferatoxin

2.1 *Synthesis of Trans-Fused Hydroazulenol* ***2.1.10***

Our first objective in the development of a synthetic route to resiniferatoxin based on our proposal in Chapter 1.5 was the rapid and scalable synthesis of a *trans*-fused hydroazulenol fragment which would enable subsequent studies of the late-stage construction of the C ring of the daphnane core (see structure **1.5.7** in Scheme 1.5.1). Our efforts began with the synthesis of (*Z*)-3-iodoacrolein **2.1.3**, envisioned to serve as a linchpin in the formation of the 7-membered ring by virtue of the aldehyde and vinyl iodide functional handles (Scheme 2.1.1). This aldehyde was obtained on gram-scale via DIBAL reduction of the corresponding methyl ester of (*Z*)-3-iodoacrylic acid **2.1.2**,[1] which is commercially available or easily accessible in one step from methyl propiolate **2.1.1**.[2] It is important to note that **2.1.3** is quite sensitive to both light and temperature in its neat form and was observed to violently decompose if stored at room temperature for more than 30 minutes even in the absence of light. Nevertheless, aldehyde **2.1.3** could be handled as a solution and was successfully employed as an electrophile in an aldol reaction with commercially available 3-methyl cyclopentenone **2.1.4** thus forging the first of the three C-C bonds necessary for formation of the B ring.

Scheme 2.1.1. Forming the first C-C bond of RTX via an aldol reaction.

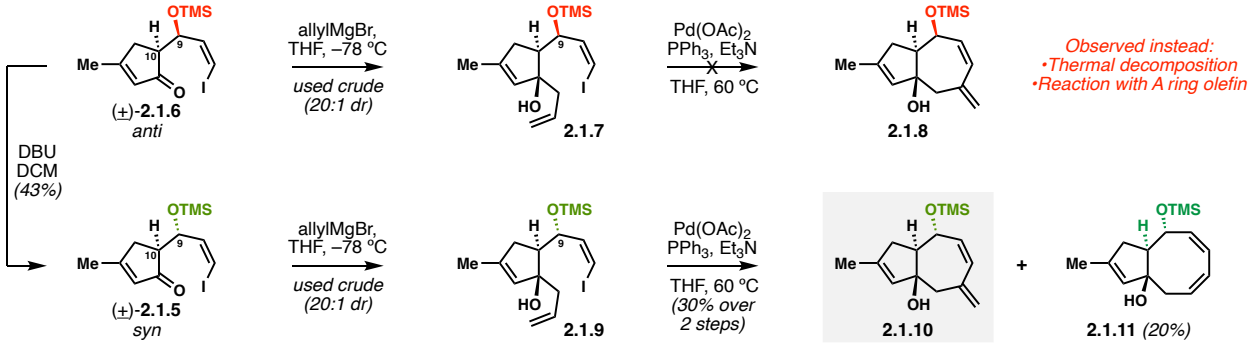


This process resulted in two diastereomeric products, *anti*-aldol product **2.1.6** and *syn*-aldol product **2.1.5**, in a 1:1 diastereomeric ratio and 76% combined yield. As a cyclic ketone, **2.1.4** can only generate an (*E*)-enolate and would therefore be expected to provide predominantly the *anti*-aldol product if reacting via a closed Zimmerman-Traxler transition state.[3,4] The diastereomeric ratio observed with LHMDS in THF is therefore consistent with an open transition state being operational. As neither reaction partner contains a chiral center, bond formation via an open transition state could occur from either face of the pro-chiral aldehyde C2 with equal probability, providing equal amounts of the two C9-epimers **2.1.5** and **2.1.6**. The *anti*-aldol product **2.1.6** could be preferentially formed in 3:1 dr with KHMDS in Et_2O, conditions under which the expected closed transition state appeared to be operational at least to some degree. While one might expect a Zimmerman-Traxler transition state to be more favored with a lithium enolate compared to a potassium one, owing to the shorter metal-oxygen bond length in the former case, the observed results are likely caused by differences in aggregation between the two sets of reaction conditions. The shorter Li-O bonds might cause the lithium enolate of **2.1.4** to form tight oligomers in solution, resulting in a coordinatively saturated Li center unable to engage in the chelation to **2.1.3** required for a closed transition state. We initially viewed the diastereomeric outcome of this transformation as inconsequential – the 5,7-fused bicyclic intermediate **1.5.7** (see Chapter 1.5) we envisioned would possess a carbonyl group at C9 and could thus arise from either epimer via an oxidation of the corresponding secondary alcohol. The diastereomeric products were therefore separated and individually subjected to the subsequent C-C bond forming steps in the hope that the two series of compounds would be reunited at a later oxidative stage.

Both C9-epimers **2.1.6** and **2.1.5** proceeded to readily react with allyl Grignard reagent with excellent diastereoselectivity at the newly formed C4 stereocenter, providing tertiary alcohols **2.1.7** and **2.1.9** respectively (Scheme 2.1.2). The presence of a silyl protecting group on the

secondary alcohol at C9 was crucial to ensure a clean reaction and stereoselective addition from the less hindered α-face of the carbonyl group. The products of this allylation reaction proved to be unstable, especially in the presence of acid or silica gel, likely due to the sensitive nature of the tertiary allylic alcohol moieties. Hence, vinyl iodides **2.1.7** and **2.1.9** were subjected the subsequent reaction without purification.

Scheme 2.1.2. Difference in reactivity between aldol products toward construction of the desired *trans*-fused hydroazulene.



With two of the three C-C bonds necessary for the B ring already constructed in only three steps from commercially available materials, the stage was set for the closure of the 7-membered ring via a Heck cyclization.[5–7] Crude iodide **2.1.7**, derived from *anti*-aldol product **2.1.6**, was subjected to a suite of classic[8] palladium catalysts and bases but no desired C-C bond formation to hydroazulene **2.1.8** was observed; instead, we noted reaction mixtures containing products stemming from decomposition of the starting materials presumably via thermal of base-mediated pathways. The residual mass balance in these studies consisted of a complex mixtures of products containing an intact mono-substituted olefin moiety. Thus, the preliminary screen did not result in the identification of reaction conditions that can bring about the desired 7-*exo*-trig cyclization of vinyl iodide **2.1.7**.

In contrast, cyclization precursor **2.1.9**, arising from *syn*-aldol product **2.1.5**, reacted successfully in the proposed 7-*exo*-trig ring formation, providing *trans*-fused hydroazulenol **2.1.10** in 30% yield over two steps. The only other product observed in this process was 5,8-fused bicycle **2.1.11**, arising from a competing 8-*endo*-trig cyclization. The formation of **2.1.11** was not too surprising as it matched observations from prior studies on a similar scaffold conducted in this laboratory and discussed in Chapter 1.[9] However, the combined yield of bicyclic products **2.1.10** and **2.1.11** did not account for the complete mass balance of the Heck reaction, with the remainder of vinyl iodide **2.1.9** presumably undergoing thermal decomposition similarly to C9-epimer **2.1.7**. The desired 5,7-fused scaffold found in **1.5.7** could thus be accessed, albeit in low yield, in only four steps from commercially available materials, thereby proving the first part of our retrosynthetic hypothesis.

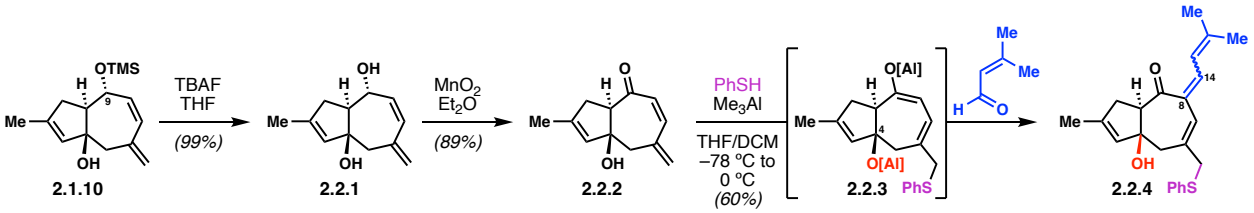
While the availability of hydroazulene **2.1.10** would allow the study of the subsequent transformations proposed in the retrosynthesis to proceed, the lack of material would necessitate lengthy and laborious scale-up efforts to bring about the desired amounts of this key intermediate. A thorough screen of the parameters of the Heck reaction could possibly alleviate the supply issues by revealing conditions that suppress formation of undesired constitutional isomer **2.1.11** in favor of the desired hydroazulenol, increase the overall mass recovery of the cyclization of reactive C9-

epimer **2.1.5**, or even allow for productive cyclization of previously unreactive C9-epimer **2.1.7**. This screening endeavor was however postponed for a later stage of the project in favor of exploring the challenging key steps for formation of the C ring as soon as possible (see Chapter 2.8 for optimization efforts that ultimately increased the yield of **2.1.10** to 51%). A temporary solution for improving material throughput was found instead by increasing the available amount of ketone **2.1.5**, the precursor to desired hydroazulenol **2.1.10**. We focused our efforts on converting the undesired aldol product **2.1.6** into the desired isomer **2.1.5**. This could be done by epimerizing ketone **2.1.6** at C10 with DBU, giving rise to the desired *syn* relative stereochemical relationship at C9 and C10. Due to the racemic nature of the two diastereomer series, such an epimerization of (±)-**2.1.6** provided (±)-**2.1.5** in 43% yield or 88% yield based on recovered undesired epimer **2.1.6**, which could be resubjected to the basic conditions. Even though the conversion in this process was partial, most likely due to both epimers having similar equilibrium concentrations under the DBU conditions, desired C9-epimer **2.1.5** could be obtained in 51% yield per aldol reaction and epimerization batch, which increased the overall material throughput and allowed the exploration of subsequent chemistry.

2.2 *Oxidative Manipulations of the Hydroazulene Fragment and Forays into Formation of the C8-C14 Bond*

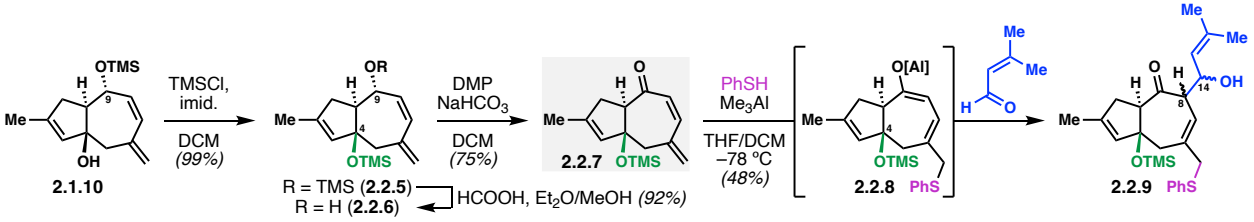
At this point, the stage was set for exploring oxidative manipulations that would provide a bicyclic ketone of the type **1.5.7**, one of two partners in the envisioned C8-C14 bond-forming event. A salient way in which this connection could be achieved while simultaneously introducing a heteroatom functional handle at C20 would be to carry out a 1,6-hetero Michael addition with vinylogous enone **2.2.2**, followed by trapping of the resulting enolate with a suitable aldehyde (Scheme 2.2.1). Heck product **2.1.10** could be elaborated into **2.2.2** in a straightforward manner via TBAF-mediated desilylation and allylic oxidation at C9 in the presence of MnO_2. However, diol **2.2.1** and ketone **2.2.2** proved to be quite unstable to purification and storage in their neat form. The latter was observed to rapidly (within 10 minutes) polymerize after concentration, necessitating its use in crude form and storage as a solution in benzene. When subjected to an excess of dimethylaluminum thiophenolate,[10–12] formed *in-situ* from PhSH and Me_3Al, vinylogous enone **2.2.2** underwent the desired conjugate 1,6-addition and aldol cascade using prenal as a test aldehyde substrate but the reaction proceeded further to yield the aldol condensation product **2.2.4**. Formation of such a triene could not be suppressed by modifying the reaction parameters and no other conditions involving a conjugate addition and aldol reaction cascade provided any productive C-C bond formation between enone **2.2.2** and prenal. In both cases the presence of a free alcohol at C4 in **2.2.2** is the likely culprit for the observed reactivity or lack thereof – in the latter instances, this OH group is not compatible with the attempted conjugate reduction[13–16] or borylation[17–19] conditions; while in the former this free alcohol, existing under the reaction conditions as an aluminum alkoxide (see enolate **2.2.3**), could act as an endogenous base to bring about an E1cB process generating triene **2.2.4** from the desired aldol product. Thus, enone **2.2.2** no longer appeared to be a desirable reaction partner in the envisioned C8-C14 bond forming step and we turned our attention to its C4-silylated counterpart (see **2.2.7** in Scheme 2.2.2) in the hopes that protecting the C4 alcohol would suppress the elimination reaction leading to triene **2.2.4** and could allow for a broader spectrum of productive reaction conditions for the proposed conjugate addition/aldol cascade.

Scheme 2.2.1. Synthesis of enone **2.2.2** and its participation in a thiol-mediated conjugate 1,6-addition/aldol reaction cascade.



In order to synthesize the new desired substrate, ketone **2.2.7**, two reaction sequences were considered – silylation of the alcohol of previously obtained ketone **2.2.2** or TMS-protection of Heck product **2.1.10** followed by selective deprotection at the C9-alcohol and oxidation (Scheme 2.2.2). While both series of reactions could be utilized to produce silanol **2.2.7**, the latter order of events was preferable as it avoided handling unstable intermediates **2.2.1** and **2.2.2**. Protection of hydroazulenol **2.1.10** proceeded without issue and selective deprotection of the secondary alcohol in **2.2.5** could be carried out with formic acid in an Et_2O/MeOH solvent mixture, resulting in mono-silylated bicycle **2.2.6**, which could be handled and purified without any issues. At first, TMS-protected enone **2.2.7** was made fresh, via oxidation of **2.2.6** with DMP, and handled without purification out of concern for instability issues similar to free alcohol **2.2.2**. Crude vinylogous enone **2.2.7** successfully underwent the conjugate 1,6-addition/aldol reaction cascade in the presence of $PhSAlMe_2$ and prenal, resulting in desired product **2.2.9** without any elimination to triene **2.2.4**. Thus, protecting the C4 alcohol in the hydroazulenol substrate successfully suppressed the undesired reactivity and provided a compound suitable for exploration of the C8-C14 bond forming event. Furthermore, enone **2.2.7** was later found to be stable to purification and storage, which simplified subsequent reaction protocols.

Scheme 2.2.2. A suitably protected hydroazulene enables C8-C14 bond formation via an aldol reaction.

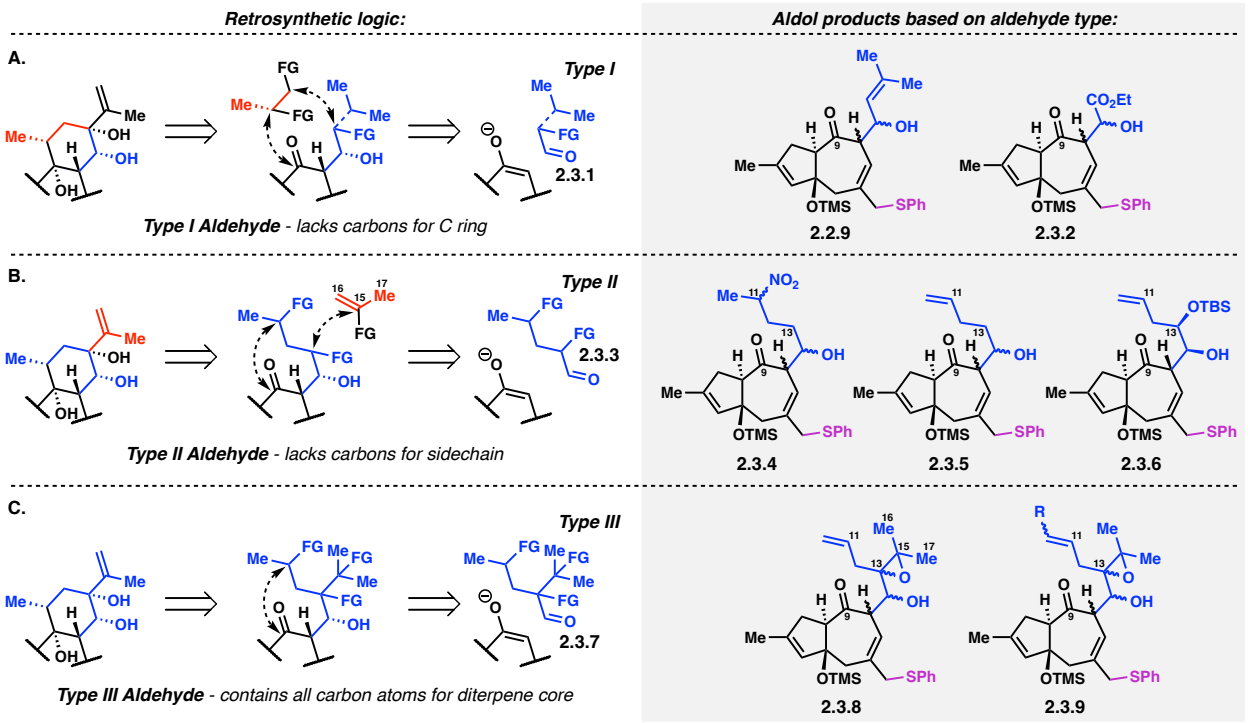


2.3 *Initial Exploration of Linear Fragments and C Ring Formation*

Having successfully identified vinylogous enone **2.2.7** as a competent *trans*-fused hydroazulenol partner of type **1.5.7**, the nature of the linear aldehyde piece for the envisioned aldol reaction was explored next. Hypothetically, three kinds of linear fragments would be feasible (Scheme 2.3.1). The first type, represented by small bifunctional compounds such as ethyl glyoxalate, would require subsequent installation of several fragments, representing both parts of the C ring and/or the isopropenyl sidechain (Scheme 2.3.1A). The second would be comprised of fragments with the general structure **2.3.3**, corresponding to the highlighted parts in **2.3.4**, **2.3.5**, or **2.3.6** that possess the carbons necessary for C ring construction but lack C15, C16, and C17 (Scheme 2.3.1B). Finally, the third type of aldehyde partner (see **2.3.7** in Scheme 2.3.1C) would contain all carbons needed for both the 6-membered ring and the sidechain decorating it, with

representative aldol products **2.3.8** and **2.3.9**. At this stage the exact reaction manifold for the closure of the C ring was yet unclear, so we explored all three types of aldehydes, theorizing that the use of a type I partner would offer the most flexibility in terms of subsequent chemistry but would require the highest number of steps to achieve the full daphnane core. In contrast, we hypothesized that the use of a type III aldehyde, while allowing for the theoretically fastest construction of the core, would be plagued with functional group compatibility issues and would limit the types of transformations that could be employed for closure of the C9-C11 bond. Subsequent experiments however would reveal that type I partners were the least amenable to further elaboration and that aldehydes of type III were uniquely suited for the completion of the daphnane core.

Scheme 2.3.1. Conceptual classification of different types of aldehyde partners (left) and examples of aldol products arising from each type (right). Type I aldehydes (**A**) lack the carbons necessary for C ring formation, type II aldehydes (**B**) lack C15, C16, C17, while type III aldehydes (**C**) contain all carbon atoms necessary for the diterpene core.

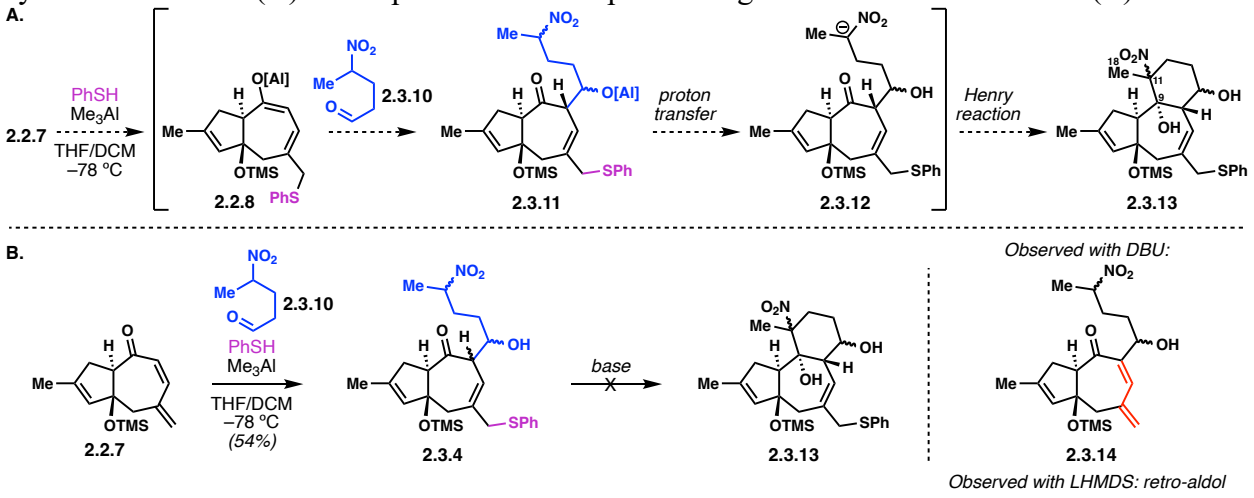


As already discussed, prenal was found to be a competent type I partner for the conjugate addition/aldol cascade. Another such aldehyde was ethyl glyoxalate, giving rise to ester **2.3.2**. These aldol products could theoretically be further elaborated via additions of nucleophiles to the C9 carbonyl and/or ester functional groups. However, such processes proved difficult in practice and substantial amounts of elimination of the C14 alcohol and retro-aldol reaction were observed. The ketone moiety on the hydroazulene core proved especially difficult to functionalize due to its sterically hindered nature. At this point it became clear that constructing further C-C bonds with the aldol products arising from reaction with a type I aldehyde was far more difficult than anticipated. An aldehyde partner of higher complexity, i.e. of type II or III that already bears all carbon atoms necessary for the six-membered ring, would hence be required. We further

hypothesized that an intramolecular process involving a sterically unencumbered intermediate would have better success at engaging the hindered C9 ketone and thereby closing the C ring.

Known[20] type II aldehyde **2.3.10** was therefore explored as a partner in the conjugate addition/aldol reaction (Scheme 2.3.2A). We hypothesized that the nitroalkane moiety in **2.3.10** could engage the C9 ketone via a Henry reaction in the presence of a base and were hopeful this could occur under the basic conditions of the aldol reaction itself, allowing for a one-step annulation to construct the C ring from bicycle **2.2.7** via aldolate **2.3.11** and stabilized carbanion **2.3.12**. A similar type of annulation process, albeit with simpler substrates, was precedented in literature to proceed well and to generate the desired *trans*-fusion of the newly formed 6-membered ring.[21] While at this stage the fate of the C11 stereocenter in tricycle **2.3.13** would be uncertain, a radical-mediated reduction of the nitro group in the putative cyclization product was expected to lead to the desired equatorial positioning of C18 under thermodynamic control. However, the only compound observed in the union of bicycle **2.2.7** and aldehyde **2.3.10** was aldol product **2.3.4** as a complex mixture of diastereomers (Scheme 2.3.2B). This result could be explained by the difference in enolate counterions – whereas in the literature precedent lithium is employed, the use of aluminum for the conjugate addition/aldol part of the proposed cascade was necessary. If deprotonation at C11 of aldolate **2.3.11** by an aluminum alkoxide is not kinetically favored, the Henry part of the desired transformation would not proceed, and the reaction would stop at aldol product **2.3.4** as observed.

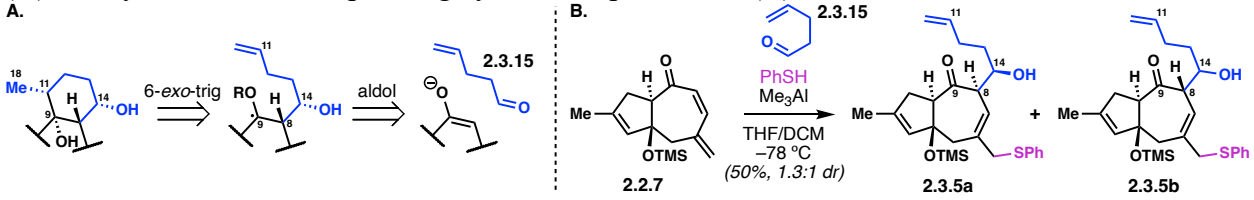
Scheme 2.3.2. Proposed 1,6-addition/aldol/Henry reaction cascade for the desired annulation of hydroazulene **2.2.7** (**A**) and experimental attempts to bring about this transformation (**B**).



Even though the proposed one-step annulation did not occur, one of the two C-C bonds necessary for formation of the six-membered ring was still successfully constructed and attempts were made to forge the remaining bond in a separate step. However, a variety of lithium bases such as LHMDS only led to a retro-aldol process, resulting in recovery of enone **2.2.7**. Milder bases such as DBU, also precedented to bring about Henry reactions,[22] provided enone **2.3.14**, arising from an E1cB process. While the former problem of a competing retro-aldol pathway could be theoretically suppressed by protection of the C14 alcohol, doing so would not address the possibility of a competing E1cB reaction. A bigger change in the retrosynthetic plan was therefore needed to suppress the issues encountered in the base-mediated attempts to forge the C9-C11 bond in substrate **2.3.4**.

To circumvent the undesired E1cB or retro-aldol reactions observed during the attempted cyclization of nitroalkane **2.3.4**, a radical-based reaction mechanism was explored next. Such a proposed one-electron reaction mechanism could bypass undesired two-electron pathways and would be highly suited for the sterically congested environment around C9 as it would involve unencumbered and reactive radical intermediates. The only one-electron side reaction we could envision, a 3-*exo*-trig cyclization between C9 and C7, would be kinetically much slower than the desired 6-*exo*-trig process,[23] and hence was not expected to pose a problem. Specifically, olefin-bearing aldehyde partner of type II **2.3.15** was chosen, as the corresponding aldol products could participate in a 6-*exo*-trig radical cyclization initiated by the formation of a ketyl radical at C9 (Scheme 2.3.3A). Cyclization precursor **2.3.5b** could be successfully constructed alongside its co-polar C8-epimer **2.3.5a** from hydroazulene **2.2.7** and 4-pentenal **2.3.15** using the standard conjugate addition/aldol procedure employed thus far (Scheme 2.3.3B). The flexible nature of the sidechain precluded a nOe-based analysis of the relative stereochemistry at this stage, with the stereochemical information shown arising from analysis of subsequent tricyclic compounds derived from these co-polar cyclization precursors.

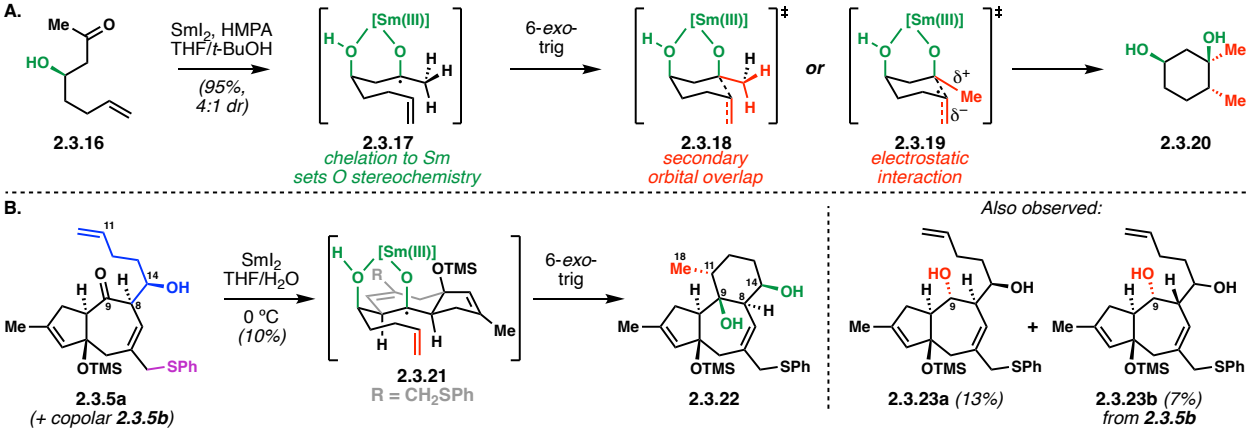
Scheme 2.3.3. Modified retrosynthetic hypothesis involving a radical-based 6-exo-trig cyclization (**A**) and synthesis of corresponding cyclization precursors (**B**).



Before the specifics of the 6-*exo*-trig cyclization of aldol products **2.3.5a** and **2.3.5b** are discussed, a general overview of the stereochemical outcome of such a transformation will be provided, specifically in the context of using Kagan's reagent (SmI_2) (Scheme 2.3.4A). Samarium (II) iodide has found wide use in the formation of ketyl radicals in complex systems[24–26] and has been observed to dictate the relative stereochemistry in subsequent 5-*exo*-trig and 6-*exo*-trig bond-forming events.[27] One way in which samarium iodide impacts the stereochemical outcome of such processes is via chelation to a hydroxyl group in proximity to the reaction center.[28] For example, after generation of ketyl radical **2.3.17** from simple β-hydroxy ketone **2.3.16**, both oxygen atoms remain coordinated to samarium and the resulting chelate cyclizes with the two oxygen atoms anchored on the same face of the ring being formed (see transition states **2.3.18** and **2.3.19** and cyclization product **2.3.20**).[29] This type of chelation-based control would be highly beneficial for us, as the secondary alcohol at C14 and the tertiary alcohol at C9 in the natural product reside on the same face (see Scheme 2.3.3A). Thus, the former stereocenter, if set correctly, would guide the selective formation of the latter during the proposed 6-*exo*-trig cyclization. The stereochemical outcome at the cyclization terminus however could prove problematic, as secondary orbital overlap between the olefin and substituents bound to the ketyl carbon atom dictates the preferential positioning of said termini *anti* to the oxygen of the ketyl radical in the proposed operative transition state **2.3.20**.[30] An alternative explanation for this observed preference has also been proposed, involving partially polarized transition state **2.3.19**, in which electrostatic interactions govern the positioning of the cyclization terminus *syn* to a C-C bond and *anti* to the C-O bond of the ketyl radical.[30] Regardless of the exact nature of the transition state, for the simple substrates in the cited study, the reaction result in the methyl and hydroxyl groups occupying opposite faces

of the ring in the products. It would be quite problematic if the proposed cyclization needed for construction of the daphnane core occurs with this *anti* selectivity, as this would position C18 on the β-face of the C ring instead of the desired α-face (see Scheme 2.3.3A) and there would be no easy way to invert the C11 stereocenter without involving the C9 alcohol as the only potential functional handle in close proximity. However, since the existing literature suggests that the stereochemical outcome at the cyclization terminus in more complex systems is more ambiguous and case-specific,[31,32] likely due to steric and electronic factors competing and potentially overriding the preference for hyperconjugative overlap, we were optimistic that we could find a substrate capable of cyclizing so that both stereocenters at C9 and C11 would be set correctly.

Scheme 2.3.4. Existing precedent for the stereochemical outcome of SmI_2-mediated 6-*exo*-trig cyclizations (**A**) and attempts at such cyclization with aldol products **2.3.5a** and **2.3.5b** (**B**).



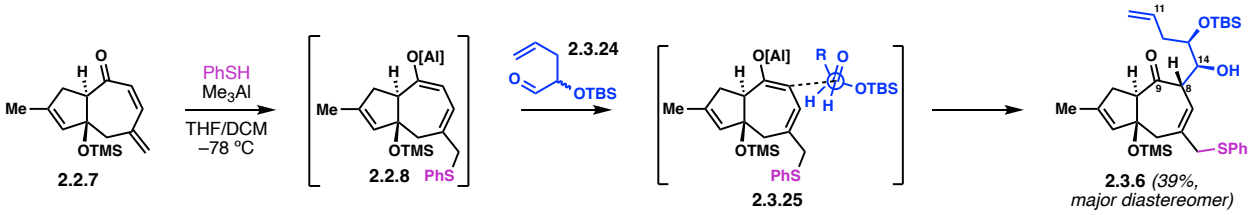
The reactivity of potential cyclization substrates **2.3.5a** and **2.3.5b** was next explored in the hopes of forging the C9-C11 linkage with the desired stereochemistry (Scheme 2.3.4B). However, under a variety of common SmI_2-based cyclization conditions no productive reaction was observed. At lower temperatures consumption of the starting material was slow, even in the presence of common additives such as alcohols or HMPA. The only products isolated were enone **2.2.7** and aldehyde **2.3.15**, arising from a retro-aldol process in which SmI_2 most likely acts as a Lewis acid. The color of the reaction solution remained blue (or purple when HMPA was used as additive), indicative of the presence of excess Sm(II), and compounds resulting from SmI_2-mediated 1,2-reduction of **2.2.7** and/or **2.3.15** were observed to varying degree, clearly indicating that a reducing environment was maintained in the reaction flask. We hypothesized that the lack of products arising from formation of the desired ketyl radical at C9 occurred because the retro-aldol process happened faster than reduction of the ketone, thereby precluding generation of appreciable amounts of this key reactive intermediate.

In order to combat these unfavorable kinetics, water was used as a co-solvent additive, since existing precedent suggested that coordination of water to Sm(II) would make this reagent a better reductant in terms of both thermodynamics and kinetics.[33,34] Indeed, in a 10:1 THF:H_2O mixture, the 1,2-reduction products **2.3.23a** and **2.3.23b** of ketones **2.3.5a** and **2.3.5b** respectively were finally observed, indicative of generation of the ketyl radical being faster than the undesired retro-aldol process in this case. A product of 6-*exo*-trig cyclization was also observed but was revealed to arise from the undesired C8 epimer **2.3.5a**. Careful analysis of the relative stereochemistry in tricycle **2.3.22** using a NOESY NMR experiment confirmed our projections around the stereocontrol that samarium could exert in this transformation, with both C9 and C14

oxygen atoms residing on the same β-face and the methyl group at C11 being placed on the opposite α-face (see ketyl radical **2.3.21** which illustrates the conformation of the reactive transition state leading to **2.3.22**). While neither **2.3.5a** or its cyclization product **2.3.22** contained the relative stereochemistry required for the daphnane core, these compounds served as proof-of-concept for several elements in our proposed retrosynthesis: a 6-*exo*-trig reaction was successfully used to connect C9 and C11 and the chiral center at C14 successfully guided the stereochemical outcome at C9. However, the relative stereochemistry at C11 in **2.3.22**, as well as the fact that no cyclization product arising from the desired C8 epimer **2.3.5b** was observed, were deeply concerning. A different cyclization precursor, arising from a different aldehyde partner in the conjugate addition/aldol cascade, was therefore called for.

Due to the possibility that productive cyclization of the ketyl radical formed from desired C14-epimer **2.3.5b** is kinetically slower relative to further reduction and protonation to provide **2.3.23b**, known[35] racemic aldehyde **2.3.24** was explored next as a type II partner (Scheme 2.3.5). The bulky OTBS substituent could render the 6-*exo*-trig cyclization kinetically more favorable via the Thorpe-Ingold effect while also being able to influence the stereochemical outcome in the initial aldol reaction between **2.2.7** and **2.3.24** in a potentially beneficial way. Indeed, the union of these two fragments proceeded with a higher degree of selectivity relative to the formation of **2.3.5a** and **2.3.5b**, resulting in diastereomer **2.3.6** as the single major reaction product alongside several minor diastereomers. A higher preference for the correct C8 epimer was therefore observed, alongside a curious case of matched-mismatched interaction, in which one enantiomer of the racemic enolate arising from **2.2.7** is preferentially joined with one enantiomer of racemic aldehyde. Aldol reaction via open transition state **2.3.25** governed by the Felkin-Anh model is the most likely explanation for the stereochemistry observed in **2.3.6**, especially based on the C14 chiral center.[36]

Scheme 2.3.5. Synthesis of modified cyclization precursor containing an OTBS group.

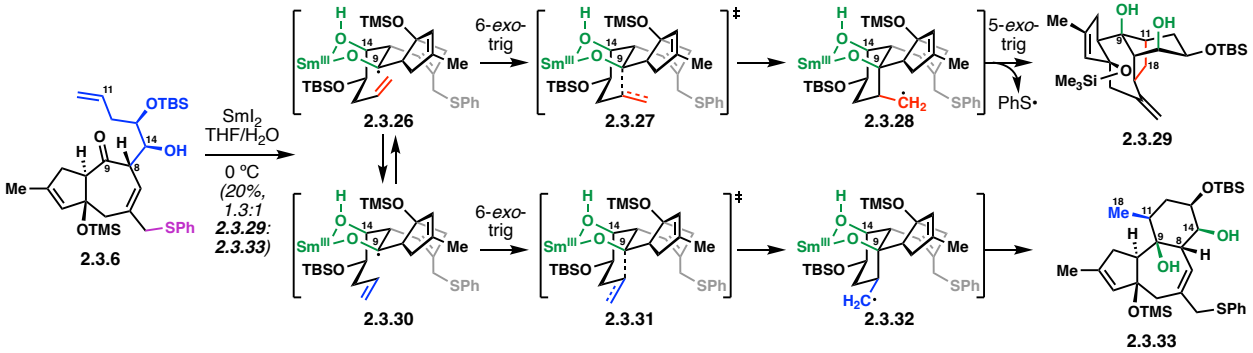


The relative configuration thereof was not confirmed until after cyclization of **2.3.6** to two copolar products, **2.3.29** and **2.3.33**, which contained rigid carbon skeletons amenable to providing definitive correlations in NOESY experiments (Scheme 2.3.6). The ready formation of these two compounds and the diminished amounts of 1,2-reduction products observed point to the beneficial effects of the OTBS group for the cyclization, thereby fully confirming our hypothesis behind the use of aldehyde **2.3.6**.

The structures of the cyclization product merit discussion in some detail. The topography and connectivity in the major component of the mixture, tetracycle **2.3.29**, are not at all surprising given the preferred stereochemical outcome of SmI_2-mediated cyclizations discussed above. In this product the oxygen atoms at C14 and C9 both reside on the β-face due to chelation to samarium during the 6-*exo*-trig bond forming event and C18 is positioned *anti* to the C9 oxygen (see transition state **2.3.27**), thereby conforming to the trend observed in literature and in the formation of **2.3.22**. However, in the current case, because of the difference in stereochemistry at C8, radical **2.3.28** arising from the initial cyclization event can undergo a subsequent 5-*exo*-trig reaction

connecting C18 and C7, since C18 is positioned sufficiently close in space to interact with the π* orbital of the olefin in the B ring.[37] This second cyclization, evidently faster than further reduction and protonation of radical **2.3.28**, would result in a tertiary radical that can be quenched by expelling phenylthiyl radical and forming an exocyclic double bond, providing tetracycle **2.3.29**. A similar two-electron mechanism centered around an anion at C18, formed by reduction of the corresponding radical, can also be proposed but is less likely as protonation of such an anion would be very rapid. Still, taken together the events leading to formation of **2.3.29** appeared to be in accordance with documented samarium reactivity. The more interesting cyclization product was **2.3.33**, in which chelation positions the hydroxy group at C9 on the same *β*-face as the one on C14, as expected, but C18 is also positioned on the *β*-face, in clear contrast with literature precedent (see transition state **2.3.31**). A possible explanation for this phenomenon is that both pseudo-axial (leading to **2.3.29**) and pseudo-equatorial (leading to **2.3.33**) orientations of the cyclization terminus allow for sufficient secondary orbital overlap, likely with the C-C or C-H bonds of the A ring, bringing the corresponding transition states **2.3.27** and **2.3.31** sufficiently close in energy that products arising from both are observed. At this stage it remained unclear whether the formation of **2.3.33** was a special case or indicated the general possibility of obtaining both relative stereochemistries at C11 regardless of the cyclization precursor. This question, combined with the fact that no tricycle with C9 and C14 oxygen atoms on the desired *α*-face of the C ring had been observed so far, prompted the exploration of even more aldehyde partners corresponding to new substrates for the 6-*exo*-trig reaction. As the hypothesis that introducing a TBSO-bearing stereocenter in the type II aldehyde would be beneficial for both the aldol reaction and cyclization, future studies focused on even more complex aldehyde congeners.

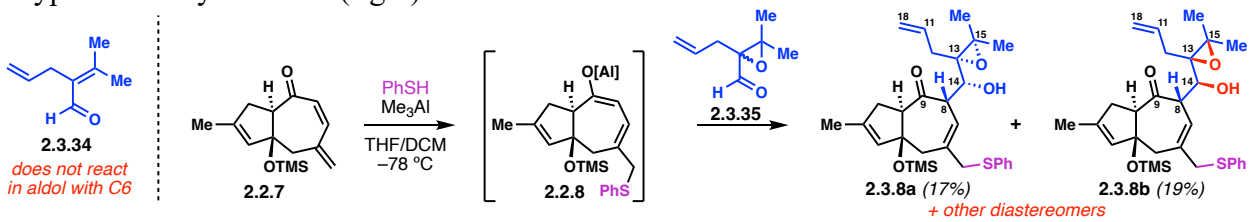
Scheme 2.3.6. SmI_2-mediated 6-*exo*-trig cyclization of ketone **2.3.6**.



The straightforward way to increase structural complexity in the aldehyde partner would be to employ a type III aldehyde, containing all carbons for both the C ring and the sidechain. First, known[38] enal **2.3.34** was envisioned as an achiral partner still capable to influencing the rate of cyclization via the Thorpe-Ingold effect and the rigidity provided by the sp^2-hybridization of C13 (Scheme 2.3.7A). However, when aldehyde **2.3.34** was subjected to the conjugate addition/aldol conditions, no reactivity was observed. This result was unexpected as prenal, a simpler enal lacking the allyl chain found in **2.3.34**, as well as all other aldehydes employed previously had successfully provided the corresponding aldol products. A possible explanation was the difference in hybridization at C13, so the corresponding epoxide **2.3.35** with a sp^3-hybridized alpha-carbon was employed next and was found to successfully engage in the construction of the desired C8-C14 bond (Scheme 2.3.7B). However, the reaction resulted in multiple diastereomeric aldol products, owing to the stereochemical complexity already present in the two racemic reaction partners and

the apparent lack of matched-mismatched reactivity as observed in the formation of **2.3.6**. Working with this more complex mixture meant that each individual constituent thereof was obtained in low yield, making analysis and subsequent chemistry more difficult. However, the greater number of diastereomeric products increased the chance of observing a compound containing the desired α-face hydroxyl group at C14, a substrate that had remained largely elusive so far.

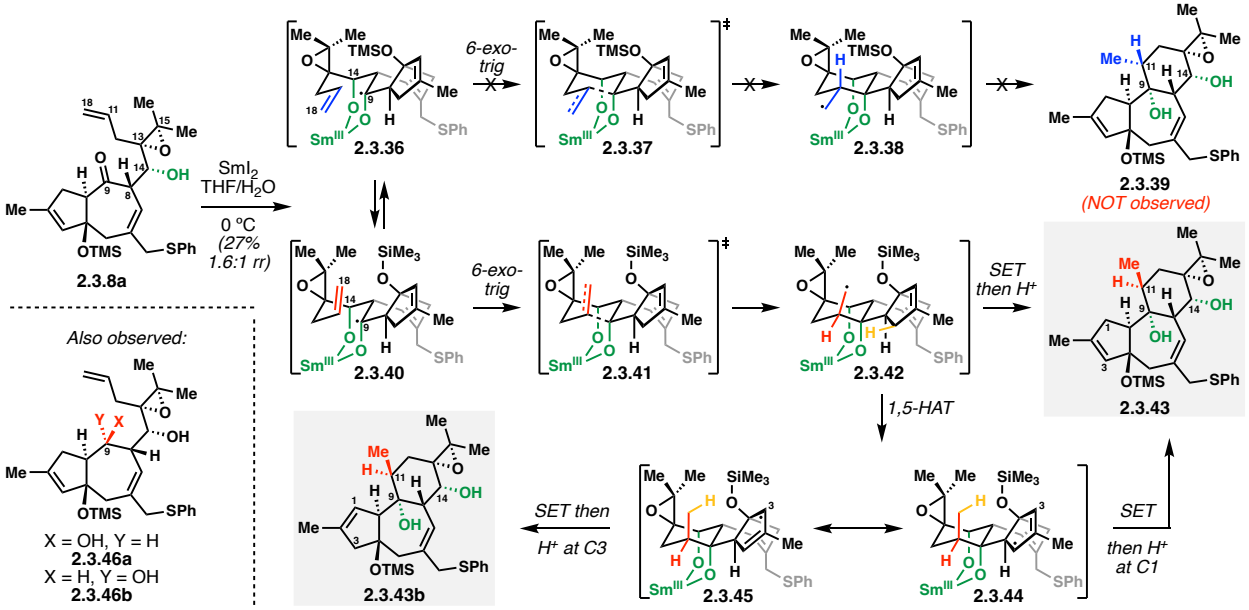
Scheme 2.3.7. Initial design of type III aldehyde (**2.3.34**, left) and productive aldol reaction with a type III aldehyde **2.3.35** (right).



Diastereomer **2.3.8a**, which was the most polar component of the product mixture and would later be revealed to bear the desired relative configuration at not only C14 but also C13, could be isolated in 17% yield and subjected to the SmI_2-mediated cyclization conditions (Scheme 2.3.8). As before, the stereochemistry around the C ring could only be confirmed after cyclization. In tricycle **2.3.43**, observed in the mixture of products from the 6-*exo*-trig cyclization, the tertiary alcohol at C9 was found to reside on the α-face as desired for the daphnane core and as expected from the chelation-based control that samarium, coordinated to the α-face C14 hydroxy group, would exert. However, the methyl substituent at C11 was positioned on the undesired β-face, meaning that once again the daphnane core remained elusive (see transition state **2.3.41**). As the chiral center at C11 was set so the methyl is *anti* to the C9 oxygen, thereby matching the predicted outcome based on existing precedent, the other components of the product mixture were explored in the hope that one of them would contain the desired stereotriad at C8, C9, and C11. The only other compound that appeared to be the result of a 6-*exo*-trig cyclization, however, was **2.3.43b** in which the A ring olefin is transposed to reside between C1 and C2. This tricycle, copolar with previously discussed **2.3.43**, unfortunately bears the same relative stereocenters and seems to arise via largely the same pathway. Coordination of SmI_2 to the oxygens at C14 and C9, followed by inner-sphere SET, would result in a ketyl radical, which could exist in one of two conformations in which the cyclization terminus is pseudo-axial (**2.3.40**) or pseudo-equatorial (**2.3.36**) respectively. These conformations would in turn give rise to two isomeric transition states for the 6-*exo*-trig cyclization. Transition state **2.3.37** which would involve a pseudo-equatorial orientation of the cyclization terminus is likely higher in energy than **2.3.41** due to fewer stabilizing secondary orbital interactions, even though the corresponding pseudo-equatorial conformation of the ketyl radical **2.3.36** would likely be lower in energy than **2.3.40**, suggesting that the Curtin-Hammett principle could be used to explain the observed diastereoselectivity at C11. Radical **2.3.42**, resulting from transition state **2.3.41** can undergo either further reduction and protonation to provide **2.3.43**, or can participate in a 1,5-hydrogen atom transfer to generate an allylic radical with resonance contributors **2.3.44** and **2.3.45**.[39] The latter intermediate is presumably further reduced and then protonated at either C1, generating more **2.3.43**, or C3, which leads to **2.3.43b**. It is unclear how much of the material in the cyclization undergoes the 1,5-HAT as the product containing C2-C3 olefin can be formed either with or without the hydrogen atom transfer. In summary, the use of type III aldehyde **2.3.35** allowed for the construction of the 5,7,6-fused tricyclic core in **2.3.43** and **2.3.43b** that resembles the desired daphnane core very closely in terms

of relative stereochemistry, and the stereocenters at C8, C9, C13, and C14 could all be set correctly as needed for the natural product scaffold. The only stereocenter that remained problematic was C11 as no desired product **2.3.39** was observed.

Scheme 2.3.8. Observed reactivity in the 6-*exo*-trig cyclization of desired aldol product **2.3.8a**.

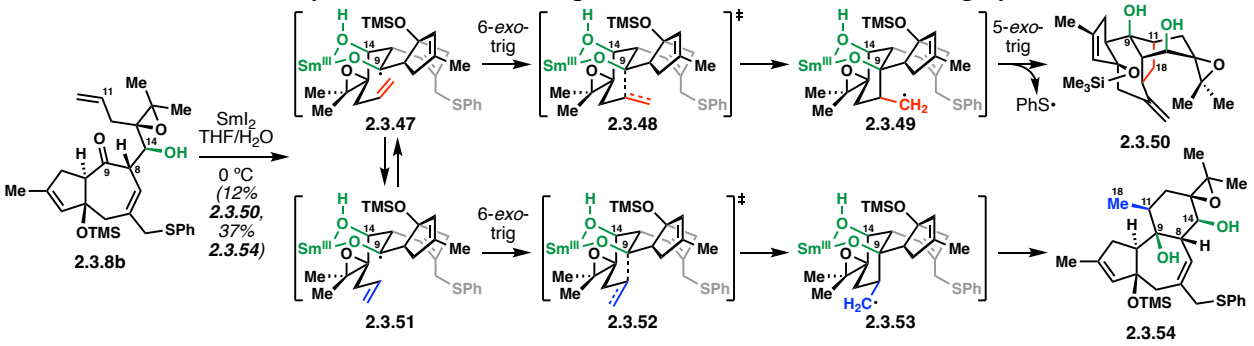


Given that **2.3.6** was observed to cyclize to both **2.3.29**, where C18 is *anti* to the C9 oxygen atom, and **2.3.33**, where these two substituents are *syn*, it is perhaps surprising that **2.3.8a** only reacted to products containing a C11-bound methyl *anti* to the C9 hydroxyl group. Indeed, the only other products identified in the cyclization reaction, **2.3.46a** and **2.3.46b**, arose from 1,2-reduction of the ketone instead of cyclization. It is possible that 6-*exo*-trig reaction via transition state **2.3.37** in which the cyclization terminus is pseudo-equatorial is too slow for substantial amounts of product to be formed; alternatively, reaction via **2.3.37** and resulting radical **2.3.38** proceeds but is followed by some unknown decomposition pathway so that no compounds related to this mode of reactivity are formed. The latter option could account for the observed low mass balance but does not point to a way in which the C11 stereocenter could be set as desired.

Since a major difference between **2.3.6** and **2.3.8a** was the C14 stereocenter, aldol product **2.3.8b**, possessing an R_f slightly higher than **2.3.8a**, was also explored as a cyclization substrate in the hopes of determining some trend regarding the stereochemical outcome at C11 (Scheme 2.3.9). Surprisingly, diastereomer **2.3.8b** provided tricycle **2.3.54** as the major product, in which C18 and the oxygen atoms at C9 and C14 are located on the β-face of the C ring. Tetracycle **2.3.50**, which would be expected to be favored based on both literature precedent for the *anti*-arrangement of C18 and the C9 hydroxyl group and the precedent observed with **2.3.29** being the major product arising from **2.3.6**, was observed only in small amounts. Comparison of the stereotriads at C8, C9, and C14 in **2.3.33**, **2.3.54**, and **2.3.43** seemed to point to an empiric rule where C18 is preferentially positioned on the β-face of any tricycle, regardless of the relative stereochemistry at C14, possibly due to a higher degree of favorable secondary orbital interactions when the cyclization terminus is positioned above the plane of the A ring, irrespective of substrate specifics. Taken together, the studies on substrates **2.3.5a**, **2.3.6**, **2.3.8a**, and **2.3.8b** confirmed the feasibility of closing the C ring via a 6-*exo*-trig reductive radical cyclization and the potential of samarium to correctly set the

C9 stereocenter in a substrate bearing an appropriately oriented C14 hydroxyl group but presented several unsolved challenges – the relative stereochemistry at C11 remained somewhat unpredictable and largely out of our control, the low yield of the cyclization, and the poor yield and diastereoselectivity in the preceding aldol reaction. Most importantly, the desired daphnane core had still yet to be realized.

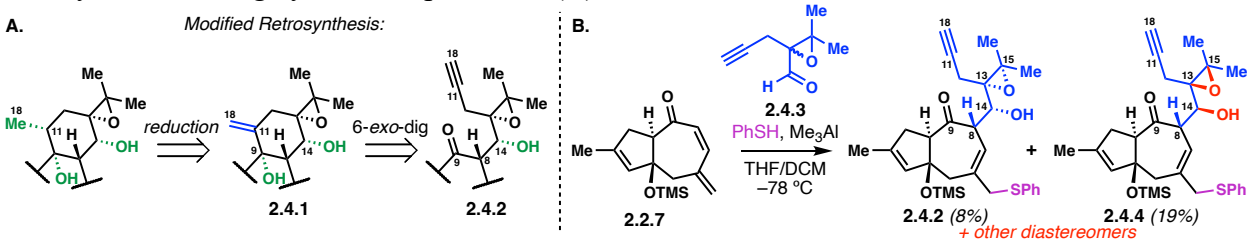
Scheme 2.3.9. Reactivity of undesired aldol product **2.3.8b** in the 6-*exo*-trig cyclization.



2.4 *SmI_2-Mediated Construction of the Daphnane Core Based on a Thiophenol-Bearing Cyclization Precursor*

The problematic stereochemical outcome at C11 was tackled first, as any optimization of the conjugate addition/aldol process would be rendered pointless if the subsequent SmI_2-mediated cyclization could not forge the desired daphnane core with all stereocenters set correctly. Since epimerizing tricycle **2.3.43** would be highly difficult without concomitantly destroying the C9 stereocenter, e.g. by forming a C9-C11 olefin, we attempted to find a different cyclization precursor that could allow for α-face selective formation of the C18 methyl group. The first intermediate that was explored was alkyne **2.4.2** (Scheme 2.4.1A), under the hypothesis that the 6-*exo*-dig cyclization of this compound would proceed in a similar manner to olefin **2.3.8a** and would afford the correct relative stereochemistry at C9 due to chelation of the ketyl oxygen atom and the C14 hydroxyl group to samarium. In contrast to the olefin case, however, the alkyne moiety in **2.4.2** would result in an exocyclic double bond at C11 in the desired cyclization product **2.4.1**. This alkene functional handle could then be used to install the correct C11 stereocenter at a later stage via reduction to the corresponding methyl group. The desired alkyne-bearing aldehyde partner **2.4.3** was easily obtained and proceeded to react with enone **2.2.7** under the previously employed conditions, resulting again in a mixture of diastereomeric products (Scheme 2.4.1B).

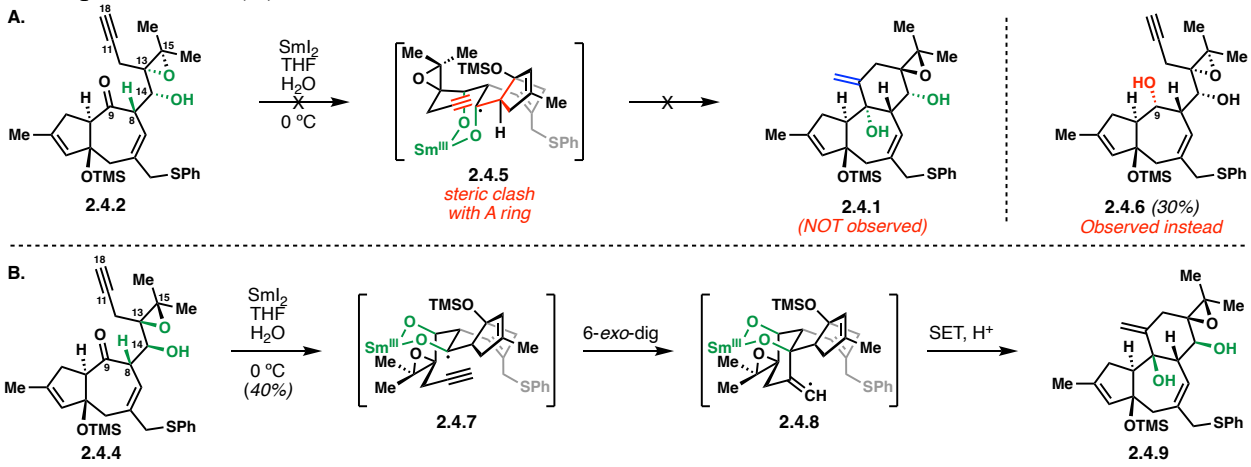
Scheme 2.4.1. Revised retrosynthetic strategy involving 6-*exo*-dig cyclization (**A**) and synthesis of alkyne-containing cyclization precursor (**B**).



Aldol product **2.4.2** was tentatively assigned to bear the desired relative stereochemistry at C14 by virtue of being the most polar constituent of the product mixture, as the desired C14-epimer

2.3.8a was the most polar product as well and the differences in structure between the two compounds were not expected to result in a drastic change in polarity. This trend in polarity would also be observed in other congeners in the series, wherein the most polar aldol product matched the relative stereochemistry found in olefin **2.3.8a** (see below). In order to confirm this stereochemical assignment and explore the 6-*exo*-dig cyclization manifold, alkyne **2.4.2** was subjected to a large excess of Kagan's reagent in the previously employed THF/H_2O mixture, but only trace cyclization product containing an exocyclic olefin was observed (Scheme 2.4.2A). The major reaction product was instead **2.4.6** via simple 1,2-reduction of the ketone. The lack of cyclization product in the crude mixture could, as discussed above, result from a kinetically unfavored 6-*exo*-dig reaction, or because the putative tricyclic intermediate undergoes some form of decomposition, with the former explanation being more likely. A brief analysis of transition state **2.4.5** required for formation of the desired cyclization product suggested that the linear nature of the cyclization terminus in this case positions C18 in close proximity to the TMS group and A ring. The resulting steric clash likely makes **2.4.5** too high in energy and therefore non-operative, which is why no appreciable amounts of tricycle **2.4.1** were observed. The proposed use of an alkyne to circumvent the undesirable stereochemical outcome at C11 was thus a dead end, likely due to unfavorable steric interactions in the transition state required for the cyclization.

Scheme 2.4.2. Attempts at 6-*exo*-dig cyclization with desired C14-epimer **2.4.2** (**A**) and undesired C14-epimer **2.4.4** (**B**).

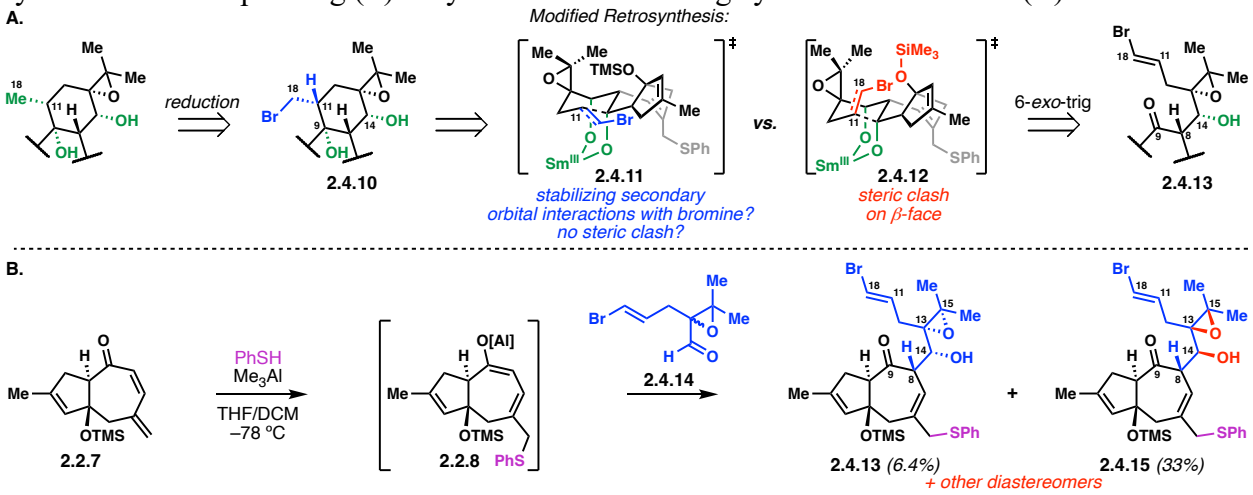


To test the feasibility of any 6-*exo*-dig cyclization with the current scaffold, diastereomer **2.4.4**, analogous to **2.3.8b** in bearing the incorrect C13 and C14 stereochemistry, was explored (Scheme 2.4.2B). This isomer could be separated from the other aldol products, was as in the previous case slightly less polar than the corresponding desired diastereomer, and was subjected to the SmI_2 conditions, resulting in allylic alcohol **2.4.9** if a large excess (10 equiv.) of samarium was used. Clearly, C9 and C11 can be united via a 6-*exo*-dig cyclization, even though this process is kinetically slower and is only operational for a substrate with undesired relative stereochemistry at C14. In the case for formation of allylic alcohol **2.4.9**, the alkyne cyclization terminus is positioned at the less hindered α-face of the bicyclic system, thereby making the corresponding transition state devoid of problematic steric interactions (see radical intermediates **2.4.7** and **2.4.8**). Chelation of the C9 and C14 oxygen atoms was observed and as expected resulted in the selective formation of the β-disposed tertiary alcohol **2.4.9**. Thus, while technically feasible with undesired

diastereomer **2.4.4**, the concept of executing a 6-*exo*-dig cyclization to access a tricycle of type **2.4.1** with desired aldol product **2.4.2** could not be realized in practice.

Given the failure of the 6-*exo*-dig idea, we reverted to exploring substrates bearing a sp^2-hybridized C18 and C11 were further explored under the hypothesis that a substituted olefin cyclization terminus could result in correct formation of both C9 and C11 stereocenters. The design of this next generation of cyclization termini would incorporate two concepts that were observed to be beneficial in the prior cyclization studies discussed above (Scheme 2.4.3A). Firstly, we sought to incorporate a substituent at C11 bearing lone electron pairs and thus capable of hyperconjugative secondary orbital interactions in a putative cyclization transition state. The degree to which such interactions seemed to govern the C11 stereochemistry in **2.3.54** suggested that secondary orbital overlap could be productively harnessed to position the cyclization terminus pseudo-equatorially, and if such overlap was not present in the native substrate, it would have to occur with a new substituent at C18 (see proposed transition state **2.4.11**). Furthermore, as sterics appeared to be the cause for one 6-*exo*-dig substrate cyclizing much more readily than the other (**2.4.4** vs. **2.4.2**), we wished to harness steric clash in a productive fashion. A substituent at C18 could be helpful in this case too, as it would cause unfavorable steric interactions with substituents on the β-face of the bicycle if the appropriately substituted cyclization terminus were positioned pseudo-axially (see proposed transition state **2.4.12**). Hence, a bulky substituent with lone pairs that, in the ideal case was easy to remove, was called for, and we envisioned that a halide would serve such a role very well – bromine and iodine atoms have large van der Waals radii relative to the other atoms in the substrate, possess multiple lone electron pairs, and can be removed under a variety of reductive conditions. Under this hypothesis we strove to access substrates such as **2.4.13** containing vinyl halides as cyclization termini.

Scheme 2.4.3. Revised retrosynthetic analysis incorporating a halide substituent at C18 (**A**) and synthesis of corresponding (*E*)-vinyl bromide-containing cyclization substrates (**B**).

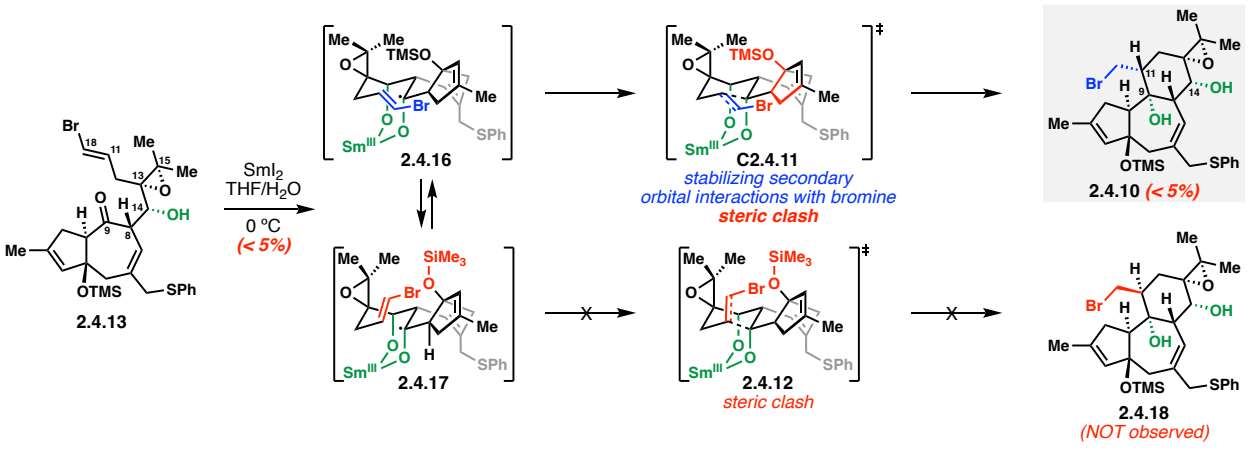


First, (*E*)-vinyl bromide **2.4.13** was targeted (Scheme 2.4.3B). The corresponding (*E*)-vinyl bromide-containing aldehyde **2.4.14** could be readily sourced from the series of intermediates leading up to aldehyde **2.4.3** (see section 2.12). With **2.4.14** in hand, the conjugate addition/aldol reaction with enone **2.2.7** was attempted and amongst the multiple diastereomeric aldol products, desired substrate **2.4.13** and its C13, C14 bis-epimer **2.4.15** were isolated. The trends in relative polarity of these compounds on TLC remained the same as for previous aldol products, but the

relative ratio of the two diastereomers was in this case much more skewed to favor formation of **2.4.15**. As a result, **2.4.13** was only isolated in 6.4% yield. The most likely explanation for this is that the aldol reaction proceeds with a different degree of stereochemical matching/mismatching between an enantiomer of enolate **2.2.8** with the enantiomers of racemic aldehyde **2.4.14**, as the two reaction products **2.4.13** and **2.4.15** discussed here arise from opposite aldehyde enantiomers (see relative stereochemistry at C13; for further discussion see Section 2.5). Irrespective of the yields, both desired cyclization precursor **2.4.13** and the diastereomer **2.4.15**, which mapped onto the undesired diastereomer series from previous substrates, could be accessed and were subjected to SmI_2.

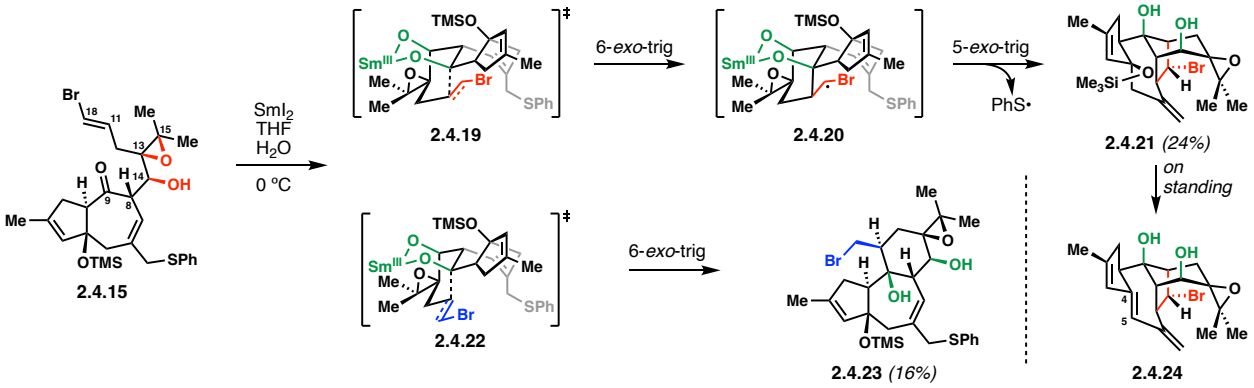
However, the cyclization of (*E*)-vinyl bromide **2.4.13** proceeded with terrible mass recovery, providing only traces of tricycle-containing products (Scheme 2.4.4). Upon scale-up and close examination with 2D NMR experiments, tricycle **2.4.10** was revealed to have exactly the desired relative stereochemistry necessary for the daphnane core. The C9 hydroxy group was correctly installed on the α-face, expected due to chelation control by samarium, and the C11 stereocenter was set appropriately as well. Thus, the elusive diastereomer where C18 and the two oxygen atoms at C9 and C14 all residing on the α-face of the 5,7,6-fused tricycle was finally achieved, and the hypothesis of using a vinyl halide to do so was largely proven correct. However, the prohibitively low yield in which **2.4.10** was obtained meant that the problem of synthesizing the daphnane diterpene core had yet to be fully solved. Upon closer examination of transition states **2.4.12** and **2.4.11**, containing a pseudo-axial and pseudo-equatorial cyclization terminus respectively, a potential reason for the very low yield was found – even in the desired transition state **2.4.11** unfavorable steric interactions involving the bulky bromine atom, positioned closely to the A ring due to the olefin geometry, could render cyclization kinetically slow. Thus, while the use of a vinyl halide seemed to successfully suppress formation of undesired diastereomer **2.4.18**, likely by lowering the energy of **2.4.11** relative to that of undesired transition state **2.4.12**, it appeared that the desired transition state was still too high in energy to provide substantial amounts of desired cyclization product. A simple solution for this issue would be changing the olefin geometry of the cyclization terminus. A (*Z*)-vinyl bromide would still be able to participate in stabilizing secondary orbital overlap as well as unfavorable steric interactions if positioned pseudo-axially. Moreover, in this case the pseudo-equatorial positioning of the (*Z*)-vinyl bromide would not result in steric clash between the bromine atom and the A ring as it seemed to be the case for the (*E*)-isomer. Before the cyclization of a substrate containing a (*Z*)-vinyl halide was explored however, an alternative hypothesis for the low yield of **2.4.10** had to be addressed.

Scheme 2.4.4. SmI_2-mediated 6-*exo*-trig cyclization of (*E*)-vinyl bromide **2.4.13**.



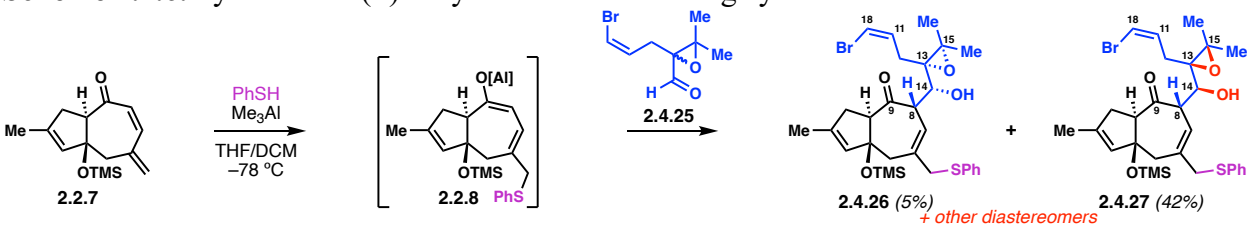
The possibility existed that a vinyl halide was simply not a suitable cyclization substituent for a SmI_2-mediated 6-*exo*-trig reaction, and indeed there was no literature precedent to suggest the feasibility of such a transformation. Aldol product **2.4.15** was thus used as a benchmark, as in previous instances compounds with a β-disposed hydroxyl group at C14 always successfully participated in the forging of the C9-C11 bond. This substrate did so as well, resulting in a mixture of tricycle **2.4.23** and tetracycle **2.4.21**, formed analogously to **2.3.54** and **2.3.50** respectively (Scheme 2.4.5). Interestingly, the tetracyclic intermediate was found to spontaneously lose TMSOH, resulting in triene **2.4.24** – a rapid process that occurred during the acquisition of 2D NMR spectra. This spontaneous elimination reaction serves to highlight the sensitivity of the synthetic intermediates involved in this project and is reminiscent of decomposition pathways observed during the attempts, not discussed herein, of further functionalizing the various tricyclic compounds synthesized thus far. The presence of cyclization products **2.4.23** and **2.4.21**, however unstable they might be, highlighted the feasibility of using a vinyl halide as a cyclization terminus and encouraged us that the use of a (*Z*)-vinyl bromide would likely solve the issues observed in the cyclization of **2.4.13**.

Scheme 2.4.5. Cyclization of undesired (*E*)-vinyl bromide **2.4.15**.



Thus, the corresponding aldehyde **2.4.25** containing a (*Z*)-vinyl bromide was synthesized in six steps (see Section 2.12) and unified with *trans*-fused hydroazulene **2.2.7** (Scheme 2.4.6). As in the case of the (*E*)-vinyl bromide isomer, the undesired diastereomer at C13 and C14 **2.4.27** was preferentially formed over desired isomer **2.4.26**.

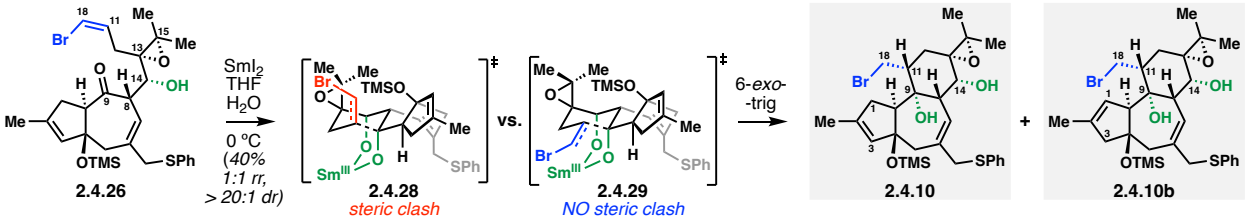
Scheme 2.4.6. Synthesis of (*Z*)-vinyl bromide-containing cyclization substrates.



The former underwent 6-exo-trig cyclization without any issue, delivering previously described tricycle **2.4.23** without formation of any tetracyclic intermediates. The fact that (*Z*)-vinyl bromide **2.4.27** reacted to provide solely a diastereomer containing a *syn*-relationship between C18 and the oxygen atoms at C9 and C14, all located on the β-face of **2.4.23**, was most encouraging and indeed, aldol product **2.4.26** cyclized to known 5,7,6-fused tricycle **2.4.10** in much higher

yield than **2.4.13** (Scheme 2.4.7). The A ring olefin isomer arising from 1,5-HAT similarly to **2.3.43b** was also observed and found to possess all C ring stereocenters as desired for the daphnane core. With a combined yield of 40% between olefin isomers **2.4.10** and **2.4.10b**, an intermediate possessing all carbons and stereocenters of the daphnane diterpenes was finally synthetically accessible in only nine steps from commercially available materials. The stereocenters at both C9 and C11 were set with greater than 20:1 dr, confirming the hypothesis that a (*Z*)-vinyl halide cyclization terminus is crucial, by virtue of both sterics and electronics, for formation of the desired diastereomer via favorable transition state **2.4.10** and reaffirming our retrosynthetic plan of using a 6-*exo*-trig radical cyclization to forge the last bond in the C ring. Before detailed exploration of the endgame of the synthesis could commence, however, a major problem – the very low yield of desired aldol product **2.4.26** – had to be solved.

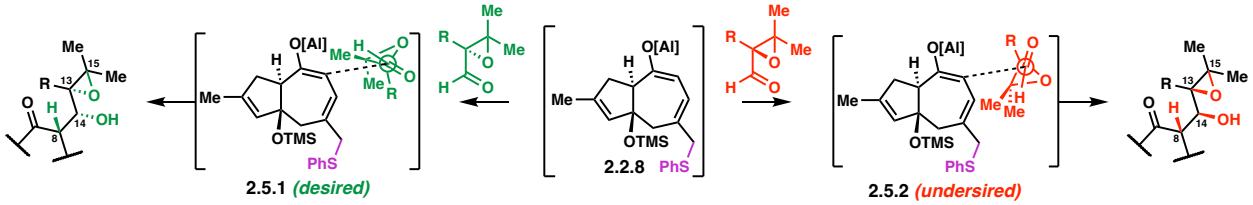
Scheme 2.4.7. Successful synthesis of the daphnane core with all requisite carbons and stereocenters.



2.5 *Identification of Stereoselective Conditions for the Formation of the C8-C14 Bond*

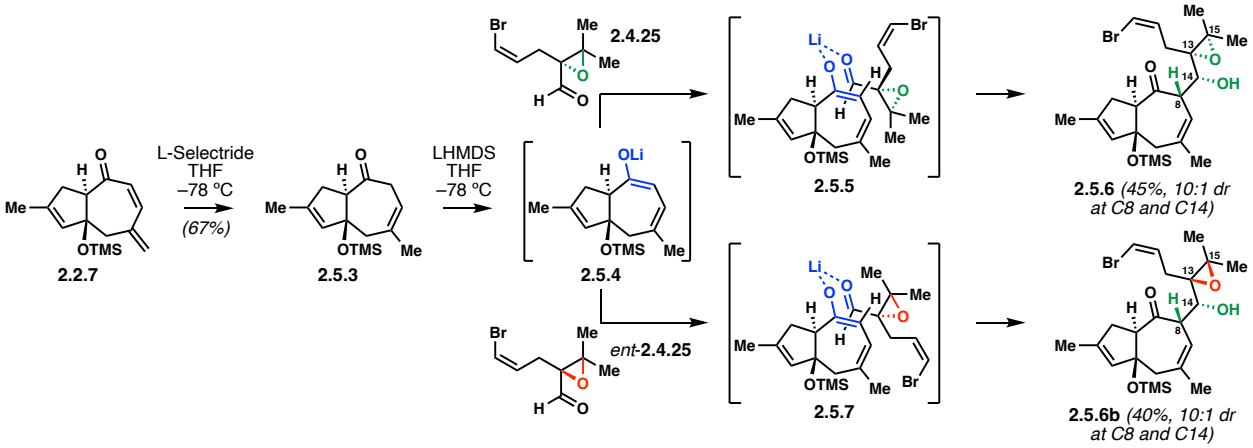
To address the low yield for the formation of the desired diastereomer of (*Z*)-vinyl halide **2.4.26**, a closer look at the product distribution in conjugate addition/aldol cascades with various aldehydes was very helpful. In contrast to aldehydes **2.3.35** and **2.4.3**, where the diastereomer with desired C13 and C14 stereochemistry (**2.3.8** and **2.4.2**) and the diastereomer with undesired C13 and C14 stereochemistry (**2.3.8b** and **2.4.4**) were formed in roughly equal amounts, with the vinyl halide-bearing aldehyde substrates the undesired C13, C14 diastereomer (**2.4.15** and **2.4.27**) was formed in much higher quantitates than the desired diastereomer **2.4.13** or **2.4.26** respectively. These results can be rationalized by the observation that all these aldol products arise from the aluminum enolate of the hydroazulene fragment reacting with either enantiomer of the aldehyde partner via open transition states **2.5.1** and **2.5.2** (Scheme 2.5.1) governed by the polar Felkin-Anh model.[36] The product distribution is thus simply a reflection of which transition state, corresponding to different pairings of the enantiomers of the two racemic reaction partners, is preferred. For formation of the desired C14-epimer reaction with the aldehyde enantiomer possessing an α-face oxygen atom is required (transition state **2.5.1**). It thus appears that in all these cases, as well as the formation of **2.3.6**, matched-mismatched reactivity between different enantiomers of hydroazulene and aldehyde is operational to a varying degree, with aldol product **2.3.6** being at one end of the spectrum, corresponding to a large degree of enantiomeric matching, while simple alkene- and alkyne-containing aldol products resided at the other end where bicycle enantiomers barely discriminate between aldehyde enantiomers. Vinyl halides, meanwhile, seemed to be positioned in between these two extremes. As the match between enantiomers of the reaction partners seemed so important, one could easily hypothesize that a change in the structure of either one would influence the relative energies of the respective transition states corresponding to **2.5.1** and **2.5.2**, thereby potentially favoring formation of the desired aldol product.

Scheme 2.5.1. Stereochemical rationale for the observed product distribution in the aluminum-mediated 1,6-addition/aldol cascade.



Such a hypothesis was however too vague, as it did not suggest any specific structural modifications and more importantly, did not address the presence of multiple other aldol products in each of the cases discussed above. Suppressing these additional diastereomers in favor of **2.4.26** would have a more marked impact on the reaction yield and could potentially be easily done if the aldol reaction were to proceed via a closed transition state. A union of a hydroazulene fragment and aldehyde **2.4.25** via a more ordered Zimmerman-Traxler would be expected to be much more selective in terms of product stereochemistry at C8 and C14, especially since the aldehyde in such a transition state would still be engaged according to the polar Felkin-Anh model. A brief sketch of such a closed transition state reveals that the stereocenters at C8 and C14 would be set exactly as desired and both enantiomers of the aldehyde partner would most likely react in the same way (see **2.5.5** and **2.5.7** in Scheme 2.5.2). Thus, we hypothesized that changing the reaction mechanism of the aldol reaction to one involving a Zimmerman-Traxler transition state would drastically increase the yield of the desired diastereomer product.

Scheme 2.5.2. Modified hydroazulene substrate engages in stereoselective aldol reaction via closed transition state.

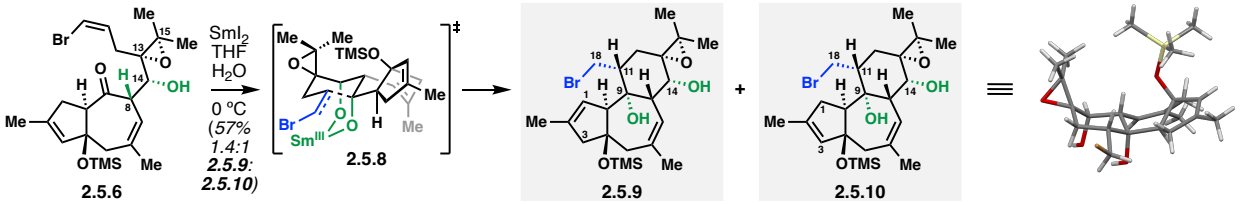


Such a change would likely occur when a different counterion was used for the enolate, with lithium being the most obvious choice given the vast amount of literature precedent on lithium enolates participating in Zimmerman-Traxler transition states.[40,41] However, the use of a lithium enolate posed a potential problem in the form of an undesired E1cB pathway that would eliminate any heteroatom substituent at C20, resulting in recovery of enone **2.2.7**. It was therefore decided to carry out the aldol reaction with enolate **2.5.4** in which such an elimination would be impossible as no suitable leaving group was present at C20, which position would later be oxidized as necessary. Ketone **2.5.3** containing an unconjugated olefin between C6 and C7 could be readily prepared from vinylogous enone **2.2.7** via a conjugate 1,6-reduction that could be carried out with

Stryker's reagent or in higher yield with L-Selectride, and in the latter case without competing 1,4-reduction. The lithium enolate of **2.5.3** was generated in a straightforward manner using LHMDS at cryogenic temperatures and upon addition of (*Z*)-vinyl bromide-bearing aldehyde **2.4.25** an aldol product containing the desired relative stereochemistry at C8 and C14 as well as an α-face epoxide at C13 and C15 was isolated in 45% yield. Thus, desired Zimmerman-Traxler transition state **2.5.5** was operational and desired diastereomer **2.5.6**, which corresponded perfectly to **2.4.26** in terms of relative stereochemistry, could be isolated in nine times greater yield. Reaction with the other enantiomer of the aldehyde via diastereomeric transition state **2.5.7** was also observed, resulting in C13,C15 epimer **2.5.6b**. Since the two products are formed in roughly equal yields, it seems that no great degree of matching between enantiomers of the two reaction partners is operational. Importantly, the relative stereochemistry at C8 and C14 in **2.5.6b** was also set correctly, as expected from a closed transition state. While in theory both aldol products could be productively harnessed, the chemistry of the desired C13 epimer **2.5.6** was explored first.

This new substrate was then successfully reacted with SmI_2 to provide tricycles **2.5.9** and **2.5.10**, with all stereocenters set correctly for the daphnane core (Scheme 2.5.3). Because of the (*Z*)-vinyl bromide cyclization terminus this transformation was once again highly stereoselective and in this case the relative stereochemistry of the cyclization products, isomeric at the A ring olefin due to yet another instance of a 1,5-HAT, was confirmed by X-ray crystallography. Since aldol product **2.5.6** could be obtained in much higher yield than previous substrates and could be used to successfully access tricyclic compounds **2.5.9** and **2.5.10** containing all carbon atoms and stereocenters of daphnane core, the endgame of the total synthesis of resiniferatoxin could finally be explored.

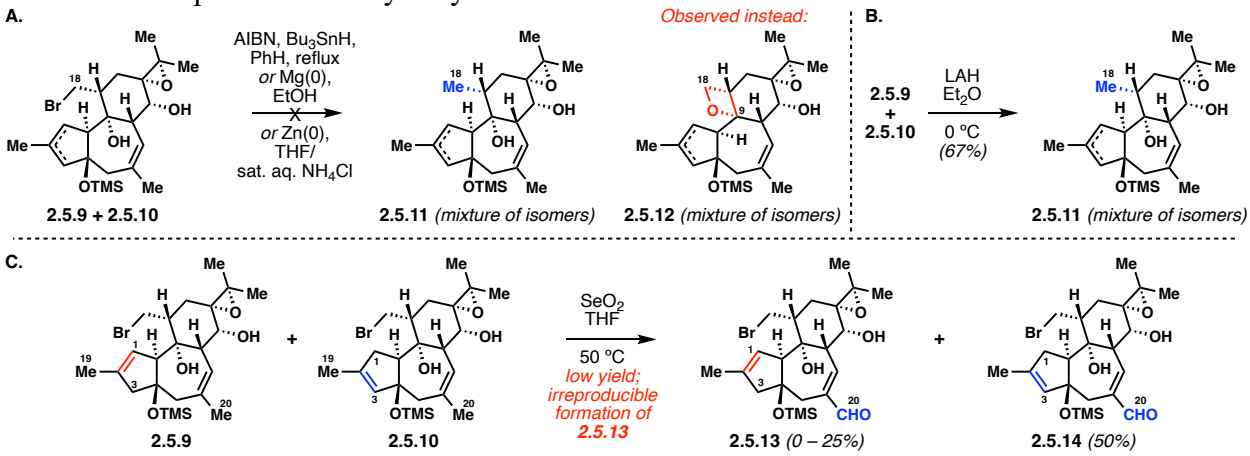
Scheme 2.5.3. Cyclization of selectively formed aldol product **2.5.6**.



The first two transformations of daphnane core-containing compounds **2.5.9** and **2.5.10** towards RTX that were investigated first were the removal of the now superfluous halide at C18 and the installation of oxidation at C20, under the hypothesis that both olefin isomers could eventually be productively oxidized to the desired A ring enone. The former transformation proved surprisingly difficult, with a variety of radical-based reduction conditions such as those involving AIBN and Bu_3SnH providing complex mixtures of products (Scheme 2.5.4A). The most likely source for this undesired reactivity was the proximity of C18 to the A ring – in the case of olefin isomer **2.5.9** a 5-*exo*-trig cyclization could take place before a putative radical at C18 can undergo hydrogen atom transfer. Indeed, the low number of olefin peaks present in the ^1H NMR spectrum of the complex mixture suggested that some compounds in it likely lack the A ring olefin. While this proposed 5-*exo*-trig pathway does not explain the fate of olefin isomer **2.5.10**, a related interaction of the C18 radical generated from **2.5.10** with functionality on the A ring, most likely a 1,5-HAT event, could lead to a variety of reactive radical species that undergo undesired transformations instead of intermolecular HAT with Bu_3SnH. Given the higher reaction temperature and different kinetics of the attempted reductions, it is not surprising that the fate of an allyl radical arising from 1,5-HAT might be different than the one observed with SmI_2 as

reductant. Using the latter reagent to remove the bromide at C18, simply by increasing the reaction time of the cyclization of **2.5.6** in order to directly observe the desired reduction product, did not prove fruitful either. The yields of tricycles **2.5.9** and **2.5.10** were diminished with reaction time, but no reduced product **2.5.11** (see Scheme 2.5.4) was observed, either due to the same kind of problematic radical-based pathways as previously observed, or because of the Lewis acidity of samarium species in the reaction mixture leading to decomposition of the acid-sensitive tricyclic products. Hence, an alternative to the one-electron reduction mechanism would have to be found in order to remove the halide substituent.

Scheme 2.5.4. Failed C18 reduction attempts (**A**), successful removal of C18 halide (**B**), and oxidative manipulations of key tricyclic intermediates **2.5.9** and **2.5.10**.



Change of reduction mechanism from one- to two-electron did not result in desired product either. The use of Mg(0) or Zn(0) as reductants resulted in formation of an undesired oxetane product **2.5.12** in which C18 is connected to the C9 oxygen atom. An extensive screen of other metal-based reducing conditions was not performed since the observation of the oxetane by-product suggested the possibility of cleaving the C-Br bond via an S_N2 mechanism (Scheme 2.5.4B). If a hydride was used as the nucleophile in such a process, the desired reduction product would be obtained and indeed, when tricycles **2.5.9** and **2.5.10** were treated with an excess of LAH at 0 ºC, the corresponding compounds containing a methyl group bound to C11, together designated as **2.5.11**, were finally observed. While the formation of the latter intermediates was not completely clean at this stage, LAH was thus identified as a promising way to remove the halide substituent from C18.

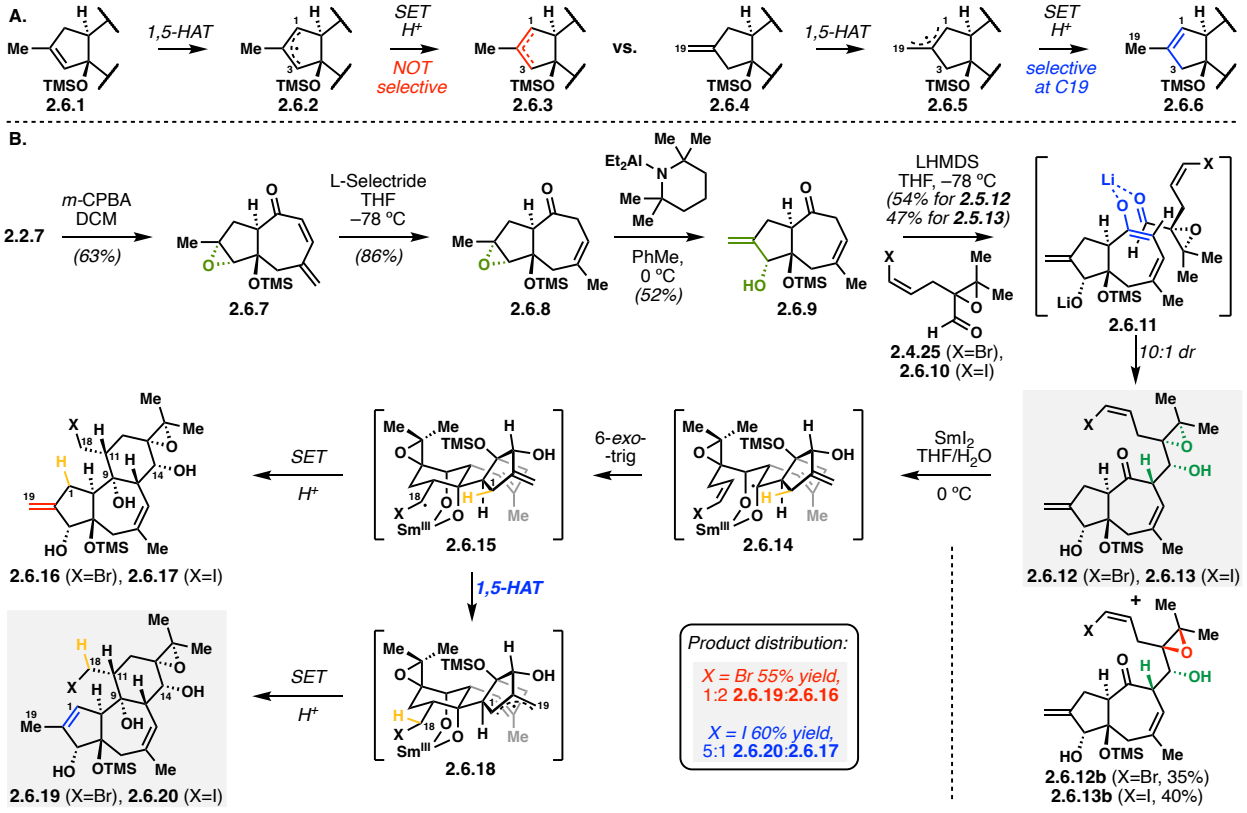
The installation of an oxygen atom at C20 was studied in parallel with the reduction experiments discussed above (Scheme 2.5.4C). Literature precedent suggested that carrying out an allylic oxidation with SeO_2 could selectively target the C20 position over the C19 methyl and other allylic carbons in the molecule. Oxidation product **2.5.14** was easily obtained when the mixture of isomers **2.5.9** and **2.5.10** was stirred with SeO_2 in THF at 50 ºC followed by direct purification of the reaction mixture on silica gel without prior concentration. While in the ideal case such an allylic oxidation would result in the desired alcohol at C20, over-oxidation to the corresponding aldehyde was not surprising. Unexpected, however, was the fate of olefin isomer **2.5.9** since little to no oxidized intermediate **2.5.13** related to this compound could be isolated, with yields varying widely between different batches. Aldehyde **2.5.14** was observed to be unstable and was only obtained in low yields when a work-up procedure different from the one

described above was used. It is likely therefore that aldehyde **2.5.13** succumbs to decomposition before or during purification more quickly than its isomer **2.5.14**. This difference in reactivity is problematic since we hypothesized that both olefin isomers could be converted to the oxidation pattern found in the A ring of the natural product. If tricycle **2.5.9** could not be reliably converted to usable late-stage intermediates, the material throughput of the synthetic daphnane core intermediates would essentially be reduced by half. In order to address this issue, as well as low yields observed in the epoxidation of the A ring olefin of aldehyde **2.5.14**, a new substrate with different functionality on the 5-membered ring was considered.

2.6 *Harnessing the Adventitious 1,5-HAT Event toward a Substrate with a More Suitably Functionalized Five-Membered Ring*

A new series of intermediates were designed to circumvent reactivity differences between olefin isomers **2.5.9** and **2.5.10** by harnessing the adventitious 1,5-HAT event observed in the SmI_2-mediated 6-*exo*-trig reaction of various substrates in a more productive way (Scheme 2.6.1A).

Scheme 2.6.1. Determination of optimal A ring substitution in order to harness 1,5-HAT event (**A**), synthesis of A ring allylic alcohol substrate **2.6.9** and elaboration thereof to a highly advanced daphnane precursor (**B**).



Specifically, we reasoned that assuming a medium to high degree of 1,5-HAT leading to formation of substantial amounts of allylic radical **2.6.2** from substrates containing an A ring olefin between C2 and C3 (see **2.6.1** as general representation), a mixture of products **2.6.3** isomeric at the A olefin would be observed. This was indeed the case with cyclization precursors **2.4.26** and **2.5.6**

and can be explained by the fact that the allylic anion arising from **2.6.2** has a similar likelihood to be protonated at either C1 or C3, both of which are secondary carbon atoms with roughly similar stereochemical environment. The lack of selectivity for the olefin geometry in the product **2.6.3** is therefore a result of the lack of kinetic preference for protonation at a particular carbon. In contrast, a cyclization precursor bearing a 1,1-disubstituted olefin between C19 and C2 (see **2.6.4**) would be expected to result in complete transposition of this double bond, giving rise to an olefin between C1 and C2 in the proposed cyclization product **2.6.6**. The crucial component of this hypothesis was that protonation of the transient allylic anion arising from allylic radical **2.6.5** would be much faster at the less hindered primary C19. Thus, a substrate containing an exocyclic A ring olefin was targeted with the expectation of a much more selective olefin transposition after 1,5-HAT. In order to circumvent stability issues such as the ones observed in the oxidation of **2.5.9**, additional oxidation at C3 would be introduced in the desired substrate, which was envisioned to contain an allylic alcohol (see **2.6.9** in Scheme 2.6.1). Upon oxidation of the C3 oxygen atom the electronic properties and thus the reactivity of the A ring olefin could be modulated, so tricyclic intermediates arising from hydroazulene **2.6.9** were expected to behave much better under allylic oxidation conditions.

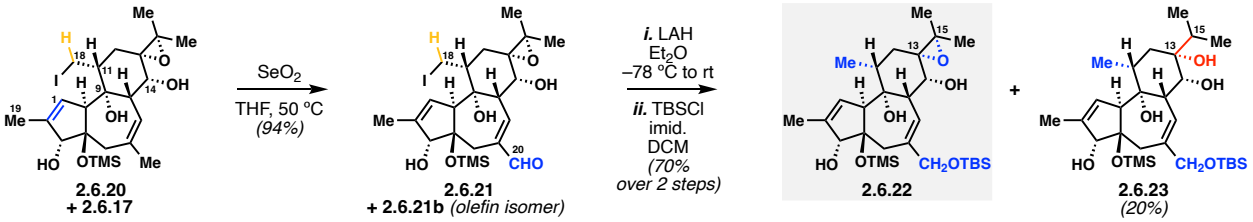
To access a hydroazulene containing the desired exocyclic allylic alcohol, enone **2.2.7** was selectively epoxidized at the most electron-rich site, namely the A-ring olefin (Scheme 2.6.1B). The resulting epoxide **2.6.7** was subjected to 1,6-reduction conditions, providing ketone **2.6.8**. This compound was elaborated to an allylic alcohol via epoxide opening mediated by diethylaluminum 2,2,6,6-tetramethylpiperidide (DATMP),[42] resulting in hydroazulene **2.6.9**, containing the desired A ring oxidation pattern. Despite the presence of a free alcohol at C3, ketone **2.6.9** was a competent substrate for the aldol reaction with aldehyde **2.4.25**, which once again proceeded via a closed transition state (see **2.6.11**) with very good diastereoselectivity at C8 and C14. Newly constructed cyclization precursor **2.6.12** was then subjected to Kagan's reagent to provide a mixture of tricyclic products **2.6.16** and **2.6.19** containing 1,1-disubstituted and trisubstituted olefins respectively. In terms of stereochemistry, both tricycles had all stereocenters set as desired, owing to the presence of the (*Z*)-vinyl bromide cyclization terminus leading to formation of radical **2.6.15**. The formation of desired cyclization product **2.6.19** arising from 1,5-HAT and olefin transposition was encouraging, but the ratio between undesired olefin isomer **2.6.16** and desired **2.6.19** was not, since the former product featuring an exocyclic olefin was favored. While in theory this product distribution might be the result of preferential protonation of the allylic anion arising from allylic radical **2.6.18** at secondary carbon C1, the more likely explanation was that **2.6.16** was the result of reduction and protonation of the C18 radical **2.6.15** before the 1,5-HAT could occur. We reasoned that changing the nature of the halide at C18 might subtly tune the reactivity of radical **2.6.15** due to differences in orbital overlap with said halide caused by the different sizes of Group 17 atoms. For instance, an iodine atom, being larger than bromine, would be expected to have a lesser stabilizing effect on the carbon-centered radical **2.6.15**, thereby increasing the reactivity of the latter, which would hopefully translate in an increased propensity for 1,5-HAT, leading in turn to a higher degree of olefin transposition during the cyclization. A cyclization substrate containing a (*Z*)-vinyl iodide was thus targeted.

The corresponding (*Z*)-vinyl iodide-containing aldehyde **2.6.10** was synthesized similarly to its vinyl bromide counterpart. The aldol reaction between **2.6.10** and the lithium enolate of **2.6.9** proceeded without any issues or differences when compared to the formation of **2.6.12**, resulting in stereoselective formation of (*Z*)-vinyl iodide **2.6.13**. Fortunately, when this aldol product was reacted with Kagan's reagent under the standard cyclization conditions, tricycle **2.6.20** containing

a transposed A ring olefin was isolated in much higher yield, alongside small amounts of its copolar isomer **2.6.17** containing an exocyclic alkene. As expected, tricycle **2.6.20** contained the desired stereochemistry at C9 and C11. Hence, substituting the bromine atom in the cyclization precursor for an iodine did indeed result in a much higher degree of 1,5-HAT, likely due to a more reactive radical **2.6.15** giving rise to much higher amounts of allylic radical **2.6.18**, which in turn led to a higher yield of transposed olefin-containing product. With our hypothesis proven, the stage was set to advance tricycle **2.6.20** to a congener containing oxidation at C20.

When the mixture of olefin isomers **2.6.20** and **2.6.17** was subjected to the previously employed allylic oxidation conditions, the major component **2.6.20** was cleanly oxidized to the expected mixture of aldehydes **2.6.21** and **2.6.21b** (Scheme 2.6.2). Aldehyde **2.6.21** was perfectly poised for a pre-meditated double reduction event, wherein the iodide substituent would be removed under the LAH conditions discussed above while simultaneously the carbonyl group at C20 would be reduced to the desired alcohol moiety. These transformations could be successfully carried out in the presence of a large excess of LAH, resulting in a C20 allylic alcohol containing a methyl substituent at C11. This highly polar compound was used without purification and after TBS protection provided silanol **2.6.22**, which could be obtained as a single olefin isomer. The fate of exocyclic olefin **2.6.21b** in this sequence is less clear, as no substantial amounts of compounds derived from this olefin isomer could be isolated, possibly due to sensitivity to Lewis acidic species in the reduction step. The LAH-mediated double reduction reaction, however rapid and selective, had some scalability issues. While reduction proceeded cleanly on small scale, resulting in pure **2.6.22** after reaction with TBSCl in a second step, when the double reduction was carried out on more than 5 mg scale a byproduct tentatively arising from reductive opening of the epoxide at C15 was also isolated. The structure of this impurity was confirmed using 2D NMR experiments as **2.6.23** after TBS protection of the primary alcohol. To suppress the unproductive epoxide opening pathway, the double reduction was carried out in multiple parallel 5 mg batches and the reaction mixtures were left to slowly warm up over 12 hours. With these modifications to the reduction procedure the material throughput ultimately yielding silanol **2.6.22** was substantially increased and with scalable access to that key intermediate the stage was set for the formation of the hallmark orthoester moiety.

Scheme 2.6.2. Oxidative manipulations of tricycle **2.6.20**.

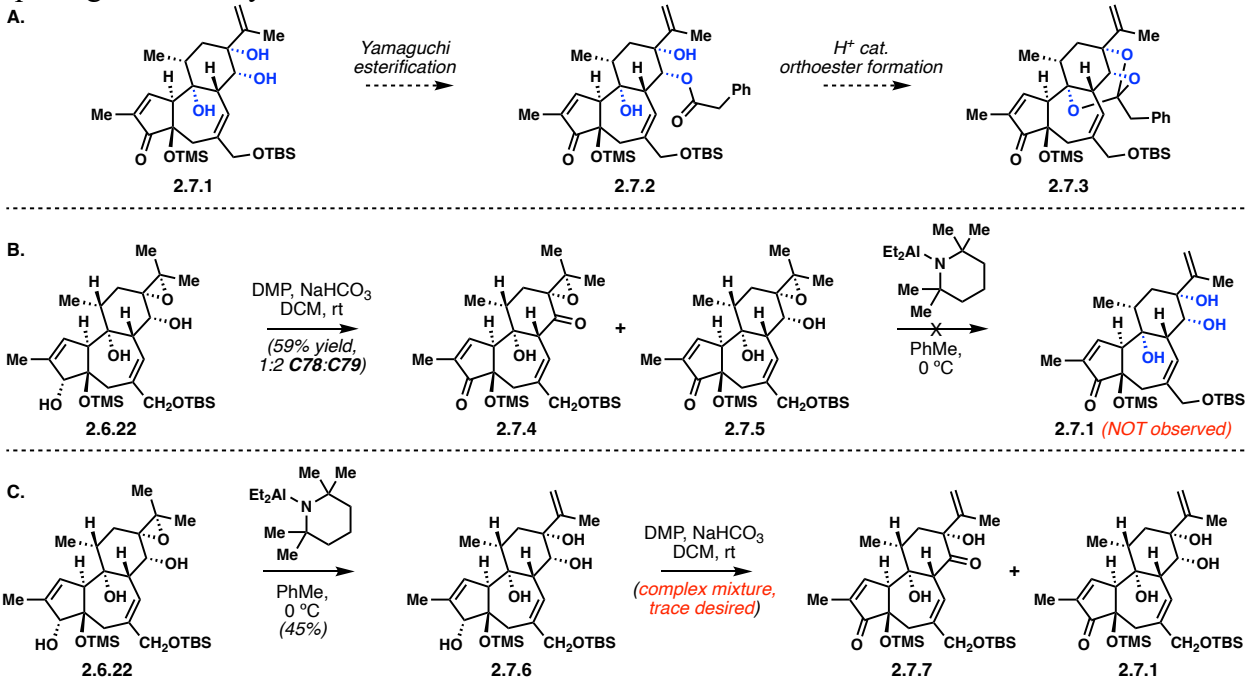


2.7 *Forging the Orthoester and Completion of the Total Synthesis of Resiniferatoxin*

Prior art suggested that the orthoester functional group can be most efficiently constructed from triol **2.7.1** via esterification of the C14 alcohol with phenylacetic acid, usually carried out under Yamaguchi conditions (see **2.7.2**), followed by acid-mediated orthoesterification (Scheme 2.7.1A).[43–46] Hence, the synthesis of triol **2.7.1** from silanol **2.6.22** was attempted by initial oxidation of the C3 alcohol followed by DATMP-mediated opening of the C13, C15 epoxide (Scheme 2.7.1B). The oxidation at C3 proved difficult, however, with a variety of common conditions resulting in low reactivity (e.g. Stahl oxidation or precedented conditions involving

AZADO) or complex mixtures (e.g. TEMPO/PIDA, likely due to acid-mediated decomposition). Out of all conditions surveyed, only DMP buffered with sodium bicarbonate delivered some of desired enone **2.7.5**, alongside double oxidation product **2.7.4**. These copolar compounds were subjected to DATMP but unfortunately, no desired reactivity was observed and several products tentatively arising from undesired reactivity of the A ring enone were observed instead as components of a complex mixture. The order of operations was inverted to circumvent this reactivity issue, so triol **2.6.22** was reacted with diethylaluminum 2,2,6,6-tetramethylpiperidide to provide tetraol **2.7.6** (Scheme 2.7.1C). However, conversion in this transformation was not complete and the product was observed to be highly unstable to acid, likely due to the presence of the newly formed tertiary allylic alcohol. The oxidation of tetraol **2.7.6** also did not proceed smoothly and in this instance the double oxidation product **2.7.7** was the major component in the reaction mixture at various levels of conversion and a lot of additional products were observed. Desired triol **2.7.1** could thus not be produced in satisfactory yield, so a new approach for the formation of the orthoester was necessary.

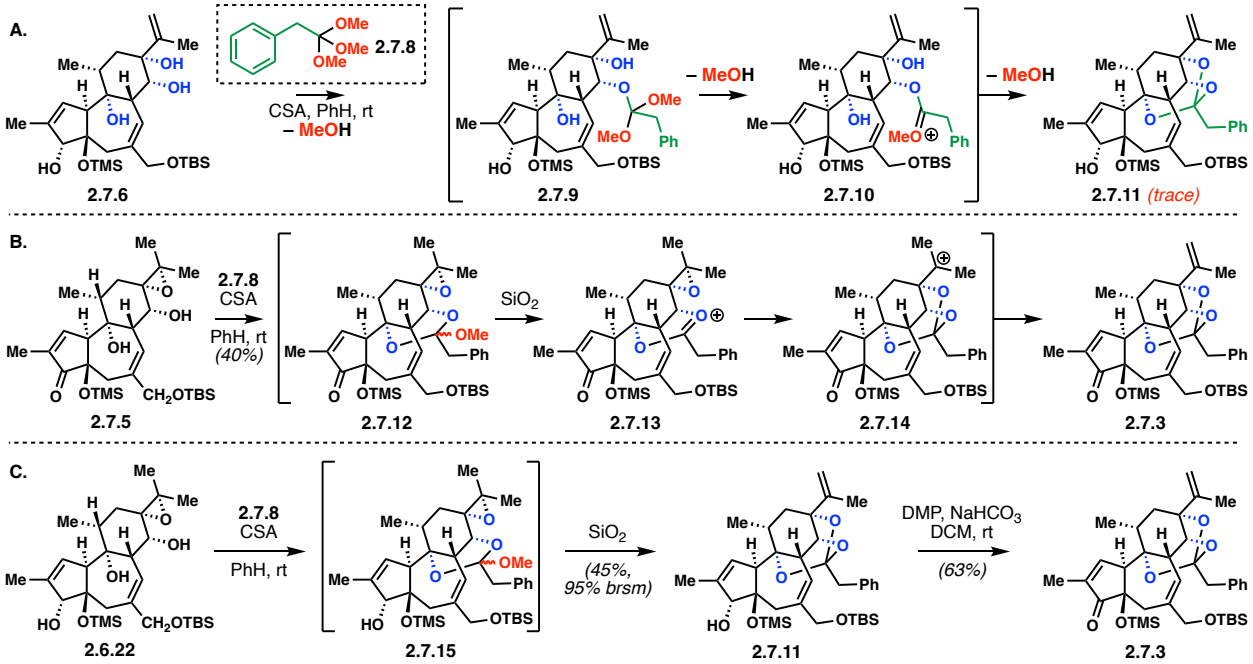
Scheme 2.7.1. (**A**) Initial retrosynthetic route for orthoester construction. (**B**) Attempts at synthesizing triol **2.7.1** via oxidation followed by epoxide opening. (**C**) Attempts at epoxide opening followed by oxidation.



As esterification of triol **2.6.22** or tetraol **2.7.6** would likely proceed at the more sterically accessible C3 hydroxy group and C3-ketone **2.7.1** could not be accessed in sufficient amounts, we turned our attention to acid-catalyzed trans-orthoesterification conditions wherein a trialkyl orthoester is attached to a pre-existing triol with concomitant loss of three simple alcohol molecules (Scheme 2.7.2A).[43,47] Tetraol **2.7.6** was envisioned as the initial reaction partner in this proposed transformation under the hypothesis that attachment of some orthoester moiety to the free C3 alcohol would be transient and that the final reaction product once equilibrium was reached would be orthoester **2.7.11** via intermediate **2.7.9** and oxonium ion **2.7.10**. However, due to the excessive acid instability of the starting material this transformation could not be carried out and

any attempts to do so resulted in mostly decomposition of **2.7.6**, with only trace amounts of **2.7.11** being isolated. Enone **2.7.5** was the next substrate with which this transformation was attempted despite the lack of a tertiary alcohol at C13 (Scheme 2.7.2B). The α-disposed oxygen atom at that carbon could feasibly still participate in the orthoesterification reaction mechanism by engaging putative oxonium ion **2.7.13** with concomitant cleavage of the C15-oxygen bond. The resulting carbocation **2.7.14** could then lose a proton to regenerate the acid catalyst in this transformation, providing the desired olefin moiety in that sector of the molecule. This proposed cascade would be a faster and more facile way to access the desired orthoester product and would circumvent the problems inherent in the construction of a C ring triol in this series of intermediates. Indeed, in the presence of an excess of (2,2,2-trimethoxyethyl)benzene (**2.7.8**) and catalytic CSA, epoxide **2.7.5** was observed to react to a new compound which was less polar on TLC and which, upon purification, reacted to form an even less polar intermediate that was identified as desired orthoester **2.7.3**. The most likely explanation for this observed reactivity is that in solution a mixed orthoester such as **2.7.12** is formed, wherein the C9 and C14 alcohols are attached to the phenylacetic sidechain but the C13 oxygen atom is still part of an epoxide. This observation is supported by the ^{1}H NMR spectrum of the crude reaction mixture which does not contain any peaks that would indicate the presence of a 1,1-disubstituted olefin. Then, upon exposure of **2.7.12** to silica gel the mixed orthoester is likely converted to desired oxonium ion **2.7.13**, which undergoes the proposed orthoesterification with concomitant epoxide opening sequence. The crucial orthoester moiety of resiniferatoxin was thus installed in a facile way.

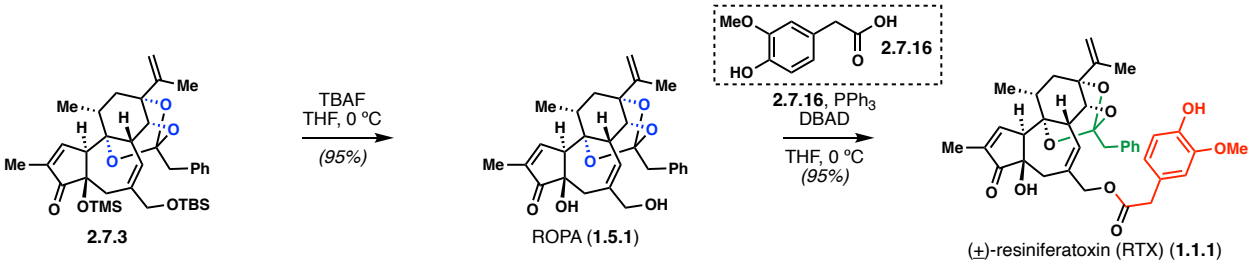
Scheme 2.7.2. Attempts at trans-orthoesterification with tetraol **2.7.6** (**A**), enone **2.7.5** (**B**), and triol **2.6.22** (**C**).



However, due to the low selectivity in the oxidation reaction leading to enone **2.7.5**, the overall material throughput to orthoester **2.7.3** was not ideal. In order to increase the supply of **2.7.3** the trans-orthoesterification reaction was attempted with triol **2.6.22** under the assumption that mixed orthoester **2.7.15** could be formed even in the presence of the free alcohol at C3, with

the latter maybe transiently engaging intermediates arising from **2.7.8** before equilibrium could be reached (Scheme 2.7.2C). This proposed orthoesterification product would then possess only one free alcohol, thereby avoiding any regioselectivity issues during the subsequent oxidation at C3. Gratifyingly, this hypothesis was correct and under the trans-orthoesterification conditions employed thus far **2.6.22** was gradually converted to a less polar compound tentatively assigned as **2.7.15** which, similarly to the previous case, was transformed in the presence of silica gel to desired orthoester **2.7.11**. While the overall yield of this reaction was modest if full conversion of the starting material was desired, a very high yield of the orthoester product based on recovered triol **2.6.22** could be obtained if the reaction was worked up once equilibrium amounts of these two compounds were reached. Allylic alcohol **2.7.11** was readily oxidized to the desired orthoester-bearing enone **2.7.3**, thereby solving the material throughput issue. Fluoride-mediated deprotection of the C20 and C4 alcohols resulted in previously known resiniferonol-9,13,14-orthophenyl acetate (ROPA, **1.5.1**), which was in turn united with the homovanillic sidechain in a single step based on a Mitsunobu reaction previously utilized by the Inoue group to provide synthetic resiniferatoxin (**1.1.1**) (Scheme 2.7.3). Hence, the flagship of the daphnane diterpene orthoesters was synthesized in 19 steps using a novel retrosynthetic logic orthogonal to previous syntheses. The odyssey of developing the modular, convergent, and highly stereoselective route to RTX was however not yet over, as the goals of reducing the step count and increasing the yields of several transformations remained.

Scheme 2.7.3. Synthesis of (±)-resiniferatoxin from orthoester **2.7.3**.

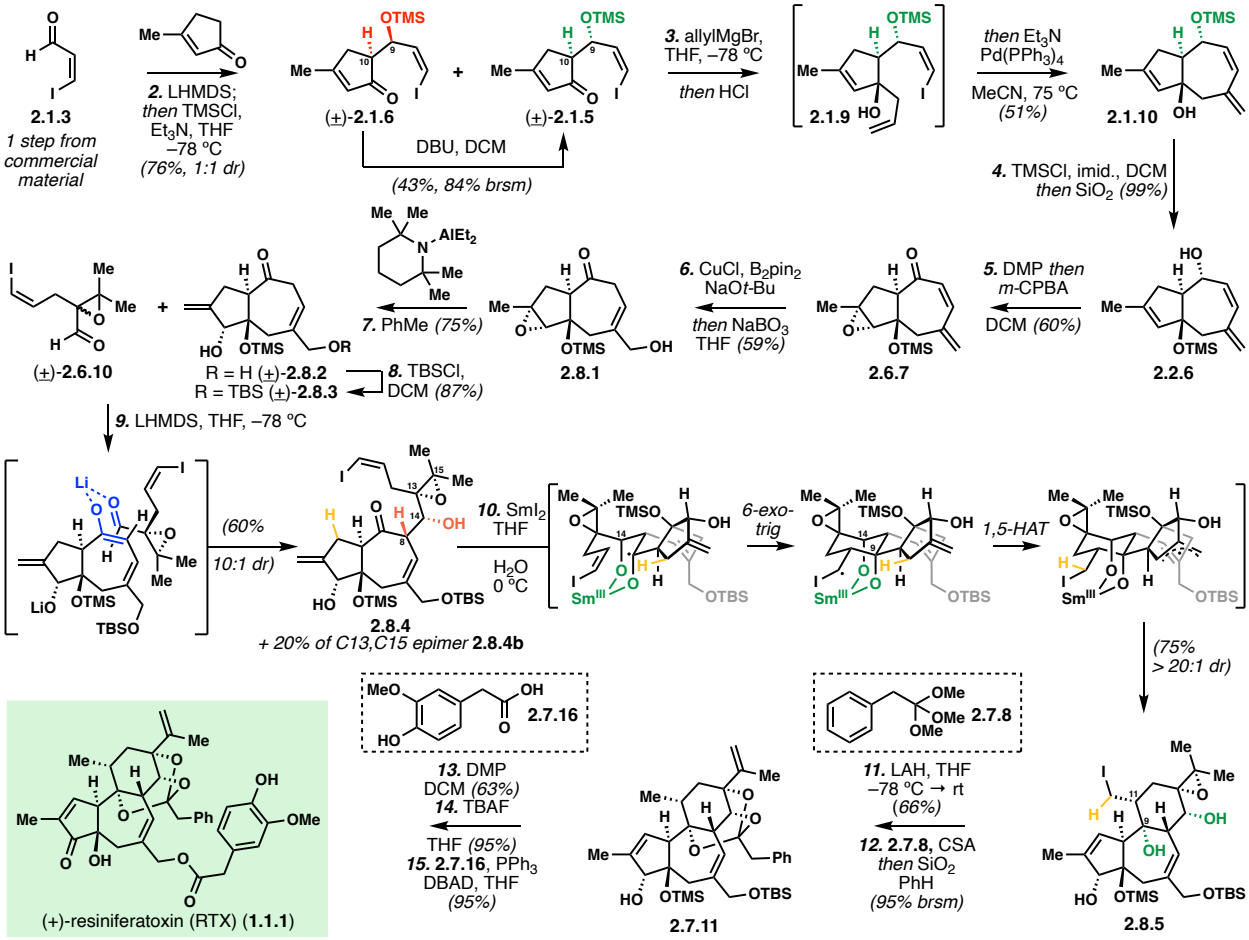


2.8 *Optimized 12-step Synthetic Route to the Daphnane Diterpene Orthoesters. A 15-Step Total Synthesis of Resiniferatoxin*

With the synthetic map to resiniferatoxin fully constructed, the final task of optimizing and shortening the route was explored. Several steps that could theoretically be carried out in the same pot were identified, namely the Grignard addition and Heck coupling to convert *syn*-aldol product **2.1.5** to hydroazulene **2.1.10**, as well as the functional group manipulations in the sequence from alcohol **2.1.10** to epoxide **2.6.7** (Scheme 2.8.1). The one-pot conversion of secondary alcohol **2.2.6** to epoxide-containing enone **2.6.7** was the most straightforward (see step 5 in Scheme 2.8.1), as simple addition of *m*-CPBA to the DMP-mediated oxidation of **2.2.6** to **2.2.7** was sufficient to bring about the desired epoxidation without any decrease in yield. Since no material or solvent left the flask in this sequence, this oxidation and epoxidation cascade can be considered as a single step in the synthetic route. The one-step conversion of Heck product **2.1.10** to secondary alcohol **2.2.6** (see step 4 in Scheme 2.8.1) was also easily carried out thanks to the adventitious observation that the C9 silanol of doubly protected intermediate **2.2.5** was spontaneously removed during purification with silica gel. In order to ensure full conversion to the free secondary alcohol, silica gel was added to the rection mixture, and the resulting suspension was concentrated to dryness. While these two optimized steps, each comprising of two functional group manipulations, could

in theory be combined into one pot, converting Heck product to **2.1.10** directly to epoxide **2.6.7** in a single flask, this was not accomplishable in practice without removing the silica gel after the crude mixture contained free alcohol **2.2.6** (end of step 4). The presence of silica gel proved detrimental for the subsequent oxidative manipulations, especially the epoxidation. Hence, the step count for the functional group manipulations from hydroazulene **2.1.10** to enone **2.6.7** could at best be reduced to two steps.

Scheme 2.8.1. Optimized 12 step synthesis of the daphnane orthoester core and 15 step total synthesis of resiniferatoxin.



The one-step transformation of ketone **2.1.5** to bicycle **2.1.10** was investigated next (see step 3 in Scheme 2.8.1). Anhydrous HCl (2 M solution in Et_2O) was quickly identified as a suitable quench for the magnesium alkoxide resulting from 1,2-addition of allyl Grignard into enone **2.1.5**. Excess acid would be neutralized by the large excess of Et_3N necessary for the Heck reaction but due to the acid sensitivity of tertiary alcohol **2.1.9**, base had to be added immediately after the acid quench while the reaction mixture was still warming up. From this point on the 7-*exo*-trig cyclization was set-up as usual and gratifyingly resulted in formation of the desired hydroazulene **2.1.10**. The yield of this Heck reaction also had to be improved as discussed in Section 2.1. Extensive screening of reaction conditions revealed that the formation of undesired 5,8-fused bicycle **2.1.11** could be suppressed if MeCN was used as reaction solvent. This solvent however proved detrimental for the desired one-step allylation/cyclization cascade. While the allylation

could be carried out at much higher concentration and the resulting mixture could be diluted with a large amount of MeCN, corresponding to a 10:1 MeCN:THF ratio, only trace desired Heck product was observed under these conditions and the reaction profile was far worse than usual. A compromise had to be struck, with the use of a 1:1 MeCN:THF mixture providing the optimal yield of Heck product **2.1.10** in the one-step reaction from ketone **2.1.5**. With that the synthetic route was shortened by yet another step and the formation of *trans*-fused hydroazulene **2.1.10** was accomplished in a satisfactory yield higher than the one obtained with the original conditions.

The optimization of the synthetic route continued with attempts to utilize a compound already bearing oxidation at C20 in the key aldol with aldehyde **2.6.10**. While concerns about an undesired E1cB reaction had prevented such studies thus far, exploring the reactivity of a substrate such as **2.8.3** was worthwhile in the context of optimizing a completed synthesis of RTX. The 1,6-reduction and subsequent allylic oxidation at C20 used in the current route could be viewed as unnecessarily lengthy functional group manipulations if a formal conjugate 1,6-addition of an oxygen atom could be carried out with enone **2.6.7**, provided that the resulting intermediate could be productively converted to the natural product. Screening of suitable conditions[48–50] for the conversion of enone **2.6.7** into allylic alcohol **2.8.1** revealed that the use of a ligandless copper catalyst in a 2:1 THF/H_2O mixture was optimal for transforming enough of the starting material into the desired product on scale. Under these conditions formation of the undesired 1,4-addition product was largely suppressed. Formation of the latter could be completely eliminated under very dilute reaction conditions, but these were not amenable to scale-up, so once again a compromise between selectivity and material throughput had to be struck. Allylic alcohol **2.8.1** was then subjected to DATMP and the concerns about a problematic E1cB pathway were partially justified, since a far less polar compound was observed alongside the desired diol **2.8.2**. However, the formation of this tentative E1cB-related byproduct could be minimized with careful control of the reaction time – the desired epoxide opening with this substrate proceeded much more rapidly than with **2.6.8**, likely due to favorable coordinative interactions with the C20 oxygen atom in the necessary transition state. With diol **2.8.2** obtained in adequate yield, an aldol reaction with aldehyde **2.6.10** was attempted but no desired product was found. Under the hypothesis that the presence of two free alcohols was too much for this transformation, the primary alcohol was protected with TBSCl. Some attempts were made to combine the epoxide opening and protection in a single step, but those efforts were thwarted by increasing amounts of E1cB-related byproducts when different non-aqueous quenches for the aluminum alkoxides formed in the first step of the sequence were investigated. Hence, silanol **2.8.3** could at best be accessed in a total of 8 steps from commercially available methyl (Z)-3-iodoacrylate.

Fortunately, no undesired E1cB reactivity was observed when ketone **2.8.3** was reacted with an excess of LHMDS to form the lithium enolate necessary for the key aldol reaction, and the desired aldol product **2.8.4** bearing oxidation at C20 was obtained in very good yield and with a high degree of stereocontrol at C8 and C14. Similar to analogous aldol products discussed, **2.8.4** could only be isolated in high yield when the aldol reaction was quenched with an excess of AcOH shortly after addition of the aldehyde. The lack of enone by-products arising from elimination of the C20 OTBS group was likely a result of the cryogenic temperature used for this transformation (cf. the epoxide opening to diol **2.8.1** being carried out at 0 ºC). The concerns about a compound with oxidation at C20 being an unsuitable substrate were thus unjustified. Moreover, the desired aldol product was observed in higher yield than previous congeners **2.5.6**, **2.6.12**, and **2.6.13**. The explanation for this lies in the different degrees of matched-mismatched reactivity between enantiomers of the corresponding bicyclic enolate and the corresponding aldehyde enantiomer

leading to the relative stereochemistry that maps onto the desired aldol product. The only by-product of the aldol reaction, which is carried out with a two-fold excess of aldehyde **2.6.10** in each of these cases, was the C13,C15 bis-epimer resulting from reaction with the opposite aldehyde enantiomer (see Section 2.12). The addition of a OTBS group at C20 clearly changes the relative energies of transition states the diastereomeric Zimmerman-Traxler transition states containing different aldehyde enantiomers to a much higher degree than the corresponding cases with a lower oxidation-state C20. As a result of this energy difference, aldol product **2.8.4** is formed preferentially than the bis-epimer at the epoxide, while in prior cases the two types of products were present in roughly equal amounts. This matching of enantiomers not only increases the yield of the desired diastereomer but also introduces the possibility of an enantioselective synthetic route wherein only one of the two reaction partners is enantioenriched while the other is racemic. While such a route will be explored in the future, it is sufficient to say for now that the desired aldol product **2.8.4** containing the requisite allylic alcohol at C20 could be successfully obtained in only nine steps with very good yield and stereocontrol.

Ketone **2.8.4** was then successfully converted to tricycle **2.8.5** in the presence of SmI_2 with a high yield and excellent stereocontrol similar to that observed with prior (*Z*)-vinyl halide-bearing substrates. The degree of A ring olefin transposition was even higher in this case compared to **2.6.20**, and the reduction of the iodine atom with LAH proceeded smoothly to deliver previously synthesized silanol **2.6.22** in a total of 11 steps from commercially available starting materials. As the yields of subsequent steps leading to orthoester **2.7.11** and from there resiniferatoxin were deemed satisfactory, no further optimization efforts were carried out and the final synthetic route requiring 12 steps to access the DDO scaffold and 15 steps to construct RTX was disclosed to the scientific community.[51]

2.9 *Conclusion*

In conclusion, the highly bioactive daphnane diterpene orthoester resiniferatoxin was synthesized in a total of 15 steps via a highly convergent and stereoselective route. This synthetic sequence conformed conceptually to the retrosynthetic hypothesis described in Section 1.5 and incorporated the novel concept of late-stage construction of the 6-membered ring, but substantial experimentation and modification were required in order to arrive at the optimized synthetic sequence. Specifically, while *trans*-fused hydroazulene **2.1.10** could be readily obtained, determining the exact substitution of this partner as well as the functionality contained in the corresponding linear partner took several rounds of hypothesis-driven improvement. Highlights from these efforts include the use of a lithium enolate instead of an aluminum one to bring about a highly diastereoselective aldol reaction occurring via a closed Zimmerman-Traxler transition state as well as the iterative investigation of the optimal cyclization terminus for the key 6-*exo*-trig reaction. In this latter transformation the inherent stereochemical preference of SmI_2-mediated cyclizations was partially harnessed and partially suppressed, and indeed inverted, to construct the stereocenters at C9 and C11 respectively. The key to the latter was the use of a (*Z*)-vinyl halide as radical acceptor which modulated the stereochemical outcome via a combination of steric and electronic factors, namely unfavorable steric interactions in the undesired transition state for this transformation coupled with beneficial secondary orbital overlap in the desired one. This vinyl halide structural fragment was proven as a suitable cyclization terminus in a variety of substrates for the SmI_2-mediated cyclization, all of which resulted in highly stereoselective formation of the desired daphnane diterpene core, thereby proving the modularity of the synthetic route. The nature of the C18 halide was further used to favor the occurrence of an adventitious 1,5-HAT event that

led to a beneficial A ring olefin isomerization. Finally, a new way to install the orthoester moiety found in the DDOs was discovered, thereby circumventing the handling of sensitive C-ring triol intermediates as well as a suite of other issues inherent to complex synthetic intermediates bearing multiple functional groups. In this way resiniferatoxin was accessed in a rapid manner and our retrosynthetic hypothesis that the stereochemically dense 6-membered ring of the daphnanes can be forged at a late stage with a high degree of selectivity was proven correct.

Given the low step count and modular nature of the synthetic route to resiniferatoxin, one could envision the synthetic logic described above being applied to a multitude of other daphnane diterpene orthoesters. Thus, the logical continuation of this project would be the synthesis of more highly oxidized daphnane natural products. Future work would also have to address the racemic nature of the current route, possibly by harnessing the matched-mismatched interactions observed in the aldol reaction between the hydroazulene enolate and the linear aldehyde. Since my time as a graduate student is coming to an end, I can only hope that such future studies will be fruitful and that despite the myriad synthetic challenges inherent in the fascinating structures of the DDOs, a way forward will be found.

2.10 *Distribution of Credit*

The synthetic strategy to access resiniferatoxin, disclosed in Section 1.5 and explored in Chapter 2, was envisioned and designed by me under the guidance of Prof. Thomas Maimone, who is credited for continuously providing helpful advice and suggestions. All frontline experiments detailed in Sections 2.1 up to 2.7 were carried out solely by me and all new compounds disclosed therein were characterized solely by me using 2D NMR experiments. Lukas Spessert is credited with scaling up the initial reaction sequence leading to hydroazulene **2.1.10** and with providing some of the aldehyde partners used to study the formation of the C9-C11 bond. The optimized route to RTX discussed in Section 2.8 is a result of a collaborative effort between me, Lukas Spessert, and Dr. Kuan Yu under the guidance of Prof. Thomas Maimone, wherein Dr. Kuan Yu is credited for some initial optimization of the 7-*exo*-trig Heck step and for finding the initial 1,6-borylation conditions to obtain allylic alcohol **2.8.1**. Lukas Spessert is credited with scaling up and initial exploration of the aldol reaction with silanol **2.8.3**. The final reaction conditions for the optimized route, including the one-step conversion of **2.1.5** to **2.1.10**, **2.1.10** to **2.2.6**, and **2.2.6** to **2.6.7** were optimized by me. Finally, the X-ray crystal structures disclosed above were obtained by Dr. Nicholas Settineri using a suitable crystalline sample prepared by me.

2.11 *References*

(1) Marek, I.; Meyer, C.; Normant, J.-F. A Simple and Convenient Method for the Preparation of (Z)-β-Iodoacrolein and of (Z)- or (E)-γ-Iodo Allylic Alcohols: (Z)- and (E)-1-Iodohept-1-En-3-Ol: 2-Propenal, 3-Iodo-, (Z)- and 1-Hepten-3-Ol, 1-Iodo-, (Z)- and (E)-. In *Organic Syntheses*; John Wiley & Sons, Inc., Ed.; John Wiley & Sons, Inc.: Hoboken, NJ, USA, 2003; pp 194–194.

(2) Piers, E.; Wong, T.; Coish, P. D.; Rogers, C. A Convenient Procedure for the Efficient Preparation of Alkyl (Z)-3-Iodo-2-Alkenoates. *Can. J. Chem.* **1994**, *72* (8), 1816–1819.

(3) Zimmerman, H. E.; Traxler, M. D. The Stereochemistry of the Ivanov and Reformatsky Reactions. I. *J. Am. Chem. Soc.* **1957**, *79* (8), 1920–1923.

(4) Heathcock, C. H.; Buse, C. T.; Kleschick, W. A.; Pirrung, M. C.; Sohn, J. E.; Lampe, J. Acyclic Stereoselection. 7. Stereoselective Synthesis of 2-Alkyl-3-Hydroxy Carbonyl Compounds by Aldol Condensation. *J. Org. Chem.* **1980**, *45* (6), 1066–1081.

(5) Beletskaya, I. P.; Cheprakov, A. V. The Heck Reaction as a Sharpening Stone of Palladium Catalysis. *Chem. Rev.* **2000**, *100* (8), 3009–3066.
(6) Gao, P.; Cook, S. P. A Reductive-Heck Approach to the Hydroazulene Ring System: A Formal Synthesis of the Englerins. *Org. Lett.* **2012**, *14* (13), 3340–3343.
(7) Overman, L. E. Application of Intramolecular Heck Reactions for Forming Congested Quaternary Carbon Centers in Complex Molecule Total Synthesis. *Pure Appl. Chem.* **1994**, *66* (7), 1423–1430.
(8) Link, J. T. The Intramolecular Heck Reaction. In *Organic Reactions*; American Cancer Society, 2004; pp 157–561.
(9) Brill, Z. G.; Zhao, Y.-M.; Vasilev, V. H.; Maimone, T. J. Synthetic Approaches to the Daphnane and Tigliane Diterpenes from Aromatic Precursors. *Tetrahedron* **2019**, *75* (32), 4212–4221.
(10) Itoh, A.; Ozawa, S.; Oshima, K.; Nozaki, H. Aldol Reaction of Aluminium Enolate Resulting from 1,4-Addition of Me2AlSPh to α,β-Unsaturated Carbonyl Compound. A 1-Acylethenyl Anion Equivalent. *Tetrahedron Lett.* **1980**, *21* (4), 361–364.
(11) Itoh, A.; Ozawa, S.; Oshima, K.; Nozaki, H. Aldol Reaction of Aluminium Enolate Resulting from 1,4-Addition of R2AlX to α,β-Unsaturated Carbonyl Compound. A 1-Acylethenyl Anion Equivalent. *Bull. Chem. Soc. Jpn.* **1981**, *54* (1), 274–278.
(12) Kamimura, A.; Mitsudera, H.; Asano, S.; Noguchi, M.; Kakehi, A. Stereoselective Michael/Aldol Tandem Reaction Triggered by Thiolate Anion or Analogues. *Chem. Commun.* **1998**, No. 10, 1095–1096.
(13) Ghosh, A. K.; Kass, J.; Anderson, D. D.; Xu, X.; Marian, C. L-Selectride-Mediated Highly Diastereoselective Asymmetric Reductive Aldol Reaction: Access to an Important Subunit for Bioactive Molecules. *Org. Lett.* **2008**, *10* (21), 4811–4814.
(14) Tsuda, T.; Satomi, H.; Hayashi, T.; Saegusa, T. Alkylation and Silylation of the Aluminum Enolates Generated by Hydroalumination of .Alpha.,.Beta.-Unsaturated Carbonyl Compounds. *J. Org. Chem.* **1987**, *52* (3), 439–443.
(15) Lipshutz, B. H.; Chrisman, W.; Noson, K.; Papa, P.; Sclafani, J. A.; Vivian, R. W.; Keith, J. M. Copper Hydride-Catalyzed Tandem 1,4-Reduction/Alkylation Reactions. *Tetrahedron* **2000**, *56* (18), 2779–2788.
(16) Miura, K.; Yamada, Y.; Tomita, M.; Hosomi, A. Indium(III) Acetate-Catalyzed 1,4-Reduction and Reductive Aldol Reactions of α-Enones with Phenylsilane. *Synlett* **2004**, *2004* (11), 1985–1989.
(17) Wu, H.; Radomkit, S.; O'Brien, J. M.; Hoveyda, A. H. Metal-Free Catalytic Enantioselective C–B Bond Formation: (Pinacolato)Boron Conjugate Additions to α,β-Unsaturated Ketones, Esters, Weinreb Amides, and Aldehydes Promoted by Chiral N-Heterocyclic Carbenes. *J. Am. Chem. Soc.* **2012**, *134* (19), 8277–8285.
(18) Lee, K.; Zhugralin, A. R.; Hoveyda, A. H. Efficient C−B Bond Formation Promoted by N-Heterocyclic Carbenes: Synthesis of Tertiary and Quaternary B-Substituted Carbons through Metal-Free Catalytic Boron Conjugate Additions to Cyclic and Acyclic α,β-Unsaturated Carbonyls. *J. Am. Chem. Soc.* **2009**, *131* (21), 7253–7255.
(19) Welle, A.; Cirriez, V.; Riant, O. Copper Catalyzed Tandem Conjugated Borylation–Aldol Reaction. *Tetrahedron* **2012**, *68* (17), 3435–3443.
(20) Motokura, K.; Tanaka, S.; Tada, M.; Iwasawa, Y. Bifunctional Heterogeneous Catalysis of Silica–Alumina-Supported Tertiary Amines with Controlled Acid–Base Interactions for Efficient 1,4-Addition Reactions. *Chem. – Eur. J.* **2009**, *15* (41), 10871–10879.

(21) Bi, X.; Xu, W.; Yao, Y.; Zhou, L.; Liang, G. Total Syntheses of a Family of Cadinane Sesquiterpenes. *J. Org. Chem.* **2018**, *83* (10), 5825–5828.
(22) Luzzio, F. A. The Henry Reaction: Recent Examples. *Tetrahedron* **2001**, *57* (6), 915–945.
(23) Sturino, C. F.; Fallis, A. G. Rate Constants for 5- and 6-Exo Secondary Alkyl Radical Cyclizations onto N,N-Diphenylhydrazones. *J. Org. Chem.* **1994**, *59* (22), 6514–6516.
(24) Heravi, M. M.; Nazari, A. Samarium(II) Iodide-Mediated Reactions Applied to Natural Product Total Synthesis. *RSC Adv.* **2022**, *12* (16), 9944–9994.
(25) Edmonds, D. J.; Johnston, D.; Procter, D. J. Samarium(II)-Iodide-Mediated Cyclizations in Natural Product Synthesis. *Chem. Rev.* **2004**, *104* (7), 3371–3404.
(26) Nicolaou, K. C.; Ellery, S. P.; Chen, J. S. Samarium Diiodide Mediated Reactions in Total Synthesis. *Angew. Chem. Int. Ed.* **2009**, *48* (39), 7140–7165.
(27) Molander, G. A.; Harris, C. R.; Charette, A. B. Samarium(II) Iodide. In *Encyclopedia of Reagents for Organic Synthesis*; American Cancer Society, 2005.
(28) Molander, G. A.; del Pozo Losada, C. Sequenced Reactions with Samarium(II) Iodide. Domino Epoxide Ring-Opening/Ketyl Olefin Coupling Reactions. *J. Org. Chem.* **1997**, *62* (9), 2935–2943.
(29) Molander, G. A.; McKie, J. A. Stereochemical Investigations of Samarium(II) Iodide-Promoted 5-Exo and 6-Exo Ketyl-Olefin Radical Cyclization Reactions. *J. Org. Chem.* **1995**, *60* (4), 872–882.
(30) Beckwith, A. L. J. Regio-Selectivity and Stereo-Selectivity in Radical Reactions. *Tetrahedron* **1981**, *37* (18), 3073–3100.
(31) Kito, M.; Sakai, T.; Yamada, K.; Matsuda, F.; Shirahama, H. Stereoselective Formation of Trans-Decalin and Cis-Decalin Skeletons via Hydroxy Group Directed Cyclization Induced by Samarium(II) Iodide. *Synlett* **1993**, *1993* (02), 158–162.
(32) Kito, M.; Sakai, T.; Haruta, N.; Shirahama, H.; Matsuda, F. Stereoselective Cyclization of Cis-Decalin Skeleton of Vinigrol via Ketyl-Olefin Coupling Promoted by Samarium(II) Iodide. *Synlett* **1996**, *1996* (11), 1057–1060.
(33) Prasad, E.; Flowers, R. A. Mechanistic Impact of Water Addition to SmI2: Consequences in the Ground and Transition State. *J. Am. Chem. Soc.* **2005**, *127* (51), 18093–18099.
(34) Szostak, M.; Spain, M.; Procter, D. J. Determination of the Effective Redox Potentials of SmI2, SmBr2, SmCl2, and Their Complexes with Water by Reduction of Aromatic Hydrocarbons. Reduction of Anthracene and Stilbene by Samarium(II) Iodide–Water Complex. *J. Org. Chem.* **2014**, *79* (6), 2522–2537.
(35) Boussonnière, A.; Bénéteau, R.; Zimmermann, N.; Lebreton, J.; Dénès, F. Radical Cyclization of α-Bromo Aluminum Acetals onto Alkenes and Alkynes (Radic[Al] Process): A Simple Access to γ-Lactols and 4-Methylene-γ-Lactols. *Chem. – Eur. J.* **2011**, *17* (20), 5613–5627.
(36) Nguyen Trong Anh, .; Eisenstein, O.; Lefour, J. M.; Tran Huu Dau, M. E. Orbital Factors and Asymmetric Induction. *J. Am. Chem. Soc.* **1973**, *95* (18), 6146–6147.
(37) Plesniak, M. P.; Huang, H.-M.; Procter, D. J. Radical Cascade Reactions Triggered by Single Electron Transfer. *Nat. Rev. Chem.* **2017**, *1* (10), 1–16.
(38) Suzuki, S.; Fujita, Y.; Nishida, T. New Diene Formation by Ene-Type Chlorination and Palladium Catalyzed Dehydrochlorination: Synthesis of Citral from Diprenyl Ether. *Tetrahedron Lett.* **1983**, *24* (51), 5737–5740.

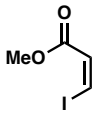
(39) Plesniak, M. P.; Garduño-Castro, M. H.; Lenz, P.; Just-Baringo, X.; Procter, D. J. Samarium(II) Folding Cascades Involving Hydrogen Atom Transfer for the Synthesis of Complex Polycycles. *Nat. Commun.* **2018**, *9* (1), 4802.
(40) Escudier, J.-M.; Baltas, M.; Gorrichon, L. Diastereoselection in the Addition of Enolates to Chiral α,β-Epoxyaldehydes. *Tetrahedron Lett.* **1991**, *32* (39), 5345–5348.
(41) Righi, G.; Spirito, F.; Bonini, C. Stereoselective Aldol Condensation of Boron Enolates to Trans α,β-Epoxy Aldehydes. *Tetrahedron Lett.* **2002**, *43* (27), 4737–4740.
(42) Yasuda, A.; Tanaka, S.; Oshima, K.; Yamamoto, H.; Nozaki, H. Organoaluminum Reagents of Type R1R2NAlEt2 Which Allow Regiospecific Isomerization of Epoxides to Allylic Alcohols. *J. Am. Chem. Soc.* **1974**, *96* (20), 6513–6514.
(43) Stanoeva, E.; He, W.; Rocchetti, M. T.; Nguyen Van, T.; De Kimpe, N. Synthesis of 1-Substituted 2,9,10-Trioxatricyclo[4.3.1.03,8]Decanes. *Tetrahedron* **2004**, *60* (23), 5077–5084.
(44) Stanoeva, E.; He, W.; De Kimpe, N. Natural and Synthetic Cage Compounds Incorporating the 2,9,10-Trioxatricyclo[4.3.1.03,8]Decane Type Moiety. *Bioorg. Med. Chem.* **2005**, *13* (1), 17–28.
(45) Bloomfield, G. C.; Ritchie, T. J.; Wrigglesworth, R. Synthesis of 2,9,10-Trioxatricyclo[4.3.1.0]Decane Analogues of Resiniferatoxin. *J. Chem. Soc. Perkin 1* **1992**, No. 10, 1229–1236.
(46) Wender, P. A.; Jesudason, C. D.; Nakahira, H.; Tamura, N.; Tebbe, A. L.; Ueno, Y. The First Synthesis of a Daphnane Diterpene: The Enantiocontrolled Total Synthesis of (+)-Resiniferatoxin. *J. Am. Chem. Soc.* **1997**, *119* (52), 12976–12977.
(47) Hirose, A.; Watanabe, A.; Ogino, K.; Nagatomo, M.; Inoue, M. Unified Total Syntheses of Rhamnofolane, Tigliane, and Daphnane Diterpenoids. *J. Am. Chem. Soc.* **2021**, *143* (31), 12387–12396.
(48) Bell, N. J.; Cox, A. J.; Cameron, N. R.; Evans, J. S. O.; Marder, T. B.; Duin, M. A.; Elsevier, C. J.; Baucherel, X.; Tulloch, A. A. D.; Tooze, R. P. Platinum Catalysed 3,4- and 1,4-Diboration of α,β-Unsaturated Carbonyl Compounds Using Bis-Pinacolatodiboron. *Chem. Commun.* **2004**, No. 16, 1854–1855.
(49) Chea, H.-S.; Sim, H.-S.; Yun, J.-S. Ligandless Copper-Catalyzed β-Boration of α,β-Unsaturated Compounds in Aqueous Solution. *Bull. Korean Chem. Soc.* **2010**, *31* (3), 551–552.
(50) Lee, J.-E.; Kwon, J.; Yun, J. Copper-Catalyzed Addition of Diboron Reagents to α,β-Acetylenic Esters: Efficient Synthesis of β-Boryl-α,β-Ethylenic Esters. *Chem. Commun.* **2008**, No. 6, 733–734.
(51) Vasilev, V. H.; Spessert, L.; Yu, K.; Maimone, T. J. Total Synthesis of Resiniferatoxin. *J. Am. Chem. Soc.* **2022**, *144* (36), 16332–16337.

2.12 *Experimental Procedures and Characterization Data.*

2.12.1 General Procedures:

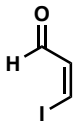
All reactions were performed in flame- or oven-dried glassware under positive pressure of nitrogen or argon, unless otherwise noted. Air- and moisture-sensitive liquids were transferred via syringe. When indicated, solvents or reagents were degassed by sparging with argon for 10 minutes in an ultrasound bath at 25 ºC. Volatile solvents were removed under reduced pressure rotary evaporation. Analytical and preparative thin-layer chromatography (TLC) were performed using glass plates coated with silica gel (0.25-mm, 60-Å pore size, Merck TLC Silicagel 60 F254) impregnated with a fluorescent indicator (254 nm). TLC plates were visualized by exposure to ultraviolet light (UV) and then were stained by submersion in an ethanolic anisaldehyde solution or potassium permanganate solution followed by brief heating on a hot plate. Flash column chromatography was performed with silica gel purchased from Fisher Scientific (230-40 mesh, Grade 60). All samples were loaded onto flash columns either as solutions in EtOAc/hexanes or dry loaded by resuspension of the crude mixture in Et_2O followed by careful concentration to dryness under reduced pressure. Triethylamine, chlorotrimethylsilane, and 2,2,6,6-tetramethylpiperidine were distilled over calcium hydride prior to use. Anhydrous acetonitrile (MeCN), tetrahydrofuran (THF), toluene (PhMe), dichloromethane (DCM) were obtained by passing these previously degassed solvents through activated alumina columns. Anhydrous benzene (PhH) was purchased from Sigma Aldrich. All other reagents were used as received from commercial sources, unless otherwise noted. Proton nuclear magnetic resonance (^{1}H NMR) spectra and carbon nuclear magnetic resonance (^{13}C NMR) spectra were recorded on Bruker AVB400, AV500, AV600, and AV700 spectrometers at 23 ºC. Proton chemical shifts are expressed as parts per million (ppm, δ scale) and are referenced to residual solvent ($CHCl_3$, δ 7.26 (s), C_6D_5H δ 7.16 (s)). Carbon chemical shifts are expressed as parts per million (ppm, δ scale) and are referenced to the solvent ($CHCl_3$, δ 77.0, C_6D_6, δ 128.06). Data is presented as follows: chemical shift, multiplicity (s = singlet, d = doublet, dd = doublet of doublets, ddd = doublet of doublet of doublet, dt = triplet of doublet, t = triplet, q = quartet, m = multiplet, br = broad, coupling constant (*J*) in Hertz (Hz), and integration. Infrared spectra were recorded on a Bruker Alpha FT-IR spectrometer as thin films and are reported as frequency of absorption (cm^{-1}). Only selected resonances are reported. High-resolution mass spectra (HRMS) were obtained by the mass spectrometry facility at the University of California, Berkeley using a Finnigan LTQFT mass spectrometer (Thermo Electron Corporation).

2.12.2 Experimental Procedures and Tabulated Characterization Data.



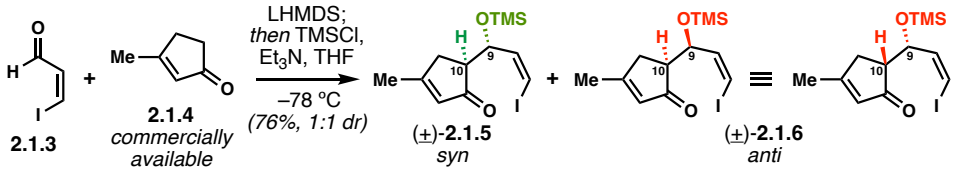
Ester 2.1.2: **2.1.2**

Ester **2.1.2** was prepared from commercially available methyl propiolate according to the procedure reported in ref. 2 (see Section 2.11) and was used without purification. The spectral data were found to match those reported in literature.[2]



Aldehyde 2.1.3: **2.1.3**

Aldehyde **2.1.3** was prepared from methyl (*Z*)-3-iodoprop-2-enoate, either freshly prepared or purchased from commercial sources, according to the procedure reported in ref. 1 (see Section 2.11) and was used without purification. The spectral data were found to match those reported in the literature.[1]



Aldol product 2.1.5:

A flame-dried 500 mL round-bottom flask was charged with THF (56 mL) and LHMDS (56 mL, 1M in THF, 56 mmol, 1.2 equiv.) and was subsequently cooled to 0 ºC. 3-methyl cyclopentenone (4.70 mL, 4.54 g, 47.2 mmol, 1.0 equiv.) was added neat and the resulting red-orange colored solution was stirred for 15 minutes before being cooled to – 78 ºC. Aldehyde **2.1.3** (8.59 g, 47.2 mmol, 1.0 equiv.) was dissolved in THF (38.0 mL) and the resulting solution was added dropwise using a syringe pump at a flow rate of 50 mL/h. After stirring for an additional 1 hour, Et_3N (14.3 g, 20.0 mL, 142 mmol, 3.0 equiv.) and TMSCl (7.69 g, 9.00 mL, 70.8 mmol, 1.5 equiv.) were added dropwise. The reaction mixture was allowed to warm to ambient temperature over 2.5 hours before being quenched by the addition of saturated *aq*. NH_4Cl (100 mL). The layers were separated, and the aqueous layer was extracted with Et_2O (3 x 100 mL). The combined organic layers were dried over Na_2SO_4 and concentrated under reduced pressure. The crude residue was passed through a short plug of silica gel (0 to 20% EtOAc/hexanes in 10% increments) to afford aldol product **2.1.5** and its C10-epimer **2.1.6** (12.5 g, 35.1 mmol, 76%, 1:1 dr) as a yellow oil. These diastereomers can be separated by careful flash column chromatography (0 to 15% EtOAc/hexanes in 2.5% increments) to provide pure **2.1.5** and **2.1.6**.

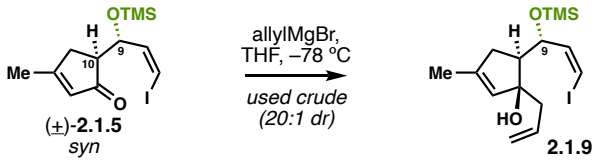
aldol product **2.1.5**:

TLC: R_f = 0.37 (10% EtOAc/hexanes)

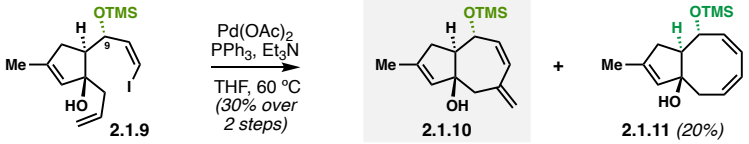
^{1}H NMR (600 MHz, C_6D_6): δ 6.01 (t, *J* = 7.7 Hz, 1H), 5.84 (dd, *J* = 7.7, 1.2 Hz, 1H), 5.76 (h, *J* = 1.5 Hz, 1H), 5.25 (ddd, *J* = 7.7, 2.4, 1.2 Hz, 1H), 2.46 (dddt, *J* = 17.7, 3.2, 2.0, 1.1 Hz, 1H), 2.37 – 2.32 (m, 1H), 1.83 – 1.75 (m, 1H), 1.45 (s, 3H), 0.17 (s, 9H).

^{13}C NMR (150 MHz, C_6D_6): δ 206.3, 176.8, 143.1, 130.7, 80.0, 74.4, 52.0, 33.2, 18.9, 0.4.

IR (thin film) ν_{max} (cm^{-1}): 2956, 2907, 1698, 1623, 1250, 1102, 1056, 1027, 856.
HRMS (m/z): (ESI) calcd. for $C_{12}H_{19}O_2{}^{127}I^{23}Na^{28}Si$ $[M+Na]^+$: 373.0091, found 373.0093.
C10-epimer **2.1.6**:
TLC: R_f = 0.31 (10% EtOAc/hexanes)
^{1}H NMR (600 MHz, C_6D_6): δ 6.76 (t, *J* = 7.8 Hz, 1H), 5.89 (dd, *J* = 7.5, 0.9 Hz, 1H), 5.69 (s, 2H), 4.70 (dd, *J* = 8.0, 3.6 Hz, 1H), 2.48 (dt, *J* = 6.7, 3.1 Hz, 1H), 2.19 – 2.12 (m, 1H), 2.02 (dd, *J* = 18.1, 7.2 Hz, 1H), 1.43 (s, 3H), 0.12 (s, 9H).
^{13}C NMR (150 MHz, C_6D_6) δ 206.1, 175.3, 142.4, 131.4, 81.3, 76.3, 51.9, 36.6, 18.6, 0.4.
The undesired aldol product **2.1.6** can be epimerized as follows: an oven-dried 500 mL round-bottom flask was charged with undesired C10-epimer **2.1.6** (8.40 g, 24 mmol, 1.0 equiv.), DCM (240 mL), and DBU (7.2 mL, 48.0 mmol, 2.0 equiv.). The resulting solution was stirred at room temperature for 12 hours before being quenched with satd. *aq*. NH_4Cl (200 mL). The organic layer was separated and the aqueous layer extracted with DCM (3 x 200 mL). The combined organic layers were dried over Na_2SO_4 and concentrated under reduced pressure to obtain a crude mixture of **2.1.5** and **2.1.6**, which was purified as detailed above to provide the desired diastereomer **2.1.5** (3.60 g, 10.3 mmol, 43% yield).

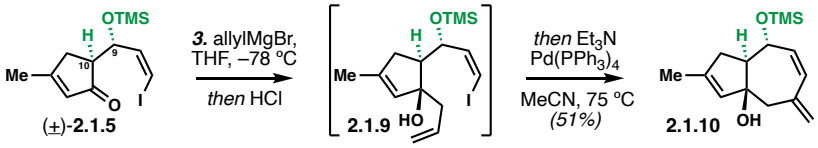


Tertiary alcohol 2.1.9:
An oven-dried 250 mL round-bottom flask was charged with *syn*-aldol product **2.1.5** (4.60 g, 13.1 mmol, 1.0 equiv.) and THF (131 mL). The resulting solution was cooled to –78 ºC and a solution of allylmagnesium bromide (15.7 mL, 1 M in Et_2O, 15.7 mmol, 1.2 equiv.) was added dropwise. After 3 minutes the reaction mixture was quenched with satd. *aq.* NH_4Cl (100 mL) and allowed to warm to room temperature. The organic layer was separated and the aqueous layer was extracted with Et_2O (3 x 100 mL). The combined organic layers were dried over Na_2SO_4 and concentrated under reduced pressure to provide crude allylic alcohol **2.1.9**, which was used in the subsequent step without purification.
TLC: R_f = 0.50 (10% EtOAc/hexanes)
^{1}H NMR: (600 MHz, C_6D_6) δ 6.12-6.07 (m, 2H), 5.79 (dd, *J* = 7.6, 1.0 Hz, 1H), 5.43 (d, *J* = 1.6 Hz, 1H), 5.20 (ddt, *J* = 17.2, 2.5, 1.4 Hz, 1H), 5.15 (d, *J* = 10.3 Hz, 1H), 4.94 (dd, *J* = 8.2, 2.4 Hz, 1H), 3.14 (br s, 1H, OH), 2.66 (dd, *J* = 13.7, 6.3 Hz, 1H), 2.62 – 2.53 (m, 2H), 2.29 (ddd, *J* = 9.3, 6.4, 3.1 Hz, 1H), 1.98 (dd, *J* = 16.2, 8.7 Hz, 1H), 1.55 (d, *J* = 1.1 Hz, 3H), 0.12 (s, 9H).



***Trans*-fused hydroazulene 2.1.10**:
*Two-step procedure with crude allylation product **2.1.9**:* An oven-dried 500 mL round-bottom flask was charged with $Pd(OAc)_2$ (540 mg, 2.4 mmol, 0.18 equiv.), PPh_3 (1.26 g, 4.8 mmol, 0.37 equiv.), and THF (100 mL). The resulting suspension was stirred at room temperature for 5 minutes, then Et_3N (9 mL, 65 mmol, 4.96 equiv.) was added and the reaction mixture was stirred at 60 ºC for 5 minutes, resulting in a deep red color. At this stage a solution of crude tertiary

alcohol **2.1.9** (assumed 13.1 mmol, 1.0 equiv.) in THF (30 mL) was added and stirring was continued at 60 ºC for 12 hours or until consumption of the starting material was complete as judged by TLC. The reaction mixture was cooled to room temperature and quenched with satd. *aq*. $NaHCO_3$ (100 mL). The organic layer was separated and the aqueous layer was extracted with Et_2O (3 x 100 mL). The combined organic layers were dried over Na_2SO_4 and concentrated under reduced pressure to provide crude hydroazulene **2.1.10**. The resulting crude mixture was purified using flash column chromatography (0 to 15% EtOAc/hexanes in 2.5% increments) to provide pure *trans*-fused hydroazulene **2.1.10** (1.04 g, 3.93 mmol, 30% from ketone **2.1.5**) as a colorless to pale yellow oil alongside 5,8-fused bicycle **2.1.11** (692 mg, 2.62 mmol, 20% from ketone **2.1.5**).



*One-step procedure from aldol product **2.1.5**:*

An oven-dried reaction tube was charged with enone **2.1.5** (100 mg, 0.285 mmol, 1.0 equiv.) and dry THF (2.8 mL). The resulting solution was cooled to –78 ºC and a solution of allylmagnesium bromide (0.34 mL, 1 M in THF, 0.34 mmol, 1.2 equiv.) was added dropwise. After stirring for 3 minutes, hydrogen chloride (0.20 mL, 2 M in Et_2O, 0.40 mmol, 1.4 equiv.) and triethylamine (0.400 mL, 2.88 mmol, 10.0 equiv.) were added sequentially. The reaction mixture was warmed to 0 ºC, diluted with acetonitrile (2.8 mL), and stirred for 10 min, at which point $Pd(PPh_3)_4$ (16 mg, 0.014 mmol, 0.05 equiv.) was added and the reaction flask placed into a pre-heated 75 ºC oil bath. Conversion was monitored by TLC and an additional portion of $Pd(PPh_3)_4$ was added after 3 hours if starting material was still present in the reaction mixture. Once conversion was complete as judged by TLC, the reaction flask was cooled to room temperature and quenched with satd. *aq*. $NaHCO_3$ (5 mL). The organic layer was separated and the aqueous layer extracted with EtOAc (3 x 5 mL). The combined organic layers were dried over Na_2SO_4 and concentrated under reduced pressure. The resulting crude mixture was purified using flash column chromatography (0 to 15% EtOAc/hexanes in 2.5% increments) to provide pure *trans*-fused hydroazulene **2.1.10** (38.0 mg, 0.144 mmol, 51%) as a colorless to pale yellow oil.

*Trans-fused hydroazulene **2.1.10**:*

TLC: R_f = 0.29 (10% EtOAc/hexanes)

^{1}H NMR (600 MHz, C_6D_6): δ 6.09 (ddd, *J* = 13.1, 2.3, 1.0 Hz, 1H), 5.74 – 5.68 (m, 1H), 5.14 (hept, *J* = 1.5 Hz, 1H), 4.99 (ddq, *J* = 2.4, 1.6, 0.8 Hz, 1H), 4.94 (td, *J* = 2.3, 1.2 Hz, 1H), 4.59 (dt, *J* = 10.3, 2.3 Hz, 1H), 2.68 (dd, *J* = 15.1, 0.9 Hz, 1H), 2.53 (dt, *J* = 15.1, 2.5 Hz, 1H), 2.49 – 2.41 (m, 1H), 2.40 – 2.35 (m, 2H), 1.54 (s, *J* = 1.2 Hz, 3H), 0.16 (s, 9H).

^{13}C NMR (150 MHz, C_6D_6): δ 144.7, 142.4, 135.8, 132.4, 129.2, 81.5, 73.1, 55.6, 47.7, 41.7, 16.9, 0.6.

IR (thin film) ν_{max} (cm^{-1}): 3500, 2956, 2911, 2850, 1441, 1249, 1054, 1043, 883, 836.

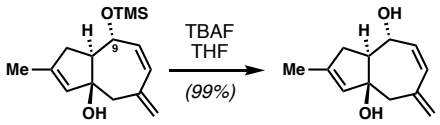
HRMS (m/z): (ESI) calcd. for $C_{15}H_{23}O_2{}^{28}Si$ $[M–H]^-$: 263.1473, found 263.1474.

*5,8-fused bicycle **2.1.11**:*

TLC: R_f = 0.32 (10% EtOAc/hexanes)

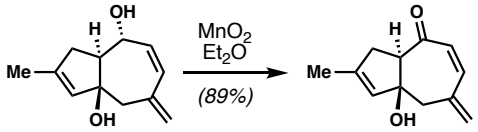
^{1}H NMR: (600 MHz, C_6D_6) δ 5.97 (dd, *J* = 11.3, 3.8 Hz, 1H), 5.94 (dd, *J* = 11.9, 5.4 Hz, 1H), 5.69 (dd, *J* = 12.0, 3.6 Hz, 1H), 5.64 (dt, *J* = 11.1, 8.0 Hz, 1H), 5.30 (s, 1H), 4.75 – 4.71 (m, 1H), 2.57 (dd, *J* = 12.9, 8.6 Hz, 1H), 2.36 (dddd, *J* = 15.2, 9.6, 2.2, 1.3 Hz, 1H), 2.28 (td, *J* = 9.7, 6.6

Hz, 1H), 2.20 (dd, *J* = 15.3, 6.6 Hz, 1H), 2.14 (dt, *J* = 12.7, 6.4 Hz, 1H), 1.53 (s, 3H), 0.18 (s, 9H).
^{13}C NMR: (151 MHz, C_6D_6) δ 146.5, 140.8, 134.2, 129.2, 128.8, 122.7, 80.5, 69.2, 55.6, 37.6, 37.2, 17.2, 0.3.
HRMS (m/z): (ESI) calcd. for $C_{15}H_{24}O_2{}^{23}Na^{28}Si$ $[M+Na]^+$: 287.1438, found 287.1438.



2.1.10 2.2.1

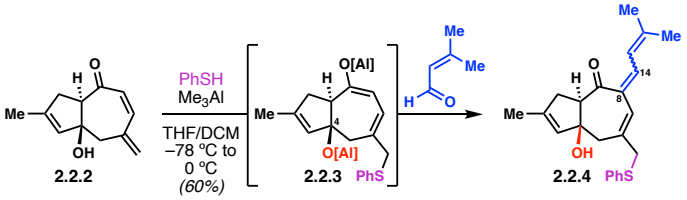
Diol 2.2.1:
An oven-dried 10 mL round-bottom flask was charged with *trans*-fused hydroazulene **2.1.10** (75 mg, 0.28 mmol, 1.0 equiv.) and THF (2.8 mL). A solution of TBAF (0.28 mL, 1 M in THF, 0.28 mmol, 1.0 equiv.) was added to the reaction mixture, resulting in an immediate color change to dark yellow. After 5 minutes conversion was complete as judged by TLC, so the solution was quenched with satd. *aq.* NH_4Cl (3 mL) and diluted with Et_2O (3 mL). The layers were separated and the aqueous layer was extracted with Et_2O (3 x 3 mL). The combined organic layers were dried over Na_2SO_4 and concentrated under reduced pressure to provide diol **2.2.1** (53 mg, 0.28 mmol, 99 %) as a dark orange oil which was used immediately without purification due to instability.
TLC: R_f = 0.10 (50% EtOAc/hexanes)
^{1}H NMR: (600 MHz, C_6D_6) δ 6.06 – 6.02 (m, 1H), 5.61 (d, *J* = 13.4 Hz, 1H), 5.12 (s, 1H), 4.98 (s, 1H), 4.93 (s, 1H), 4.30 (d, *J* = 10.7 Hz, 1H), 2.70 (d, *J* = 15.2 Hz, 1H), 2.48 (dt, *J* = 15.4, 2.3 Hz, 1H), 2.30 – 2.25 (m, 1H), 2.20 (dd, *J* = 16.2, 7.5 Hz, 1H), 2.09 (dt, *J* = 10.5, 8.2 Hz, 1H), 1.52 – 1.51 (m, 3H).
^{13}C NMR: (151 MHz, C_6D_6) δ 144.4, 142.1, 134.9, 132.1, 129.5, 120.9, 81.4, 72.0, 55.3, 47.4, 40.9, 16.6.
HRMS (m/z): (ESI) calcd. for $C_{12}H_{16}O_2{}^{23}Na$ $[M+Na]^+$: 215.1043, found 215.1042.



2.2.1 2.2.2

Enone 2.2.2:
A small reaction tube was charged with crude diol **2.2.1** (48 mg, 0.25 mmol, 1.0 equiv.) and Et_2O (2.5 mL). Activated MnO_2 (217 mg, 2.5 mmol, 10.0 equiv.) was added and the resulting suspension was stirred vigorously at room temperature. The reaction progress was monitored by TLC at 1-hour intervals and additional portions of MnO_2 (108 mg, 1.25 mmol, 5.0 equiv.) were added as necessary. Once all starting material was consumed, the reaction mixture was filtered through a pad of Celite in order to remove the solid components of the mixture and the filter pad was washed with DCM (5 mL). The resulting pale-yellow solution was concentrated under reduced pressure to provide crude enone **2.2.2** (43 mg, 0.22 mmol, 89%) as a yellow gum, which was immediately re-dissolved in THF (2.2 mL) to avoid polymerization and/or decomposition of the neat enone. The THF solution obtained in this way was used in the next step without additional manipulations.
TLC: R_f = 0.40 (50% EtOAc/hexanes)

^{1}H NMR: (600 MHz, C_6D_6) δ 6.31 (d, *J* = 12.9 Hz, 1H), 6.01 (d, *J* = 12.9 Hz, 1H), 5.04 (s, 1H), 4.98 (s, 1H), 4.96 (s, 1H), 3.13 (ddd, *J* = 17.1, 8.2, 1.1 Hz, 1H), 2.97 (t, *J* = 8.0 Hz, 1H), 2.79 (d, *J* = 16.1 Hz, 1H), 2.48 (d, *J* = 16.1 Hz, 1H), 1.99 (dd, *J* = 16.9, 7.8 Hz, 1H), 1.43 (s, 3H).

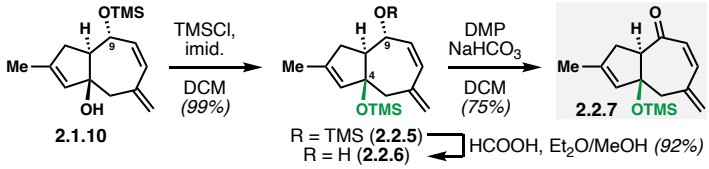


Triene 2.2.4:

An oven-dried 25 mL round-bottom flask was charged with Me_3Al (0.440 mL, 2 M in PhMe, 0.88 mmol, 4.0 equiv.) and DCM (2.2 mL). Then, PhSH (0.089 mL, 0.88 mmol, 4.0 equiv.) was added dropwise at 0 °C and the resulting solution was stirred for 15 minutes at that temperature. At this point the reaction mixture was cooled to –78 °C and a solution of enone **2.2.2** (0.22 mmol) in THF (2.2 mL) was added dropwise. Stirring was continued for 15 minutes, when consumption of enone **2.2.2** was complete as judged by TLC. A solution of prenal (0.042 mL, 0.44 mmol, 2.0 equiv.) in DCM (2 mL) was added and the reaction mixture was stirred at 0 °C for 5 minutes before being quenched with satd. *aq.* NH_4Cl (5 mL). The resulting mixture was diluted with Et_2O (10 mL) and satd. *aq.* Rochelle's salt (10 mL) and was then stirred vigorously for 10 minutes. The layers were separated and the aqueous layer was extracted with Et_2O (3 x 10 mL). The combined organic layers were dried over Na_2SO_4 and concentrated under reduced pressure. The crude reaction product was purified by column chromatography (10 to 60% EtOAc/hexanes) to provide pure triene **2.2.4** (48 mg, 0.13 mmol, 60%) as a yellow oil.

TLC: R_f = 0.62 (50% EtOAc/hexanes)

^{1}H NMR: (600 MHz, C_6D_6) δ 7.96 (d, *J* = 12.3 Hz, 1H), 7.43 – 7.37 (m, 2H), 7.00 (t, *J* = 7.6 Hz, 2H), 6.94 – 6.90 (m, 1H), 6.39 (s, 1H), 6.01 (d, *J* = 12.3 Hz, 1H), 5.05 (s, 1H), 3.47 – 3.34 (m, 3H), 3.26 (m, 1H), 2.93 (d, *J* = 18.6 Hz, 1H), 2.49 (d, *J* = 18.5 Hz, 1H), 2.00 (dd, *J* = 17.1, 8.3 Hz, 1H), 1.54 (s, 3H), 1.54 (s, 3H), 1.48 (s, 3H).



Silanol 2.2.5:

An oven-dried 10 mL round-bottom flask was charged with *trans*-fused hydroazulene **2.1.10** (100 mg, 0.379 mmol, 1.0 equiv.) and DCM (4 mL). Imidazole (77 mg, 1.14 mmol, 3.0 equiv.) was added, followed by dropwise addition of TMSCl (72 µL, 0.57 mmol, 1.5 equiv.), resulting in formation of a white precipitate. The reaction mixture was stirred for 1 hour, at which point conversion was complete as judged by TLC. The suspension was quenched with satd. *aq.* $NaHCO_3$ (4 mL) and the layers were separated. The aqueous layer was extracted with DCM (3 x 4 mL) and the combined organic layers were dried over Na_2SO_4 and concentrated under reduced pressure to provide crude silanol **2.2.5**. This compound was purified by a short silica plug (0 to 15% EtOAc/hexanes), resulting in pure bicycle **2.2.5** (126 mg, 0.375 mmol, 99%) as a pale yellow oil.

TLC: R_f = 0.92 (25% EtOAc/hexanes).

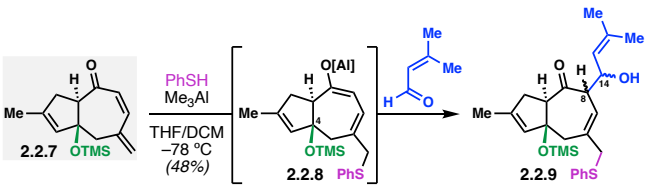
^{1}H NMR: (600 MHz, C_6D_6) δ 6.12 (d, *J* = 13.0 Hz, 1H), 5.74 (d, *J* = 13.0 Hz, 1H), 5.24 (s, 1H), 4.99 (d, *J* = 2.1 Hz, 1H), 4.92 (s, 1H), 4.67 (d, *J* = 9.1 Hz, 1H), 2.76 (d, *J* = 15.2 Hz, 1H), 2.53 (dt, *J* = 15.2, 2.2 Hz, 1H), 2.48 – 2.36 (m, 3H), 1.55 (s, 3H), 0.19 (s, 9H), 0.11 (s, 9H).
^{13}C NMR: (151 MHz, C_6D_6) δ 145.3, 143.3, 135.6, 132.0, 129.1, 119.3, 84.3, 73.1, 57.0, 48.4, 41.5, 16.7, 2.1, 0.5.

Secondary alcohol 2.2.6:
*Via deprotection of **2.2.5**:* A small reaction tube was charged with silanol **2.2.5** (62 mg, 0.18 mmol, 1.0 equiv.), Et_2O (1.4 mL) and MeOH (1.4 mL). Neat formic acid (10 μL, 0.27 mmol, 1.5 equiv.) was added and the resulting mixture was stirred at room temperature. Conversion was monitored by TLC and additional HCOOH (3.3 μL, 0.09 mmol, 0.5 equiv.) was added if there was still starting material present after 1 hour. Once all silanol **2.2.5** was consumed, the reaction mixture was *carefully* quenched by dropwise addition of satd. *aq.* $NaHCO_3$ (5 mL or until all formic acid was neutralized). The layers were separated and the aqueous layer was extracted with Et_2O (3 x 5 mL). The combined organic layers were washed with brine, dried over Na_2SO_4, and concentrated under reduced pressure to provide crude alcohol **2.2.6**. Purification by column chromatography (0 to 25% EtOAc/hexanes in 5% increments) resulted in pure secondary alcohol **2.2.6** (45 mg, 0.17 mmol, 92%) as a colorless oil.
*One-step procedure from Heck product **2.1.10**:* An oven-dried 25 mL round-bottom flask was charged with *trans*-fused hydroazulene **2.1.10** (105 mg, 0.398 mmol, 1.0 equiv.) and DCM (4.0 mL). To this solution were added imidazole (54.1 mg, 0.796 mmol, 2.0 equiv.) and TMSCl (0.060 mL, 0.48 mmol, 1.2 equiv.) and the resulting suspension was stirred for 3 hours at room temperature until full consumption of the starting material was observed by TLC. At this stage, silica gel (5.0 g) was added and stirring was continued for another 3 h to liberate the C9 alcohol. The resulting suspension was concentrated under reduced pressure and the crude residue was loaded onto a flash column and purified (0 to 25% EtOAc/hexanes in 5% increments) to obtain the pure free secondary alcohol **2.2.6** (104 mg, 0.394 mmol, 99% yield) as a colorless oil.
TLC: R_f = 0.26 (10% EtOAc/hexanes)
^{1}H NMR (600 MHz, C_6D_6): δ 6.07 (ddd, *J* = 13.0, 2.4, 1.1 Hz, 1H), 5.66 – 5.60 (m, 1H), 5.22 (hept, *J* = 1.3 Hz, 1H), 4.99 (tt, *J* = 2.4, 0.9 Hz, 1H), 4.91 (td, *J* = 2.4, 1.2 Hz, 1H), 4.37 (ddt, *J* = 10.1, 7.8, 2.4 Hz, 1H), 2.76 (d, *J* = 15.2 Hz, 1H), 2.49 (dt, *J* = 15.2, 2.5 Hz, 1H), 2.38 – 2.30 (m, 1H), 2.23 (dd, *J* = 16.1, 7.3 Hz, 1H), 2.07 (ddd, *J* = 10.5, 8.9, 7.2 Hz, 1H), 1.56 – 1.51 (s, 3H), 0.88 (br s, 1H of OH), 0.08 (s, 8H).
^{13}C NMR (150 MHz, C_6D_6): δ 145.4, 143.4, 134.9, 131.9, 129.6, 119.7, 84.5, 72.3, 57.2, 48.5, 41.2, 16.8, 2.2.
IR (thin film) ν_{max} (cm^{-1}): 3304, 2959, 2931, 2910, 1594, 1438, 1248, 1140, 1020, 865, 762.
HRMS (m/z): (ESI) calcd. for $C_{15}H_{23}O_2{}^{28}Si$ $[M–H]^-$: 263.1473, found 263.1479.

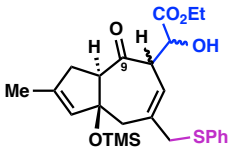
Enone 2.2.7:
An oven-dried 10 mL round-bottom flask was charged with secondary alcohol **2.2.6** (100 mg, 0.379 mmol, 1.0 equiv.) and DCM (4 mL). Then, solid $NaHCO_3$ (63.6 mg, 0.756 mmol, 2.0 equiv.) was added, followed by Dess-Martin periodinane (193 mg, 0.455 mmol, 1.2 equiv.). After 5 minutes conversion was complete as judged by TLC. The reaction mixture was quenched with satd. *aq*. $NaHCO_3$ (3 mL) and satd. *aq*. $Na_2S_2O_3$ (3 mL) and the layers were separated. The aqueous layer was extracted with DCM (3 x 6 mL) and the combined organic layers were dried over Na_2SO_4 and concentrated under reduced pressure to provide crude enone **2.2.7**. This

compound can be used in its crude form or, alternatively, can be purified by column chromatography (0 to 20% EtOAc/hexanes) to provide pure enone **2.2.7** (74.5 mg, 0.284 mmol, 75%) as a pale-yellow oil.
TLC: R_f = 0.75 (25% EtOAc/hexanes)
^{1}H NMR: (600 MHz, C_6D_6) δ 6.32 (d, *J* = 12.9 Hz, 1H), 5.99 (d, *J* = 12.9 Hz, 1H), 5.12 (s, 1H), 5.06 (s, 1H), 4.96 (s, 1H), 3.22 (dd, *J* = 16.8, 8.3 Hz, 1H), 2.95 (t, *J* = 8.0 Hz, 1H), 2.82 (d, *J* = 16.1 Hz, 1H), 2.54 (dt, *J* = 16.1, 2.2 Hz, 1H), 1.49 (s, 3H), 0.02 (s, 9H).
^{13}C NMR: (151 MHz, C_6D_6) δ 196.1, 145.7, 143.1, 141.2, 129.5, 128.9, 125.7, 83.8, 63.2, 47.4, 36.3, 16.5, 1.7.
HRMS (m/z): (ESI) calcd. for $C_{15}H_{22}O_2{}^{23}Na^{28}Si$ [M+Na]$^+$: 285.1281, found 285.1284.

General procedure A: *1,6-addition/aldol cascade with enone **2.2.7**.*
An oven-dried round-bottom flask was charged with Me_3Al solution (2 M in PhMe, 3.0 equiv.) and DCM (0.3 M). The resulting solution was cooled to 0 ºC and neat PhSH (3.0 equiv.) was added dropwise and stirring was continued for 15 minutes at 0 ºC. Then, the reaction mixture was cooled to –78 ºC and a solution of enone **2.2.7** (1.0 equiv.) in THF (0.1 M) was added dropwise. After stirring the resulting solution for 20 minutes at –78 ºC, full consumption of enone **2.2.7** was checked by TLC and a solution of the appropriate aldehyde partner (2 equiv.) in DCM (0.2 M) was added dropwise. After another 15 minutes of stirring at –78 ºC, the reaction mixture was quenched with satd. *aq.* Rochelle's salt (volume equal to total reaction volume) and diluted with Et_2O (volume equal to total reaction volume). The resulting mixture was allowed to warm to room temperature and was vigorously stirred for 5 minutes. The layers were separated and the aqueous layer was extracted three times with Et_2O. The organic layers were combined, dried over Na_2SO_4 and concentrated under reduced pressure. The resulting crude residue was purified by column chromatography.



Allylic alcohol 2.2.9:
Synthesized according to general procedure A from enone **2.2.7** (14.5 mg, 0.055 mmol) and commercially available prenal (10 µL, 0.11 mmol). Column chromatography (0 to 40% EtOAc/hexanes) provided pure alcohol **2.2.9** (12 mg, 0.027 mmol, 48%, mixture of diastereomers) as a colorless oil.
TLC: R_f = 0.45 (25% EtOAc/hexanes)
^{1}H NMR: (600 MHz, C_6D_6) δ 7.35 – 7.31 (m, 2H), 7.05 – 7.00 (m, 2H), 6.96 – 6.91 (m, 1H), 5.50 (s, 1H), 5.31 (dt, *J* = 8.1, 1.3 Hz, 1H), 5.19 – 5.16 (m, 1H), 5.16 – 5.11 (m, 1H), 3.83 (s, 1H), 3.34 (d, *J* = 13.2 Hz, 1H), 3.28 (d, *J* = 13.0 Hz, 1H), 3.14 (t, *J* = 8.1 Hz, 1H), 3.10 – 3.03 (m, 2H), 2.82 (d, *J* = 18.3 Hz, 1H), 2.56 – 2.50 (m, 1H), 2.42 (d, *J* = 6.6 Hz, 1H), 2.00 (dd, *J* = 16.9, 8.1 Hz, 1H), 1.56 (d, *J* = 1.0 Hz, 3H), 1.55 (s, 3H), 1.54 (s, 3H), 1.45 (s, 3H), 0.04 (s, 9H).
^{13}C NMR: (151 MHz, C_6D_6) δ 209.3, 144.2, 134.6, 131.6, 131.4, 130.2, 129.5, 128.8, 126.7, 126.4, 124.0, 85.1, 69.6, 61.0, 57.8, 45.7, 45.6, 35.8, 25.7, 18.2, 16.4, 1.9, 1.8.
HRMS (m/z): (ESI) calcd. for $C_{26}H_{36}O_3{}^{23}Na^{32}S^{28}Si$ [M+Na]$^+$: 479.2047, found 479.2051.



2.3.2

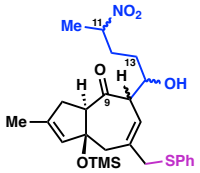
Ester 2.3.2:

Synthesized according to general procedure A from enone **2.2.7** (14.5 mg, 0.055 mmol) and commercially available ethyl glyoxalate (22 µL, 50% in PhMe, 0.11 mmol). Column chromatography (0 to 40% EtOAc/hexanes) provided pure alcohol **2.3.2** (3.9 mg, 8.3 µmol, 15%, one major diastereomer contaminated with copolar impurities derived from ethyl glyoxalate) as a colorless oil.

TLC: R_f = 0.35 (25% EtOAc/hexanes)

^{1}H NMR: (600 MHz, C_6D_6) δ 7.32 (dd, *J* = 8.3, 1.2 Hz, 2H), 7.05 (t, *J* = 7.8 Hz, 1H), 6.94 – 6.91 (m, 2H), 5.47 – 5.39 (m, 1H), 5.20 (dd, *J* = 5.4, 2.1 Hz, 1H), 5.14 (s, 1H), 4.07 (s, 1H), 3.83 – 3.78 (m, 1H), 3.78 – 3.71 (m, 1H), 3.40 (d, *J* = 10.0 Hz, 0H), 3.31 (d, *J* = 13.3 Hz, 1H), 3.25 (d, *J* = 13.4 Hz, 1H), 3.20 (t, *J* = 8.0 Hz, 1H), 3.12 (dd, *J* = 16.9, 7.7 Hz, 1H), 2.96 (d, *J* = 5.5 Hz, 1H), 2.80 (d, *J* = 18.6 Hz, 1H), 2.53 – 2.44 (m, 1H), 1.98 (dd, *J* = 17.0, 8.1 Hz, 1H), 1.43 (s, 3H), 0.83 (t, *J* = 7.1 Hz, 3H), 0.05 (s, 9H).

^{13}C NMR: (151 MHz, C_6D_6) δ 205.8, 174.7, 144.5, 135.7, 134.5, 131.3, 129.0, 128.9, 126.6, 122.0, 85.3, 77.1, 71.5, 62.0, 61.5, 60.7, 55.3, 45.9, 45.2, 35.9, 16.4, 13.8, 1.7.



2.3.4

Nitroalkane 2.3.4:

Synthesized according to general procedure A from enone **2.2.7** (30 mg, 0.11 mmol) and known[20] 4-nitropentanal (28.8 mg, 0.22 mmol). Column chromatography (10 to 50% EtOAc/hexanes) provided pure alcohol **2.3.4** (30 mg, 59 µmol, 54%, mixture of diastereomers) as a colorless oil alongside some residual 4-nitropentanal (6 mg), which was copolar.

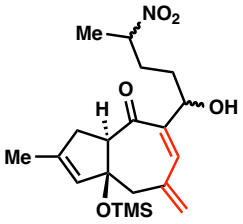
TLC: R_f = 0.75 (50% EtOAc/hexanes)

Selected NMR shifts of the diastereomeric mixture are reported:

^{1}H NMR: (600 MHz, C_6D_6) δ 7.38 – 7.33 (m), 7.30 – 7.26 (m), 7.08 – 7.04 (m), 7.02 – 6.92 (m), 5.12 (d, *J* = 7.3 Hz, 1H), 5.08 (s, 1H), 4.69 (s, 1H), 4.55 (s, 1H), 4.26 – 4.19 (m, 1H), 4.13 (dtd, *J* = 9.0, 4.9, 2.4 Hz, 2H), 4.05 (dqd, *J* = 12.5, 6.1, 3.2 Hz, 1H), 3.90 (dddt, *J* = 13.3, 6.7, 4.5, 2.5 Hz, 1H), 3.76 – 3.72 (m), 3.30 – 3.22 (m), 3.00 – 2.95 (m, 3H), 2.81 (d, *J* = 17.0 Hz, 3H), 2.54 (q, *J* = 7.4 Hz, 1H), 2.50 – 2.42 (m, 1H), 2.34 (dd, *J* = 17.9, 9.7 Hz, 1H), 2.01 – 1.92 (m, 4H), 1.76 (dd, *J* = 17.0, 7.3 Hz, 1H), 1.60 – 1.54 (m, 7H), 1.46 (s, 8H), 1.05 (d, *J* = 5.1 Hz, 3H), 1.04 (d, *J* = 5.1 Hz, 3H), 0.97 (d, *J* = 6.2 Hz, 3H), 0.95 (d, 3H), 0.06 (s, 9H), 0.04 (d, *J* = 2.9 Hz, 9H), 0.03 (s, 9H), 0.02 (s, 9H).

^{13}C NMR: (151 MHz, C_6D_6) δ 210.5, 210.3, 210.0, 209.6, 145.1, 144.1, 135.7, 135.3, 135.3, 133.3, 132.1, 131.9, 131.6, 131.3, 129.5, 129.0, 127.2, 127.1, 126.9, 126.9, 122.9, 122.0, 121.8, 86.2, 86.2, 84.9, 83.7, 83.6, 82.7, 82.1, 72.2, 72.1, 71.4, 71.3, 61.4, 61.2, 60.9, 57.4, 56.7, 56.2, 56.2, 46.1, 46.0, 45.5, 39.2, 35.7, 34.9, 34.9, 32.4, 32.0, 31.5, 30.9, 30.6, 30.5, 30.1, 29.6, 26.8, 19.3, 19.2, 18.8, 18.8, 18.6, 16.4, 1.9, 1.9, 1.8, 1.8, 1.7.

HRMS (m/z): (ESI) calcd. for $C_{26}H_{37}O_5N^{23}Na^{32}S^{28}Si$ $[M+Na]^+$: 526.2054, found 526.2059.



2.3.14

Enone 2.3.14:

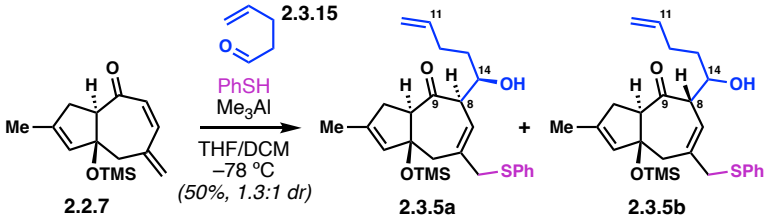
An oven-dried small reaction tube was charged with aldol products **2.3.4** (13 mg, 26 μmol, 1.0 equiv.). This mixture of diastereomers was dissolved in DCM (0.26 mL) and DBU (10 μL, 0.067 mmol, 2.6 equiv.) was added. The reaction mixture was stirred at room temperature and gradually changed color to deep red over 10 minutes. At this point the starting material was consumed as judged by TLC, so the reaction mixture was quenched with satd. *aq*. NH_4Cl (0.5 mL). The layers were separated and the aqueous layer was extracted with DCM (3 x 0.5 mL). The combined organic layers were dried over Na_2SO_4 and concentrated under reduced pressure. The crude reaction product was purified by column chromatography (10 to 60% EtOAc/hexanes) to provide pure enone **2.3.14** as a mixture of diastereomers (5.4 mg, 14 μmol, 53%).

TLC: R_f = 0.8 (50% EtOAc/hexanes)

Selected NMR resonances for this mixture of diastereomers are reported.

^{1}H NMR: (600 MHz, C_6D_6) δ 6.81 (s, 1H), 6.76 (s, 1H), 5.19 (s, 1H), 5.12 – 5.09 (m, 1H), 5.04 – 4.99 (m, 1H), 4.39 (s, 1H), 4.33 – 4.27 (m, 1H), 4.16 (dq, *J* = 13.6, 7.5 Hz, 1H), 3.30 – 3.22 (m, 1H), 2.97 (q, *J* = 7.5 Hz, 1H), 2.81 (dd, *J* = 16.3, 4.5 Hz, 1H), 2.55 – 2.50 (m, 1H), 2.39 (d, *J* = 6.6 Hz, 1H), 2.20 (d, *J* = 6.2 Hz, 1H), 1.98 (dd, *J* = 17.4, 8.4 Hz, 1H), 1.50 (s, 3H), 1.50 (s, 3H), 1.02 (d, *J* = 6.6 Hz, 3H), 0.99 (d, *J* = 6.6 Hz, 3H), 0.03 (s, 9H), 0.01 (s, 9H).

^{13}C NMR: (151 MHz, C_6D_6) δ 197.8, 197.4, 145.4, 145.3, 142.7, 139.9, 139.7, 132.1, 129.0, 126.3, 84.5, 83.5, 83.0, 73.4, 72.8, 62.8, 62.7, 47.4, 35.9, 34.2, 33.9, 32.0, 31.9, 18.9, 18.6, 16.5, 1.7.



2.2.7 **2.3.5a** **2.3.5b**

Olefins 2.3.5a and 2.3.5b:

Synthesized according to general procedure A from enone **2.2.7** (59 mg, 0.22 mmol) and known 4-pentenal **2.3.15** (37 mg, 0.44 mmol). Column chromatography (5 to 50% EtOAc/hexanes) provided pure alcohols **2.3.5a** and **2.3.5b** (50 mg, 0.11 mmol, 50%, 1.3:1 dr) as a colorless oil.

TLC: R_f = 0.22 (25% EtOAc/hexanes)

2.3.5a – **bold**

2.3.5b – underlined

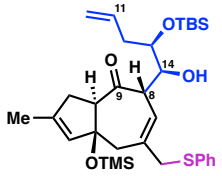
Overlapping signals from both - normal

^{1}H NMR: (600 MHz, C_6D_6) δ **7.32** (dt, *J* = 8.5, 1.7 Hz, 2H), 7.31 – 7.28 (m, 2H), **7.07 – 7.04** (m, 2H), 7.04 – 7.00 (m, 2H), 6.97 – 6.91 (m), **5.90** (ddt, *J* = 17.0, 10.2, 6.7 Hz, 1H), 5.76 (ddt, *J* = 17.0, 10.2, 6.7 Hz, 1H), 5.32 – 5.26 (m), 5.18 (s, 1H), 5.14 – 5.09 (m), 5.06 – 5.03 (m), 5.02 –

5.00 (m), 4.99 – 4.96 (m), **4.30** (s, 1H), 4.19 (s), 3.75 (s, 1H), 3.32 – 3.23 (m, 4H), **3.22 – 3.15** (m, 1H), 3.07 – 2.99 (m), 2.86 – 2.78 (m), **2.71** (t, *J* = 6.1 Hz, 1H), 2.52 (d, *J* = 17.7 Hz, 1H), **2.48 – 2.41** (m, 1H), **2.37 – 2.32** (m, 1H), 2.32 – 2.23 (m), 2.08 – 2.01 (m, 1H), 1.98 (dd, *J* = 16.5, 7.7 Hz, 1H), **1.76** (dd, *J* = 16.8, 7.8 Hz, 1H), 1.57 (dddd, *J* = 13.1, 9.5, 6.5, 2.6 Hz, 1H), **1.47** (s, 3H), 1.46 (s, 3H), **1.42** (dq, *J* = 13.7, 4.6 Hz, 1H), 1.27 (dddd, *J* = 12.0, 9.4, 6.5, 3.3 Hz, 1H), **0.06** (s, 9H), 0.03 (s, 9H).

^{13}C NMR: (151 MHz, C_6D_6) δ 210.0, 208.9, 145.1, 144.2, 139.2, 138.6, 136.3, 135.9, 134.7, 132.4, 131.9, 131.2, 129.6, 129.2, 129.0, 128.9, 128.9, 123.6, 122.6, 114.8, 114.6, 86.0, 85.0, 71.9, 71.8, 61.3, 60.9, 58.2, 56.4, 46.2, 45.6, 45.6, 45.5, 35.7, 35.0, 34.3, 33.4, 30.9, 30.2, 16.4, 2.0, 1.8.

HRMS (m/z): (ESI) calcd. for $C_{26}H_{36}O_3{}^{23}Na^{32}S^{28}Si$ $[M+Na]^+$: 479.2047, found 479.2051.



2.3.6 *(39%, major diastereomer)*

Silanol 2.3.6:

Synthesized according to general procedure A from enone **2.2.7** (29 mg, 0.11 mmol) and known[35] aldehyde **2.3.24** (47 mg, 0.22 mmol). Column chromatography (5 to 40% EtOAc/hexanes) provided pure alcohol **2.3.6** (25 mg, 43 μmol, 39%) as a colorless oil.

TLC: R_f = 0.33 (25% EtOAc/hexanes)

^{1}H NMR: (600 MHz, C_6D_6) δ 7.34 (dd, *J* = 8.3, 1.1 Hz, 2H), 7.03 (t, *J* = 7.7 Hz, 2H), 6.94 – 6.91 (m, 1H), 6.00 – 5.91 (m, 1H), 5.90 (s, 1H), 5.20 (s, 1H), 5.11 (dd, *J* = 17.2, 1.8 Hz, 1H), 5.06 – 5.03 (m, 1H), 4.50 (td, *J* = 6.6, 3.0 Hz, 1H), 4.05 (s, 1H), 3.95 (dt, *J* = 6.8, 5.1 Hz, 1H), 3.58 – 3.50 (m, 1H), 3.41 – 3.33 (m, 1H), 3.21 (t, *J* = 8.1 Hz, 1H), 3.03 (dd, *J* = 15.8, 8.0 Hz, 1H), 2.80 (d, *J* = 18.2 Hz, 1H), 2.70 (d, *J* = 18.2 Hz, 1H), 2.54 – 2.48 (m, 1H), 2.36 – 2.32 (m, 1H), 2.01 (dd, *J* = 16.9, 8.1 Hz, 1H), 1.46 (s, 3H), 0.97 (s, 9H), 0.12 (s, 3H), 0.09 (s, 3H), 0.07 (d, *J* = 1.9 Hz, 9H).

^{13}C NMR: (151 MHz, C_6D_6) δ 208.6, 144.2, 136.7, 134.8, 134.7, 131.1, 129.9, 129.0, 126.6, 124.5, 117.5, 85.2, 73.3, 73.3, 60.7, 53.5, 45.7, 45.4, 38.4, 35.8, 26.1, 18.3, 16.5, 2.0, 1.8, -4.2, -4.3.

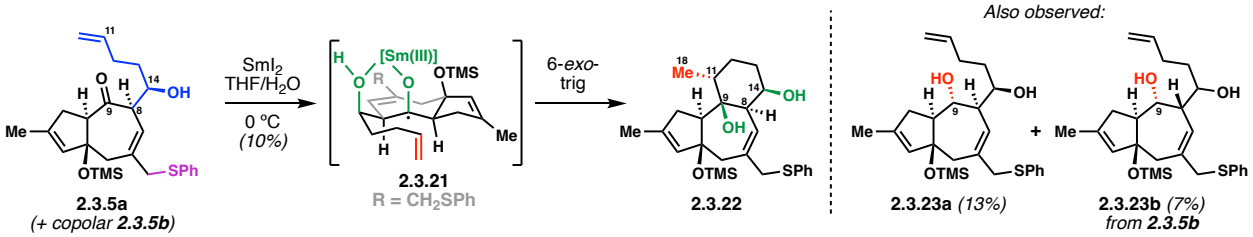
HRMS (m/z): (ESI) calcd. for $C_{32}H_{50}O_4{}^{23}Na^{32}S^{28}Si$ $[M+Na]^+$: 609.2861, found 609.2867.

Samarium (II) iodide, solution in THF: *(CAUTION: SmI_2 is a very air-sensitive reagent. Careful Schlenk technique should be used at all times.)*

Solutions of SmI_2 in THF were prepared fresh from Sm(0) and I_2 via a modified procedure by Procter et al. (see ref. SI-1 in Section 2.12.4) wherein a 100 mL Schlenk storage flask equipped with a single outlet stoppered by a Teflon-coated screw was charged with Sm(0) powder (700 mg, 4.66 mmol, 2.1 equiv.), evacuated and back-filled with argon. The evacuation and back-filling was repeated 4 more times. THF was degassed by sparging with argon in a sonicator for 15 minutes (note a 20 gauge inlet needle and 22 gauge outlet needle was used). Then, the Sm(0) powder was suspended in 20 mL of degassed THF with vigorous stirring. A solution of iodine (560 mg, 2.21 mmol, 1.0 equiv.) in degassed THF (4 mL) was added to the Sm(0) suspension, resulting in a dark brown mixture. At this point the Teflon stopcock was closed and the reaction mixture was stirred vigorously at 60 ºC for 18 hours. A gradual color change to light brown, then

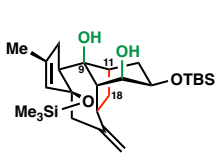
green, and finally dark blue was observed, with the dark blue color indicating the presence of Sm(II). Note that the intensity of the blue color does not correlate to Sm(II) concentration, so even if the dark blue color is observed within the first hour, heating of the reaction mixture should be continued for the full duration state above. Once the 18-hour interval had elapsed, the deep blue solution was allowed to cool to room temperature and the remaining solid Sm(0) powder was allowed to settle. At this point the SmI_2 solution in THF was ready to use with an assumed concentration of 0.1 M. This solution can be stored outside of a glovebox for several weeks in the previously described reaction vessel.

General procedure B: *SmI_2-mediated 6-exo-trig cyclization.*
An oven-dried round-bottom flask was charged with neat starting material (1.0 equiv.) and was evacuated then back-filled with argon. The evacuation and back-filling was repeated two more times. THF was degassed by sparging with argon in a sonicator for 5 minutes. The neat starting material was dissolved in degassed THF (0.07M) and H_2O (10% of THF volume) was added to the resulting solution. The reaction mixture was degassed by sparging with argon in a sonicator for 5 minutes and was then cooled to 0 ºC. Then, a solution of SmI_2 in THF (0.1 M, 5.0 equiv.) was added (rapid drops) with vigorous stirring. After 1 minute, conversion of the starting material was checked by TLC and more SmI_2 was added if necessary. Once all starting ketone was consumed, the reaction mixture was quenched with satd. *aq.* Rochelle's salt (volume equal to THF volume in reaction mixture) and diluted with Et_2O (volume equal to THF volume in reaction mixture). A color change from dark blue/purple to dark green was observed. The resulting biphasic mixture was vigorously stirred for 10 minutes at room temperature, during which time the intensity of the green color decreased, and the layers were separated. The aqueous layer was extracted with Et_2O or EtOAc for more polar products and the combined organic layers were dried over Na_2SO_4 and concentrated under reduced pressure. The resulting crude product was purified by column chromatography.

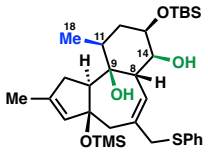


Tricycle 2.3.22:
Synthesized by subjecting a mixture of diastereomers **2.3.5a** and **2.3.5b** (40 mg, 88 µmol, 1.3:1 dr) to general procedure B. The tricyclic product **2.3.22** (10 mg, 22 µmol) was isolated alongside diols **2.3.23a** and **2.3.23b** (20 mg, 44 µmol, 2:1 **2.3.23a**:**2.3.23b**).
*Tricycle **2.3.22**:*
TLC: R_f = 0.78 (50%EtOAc/hexanes)
^{1}H NMR: (600 MHz, C_6D_6) δ 7.40 (dd, *J* = 8.2, 1.0 Hz, 2H), 7.06 (t, *J* = 7.8 Hz, 2H), 6.94 (t, *J* = 7.4 Hz, 1H), 6.25 (s, 1H), 6.02 (s, 1H), 5.15 (s, 1H), 5.08 (d, *J* = 10.3 Hz, 1H), 3.88 – 3.82 (m, 1H), 3.73 (d, *J* = 12.7 Hz, 1H), 3.49 (d, *J* = 12.7 Hz, 1H), 2.71 (d, *J* = 15.5 Hz, 1H), 2.66 – 2.55 (m, 2H), 2.30 (dt, *J* = 15.5, 2.3 Hz, 1H), 1.94 (s, 1H), 1.93 – 1.89 (m, 1H), 1.88 – 1.82 (m, 2H), 1.67 (dd, *J* = 9.8, 6.4 Hz, 1H), 1.52 (tt, *J* = 13.8, 3.8 Hz, 1H), 1.49 (s, 3H), 1.10 (dd, *J* = 13.5, 3.3 Hz, 1H), 0.63 (d, *J* = 7.2 Hz, 3H), -0.01 (s, 9H).

^{13}C NMR: (151 MHz, C_6D_6) δ 147.3, 137.3, 133.1, 132.7, 131.4, 130.1, 128.9, 126.1, 86.9, 77.3, 72.8, 56.7, 46.8, 43.6, 43.3, 37.8, 35.8, 27.8, 21.7, 16.9, 15.2, 1.6.
HRMS (m/z): (ESI) calcd. for $C_{26}H_{38}O_3{}^{23}Na^{32}S^{28}Si$ $[M+Na]^+$: 481.2203, found 481.2209.
*Diols **2.3.23a** and **2.3.23b**:*
TLC: R_f = 0.56 (50% EtOAc/hexanes)
2.3.23a – **bold**
2.3.23b – underlined
Overlap – normal
^{1}H NMR: (600 MHz, C_6D_6) δ 7.40 – 7.36 (m, 2H), **7.30** (dd, *J* = 8.2, 1.2 Hz, 2H), 7.06 (t, *J* = 7.7 Hz, 2H), **7.02 – 6.98** (m, 2H), 6.92 – 6.88 (m, 1H), 5.87 (dtd, *J* = 10.4, 6.9, 3.5 Hz, 1H), 5.67 (s, 1H), **5.31** (s, 1H), 5.17 (s, 1H), 5.13 (dq, *J* = 3.5, 1.7 Hz, 1H), 5.11 – 5.09 (m), 5.02 – 5.00 (m, 1H), 4.32 (d, *J* = 9.8 Hz, 1H), **4.05** (t, 1H), **3.81** (dd, *J* = 8.5, 4.4 Hz, 1H), 3.74 (s, 1H), 3.69 (d, *J* = 13.0 Hz, 1H), 3.45 (d, *J* = 13.0 Hz, 1H), 3.42 (d, *J* = 13.0 Hz, 1H), 3.25 (d, *J* = 13.1 Hz, 1H), 2.75 (d, *J* = 15.1 Hz, 1H), 2.70 (d, *J* = 18.0 Hz, 1H), 2.58 (d, *J* = 18.0 Hz, 1H), 2.30 (td, *J* = 15.0, 7.9 Hz, 1H), 2.19 (dq, *J* = 14.4, 6.4 Hz, 1H), 2.08 (d, *J* = 8.1 Hz, 1H), 1.78 – 1.67 (m, 2H), **1.53** (s, 2H), 1.51 (s, 1H), **0.05** (d, *J* = 1.5 Hz, 9H), -0.02 (s, 9H).
^{13}C NMR: (151 MHz, C_6D_6) δ 143.2, 139.1, 138.9, 136.4, 134.8, 134.5, 132.2, 131.6, 131.2, 130.8, 130.4, 126.5, 126.4, 125.8, 114.6, 114.6, 86.1, 84.3, 79.6, 74.5, 73.0, 69.6, 56.5, 54.2, 50.2, 46.7, 45.8, 44.6, 43.9, 42.8, 40.4, 38.7, 35.6, 35.3, 31.1, 30.5, 16.9, 16.6, 2.0, 1.7.
HRMS (m/z): (ESI) calcd. for $C_{26}H_{38}O_3{}^{23}Na^{32}S^{28}Si$ $[M+Na]^+$: 481.2203, found 481.2207.



2.3.29



2.3.33

Tricycle 2.3.33 and tetracycle 2.3.29:
Synthesized from **2.3.6** (25 mg, 43 μmol) according to general procedure B. The two cyclization products were copolar (5 mg, 8.5 μmol, 20%, 1.3:1 **2.3.29**:**2.3.33**).
*Tetracycle **2.3.29**:*
TLC: R_f = 0.67 (50% EtOAc/hexanes)
^{1}H NMR: (700 MHz, C_6D_6) δ 6.13 (s, 1H), 5.27 (s, 1H), 4.85 (s, 1H), 4.74 (s, 1H), 3.97 – 3.91 (m, 2H), 3.80 – 3.77 (m, 1H), 3.33 (dd, *J* = 29.6, 12.2 Hz, 1H), 3.27 (s, 1H), 2.68 – 2.65 (m, 1H), 2.47 (d, *J* = 15.1 Hz, 1H), 2.46 – 2.43 (m, 1H), 2.42 (d, *J* = 11.7 Hz, 1H), 2.32 (dd, *J* = 16.2, 7.1 Hz, 1H), 1.95 (dd, *J* = 9.7, 7.3 Hz, 1H), 1.78 (s, 1H), 1.74 (dd, *J* = 12.9, 7.4 Hz, 1H), 1.66 (s, 3H), 1.55 (dd, *J* = 14.5, 9.9 Hz, 2H), 0.82 (s, 9H), 0.22 (s, 9H), -0.04 (s, 3H), -0.07 (s, 3H).
HRMS (m/z): (ESI) calcd. for $C_{26}H_{46}O_4{}^{23}Na^{28}Si_2$ $[M+Na]^+$: 501.2827, found 501.2836.
*Tricycle **2.3.33**:*
TLC: R_f = 0.67 (50% EtOAc/hexanes)
^{1}H NMR: (600 MHz, C_6D_6) δ 7.24 (d, *J* = 7.4 Hz, 2H), 7.01 (t, *J* = 7.7 Hz, 2H), 6.95 – 6.89 (m, 1H), 5.31 (s, 1H), 4.82 (s, 1H), 4.66 (s, 1H), 4.34 (br s, 1H, OH), 3.69 – 3.63 (m, 1H), 3.30 (m, 1H), 3.18 (s, 1H), 2.97 (m, 1H), 2.91 (br s, 1H, OH), 2.64 (m, 1H), 2.45 (m, 1H), 2.10 (dd, *J* = 14.7, 8.7 Hz, 1H), 1.92 (m, 1H), 1.82 (m, 1H), 1.62 (s, 3H), 1.19 – 1.13 (m, 1H), 0.98 (m, 1H), 0.91 (d, 3H), 0.90 (s, 9H), 0.28 (s, 9H), 0.05 (s, 3H), 0.02 (s, 3H).
HRMS (m/z): (ESI) calcd. for $C_{32}H_{52}O_4{}^{23}Na^{32}S^{28}Si_2$ $[M+Na]^+$: 611.3017, found 611.3025.

^{13}C NMR: (151 MHz, C_6D_6) δ 150.5, 146.2, 134.5, 132.3, 131.2, 130.7, 128.7, 126.6, 112.7, 86.6, 85.9, 79.1, 76.2, 68.0, 60.3, 46.9, 46.6, 45.6, 45.1, 38.2, 32.2, 29.8, 25.8, 25.7, 18.0, 17.0, 16.8, 2.3, 2.1, -4.4, -4.6, -4.8, -5.2.
*Note ^{13}C shifts for the mixture of **2.3.33** and **2.3.29** are reported; for additional structural information see 2D spectra.*

General procedure C: Synthesis of type III aldehydes.

Step C1: Michael addition of a methyl Gilman reagent to ethyl 2-butynoate followed by alkylation of the resulting cuprate.

An oven-dried round-bottom flask was charged with CuBr•DMS (1.0 equiv.) inside a glovebox. THF (0.14 M, degassed) was added, and the resulting suspension was cooled to 0 ºC. Methyllithium (1.6 M in Et_2O, 2.0 equiv.) was added and the resulting clear solution was cooled to –78 ºC. Ethyl 2-butynoate (1.0 equiv.) in THF (0.56 M, degassed) was added dropwise and the reaction mixture was stirred for 1 hour. Then, the corresponding allyl or propargyl halide (2.0 equiv.) in THF (2 M, degassed) was added dropwise and the reaction mixture was stirred overnight while being allowed to slowly warm to ambient temperature. The reaction mixture was quenched by addition of satd. *aq.* NH_4Cl (volume equal to total THF volume). The organic layer was separated and the aqueous layer was extracted with Et_2O (3 x volume equal to total THF volume). The combined organic layers were dried over Na_2SO_4 and concentrated under reduced pressure. The crude residue was purified by silica gel chromatography (0 to 40% Et_2O/hexanes) to give the corresponding alkylated Michael addition product.

Step C2: Reduction of alkylation products.

A flame-dried round-bottom flask was charged with the ester product from step C1 (1.0 equiv.) and DCM (0.1 M) and was subsequently cooled to –78 ºC. A solution of DIBAL (1 M in hexanes, 3.5 equiv.) was added and the reaction mixture was stirred for 3 hours before being quenched by addition of EtOAc (10% of DIBAL solution volume) and satd. *aq.* NH_4Cl (40% of DIBAL solution volume). The resulting mixture was allowed to warm to ambient temperature and was then stirred for 1 hour. The resulting suspension was filtered over a pad of celite, and the filter cake was generously washed with Et_2O and the filtrate was concentrated under reduced pressure. The crude residue was purified by silica gel chromatography (10 to 70% Et_2O/hexanes) to afford the corresponding alcohol products.

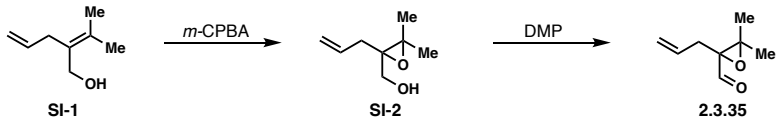
Step C3: Epoxidation of reduction products.

A flame-dried round-bottom flask was charged with the alcohol obtained in step C2 (1.0 equiv.), DCM (0.1 M), and $NaHCO_3$ (5.0 equiv.). Then, *m*-CPBA (1.4 equiv.) was added and the reaction mixture was stirred for 10 minutes or until conversion was completed as judged by TLC. After quenching with satd. *aq.* $NaHCO_3$ (volume equal to DCM volume) and satd. *aq.* $Na_2S_2O_3$ (volume equal to DCM volume), the layers were separated and the aqueous layer was extracted three times with DCM. The combined organic layers were dried over Na_2SO_4 and concentrated under reduced pressure. The crude reaction product was purified by column chromatography (10 to 70% Et_2O/hexanes) to provide pure epoxide product.

Step C4: Oxidation to form type III aldehydes.

An oven-dried round-bottom flask was charged with the corresponding α,β-epoxy alcohol arising from step C3 (1.0 equiv.), DCM (0.1 M), and $NaHCO_3$ (2.0 equiv.). Then, DMP (1.3 equiv.) was added and the reaction mixture was stirred at room temperature for 5 minutes or until conversion was complete as judged by TLC. After quenching with satd. *aq.* $NaHCO_3$ (volume equal to DCM volume) and satd. *aq.* $Na_2S_2O_3$ (volume equal to DCM volume), the layers were

separated and the aqueous layer was extracted three times with DCM. The combined organic layers were dried over Na_2SO_4 and concentrated under reduced pressure. The crude reaction product was purified by column chromatography (0 to 40% Et_2O/hexanes) to provide pure aldehyde product.



Type III aldehyde 2.3.35:

Synthesized according to general procedure C, steps C3 and C4, from known alcohol **SI-1**.[SI-2]

Step C3: Epoxide **SI-2** was synthesized from known olefin **SI-1** (1 g, 7.9 mmol) according to general procedure C, step C3. After purification, desired α,β-epoxy alcohol **SI-2** (824 mg, 5.9 mmol, 75%) was obtained as a colorless oil.

*Epoxide **SI-2**:*

TLC: R_f = 0.20 (25% EtOAc/hexanes)

^{1}H NMR: (600 MHz, $CDCl_3$) δ 5.83 (ddt, *J* = 14.2, 10.3, 6.9 Hz, 1H), 5.19 – 5.11 (m, 2H), 3.78 – 3.68 (m, 2H), 2.72 (ddt, *J* = 14.8, 7.2, 1.3 Hz, 1H), 2.27 (dd, *J* = 14.7, 6.2 Hz, 1H), 1.39 (s, 3H), 1.38 (s, 3H).

^{13}C NMR: (151 MHz, $CDCl_3$) δ 133.2, 118.0, 66.1, 62.9, 62.6, 35.2, 21.2, 20.7.

HRMS (m/z): (ESI) calcd. for $C_8H_{14}O_2{}^{23}Na$ $[M+Na]^+$: 165.0886, found 165.0885.

Step C4: Epoxide **SI-2** (361 mg, 2.54 mmol) was subjected to general procedure C, step C4, to provide type III aldehyde **2.3.35** (256 mg, 1.82 mmol, 72%).

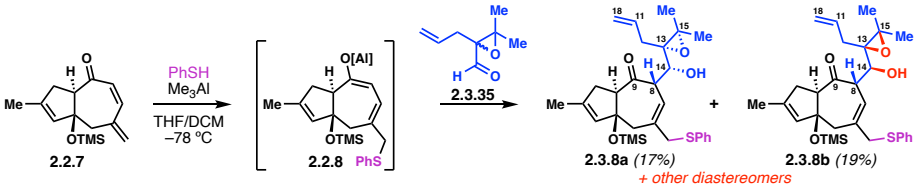
*Aldehyde **2.3.35**:*

TLC: R_f = 0.70 (25% EtOAc/hexanes)

^{1}H NMR: (600 MHz, $CDCl_3$) δ 9.51 (s, 1H), 5.81 (ddt, *J* = 17.2, 10.2, 6.6 Hz, 1H), 5.17 – 5.09 (m, 3H), 2.76 (dd, *J* = 15.2, 7.1 Hz, 1H), 2.42 (dd, *J* = 15.2, 6.1 Hz, 1H), 1.43 (s, 6H).

^{13}C NMR: (151 MHz, $CDCl_3$) δ 201.8, 131.9, 118.4, 68.7, 64.2, 31.9, 21.8, 20.6.

HRMS (m/z): (EI+) calcd. for $C_8H_{12}O_2$: 140.0837, found 140.0835.



Cyclization precursors 2.3.8a and 2.3.8b:

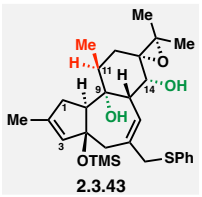
Synthesized from **2.2.7** (132 mg, 0.500 mmol) and type III aldehyde **2.3.35** (141 mg, 1.0 mmol) according to general procedure A, resulting in **2.3.8a** (44 mg, 0.086 mg, 17%) and **2.3.8b** (48 mg, 0.093 mmol, 19%) after purification by column chromatography (5 to 50% EtOAc/hexanes) alongside other tentative diastereomer products.

*Desired C14 epimer **2.3.8a**:*

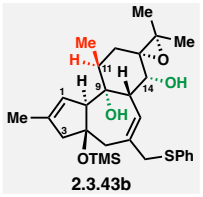
TLC: R_f = 0.53 (50% EtOAc/hexanes)

^{1}H NMR: (600 MHz, C_6D_6) δ 7.32 – 7.26 (m, 2H), 7.03 – 6.98 (m, 2H), 6.94 – 6.88 (m, 1H), 5.34 (d, *J* = 3.7 Hz, 1H), 5.16 (d, *J* = 6.3 Hz, 1H), 5.04 (dd, *J* = 17.2, 1.6 Hz, 1H), 5.00 – 4.97 (m, 1H), 4.14 (dd, *J* = 8.9, 1.8 Hz, 1H), 4.09 – 4.03 (m, 0H), 3.88 (s, 1H), 3.31 (d, *J* = 13.7 Hz, 1H), 3.25 (d, *J* = 13.7 Hz, 1H), 3.07 (t, *J* = 8.1 Hz, 1H), 2.98 – 2.89 (m, 1H), 2.78 (d, *J* = 18.1

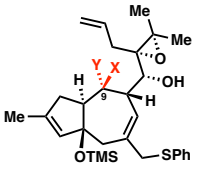
Hz, 1H), 2.70 (dd, *J* = 15.6, 7.8 Hz, 1H), 2.59 – 2.50 (m, 1H), 2.40 (d, *J* = 18.0 Hz, 1H), 1.99 (dd, *J* = 16.8, 8.0 Hz, 1H), 1.46 (s, 3H), 1.24 (s, 3H), 1.21 (s, 3H), 0.07 (s, 9H).
^{13}C NMR: (151 MHz, C_6D_6) δ 209.9, 144.3, 136.3, 135.6, 134.6, 131.0, 129.7, 129.0, 126.8, 122.9, 116.1, 84.7, 74.6, 66.2, 62.0, 60.3, 55.3, 45.8, 45.4, 36.0, 33.9, 22.0, 21.7, 16.4, 1.9.
HRMS (m/z): (ESI) calcd. for $C_{29}H_{40}O_4{}^{23}Na^{32}S^{28}Si$ $[M+Na]^+$: 535.2309, found 535.2312.
*Undesired C14 epimer **2.3.8b**:*
TLC: R_f = 0.59 (50% EtOAc/hexanes)
^{1}H NMR: (600 MHz, C_6D_6) δ 7.38 (dd, *J* = 8.3, 1.2 Hz, 2H), 7.05 (t, *J* = 7.8 Hz, 2H), 6.96 – 6.91 (m, 1H), 5.96 – 5.89 (m, 1H), 5.88 (s, 1H), 5.19 (s, 1H), 5.02 – 4.99 (m, 1H), 4.98 (dt, *J* = 5.1, 1.7 Hz, 1H), 4.74 (dd, *J* = 5.0, 3.5 Hz, 1H), 4.05 (br s, 1H, OH), 3.46 (d, *J* = 13.2 Hz, 1H), 3.35 (d, *J* = 13.2 Hz, 1H), 3.25 (t, *J* = 8.1 Hz, 1H), 3.12 – 3.06 (m, 1H), 2.83 (d, *J* = 18.3 Hz, 1H), 2.70 (dd, *J* = 15.8, 6.2 Hz, 1H), 2.59 (d, *J* = 18.0 Hz, 1H), 2.33 (d, *J* = 5.1 Hz, 1H), 2.27 (ddt, *J* = 15.8, 6.9, 1.5 Hz, 1H), 2.02 (dd, *J* = 16.9, 8.1 Hz, 1H), 1.47 – 1.45 (m, 3H), 1.32 (s, 3H), 1.16 (s, 3H), 0.08 (s, 9H).
^{13}C NMR: (151 MHz, C_6D_6) δ 208.0, 144.2, 136.7, 135.1, 134.1, 131.2, 129.5, 129.0, 126.5, 123.9, 116.7, 85.1, 72.6, 65.9, 62.5, 60.8, 54.7, 45.7, 35.9, 35.7, 22.0, 21.0, 16.4, 1.9.
HRMS (m/z): (ESI) calcd. for $C_{29}H_{40}O_4{}^{23}Na^{32}S^{28}Si$ $[M+Na]^+$: 535.2309, found 535.2301.



2.3.43



2.3.43b



X = OH, Y = H
2.3.46a
X = H, Y = OH
2.3.46b

Tricycles 2.3.43 and 2.3.43b; alcohols 2.3.46a and 2.3.46b:
Synthesized from alkene **2.3.8a** (44 mg, 86 µmol) using general procedure B. After purification (5 to 60% EtOAc/hexanes), a mixture of copolar olefin isomers **2.3.43** and **2.3.43b** and secondary alcohol **2.3.46b** (12 mg, 23 µmol, 27%, 3.3:2:1 **2.3.43**:**2.3.43b**:**2.3.46b**) was isolated alongside a mixture of copolar products containing alcohol **2.3.46a** (12 mg, 23 µmol, 27%) as the major constituent.
*Tricycle **2.3.43**:*
TLC: R_f = 0.39 (50% EtOAc/hexanes)
^{1}H NMR: (700 MHz, C_6D_6) δ 7.41 (dd, *J* = 6.0, 1.2 Hz, 2H), 7.05 (d, *J* = 7.7 Hz, 2H), 6.96 – 6.93 (m, 1H), 5.64 (s, 1H), 5.28 (s, 1H), 4.02 (s, 1H), 3.59 (s, 2H), 3.33 (d, *J* = 12.9 Hz, 1H), 3.28 (d, *J* = 13.0 Hz, 1H), 2.98 (s, 1H), 2.90 (d, *J* = 14.3 Hz, 1H), 2.87 (d, *J* = 19.4 Hz, 1H), 2.65 (t, *J* = 8.9 Hz, 1H), 2.45 (d, *J* = 7.3 Hz, 1H), 2.32 (d, *J* = 16.6 Hz, 1H), 2.28 (dd, *J* = 16.2, 8.4 Hz, 2H), 2.10 – 2.07 (m, 1H), 1.54 (s, 3H), 1.24 (d, *J* = 3.6 Hz, 1H), 1.21 (s, 3H), 1.20 (s, 3H), 0.96 (d, *J* = 7.4 Hz, 3H), 0.10 (s, 9H).
HRMS (m/z): (ESI) calcd. for $C_{29}H_{42}O_4{}^{23}Na^{32}S^{28}Si$ $[M+Na]^+$: 537.2465, found 537.2472.
*Tricycle **2.3.43b**:*
TLC: R_f = 0.39 (50% EtOAc/hexanes)
^{1}H NMR: (700 MHz, C_6D_6) δ 7.39 (d, *J* = 1.0 Hz, 2H), 7.04 (d, *J* = 7.6 Hz, 2H), 7.01 (d, *J* = 8.1 Hz, 1H), 5.63 (s, 1H), 5.61 (d, *J* = 3.9 Hz, 1H), 4.15 (s, 1H), 3.57 (s, 1H), 3.52 (s, 1H), 3.36 (d, *J* = 13.0 Hz, 1H), 3.25 (d, *J* = 13.0 Hz, 1H), 3.18 (s, 1H), 2.95 – 2.92 (m, 2H), 2.47 (d, *J* = 9.4 Hz, 2H), 2.41 (s, 1H), 2.28 – 2.26 (m, 2H), 2.17 (d, *J* = 16.4 Hz, 1H), 1.61 (s, 3H), 1.20 (s, 3H), 1.19

(s, 3H), 0.99 (d, *J* = 7.4 Hz, 3H), 0.09 (s, 9H). *Note only select peaks are reported due to overlap.*

*Assorted 13C peaks for **2.3.43** and **2.3.43b**:*

^{13}C NMR: (151 MHz, C_6D_6) δ 142.2, 136.5, 133.4, 132.2, 131.9, 131.2, 130.1, 128.9, 128.8, 128.7, 126.7, 125.1, 85.1, 84.6, 81.6, 80.3, 75.0, 74.9, 66.3, 65.8, 64.2, 58.6, 53.8, 47.7, 47.3, 45.1, 39.8, 39.6, 39.2, 39.1, 36.7, 30.0, 27.7, 27.6, 22.4, 22.3, 20.6, 20.5, 17.8, 17.2, 16.6, 2.3, 2.1, 2.0.

*Alcohol **2.3.46a**:*

TLC: R_f = 0.65 (50% EtOAc/hexanes)

^{1}H NMR: (700 MHz, C_6D_6) δ 7.28 (d, *J* = 7.3 Hz, 2H), 7.02 – 6.99 (m, 2H), 6.91 – 6.88 (m, 1H), 6.06 – 5.99 (m, 1H), 5.49 (d, *J* = 6.5 Hz, 1H), 5.22 (s, 1H), 5.07 (dd, *J* = 17.2, 1.6 Hz, 1H), 4.98 (d, *J* = 10.1 Hz, 1H), 4.53 (d, *J* = 9.1 Hz, 1H), 4.20 (s, 1H), 3.69 (d, 1H), 3.40 (dt, *J* = 10.8, 5.6 Hz, 2H), 3.30 (d, *J* = 13.5 Hz, 1H), 3.19 (dd, *J* = 13.0, 8.1 Hz, 1H), 2.95 (dd, *J* = 16.1, 9.5 Hz, 1H), 2.89 (dd, *J* = 15.7, 7.9 Hz, 1H), 2.67 (s, 1H), 2.50 (dd, *J* = 15.7, 5.8 Hz, 1H), 2.15 – 2.08 (m, 1H), 1.85 (dd, *J* = 15.9, 7.2 Hz, 1H), 1.56 (s, 3H), 1.25 (s, 3H), 1.19 (s, 3H), 0.10 (s, 9H).

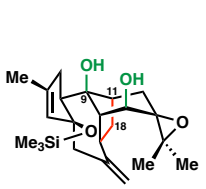
^{13}C NMR: (151 MHz, C_6D_6) δ 146.8, 135.7, 131.3, 131.0, 129.7, 129.0, 128.7, 126.2, 126.0, 116.2, 86.5, 76.9, 72.8, 67.8, 63.7, 50.2, 47.4, 45.3, 45.2, 37.4, 33.9, 22.3, 21.9, 16.9, 16.6, 2.1, 2.0.

HRMS (m/z): (ESI) calcd. for $C_{29}H_{42}O_4{}^{23}Na^{32}S^{28}Si$ $[M+Na]^+$: 537.2465, found 537.2471.

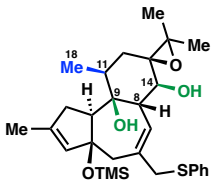
*Alcohol **2.3.46b**:*

TLC: R_f = 0.39 (50% EtOAc/hexanes)

^{1}H NMR: (600 MHz, C_6D_6) δ 5.96 (ddt, *J* = 17.2, 10.2, 6.8 Hz, 1H), 5.38 (d, *J* = 6.0 Hz, 1H), 5.33 (s, 1H), 5.06 (dd, *J* = 17.1, 1.8 Hz, 1H), 4.99 (dd, *J* = 10.2, 1.7 Hz, 2H), 4.33 (s, 1H), 3.94 (d, *J* = 11.2 Hz, 1H), 0.13 (s, 9H). *Note only select peaks are reported as the others are obscured.*



2.3.50



2.3.54

Tricycle 2.3.54 and tetracycle 2.3.50:

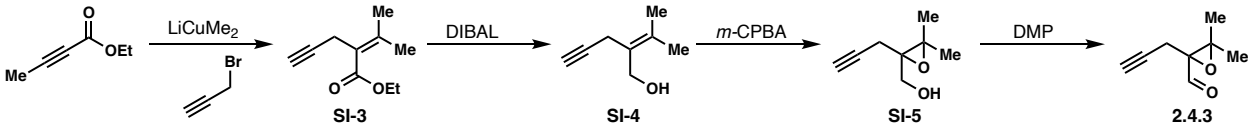
Synthesized from alkene **2.3.8b** (30 mg, 59 μmol) using general procedure B. After purification (5 to 60% EtOAc/hexanes) the major product, tricycle **2.3.54** (11 mg, 21 μmol, 37%) was separated from tetracycle **2.3.50** (3 mg, 7 μmol, 12%).

*Tricycle **2.3.54**:*

TLC: R_f = 0.72 (50% EtOAc/hexanes)

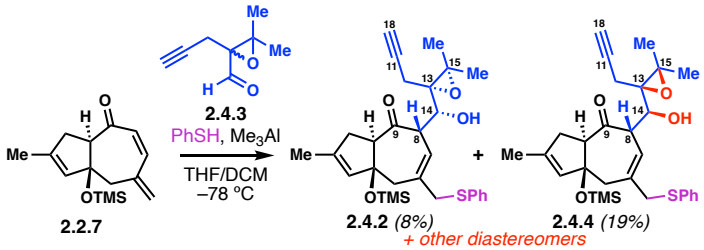
^{1}H NMR: (600 MHz, C_6D_6) δ 7.22 (dt, *J* = 8.3, 1.5 Hz, 2H), 7.03 – 6.97 (m, 2H), 6.89 (tt, *J* = 7.1, 1.2 Hz, 1H), 5.92 (dd, *J* = 7.3, 1.9 Hz, 1H), 5.22 (s, 1H), 4.58 (d, *J* = 10.0 Hz, 1H), 3.96 (d, *J* = 7.2 Hz, 1H), 3.79 (dt, *J* = 10.0, 2.0 Hz, 1H), 3.68 (s, 1H), 3.45 (d, *J* = 13.3 Hz, 1H), 2.97 – 2.92 (m, 1H), 2.75 (d, *J* = 17.6 Hz, 1H), 2.69 (d, *J* = 17.8 Hz, 1H), 2.59 (dd, *J* = 16.2, 8.2 Hz, 1H), 2.53 – 2.46 (m, 1H), 1.81 (dd, *J* = 16.2, 7.6 Hz, 1H), 1.66 (t, *J* = 8.2 Hz, 1H), 1.56 – 1.51 (m, 1H), 1.50 (s, 3H), 1.46 (s, 3H), 1.26 (s, 3H), 1.16 (ddd, *J* = 14.3, 3.8, 1.6 Hz, 1H), 0.90 (d, *J* = 6.7 Hz, 3H), 0.05 (s, 9H).

^{13}C NMR: (151 MHz, C_6D_6) δ 144.3, 135.6, 134.9, 131.5, 131.2, 129.0, 128.7, 126.3, 88.2, 77.6, 72.7, 65.7, 60.3, 54.5, 49.5, 43.9, 42.3, 37.7, 36.2, 30.7, 20.6, 20.3, 17.9, 16.6, 2.0.
HRMS (m/z): (ESI) calcd. for $C_{29}H_{42}O_4{}^{23}Na^{32}S^{28}Si$ $[M+Na]^+$: 537.2465, found 537.2461.
*Tetracycle **2.3.50**:*
TLC: R_f = 0.49 (50% EtOAc/hexanes)
^{1}H NMR: (600 MHz, C_6D_6) δ 5.22 (s, 1H), 4.86 (t, *J* = 2.0 Hz, 1H), 4.68 (t, *J* = 2.0 Hz, 1H), 3.79 (s, 1H), 3.54 (d, *J* = 2.5 Hz, 1H), 3.25 (br s, 1H), 3.18 (dd, *J* = 10.1, 4.3 Hz, 1H), 2.85 – 2.71 (m, 1H), 2.66 (d, *J* = 14.4 Hz, 1H), 2.60 (d, *J* = 14.9 Hz, 1H), 2.43 (d, *J* = 14.9 Hz, 1H), 2.35 (dd, *J* = 13.9, 10.2 Hz, 1H), 1.97 – 1.86 (m, 2H), 1.72 (m, 1H), 1.68 (dd, *J* = 13.1, 5.6 Hz, 1H), 1.60 (s, 3H), 1.29 (s, 3H), 1.28 (m, 1H), 1.15 (s, 3H), 0.16 (s, 9H).
^{13}C NMR: (151 MHz, C_6D_6) δ 150.4, 144.9, 132.0, 112.9, 86.0, 80.3, 79.1, 63.5, 60.2, 58.3, 48.3, 46.7, 46.7, 43.3, 37.1, 30.0, 20.6, 20.4, 16.9, 2.1.
HRMS (m/z): (ESI) calcd. for $C_{23}H_{36}O_4{}^{23}Na^{28}Si$ $[M+Na]^+$: 427.2275, found 427.2270.

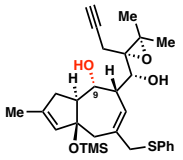


Alkyne-containing type III aldehyde 2.4.3:
Synthesized using general procedure C as follows:
*Ester **SI-3**:*
Propargyl bromide was used to quench the cuprate arising from ethyl 2-butynoate (4.75 g, 42. 4 mmol) in step C1 of general procedure C, resulting in ester **SI-3** (6.76 g, 40.7 mmol, 96%).
TLC: R_f = 0.77 (25% EtOAc/hexanes)
^{1}H NMR: (600 MHz, $CDCl_3$) δ 4.21 (q, *J* = 7.1 Hz, 2H), 3.20 (d, *J* = 2.5 Hz, 2H), 2.06 (s, 3H), 1.94 (t, *J* = 2.7 Hz, 1H), 1.90 (s, 3H), 1.29 (t, *J* = 7.1 Hz, 3H).
^{13}C NMR: (151 MHz, $CDCl_3$) δ 167.7, 147.1, 122.5, 81.7, 67.9, 60.3, 23.1, 22.7, 19.3, 14.2.
*Allylic alcohol **SI-4**:*
Reduction of ester **SI-3** (4.76 g, 28.7 mmol) according to step C2 of general procedure C resulted in allylic alcohol **SI-4** (2.96 g, 23.9 mmol, 83%).
TLC: R_f = 0.26 (25% EtOAc/hexanes)
^{1}H NMR: (600 MHz, $CDCl_3$) δ 4.25 (s, 2H), 3.06 (s, 2H), 1.98 (t, *J* = 2.7 Hz, 1H), 1.77 (s, 3H), 1.74 (s, 3H), 1.71 (br s, 1H).
^{13}C NMR: (151 MHz, $CDCl_3$) δ 132.0, 126.8, 82.8, 68.2, 61.7, 20.7, 20.3, 19.8.
HRMS (m/z): (ESI) calcd. for $C_8H_{12}O^{23}Na$ $[M+Na]^+$: 147.0780, found 147.0780.
*Epoxide **SI-5**:*
Epoxidation of allylic alcohol **SI-4** (1.4 g, 11 mmol) according to step C3 of general procedure C resulted in epoxide **SI-5** (600 mg, 4.30 mmol, 39%).
TLC: R_f = 0.22 (25% EtOAc/hexanes)
^{1}H NMR: (600 MHz, $CDCl_3$) δ 3.89 (d, *J* = 12.0 Hz, 1H), 3.78 (d, *J* = 12.0 Hz, 1H), 2.91 (dd, *J* = 17.1, 2.7 Hz, 1H), 2.32 (br s, 1H, OH), 2.29 (m, 1H), 2.04 (t, *J* = 2.7 Hz, 1H), 1.39 (s, 3H), 1.36 (s, 3H).
^{13}C NMR: (151 MHz, $CDCl_3$) δ 79.6, 70.6, 65.8, 62.9, 62.4, 20.9, 20.6, 20.5.
HRMS (m/z): (ESI) calcd. for $C_8H_{12}O_2{}^{23}Na$ $[M+Na]^+$: 163.0730, found 163.0729.
*Type III aldehyde **2.4.3**:*
Oxidation of epoxide **SI-5** (600 mg, 4.30 mmol) according to step C4 of general procedure C resulted in type III aldehyde **2.4.3** (370 mg, 2.65 mmol, 62%).

TLC: R_f = 0.69 (25% EtOAc/hexanes)
^{1}H NMR: (600 MHz, $CDCl_3$) δ 9.53 (s, 1H), 2.74 (dd, *J* = 17.3, 2.8 Hz, 1H), 2.65 (dd, *J* = 17.3, 2.7 Hz, 1H), 2.05 (t, *J* = 2.7 Hz, 1H), 1.47 (s, 3H), 1.46 (s, 3H).
^{13}C NMR: (151 MHz, $CDCl_3$) δ 199.9, 78.1, 70.9, 67.3, 64.5, 21.5, 20.3, 18.3.

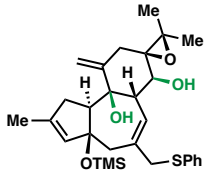


Alkyne-containing cyclization precursors 2.4.2 and 2.4.4:
Synthesized from **2.2.7** (767 mg, 2.9 mmol) and type III aldehyde **2.4.3** (800 mg, 5.8 mmol) according to general procedure A. Purification with column chromatography (5 to 60% EtOAc/hexanes) resulted in tentative desired C14-epimer **2.4.2** (115 mg, 0.228 mmol, 8%) and undesired C14-epimer **2.4.4** (274 mg, 0.540 mmol, 19%) alongside other tentative diastereomeric products.
*Aldol product **2.4.2**:*
TLC: R_f = 0.55 (50% EtOAc/hexanes)
^{1}H NMR: (600 MHz, C_6D_6) δ 7.30 (dd, *J* = 8.3, 1.2 Hz, 2H), 7.02 – 6.95 (m, 2H), 6.94 – 6.87 (m, 1H), 5.58 (s, 1H), 5.19 (s, 1H), 4.27 (dd, *J* = 7.3, 1.8 Hz, 1H), 4.08 (dd, *J* = 9.3, 2.2 Hz, 1H), 4.01 (d, *J* = 2.6 Hz, 1H), 3.39 (d, *J* = 13.4 Hz, 1H), 3.35 (dd, *J* = 17.8, 2.7 Hz, 1H), 3.31 (d, *J* = 13.4 Hz, 1H), 3.10 (t, *J* = 8.0 Hz, 1H), 3.00 – 2.90 (m, 1H), 2.75 (d, *J* = 18.0 Hz, 1H), 2.48 (d, *J* = 17.9 Hz, 1H), 2.25 (dd, *J* = 17.8, 2.4 Hz, 1H), 2.00 (dd, *J* = 16.8, 8.0 Hz, 1H), 1.65 (t, *J* = 2.8 Hz, 1H), 1.48 (s, 3H), 1.33 (s, 3H), 1.21 (s, 3H), 0.10 (s, 9H).
^{13}C NMR: (151 MHz, C_6D_6) δ 209.7, 144.3, 136.7, 134.0, 130.7, 129.7, 129.0, 126.6, 123.6, 84.7, 80.5, 73.6, 71.1, 66.2, 62.3, 60.2, 55.0, 45.5, 45.5, 36.0, 21.7, 21.7, 19.9, 16.4, 1.9.
HRMS (m/z): (ESI) calcd. for $C_{29}H_{39}O_4{}^{32}S^{28}Si$ $[M+H]^+$: 511.2333, found 511.2343.
*Undesired C14 epimer **2.4.4**:*
TLC: R_f = 0.60 (50% EtOAc/hexanes)
^{1}H NMR: (600 MHz, C_6D_6) δ 7.39 (dd, *J* = 8.2, 1.0 Hz, 2H), 7.10 – 7.02 (m, 2H), 6.94 (t, *J* = 7.4 Hz, 1H), 5.95 (s, 1H), 5.19 (s, 1H), 4.88 (dd, *J* = 5.5, 3.1 Hz, 1H), 4.05 (s, 1H), 3.47 (d, *J* = 13.3 Hz, 1H), 3.38 (d, *J* = 13.3 Hz, 1H), 3.26 (t, *J* = 8.0 Hz, 1H), 3.11 (dd, *J* = 16.3, 7.3 Hz, 1H), 2.85 (d, *J* = 18.1 Hz, 1H), 2.77 (dd, *J* = 17.4, 2.7 Hz, 1H), 2.58 (d, *J* = 18.1 Hz, 1H), 2.39 (d, *J* = 5.5 Hz, 1H), 2.24 (dd, *J* = 17.4, 2.8 Hz, 1H), 2.03 (dd, *J* = 16.9, 8.1 Hz, 1H), 1.71 (t, *J* = 2.7 Hz, 1H), 1.46 (s, 3H), 1.28 (s, 3H), 1.21 (s, 3H), 0.08 (s, 9H).
^{13}C NMR: (151 MHz, C_6D_6) δ 207.4, 144.2, 136.7, 134.3, 131.1, 129.5, 129.0, 126.5, 123.7, 85.2, 80.6, 72.1, 71.1, 65.5, 62.6, 60.8, 54.8, 45.7, 45.7, 36.0, 21.7, 21.6, 20.7, 16.4, 1.8.



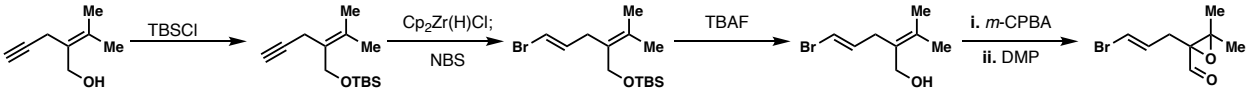
Secondary alcohol 2.4.6:

This product was observed when desired cyclization precursor **2.4.2** (30 mg, 59 μmol) was subjected to general procedure B. After purification by column chromatography (20 to 60% EtOAc/hexanes) reduction product **2.4.6** (9 mg, 18 μmol, 30%) was isolated.
TLC: R_f = 0.45 (50% EtOAc/hexanes)
^{1}H NMR: (600 MHz, C_6D_6) δ 7.31 (dd, *J* = 8.3, 1.1 Hz, 2H), 7.04 – 6.98 (m, 2H), 6.94 – 6.88 (m, 1H), 5.54 (d, *J* = 6.3 Hz, 1H), 5.36 (s, 1H), 4.36 – 4.31 (m, 1H), 3.87 (d, *J* = 11.2 Hz, 1H), 3.64 (dt, *J* = 10.9, 5.3 Hz, 1H), 3.39 (d, *J* = 13.6 Hz, 1H), 3.31 (d, *J* = 13.5 Hz, 1H), 3.17 (dd, *J* = 17.6, 2.7 Hz, 1H), 2.66 (d, *J* = 17.2 Hz, 1H), 2.47 – 2.37 (m, 3H), 2.25 – 2.16 (m, 3H), 1.71 (t, *J* = 2.8 Hz, 1H), 1.57 (s, 3H), 1.29 (s, 3H), 1.22 (s, 3H), 0.16 (s, 9H).
^{13}C NMR: (151 MHz, C_6D_6) δ 144.7, 137.6, 134.6, 132.1, 129.9, 129.0, 126.1, 125.2, 84.0, 80.4, 73.4, 73.0, 71.0, 67.9, 64.7, 53.1, 45.9, 44.9, 42.9, 41.0, 21.8, 21.8, 19.8, 16.7, 2.1.
HRMS (m/z): (ESI) calcd. for $C_{29}H_{40}O_4{}^{23}Na^{32}S^{28}Si$ $[M+Na]^+$: 535.2309, found 535.2315.



2.4.9

Tricycle 2.4.9:
This product was obtained when undesired C14-epimer **2.4.4** (128 mg, 0.25 mmol) was subjected to general procedure B. Note that 10 equiv. of SmI_2 were used, without a change in the other reaction parameters. After purification (10 to 50% EtOAc/hexanes, note the allylic alcohol product **2.4.9** is unstable on silica) the titular compound **2.4.9** (73 mg, 0.14 mmol, 40%) was isolated.
TLC: 0.61 (50% EtOAc/hexanes)
^{1}H NMR: (600 MHz, C_6D_6) δ 7.26 (dd, *J* = 8.3, 1.1 Hz, 2H), 7.05 – 7.00 (m, 2H), 6.92 – 6.89 (m, 1H), 5.77 (d, *J* = 5.5 Hz, 1H), 5.26 (s, 1H), 5.00 (d, *J* = 1.2 Hz, 1H), 4.94 (s, 1H), 4.71 (s, 1H), 4.37 (d, *J* = 8.8 Hz, 1H), 3.94 (dd, *J* = 8.8, 3.4 Hz, 1H), 3.74 (s, 1H), 3.37 (d, *J* = 13.3 Hz, 1H), 3.06 (d, *J* = 13.3 Hz, 1H), 2.90 (d, *J* = 14.2 Hz, 1H), 2.79 – 2.74 (m, 1H), 2.73 (s, 1H), 2.72 (s, 1H), 2.37 (t, *J* = 8.8 Hz, 1H), 2.08 (d, *J* = 14.2 Hz, 1H), 1.87 (dd, *J* = 16.5, 7.6 Hz, 1H), 1.55 (s, 3H), 1.51 (s, 3H), 1.26 (s, 3H), 0.04 (s, 9H).
^{13}C NMR: (151 MHz, C_6D_6) δ 146.1, 144.7, 136.3, 134.9, 131.4, 130.5, 129.0, 126.2, 112.9, 87.1, 77.9, 75.2, 67.6, 61.2, 51.4, 51.1, 44.7, 43.3, 35.2, 32.6, 21.3, 21.1, 16.7, 1.9.
HRMS (m/z): (ESI) calcd. for $C_{29}H_{40}O_4{}^{23}Na^{32}S^{28}Si$ $[M+Na]^+$: 535.2309, found 535.2302.



SI-4 **SI-6** **SI-7** **SI-8** **2.4.14**

(*E*)-vinyl bromide-containing type III aldehyde 2.4.14:
This aldehyde was synthesized in 5 steps from allylic alcohol **SI-4** as follows:
*Allylic silanol **SI-6**:*
An oven-dried 250 mL round-bottom flask was charged with allylic alcohol **SI-4** (960 mg, 7.70 mmol, 1.0 equiv.), DCM (77 mL), and imidazole (1.30 g, 15.4 mmol, 2.0 equiv.). Then, TBSCl (1.4 g, 9.2 mmol, 1.2 equiv.) was added, upon which the clear reaction mixture turned into a white suspension. The reaction mixture was stirred at room temperature until conversion was complete, as judged by TLC, and was then quenched with satd. *aq.* $NaHCO_3$ (70 mL). The layers

were separated and the aqueous layer was extracted with DCM (3 x 70 mL). The combined organic layers were dried over Na_2SO_4 and concentrated under reduced pressure. The crude reaction product was purified by column chromatography (0 to 40% Et_2O/hexanes) to yield pure silanol **SI-6** (1.6 g, 6.7 mmol, 87%) as a pale yellow oil.

TLC: 0.75 (10% EtOAc/hexanes)

^{1}H NMR: (600 MHz, $CDCl_3$) δ 4.26 (s, 2H), 3.03 (d, *J* = 2.4 Hz, 2H), 1.91 (t, *J* = 2.7 Hz, 1H), 1.75 (s, 3H), 1.73 (s, 3H), 0.91 (s, 9H), 0.08 (s, 6H).

^{13}C NMR: (151 MHz, $CDCl_3$) δ 130.0, 127.2, 83.1, 67.3, 61.2, 26.0, 20.8, 20.2, 18.5, 18.4, -5.3.

*(E)-vinyl bromide **SI-7**:*

An oven-dried 100 mL round-bottom flask was charged with solid Schwartz's reagent (790 mg, 3.06 mmol, 1.25 equiv.) and PhH (20 mL). A solution of silanol **SI-6** (578 mg, 2.42 mmol, 1.0 equiv.) in PhH (10 mL) was added dropwise and the resulting beige suspension was stirred at room temperature for 90 minutes, during which time a gradual change to an orange solution was observed. At this point solid NBS (550 mg, 3.09 mmol, 1.25 equiv.) was added and the reaction mixture, which changed color from orange to yellow, was stirred for 30 minutes before being quenched with H_2O (30 mL). The layers were separated and the aqueous layer was extracted with Et_2O (3 x 30 mL). The combined organic layers were dried over Na_2SO_4 and concentrated under reduced pressure. The crude reaction product was purified by column chromatography (0 to 40% Et_2O/hexanes) to yield pure (*E*)-vinyl bromide **SI-7** (700 mg, 2.19 mmol, 90%) as a pale yellow oil.

TLC: 0.75 (10% EtOAc/hexanes)

^{1}H NMR: (600 MHz, $CDCl_3$) δ 6.14 (dt, *J* = 13.6, 6.8 Hz, 1H), 5.98 (dt, *J* = 13.5, 1.5 Hz, 1H), 4.13 (s, 1H), 4.13 (s, 1H), 2.88 (s, 1H), 2.87 (s, 1H), 1.71 (s, 3H), 1.68 (s, 3H), 0.90 (s, 9H), 0.06 (s, 6H).

^{13}C NMR: (151 MHz, $CDCl_3$) δ 135.9, 129.9, 128.3, 104.5, 61.7, 33.1, 26.0, 20.6, 20.1, 18.4, -5.3.

*Allylic alcohol **SI-8**:*

An oven-dried 100 mL round-bottom flask was charged with (*E*)-vinyl bromide **SI-7** (700 mg, 2.2 mmol, 1.0 equiv.) and THF (22 mL). A solution of TBAF (2.2 mL, 1.0 M in THF, 2.2 mmol, 1.0 equiv.) was added and stirring was continued until all silanol **SI-7** was consumed. The reaction mixture was quenched with H_2O (20 mL) and the layers were separated. The aqueous layer was extracted with Et_2O (3 x 20 mL) and the combined organic layers were dried over Na_2SO_4 and concentrated under reduced pressure. The crude residue was purified by column chromatography (20 to 80% Et_2O/hexanes) to provide pure allylic alcohol **SI-8** (400 mg, 2.0 mmol, 90%) as a yellow oil.

TLC: 0.33 (25% EtOAc/hexanes)

^{1}H NMR: (600 MHz, $CDCl_3$) δ 6.15 (dt, *J* = 13.6, 6.8 Hz, 1H), 6.04 (d, *J* = 13.5 Hz, 1H), 4.13 (s, 1H), 4.13 (s, 1H), 2.91 (s, 1H), 2.90 (s, 1H), 1.77 (s, 3H), 1.71 (s, 3H).

^{13}C NMR: (151 MHz, $CDCl_3$) δ 135.6, 132.5, 128.2, 105.0, 61.9, 34.0, 20.6, 20.2.

*Epoxide **SI-9**:*

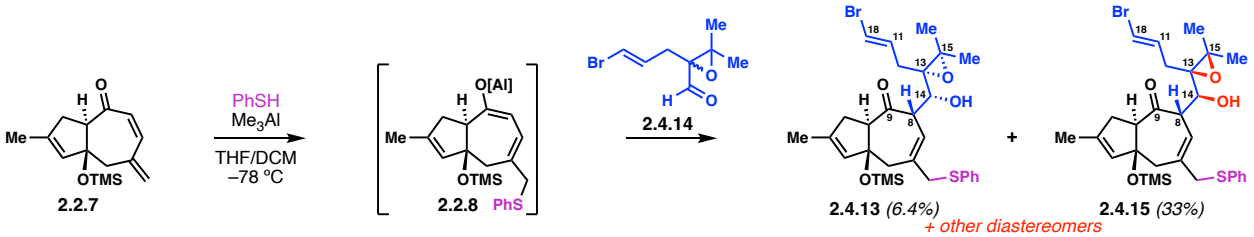
Allylic alcohol **SI-8** (400 mg, 2.0 mmol) was epoxidized according to step C3 of general procedure C, resulting in epoxide **SI-9** (220 mg, 1.0 mmol, 50%) as a yellow oil.

TLC: 0.28 (25% EtOAc/hexanes)

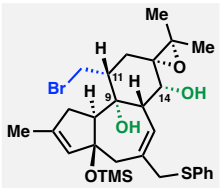
^{1}H NMR: (600 MHz, $CDCl_3$) δ 6.24 – 6.15 (m, 2H), 3.72 (q, *J* = 11.8 Hz, 2H), 2.75 – 2.70 (m, 1H), 2.28 – 2.22 (m, 1H), 1.39 (s, 3H), 1.37 (s, 3H).

^{13}C NMR: (151 MHz, $CDCl_3$) δ 132.4, 107.5, 65.6, 62.9, 62.4, 33.9, 21.2, 20.6.

*Aldehyde **2.4.14**:*
Epoxide **SI-9** (220 mg, 1.0 mmol) was oxidized according to step C4 of general procedure C, resulting in desired (*E*)-vinyl bromide-containing type III aldehyde **2.4.14** (110 mg, 0.50 mmol, 50%) as a yellow oil.
TLC: 0.75 (25% EtOAc/hexanes)
^{1}H NMR: (600 MHz, $CDCl_3$) δ 9.46 (s, 1H), 6.18 (dd, *J* = 4.2, 0.9 Hz, 2H), 2.78 – 2.72 (m, 1H), 2.36 (dd, *J* = 15.2, 4.9 Hz, 1H), 1.46 (s, 3H), 1.43 (s, 3H).
^{13}C NMR: (151 MHz, $CDCl_3$) δ 201.4, 131.2, 108.2, 67.9, 64.4, 30.9, 21.9, 20.6.



(*E*)-vinyl bromide-containing cyclization substrates 2.4.13 and 2.4.15:
Reaction of enone **2.2.7** (132 mg, 0.500 mmol) and type III aldehyde **2.4.14** (219 mg, 1.00 mmol) according to general procedure A followed by purification via column chromatography (5 to 60% EtOAc/hexanes) resulted in formation of desired C14-epimer **2.4.13** (19 mg, 0.032 mmol, 6.4%) and undesired C14-epimer **2.4.15** (100 mg, 0.169 mmol, 33%) alongside other tentative diastereomer products.
*Desired cyclization substrate **2.4.13**:*
TLC: R_f = 0.56 (50% EtOAc/hexanes)
^{1}H NMR: (600 MHz, C_6D_6) δ 7.25 (d, *J* = 7.5 Hz, 2H), 6.98 (t, *J* = 7.7 Hz, 2H), 6.88 (t, *J* = 7.4 Hz, 1H), 6.34 (ddd, *J* = 13.6, 8.9, 6.0 Hz, 1H), 5.91 (d, *J* = 13.6 Hz, 1H), 5.25 (s, 1H), 5.19 (s, 1H), 4.08 (s, 2H), 3.90 (s, 1H), 3.37 (d, *J* = 14.0 Hz, 1H), 3.25 (d, *J* = 14.0 Hz, 1H), 3.09 – 2.99 (m, 2H), 2.86 (dd, *J* = 17.0, 8.2 Hz, 1H), 2.80 (d, *J* = 18.0 Hz, 1H), 2.69 (dd, *J* = 15.8, 8.9 Hz, 1H), 2.46 (d, *J* = 18.0 Hz, 1H), 2.17 (ddd, *J* = 15.7, 6.0, 1.8 Hz, 1H), 2.01 (dd, *J* = 16.8, 8.1 Hz, 1H), 1.46 (s, 3H), 1.14 (s, 3H), 1.06 (s, 3H), 0.08 (s, 9H).
^{13}C NMR: (151 MHz, C_6D_6) δ 210.4, 144.1, 136.3, 135.5, 134.8, 131.5, 130.7, 129.8, 129.1, 122.2, 106.2, 84.5, 74.1, 65.7, 62.1, 60.0, 55.0, 45.9, 44.7, 35.9, 32.7, 21.8, 21.5, 16.4, 1.9.
*Undesired C14-epimer **2.4.15**:*
TLC: R_f = 0.59 (50% EtOAc/hexanes)
^{1}H NMR: (600 MHz, C_6D_6) δ 7.37 (dt, *J* = 8.3, 1.6 Hz, 2H), 7.07 – 7.02 (m, 2H), 6.94 (tt, *J* = 7.0, 1.2 Hz, 1H), 6.33 (ddd, *J* = 14.1, 8.0, 6.3 Hz, 1H), 5.85 (dt, *J* = 13.7, 1.5 Hz, 1H), 5.83 – 5.81 (m, 1H), 5.20 (s, 1H), 4.60 (dd, *J* = 5.4, 3.1 Hz, 1H), 4.11 (s, 1H), 3.49 (d, *J* = 13.2 Hz, 1H), 3.33 (d, *J* = 13.2 Hz, 1H), 3.14 (t, *J* = 8.1 Hz, 1H), 2.99 (ddd, *J* = 16.8, 8.1, 1.1 Hz, 1H), 2.82 (d, *J* = 18.3 Hz, 1H), 2.60 (d, *J* = 18.1 Hz, 1H), 2.46 (ddd, *J* = 15.7, 6.3, 1.7 Hz, 1H), 2.12 (ddd, *J* = 15.7, 8.1, 1.3 Hz, 1H), 2.09 – 2.03 (m, 2H), 1.46 (s, 3H), 1.16 (s, 3H), 1.00 (s, 3H), 0.07 (s, 9H).
^{13}C NMR: (151 MHz, C_6D_6) δ 208.4, 143.9, 136.6, 134.7, 134.3, 131.3, 129.8, 129.0, 126.6, 123.6, 106.5, 84.9, 70.9, 65.2, 62.5, 60.6, 54.6, 45.6, 36.0, 34.0, 21.6, 20.7, 16.4, 1.9.
HRMS (m/z): (ESI) calcd. for $C_{29}H_{40}O_4{}^{79}Br^{32}S^{28}Si$ $[M+H]^+$: 591.1594, found 591.1592.



2.4.10 *(< 5%)*

Tricycle 2.4.10:

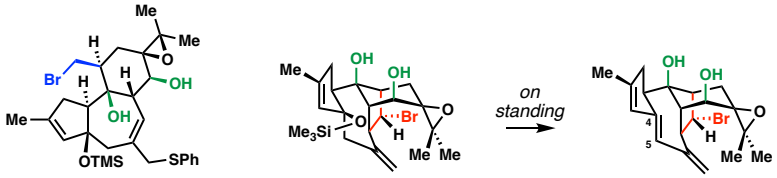
Reaction of desired C14-epimer **2.4.13** (15 mg, 25 μmol) according to general procedure B resulted in trace amounts of tricycle **2.4.10** (0.6 mg, 1 μmol, 4%) detected after preparative TLC. Note the mass recovery in this transformation was very low; although trace olefin isomer **2.4.10b** (see below) was also observed, it could not be isolated as a pure compound in sufficient quantities.

TLC: R_f = 0.62 (50% EtOAc/hexanes)

^{1}H NMR: (600 MHz, C_6D_6) δ 7.25 (dd, *J* = 8.2, 1.2 Hz, 2H), 6.98 (t, *J* = 7.7 Hz, 2H), 6.91 – 6.87 (m, 1H), 5.86 (d, *J* = 4.8 Hz, 1H), 5.24 (s, 1H), 3.97 (d, *J* = 9.7 Hz, 1H), 3.64 – 3.58 (m, 2H), 3.39 (d, *J* = 13.1 Hz, 1H), 3.24 (d, *J* = 3.0 Hz, 1H), 3.17 (d, *J* = 13.1 Hz, 1H), 2.78 (s, 1H), 2.71 – 2.68 (m, 1H), 2.68 (s, 1H), 2.67 (s, 1H), 2.54 (d, *J* = 4.9 Hz, 1H), 2.50 – 2.43 (m, 2H), 2.27 (dd, *J* = 14.6, 6.6 Hz, 1H), 2.10 – 2.04 (m, 1H), 2.01 (dd, *J* = 9.7, 7.0 Hz, 1H), 1.47 (s, 3H), 1.26 (s, 3H), 1.10 (s, 3H), 0.10 (s, 9H).

^{13}C NMR: (151 MHz, C_6D_6) δ 143.9, 136.1, 131.9, 131.4, 128.7, 127.1, 126.5, 84.7, 77.2, 70.1, 66.0, 61.4, 58.2, 46.3, 45.6, 44.2, 43.3, 38.9, 37.2, 29.9, 26.7, 20.7, 19.6, 16.5, 2.1.

HRMS (m/z): (ESI) calcd. for $C_{29}H_{41}O_4{}^{79}Br^{23}Na^{32}S^{28}Si$ $[M+Na]^+$: 615.1570, found 615.1561.



2.4.23 *(16%)* **2.4.21** *(24%)* **2.4.24**

Tricycle 2.4.23, tetracycle 2.4.21, and triene 2.4.24:

Reaction of undesired C14-epimer **2.4.15** (50 mg, 84 μmol) according to general procedure B followed by column chromatography (10 to 60% EtOAc/hexanes) resulted in tricycle **2.4.23** (8 mg, 13 μmol, 16%) and tetracycle **2.4.21** (12 mg, 20 μmol, 24%) as colorless oils. The latter compound was observed to partially decompose to triene **2.4.24** in solution of C_6D_6 while 2D NMR spectra were being obtained.

*Tricycle **2.4.23**:*

TLC: R_f = 0.67 (50% EtOAc/hexanes)

^{1}H NMR: (600 MHz, C_6D_6) δ 7.17 (d, *J* = 3.0 Hz, 2H), 7.09 – 7.01 (m, 3H), 5.82 (d, *J* = 7.4 Hz, 1H), 5.16 (s, 1H), 4.21 (d, *J* = 9.9 Hz, 1H), 3.89 (d, *J* = 7.1 Hz, 1H), 3.73 (d, *J* = 9.9 Hz, 1H), 3.69 (s, 1H), 3.55 (dd, *J* = 9.9, 3.6 Hz, 1H), 3.44 (d, *J* = 13.6 Hz, 1H), 3.25 (t, *J* = 10.2 Hz, 1H), 2.85 (d, *J* = 13.6 Hz, 1H), 2.73 (d, *J* = 17.5 Hz, 1H), 2.57 (d, *J* = 17.5 Hz, 1H), 2.36 (dd, *J* = 17.5, 8.8 Hz, 1H), 2.34 (dd, *J* = 14.3, 12.9 Hz, 1H), 2.12 (dd, *J* = 14.4, 2.1 Hz, 1H), 1.72 (tdd, *J* = 13.0, 4.8, 2.5 Hz, 2H), 1.53 – 1.48 (m, 2H), 1.44 (s, 3H), 1.42 (s, 3H), 1.39 – 1.36 (m, 1H), 1.32 (s, 3H), 0.02 (s, 9H).

^{13}C NMR: (151 MHz, C_6D_6) δ 143.8, 135.6, 134.9, 131.5, 131.5, 128.9, 128.4, 126.9, 88.0, 78.1, 72.7, 65.1, 60.7, 53.8, 49.7, 43.6, 43.5, 41.8, 37.6, 37.5, 26.2, 20.7, 20.1, 16.5, 1.9.

HRMS (m/z): (ESI) calcd. for $C_{29}H_{41}O_4{}^{79}Br^{23}Na^{32}S^{28}Si$ $[M+Na]^+$: 615.1570, found 615.1564.

*Tetracycle **2.4.21**:*

TLC: R_f = 0.44 (50% EtOAc/hexanes)

^{1}H NMR: (600 MHz, C_6D_6) δ 5.45 (d, *J* = 9.8 Hz, 1H), 5.25 (s, 1H), 4.87 (s, 1H), 4.74 (t, *J* = 2.0 Hz, 1H), 3.88 (t, *J* = 3.0 Hz, 1H), 3.68 – 3.63 (m, 1H), 3.37 (d, *J* = 9.8 Hz, 1H), 3.29 (d, *J* = 7.9 Hz, 1H), 3.25 – 3.19 (m, 2H), 3.13 (dd, *J* = 9.7, 7.5 Hz, 1H), 2.80 (d, *J* = 16.0 Hz, 1H), 2.75 – 2.69 (m, 1H), 2.56 (dd, *J* = 14.5, 2.5 Hz, 1H), 2.48 (dt, *J* = 4.7, 2.6 Hz, 1H), 2.04 (dd, *J* = 15.4, 7.4 Hz, 1H), 1.57 (s, 3H), 1.36 (ddd, *J* = 14.4, 4.1, 1.8 Hz, 1H), 1.24 (s, 3H), 1.04 (s, 3H), 0.15 (s, 9H).

^{13}C NMR: (151 MHz, C_6D_6) δ 147.1, 144.2, 131.7, 117.7, 86.5, 79.6, 78.6, 63.3, 59.3, 56.2, 55.4, 53.0, 50.4, 49.3, 49.0, 36.0, 30.0, 20.6, 20.2, 16.8, 2.1.

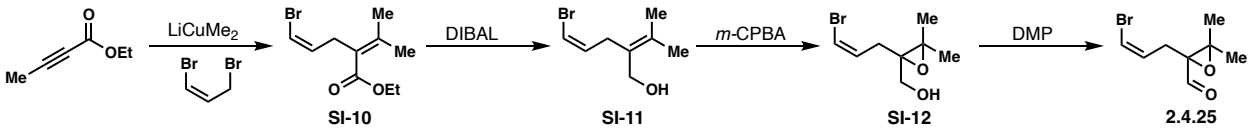
*Triene **2.4.24**:*

^{1}H NMR: (700 MHz, C_6D_6) δ 6.09 (s, 1H), 5.73 (s, 1H), 5.14 (d, *J* = 10.0 Hz, 1H), 4.97 (s, 1H), 4.74 (s, 1H), 3.94 (t, *J* = 6.1 Hz, 1H), 3.91 (s, 1H), 3.47 (s, 1H), 3.34 (d, *J* = 10.0 Hz, 1H), 3.25 – 3.21 (m, 1H), 3.06 (dd, *J* = 17.0, 6.1 Hz, 1H), 2.85 (d, *J* = 6.5 Hz, 1H), 2.61 – 2.59 (m, 1H), 2.56 – 2.54 (m, 1H), 2.51 (d, *J* = 2.7 Hz, 1H), 2.26 (dd, *J* = 17.0, 8.3 Hz, 1H), 1.68 (s, 3H), 1.20 (s, 3H), 1.03 (s, 3H).

^{13}C NMR: (151 MHz, C_6D_6) δ 148.5, 148.1, 146.5, 130.9, 119.9, 115.7, 79.6, 78.8, 62.7, 59.2, 57.5, 53.9, 53.3, 49.4, 48.3, 40.0, 31.5, 20.6, 20.2, 17.0.

TLC: R_f = 0.55 (50% EtOAc/hexanes)

HRMS (m/z): (ESI) calcd. for $C_{20}H_{25}O_3{}^{79}Br^{23}Na^{28}Si$ $[M+Na]^+$: 415.0879, found 415.0878.



(*Z*)-vinyl bromide-containing aldehyde 2.4.25:

Synthesized using general procedure C as follows:

*Ester **SI-10**:*

Known[SI-3] (*Z*)-1,3-dibromoprop-1-ene was used to quench the cuprate arising from ethyl 2-butynoate (1.48 g, 13.2 mmol) in step C1 of general procedure C, resulting in ester **SI-10** (1.75 g, 7.11 mmol, 54%).

TLC: 0.72 (25% EtOAc/hexanes)

^{1}H NMR: (600 MHz, $CDCl_3$) δ 6.15 (dt, *J* = 7.0, 1.8 Hz, 1H), 6.04 (q, *J* = 6.7 Hz, 1H), 4.18 (q, *J* = 7.1 Hz, 2H), 3.19 (d, *J* = 6.6 Hz, 2H), 2.02 (s, 3H), 1.85 (s, 3H), 1.29 (t, *J* = 7.1 Hz, 3H).

^{13}C NMR: (151 MHz, $CDCl_3$) δ 168.7, 145.7, 132.7, 124.2, 107.5, 60.2, 30.8, 23.1, 22.6, 14.3.

*Allylic alcohol **SI-11**:*

Reduction of ester **SI-10** (1.60 g, 6.50 mmol) according to step C2 of general procedure C resulted in allylic alcohol **SI-11** (926 mg, 4.54 mmol, 70%).

TLC: 0.27 (25% EtOAc/hexanes)

^{1}H NMR: (600 MHz, $CDCl_3$) δ 6.16 (dt, *J* = 6.9, 1.6 Hz, 1H), 6.05 (q, *J* = 7.0 Hz, 1H), 4.13 (s, 2H), 3.06 (s, 1H), 3.05 (s, 1H), 1.75 (s, 3H), 1.72 (s, 3H).

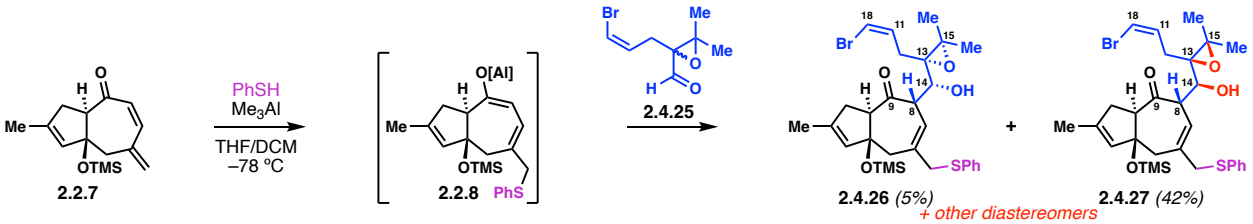
^{13}C NMR: (151 MHz, $CDCl_3$) δ 133.2, 132.0, 128.8, 107.5, 62.0, 31.4, 20.8, 20.2.

HRMS (m/z): (ESI) calcd. for $C_8H_{13}O_1{}^{79}Br^{23}Na$ $[M+Na]^+$: 227.0042, found 227.0043.

*Epoxide **SI-12**:*

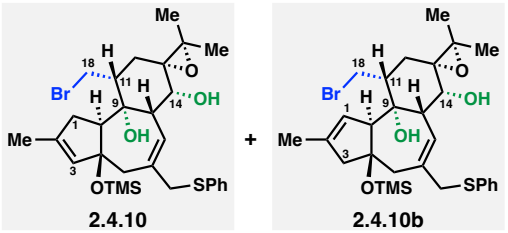
Epoxidation of allylic alcohol **SI-11** (926 mg, 4.54 mmol) according to step C3 of general procedure C resulted in epoxide **SI-12** (805 mg, 3.66 mmol, 81%).

TLC: 0.21 (25% EtOAc/hexanes)
^{1}H NMR: (600 MHz, $CDCl_3$) δ 6.32 (dt, *J* = 7.1, 1.7 Hz, 1H), 6.20 (td, *J* = 7.2, 6.5 Hz, 1H), 3.74 (dd, *J* = 11.8, 4.5 Hz, 1H), 3.69 (dd, *J* = 11.8, 6.2 Hz, 1H), 2.74 (ddd, *J* = 15.4, 6.5, 1.7 Hz, 1H), 2.56 (ddd, *J* = 15.4, 7.5, 1.4 Hz, 1H), 1.85 (t, *J* = 5.7 Hz, 1H), 1.40 (s, 3H), 1.39 (s, 3H).
^{13}C NMR: (151 MHz, $CDCl_3$) δ 129.8, 110.2, 65.7, 63.0, 63.0, 31.2, 21.4, 20.5.
HRMS (m/z): (ESI) calcd. for $C_8H_{13}O_2{}^{79}Br^{23}Na$ $[M+Na]^+$: 242.9991, found 242.9994.
*Type III aldehyde **2.4.25**:*
Oxidation of epoxide **SI-12** (780 mg, 3.55 mmol) according to step C4 of general procedure C resulted in type III aldehyde **2.4.25** (634 mg, 2.91 mmol, 82%).
TLC: 0.68 (25% EtOAc/hexanes)
^{1}H NMR: (600 MHz, $CDCl_3$) δ 9.48 (s, 1H), 6.28 (dt, *J* = 7.1, 1.7 Hz, 1H), 6.14 (td, *J* = 7.2, 6.3 Hz, 1H), 2.92 (ddd, *J* = 15.8, 7.3, 1.6 Hz, 1H), 2.55 (ddd, *J* = 15.8, 6.2, 1.8 Hz, 1H), 1.44 (s, 6H).
^{13}C NMR: (151 MHz, $CDCl_3$) δ 201.4, 128.7, 110.4, 68.1, 64.5, 28.4, 21.8, 20.5.

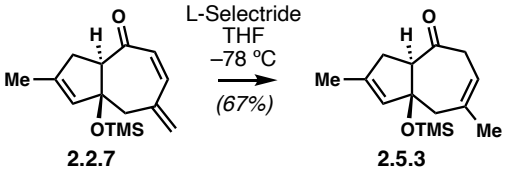


(*Z*)-vinyl bromide-containing cyclization substrates 2.4.26 and 2.4.27:
Reaction of enone **2.2.7** (115 mg, 0.44 mmol) and type III aldehyde **2.4.25** (193 mg, 0.88 mmol) according to general procedure A followed by purification via column chromatography (5 to 60% EtOAc/hexanes) resulted in formation of desired C14-epimer **2.4.26** (12 mg, 0.020 mmol, 4.6%) and undesired C14-epimer **2.4.27** (110 mg, 0.186 mmol, 42%) alongside other tentative diastereomer products.
*Desired C14-epimer **2.4.26**:*
TLC: 0.54 (50% EtOAc/hexanes)
^{1}H NMR: (600 MHz, C_6D_6) δ 7.27 (dd, *J* = 8.1, 1.0 Hz, 2H), 7.07 – 7.01 (m, 2H), 6.97 – 6.91 (m, 1H), 6.48 (td, *J* = 6.9, 5.6 Hz, 1H), 5.85 (dt, *J* = 7.0, 2.1 Hz, 1H), 5.25 – 5.21 (m, 1H), 5.16 (s, 1H), 4.09 (dd, *J* = 9.1, 2.5 Hz, 1H), 4.03 – 3.98 (m, 1H), 3.96 (d, *J* = 2.3 Hz, 1H), 3.25 (d, *J* = 14.0 Hz, 1H), 3.20 (d, *J* = 13.9 Hz, 1H), 3.04 (t, *J* = 8.0 Hz, 1H), 2.96 – 2.90 (m, 1H), 2.78 (d, *J* = 18.3 Hz, 1H), 2.70 (ddd, *J* = 8.2, 6.2, 2.1 Hz, 2H), 2.34 (d, *J* = 18.2 Hz, 1H), 2.01 (dd, *J* = 16.8, 8.1 Hz, 1H), 1.46 (s, 3H), 1.17 (s, 3H), 1.16 (s, 3H), 0.07 (s, 9H).
^{13}C NMR: (151 MHz, C_6D_6) δ 210.3, 144.3, 136.1, 135.3, 132.5, 131.0, 129.5, 129.1, 127.0, 121.6, 107.5, 84.6, 74.7, 65.9, 62.1, 60.3, 55.3, 45.9, 45.3, 36.0, 29.1, 21.8, 21.7, 16.4, 1.8.
HRMS (m/z): (ESI) calcd. for $C_{29}H_{40}O_4{}^{79}Br^{32}S^{28}Si$ $[M+H]^+$: 591.1594, found 591.1607.
*Undesired C14-epimer **2.4.27**:*
TLC: 0.59 (50% EtOAc/hexanes)
^{1}H NMR: (600 MHz, C_6D_6) δ 7.36 (dd, *J* = 8.2, 1.0 Hz, 2H), 7.07 (t, *J* = 7.7 Hz, 2H), 6.95 (t, *J* = 7.4 Hz, 1H), 6.15 (td, *J* = 6.9, 5.4 Hz, 1H), 5.86 (dt, *J* = 7.0, 2.1 Hz, 1H), 5.78 (s, 1H), 5.19 (s, 1H), 4.58 (dd, *J* = 5.2, 3.7 Hz, 1H), 4.12 (s, 1H), 3.48 (d, *J* = 13.2 Hz, 1H), 3.30 (d, *J* = 13.3 Hz, 1H), 3.22 (t, *J* = 8.1 Hz, 1H), 3.04 (dd, *J* = 16.9, 7.9 Hz, 1H), 2.81 (d, *J* = 18.2 Hz, 1H), 2.69 – 2.64 (m, 1H), 2.63 (s, 1H), 2.61 – 2.53 (m, 2H), 2.08 (dd, *J* = 16.9, 8.1 Hz, 1H), 1.46 (s, 3H), 1.28 (s, 3H), 1.12 (s, 3H), 0.08 (s, 9H).

^{13}C NMR: (151 MHz, C_6D_6) δ 208.7, 144.1, 136.4, 134.7, 131.8, 131.4, 129.6, 129.0, 126.7, 123.4, 108.4, 85.0, 72.2, 65.5, 62.7, 60.7, 54.4, 45.6, 36.0, 31.8, 21.7, 20.9, 16.4, 1.8.
HRMS (m/z): (ESI) calcd. for $C_{29}H_{39}O_4{}^{79}Br^{23}Na^{32}S^{28}Si$ $[M+Na]^+$: 613.1414, found 613.1422.

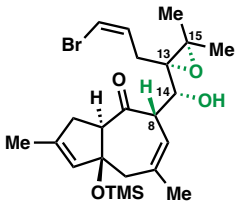


Tricycles 2.4.10 and 2.4.10b:
Reaction of desired C14-epimer **2.4.26** (12 mg, 20 μmol) according to general procedure B generated, after purification by column chromatography (5 to 60% EtOAc/hexanes) tricycles **2.4.20** and **2.4.10b** (4.8 mg, 8 μmol, 40%, 1:1 rr, > 20:1 dr) as a colorless oil.
*Tricycle **2.4.10**:* see above for characterization data.
*Tricycle **2.4.10b**:*
TLC: R_f = 0.62 (50% EtOAc/hexanes)
^{1}H NMR: (700 MHz, C_6D_6) δ 7.25 (dd, *J* = 8.2, 1.2 Hz, 2H), 6.98 (td, *J* = 7.8, 2.3 Hz, 2H), 6.90 – 6.88 (m, 1H), 5.73 (d, *J* = 7.1 Hz, 1H), 5.38 (s, 1H), 4.36 (dd, *J* = 9.4, 3.4 Hz, 1H), 3.66 (s, 1H), 3.46 (dd, *J* = 11.3, 9.4 Hz, 1H), 3.35 (d, *J* = 13.0 Hz, 1H), 3.15 (s, 1H), 2.87 (s, 1H), 2.64 (t, *J* = 5.7 Hz, 1H), 2.62 (s, 1H), 2.60 (d, *J* = 6.8 Hz, 1H), 2.53 (d, *J* = 12.7 Hz, 1H), 2.46 (m, 1H), 2.37 (d, *J* = 16.7 Hz, 1H), 2.30 (d, *J* = 7.0 Hz, 1H), 2.02 (dd, *J* = 9.7, 7.0 Hz, 1H), 1.48 (s, 3H), 1.42 (s, 3H), 1.12 (s, 3H), 0.12 (s, 9H).
^{13}C NMR: (151 MHz, C_6D_6) δ 138.1, 136.1, 135.9, 133.0, 131.0, 128.7, 126.5, 125.5, 83.6, 77.3, 73.7, 67.4, 63.1, 62.7, 53.7, 48.2, 46.9, 46.4, 43.1, 37.8, 26.7, 20.9, 20.7, 16.4, 2.0.
HRMS (m/z): (ESI) calcd. for $C_{29}H_{40}O_4{}^{79}Br^{32}S^{28}Si$ $[M+H]^+$: 591.1594, found 591.1607.



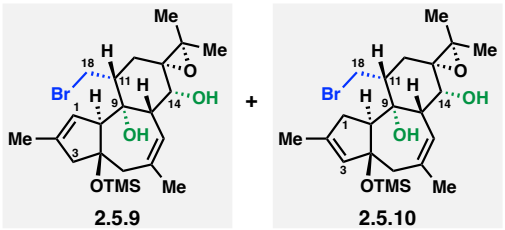
Ketone 2.5.3:
An oven-dried 100 mL round-bottom flask was charged with enone **2.2.7** (274 mg, 1.05 mmol, 1.0 equiv.) and THF (10.5 mL). The resulting solution was cooled to –78 °C and a solution of L-Selectride (1.26 mL, 1.0 M, 1.26 mmol, 1.2 equiv.) was added dropwise down the side of the flask. After conversion of enone **2.2.7** was complete as judged by TLC, the reaction mixture was quenched with satd. *aq.* NH_4Cl (10 mL) and allowed to warm to room temperature. The layers were separated and the aqueous layer was extracted with Et_2O (3 x 10 mL). The combined organic layers were dried over Na_2SO_4 and concentrated under reduced pressure. The resulting crude material was purified by column chromatography (0 to 20% EtOAc/hexanes) to provide pure ketone **2.5.3** (184 mg, 0.70 mmol, 67%) as a colorless oil.
TLC: R_f = 0.77 (25% EtOAc/hexanes)
^{1}H NMR: (600 MHz, C_6D_6) δ 5.14 (s, 1H), 5.12 (ddt, *J* = 6.0, 2.8, 1.4 Hz, 1H), 3.51 (dp, *J* = 20.6, 2.6 Hz, 1H), 3.21 – 3.12 (m, 1H), 3.07 (t, *J* = 7.9 Hz, 1H), 2.93 (dd, *J* = 20.6, 7.8 Hz, 1H),

2.49 (d, J = 18.1 Hz, 1H), 2.10 – 2.03 (m, 1H), 2.00 (dd, J = 16.9, 8.2 Hz, 1H), 1.59 (s, 3H), 1.49 (s, 3H), 0.04 (s, 9H).
^{13}C NMR: (151 MHz, C_6D_6) δ 206.0, 144.3, 132.9, 129.5, 117.5, 85.1, 60.5, 48.8, 43.2, 35.8, 26.8, 16.5, 1.8.
HRMS (m/z): (ESI) calcd. for $C_{15}H_{25}O_2{}^{28}Si$ $[M+H]^+$: 265.1618, found 265.1619.



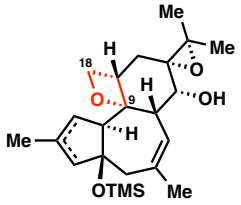
2.5.6 *(45%, 10:1 dr at C8 and C14)*

Aldol product 2.5.6:
A small reaction tube was charged with ketone **2.5.3** (17 mg, 65 µmol, 1.0 equiv.) and THF (0. 65 mL) and the resulting solution was cooled to –78 ºC. A solution of LHMDS (0.078 mL, 1.0 M in THF, 78 µmol, 1.2 equiv.) was added and stirring was continued for 30 minutes, after which time a solution of aldehyde **2.4.25** (28 mg, 0.13 mmol, 2.0 equiv.) in THF (0.4 mL) was added dropwise. After 5 minutes the reaction mixture was quenched with AcOH (20 µL, 0.33 mmol, 5 equiv.) and satd. *aq*. $NaHCO_3$ (1.5 mL) and was allowed to warm to room temperature. The layers were separated and the aqueous layer was extracted with EtOAc (3 x 1.5 mL). The combined organic layers were dried over Na_2SO_4 and concentrated under reduced pressure. Purification by column chromatography (10 to 60% EtOAc/hexanes) provided pure desired aldol product **2.5.6** (14 mg, 29 µmol, 45%) alongside the C13,C15 bis-epimer **2.5.6b** (12 mg, 26 µmol, 40%) as yellow oils.
*Desired aldol product **2.5.6**:*
TLC: R_f = 0.60 (50% EtOAc/hexanes)
^{1}H NMR: (600 MHz, C_6D_6) δ 6.52 (td, J = 6.9, 5.3 Hz, 1H), 5.87 (dt, J = 7.0, 2.1 Hz, 1H), 5.16 (dd, J = 3.4, 1.6 Hz, 1H), 5.13 (s, 1H), 4.16 (dd, J = 9.2, 2.4 Hz, 1H), 4.01 (d, J = 7.5 Hz, 2H), 3.06 (t, J = 8.0 Hz, 1H), 2.98 (dd, J = 16.7, 8.0 Hz, 1H), 2.90 (ddd, J = 16.8, 7.0, 1.8 Hz, 1H), 2.84 (ddd, J = 16.9, 5.4, 2.3 Hz, 1H), 2.50 (d, J = 18.2 Hz, 1H), 2.05 – 1.97 (m, 2H), 1.58 (s, 3H), 1.47 (s, 3H), 1.23 (s, 3H), 1.23 (s, 3H), 0.06 (s, 9H).
^{13}C NMR: (151 MHz, C_6D_6) δ 210.6, 144.1, 135.5, 132.5, 129.6, 118.2, 107.6, 84.7, 74.8, 66.0, 62.1, 60.2, 55.3, 48.3, 36.0, 29.2, 27.4, 21.9, 21.6, 16.4, 1.8.



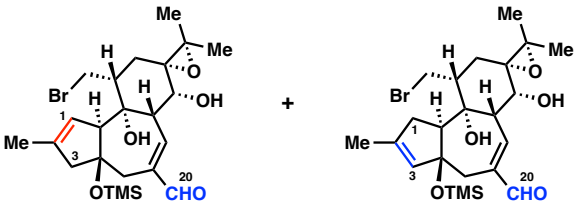
Tricycles 2.5.9 and 2.5.10:
Aldol product **2.5.6** (37 mg, 77 µmol) was subjected to general procedure B, resulting in tricycles **2.5.9** and **2.5.10** (21 mg, 44 µmol, 57%, 1.4:1 **2.5.9**:**2.5.10**) after purification (5 to 60% EtOAc/hexanes).
TLC: R_f = 0.52 (50% EtOAc/hexanes)

2.5.9 – **bold**
2.5.10 – underlined
Overlap of **2.5.9** and **2.5.10** signals/ambiguous - normal
^{1}H NMR: (700 MHz, C_6D_6) δ 5.93 (d, *J* = 6.1 Hz, 1H), **5.82** (d, *J* = 7.1 Hz, 1H), **5.57** (s, 1H), 5.18 (s, 1H), **4.87** (br s, 1H), **4.48** (dd, *J* = 9.3, 3.4 Hz, 1H), 4.10 (d, *J* = 10.8 Hz, 1H), 3.90 (br s, 1H), **3.84** (s, 1H), 3.79 (s, 1H), 3.61 (t, 1H), **3.57** (dd, *J* = 11.3, 9.4 Hz, 1H), 3.41 (s, 1H), **3.31** (s, 1H), 2.93 (br s, 1H), 2.88 (br s, 1H), **2.77** (d, *J* = 6.7 Hz, 1H), 2.73 – 2.67 (m), 2.64 – 2.55 (m), 2.51 (m), 2.40 – 2.31 (m), 2.28 (m), 2.20 (d, *J* = 18.1 Hz, 1H), 2.16 (m), **1.97** (d, *J* = 19.6 Hz, 1H), 1.63 (s, 3H), **1.59** (s, 3H), **1.49** (s, 3H), 1.47 (s, 3H), **1.44** (s, 3H), 1.28 (s, 3H), **1.15** (s, 3H), 1.10 (s, 3H), **0.12** (s, 9H), 0.10 (s, 9H).
^{13}C NMR: (151 MHz, C_6D_6) δ 143.9, **138.7**, 136.6, **132.8**, 131.9, **126.2**, **123.4**, 122.9, 85.1, **83.5**, 77.9, 77.6, **74.2**, 71.1, 67.8, 66.5, 63.5, 62.9, 62.1, 58.3, **54.8**, 49.7, 49.4, 48.4, **46.6**, 46.3, 43.7, 39.3, 38.1, 37.7, 27.0, 26.8, 25.4, 25.3, 20.9, 20.7, 20.7, 19.8, 16.5, 16.4, 2.2, 2.0.
HRMS (m/z): (ESI) calcd. for $C_{23}H_{37}O_4{}^{79}Br^{23}Na^{28}Si$ $[M+Na]^+$: 507.1537, found 507.1537.



2.5.12 *(mixture of isomers)*

Oxetane 2.5.12:
An oven-dried reaction tube was charged with tricycles **2.5.9** and **2.5.10** (5.3 mg, 11 μmol, 1.0 equiv.) and MeOH (0.2 mL). An excess of freshly ground Mg^0 turnings (5.3 mg, 220 μmol, 20 equiv.) were added and the reaction mixture was stirred vigorously at room temperature. After 60 minutes the reaction mixture was diluted with Et_2O (2 mL) and quenched with satd. aq. NH_4Cl (2 mL). The layers were separated and the aqueous layer was extracted with Et_2O (3 x 2 mL). The combined organic layers were dried over Na_2SO_4 and concentrated under reduced pressure. The crude reaction residue was purified by column chromatography (5 to 50 % EtOAc/hexanes) to provide oxetane **2.5.12** (1.2 mg, 3.9 μmol, 35%) as a mixture of olefin isomers.
TLC: R_f = 0.59 (50% EtOAc/hexanes)
Major isomer – **bold**
Minor isomer – underlined
Overlap – normal
^{1}H NMR: (600 MHz, C_6D_6) δ **6.24** (s, 1H), 6.21 (s, 1H), 5.82 (s, 1H), **5.24** (s, 1H), 4.94 (dd, *J* = 6.2, 4.4 Hz, 1H), **4.87** (dd, *J* = 6.1, 4.1 Hz, 1H), 4.55 (t, *J* = 6.9 Hz, 1H), **4.44** (t, *J* = 6.7 Hz, 1H), 4.15 (dd, *J* = 11.7, 4.1 Hz, 1H), 4.11 – 4.07 (m), **3.98** (d, *J* = 11.3 Hz, 1H), 3.35 (m), 3.27 (s, 1H), 2.85 (m), 2.81 (m), 2.70 – 2.64 (m), 2.58 (s, 1H), 2.55 (s, 2H), 2.40 – 2.32 (m), 2.18 (d, *J* = 18.3 Hz, 2H), 2.12 (d, *J* = 4.3 Hz, 1H), **2.10** (d, *J* = 4.2 Hz, 1H), **2.07** (d, *J* = 4.4 Hz, 1H), 2.05 (s, 1H), 1.67 (s, 3H), **1.65** (s, 3H), 1.63 (s, 3H), **1.57** (s, 3H), **1.49** (d, *J* = 2.5 Hz, 1H), 1.47 (d, *J* = 2.6 Hz, 1H), **1.42** (s, 3H), 1.42 (s, 3H), **1.21** (s, 3H), 1.19 (s, 3H), **0.04** (s, 9H), 0.04 (s, 9H).
^{13}C NMR: (151 MHz, C_6D_6) δ 143.5, 137.8, 135.4, 135.1, 131.8, 124.7, 123.0, 122.9, 93.0, 91.9, 85.0, 83.6, 71.6, 71.1, 68.7, 68.5, 63.9, 62.6, 58.3, 54.8, 54.2, 49.1, 43.3, 42.7, 36.5, 35.9, 35.7, 27.8, 27.7, 26.1, 26.0, 20.1, 20.0, 19.9, 16.8, 16.7, 2.2, 2.0.



2.5.13 *(0 – 25%)* **2.5.14** *(50%)*

Aldehydes 2.5.13 and 2.5.14:

An oven-dried reaction tube was charged with copolar tricycles 2.5.9 and 2.5.10 (6 mg, 12 µmol, 1.0 equiv.), THF (0.2 mL), and SeO_2 (10 mg, 90 µmol, 7.5 equiv.). The resulting mixture was stirred at 50 ºC for 90 minutes or until conversion was complete as judged by TLC. The reaction mixture was transferred directly onto a silica gel column; EtOAc (0.2 mL) was used to wash the reaction vessel and ensure quantitative transfer. Elution with 0 to 80% EtOAc/hexanes resulted in a mixture of aldehydes **2.5.13** and **2.5.14** (1.8 mg, 3.6 µmol, 30% combined yield) as a dark yellow oil.

TLC: R_f = 0.38 (50% EtOAc/hexanes).

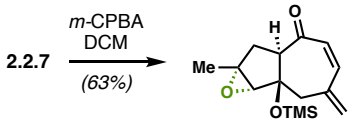
2.5.14 – **bold**

2.5.13 – underlined

Overlapping peaks - normal

^{1}H NMR: (600 MHz, C_6D_6) δ **9.34** (s, 1H), 9.26 (s, 1H), **6.80** (dd, *J* = 5.8, 2.4 Hz, 1H), 6.59 (dd, *J* = 6.9, 2.7 Hz, 1H), 5.40 (s, 1H), **5.14** (s, 1H), 4.51 (s, 1H), 4.35 (dd, *J* = 9.5, 3.4 Hz, 1H), 4.24 (t, *J* = 6.7 Hz, 1H), **3.93** (d, *J* = 10.6 Hz, 1H), **3.64 – 3.58** (m), 3.45 (dd, *J* = 11.3, 9.6 Hz, 1H), **3.34** (s, 1H), 3.24 (s, 1H), **3.15** (d, *J* = 18.6 Hz, 1H), 3.04 (d, *J* = 6.8 Hz, 1H), 2.89 (s, 1H), 2.73 – 2.67 (m), 2.66 – 2.62 (m), 2.55 (m), 2.48 – 2.41 (m), 2.36 – 2.22 (m), 2.14 – 2.00 (m), 1.98 (d, *J* = 18.4 Hz, 1H), **1.39** (s, 3H), 1.39 (s, 3H), 1.39 (s, 3H), **1.23** (s, 3H), 1.10 (s, 3H), **1.08** (s, 3H), 0.29 (s, 9H), **0.21** (s, 9H).

^{13}C NMR: (151 MHz, C_6D_6) δ 193.1, 192.2, 150.0, 145.1, 143.8, 143.5, 134.2, 131.2, 130.6, 124.9, 84.1, 82.5, 78.2, 77.8, 72.9, 69.2, 66.9, 65.5, 63.3, 63.0, 61.6, 58.0, 54.0, 48.3, 47.3, 45.8, 44.8, 40.2, 39.7, 38.4, 37.4, 26.5, 26.4, 20.8, 20.6, 19.5, 16.4, 16.2, 2.0, 1.7.



2.6.7

Epoxide 2.6.7:

*From enone **2.2.7**:*

An oven-dried reaction tube was charged with enone **2.2.7** (75 mg, 0.28 mmol, 1.0 equiv.), $NaHCO_3$ (47 mg, 0.56 mmol, 2.0 equiv.) and DCM (2.8 mL). Then, *m*-CPBA (62.6 mg, 0.364 mmol, 1.3 equiv.) was added and stirring was continued at room temperature until conversion was complete as judged by TLC. At this point the reaction mixture was quenched with satd. *aq.* $NaHCO_3$ (3 mL) and satd. *aq.* $Na_2S_2O_3$ (3 mL). The organic layer was separated and the aqueous layer was extracted with DCM (3 x 3 mL). The combined organic layers were dried over Na_2SO_4 and concentrated under reduced pressure. The crude reaction product was purified by flash column chromatography (10 to 30% EtOAc/hexanes in 5% increments) to provide pure epoxide **2.6.7** (49.0 mg, 0.175 mmol, 63% yield) as a colorless oil.

*One-step procedure from secondary alcohol **2.2.6**:* An oven-dried 50 mL round-bottom flask was charged with secondary alcohol **2.2.6** (215 mg, 0.814 mmol, 1.0 equiv.), $NaHCO_3$ (138 mg, 1.62 mmol, 2.0 equiv.) and DCM (8.0 mL). Dess-Martin periodinane (385 mg, 0.908 mmol, 1.1 equiv.) was added and within 3 minutes full conversion to the enone was observed by TLC. At this point *m*-CPBA (224 mg, 1.30 mmol, 1.6 equiv.) was added and stirring was continued at room temperature until conversion to the A ring epoxide was complete as judged by TLC. The reaction mixture was quenched with satd. *aq.* $NaHCO_3$ (5 mL) and satd. *aq.* $Na_2S_2O_3$ (5 mL). The organic layer was separated and the aqueous layer was extracted with DCM (3 x 10 mL). The combined organic layers were dried over Na_2SO_4 and concentrated under reduced pressure. The crude reaction product was purified by flash column chromatography (10 to 30% EtOAc/hexanes in 5% increments) to provide pure epoxide **2.6.7** (136 mg, 0.489 mmol, 60% yield) as a colorless oil.

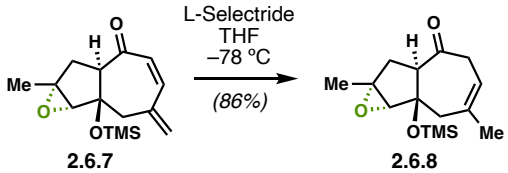
TLC: R_f = 0.52 (25% EtOAc/hexanes)

^{1}H NMR (600 MHz, C_6D_6): δ 6.20 (dd, *J* = 13.1, 0.9 Hz, 1H), 5.89 (d, *J* = 12.9 Hz, 1H), 4.97 (d, *J* = 2.3 Hz, 1H), 4.88 (dt, *J* = 2.2, 1.1 Hz, 1H), 2.96 (s, 1H), 2.84 (dt, *J* = 16.4, 2.5 Hz, 1H), 2.76 – 2.68 (m, 2H), 2.49 (dd, *J* = 14.2, 9.9 Hz, 1H), 2.04 (dd, *J* = 14.2, 7.4 Hz, 1H), 1.25 (s, 3H), -0.03 (s, 8H).

^{13}C NMR (150 MHz, C_6D_6): δ 196.4, 142.0, 140.9, 128.9, 126.5, 80.7, 67.6, 63.3, 59.2, 43.1, 32.5, 17.4, 2.0.

IR (thin film) ν_{max} (cm^{-1}): 2959, 2935, 1663, 1595, 1446, 1249, 1111, 1050, 838.

HRMS (m/z): (EI) calcd. for $C_{15}H_{22}O_3Si$ $[M]^+$: 278.1338, found 278.1339.



2.6.7 **2.6.8**

Ketone 2.6.8:

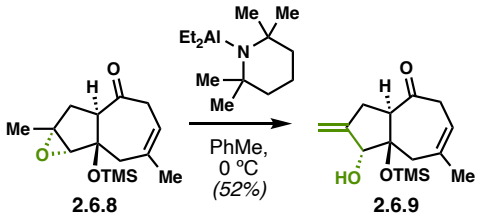
An oven-dried 50 mL round-bottom flask was charged with enone **2.6.7** (210 mg, 0.76 mmol, 1.0 equiv.) and THF (7.6 mL). The resulting solution was cooled to –78 ºC and a solution of L-Selectride (0.90 mL, 1.0 M, 0.90 mmol, 1.2 equiv.) was added dropwise down the side of the flask. After conversion of enone **2.6.7** was complete as judged by TLC, the reaction mixture was quenched with satd. *aq.* NH_4Cl (10 mL) and allowed to warm to room temperature. The layers were separated and the aqueous layer was extracted with Et_2O (3 x 10 mL). The combined organic layers were dried over Na_2SO_4 and concentrated under reduced pressure. The resulting crude material was purified by column chromatography (0 to 25% EtOAc/hexanes) to provide pure ketone **2.6.8** (180 mg, 0.65 mmol, 86%) as a colorless oil.

TLC: R_f = 0.55 (25% EtOAc/hexanes)

^{1}H NMR: (600 MHz, C_6D_6) δ 5.00 (ddt, *J* = 6.0, 2.9, 1.4 Hz, 1H), 3.27 (dt, *J* = 20.2, 2.6 Hz, 1H), 3.01 (s, 1H), 2.85 (dd, *J* = 20.2, 7.8 Hz, 1H), 2.80 (t, *J* = 8.7 Hz, 1H), 2.59 (d, *J* = 18.5 Hz, 1H), 2.46 (dd, *J* = 14.3, 9.4 Hz, 1H), 2.34 (d, *J* = 18.4 Hz, 1H), 2.01 (dd, *J* = 14.3, 7.9 Hz, 1H), 1.52 (s, 3H), 1.24 (s, 3H), -0.01 (s, 9H).

^{13}C NMR: (151 MHz, C_6D_6) δ 206.0, 132.7, 116.8, 81.6, 67.5, 64.5, 57.7, 43.5, 42.9, 32.3, 26.5, 17.4, 1.9.

HRMS (m/z): (ESI) calcd. for $C_{15}H_{24}O_3{}^{23}Na^{28}Si$ $[M+Na]^+$: 303.1387, found 303.1385.



2.6.8 2.6.9

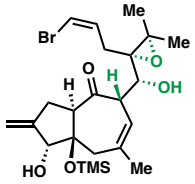
Allylic alcohol 2.6.9:

Diethylaluminum 2,2,6,6-tetramethylpiperidide was prepared according to a modified literature procedure.[SI-4] An oven-dried 25 mL round-bottom flask was charged with 2,2,6,6-tetramethylpiperidine (0.322 mL, 1.9 mmol, 3 equiv.) and toluene (4.0 mL). This solution was cooled to 0 ºC and a solution of *n*-BuLi (0.770 mL, 2.5 M in hexanes, 1.9 mmol, 3.0 equiv.) was added dropwise and stirring was continued for 30 minutes at 0 ºC, during which time the reaction mixture transitions from clear colorless solution to bright yellow suspension. Then, a solution of diethylaluminum chloride (1.9 mL, 1 M in hexanes, 1.9 mmol, 3.0 equiv.) was added, upon which the yellow color disappeared. The resulting white suspension was stirred for 40 minutes at 0 ºC and a solution of epoxide **2.6.8** (180 mg, 0.640 mmol, 1.0 equiv.) in toluene (2 mL) was added. Stirring at 0 ºC was continued for 15 minutes or until consumption of the starting material was complete as judged by TLC, at which point the reaction mixture was quenched with satd. *aq.* Rochelle's salt (15 mL) and diluted with EtOAc (8 mL). The resulting suspension was stirred vigorously for 30 minutes and allowed to settle in order for phase separation to occur. The layers were separated and the aqueous layer was extracted with EtOAc (3 x 10 mL). The combined organic layers were dried over Na_2SO_4 and concentrated under reduced pressure. Purification by column chromatography (10 to 50% EtOAc/hexanes) resulted in pure allylic alcohol **2.6.9** (93 mg, 0.333 mmol, 52%) as a yellow oil.

TLC: R_f = 0.73 (50% EtOAc/hexanes)

^{1}H NMR: (600 MHz, C_6D_6) δ 5.12 (ddq, *J* = 7.2, 4.3, 1.3 Hz, 1H), 4.92 (t, *J* = 2.4 Hz, 1H), 4.86 (s, 1H), 3.92 (d, *J* = 3.0 Hz, 1H), 3.27 (ddq, *J* = 18.0, 4.1, 2.0 Hz, 1H), 3.12 (ddt, *J* = 16.6, 9.7, 2.4 Hz, 1H), 3.08 – 3.02 (m, 1H), 2.89 (dd, *J* = 18.0, 7.0 Hz, 1H), 2.82 (d, *J* = 17.9 Hz, 1H), 2.48 (ddt, *J* = 17.3, 9.4, 2.1 Hz, 1H), 2.36 (d, *J* = 17.8 Hz, 1H), 1.64 (s, 3H), 0.90 (br s, 1H, OH), 0.03 (s, 9H).

^{13}C NMR: (151 MHz, C_6D_6) δ 205.6, 152.5, 134.6, 116.8, 110.7, 84.8, 82.7, 58.8, 43.4, 40.8, 30.1, 26.7, 1.9.



2.6.12 (X=Br)

Aldol product 2.6.12:

An oven-dried 10 mL round-bottom flask was charged with allylic alcohol **2.6.9** (40 mg, 0.14 mmol, 1.0 equiv.) and THF (1.4 mL) and the resulting solution was cooled to –78 ºC. A solution of LHMDS (0.36 mL, 1.0 M in THF, 0.36 µmol, 2.5 equiv.) was added and stirring was continued for 30 minutes, after which time a solution of aldehyde **2.4.25** (60 mg, 0.28 mmol, 2.0 equiv.) in THF (0.5 mL) was added dropwise. After 5 minutes the reaction mixture was quenched with AcOH (40 µL, 0.70 mmol, 5 equiv.) and satd. *aq.* $NaHCO_3$ (3 mL) and was allowed to warm to room temperature. The layers were separated and the aqueous layer was

extracted with EtOAc (3 x 3 mL). The combined organic layers were dried over Na_2SO_4 and concentrated under reduced pressure. Purification by column chromatography (10 to 70% EtOAc/hexanes) provided pure desired aldol product **2.6.12** (40 mg, 80 µmol, 54%) alongside the C13,C15 bis-epimer **2.6.12b** (24 mg, 49 µmol, 35%) as yellow oils.

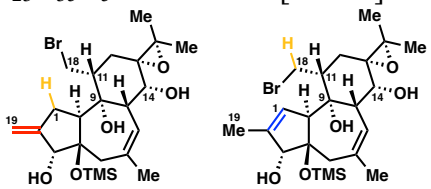
*Desired aldol product **2.6.12**:*

TLC: R_f = 0.49 (50% EtOAc/hexanes)

^{1}H NMR: (600 MHz, C_6D_6) δ 6.34 (td, *J* = 7.0, 5.5 Hz, 1H), 5.84 (dt, *J* = 7.1, 2.0 Hz, 2H), 5.10 (d, *J* = 6.3 Hz, 1H), 4.94 (s, 1H), 4.88 (s, 1H), 4.20 (d, *J* = 10.1 Hz, 1H), 3.91 (s, 1H), 3.74 – 3.64 (m, 1H), 3.32 (dd, *J* = 10.6, 8.5 Hz, 1H), 3.22 (br s, 1H, OH), 3.04 (ddt, *J* = 16.7, 10.7, 2.6 Hz, 1H), 2.93 – 2.86 (m, 2H), 2.69 (ddd, *J* = 16.9, 5.4, 2.3 Hz, 1H), 2.52 – 2.41 (m, 2H), 1.66 (s, 3H), 1.20 (s, 3H), 1.14 (s, 3H), 0.10 (s, 9H).

^{13}C NMR: (151 MHz, C_6D_6) δ 207.4, 152.2, 137.9, 132.1, 118.3, 111.8, 107.9, 85.2, 82.0, 73.5, 66.5, 62.9, 56.7, 56.0, 40.6, 29.9, 29.5, 27.0, 21.9, 21.5, 2.1.

HRMS (m/z): (ESI) calcd. for $C_{23}H_{35}O_5{}^{79}Br^{23}Na^{28}Si$ $[M+Na]^+$: 521.1329, found 521.1332.



Tricycles 2.6.16 and 2.6.19:

When ketone **2.6.12** (33 mg, 0.066 mmol) was subjected to general procedure B, a mixture of tricyclic products was obtained. After purification by column chromatography (10 to 70% EtOAc/hexanes), exocyclic olefin **2.6.16** (12 mg, 0.024 mmol, 37%) was separated from desired trisubstituted olefin **2.6.19** (6 mg, 0.012 mmol, 18%).

*Exocyclic olefin **2.6.16**:*

TLC: R_f = 0.55 (50% EtOAc/hexanes)

^{1}H NMR: (600 MHz, C_6D_6) δ 5.46 (s, 1H), 4.98 (s, 1H), 4.93 (s, 1H), 3.83 (dd, *J* = 10.6, 1.5 Hz, 1H), 3.75 (s, 1H), 3.61 (s, 1H), 3.45 – 3.33 (m, 2H), 2.82 (m, 2H), 2.61 – 2.53 (m, 1H), 2.49 (dd, *J* = 15.0, 6.6 Hz, 1H), 2.34 (t, *J* = 6.8 Hz, 1H), 2.33 – 2.26 (m, 1H), 2.22 (td, *J* = 9.8, 5.4 Hz, 1H), 2.15 (s, 1H), 2.02 (dd, *J* = 13.4, 3.6 Hz, 1H), 1.78 (s, 3H), 1.26 (s, 3H), 1.12 (s, 3H), 0.04 (s, 9H).

^{13}C NMR: (151 MHz, C_6D_6) δ 152.3, 136.0, 124.0, 111.9, 86.0, 81.3, 76.5, 73.6, 66.6, 61.8, 55.0, 47.9, 45.4, 40.8, 38.4, 32.5, 25.7, 25.6, 20.5, 20.0, 1.9.

HRMS (m/z): (ESI) calcd. for $C_{23}H_{37}O_5{}^{79}Br^{23}Na^{28}Si$ $[M+Na]^+$: 523.1486, found 523.1482.

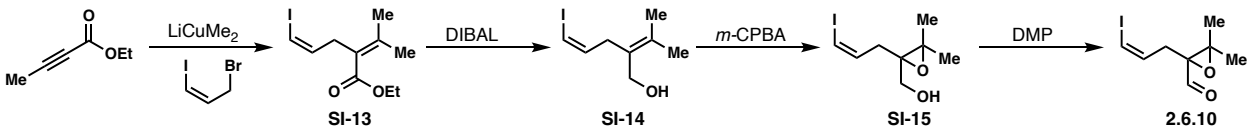
*Trisubstituted olefin **2.6.19**:*

TLC: R_f = 0.50 (50% EtOAc/hexanes)

^{1}H NMR: (600 MHz, $CDCl_3$) δ 5.73 (s, 1H), 5.65 (d, *J* = 7.4 Hz, 1H), 3.99 (dd, *J* = 9.3, 3.5 Hz, 1H), 3.91 (s, 1H), 3.88 (s, 1H), 3.35 – 3.30 (m, 1H), 3.20 (s, 1H), 2.93 (d, *J* = 16.4 Hz, 1H), 2.55 (d, *J* = 8.1 Hz, 1H), 2.51 (d, *J* = 10.8 Hz, 1H), 2.38 (d, *J* = 17.5 Hz, 1H), 2.33 (d, *J* = 13.2 Hz, 1H), 2.00 (d, *J* = 14.1 Hz, 1H), 1.83 (s, 3H), 1.83 (s, 3H), 1.45 (s, 3H), 1.37 (s, 3H), 0.15 (s, 9H).

^{13}C NMR: (151 MHz, $CDCl_3$) δ 141.6, 136.5, 130.2, 121.7, 85.1, 84.7, 76.6, 73.9, 67.6, 64.3, 59.5, 47.8, 47.0, 42.3, 37.1, 26.2, 24.5, 21.0, 20.8, 14.7, 2.2.

HRMS (m/z): (ESI) calcd. for $C_{23}H_{37}O_5{}^{79}Br^{23}Na^{28}Si$ $[M+Na]^+$: 523.1486, found 523.1487.



(Z)-vinyl iodide-containing type III aldehyde 2.6.10:

Synthesized using general procedure C as follows:

*Ester **SI-13**:*

Known[SI-5] (*Z*)-3-bromo-1-iodoprop-1-ene was used to quench the cuprate arising from ethyl 2-butynoate (0.650 mL, 5.59 mmol) in step C1 of general procedure C, resulting in ester **SI-13** (1.29 g, 4.38 mmol, 78%).

TLC: R_f = 0.62 (25% EtOAc/hexanes)

^{1}H NMR (400 MHz, $CDCl_3$): δ 6.22 (dt, *J* = 7.4, 1.7 Hz, 1H), 6.12 (ddd, *J* = 7.6, 6.8, 6.0 Hz, 1H), 4.19 (q, *J* = 7.1 Hz, 2H), 3.17 – 3.10 (m, 2H), 2.03 (s, 3H), 1.86 (s, 3H), 1.30 (t, *J* = 7.1 Hz, 3H).

^{13}C NMR (150 MHz, C_6D_6) δ 168.0, 146.1, 139.7, 124.7, 82.0, 60.0, 36.3, 23.2, 22.7, 14.4.

IR (thin film) ν_{max} (cm^{-1}): 2980, 2932, 1709, 1472, 1369, 1286, 1203, 1166, 1074, 949.

HRMS (m/z): (EI) calcd. for $C_{10}H_{15}O_2{}^{127}I$: 294.0117, found 294.0119.

*Allylic alcohol **SI-14**:*

Reduction of ester **SI-13** (1.29 g, 4.38 mmol) according to step C2 of general procedure C resulted in allylic alcohol **SI-14** (843 mg, 3.34 mmol, 76%).

TLC: R_f = 0.32 (25% EtOAc/hexanes)

^{1}H NMR (600 MHz, $CDCl_3$): δ 6.23 (dt, *J* = 7.3, 1.6 Hz, 1H), 6.14 (q, *J* = 6.9 Hz, 1H), 4.15 (d, *J* = 3.1 Hz, 2H), 3.04 – 3.00 (m, 2H), 1.77 (s, 3H), 1.74 (s, 3H), 1.26 (br s, 1H).

^{13}C NMR (150 MHz, $CDCl_3$): δ 139.8, 132.5, 128.9, 82.5, 62.4, 36.8, 21.2, 20.4.

IR (thin film) ν_{max} (cm^{-1}): 3500, 2978, 2931, 1374, 1254, 1151, 1039, 758.

HRMS (m/z): (EI) calcd. for $C_8H_{13}O_2{}^{127}I$: 252.0011, found 252.0010.

*Epoxide **SI-15**:*

Epoxidation of allylic alcohol **SI-14** (563 mg, 2.33 mmol) according to step C3 of general procedure C resulted in epoxide **SI-15** (455 mg, 1.70 mmol, 81%).

TLC: R_f = 0.31 (25% EtOAc/hexanes)

^{1}H NMR (400 MHz, $CDCl_3$): δ 6.41 (dq, *J* = 7.6, 1.5 Hz, 1H), 6.29 (td, *J* = 7.3, 6.3 Hz, 1H), 3.74 (dd, *J* = 11.8, 1.4 Hz, 1H), 3.68 (dd, *J* = 11.8, 1.1 Hz, 1H), 2.71 (ddd, *J* = 15.5, 6.3, 1.7 Hz, 1H), 2.48 (ddt, *J* = 15.5, 7.2, 1.6 Hz, 1H), 1.41 (s, 3H), 1.39 (s, 3H).

^{13}C NMR (150 MHz, $CDCl_3$): δ 136.6, 85.2, 65.9, 63.2, 63.2, 36.4, 21.7, 20.7.

IR (thin film) ν_{max} (cm^{-1}): 3411, 3002, 2960, 2928, 1412, 1320, 1277, 1121, 1033, 844.

HRMS (m/z): (EI) calcd. for $C_8H_{13}O_2{}^{127}I$: 267.9960, found 267.9958.

*Type III aldehyde **2.6.10**:*

Oxidation of epoxide **SI-15** (400 mg, 1.49 mmol) according to step C4 of general procedure C resulted in type III aldehyde **2.6.10** (304 mg, 1.14 mmol, 77%).

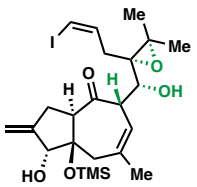
TLC: R_f = 0.64 (25% EtOAc/hexanes)

^{1}H NMR (700 MHz, $CDCl_3$): δ 9.49 (s, 1H), 6.40 (dt, *J* = 7.5, 1.7 Hz, 1H), 6.27 – 6.22 (m, 1H), 2.87 (ddd, *J* = 15.8, 7.1, 1.5 Hz, 1H), 2.51 (ddd, *J* = 15.8, 6.1, 1.7 Hz, 1H), 1.46 (s, 3H), 1.45 (s, 2H).

^{13}C NMR (150 MHz, C_6D_6): δ 201.6, 135.4, 85.5, 68.3, 64.7, 33.6, 22.2, 20.7.

IR (thin film) ν_{max} (cm^{-1}): 3001, 2928, 2831, 1710, 1400, 1278, 1120, 837, 764.

HRMS (m/z): (EI) calcd. for $C_8H_{11}O_2{}^{127}I$: 265.9804, found 265.9803.



2.6.13

Aldol product 2.6.13:

Prepared analogously to **2.6.12** from **2.6.9** (23 mg, 82 μmol) and aldehyde **2.6.10** (41.4 mg, 0.164 mmol) to provide desired C13,C15 epimer **2.6.13** (20 mg, 39 μmol, 47%) and undesired C13,C15 epimer **2.6.13b** (18 mg, 33 μmol, 40%).

*Desired aldol product **2.6.13**:*

TLC: R_f = 0.45 (50% EtOAc/hexanes)

^{1}H NMR: (600 MHz, C_6D_6) δ 6.43 (td, *J* = 7.1, 5.3 Hz, 1H), 5.92 (dt, *J* = 7.4, 2.1 Hz, 1H), 5.14 – 5.09 (m, 1H), 4.94 (t, *J* = 2.4 Hz, 1H), 4.89 (s, 1H), 4.19 (dd, *J* = 10.1, 2.9 Hz, 1H), 3.92 (d, *J* = 1.9 Hz, 2H), 3.68 (dd, *J* = 9.0, 6.6 Hz, 1H), 3.33 (dd, *J* = 10.6, 8.5 Hz, 1H), 3.21 (d, *J* = 3.0 Hz, 1H), 3.05 (ddt, *J* = 16.3, 10.6, 2.7 Hz, 1H), 2.91 (d, *J* = 17.0 Hz, 1H), 2.80 (ddd, *J* = 16.9, 6.9, 1.7 Hz, 1H), 2.63 (ddd, *J* = 16.9, 5.2, 2.3 Hz, 1H), 2.51 – 2.42 (m, 2H), 1.67 (s, 3H), 1.67 (s, 3H), 1.20 (s, 3H), 1.14 (s, 3H), 0.10 (s, 9H).

^{13}C NMR: (151 MHz, C_6D_6) δ 207.2, 152.2, 138.5, 137.9, 118.3, 111.8, 85.3, 82.9, 82.1, 73.5, 66.6, 63.0, 56.7, 56.0, 40.7, 34.7, 29.9, 27.1, 21.9, 21.6, 2.2, 2.1.

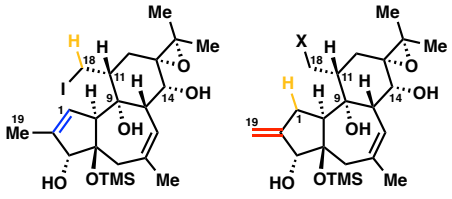
HRMS (m/z): (ESI) calcd. for $C_{23}H_{35}O_5{}^{127}I{}^{23}Na{}^{28}Si$ $[M+Na]^+$: 569.1191, found 569.1194.

*Undesired C13,C15 epimer **2.6.13b**:*

TLC: R_f = 0.53 (50% EtOAc/hexanes)

^{1}H NMR: (600 MHz, C_6D_6) δ 6.72 – 6.66 (m, 1H), 5.98 (dt, *J* = 7.4, 2.2 Hz, 1H), 5.77 (dd, *J* = 3.3, 1.8 Hz, 1H), 4.91 (t, *J* = 2.4 Hz, 1H), 4.87 (s, 1H), 4.58 – 4.54 (m, 1H), 4.21 (d, *J* = 9.8 Hz, 1H), 3.90 – 3.84 (m, 1H), 3.79 – 3.72 (m, 1H), 3.29 (dd, *J* = 10.6, 8.6 Hz, 1H), 2.87 – 2.77 (m, 3H), 2.68 (d, *J* = 16.5 Hz, 1H), 2.60 – 2.55 (m, 1H), 2.54 – 2.45 (m, 1H), 2.42 (d, *J* = 8.6 Hz, 1H), 2.40 – 2.37 (m, 1H), 1.77 (s, 3H), 1.64 (s, 1H), 1.42 (s, 3H), 1.19 (s, 3H), 0.11 (s, 9H).

^{13}C NMR: (151 MHz, C_6D_6) δ 213.8, 151.9, 139.5, 138.6, 120.0, 111.9, 85.2, 82.6, 81.4, 74.7, 64.9, 60.9, 56.5, 55.0, 41.4, 36.0, 29.3, 25.4, 21.7, 20.4, 2.2, 1.9.



2.6.20 2.6.17

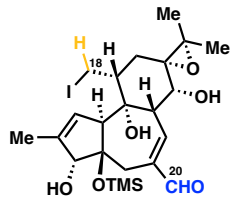
Tricycle 2.6.20:

Prepared analogously to tricycle **2.6.19** from subjecting (*Z*)-vinyl iodide **2.6.13** (46 mg, 84 μmol) to general procedure B. After column chromatography (20 to 80% EtOAc/hexanes) desired trisubstituted olefin **2.6.20** was isolated alongside small amounts of copolar exocyclic olefin **2.6.17** (28 mg, 51 μmol, 60%, 5:1 rr).

TLC: R_f = 0.33 (50% EtOAc/hexanes)

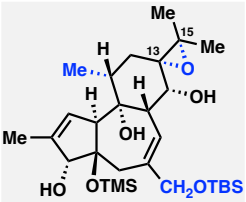
^{1}H NMR: (600 MHz, $CDCl_3$) δ 5.75 (s, 1H), 5.65 (d, *J* = 6.9 Hz, 1H), 4.49 (s, 1H), 3.92 (s, 1H), 3.88 (dd, *J* = 9.1, 3.3 Hz, 1H), 3.86 (s, 1H), 3.20 (s, 1H), 3.09 (dd, *J* = 11.5, 9.3 Hz, 1H), 2.93 (d, *J* = 16.3 Hz, 1H), 2.59 (s, 1H), 2.51 (d, *J* = 7.5 Hz, 1H), 2.44 (dd, *J* = 24.2, 12.0 Hz, 1H), 2.37 (d,

J = 16.3 Hz, 1H), 2.31 (t, J = 13.4 Hz, 1H), 1.97 (d, J = 14.0 Hz, 1H), 1.83 (s, 3H), 1.83 (s, 3H), 1.48 (s, 3H), 1.37 (s, 3H), 0.17 (s, 9H).
^{13}C NMR: (151 MHz, $CDCl_3$) δ 141.6, 136.2, 130.3, 121.6, 85.1, 84.7, 76.6, 74.1, 67.9, 64.5, 59.5, 48.2, 47.1, 42.4, 28.9, 24.4, 21.0, 14.7, 12.4, 2.3, 2.0.
HRMS (m/z): (ESI) calcd. for $C_{23}H_{37}O_5{}^{127}I^{23}Na^{28}Si$ $[M+Na]^+$: 571.1347, found 571.1355.



2.6.21
+ 2.6.21b *(olefin isomer)*

Aldehyde 2.6.21:
An oven-dried reaction tube was charged with tricycle **2.6.20** (50 mg, 91 µmol, 1.0 equiv.) and THF (0.90 mL). Then, SeO_2 (75 mg, 0.67 mmol, 7.5 equiv.) was added and the reaction mixture was stirred at 50 ºC until consumption of the starting material was complete as judged by TLC. The reaction mixture was transferred to a silica gel column without drying or concentration *in vacuo*; EtOAc (0.3 mL) was used to render the transfer quantitative. Elution with 0 to 100% EtOAc/hexanes in 20% increments resulted in pure aldehyde **2.6.21** and copolar olefin isomer **2.6.21b** (48 mg, 84 µmol, 94%, 5:1 rr) as an off-white solid.
TLC: R_f = 0.26 (50% EtOAc/hexanes)
^{1}H NMR: (600 MHz, $CDCl_3$) δ 9.49 (s, 1H), 6.96 (dd, J = 7.3, 2.7 Hz, 1H), 5.69 (s, 1H), 4.09 (s, 1H), 3.97 (d, J = 9.2 Hz, 1H), 3.90 (dd, J = 9.3, 3.3 Hz, 1H), 3.82 (d, J = 17.4 Hz, 1H), 3.11 – 3.03 (m, 1H), 2.99 (d, J = 7.9 Hz, 2H), 2.52 – 2.45 (m, 1H), 2.37 – 2.30 (m, 1H), 2.17 – 2.12 (m, 1H), 2.03 (d, J = 13.6 Hz, 1H), 1.82 (s, 3H), 1.50 (s, 3H), 1.37 (s, 3H), 0.18 (s, 9H).
^{13}C NMR: (151 MHz, $CDCl_3$) δ 192.7, 150.2, 146.1, 136.9, 129.1, 85.2, 83.6, 77.1, 72.7, 67.4, 64.6, 59.8, 48.4, 47.9, 32.7, 28.7, 21.0, 20.9, 14.7, 11.4, 2.2, 1.7.



2.6.22

Silanol 2.6.22:
An oven-dried reaction tube was charged with aldehyde **2.6.21** (5.0 mg, 8.9 µmol, 1.0 equiv.) and THF (0.5 mL). The resulting solution was cooled to –78 ºC and a solution of LAH (0.050 mL, 1 M in THF, 50 µmol, 5.6 equiv.) was added. The reaction mixture was allowed to slowly warm up to room temperature over the course of 12 hours, at which point it was quenched with EtOAc (1 mL) and satd. *aq.* Rochelle's salt (1.5 mL). After vigorously stirring the biphasic mixture for 30 minutes, the layers were separated and the aqueous layer was extracted with EtOAc (4 x 1.5 mL). The combined organic layers were dried over Na_2SO_4 and concentrated under reduced pressure. The resulting crude material was used in the next step without purification.
TLC: R_f = 0.11 (50% EtOAc/hexanes)

An oven-dried reaction tube was charged with the crude material from the LAH reduction reaction (assumed 8.9 μmol) and DCM (0.2 mL). Then, imidazole (1.8 mg, 27 μmol, 3 equiv.) and TBSCl (2.0 mg, 13.4 μmol, 1.5 equiv.) were added and the reaction mixture was stirred for 15 minutes or until conversion was complete. After a quench with satd. *aq.* $NaHCO_3$ (1 mL) the layers were separated and the aqueous layer was extracted with DCM (3 x 1 mL). The combined organic layers were dried over Na_2SO_4 and concentrated under reduced pressure. The crude reaction product was purified by column chromatography (5 to 50% EtOAc/hexanes) to provide pure silanol **2.6.22** (3.4 mg, 6.3 μmol, 70% from aldehyde **2.6.21**) alongside undesired reductive opening product **2.6.23** (0.9 mg, 1.8 μmol, 20% over 2 steps).

*Desired silanol **2.6.22**:*

TLC: R_f = 0.89 (50% EtOAc/hexanes)

^{1}H NMR (600 MHz, $CDCl_3$): δ 5.92 (d, *J* = 7.7 Hz, 1H), 5.78 (s, 1H), 4.12 (d, *J* = 6.2 Hz, 2H), 3.92 (s, 1H), 3.86 (s, 1H), 3.11 (m, 1H), 3.05 (d, *J* = 16.6 Hz, 1H), 2.65 (d, *J* = 6.1 Hz, 1H), 2.40 – 2.31 (m, 2H), 2.28 (ddd, *J* = 13.4, 6.6, 3.1 Hz, 1H), 1.79 (dd, *J* = 2.8, 1.5 Hz, 3H), 1.39 (s, 3H), 1.35 (s, 3H), 1.19 (d, *J* = 12.7 Hz, 1H), 1.01 (d, *J* = 6.6 Hz, 3H), 0.91 (s, 9H), 0.12 (s, 9H), 0.09 (s, 3H), 0.08 (s, 3H).

^{13}C NMR (150 MHz, $CDCl_3$): δ 143.1, 135.2, 130.8, 123.4, 85.7, 84.7, 76.5, 73.7, 67.9, 67.6, 64.2, 60.2, 46.4, 39.2, 38.4, 31.1, 26.2, 21.2, 21.1, 18.7, 17.9, 14.7, 2.4, -5.1.

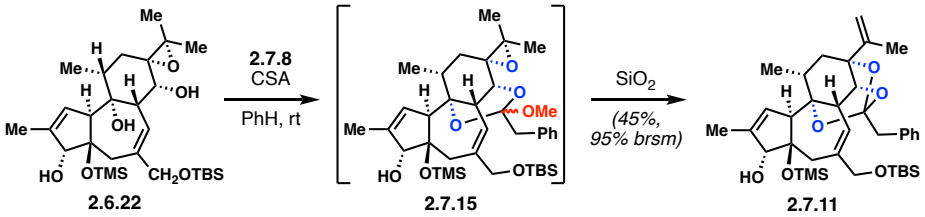
IR (thin film) ν_{max} (cm^{-1}): 3380, 2929, 2856, 1406, 1251, 1120, 1054, 963, 830.

HRMS (m/z): (ESI) calcd. for $C_{29}H_{52}O_6{}^{23}Na^{28}Si_2$ $[M+Na]^+$: 575.3195, found 575.3198.

*Undesired triol **2.6.23**:*

TLC: R_f = 0.84 (50% EtOAc/hexanes)

^{1}H NMR: (700 MHz, $CDCl_3$) δ 5.95 (d, *J* = 7.1 Hz, 1H), 5.72 (d, *J* = 7.6 Hz, 1H), 4.17 – 4.09 (m, 3H), 3.96 (s, 1H), 3.84 (s, 1H), 3.07 (s, 1H), 3.04 (d, *J* = 16.6 Hz, 1H), 2.73 (d, *J* = 7.1 Hz, 1H), 2.36 (d, *J* = 15.6 Hz, 1H), 2.24 (d, *J* = 17.8 Hz, 2H), 2.05 – 1.99 (m, 1H), 1.78 (s, 3H), 0.98 (d, *J* = 6.8 Hz, 3H), 0.95 (d, *J* = 6.7 Hz, 3H), 0.91 (s, 9H), 0.89 (d, *J* = 9.6 Hz, 3H), 0.11 (s, 9H), 0.08 (s, 3H), 0.08 (s, 3H).



Orthoester 2.7.11:

An oven-dried reaction tube was charged with silanol **26.22** (5.0 mg, 9.0 μmol, 1.0 equiv.), benzene (0.5 mL), (2,2,2-trimethoxyethyl)benzene (5.3 mg, 27 μmol, 3.0 equiv.), and (+)-camphorsulfonic acid (0.5 mg, 2.0 μmol, 0.24 equiv.). The resulting solution was stirred at room temperature until conversion was complete as judged by TLC; additional portions of (2,2,2-trimethoxyethyl)benzene (5.3 mg) and (+)-camphorsulfonic acid (1.0 mg) were added as necessary for full consumption of diol **2.6.22**. At this stage the reaction mixture was quenched with satd. *aq.* $NaHCO_3$ (1.5 mL), the organic layer was separated, and the aqueous layer was extracted with Et_2O (4 x 1 mL). The combined organic layers were dried over Na_2SO_4 and combined with silica gel (2 g) and the resulting suspension was concentrated to dryness under reduced pressure. The silica-gel absorbed material was then chromatographically purified (0 to 15% EtOAc/hexanes in 2.5% increments) to obtain pure orthoester **2.7.11** (2.4 mg, 3.6 μmol,

40% yield) as a colorless oil. [**Note**: As an alternative to the procedure above, the same reaction can be carried out on larger scale (13 mg of **2.6.22**, 24 μmol) but quenched at ~25% conversion to obtain **27.11** (2.5 mg, 3.8 μmol, 95% brsm) as well as recovered **2.6.22** (11 mg, 20 μmol), which can be recycled repeatedly to increase the overall material throughput of the orthoester product. In this case, flash column chromatography is carried out as follows: 0 to 15% EtOAc/hexanes in 2.5% increments to isolate desired **2.7.11**; then 20 to 50% EtOAc/hexanes in 10% increments to recover unreacted **2.6.22**.]

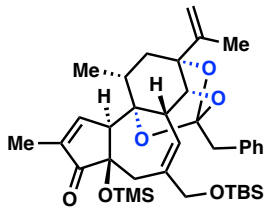
TLC: R_f = 0.78 (25% EtOAc/hexanes)

^{1}H NMR (600 MHz, $CDCl_3$): δ 7.34 (dd, *J* = 6.6, 1.4 Hz, 2H), 7.25 (d, *J* = 7.8 Hz, 2H), 7.22 – 7.18 (t, 1H), 5.79 (s, 1H), 5.71 (t, *J* = 1.8 Hz, 1H), 4.72 (s, 1H), 4.71 (t, *J* = 1.6 Hz, 1H), 4.20 (d, *J* = 2.8 Hz, 1H), 4.13 (s, 1H), 4.10 (d, *J* = 3.3 Hz, 2H), 3.16 (s, 2H), 2.95 (s, 1H), 2.77 – 2.72 (m, 2H), 2.65 (p, *J* = 7.2 Hz, 1H), 2.41 (d, *J* = 18.4 Hz, 1H), 2.05 (dd, *J* = 14.1, 8.6 Hz, 1H), 1.81 – 1.78 (m, 3H), 1.54 – 1.51 (m, 4H), 1.00 (d, *J* = 7.1 Hz, 3H), 0.92 (s, 9H), 0.12 (s, 9H), 0.09 (s, 3H), 0.08 (s, 3H).

^{13}C NMR (150 MHz, $CDCl_3$): δ 147.0, 139.8, 137.3, 135.5, 131.0, 130.6, 127.8, 126.5, 123.6, 117.9, 110.6, 87.7, 84.3, 84.2, 82.3, 80.8, 69.4, 59.2, 41.3, 39.1, 39.1, 36.6, 33.3, 26.2, 20.9, 18.9, 18.6, 14.5, 2.2, -5.0, -5.1.

IR (thin film) ν_{max} (cm^{-1}): 3500, 2952, 2924, 2854, 1602, 1497, 1465, 1436, 1254, 1158, 1102, 948.

HRMS (m/z): (ESI) calcd. for $C_{37}H_{56}O_6{}^{23}Na^{28}Si_2$ $[M+Na]^+$: 675.3508, found 675.3507.



2.7.3

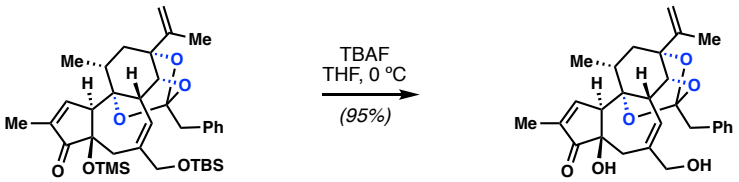
Enone 2.7.3:

An oven-dried reaction tube was charged with orthoester **2.7.11** (10 mg, 15 μmol, 1.0 equiv.) and DCM (0.3 mL). A stock solution of acid-free Dess-Martin periodinane (DMP) was prepared by suspending DMP (70.0 mg, 165 μmol, 11 equiv.) and $NaHCO_3$ (20.0 mg) in DCM (1.0 mL), shaking vigorously, and allowing the inorganic solids to settle. An appropriate aliquot of the supernatant (0.100 mL, containing 16.5 μmol of DMP, 1.1 equiv.) was added to the DCM solution of orthoester **2.7.11** and the resulting mixture was stirred at room temperature for 1 hour. If conversion was incomplete at this point, an additional amount of DMP solution (20 μL, 0.22 equiv. DMP) was added as necessary. Once all **2.7.11** was consumed as judged by TLC, the reaction was quenched with satd. *aq.* $NaHCO_3$ (0.5 mL) and satd. *aq.* $Na_2S_2O_3$ (0.5 mL). The organic layer was separated and the aqueous layer was extracted with DCM (3 x 1 mL). The combined organic layers were dried over Na_2SO_4 and concentrated under reduced pressure. The crude reaction product was purified by flash column chromatography (0 to 20% Et_2O/hexanes) to provide pure enone **2.7.3** (6.3 mg, 9.6 μmol, 63%) as a colorless amorphous solid.

TLC: R_f = 0.62 (10% EtOAc/hexanes)

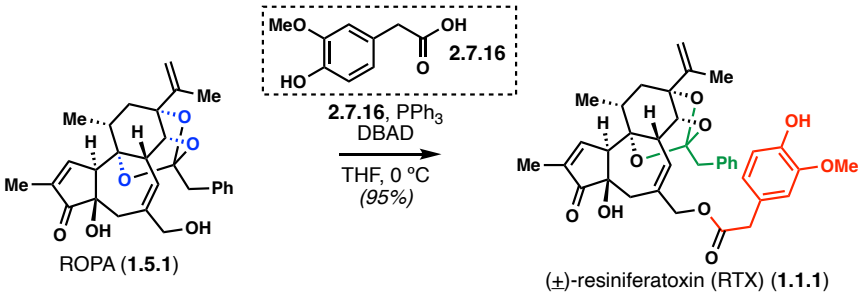
^{1}H NMR (600 MHz, C_6D_6): δ 7.49 (s, 1H), 7.48 (s, 1H), 7.21 (t, *J* = 7.6 Hz, 3H), 7.14 – 7.09 (m, 1H), 6.00 (s, 1H), 4.89 (s, 1H), 4.75 (s, 1H), 4.21 (d, *J* = 2.7 Hz, 1H), 3.99 (d, *J* = 12.6 Hz, 1H), 3.97 (d, *J* = 12.6 Hz, 1H), 3.40 (d, *J* = 14.0 Hz, 1H), 3.37 (d, *J* = 14.1 Hz, 1H), 3.15 (s, 1H), 3.05

(s, 1H), 2.89 (d, J = 18.7 Hz, 1H), 2.64 (p, J = 7.3 Hz, 1H), 2.13 – 2.03 (m, 2H), 1.62 – 1.59 (m, 4H), 1.50 (s, 3H), 1.17 (d, J = 7.2 Hz, 3H), 1.00 (s, 9H), 0.19 (s, 9H), 0.10 (s, 3H), 0.09 (s, 3H).
^{13}C NMR (150 MHz, C_6D_6): δ 206.3, 156.4, 147.0, 139.1, 137.4, 135.7, 131.4, 126.9, 124.5, 118.4, 110.9, 84.7, 82.0, 81.3, 76.8, 69.7, 56.6, 41.8, 39.9, 39.2, 36.5, 33.7, 26.2, 20.6, 18.9, 18.6, 10.3, 1.7, 1.4, -5.0.
IR (thin film) ν_{max} (cm^{-1}): 2952, 2924, 2854, 1716, 1457, 1360, 1252, 1076, 1014, 843.
HRMS (m/z): (ESI) calcd. for $C_{37}H_{54}O_6{}^{23}Na^{28}Si_2$ $[M+Na]^+$: 673.3351, found 673.3345.



2.7.3 ROPA (**1.5.1**)

Resiniferonol-9,13,14-orthophenyl acetate (1.5.1)
Resiniferonol-9,13,14-orthophenyl acetate (ROPA, **1.5.1**) was prepared by deprotecting enone **2.7.3** with TBAF according to a modified literature procedure.[SI-6] An oven-dried reaction tube was charged with enone **2.7.3** (6.9 mg, 11 μmol, 1.0 equiv.) and THF (300 μL). The resulting solution was cooled to 0 ºC and a solution of TBAF (50 μL, 1 M in THF, 50 μmol, 4.7 equiv.) was added. The reaction mixture was stirred for 2 hours, at which point conversion was complete as judged by TLC and was quenched with satd. *aq.* NH_4Cl (1 mL) and diluted with EtOAc (1 mL). The organic layer was separated and the aqueous layer was extracted with EtOAc (5 x 1 mL). The combined organic layers were washed with satd. *aq.* $NaHCO_3$ (1 mL), dried over Na_2SO_4 and concentrated under reduced pressure. The crude product was purified by column chromatography (20 to 100% Et_2O/hexanes then 50 to 80% EtOAc/hexanes) to provide pure ROPA (**1.5.1**) (4.9 mg, 11 μmol) as a colorless amorphous solid.
TLC: R_f = 0.33 (50% EtOAc/hexanes)
^{1}H NMR (600 MHz, $CDCl_3$): ^{1}H NMR (600 MHz, $CDCl_3$) δ 7.45 (dd, J = 2.4, 1.4 Hz, 1H), 7.38 – 7.34 (m, 2H), 7.28 (dd, J = 8.2, 6.6 Hz, 2H), 7.24 – 7.20 (m, 1H), 5.87 (s, 1H), 4.71 (dd, J = 3.0, 1.4 Hz, 2H), 4.26 (d, J = 2.8 Hz, 1H), 4.11 (d, J = 12.8 Hz, 1H), 4.08 (d, J = 12.8 Hz, 1H), 3.22 (d, J = 14.2 Hz, 1H), 3.19 (d, J = 14.2 Hz, 1H), 3.13 (br s, 1H), 3.10 (s, 1H), 2.60 – 2.51 (m, 2H), 2.28 (br s, 1H), 2.16 (dd, J = 14.4, 8.9 Hz, 1H), 1.82 (dd, J = 2.8, 1.4 Hz, 3H), 1.54 (m, 1H), 1.52 (s, 3H), 0.96 (d, J = 7.2 Hz, 3H).
^{13}C NMR (150 MHz, $CDCl_3$): δ 208.7, 158.3, 146.4, 138.9, 136.5, 135.0, 130.8, 127.7, 126.5, 125.4, 117.8, 110.7, 84.5, 81.2, 80.8, 73.5, 69.3, 55.5, 41.0, 39.8, 38.9, 35.7, 33.1, 19.9, 18.8, 10.2.
IR (thin film) ν_{max} (cm^{-1}): 3347, 3319, 2958, 2925, 2855, 1708, 1447, 1378, 1287, 1238, 1159, 1048, 948.
HRMS (m/z): (ESI) calcd. for $C_{28}H_{33}O_6$ $[M+H]^+$: 465.2272, found 465.2271.



Resiniferatoxin (1.1.1)

Resiniferatoxin (**1.1.1**) was synthesized from ROPA (**1.5.1**) via a modified literature procedure.[SI-6] An oven-dried reaction tube was charged with ROPA (4.9 mg, 11 μmol), DBAD (6.3 mg, 27 μmol, 2.6 equiv.), homovanillic acid (5.0 mg, 27 μmol, 2.6 equiv.), and PPh_3 (7.1 mg, 27 μmol, 2.6 equiv.) and was cooled to 0 ºC. THF (0.3 mL) was added down the side of the tube and the reaction mixture was stirred at 0 ºC for 15 minutes, during which time a change from a bright yellow solution to pale yellow suspension was observed. At this time conversion was complete as judged by TLC, so the reaction mixture was transferred onto a silica (4.0 g) column. The reaction tube was washed twice with 10% Et_2O/hexanes (0.2 mL) to render the transfer quantitative. The column was eluted with 20 to 100% Et_2O/hexanes followed by 50 to 75% EtOAc/hexanes. The fractions containing the desired product were combined and re-purified with another chromatography column (10 to 60% EtOAc/hexanes in 10% increments) to provide pure resiniferatoxin (**1.1.1**) (6.2 mg, 10 μmol, 95% over 2 steps) as a white solid.

TLC: R_f = 0.58 (50% EtOAc/hexanes)

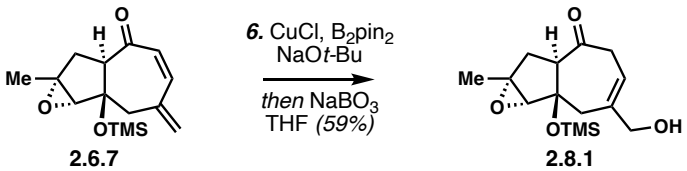
^{1}H NMR (600 MHz, $CDCl_3$): δ 7.44 (s, 1H), 7.37 (d, *J* = 7.1 Hz, 2H), 7.28 (t, *J* = 7.4 Hz, 2H), 7.23 (t, *J* = 7.3 Hz, 1H), 6.84 (d, *J* = 8.0 Hz, 1H), 6.80 (d, *J* = 1.9 Hz, 1H), 6.76 (dd, *J* = 8.0, 1.9 Hz, 1H), 5.87 (s, 1H), 5.54 (s, 1H), 4.71 (s, 2H), 4.59 (d, *J* = 12.2 Hz, 1H), 4.54 (d, *J* = 12.2 Hz, 1H), 4.20 (d, *J* = 2.7 Hz, 1H), 3.88 (s, 3H), 3.56 (s, 2H), 3.22 (d, *J* = 14.5 Hz, 1H), 3.19 (d, *J* = 14.5 Hz, 1H), 3.08 (s, 1H), 3.04 (s, 1H), 2.55 (p, *J* = 7.3 Hz, 1H), 2.43 (d, *J* = 18.9 Hz, 1H), 2.18 – 2.10 (dd, *J* = 14.3, 8.8 Hz, 1H), 2.15 (br s, 1H), 2.04 (d, *J* = 18.9 Hz, 1H), 1.82 (dd, *J* = 2.7, 1.3 Hz, 3H), 1.55 (d, *J* = 14.3 Hz, 1H), 1.51 (s, 3H), 0.96 (d, *J* = 7.2 Hz, 3H).

^{13}C NMR (150 MHz, $CDCl_3$): δ 208.4, 171.5, 158.2, 146.5, 146.3, 144.8, 136.5, 134.9, 134.1, 130.8, 128.6, 127.7, 126.5, 125.6, 122.2, 117.8, 114.4, 111.7, 110.7, 84.4, 81.1, 80.6, 73.3, 70.5, 56.0, 55.3, 41.0, 40.9, 39.9, 39.1, 35.7, 33.0, 19.8, 18.8, 10.2.

IR (thin film) ν_{max} (cm^{-1}): 3447, 2971, 2926, 1724, 1629, 1604, 1515, 1271, 1149, 1029, 982.

HRMS (m/z): (ESI) calcd. for $C_{37}H_{41}O_9$ $[M+H]^+$: 629.2745, found 629.2754.

Compounds from optimized route:



Allylic alcohol 2.8.1:

An oven-dried 25 mL round-bottom flask was charged with CuCl (6.3 mg, 0.064 mmol, 0.1 equiv.), NaO*t*-Bu (6.3 mg, 0.064 mmol, 0.1 equiv.), and THF (2.8 mL). These reagents were stirred together for 15 min at room temperature, at which point a solution of B_2pin_2 (178 mg, 0.701 mmol, 1.1 equiv.) in THF (2.8 mL) was added and stirring was continued for another 15 minutes. Then, enone **2.6.7** (178 mg, 0.636 mmol, 1.0 equiv.) in THF (2.8 mL) was added,

followed by H_2O (4.8 mL). The resulting mixture was stirred at room temperature for 1.5 hours, at which point conversion was complete as judged by TLC. Solid $NaBO_3$•$4H_2O$ (310 mg, 2.00 mmol, 3.2 equiv.) was added and stirring was continued for 1 hour or until all boronate was oxidized. The reaction mixture was quenched with satd. *aq.* $Na_2S_2O_3$ (10 mL). The organic layer was separated and the aqueous layer was extracted with EtOAc (3 x 10 mL). The combined organic layers were dried over Na_2SO_4 and concentrated under reduced pressure. The crude reaction product was loaded on a chromatography column, which was eluted with 10 to 50% Et_2O/DCM. The fractions containing the product were combined, concentrated, and re-purified using another chromatography column (25 to 45% EtOAc/hexanes) to provide pure allylic alcohol **2.8.1** (109 mg, 0.369 mmol, 59% yield) as a colorless oil.

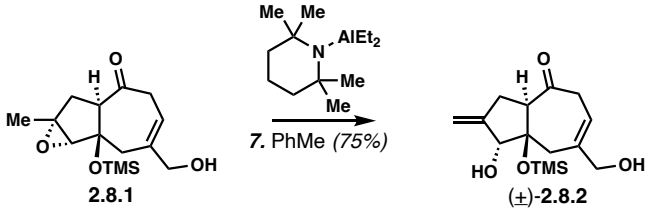
TLC: R_f = 0.48 (50% EtOAc/hexanes)

^{1}H NMR (700 MHz, C_6D_6): δ 5.16 (ddd, *J* = 7.8, 3.2, 1.7 Hz, 1H), 3.61 (s, 2H), 3.26 (dq, *J* = 20.6, 2.5 Hz, 1H), 3.03 (s, 1H), 2.87 (dd, *J* = 20.2, 7.6 Hz, 1H), 2.77 (t, *J* = 8.6 Hz, 1H), 2.68 (d, *J* = 18.4 Hz, 1H), 2.51 – 2.45 (m, 2H), 2.02 (dd, *J* = 14.3, 7.9 Hz, 1H), 1.24 (s, 3H), -0.01 (d, *J* = 0.8 Hz, 9H).

^{13}C NMR (175 MHz, C_6D_6): δ 205.8, 137.0, 117.4, 81.6, 69.3, 67.6, 64.6, 60.0, 42.8, 39.5, 32.5, 17.5, 2.1.

IR (thin film) ν_{max} (cm^{-1}): 3420, 2957, 2932, 1707, 1252, 1104, 1063, 986, 840.

HRMS (m/z): (ESI) calcd. for $C_{15}H_{24}O_4{}^{23}Na^{28}Si$ $[M+Na]^+$: 319.1336, found 319.1337.



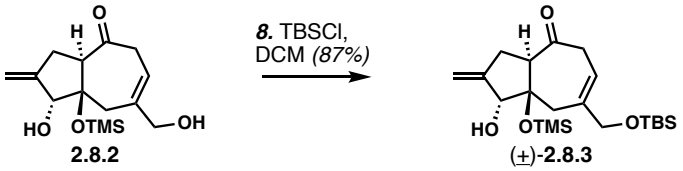
Diol 2.8.2:

Diethylaluminum 2,2,6,6-tetramethylpiperidide was prepared according to a modified literature procedure.[SI-4] An oven-dried 25 mL round-bottom flask was charged with 2,2,6,6-tetramethylpiperidine (0.24 mL, 1.4 mmol, 4.0 equiv.) and toluene (3.0 mL). This solution was cooled to 0 ºC and a solution of *n*-BuLi (0.56 mL, 2.5 M in hexanes, 1.4 mmol, 4.0 equiv.) was added dropwise and stirring was continued for 30 minutes at 0 ºC, during which time the reaction mixture transitions from clear colorless solution to bright yellow suspension. Then, a solution of diethylaluminum chloride (1.4 mL, 1 M in hexanes, 1.4 mmol, 4.0 equiv.) was added, upon which the yellow color disappeared. The resulting white suspension was stirred for 40 minutes at 0 ºC and a solution of allylic alcohol **2.8.1** (104 mg, 0.350 mmol, 1.0 equiv.) in toluene (2.0 mL) was added dropwise. Conversion after 2 minutes was complete as judged by TLC, so the reaction mixture was quenched with satd. *aq.* Rochelle salt (20 mL) and diluted with EtOAc (10 mL). This biphasic mixture was vigorously stirred for 30 minutes, at which point the organic layer was separated and the aqueous layer was extracted with EtOAc (4 x 20 mL). The combined organic layers were dried over Na_2SO_4 and concentrated *in vacuo*. The crude reaction product was purified with flash column chromatography (50 to 100% EtOAc/hexanes) to provide pure diol **2.8.2** (78.0 mg, 0.264 mmol, 75% yield) as a colorless oil.

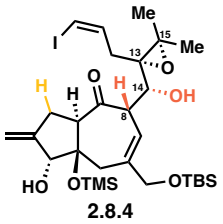
TLC: R_f = 0.23 (50% EtOAc/hexanes)

^{1}H NMR (400 MHz, C_6D_6): δ 5.35 (t, *J* = 5.6 Hz, 1H), 5.02 – 4.96 (m, 1H), 4.91 (d, *J* = 2.4 Hz, 1H), 4.00 (s, 1H), 3.85 (t, *J* = 5.0 Hz, 2H), 3.30 – 3.04 (m, 3H), 2.98 – 2.84 (m, 2H), 2.53 – 2.41 (m, 2H), 0.03 (d, *J* = 1.5 Hz, 9H).

^{13}C NMR (150 MHz, C_6D_6): δ 205.0, 152.2, 139.7, 119.1, 111.4, 85.2, 83.0, 68.9, 58.3, 43.0, 37.1, 29.8, 2.2.
IR (thin film) ν_{max} (cm^{-1}): 3350, 2955, 2923, 2854, 1706, 1252, 1116, 1041, 841.
HRMS (m/z): (ESI) calcd. for $C_{15}H_{24}O_4{}^{23}Na^{28}Si$ $[M+Na]^+$: 319.1336, found 319.1336.

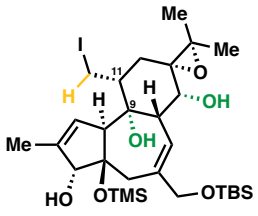


Protected allylic alcohol 2.8.3:
An oven-dried reaction tube was charged with diol **2.8.2** (78.0 mg, 0.264 mmol, 1.0 equiv.) and DCM (2.6 mL). Imidazole (40 mg, 0.59 mmol, 2.2 equiv.) and TBSCl (48 mg, 0.32 mmol, 1.2 equiv.) were added and stirring was continued for 15 minutes, at which point conversion was complete as judged by TLC. The reaction mixture was quenched with satd. *aq.* $NaHCO_3$ (3 mL), the organic layer was separated, and the aqueous layer was extracted with EtOAc (3 x 3 mL). The combined organic layers were dried over Na_2SO_4 and concentrated under reduced pressure. The crude reaction product was purified by column chromatography (10% to 50% EtOAc/hexanes) to provide pure TBS-protected primary allylic alcohol **2.8.3** (94 mg, 0.23 mmol, 87% yield) as a colorless oil.
TLC: R_f = 0.43 (25% EtOAc/hexanes)
^{1}H NMR (400 MHz, C_6D_6): δ 5.60 – 5.52 (m, 1H), 4.92 (d, *J* = 2.5 Hz, 1H), 4.86 (dq, *J* = 2.1, 1.1 Hz, 1H), 4.05 – 3.98 (m, 2H), 3.96 (d, *J* = 3.3 Hz, 1H), 3.32 (ddt, *J* = 18.1, 4.4, 2.0 Hz, 1H), 3.20 – 3.07 (m, 2H), 3.02 – 2.91 (m, 2H), 2.57 – 2.41 (m, 2H), 1.00 (s, 9H), 0.09 (s, 6H), 0.05 (s, *J* = 0.7 Hz, 9H).
^{13}C NMR (150 MHz, C_6D_6): δ 205.4, 152.5, 138.3, 116.9, 111.0, 85.0, 82.9, 69.1, 58.8, 43.2, 36.8, 30.1, 26.2, 18.6, 2.1, -5.1.
IR (thin film) ν_{max} (cm^{-1}): 3420, 2924, 2854, 1740, 1436, 1254, 1158, 1012, 948.
HRMS (m/z): (ESI) calcd. for $C_{21}H_{38}O_4{}^{23}Na^{28}Si_2$ $[M+Na]^+$: 433.2201, found 433.2203.



Aldol product 2.8.4:
An oven-dried reaction tube was charged with ketone **2.8.3** (26 mg, 63 μmol, 1.0 equiv.) and THF (0.4 mL). The resulting solution was cooled to –78 ºC and a solution of LHMDS (160 μL, 1 M in THF, 0.160 mmol, 2.5 equiv.) was added. The reaction mixture was stirred at –78 ºC for 30 minutes, at which point a solution of aldehyde **2.6.10** (33.0 mg, 0.126 mmol, 2.0 equiv.) in THF (0.4 mL) was added dropwise. After 5 minutes, conversion was complete as judged by TLC and the reaction was quenched with neat acetic acid (20 μL) before being quickly warmed up to room temperature. Then, satd. *aq.* $NaHCO_3$ (2 mL) was added carefully, the organic layer was separated, and the aqueous layer was extracted with EtOAc (5 x 2 mL). The combined organic layers were dried over Na_2SO_4 and concentrated under reduced pressure. The crude reaction

product was purified by flash column chromatography (0 to 60% EtOAc/hexanes) to provide pure vinyl iodide **2.8.3** (26 mg, 38 μmol, 60% yield) as a white solid.
TLC: R_f = 0.67 (50% EtOAc/hexanes)
^{1}H NMR (600 MHz, C_6D_6): δ 6.47 (td, *J* = 7.1, 5.3 Hz, 1H), 5.98 (dt, *J* = 7.4, 2.1 Hz, 1H), 5.69 (dt, *J* = 7.3, 1.5 Hz, 1H), 5.01 (t, *J* = 2.5 Hz, 1H), 4.94 (qd, *J* = 2.1, 1.1 Hz, 1H), 4.30 (dd, *J* = 10.3, 2.5 Hz, 1H), 4.04 – 4.01 (m, 2H), 3.99 (s, 1H), 3.76 (dd, *J* = 10.4, 7.1 Hz, 1H), 3.53 – 3.45 (m, 2H), 3.11 (ddt, *J* = 16.7, 10.8, 2.8 Hz, 1H), 2.97 (d, *J* = 16.6 Hz, 1H), 2.94 – 2.88 (m, 1H), 2.64 (ddd, *J* = 17.0, 5.3, 2.4 Hz, 1H), 2.47 (ddd, *J* = 16.6, 11.8, 3.6 Hz, 2H), 1.53 (s, 1H), 1.34 (s, 3H), 1.25 (s, 3H), 0.97 (s, 9H), 0.11 (s, 9H), 0.08 (d, *J* = 2.0 Hz, 6H).
^{13}C NMR (150 MHz, C_6D_6): δ 206.8, 152.3, 140.7, 138.6, 116.8, 112.2, 85.7, 83.2, 82.4, 73.6, 67.9, 67.1, 63.7, 56.6, 56.2, 36.9, 34.9, 30.0, 26.2, 26.2, 22.2, 21.9, 18.6, 2.4, -5.2.
IR (thin film) ν_{max} (cm^{-1}): 3450, 2954, 2928, 2856, 1707, 1405, 1251, 1103, 1008, 837.
HRMS (m/z): (ESI) calcd. for $C_{29}H_{49}O_6{}^{127}I^{23}Na^{28}Si_2$ $[M+Na]^+$: 699.2005, found 699.2008.



2.8.5

5,7,6-fused tricycle 2.8.5:
An oven-dried 10 mL round-bottom flask was charged with vinyl iodide **2.8.4** (43 mg, 63 μmol, 1.0 equiv.), degassed THF (900 μL), and H_2O (90 μL). The resulting solution was degassed for 5 minutes with sonication and argon sparging and was then cooled to 0 ºC. A solution of SmI_2 (3.2 mL, 0.1 M in THF, 0.32 mmol, 5.0 equiv.) was added dropwise until the blue color persisted, at which point conversion was complete as judged by TLC. The reaction mixture was quenched with satd. *aq.* Rochelle salt (10 mL) and diluted with EtOAc (10 mL). The resulting biphasic mixture was vigorously stirred for 30 minutes at room temperature and then the organic layer was separated. The aqueous layer was extracted with EtOAc (5 x 10 mL). The combined organic layers were dried over Na_2SO_4 and concentrated under reduced pressure. The crude reaction product was purified by flash column chromatography (10 to 60% EtOAc/hexanes) to provide pure 5,7,6-fused tricycle **2.8.5** (32 mg, 47 μmol, 75% yield, > 20:1 dr) as a white solid.
TLC: R_f = 0.82 (50% EtOAc/hexanes)
^{1}H NMR (600 MHz, $CDCl_3$): δ 5.92 (d, *J* = 7.0 Hz, 1H), 5.71 (s, 1H), 4.52 (br s, 1H), 4.15 (d, *J* = 12.8 Hz, 1H), 4.11 (d, *J* = 12.7 Hz, 1H), 3.94 (s, 1H), 3.90 – 3.86 (m, 2H), 3.20 (s, 1H), 3.11 – 3.04 (m, 2H), 2.72 (br s, 1H), 2.54 – 2.43 (m, 2H), 2.37 – 2.28 (m, 2H), 1.97 (d, *J* = 13.7 Hz, 1H), 1.81 (s, 3H), 1.65 (br s, 1H), 1.48 (s, 3H), 1.36 (s, 3H), 0.90 (s, 9H), 0.17 (s, 9H), 0.08 (s, 3H), 0.08 (s, 3H).
^{13}C NMR (150 MHz, $CDCl_3$): δ 144.2, 136.4, 129.7, 122.8, 85.5, 84.3, 76.5, 73.9, 68.1, 67.3, 64.6, 59.6, 48.5, 46.9, 38.5, 29.0, 26.1, 21.2, 18.7, 14.8, 12.4, 2.4, -5.1.
IR (thin film) ν_{max} (cm^{-1}): 3400, 2926, 2855, 1580, 1252, 1126, 1034, 936, 906, 839.
HRMS (m/z): (ESI) calcd. for $C_{29}H_{51}O_6{}^{127}I^{23}Na^{28}Si_2$ $[M+Na]^+$: 701.2161, found 701.2164.

Reduction product 2.6.22 from iodide 2.8.5:

An oven-dried reaction tube was charged with iodide **2.8.5** (5.0 mg, 7.3 μmol, 1.0 equiv.) and THF (0.5 mL). The mixture was cooled to –78 ºC and a solution of lithium aluminum hydride in THF (100 μL, 0.5 M in THF, 50.0 μmol, 6.8 equiv.) was added dropwise. The resulting solution was left to slowly warm up to room temperature over the course of 12 hours. At this point, the reaction mixture was quenched with EtOAc (1 mL) and stirred vigorously with satd. *aq.* Rochelle salt (2 mL) for 30 minutes. The organic layer was separated and the aqueous layer was extracted with EtOAc (5 x 5 mL). The combined organic layers were dried over Na_2SO_4 and concentrated under reduced pressure. The resulting crude mixture was purified by flash column chromatography (10 to 50% EtOAc/hexanes) to provide reduction product **2.6.22** (2.7 mg, 4.8 μmol, 66% yield) as a white solid.

2.12.3. Natural Product Spectral Comparisons

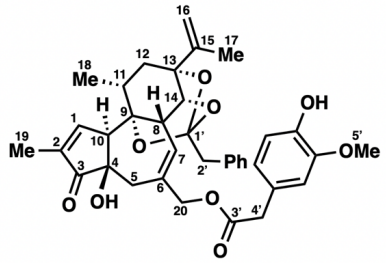


Table S1. Comparison of ^{1}H NMR data of natural, reported, and synthetic RTX.

Position	*^{1}H (δ) Natural RTX* (ref. SI-7)	*^{1}H (δ) Reported RTX* (ref. SI-6) *(500 MHz, $CDCl_3$)*	*^{1}H (δ) Synthetic RTX (600 MHz, $CDCl_3$)*
1-H	7.42 (m, 1H)	7.44 (br s, 1H)	7.44 (s, 1H)
5-H_a	2.12 (AB, 1H)	2.04 (d, *J* = 18.3 Hz, 1H)	2.04 (d, *J* = 18.9 Hz, 1H)
5-H_b	2.12 (AB, 1H)	2.43 (d, *J* = 18.3 Hz, 1H)	2.43 (d, *J* = 18.9 Hz, 1H)
7-H	5.84 (m, 1H)	5.87 (br s, 1H)	5.87 (s, 1H)
8-H	3.05 (m, 1H)	3.08 (br s, 1H)	3.08 (s, 1H)
10-H	3.05 (m, 1H)	3.04 (br s, 1H)	3.04 (s, 1H)
11-H	2.6 (m, 1H)	2.55 (dq, *J* = 8.6, 7.5 Hz, 1H)	2.55 (p, *J* = 7.3 Hz, 1H)
12-H_a	1.9 – 2.2 (m, 2H)	1.56 (d, *J* = 14.9 Hz, 1H)	1.55 (d, *J* = 14.3 Hz, 1H)
12-H_b		2.13 (dd, *J* = 14.9, 8.6 Hz, 1H)	2.18 – 2.10 (dd, *J* = 14.3, 8.8 Hz, 1H) {overlaps with C4-O*H*}
14-H	4.18 (d, *J* = 7 Hz, 1H)	4.20 (d, *J* = 2.3 Hz, 1H)	4.20 (d, *J* = 2.7 Hz, 1H)
16-$H_{a,b}$	4.7 (AB, 2H)	4.72 – 4.69 (m, 2H)	4.71 (s, 2H)
17-H	1.52 (br s, 3H)	1.51 (s, 3H)	1.51 (s, 3H)
18-H	0.96 (d, *J* = 7.5 Hz, 3H)	0.96 (d, *J* = 7.5 Hz, 3H)	0.96 (d, *J* = 7.2 Hz, 3H)
19-H	1.81 (m, 3H)	1.81 – 1.84 (m, 3H)	1.82 (dd, *J* = 2.7, 1.3 Hz, 3H)
20-H_a	4.53 (AB, 1H)	4.53 (d, *J* = 12.6 Hz, 1H)	4.54 (d, *J* = 12.2 Hz, 1H)
20-H_b	4.53 (AB, 1H)	4.59 (d, *J* = 12.6 Hz, 1H)	4.59 (d, *J* = 12.2 Hz, 1H)
2'-H_a	3.2 (s, 1H)	3.19 (d, *J* = 14.9 Hz, 1H)	3.19 (d, *J* = 14.5 Hz, 1H)
2'-H_b	3.2 (s, 1H)	3.22 (d, *J* = 14.9 Hz, 1H)	3.22 (d, *J* = 14.5 Hz, 1H)
4'-$H_{a,b}$	3.55 (s, 2H)	3.56 (s, 2H)	3.56 (s, 2H)
5'-H	3.85 (s, 3H)	3.88 (s, 3H)	3.88 (s, 3H)
C4-O*H*	2.0 – 2.5	2.04 (s, 1H)	2.15 (br s, 1H)
Ar-O*H*	5.5	5.53 (s, 1H)	5.54 (s, 1H)
Ph	7.27 (m, 5H)	7.35-7.39 (m, 2H)	7.37 (d, *J* = 7.1 Hz, 2H)
		7.20-7.31 (m, 3H)	7.28 (t, *J* = 7.4 Hz, 2H)
			7.23 (t, *J* = 7.3 Hz, 1H)
Ar	6.76 (AB, 3H)	6.74-6.85 (m, 3H)	6.84 (d, *J* = 8.0 Hz, 1H)
			6.80 (d, *J* = 1.9 Hz, 1H)
			6.76 (dd, *J* = 8.0, 1.9 Hz, 1H)

Table S2. Comparison of ^{13}C NMR data of reported[SI-6] and synthetic RTX.

Position	*^{13}C (δ) Reported RTX* (ref. SI-6) *(125 MHz, $CDCl_3$)*	*^{13}C (δ) Synthetic RTX (150 MHz, $CDCl_3$)*
1	158.3	158.2
2	136.5	136.5
3	208.5	208.4
4	73.3	73.3
5	39.9	39.9
6	134.0	134.1
7	128.5	128.6
8	39.1	39.1
9	81.1	81.1
10	55.3	55.3
11	33.0	33.0
12	35.6	35.7
13	84.4	84.4
14	80.6	80.6
15	146.3	146.3
16	110.7	110.7
17	18.8	18.8
18	19.8	19.8
19	10.2	10.2
20	70.5	70.5
1'	117.8	117.8
2'	40.9	40.9
3'	171.5	171.5
4'	41.0	41.0
5'	55.9	56.0
Ph	126.5	126.5
	127.7	127.7
	130.8	130.8
	134.9	134.9
Ar	111.7	111.7
	114.3	114.3
	122.2	122.2
	125.6	125.6
	144.8	144.8
	146.5	146.5

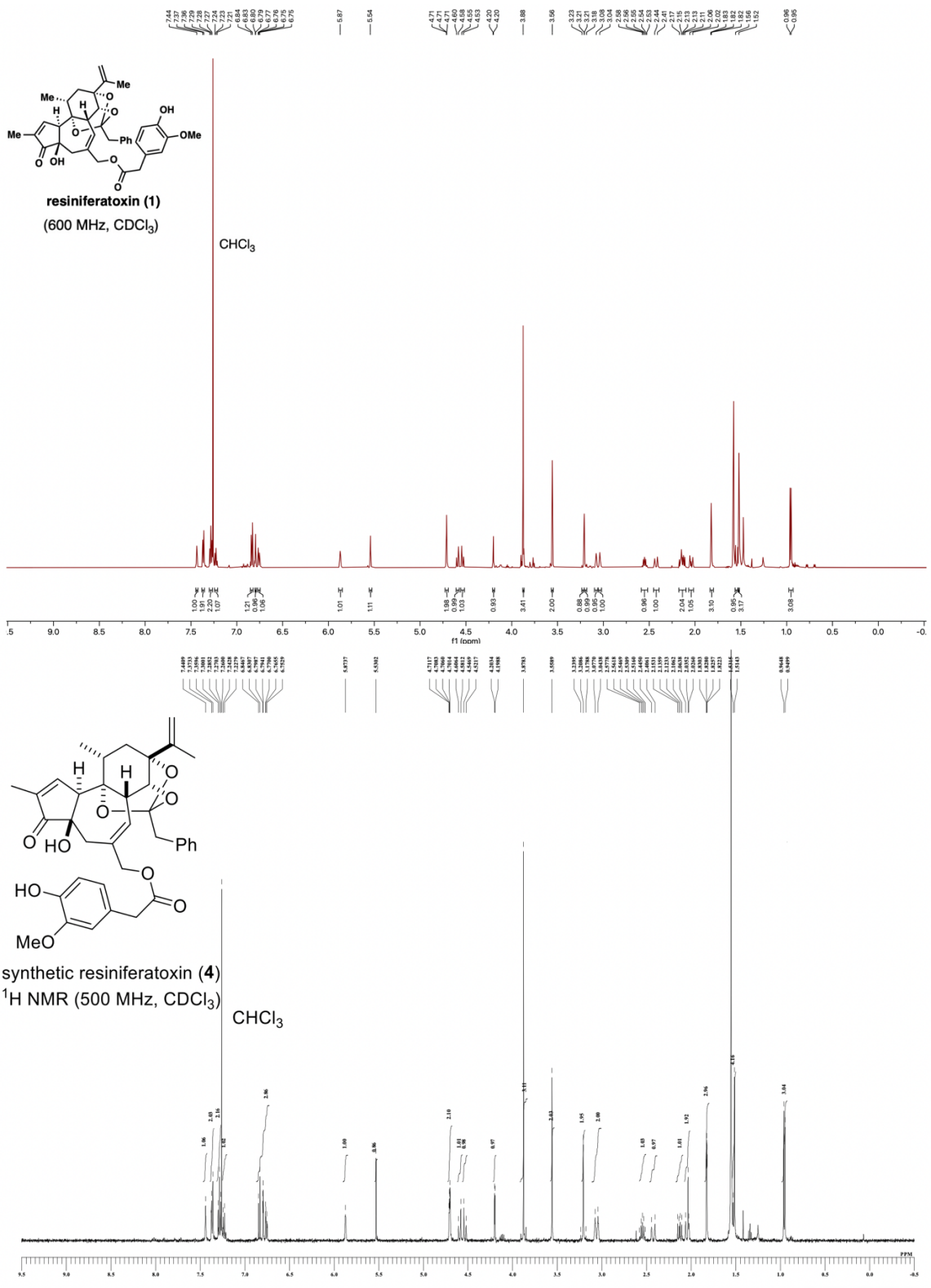


Figure SI-1. ^{1}H NMR spectra of synthetic and reported[4] RTX.

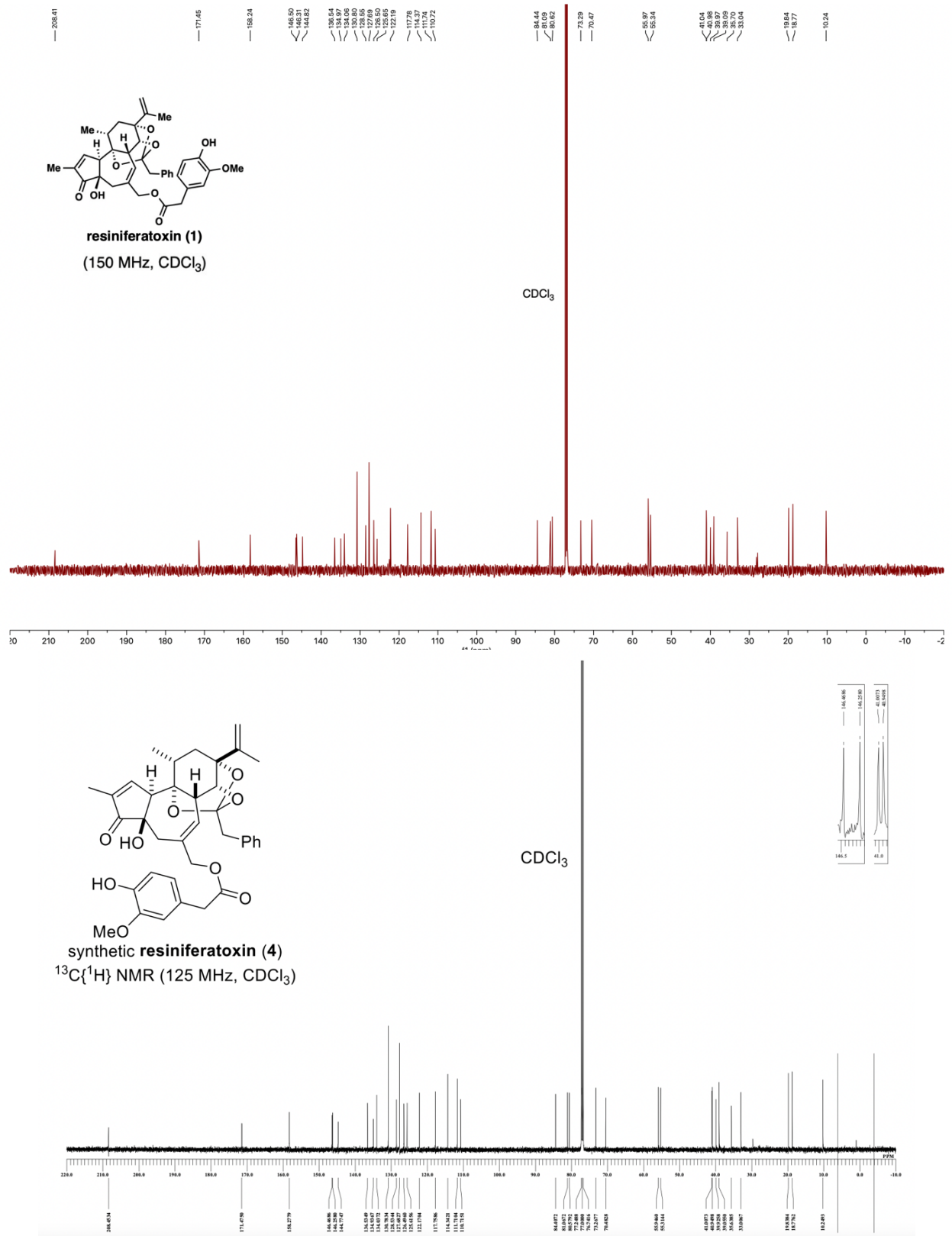


Figure SI-2. ^{13}C NMR spectra of synthetic and reported[4] RTX.

2.12.4. References for section 2.12.

SI-1. Szostak, M.; Spain, M.; Procter, D. J. *J. Org. Chem.* **2012**, *77*, 3049.

SI-2. Mitasev, B.; Porco, J. A. *Org. Lett.* **2009**, *11*, 2285.

SI-3. Shen, Z.; Ni, Z.; Mo, S.; Wang, J.; Zhu, Y. *Chem. Eur. J.* **2012**, *18*, 4859.

SI-4. Maruoka, K.; Yamamoto, H. "Diethylaluminum 2,2,6,6-tetramethylpiperidide" *e-EROS Encyclopedia of Reagents for Organic Synthesis* **2001**.

SI-5. Piers, E.; Rogers, C. "(*Z*)-3-bromo-1-iodopropene" *e-EROS Encyclopedia of Reagents for Organic Synthesis* **2001**.

SI-6. Hirose, A.; Watanabe, A.; Ogino, K.; Nagatomo, M.; Inoue, M. Unified Total Synthesis of Rhamnofolane, Tigliane, and Daphnane Diterpenoids. *J. Am. Chem. Soc.* **2021**, *143*, 12387.

SI-7. Hergenhahn, M.; Adolf, W.; Hecker, E. Resiniferatoxin and Other Esters of Novel Polyfunctional Diterpenes from *Euphorbia resinifera* and *unispina*. *Tetrahedron Lett.* **1975**, *16*, 1595.

2.12.5 – X-ray data for tricycle ***2.5.10***

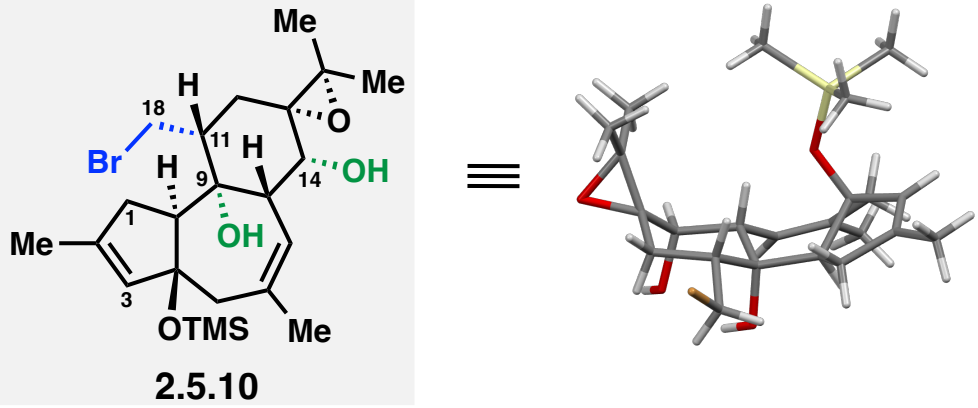


Table 1. Crystal data and structure refinement for VHV_08_202.

Identification code	VHV_08_202	
Empirical formula	C23 H37 Br O4 Si	
Formula weight	485.52	
Temperature	100(2) K	
Wavelength	1.54184 Å	
Crystal system	Triclinic	
Space group	P -1	
Unit cell dimensions	a = 9.75240(10) Å	α= 93.2890(10)°.
	b = 15.7301(2) Å	β= 106.2130(10)°.
	c = 17.2345(2) Å	γ = 104.1180(10)°.
Volume	2439.60(5) Å^3	
Z	4	
Density (calculated)	1.322 Mg/m^3	
Absorption coefficient	2.964 mm^{-1}	
F(000)	1024	
Crystal size	0.170 x 0.070 x 0.050 mm^3	
Theta range for data collection	2.923 to 74.497°.	
Index ranges	-12<=h<=12, -19<=k<=19, -21<=l<=20	
Reflections collected	105336	
Independent reflections	9968 [R(int) = 0.0684]	
Completeness to theta = 74.000°	99.8 %	
Absorption correction	Semi-empirical from equivalents	
Max. and min. transmission	1.00000 and 0.81098	
Refinement method	Full-matrix least-squares on F^2	
Data / restraints / parameters	9968 / 2 / 563	

Goodness-of-fit on F^2	1.055
Final R indices [I>2sigma(I)]	R1 = 0.0469, wR2 = 0.1212
R indices (all data)	R1 = 0.0526, wR2 = 0.1251
Extinction coefficient	n/a
Largest diff. peak and hole	0.528 and -1.179 e.$Å^{-3}$

Table 2. Atomic coordinates (x 10^4) and equivalent isotropic displacement parameters ($Å^2$x 10^3) for vhv_08_202. U(eq) is defined as one third of the trace of the orthogonalized U^{ij} tensor.

	x	y	z	U(eq)
Br(1)	3245(11)	2022(12)	4320(6)	86(2)
Br(1B)	3046(2)	1836(1)	4405(1)	53(1)
Si(1B)	-1230(1)	1292(1)	5669(1)	44(1)
O(1B)	6091(2)	3741(2)	7366(2)	55(1)
O(2B)	4646(3)	5287(2)	6693(2)	49(1)
O(3B)	2521(2)	4709(1)	5233(1)	41(1)
O(4B)	-298(2)	2327(1)	5713(1)	38(1)
C(1B)	4402(4)	3150(2)	8174(2)	49(1)
C(2B)	4781(3)	3075(2)	7382(2)	42(1)
C(3B)	4643(4)	2129(2)	7067(2)	56(1)
C(4B)	4654(3)	3750(2)	6822(2)	41(1)
C(5B)	4022(3)	4502(2)	6994(2)	37(1)
C(6B)	2352(3)	4187(2)	6556(2)	31(1)
C(7B)	1513(3)	4783(2)	6804(2)	34(1)
C(8B)	101(3)	4480(2)	6790(2)	34(1)
C(9B)	-774(4)	5057(2)	7035(2)	44(1)
C(10B)	-695(3)	3510(2)	6515(2)	34(1)
C(11B)	-741(3)	3139(2)	5653(2)	32(1)
C(12B)	-2257(3)	2985(2)	5015(2)	42(1)
C(13B)	-1952(3)	3045(2)	4229(2)	44(1)
C(14B)	-3144(4)	2763(2)	3428(2)	56(1)
C(15B)	-496(3)	3436(2)	4346(2)	41(1)
C(16B)	271(3)	3752(2)	5247(2)	32(1)
C(17B)	1973(3)	3961(2)	5609(2)	32(1)
C(18B)	2710(3)	3217(2)	5463(2)	38(1)
C(19B)	2410(5)	2918(3)	4568(2)	63(1)
C(20B)	4385(3)	3520(2)	5918(2)	45(1)
C(21B)	-2438(5)	1186(3)	6342(3)	75(1)
C(22B)	-2391(5)	784(2)	4610(3)	69(1)
C(23B)	227(5)	721(2)	6044(3)	60(1)
Br(1A)	11234(1)	8585(1)	7921(1)	47(1)

Si(1A)	7492(1)	9041(1)	10398(1)	25(1)
O(1A)	11479(2)	6264(1)	10318(1)	25(1)
O(2A)	8584(2)	5258(1)	8965(1)	28(1)
O(3A)	7272(2)	6203(1)	7869(1)	25(1)
O(008)	7117(2)	8117(1)	9776(1)	26(1)
C(1A)	12171(3)	7867(2)	10860(2)	32(1)
C(2A)	11038(2)	6981(2)	10686(1)	24(1)
C(3A)	10441(3)	6752(2)	11386(2)	30(1)
C(4A)	10242(2)	6565(1)	9834(1)	21(1)
C(5A)	8725(2)	5921(1)	9612(1)	22(1)
C(6A)	7570(2)	6440(1)	9330(1)	21(1)
C(7A)	6033(2)	5852(2)	9220(1)	23(1)
C(8A)	4814(3)	6108(2)	9173(1)	25(1)
C(9A)	3357(3)	5446(2)	9090(2)	30(1)
C(10A)	4697(3)	7046(2)	9168(2)	30(1)
C(11A)	5935(3)	7765(2)	9019(2)	24(1)
C(12A)	5335(3)	8506(2)	8661(2)	28(1)
C(13A)	5915(3)	8803(2)	8084(2)	31(1)
C(14A)	5677(4)	9572(2)	7639(2)	43(1)
C(15A)	6927(3)	8288(2)	7932(2)	31(1)
C(16A)	6554(2)	7447(2)	8345(1)	24(1)
C(17A)	7694(2)	6884(1)	8564(1)	21(1)
C(18A)	9319(2)	7425(1)	8677(1)	23(1)
C(19A)	9528(3)	7588(2)	7837(2)	30(1)
C(20A)	10500(3)	6964(2)	9096(2)	25(1)
C(21A)	5896(3)	9141(2)	10756(2)	35(1)
C(22A)	9020(3)	8953(2)	11291(2)	35(1)
C(23A)	8092(3)	10041(2)	9921(2)	34(1)

Table 3. Bond lengths [Å] and angles [°] for vhv_08_202.

Br(1)-C(19B)	1.876(9)
Br(1B)-C(19B)	1.979(4)
Si(1B)-O(4B)	1.647(2)
Si(1B)-C(23B)	1.849(4)
Si(1B)-C(21B)	1.857(4)
Si(1B)-C(22B)	1.868(4)
O(1B)-C(2B)	1.449(4)
O(1B)-C(4B)	1.456(3)
O(2B)-C(5B)	1.430(3)
O(2B)-H(2B)	0.74(4)
O(3B)-C(17B)	1.437(3)
O(3B)-H(3B)	0.79(4)
O(4B)-C(11B)	1.444(3)
C(1B)-C(2B)	1.517(5)
C(1B)-H(1BA)	0.9800
C(1B)-H(1BB)	0.9800
C(1B)-H(1BC)	0.9800
C(2B)-C(4B)	1.479(4)
C(2B)-C(3B)	1.516(4)
C(3B)-H(3BA)	0.9800
C(3B)-H(3BB)	0.9800
C(3B)-H(3BC)	0.9800
C(4B)-C(5B)	1.511(4)
C(4B)-C(20B)	1.513(4)
C(5B)-C(6B)	1.531(4)
C(5B)-H(5B)	1.0000
C(6B)-C(7B)	1.502(4)
C(6B)-C(17B)	1.568(3)
C(6B)-H(6B)	1.0000
C(7B)-C(8B)	1.337(4)
C(7B)-H(7B)	0.9500
C(8B)-C(9B)	1.504(4)
C(8B)-C(10B)	1.514(4)
C(9B)-H(9BA)	0.9800

C(9B)-H(9BB)	0.9800
C(9B)-H(9BC)	0.9800
C(10B)-C(11B)	1.550(4)
C(10B)-H(10A)	0.9900
C(10B)-H(10B)	0.9900
C(11B)-C(12B)	1.530(4)
C(11B)-C(16B)	1.547(4)
C(12B)-C(13B)	1.469(4)
C(12B)-H(12A)	0.9900
C(12B)-H(12B)	0.9900
C(13B)-C(15B)	1.355(4)
C(13B)-C(14B)	1.495(4)
C(14B)-H(14A)	0.9800
C(14B)-H(14B)	0.9800
C(14B)-H(14C)	0.9800
C(15B)-C(16B)	1.517(4)
C(15B)-H(15B)	0.9500
C(16B)-C(17B)	1.544(4)
C(16B)-H(16B)	1.0000
C(17B)-C(18B)	1.557(4)
C(18B)-C(19B)	1.511(4)
C(18B)-C(20B)	1.540(4)
C(18B)-H(18B)	1.0000
C(19B)-H(19C)	0.9900
C(19B)-H(19D)	0.9900
C(19B)-H(19A)	0.9900
C(19B)-H(19B)	0.9900
C(20B)-H(20A)	0.9900
C(20B)-H(20B)	0.9900
C(21B)-H(21A)	0.9800
C(21B)-H(21B)	0.9800
C(21B)-H(21C)	0.9800
C(22B)-H(22A)	0.9800
C(22B)-H(22B)	0.9800
C(22B)-H(22C)	0.9800
C(23B)-H(23A)	0.9800

C(23B)-H(23B)	0.9800
C(23B)-H(23C)	0.9800
Br(1A)-C(19A)	1.953(2)
Si(1A)-O(008)	1.6538(17)
Si(1A)-C(22A)	1.859(3)
Si(1A)-C(23A)	1.860(3)
Si(1A)-C(21A)	1.864(3)
O(1A)-C(4A)	1.462(2)
O(1A)-C(2A)	1.472(3)
O(2A)-C(5A)	1.436(3)
O(2A)-H(2A)	0.777(18)
O(3A)-C(17A)	1.455(3)
O(3A)-H(3A)	0.799(18)
O(008)-C(11A)	1.451(3)
C(1A)-C(2A)	1.506(3)
C(1A)-H(1AA)	0.9800
C(1A)-H(1AB)	0.9800
C(1A)-H(1AC)	0.9800
C(2A)-C(4A)	1.480(3)
C(2A)-C(3A)	1.505(3)
C(3A)-H(3AA)	0.9800
C(3A)-H(3AB)	0.9800
C(3A)-H(3AC)	0.9800
C(4A)-C(20A)	1.506(3)
C(4A)-C(5A)	1.507(3)
C(5A)-C(6A)	1.535(3)
C(5A)-H(5A)	1.0000
C(6A)-C(7A)	1.511(3)
C(6A)-C(17A)	1.549(3)
C(6A)-H(6A)	1.0000
C(7A)-C(8A)	1.329(3)
C(7A)-H(7A)	0.9500
C(8A)-C(9A)	1.507(3)
C(8A)-C(10A)	1.507(3)
C(9A)-H(9AA)	0.9800
C(9A)-H(9AB)	0.9800

C(9A)-H(9AC)	0.9800
C(10A)-C(11A)	1.532(3)
C(10A)-H(10C)	0.9900
C(10A)-H(10D)	0.9900
C(11A)-C(12A)	1.515(3)
C(11A)-C(16A)	1.561(3)
C(12A)-C(13A)	1.328(4)
C(12A)-H(12C)	0.9500
C(13A)-C(15A)	1.486(3)
C(13A)-C(14A)	1.501(3)
C(14A)-H(14D)	0.9800
C(14A)-H(14E)	0.9800
C(14A)-H(14F)	0.9800
C(15A)-C(16A)	1.552(3)
C(15A)-H(15A)	0.9900
C(15A)-H(15C)	0.9900
C(16A)-C(17A)	1.564(3)
C(16A)-H(16A)	1.0000
C(17A)-C(18A)	1.557(3)
C(18A)-C(20A)	1.541(3)
C(18A)-C(19A)	1.544(3)
C(18A)-H(18A)	1.0000
C(19A)-H(19E)	0.9900
C(19A)-H(19F)	0.9900
C(20A)-H(20C)	0.9900
C(20A)-H(20D)	0.9900
C(21A)-H(21D)	0.9800
C(21A)-H(21E)	0.9800
C(21A)-H(21F)	0.9800
C(22A)-H(22D)	0.9800
C(22A)-H(22E)	0.9800
C(22A)-H(22F)	0.9800
C(23A)-H(23D)	0.9800
C(23A)-H(23E)	0.9800
C(23A)-H(23F)	0.9800

O(4B)-Si(1B)-C(23B)	104.03(15)
O(4B)-Si(1B)-C(21B)	111.66(15)
C(23B)-Si(1B)-C(21B)	109.7(2)
O(4B)-Si(1B)-C(22B)	112.54(16)
C(23B)-Si(1B)-C(22B)	109.94(18)
C(21B)-Si(1B)-C(22B)	108.9(2)
C(2B)-O(1B)-C(4B)	61.20(19)
C(5B)-O(2B)-H(2B)	105(3)
C(17B)-O(3B)-H(3B)	107(3)
C(11B)-O(4B)-Si(1B)	132.51(17)
C(2B)-C(1B)-H(1BA)	109.5
C(2B)-C(1B)-H(1BB)	109.5
H(1BA)-C(1B)-H(1BB)	109.5
C(2B)-C(1B)-H(1BC)	109.5
H(1BA)-C(1B)-H(1BC)	109.5
H(1BB)-C(1B)-H(1BC)	109.5
O(1B)-C(2B)-C(4B)	59.64(19)
O(1B)-C(2B)-C(3B)	116.9(3)
C(4B)-C(2B)-C(3B)	121.0(3)
O(1B)-C(2B)-C(1B)	114.2(3)
C(4B)-C(2B)-C(1B)	121.6(3)
C(3B)-C(2B)-C(1B)	112.5(3)
C(2B)-C(3B)-H(3BA)	109.5
C(2B)-C(3B)-H(3BB)	109.5
H(3BA)-C(3B)-H(3BB)	109.5
C(2B)-C(3B)-H(3BC)	109.5
H(3BA)-C(3B)-H(3BC)	109.5
H(3BB)-C(3B)-H(3BC)	109.5
O(1B)-C(4B)-C(2B)	59.15(19)
O(1B)-C(4B)-C(5B)	117.8(2)
C(2B)-C(4B)-C(5B)	120.5(3)
O(1B)-C(4B)-C(20B)	117.1(2)
C(2B)-C(4B)-C(20B)	121.2(3)
C(5B)-C(4B)-C(20B)	111.6(3)
O(2B)-C(5B)-C(4B)	112.2(3)
O(2B)-C(5B)-C(6B)	109.1(2)

C(4B)-C(5B)-C(6B)	106.4(2)
O(2B)-C(5B)-H(5B)	109.7
C(4B)-C(5B)-H(5B)	109.7
C(6B)-C(5B)-H(5B)	109.7
C(7B)-C(6B)-C(5B)	112.8(2)
C(7B)-C(6B)-C(17B)	113.7(2)
C(5B)-C(6B)-C(17B)	113.2(2)
C(7B)-C(6B)-H(6B)	105.4
C(5B)-C(6B)-H(6B)	105.4
C(17B)-C(6B)-H(6B)	105.4
C(8B)-C(7B)-C(6B)	122.0(2)
C(8B)-C(7B)-H(7B)	119.0
C(6B)-C(7B)-H(7B)	119.0
C(7B)-C(8B)-C(9B)	123.5(3)
C(7B)-C(8B)-C(10B)	119.7(2)
C(9B)-C(8B)-C(10B)	116.9(3)
C(8B)-C(9B)-H(9BA)	109.5
C(8B)-C(9B)-H(9BB)	109.5
H(9BA)-C(9B)-H(9BB)	109.5
C(8B)-C(9B)-H(9BC)	109.5
H(9BA)-C(9B)-H(9BC)	109.5
H(9BB)-C(9B)-H(9BC)	109.5
C(8B)-C(10B)-C(11B)	116.0(2)
C(8B)-C(10B)-H(10A)	108.3
C(11B)-C(10B)-H(10A)	108.3
C(8B)-C(10B)-H(10B)	108.3
C(11B)-C(10B)-H(10B)	108.3
H(10A)-C(10B)-H(10B)	107.4
O(4B)-C(11B)-C(12B)	110.7(2)
O(4B)-C(11B)-C(16B)	107.5(2)
C(12B)-C(11B)-C(16B)	101.0(2)
O(4B)-C(11B)-C(10B)	108.1(2)
C(12B)-C(11B)-C(10B)	113.5(2)
C(16B)-C(11B)-C(10B)	115.8(2)
C(13B)-C(12B)-C(11B)	105.4(2)
C(13B)-C(12B)-H(12A)	110.7

C(11B)-C(12B)-H(12A)	110.7
C(13B)-C(12B)-H(12B)	110.7
C(11B)-C(12B)-H(12B)	110.7
H(12A)-C(12B)-H(12B)	108.8
C(15B)-C(13B)-C(12B)	110.5(3)
C(15B)-C(13B)-C(14B)	126.6(3)
C(12B)-C(13B)-C(14B)	122.8(3)
C(13B)-C(14B)-H(14A)	109.5
C(13B)-C(14B)-H(14B)	109.5
H(14A)-C(14B)-H(14B)	109.5
C(13B)-C(14B)-H(14C)	109.5
H(14A)-C(14B)-H(14C)	109.5
H(14B)-C(14B)-H(14C)	109.5
C(13B)-C(15B)-C(16B)	109.3(3)
C(13B)-C(15B)-H(15B)	125.4
C(16B)-C(15B)-H(15B)	125.4
C(15B)-C(16B)-C(17B)	121.2(2)
C(15B)-C(16B)-C(11B)	102.7(2)
C(17B)-C(16B)-C(11B)	119.6(2)
C(15B)-C(16B)-H(16B)	103.7
C(17B)-C(16B)-H(16B)	103.7
C(11B)-C(16B)-H(16B)	103.7
O(3B)-C(17B)-C(16B)	103.8(2)
O(3B)-C(17B)-C(18B)	109.4(2)
C(16B)-C(17B)-C(18B)	117.4(2)
O(3B)-C(17B)-C(6B)	112.7(2)
C(16B)-C(17B)-C(6B)	107.1(2)
C(18B)-C(17B)-C(6B)	106.8(2)
C(19B)-C(18B)-C(20B)	111.7(3)
C(19B)-C(18B)-C(17B)	112.7(2)
C(20B)-C(18B)-C(17B)	110.0(2)
C(19B)-C(18B)-H(18B)	107.4
C(20B)-C(18B)-H(18B)	107.4
C(17B)-C(18B)-H(18B)	107.4
C(18B)-C(19B)-Br(1)	116.3(4)
C(18B)-C(19B)-Br(1B)	111.4(2)

C(18B)-C(19B)-H(19C)	108.2
Br(1)-C(19B)-H(19C)	108.2
C(18B)-C(19B)-H(19D)	108.2
Br(1)-C(19B)-H(19D)	108.2
H(19C)-C(19B)-H(19D)	107.4
C(18B)-C(19B)-H(19A)	109.4
Br(1B)-C(19B)-H(19A)	109.4
C(18B)-C(19B)-H(19B)	109.4
Br(1B)-C(19B)-H(19B)	109.4
H(19A)-C(19B)-H(19B)	108.0
C(4B)-C(20B)-C(18B)	110.6(2)
C(4B)-C(20B)-H(20A)	109.5
C(18B)-C(20B)-H(20A)	109.5
C(4B)-C(20B)-H(20B)	109.5
C(18B)-C(20B)-H(20B)	109.5
H(20A)-C(20B)-H(20B)	108.1
Si(1B)-C(21B)-H(21A)	109.5
Si(1B)-C(21B)-H(21B)	109.5
H(21A)-C(21B)-H(21B)	109.5
Si(1B)-C(21B)-H(21C)	109.5
H(21A)-C(21B)-H(21C)	109.5
H(21B)-C(21B)-H(21C)	109.5
Si(1B)-C(22B)-H(22A)	109.5
Si(1B)-C(22B)-H(22B)	109.5
H(22A)-C(22B)-H(22B)	109.5
Si(1B)-C(22B)-H(22C)	109.5
H(22A)-C(22B)-H(22C)	109.5
H(22B)-C(22B)-H(22C)	109.5
Si(1B)-C(23B)-H(23A)	109.5
Si(1B)-C(23B)-H(23B)	109.5
H(23A)-C(23B)-H(23B)	109.5
Si(1B)-C(23B)-H(23C)	109.5
H(23A)-C(23B)-H(23C)	109.5
H(23B)-C(23B)-H(23C)	109.5
O(008)-Si(1A)-C(22A)	104.20(10)
O(008)-Si(1A)-C(23A)	112.00(11)

C(22A)-Si(1A)-C(23A)	110.60(13)
O(008)-Si(1A)-C(21A)	112.94(11)
C(22A)-Si(1A)-C(21A)	108.45(13)
C(23A)-Si(1A)-C(21A)	108.55(12)
C(4A)-O(1A)-C(2A)	60.58(14)
C(5A)-O(2A)-H(2A)	109(3)
C(17A)-O(3A)-H(3A)	109(3)
C(11A)-O(008)-Si(1A)	130.04(14)
C(2A)-C(1A)-H(1AA)	109.5
C(2A)-C(1A)-H(1AB)	109.5
H(1AA)-C(1A)-H(1AB)	109.5
C(2A)-C(1A)-H(1AC)	109.5
H(1AA)-C(1A)-H(1AC)	109.5
H(1AB)-C(1A)-H(1AC)	109.5
O(1A)-C(2A)-C(4A)	59.38(13)
O(1A)-C(2A)-C(3A)	114.34(18)
C(4A)-C(2A)-C(3A)	122.8(2)
O(1A)-C(2A)-C(1A)	113.95(19)
C(4A)-C(2A)-C(1A)	120.2(2)
C(3A)-C(2A)-C(1A)	113.5(2)
C(2A)-C(3A)-H(3AA)	109.5
C(2A)-C(3A)-H(3AB)	109.5
H(3AA)-C(3A)-H(3AB)	109.5
C(2A)-C(3A)-H(3AC)	109.5
H(3AA)-C(3A)-H(3AC)	109.5
H(3AB)-C(3A)-H(3AC)	109.5
O(1A)-C(4A)-C(2A)	60.05(13)
O(1A)-C(4A)-C(20A)	114.30(18)
C(2A)-C(4A)-C(20A)	124.2(2)
O(1A)-C(4A)-C(5A)	116.53(17)
C(2A)-C(4A)-C(5A)	121.2(2)
C(20A)-C(4A)-C(5A)	110.38(19)
O(2A)-C(5A)-C(4A)	109.27(18)
O(2A)-C(5A)-C(6A)	110.13(18)
C(4A)-C(5A)-C(6A)	107.88(17)
O(2A)-C(5A)-H(5A)	109.8

C(4A)-C(5A)-H(5A)	109.8
C(6A)-C(5A)-H(5A)	109.8
C(7A)-C(6A)-C(5A)	109.94(18)
C(7A)-C(6A)-C(17A)	112.70(18)
C(5A)-C(6A)-C(17A)	112.96(18)
C(7A)-C(6A)-H(6A)	106.9
C(5A)-C(6A)-H(6A)	106.9
C(17A)-C(6A)-H(6A)	106.9
C(8A)-C(7A)-C(6A)	127.0(2)
C(8A)-C(7A)-H(7A)	116.5
C(6A)-C(7A)-H(7A)	116.5
C(7A)-C(8A)-C(9A)	121.2(2)
C(7A)-C(8A)-C(10A)	125.8(2)
C(9A)-C(8A)-C(10A)	113.0(2)
C(8A)-C(9A)-H(9AA)	109.5
C(8A)-C(9A)-H(9AB)	109.5
H(9AA)-C(9A)-H(9AB)	109.5
C(8A)-C(9A)-H(9AC)	109.5
H(9AA)-C(9A)-H(9AC)	109.5
H(9AB)-C(9A)-H(9AC)	109.5
C(8A)-C(10A)-C(11A)	119.8(2)
C(8A)-C(10A)-H(10C)	107.4
C(11A)-C(10A)-H(10C)	107.4
C(8A)-C(10A)-H(10D)	107.4
C(11A)-C(10A)-H(10D)	107.4
H(10C)-C(10A)-H(10D)	106.9
O(008)-C(11A)-C(12A)	109.68(18)
O(008)-C(11A)-C(10A)	110.21(19)
C(12A)-C(11A)-C(10A)	110.52(19)
O(008)-C(11A)-C(16A)	110.93(18)
C(12A)-C(11A)-C(16A)	101.92(18)
C(10A)-C(11A)-C(16A)	113.29(19)
C(13A)-C(12A)-C(11A)	111.9(2)
C(13A)-C(12A)-H(12C)	124.1
C(11A)-C(12A)-H(12C)	124.1
C(12A)-C(13A)-C(15A)	111.3(2)

C(12A)-C(13A)-C(14A)	127.1(2)
C(15A)-C(13A)-C(14A)	121.6(2)
C(13A)-C(14A)-H(14D)	109.5
C(13A)-C(14A)-H(14E)	109.5
H(14D)-C(14A)-H(14E)	109.5
C(13A)-C(14A)-H(14F)	109.5
H(14D)-C(14A)-H(14F)	109.5
H(14E)-C(14A)-H(14F)	109.5
C(13A)-C(15A)-C(16A)	104.1(2)
C(13A)-C(15A)-H(15A)	110.9
C(16A)-C(15A)-H(15A)	110.9
C(13A)-C(15A)-H(15C)	110.9
C(16A)-C(15A)-H(15C)	110.9
H(15A)-C(15A)-H(15C)	109.0
C(15A)-C(16A)-C(11A)	102.89(18)
C(15A)-C(16A)-C(17A)	119.57(19)
C(11A)-C(16A)-C(17A)	119.19(19)
C(15A)-C(16A)-H(16A)	104.5
C(11A)-C(16A)-H(16A)	104.5
C(17A)-C(16A)-H(16A)	104.5
O(3A)-C(17A)-C(6A)	109.14(17)
O(3A)-C(17A)-C(18A)	107.27(17)
C(6A)-C(17A)-C(18A)	111.11(18)
O(3A)-C(17A)-C(16A)	105.78(17)
C(6A)-C(17A)-C(16A)	110.11(18)
C(18A)-C(17A)-C(16A)	113.19(17)
C(20A)-C(18A)-C(19A)	106.58(18)
C(20A)-C(18A)-C(17A)	114.14(18)
C(19A)-C(18A)-C(17A)	109.85(19)
C(20A)-C(18A)-H(18A)	108.7
C(19A)-C(18A)-H(18A)	108.7
C(17A)-C(18A)-H(18A)	108.7
C(18A)-C(19A)-Br(1A)	112.26(17)
C(18A)-C(19A)-H(19E)	109.2
Br(1A)-C(19A)-H(19E)	109.2
C(18A)-C(19A)-H(19F)	109.2

Br(1A)-C(19A)-H(19F)	109.2
H(19E)-C(19A)-H(19F)	107.9
C(4A)-C(20A)-C(18A)	113.80(18)
C(4A)-C(20A)-H(20C)	108.8
C(18A)-C(20A)-H(20C)	108.8
C(4A)-C(20A)-H(20D)	108.8
C(18A)-C(20A)-H(20D)	108.8
H(20C)-C(20A)-H(20D)	107.7
Si(1A)-C(21A)-H(21D)	109.5
Si(1A)-C(21A)-H(21E)	109.5
H(21D)-C(21A)-H(21E)	109.5
Si(1A)-C(21A)-H(21F)	109.5
H(21D)-C(21A)-H(21F)	109.5
H(21E)-C(21A)-H(21F)	109.5
Si(1A)-C(22A)-H(22D)	109.5
Si(1A)-C(22A)-H(22E)	109.5
H(22D)-C(22A)-H(22E)	109.5
Si(1A)-C(22A)-H(22F)	109.5
H(22D)-C(22A)-H(22F)	109.5
H(22E)-C(22A)-H(22F)	109.5
Si(1A)-C(23A)-H(23D)	109.5
Si(1A)-C(23A)-H(23E)	109.5
H(23D)-C(23A)-H(23E)	109.5
Si(1A)-C(23A)-H(23F)	109.5
H(23D)-C(23A)-H(23F)	109.5
H(23E)-C(23A)-H(23F)	109.5

Symmetry transformations used to generate equivalent atoms:

Table 4. Anisotropic displacement parameters ($Å^2 x\ 10^3$)for vhv_08_202. The anisotropic displacement factor exponent takes the form: $-2\pi^2[\ h^2 a^{*2} U^{11} + ... + 2\ h\ k\ a^*\ b^*\ U^{12}\ ]$

	U^{11}	U^{22}	U^{33}	U^{23}	U^{13}	U^{12}
Br(1)	45(2)	169(5)	42(2)	-28(3)	10(2)	38(3)
Br(1B)	62(1)	54(1)	50(1)	-7(1)	26(1)	21(1)
Si(1B)	52(1)	32(1)	55(1)	6(1)	25(1)	12(1)
O(1B)	30(1)	73(2)	53(1)	2(1)	0(1)	15(1)
O(2B)	41(1)	43(1)	45(1)	6(1)	-2(1)	-4(1)
O(3B)	40(1)	43(1)	34(1)	9(1)	11(1)	0(1)
O(4B)	44(1)	32(1)	46(1)	5(1)	24(1)	14(1)
C(1B)	61(2)	44(2)	41(2)	8(1)	5(2)	24(2)
C(2B)	36(1)	48(2)	40(2)	0(1)	0(1)	18(1)
C(3B)	62(2)	57(2)	50(2)	-1(2)	1(2)	37(2)
C(4B)	27(1)	51(2)	41(2)	-1(1)	3(1)	10(1)
C(5B)	36(1)	34(1)	32(1)	1(1)	4(1)	4(1)
C(6B)	34(1)	31(1)	26(1)	1(1)	7(1)	8(1)
C(7B)	45(2)	29(1)	26(1)	1(1)	7(1)	11(1)
C(8B)	48(2)	33(1)	27(1)	5(1)	16(1)	18(1)
C(9B)	63(2)	40(2)	44(2)	10(1)	30(2)	25(1)
C(10B)	40(1)	35(1)	34(1)	5(1)	18(1)	13(1)
C(11B)	35(1)	30(1)	32(1)	2(1)	13(1)	11(1)
C(12B)	35(1)	45(2)	45(2)	0(1)	12(1)	8(1)
C(13B)	44(2)	43(2)	38(2)	-4(1)	-1(1)	19(1)
C(14B)	51(2)	51(2)	49(2)	-2(2)	-10(2)	13(2)
C(15B)	39(2)	54(2)	27(1)	3(1)	9(1)	11(1)
C(16B)	34(1)	35(1)	26(1)	3(1)	9(1)	9(1)
C(17B)	33(1)	34(1)	27(1)	5(1)	11(1)	6(1)
C(18B)	36(1)	48(2)	31(1)	-1(1)	10(1)	14(1)
C(19B)	77(3)	87(3)	37(2)	-3(2)	13(2)	51(2)
C(20B)	35(2)	61(2)	42(2)	2(1)	14(1)	15(1)
C(21B)	88(3)	50(2)	107(4)	23(2)	66(3)	13(2)
C(22B)	72(3)	39(2)	82(3)	-7(2)	7(2)	12(2)
C(23B)	72(2)	41(2)	72(2)	8(2)	21(2)	22(2)
Br(1A)	44(1)	47(1)	48(1)	7(1)	23(1)	-3(1)

Si(1A)	25(1)	22(1)	31(1)	4(1)	13(1)	9(1)
O(1A)	24(1)	26(1)	31(1)	6(1)	9(1)	15(1)
O(2A)	35(1)	20(1)	28(1)	1(1)	10(1)	11(1)
O(3A)	26(1)	23(1)	25(1)	0(1)	9(1)	7(1)
O(008)	27(1)	25(1)	29(1)	3(1)	9(1)	12(1)
C(1A)	25(1)	28(1)	38(1)	2(1)	6(1)	5(1)
C(2A)	23(1)	23(1)	28(1)	4(1)	8(1)	12(1)
C(3A)	34(1)	30(1)	27(1)	3(1)	10(1)	12(1)
C(4A)	20(1)	22(1)	27(1)	6(1)	9(1)	11(1)
C(5A)	25(1)	20(1)	24(1)	2(1)	8(1)	8(1)
C(6A)	20(1)	21(1)	24(1)	3(1)	9(1)	7(1)
C(7A)	24(1)	22(1)	25(1)	4(1)	9(1)	5(1)
C(8A)	23(1)	26(1)	26(1)	4(1)	9(1)	5(1)
C(9A)	23(1)	32(1)	35(1)	6(1)	12(1)	4(1)
C(10A)	24(1)	29(1)	40(1)	5(1)	15(1)	9(1)
C(11A)	24(1)	25(1)	28(1)	5(1)	11(1)	10(1)
C(12A)	26(1)	27(1)	35(1)	5(1)	9(1)	14(1)
C(13A)	35(1)	29(1)	33(1)	8(1)	8(1)	14(1)
C(14A)	57(2)	38(2)	44(2)	16(1)	19(1)	25(1)
C(15A)	33(1)	34(1)	30(1)	10(1)	12(1)	14(1)
C(16A)	22(1)	25(1)	26(1)	4(1)	8(1)	9(1)
C(17A)	21(1)	19(1)	23(1)	1(1)	7(1)	6(1)
C(18A)	22(1)	22(1)	28(1)	7(1)	10(1)	5(1)
C(19A)	28(1)	31(1)	33(1)	8(1)	13(1)	7(1)
C(20A)	23(1)	28(1)	29(1)	8(1)	11(1)	9(1)
C(21A)	35(1)	33(1)	43(2)	1(1)	19(1)	12(1)
C(22A)	34(1)	36(1)	37(1)	4(1)	11(1)	15(1)
C(23A)	30(1)	27(1)	44(2)	7(1)	12(1)	6(1)

Table 5. Hydrogen coordinates (x 10^4) and isotropic displacement parameters ($Å^2$x 10^3) for vhv_08_202.

	x	y	z	U(eq)
H(1BA)	4990	2855	8572	73
H(1BB)	3344	2867	8075	73
H(1BC)	4627	3776	8389	73
H(3BA)	5032	2123	6601	85
H(3BB)	3597	1790	6896	85
H(3BC)	5211	1862	7501	85
H(5B)	4199	4630	7594	44
H(6B)	1997	3612	6752	38
H(7B)	2001	5394	6975	41
H(9BA)	-1565	5101	6555	65
H(9BB)	-115	5648	7267	65
H(9BC)	-1213	4797	7443	65
H(10A)	-1728	3412	6532	41
H(10B)	-210	3163	6914	41
H(12A)	-2908	2395	5018	51
H(12B)	-2746	3442	5124	51
H(14A)	-3854	3117	3389	84
H(14B)	-3659	2136	3387	84
H(14C)	-2701	2852	2984	84
H(15B)	-29	3502	3929	49
H(16B)	65	4337	5331	38
H(18B)	2267	2696	5705	46
H(19C)	2783	3439	4313	76
H(19D)	1322	2709	4312	76
H(19A)	2948	3397	4327	76
H(19B)	1336	2800	4284	76
H(20A)	4843	3042	5828	54
H(20B)	4855	4044	5699	54
H(21A)	-1836	1443	6901	112
H(21B)	-2920	559	6332	112

H(21C)	-3197	1499	6147	112
H(22A)	-3253	1022	4449	104
H(22B)	-2728	141	4592	104
H(22C)	-1801	922	4235	104
H(23A)	888	801	5702	91
H(23B)	-236	89	6020	91
H(23C)	800	971	6609	91
H(1AA)	12919	7910	11387	47
H(1AB)	11679	8339	10876	47
H(1AC)	12653	7928	10430	47
H(3AA)	9786	6148	11255	45
H(3AB)	9881	7166	11480	45
H(3AC)	11267	6792	11878	45
H(5A)	8584	5636	10098	27
H(6A)	7774	6925	9781	25
H(7A)	5927	5233	9180	28
H(9AA)	2664	5426	8549	44
H(9AB)	2942	5622	9510	44
H(9AC)	3517	4860	9155	44
H(10C)	4590	7237	9700	36
H(10D)	3761	7033	8746	36
H(12C)	4629	8732	8828	34
H(14D)	4941	9806	7802	65
H(14E)	5319	9377	7050	65
H(14F)	6616	10036	7773	65
H(15A)	7978	8628	8179	37
H(15C)	6738	8131	7340	37
H(16A)	5666	7041	7931	28
H(18A)	9516	8009	9008	28
H(19E)	8622	7704	7481	36
H(19F)	9664	7048	7579	36
H(20C)	10515	6491	8696	30
H(20D)	11486	7400	9261	30
H(21D)	5055	9146	10287	53
H(21E)	6184	9692	11129	53
H(21F)	5609	8637	11042	53

H(22D)	8674	8435	11546	52
H(22E)	9329	9488	11687	52
H(22F)	9863	8890	11111	52
H(23D)	8657	9913	9561	50
H(23E)	8718	10529	10348	50
H(23F)	7217	10207	9603	50
H(2B)	5300(50)	5530(30)	7030(30)	57(12)
H(3B)	3160(50)	5050(30)	5580(30)	62(12)
H(2A)	8550(40)	4805(15)	9130(20)	46(10)
H(3A)	7590(40)	5797(18)	8020(20)	53(11)

Table 6. Torsion angles [°] for vhv_08_202.

C(23B)-Si(1B)-O(4B)-C(11B)	-166.8(2)
C(21B)-Si(1B)-O(4B)-C(11B)	-48.6(3)
C(22B)-Si(1B)-O(4B)-C(11B)	74.2(3)
C(4B)-O(1B)-C(2B)-C(3B)	111.9(3)
C(4B)-O(1B)-C(2B)-C(1B)	-113.8(3)
C(2B)-O(1B)-C(4B)-C(5B)	110.7(3)
C(2B)-O(1B)-C(4B)-C(20B)	-111.8(3)
C(3B)-C(2B)-C(4B)-O(1B)	-105.1(3)
C(1B)-C(2B)-C(4B)-O(1B)	101.4(3)
O(1B)-C(2B)-C(4B)-C(5B)	-106.2(3)
C(3B)-C(2B)-C(4B)-C(5B)	148.7(3)
C(1B)-C(2B)-C(4B)-C(5B)	-4.9(4)
O(1B)-C(2B)-C(4B)-C(20B)	105.0(3)
C(3B)-C(2B)-C(4B)-C(20B)	-0.1(4)
C(1B)-C(2B)-C(4B)-C(20B)	-153.7(3)
O(1B)-C(4B)-C(5B)-O(2B)	80.7(3)
C(2B)-C(4B)-C(5B)-O(2B)	149.5(3)
C(20B)-C(4B)-C(5B)-O(2B)	-59.0(3)
O(1B)-C(4B)-C(5B)-C(6B)	-160.0(3)
C(2B)-C(4B)-C(5B)-C(6B)	-91.3(3)
C(20B)-C(4B)-C(5B)-C(6B)	60.3(3)
O(2B)-C(5B)-C(6B)-C(7B)	-70.5(3)
C(4B)-C(5B)-C(6B)-C(7B)	168.3(2)
O(2B)-C(5B)-C(6B)-C(17B)	60.4(3)
C(4B)-C(5B)-C(6B)-C(17B)	-60.8(3)
C(5B)-C(6B)-C(7B)-C(8B)	-150.9(3)
C(17B)-C(6B)-C(7B)-C(8B)	78.5(3)
C(6B)-C(7B)-C(8B)-C(9B)	179.9(2)
C(6B)-C(7B)-C(8B)-C(10B)	-0.3(4)
C(7B)-C(8B)-C(10B)-C(11B)	-56.6(3)
C(9B)-C(8B)-C(10B)-C(11B)	123.2(3)
Si(1B)-O(4B)-C(11B)-C(12B)	-38.1(3)
Si(1B)-O(4B)-C(11B)-C(16B)	-147.5(2)
Si(1B)-O(4B)-C(11B)-C(10B)	86.8(3)

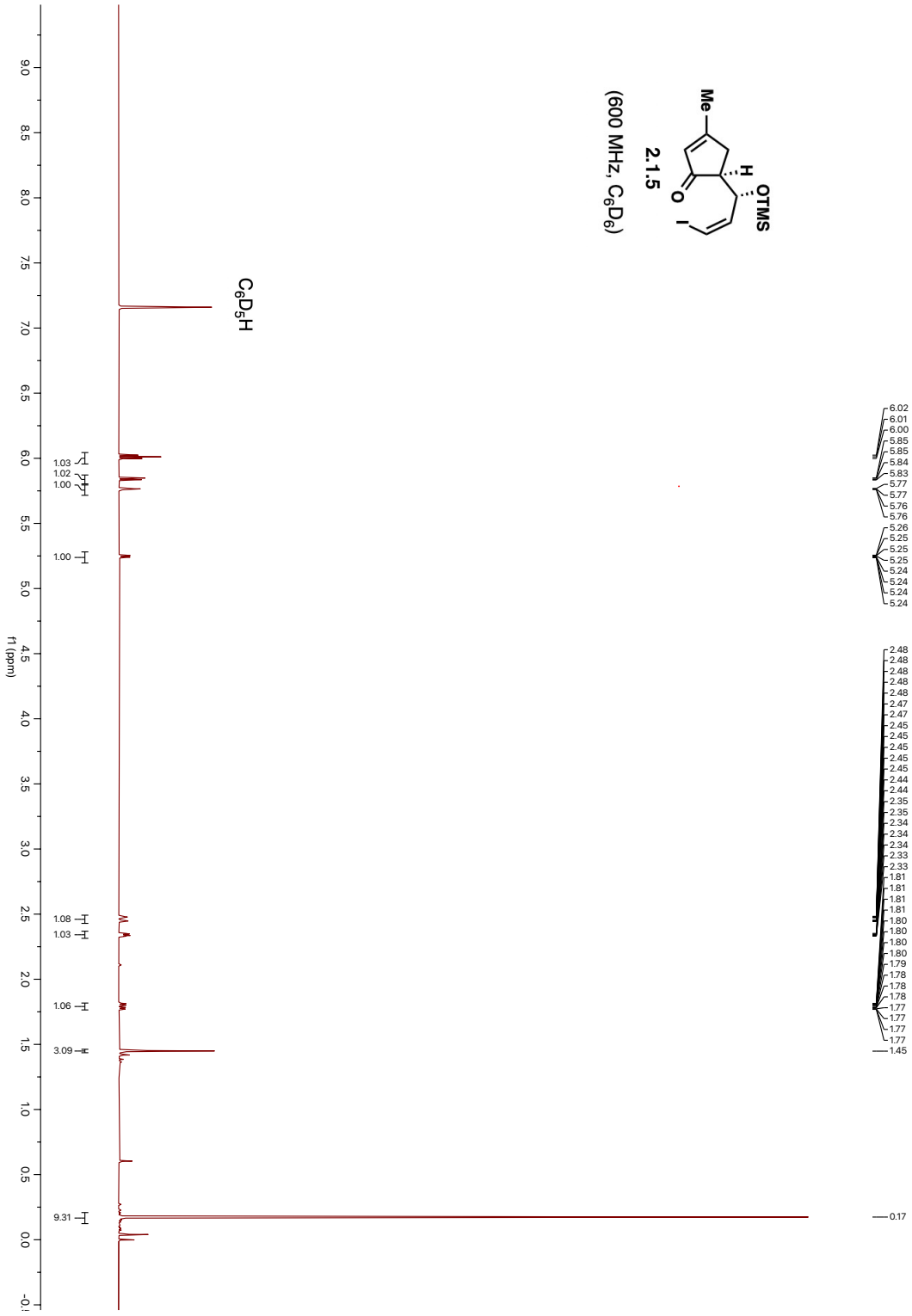
C(8B)-C(10B)-C(11B)-O(4B)	131.6(2)
C(8B)-C(10B)-C(11B)-C(12B)	-105.1(3)
C(8B)-C(10B)-C(11B)-C(16B)	11.0(3)
O(4B)-C(11B)-C(12B)-C(13B)	-83.7(3)
C(16B)-C(11B)-C(12B)-C(13B)	29.9(3)
C(10B)-C(11B)-C(12B)-C(13B)	154.5(2)
C(11B)-C(12B)-C(13B)-C(15B)	-16.3(3)
C(11B)-C(12B)-C(13B)-C(14B)	167.8(3)
C(12B)-C(13B)-C(15B)-C(16B)	-5.3(3)
C(14B)-C(13B)-C(15B)-C(16B)	170.3(3)
C(13B)-C(15B)-C(16B)-C(17B)	161.1(3)
C(13B)-C(15B)-C(16B)-C(11B)	24.3(3)
O(4B)-C(11B)-C(16B)-C(15B)	84.0(2)
C(12B)-C(11B)-C(16B)-C(15B)	-32.1(3)
C(10B)-C(11B)-C(16B)-C(15B)	-155.0(2)
O(4B)-C(11B)-C(16B)-C(17B)	-53.7(3)
C(12B)-C(11B)-C(16B)-C(17B)	-169.7(2)
C(10B)-C(11B)-C(16B)-C(17B)	67.3(3)
C(15B)-C(16B)-C(17B)-O(3B)	65.4(3)
C(11B)-C(16B)-C(17B)-O(3B)	-164.9(2)
C(15B)-C(16B)-C(17B)-C(18B)	-55.4(3)
C(11B)-C(16B)-C(17B)-C(18B)	74.4(3)
C(15B)-C(16B)-C(17B)-C(6B)	-175.3(2)
C(11B)-C(16B)-C(17B)-C(6B)	-45.5(3)
C(7B)-C(6B)-C(17B)-O(3B)	69.8(3)
C(5B)-C(6B)-C(17B)-O(3B)	-60.7(3)
C(7B)-C(6B)-C(17B)-C(16B)	-43.7(3)
C(5B)-C(6B)-C(17B)-C(16B)	-174.1(2)
C(7B)-C(6B)-C(17B)-C(18B)	-170.2(2)
C(5B)-C(6B)-C(17B)-C(18B)	59.4(3)
O(3B)-C(17B)-C(18B)-C(19B)	-58.9(3)
C(16B)-C(17B)-C(18B)-C(19B)	58.9(4)
C(6B)-C(17B)-C(18B)-C(19B)	178.9(3)
O(3B)-C(17B)-C(18B)-C(20B)	66.3(3)
C(16B)-C(17B)-C(18B)-C(20B)	-175.9(2)
C(6B)-C(17B)-C(18B)-C(20B)	-55.8(3)

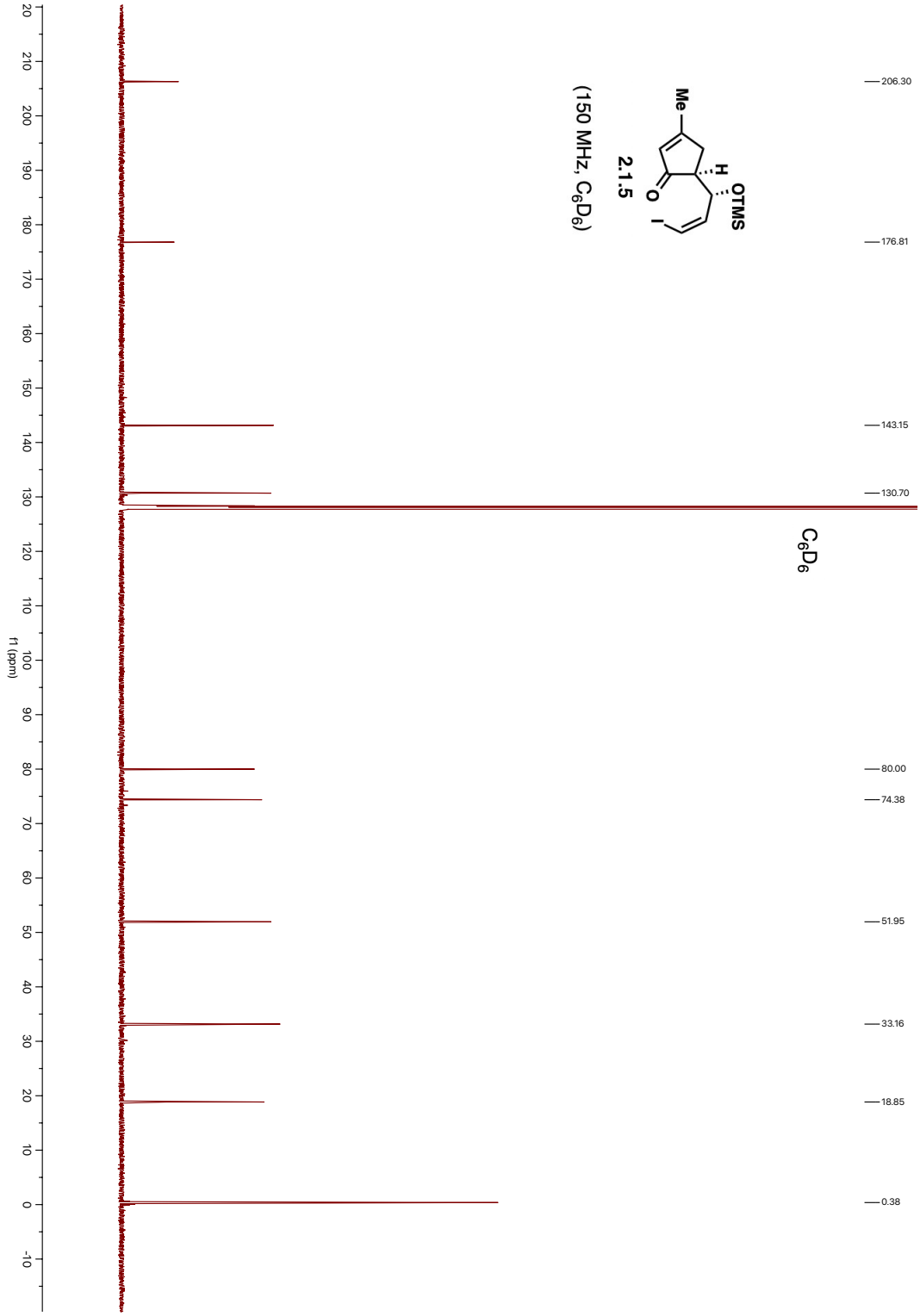
C(20B)-C(18B)-C(19B)-Br(1)	55.7(7)
C(17B)-C(18B)-C(19B)-Br(1)	-180.0(7)
C(20B)-C(18B)-C(19B)-Br(1B)	66.0(4)
C(17B)-C(18B)-C(19B)-Br(1B)	-169.7(2)
O(1B)-C(4B)-C(20B)-C(18B)	158.7(3)
C(2B)-C(4B)-C(20B)-C(18B)	90.0(3)
C(5B)-C(4B)-C(20B)-C(18B)	-61.3(3)
C(19B)-C(18B)-C(20B)-C(4B)	-175.7(3)
C(17B)-C(18B)-C(20B)-C(4B)	58.5(3)
C(22A)-Si(1A)-O(008)-C(11A)	173.14(19)
C(23A)-Si(1A)-O(008)-C(11A)	-67.3(2)
C(21A)-Si(1A)-O(008)-C(11A)	55.6(2)
C(4A)-O(1A)-C(2A)-C(3A)	115.0(2)
C(4A)-O(1A)-C(2A)-C(1A)	-112.2(2)
C(2A)-O(1A)-C(4A)-C(20A)	116.9(2)
C(2A)-O(1A)-C(4A)-C(5A)	-112.4(2)
C(3A)-C(2A)-C(4A)-O(1A)	-100.9(2)
C(1A)-C(2A)-C(4A)-O(1A)	101.6(2)
O(1A)-C(2A)-C(4A)-C(20A)	-100.5(2)
C(3A)-C(2A)-C(4A)-C(20A)	158.6(2)
C(1A)-C(2A)-C(4A)-C(20A)	1.1(3)
O(1A)-C(2A)-C(4A)-C(5A)	104.7(2)
C(3A)-C(2A)-C(4A)-C(5A)	3.8(3)
C(1A)-C(2A)-C(4A)-C(5A)	-153.7(2)
O(1A)-C(4A)-C(5A)-O(2A)	-76.1(2)
C(2A)-C(4A)-C(5A)-O(2A)	-145.59(19)
C(20A)-C(4A)-C(5A)-O(2A)	56.5(2)
O(1A)-C(4A)-C(5A)-C(6A)	164.20(18)
C(2A)-C(4A)-C(5A)-C(6A)	94.7(2)
C(20A)-C(4A)-C(5A)-C(6A)	-63.3(2)
O(2A)-C(5A)-C(6A)-C(7A)	69.2(2)
C(4A)-C(5A)-C(6A)-C(7A)	-171.57(18)
O(2A)-C(5A)-C(6A)-C(17A)	-57.6(2)
C(4A)-C(5A)-C(6A)-C(17A)	61.6(2)
C(5A)-C(6A)-C(7A)-C(8A)	162.8(2)
C(17A)-C(6A)-C(7A)-C(8A)	-70.3(3)

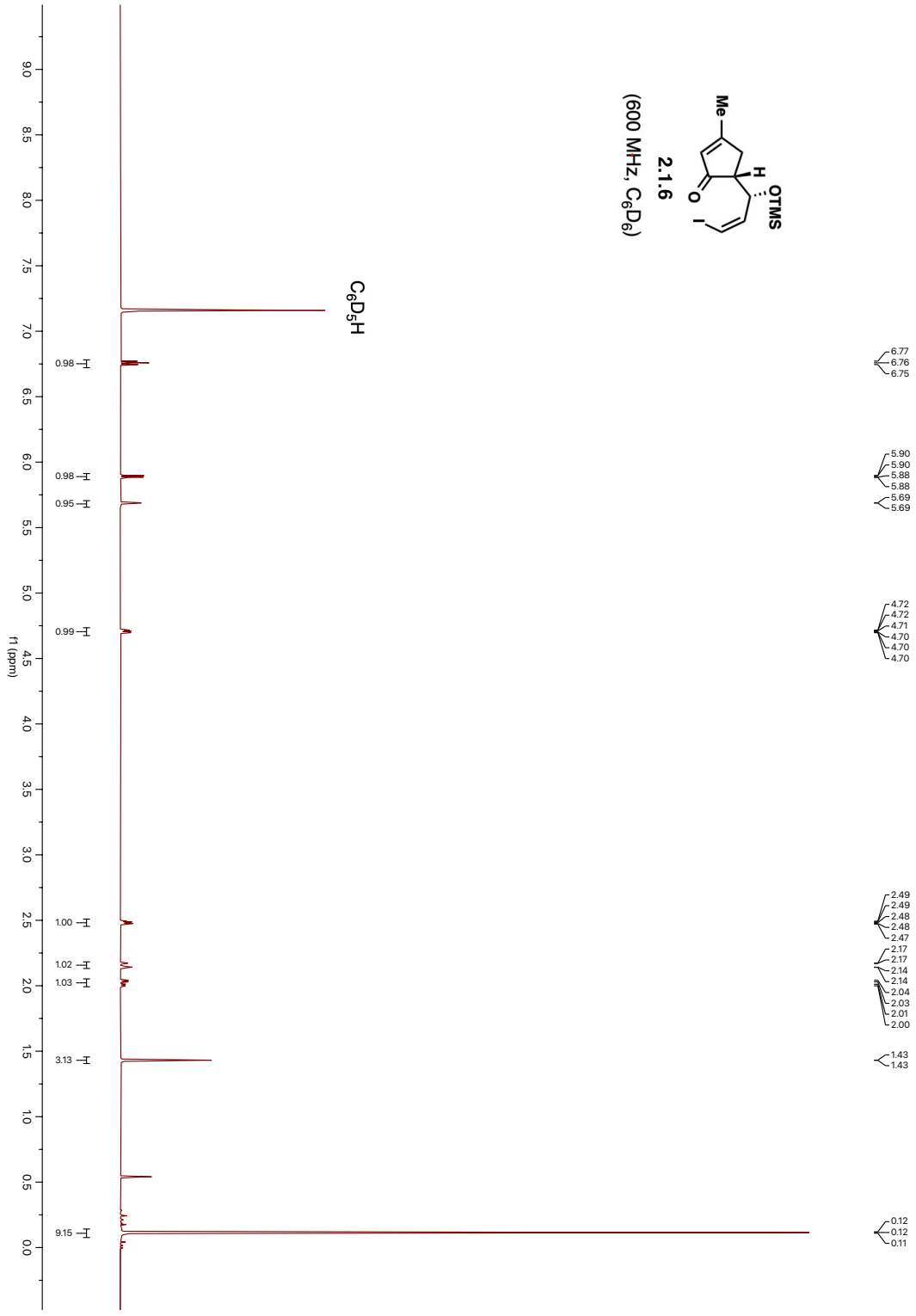
C(6A)-C(7A)-C(8A)-C(9A)	-178.0(2)
C(6A)-C(7A)-C(8A)-C(10A)	4.1(4)
C(7A)-C(8A)-C(10A)-C(11A)	14.3(4)
C(9A)-C(8A)-C(10A)-C(11A)	-163.8(2)
Si(1A)-O(008)-C(11A)-C(12A)	21.3(3)
Si(1A)-O(008)-C(11A)-C(10A)	-100.6(2)
Si(1A)-O(008)-C(11A)-C(16A)	133.09(17)
C(8A)-C(10A)-C(11A)-O(008)	-84.6(3)
C(8A)-C(10A)-C(11A)-C(12A)	154.0(2)
C(8A)-C(10A)-C(11A)-C(16A)	40.4(3)
O(008)-C(11A)-C(12A)-C(13A)	98.3(2)
C(10A)-C(11A)-C(12A)-C(13A)	-140.0(2)
C(16A)-C(11A)-C(12A)-C(13A)	-19.3(3)
C(11A)-C(12A)-C(13A)-C(15A)	2.9(3)
C(11A)-C(12A)-C(13A)-C(14A)	-175.1(3)
C(12A)-C(13A)-C(15A)-C(16A)	15.1(3)
C(14A)-C(13A)-C(15A)-C(16A)	-166.8(2)
C(13A)-C(15A)-C(16A)-C(11A)	-25.8(2)
C(13A)-C(15A)-C(16A)-C(17A)	-160.6(2)
O(008)-C(11A)-C(16A)-C(15A)	-90.0(2)
C(12A)-C(11A)-C(16A)-C(15A)	26.7(2)
C(10A)-C(11A)-C(16A)-C(15A)	145.4(2)
O(008)-C(11A)-C(16A)-C(17A)	45.0(3)
C(12A)-C(11A)-C(16A)-C(17A)	161.74(19)
C(10A)-C(11A)-C(16A)-C(17A)	-79.5(3)
C(7A)-C(6A)-C(17A)-O(3A)	-57.5(2)
C(5A)-C(6A)-C(17A)-O(3A)	67.8(2)
C(7A)-C(6A)-C(17A)-C(18A)	-175.62(18)
C(5A)-C(6A)-C(17A)-C(18A)	-50.3(2)
C(7A)-C(6A)-C(17A)-C(16A)	58.2(2)
C(5A)-C(6A)-C(17A)-C(16A)	-176.48(18)
C(15A)-C(16A)-C(17A)-O(3A)	-92.9(2)
C(11A)-C(16A)-C(17A)-O(3A)	139.43(19)
C(15A)-C(16A)-C(17A)-C(6A)	149.3(2)
C(11A)-C(16A)-C(17A)-C(6A)	21.6(3)
C(15A)-C(16A)-C(17A)-C(18A)	24.3(3)

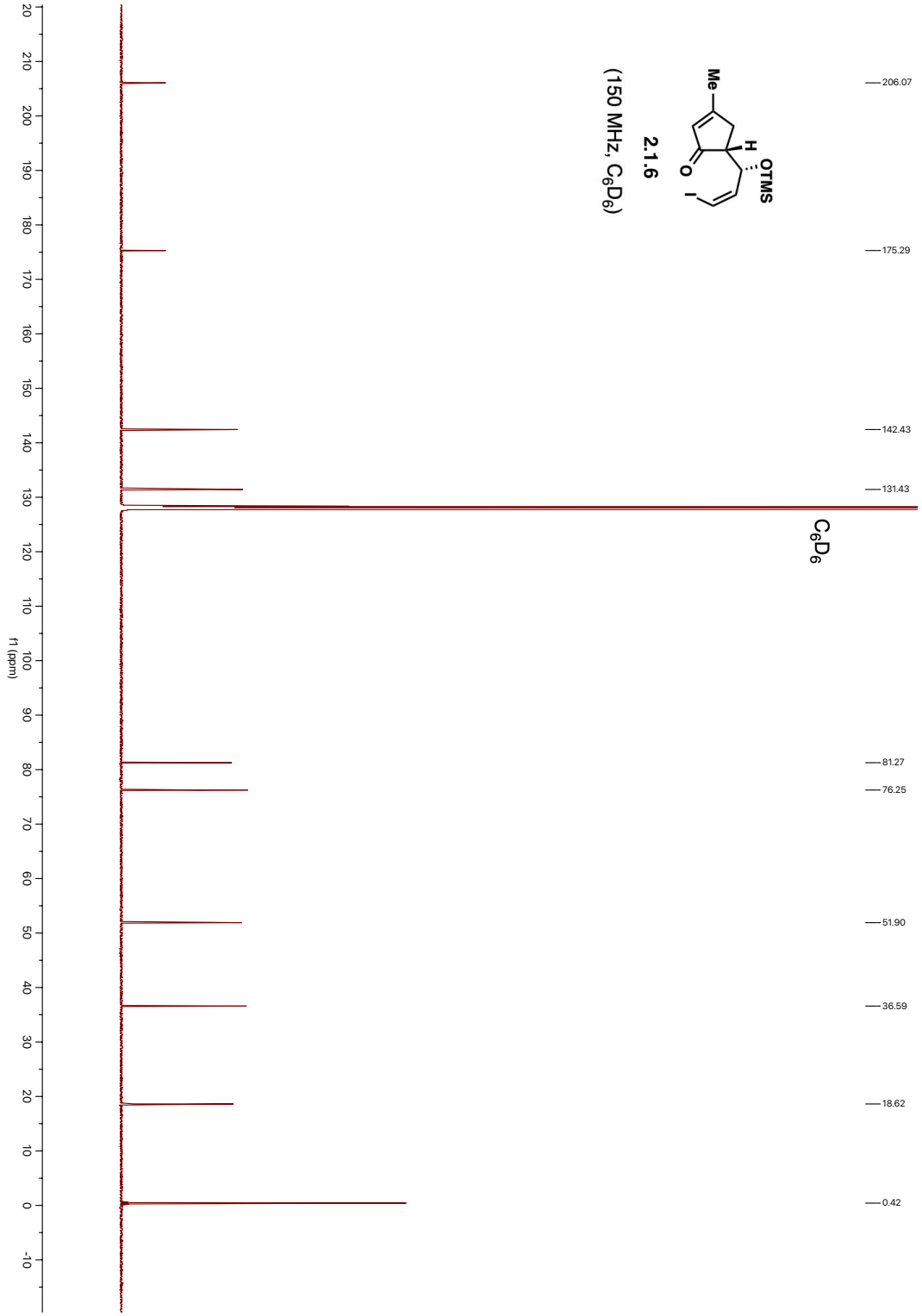
C(11A)-C(16A)-C(17A)-C(18A)	-103.4(2)
O(3A)-C(17A)-C(18A)-C(20A)	-78.1(2)
C(6A)-C(17A)-C(18A)-C(20A)	41.1(3)
C(16A)-C(17A)-C(18A)-C(20A)	165.57(19)
O(3A)-C(17A)-C(18A)-C(19A)	41.5(2)
C(6A)-C(17A)-C(18A)-C(19A)	160.70(18)
C(16A)-C(17A)-C(18A)-C(19A)	-74.8(2)
C(20A)-C(18A)-C(19A)-Br(1A)	-76.6(2)
C(17A)-C(18A)-C(19A)-Br(1A)	159.31(15)
O(1A)-C(4A)-C(20A)-C(18A)	-169.89(18)
C(2A)-C(4A)-C(20A)-C(18A)	-100.7(2)
C(5A)-C(4A)-C(20A)-C(18A)	56.4(2)
C(19A)-C(18A)-C(20A)-C(4A)	-166.60(19)
C(17A)-C(18A)-C(20A)-C(4A)	-45.2(3)

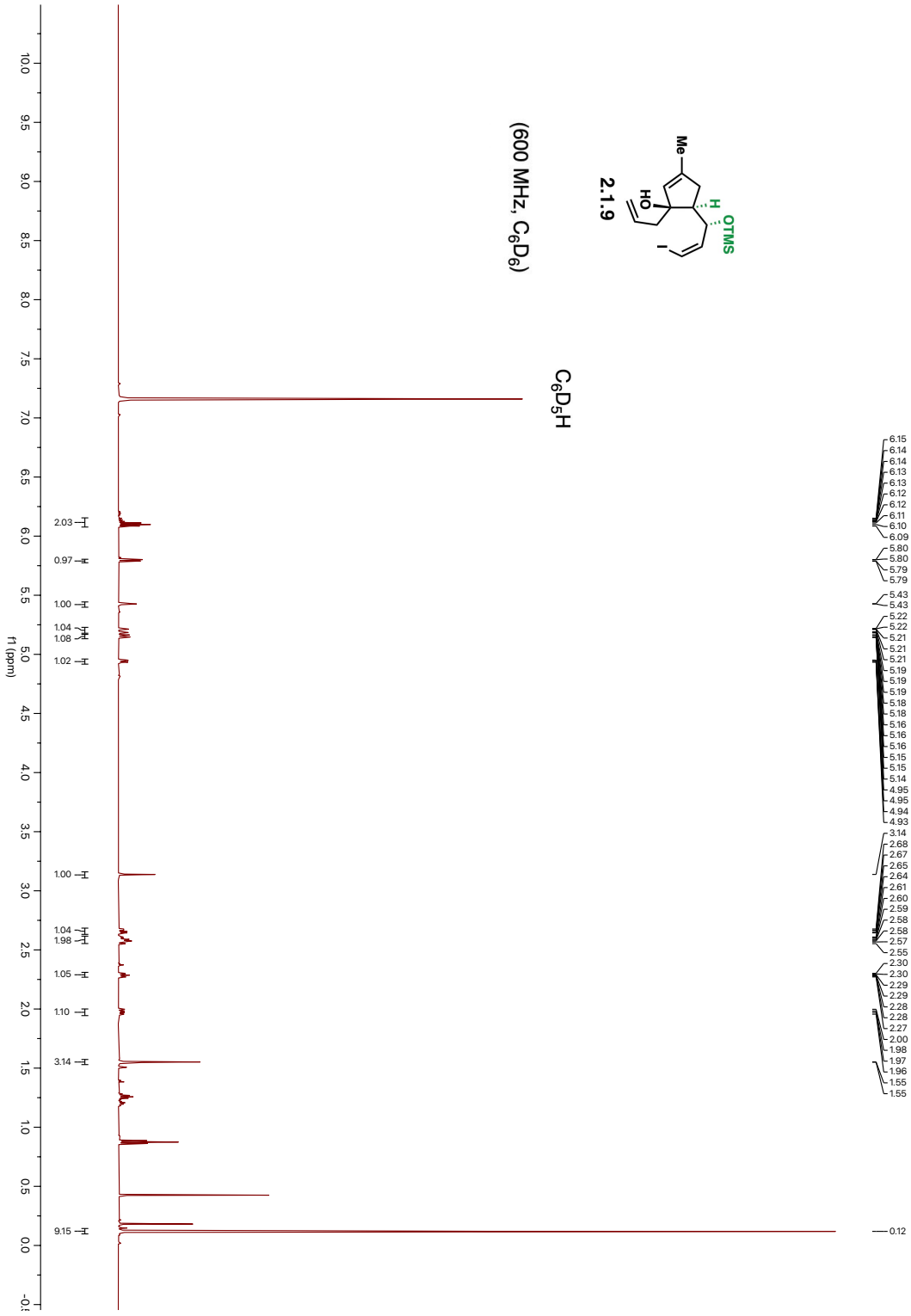
Symmetry transformations used to generate equivalent atoms:

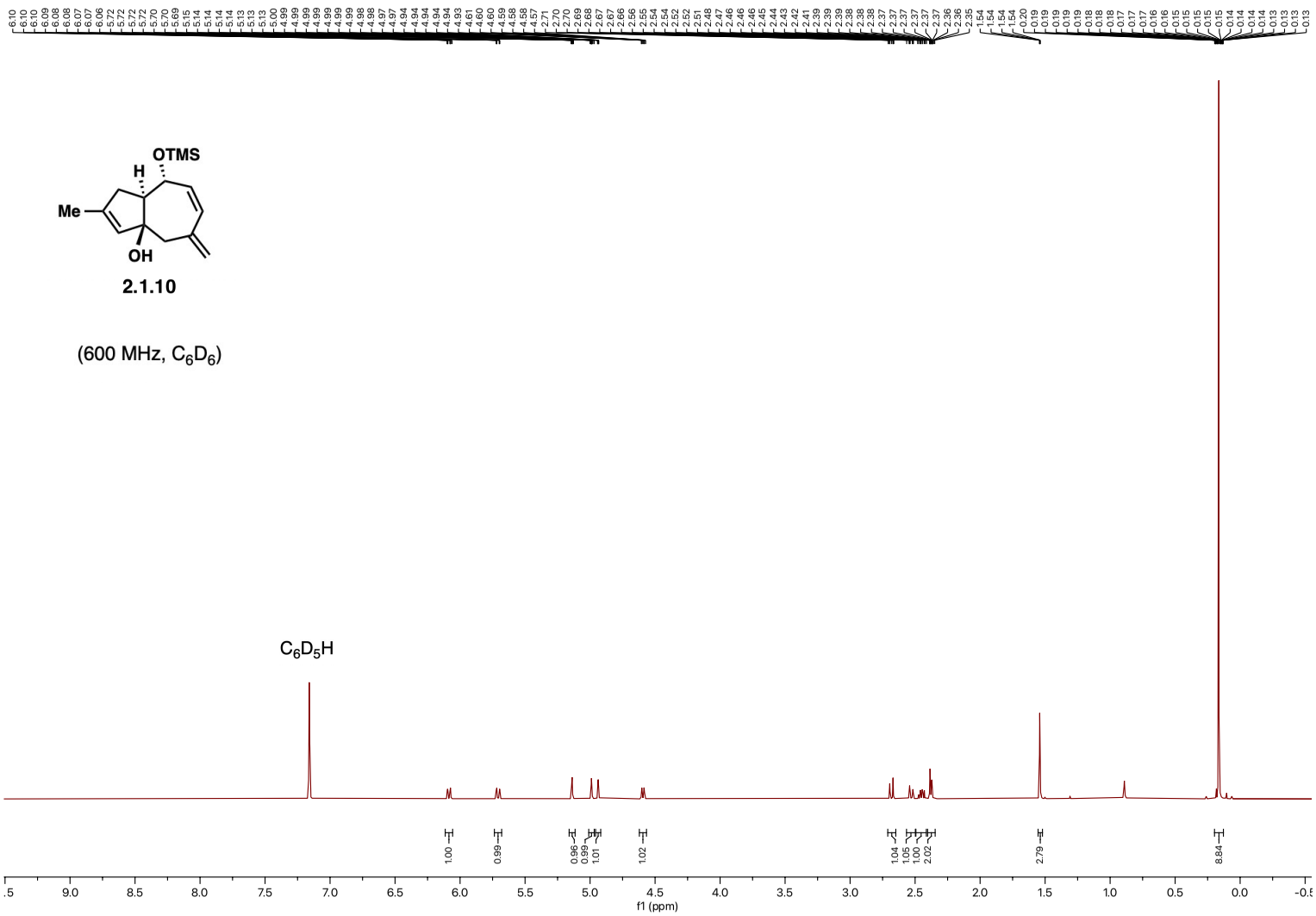

Me
H
OTMS
O
2.1.5
(600 MHz, C6D6)
C6D5H
f1 (ppm)
9.0
8.5
8.0
7.5
7.0
6.5
6.0
5.5
5.0
4.5
4.0
3.5
3.0
2.5
2.0
1.5
1.0
0.5
0.0
1.03
1.02
1.00
1.00
1.08
1.03
1.06
3.09
9.31
6.02
6.01
6.00
5.85
5.85
5.84
5.83
5.77
5.77
5.76
5.76
5.26
5.25
5.25
5.25
5.24
5.24
5.24
5.24
2.48
2.48
2.48
2.48
2.48
2.47
2.47
2.45
2.45
2.45
2.45
2.45
2.44
2.44
2.35
2.35
2.34
2.34
2.34
2.33
2.33
1.81
1.81
1.81
1.81
1.80
1.80
1.80
1.80
1.79
1.78
1.78
1.78
1.77
1.77
1.77
1.77
1.45
0.17

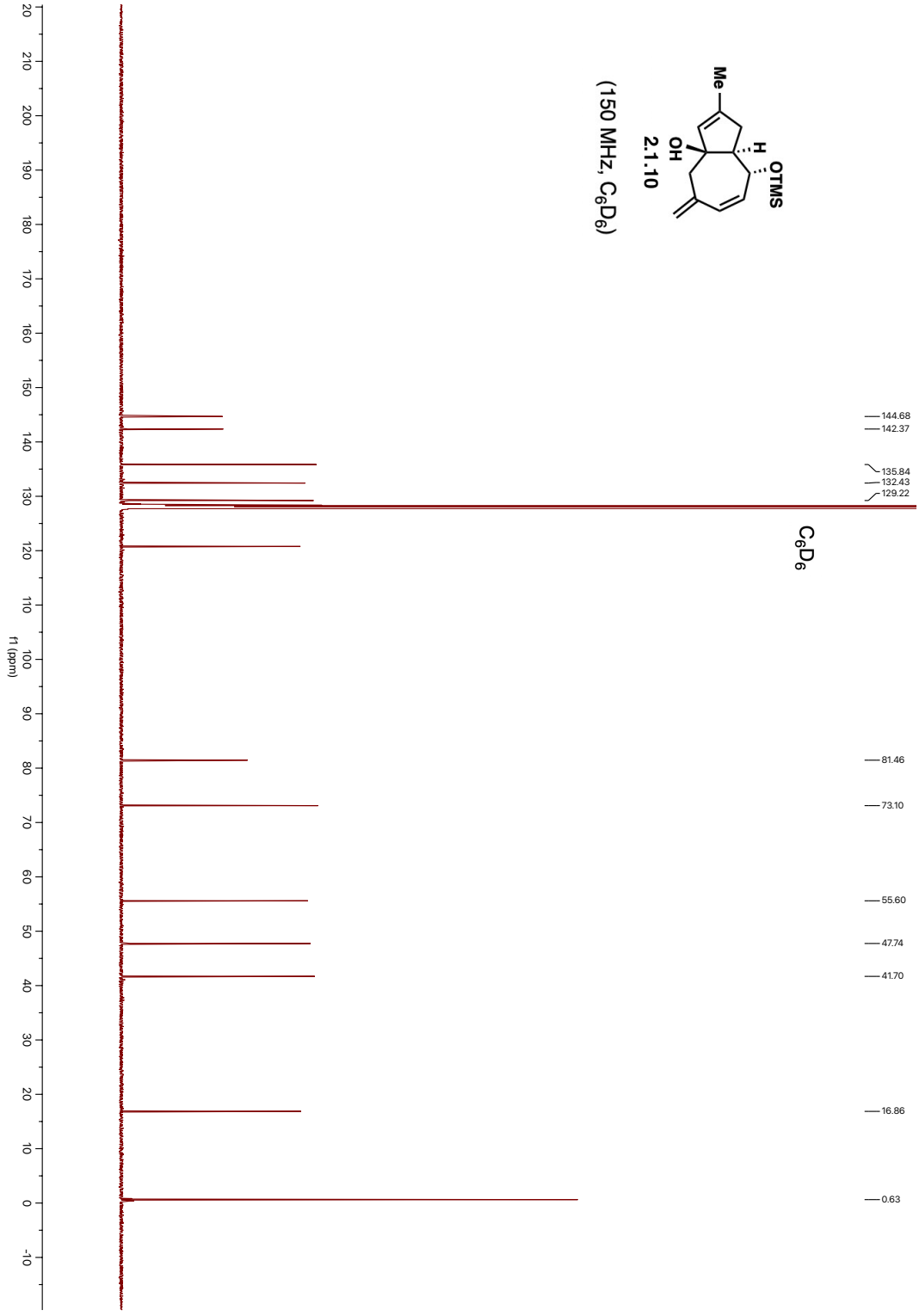

Me
H
OTMS
O
2.1.5
(150 MHz, C6D6)
206.30
176.81
143.15
130.70
C6D6
80.00
74.38
51.95
33.16
18.85
0.38
f1 (ppm)

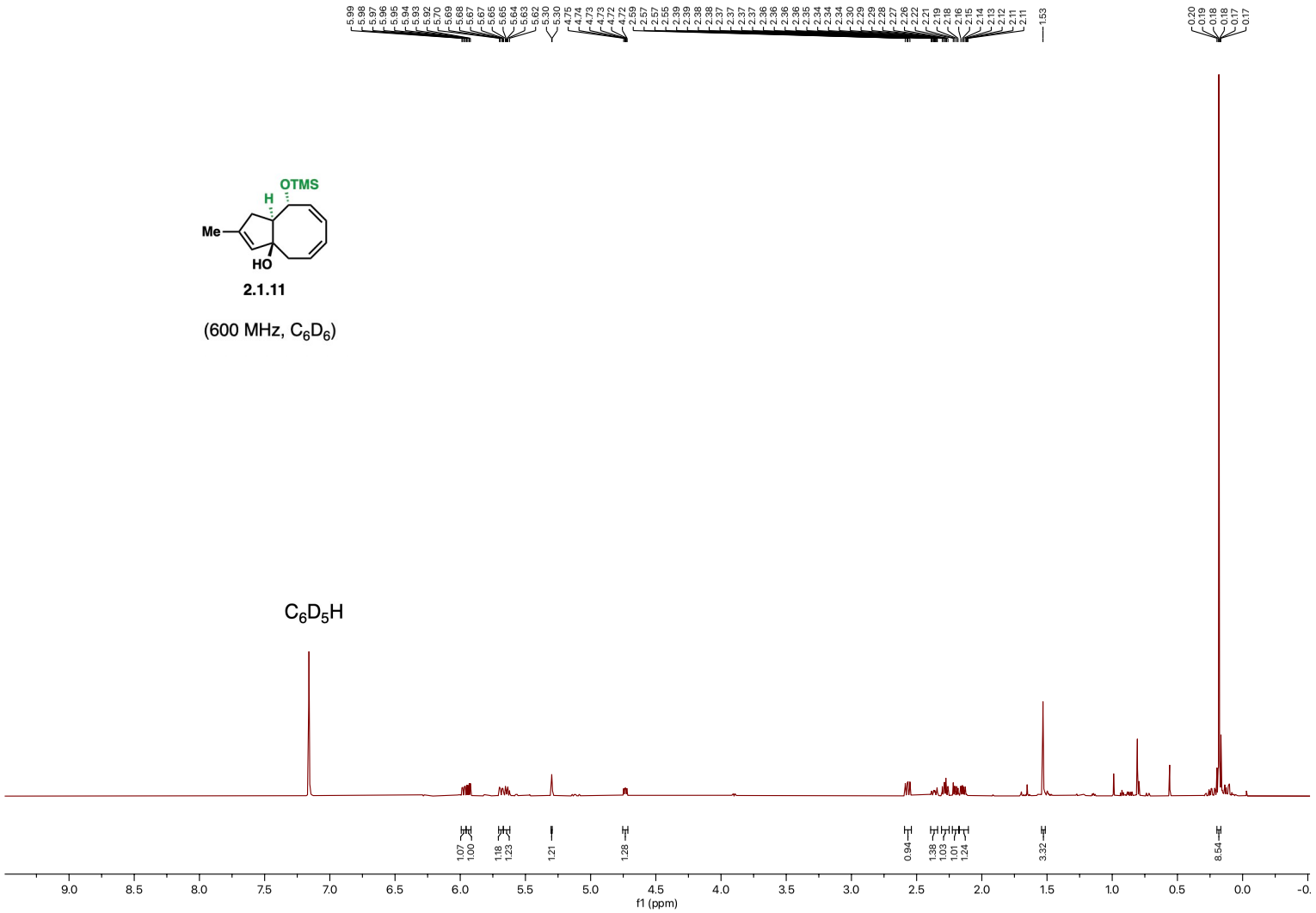

2.1.6
(600 MHz, C_6D_6)
Me
H
OTMS
O
I
C_6D_5H
f1 (ppm)
9.0
8.5
8.0
7.5
7.0
6.5
6.0
5.5
5.0
4.5
4.0
3.5
3.0
2.5
2.0
1.5
1.0
0.5
0.0
0.98
0.98
0.95
0.99
1.00
1.02
1.03
3.13
9.15
6.77
6.76
6.75
5.90
5.90
5.88
5.88
5.69
5.69
4.72
4.72
4.71
4.70
4.70
4.70
2.49
2.49
2.48
2.48
2.47
2.17
2.17
2.14
2.14
2.04
2.03
2.01
2.00
1.43
1.43
0.12
0.12
0.11

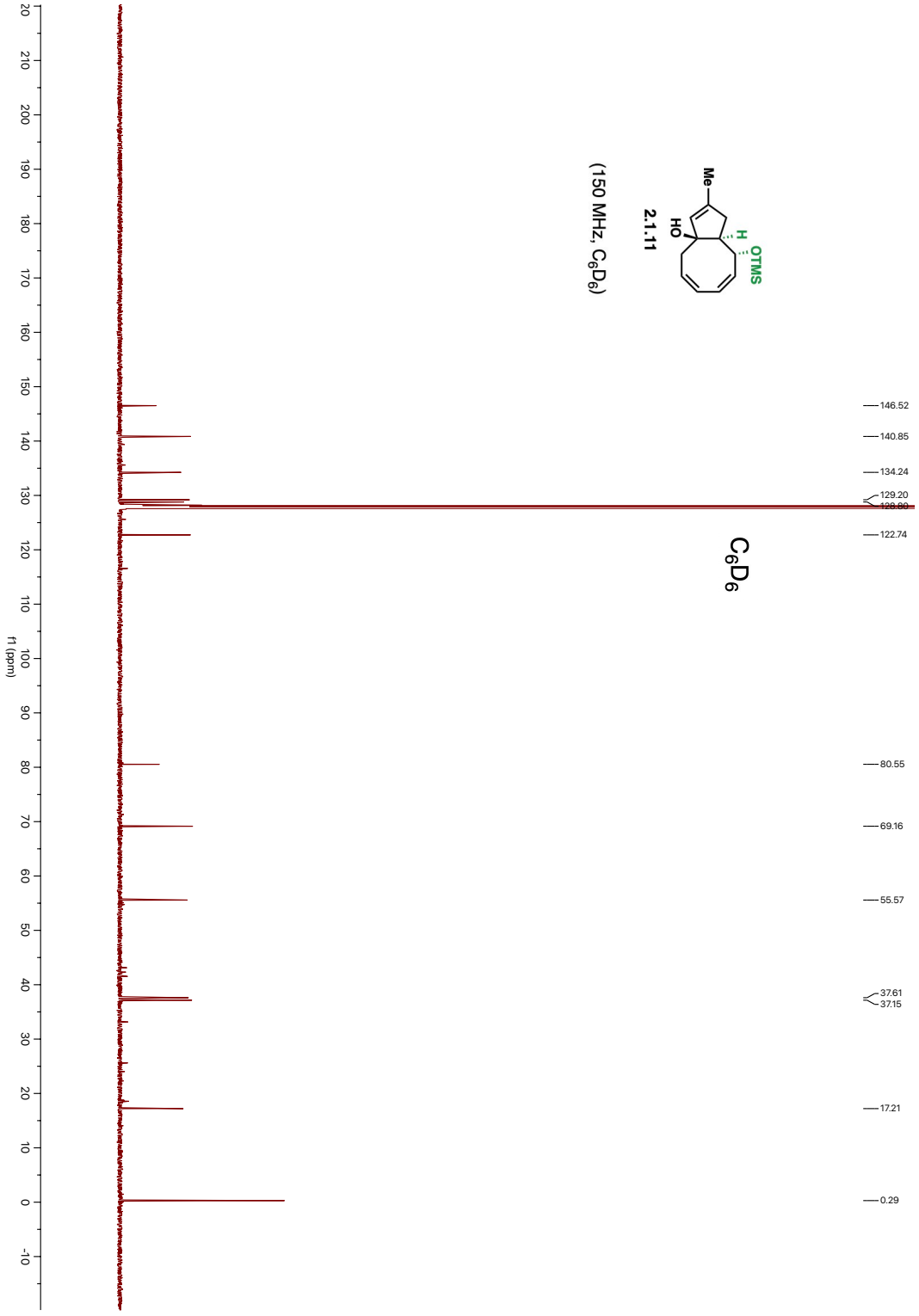

Me
H
OTMS
O
I
2.1.6
(150 MHz, C6D6)
206.07
175.29
142.43
131.43
C6D6
81.27
76.25
51.90
36.59
18.62
0.42
f1 (ppm)

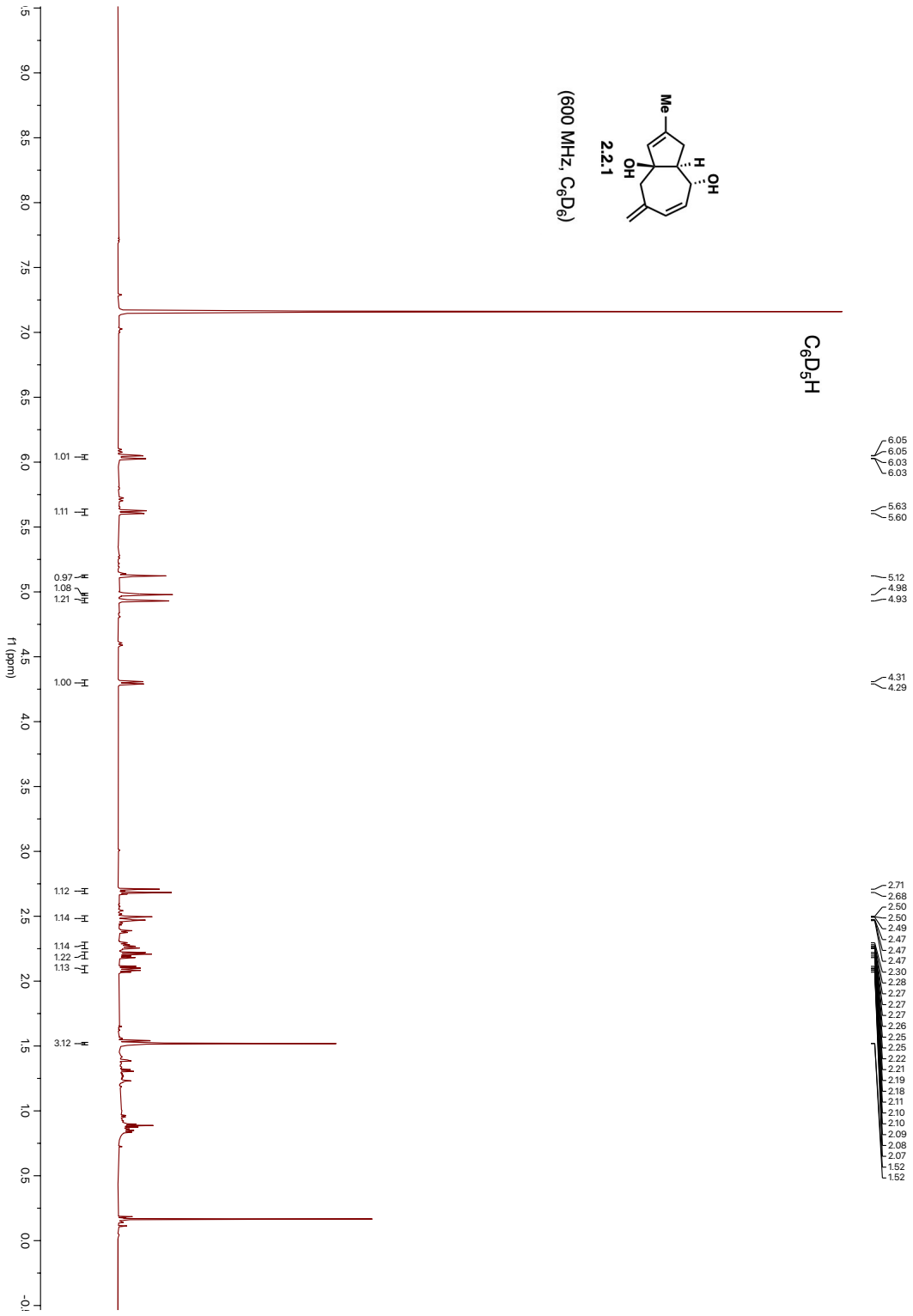

2.1.9
(600 MHz, C_6D_6)
C_6D_5H
Me
HO
H
OTMS
f1 (ppm)
2.03
0.97
1.00
1.04
1.08
1.02
1.00
1.04
1.98
1.05
1.10
3.14
9.15
0.12

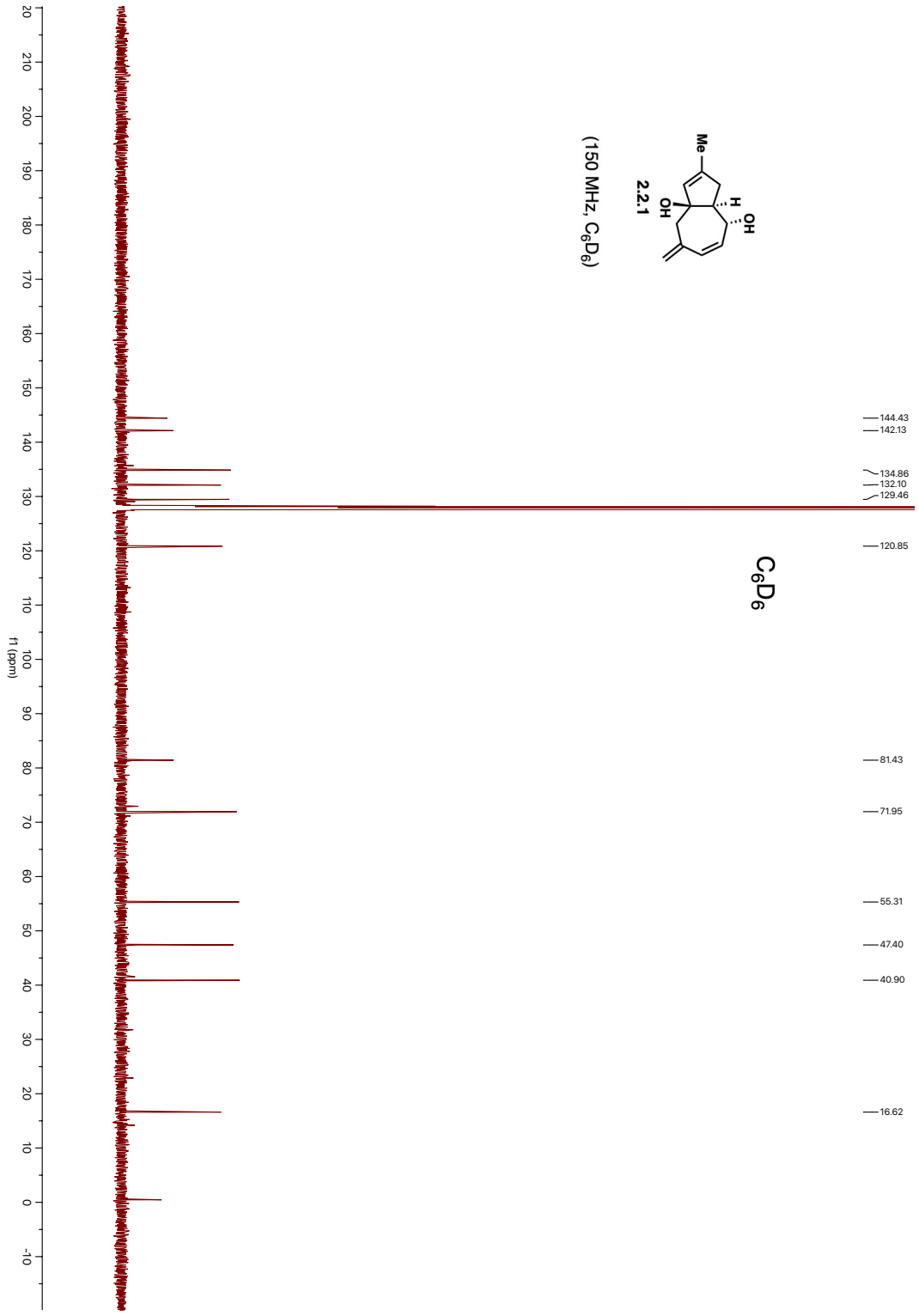

OTMS
H
Me
OH
2.1.10
(600 MHz, C6D6)
C6D5H
1.00
0.99
0.96
0.99
1.01
1.02
1.04
1.05
1.00
2.02
2.79
8.84
f1 (ppm)

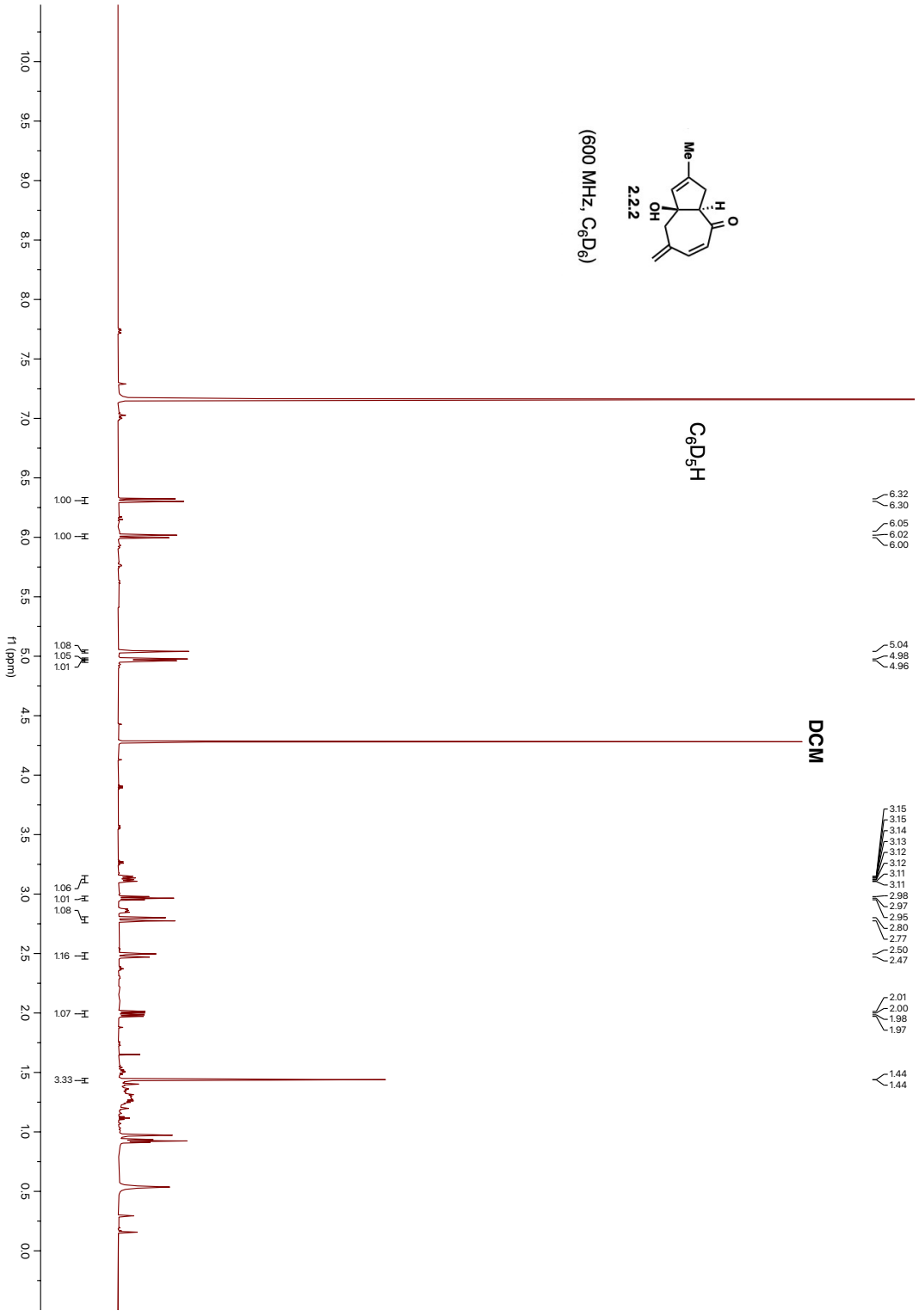

Me
H
OTMS
OH
2.1.10
(150 MHz, C6D6)
144.68
142.37
135.84
132.43
129.22
C6D6
81.46
73.10
55.60
47.74
41.70
16.86
0.63
f1 (ppm)

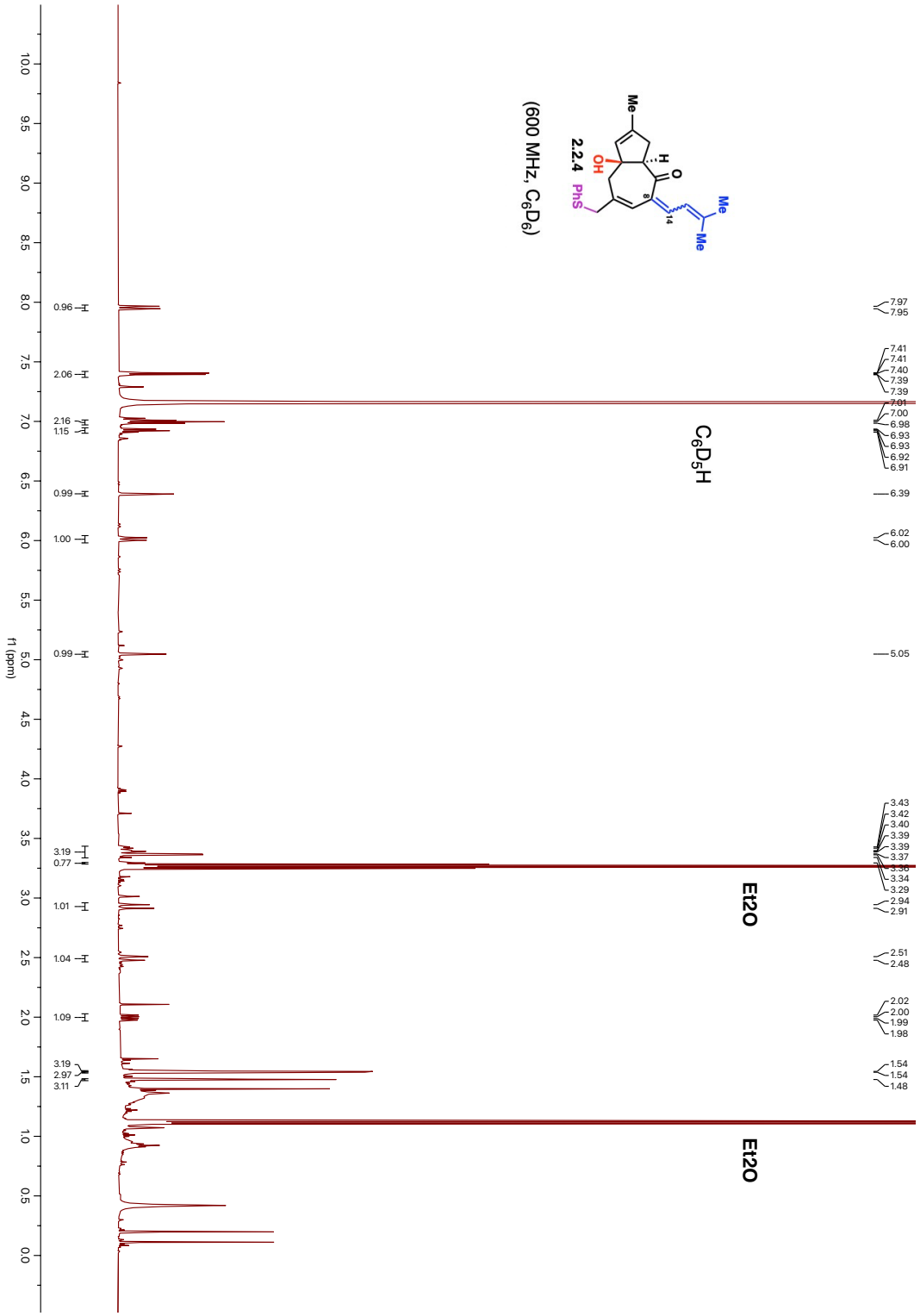

OTMS
H
Me
HO
2.1.11
(600 MHz, C6D6)
C6D5H
f1 (ppm)

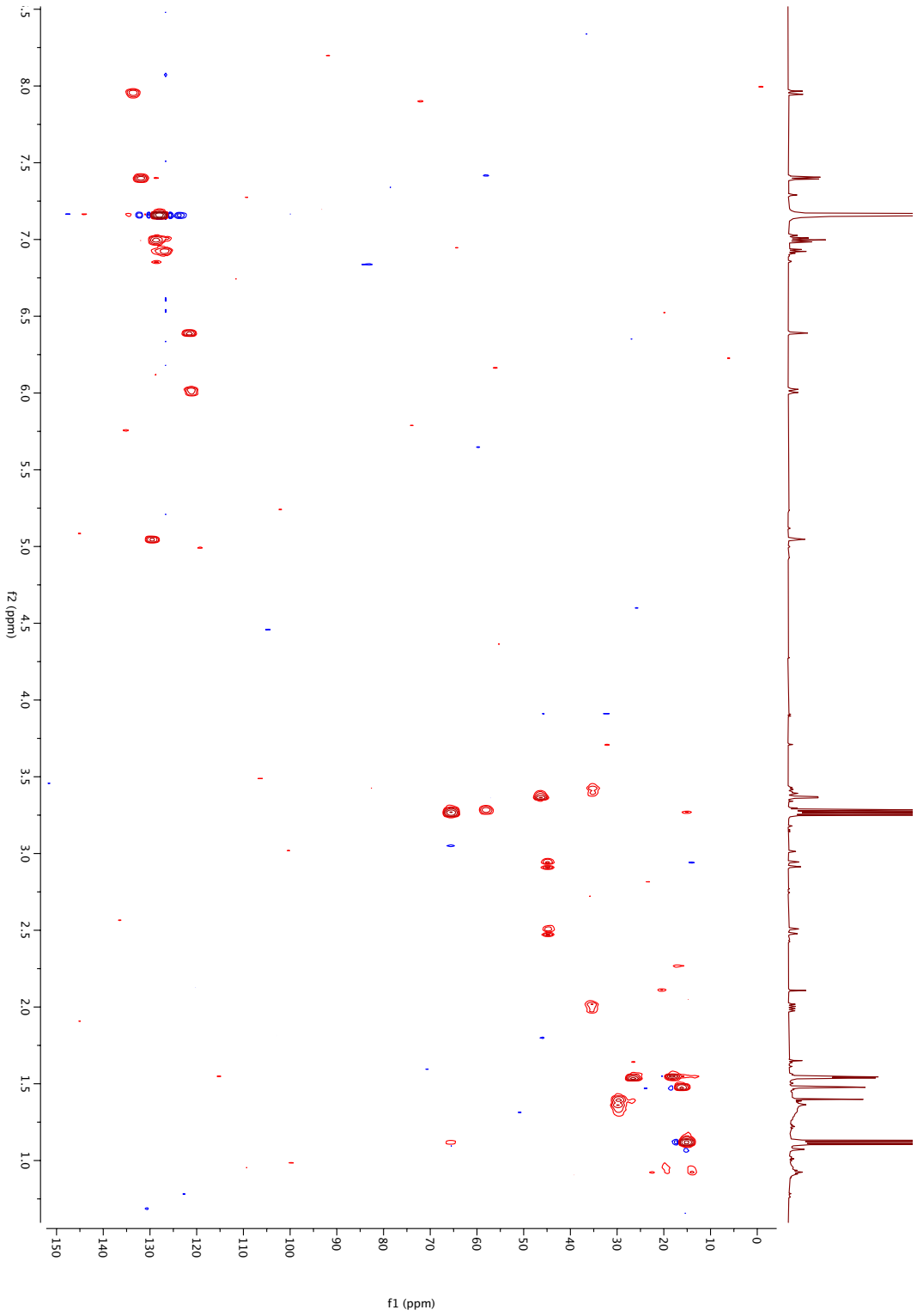

Me
HO
H
OTMS
2.1.11
(150 MHz, C6D6)
C6D6
146.52
140.85
134.24
129.20
128.80
122.74
80.55
69.16
55.57
37.61
37.15
17.21
0.29
f1 (ppm)

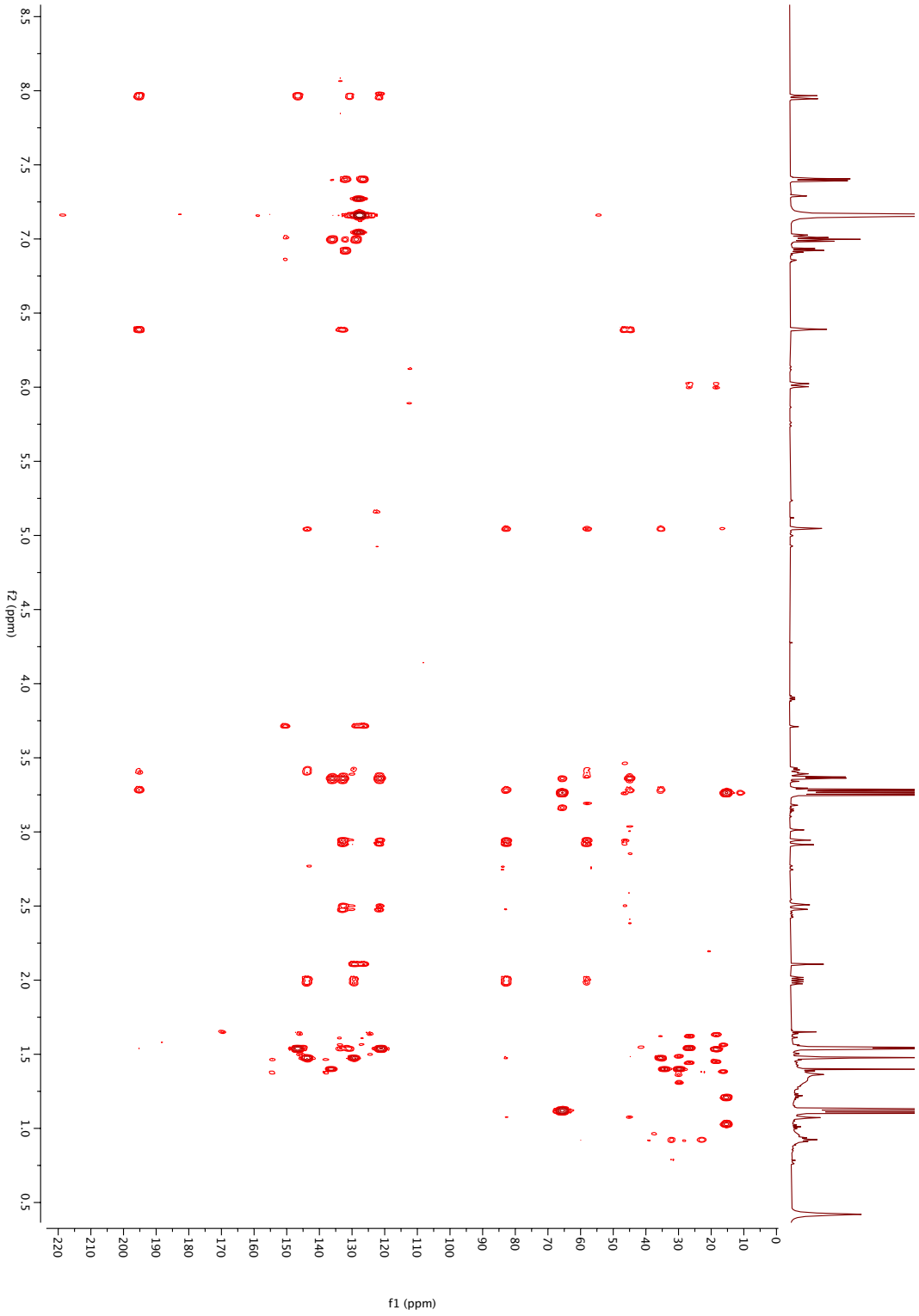

2.2.1
(600 MHz, C_6D_6)
C_6D_5H
f1 (ppm)

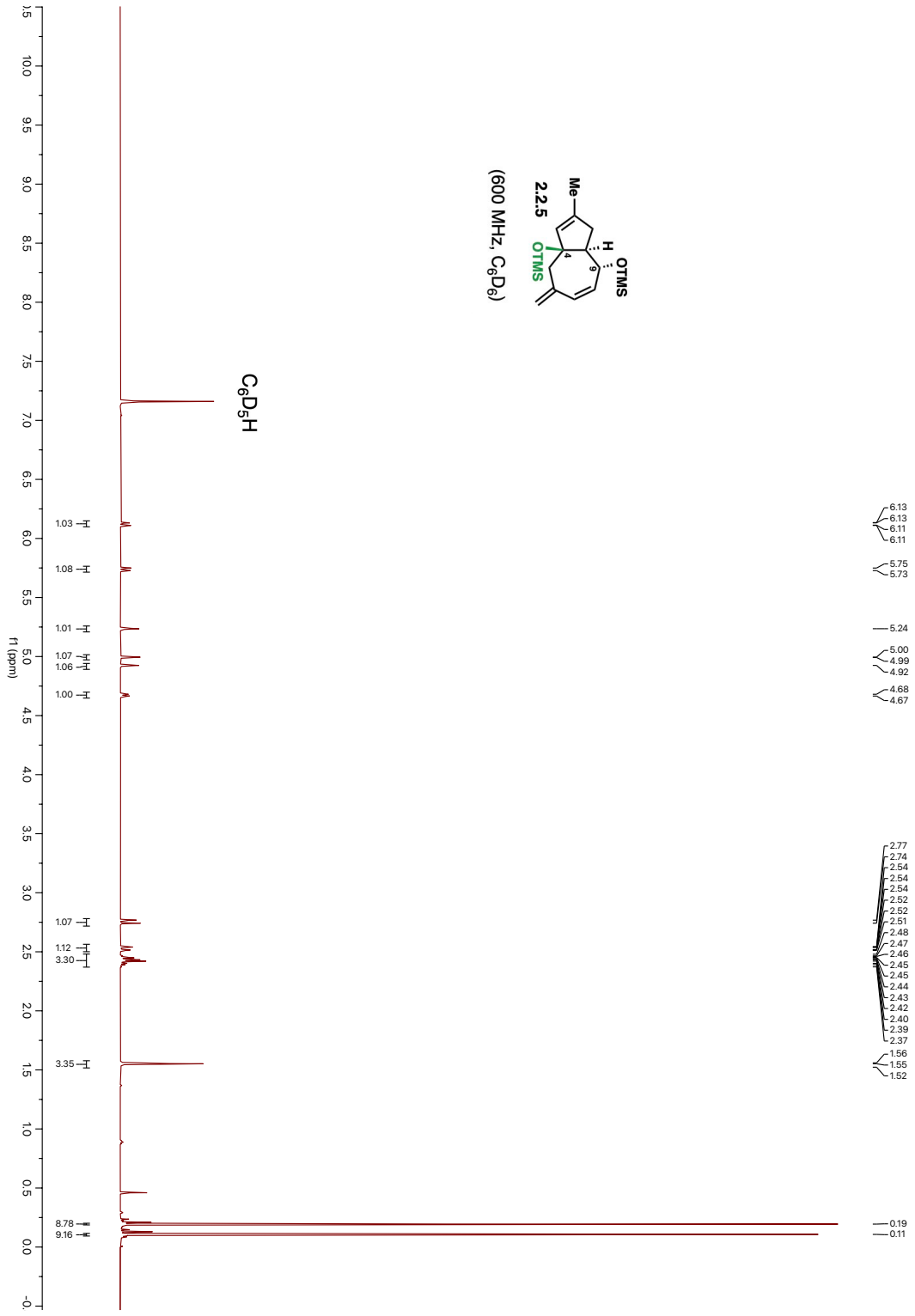

2.2.1
(150 MHz, C6D6)
C6D6
144.43
142.13
134.86
132.10
129.46
120.85
81.43
71.95
55.31
47.40
40.90
16.62
f1 (ppm)

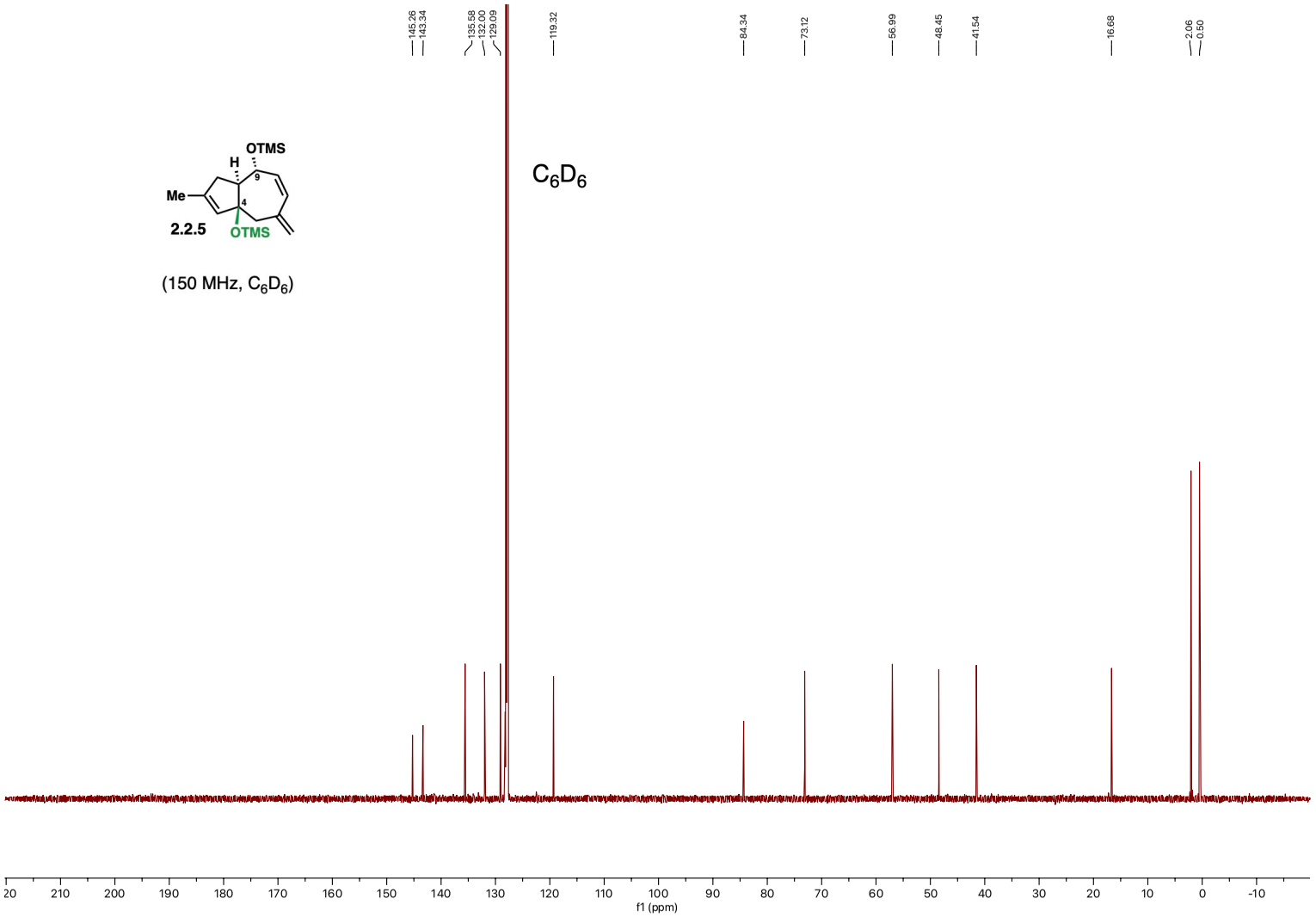

(600 MHz, C_6D_6)
2.2.2
Me
OH
H
O
C_6D_5H
DCM
f1 (ppm)
10.0
9.5
9.0
8.5
8.0
7.5
7.0
6.5
6.0
5.5
5.0
4.5
4.0
3.5
3.0
2.5
2.0
1.5
1.0
0.5
0.0
1.00 H
1.00 H
1.08 H
1.05 H
1.01 H
1.06 H
1.01 H
1.08 H
1.16 H
1.07 H
3.33 H
6.32
6.30
6.05
6.02
6.00
5.04
4.98
4.96
3.15
3.15
3.14
3.13
3.12
3.12
3.11
3.11
2.98
2.97
2.95
2.80
2.77
2.50
2.47
2.01
2.00
1.98
1.97
1.44
1.44

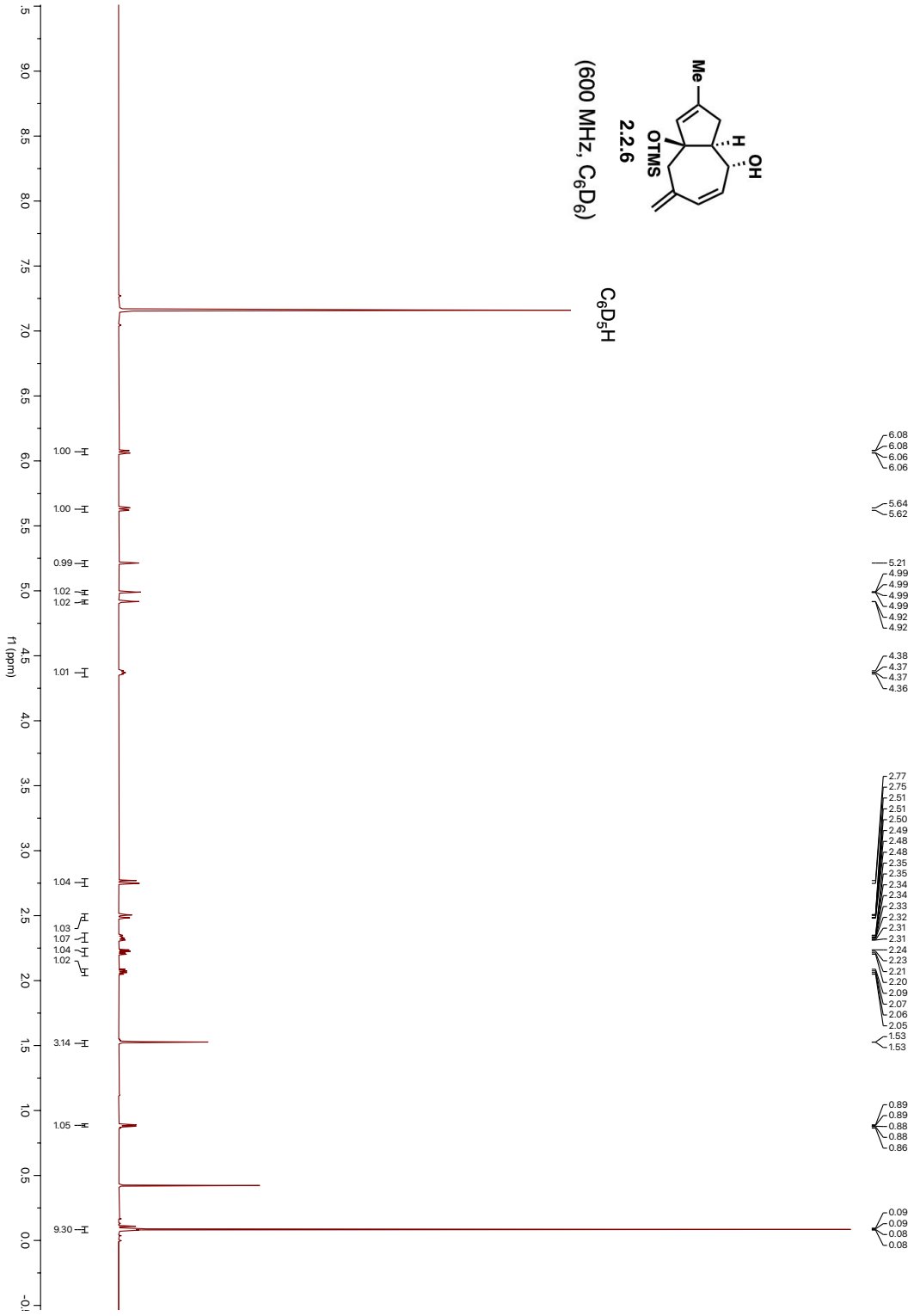

(600 MHz, C6D6)
2.2.4
Me
OH
PhS
H
O
8
14
Me
Me
C6D5H
Et2O
Et2O
f1 (ppm)
0.96
2.06
2.16
1.15
0.99
1.00
0.99
3.19
0.77
1.01
1.04
1.09
3.19
2.97
3.11
7.97
7.95
7.41
7.41
7.40
7.39
7.39
7.01
7.00
6.98
6.93
6.93
6.92
6.91
6.39
6.02
6.00
5.05
3.43
3.42
3.40
3.39
3.39
3.37
3.36
3.34
3.29
2.94
2.91
2.51
2.48
2.02
2.00
1.99
1.98
1.54
1.54
1.48

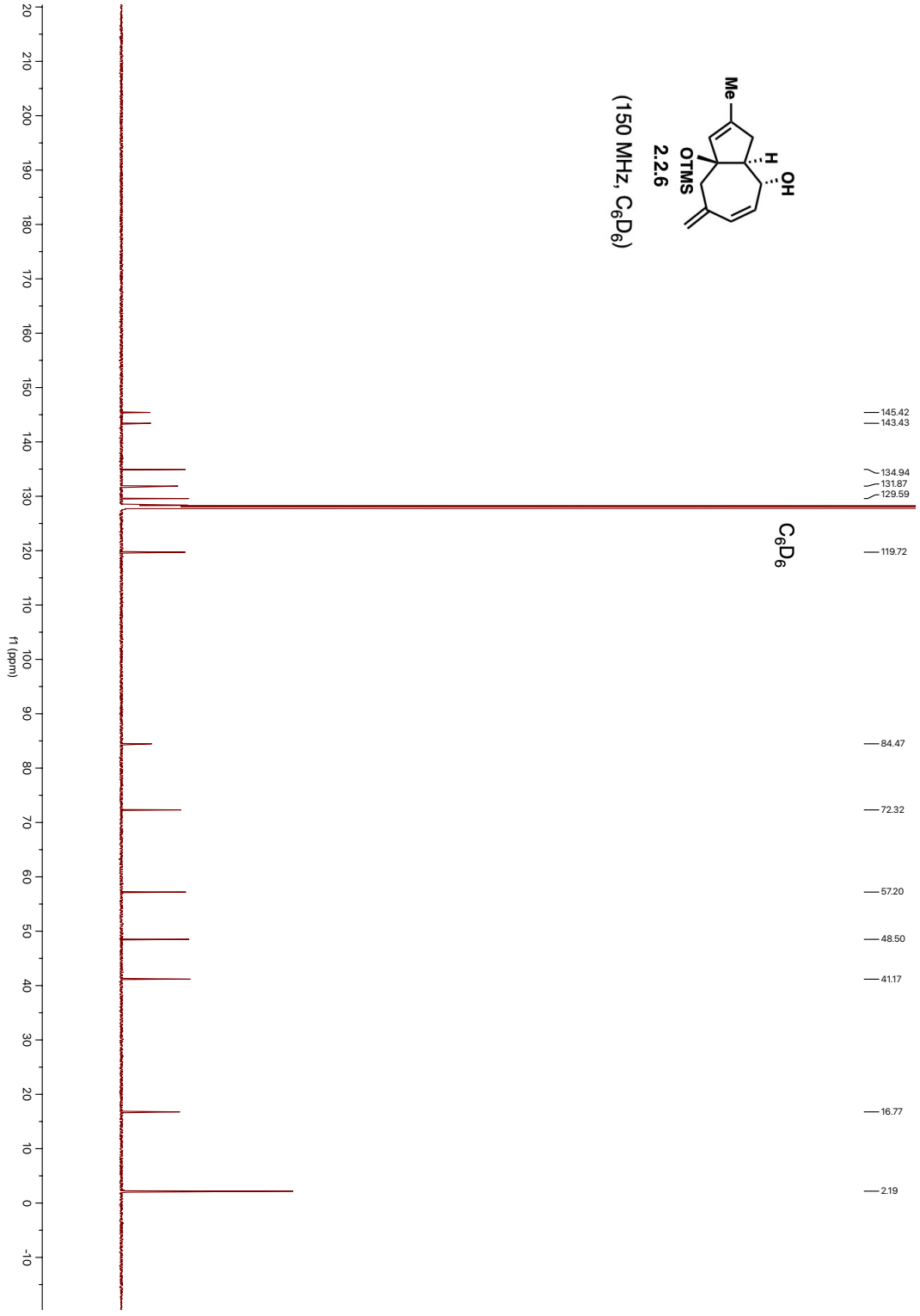

f2 (ppm)
f1 (ppm)

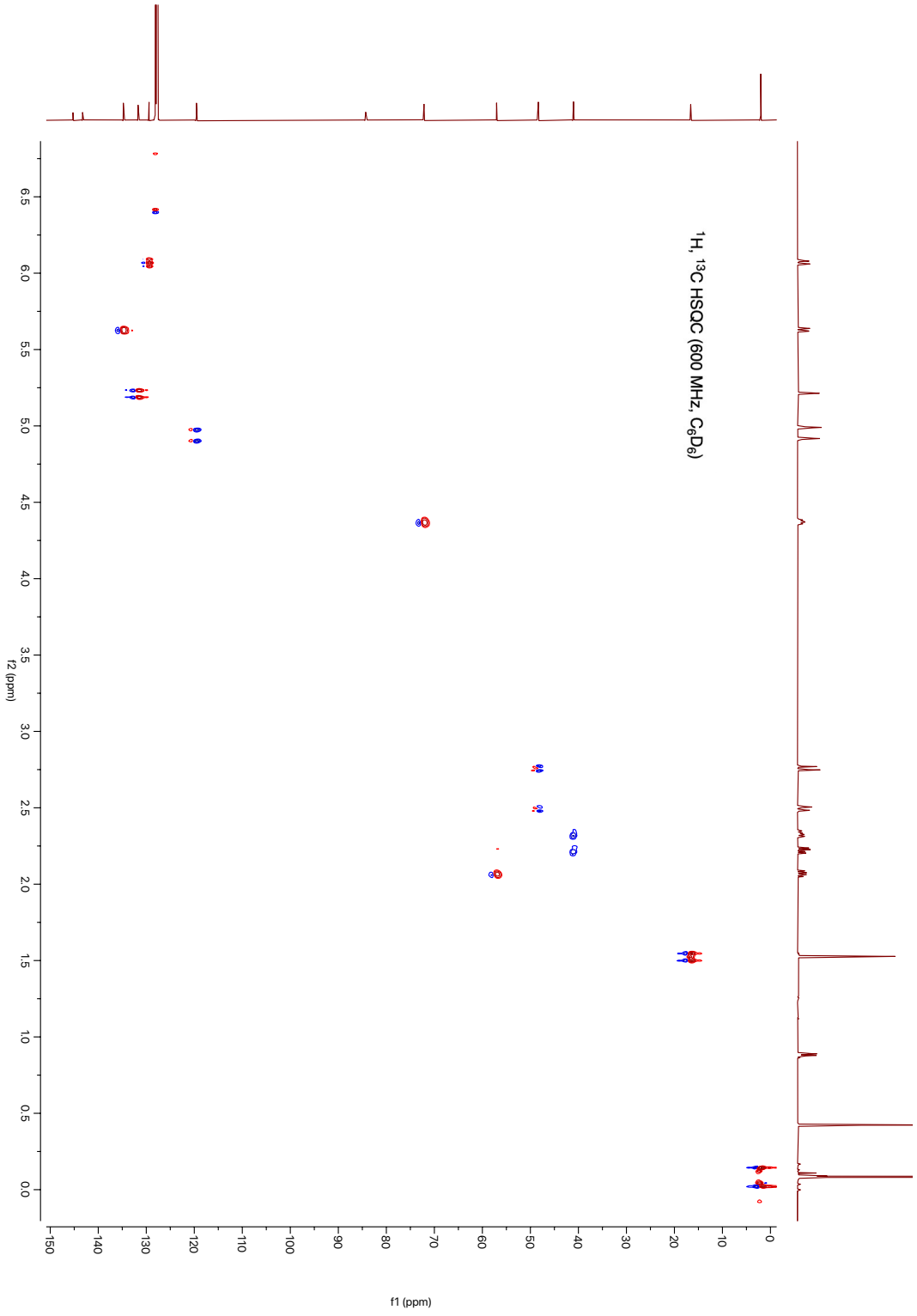

f2 (ppm)
f1 (ppm)

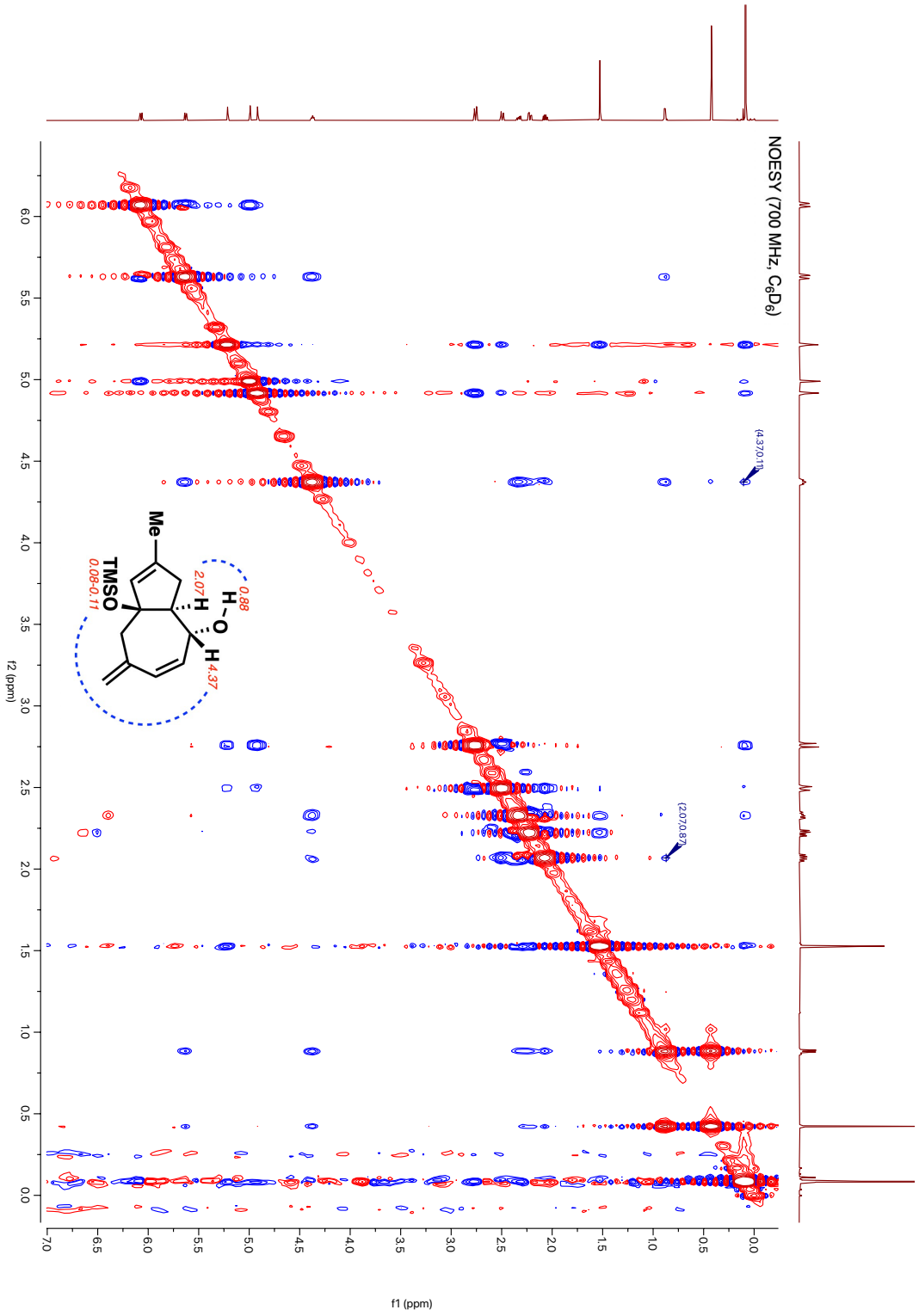

2.2.5
Me
H
OTMS
OTMS
(600 MHz, C6D6)
C6D5H
f1 (ppm)
1.03
1.08
1.01
1.07
1.06
1.00
1.07
1.12
3.30
3.35
8.78
9.16
6.13
6.13
6.11
6.11
5.75
5.73
5.24
5.00
4.99
4.92
4.68
4.67
2.77
2.74
2.54
2.54
2.54
2.52
2.52
2.51
2.48
2.47
2.46
2.45
2.45
2.44
2.43
2.42
2.40
2.39
2.37
1.56
1.55
1.52
0.19
0.11

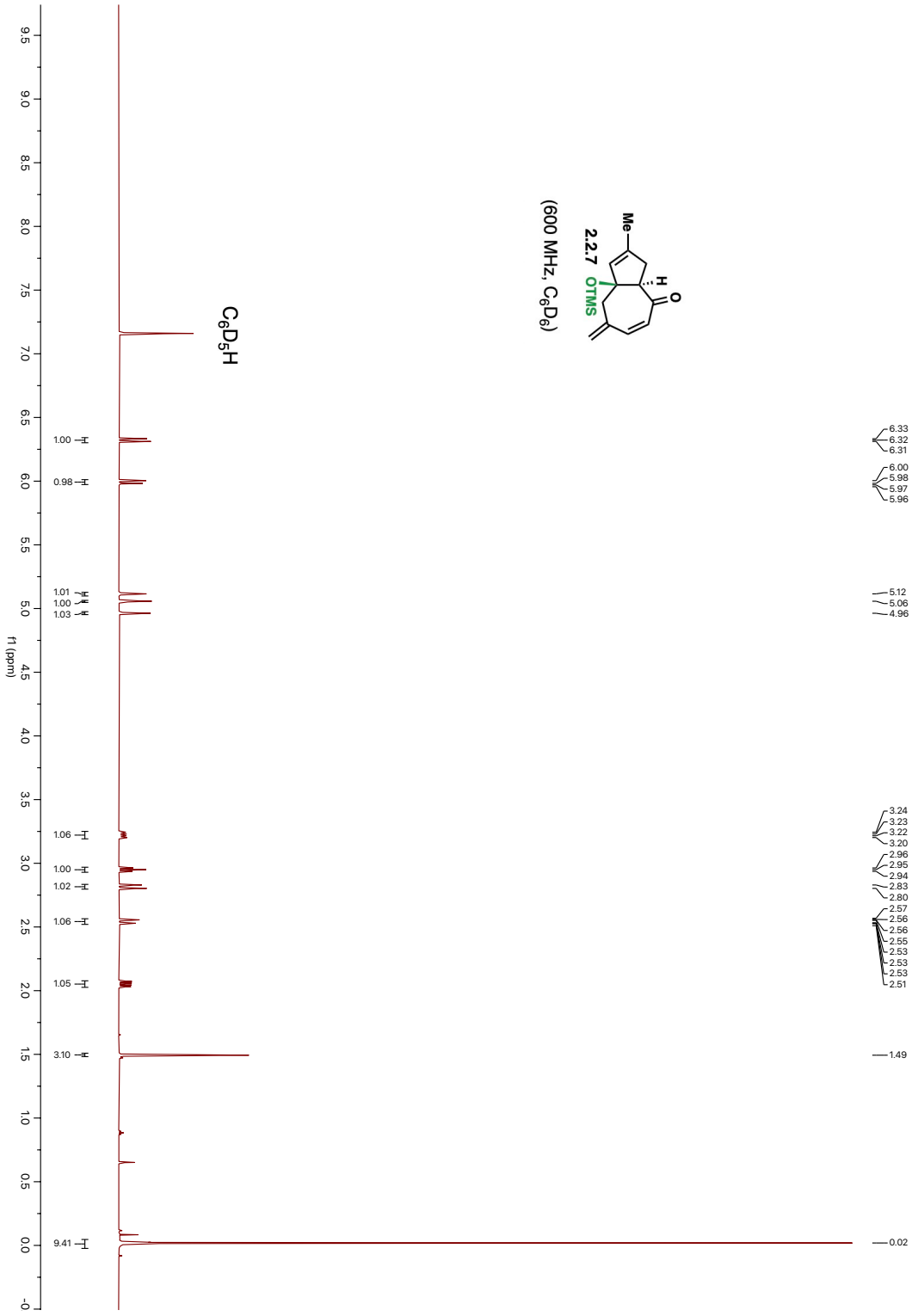

145.26
143.34
135.58
132.00
129.09
119.32
84.34
73.12
56.99
48.45
41.54
16.68
2.06
0.50
OTMS
H
9
Me
4
2.2.5
OTMS
(150 MHz, C6D6)
C6D6
f1 (ppm)

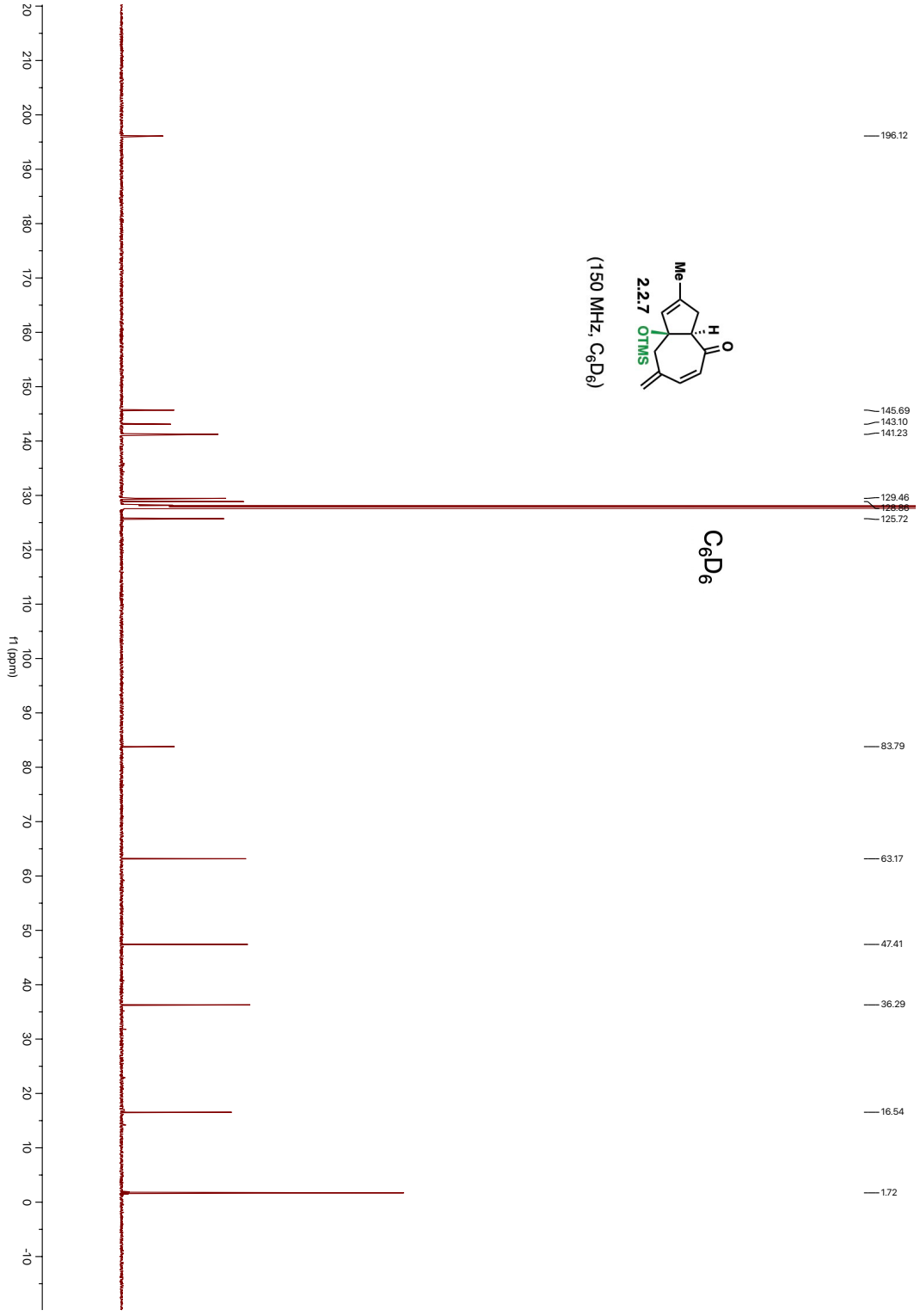

2.2.6
(600 MHz, C6D6)
C6D5H
Me
H
OH
OTMS
f1 (ppm)
1.00
1.00
0.99
1.02
1.02
1.01
1.04
1.03
1.07
1.04
1.02
3.14
1.05
9.30
6.08
6.08
6.06
6.06
5.64
5.62
5.21
4.99
4.99
4.99
4.99
4.92
4.92
4.38
4.37
4.37
4.36
2.77
2.75
2.51
2.51
2.50
2.49
2.48
2.48
2.35
2.35
2.34
2.34
2.33
2.32
2.31
2.31
2.24
2.23
2.21
2.20
2.09
2.07
2.06
2.05
1.53
1.53
0.89
0.89
0.88
0.88
0.86
0.09
0.09
0.08
0.08

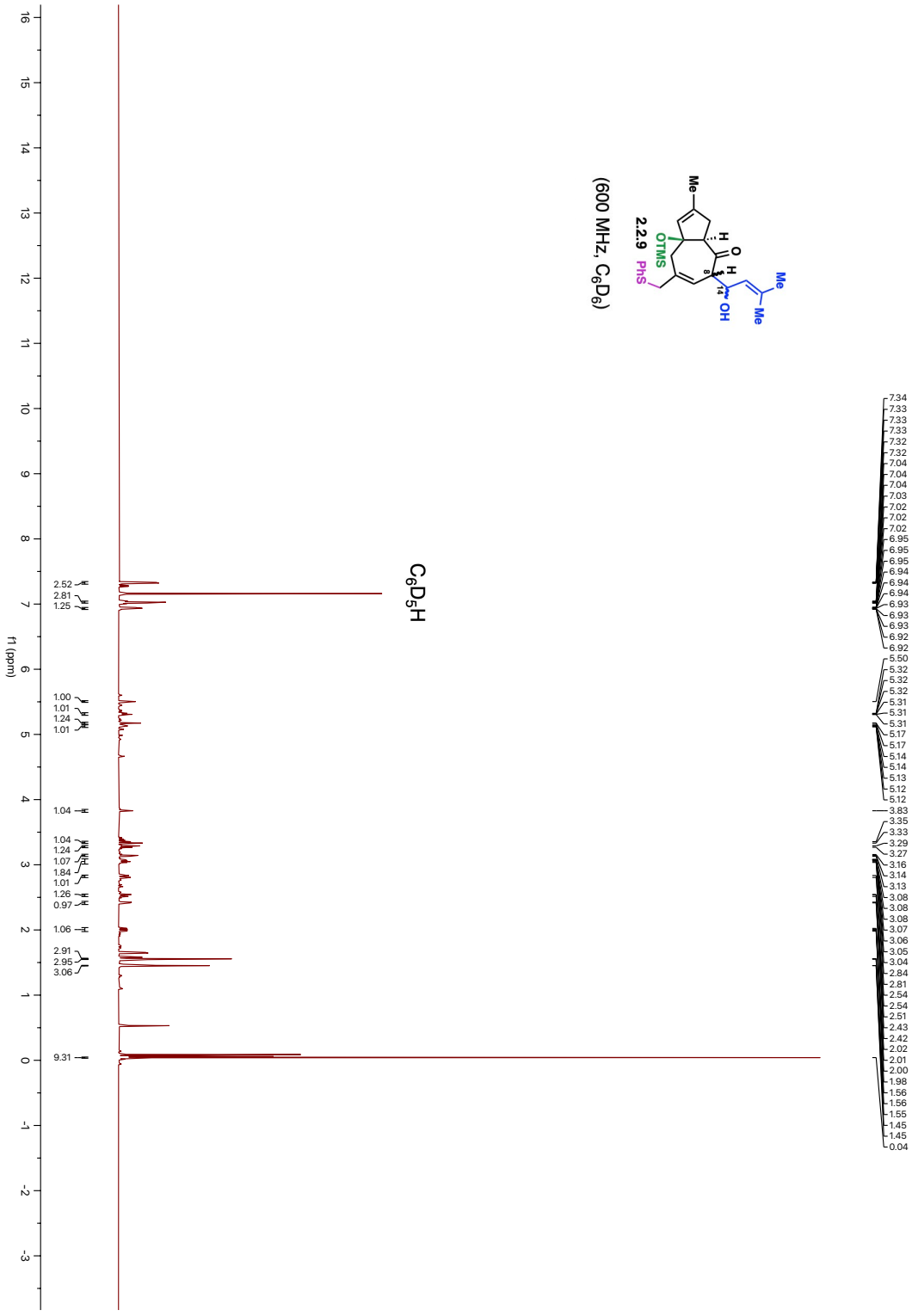

Me
H
OH
OTMS
2.2.6
(150 MHz, C6D6)
145.42
143.43
134.94
131.87
129.59
C6D6
119.72
84.47
72.32
57.20
48.50
41.17
16.77
2.19
f1 (ppm)

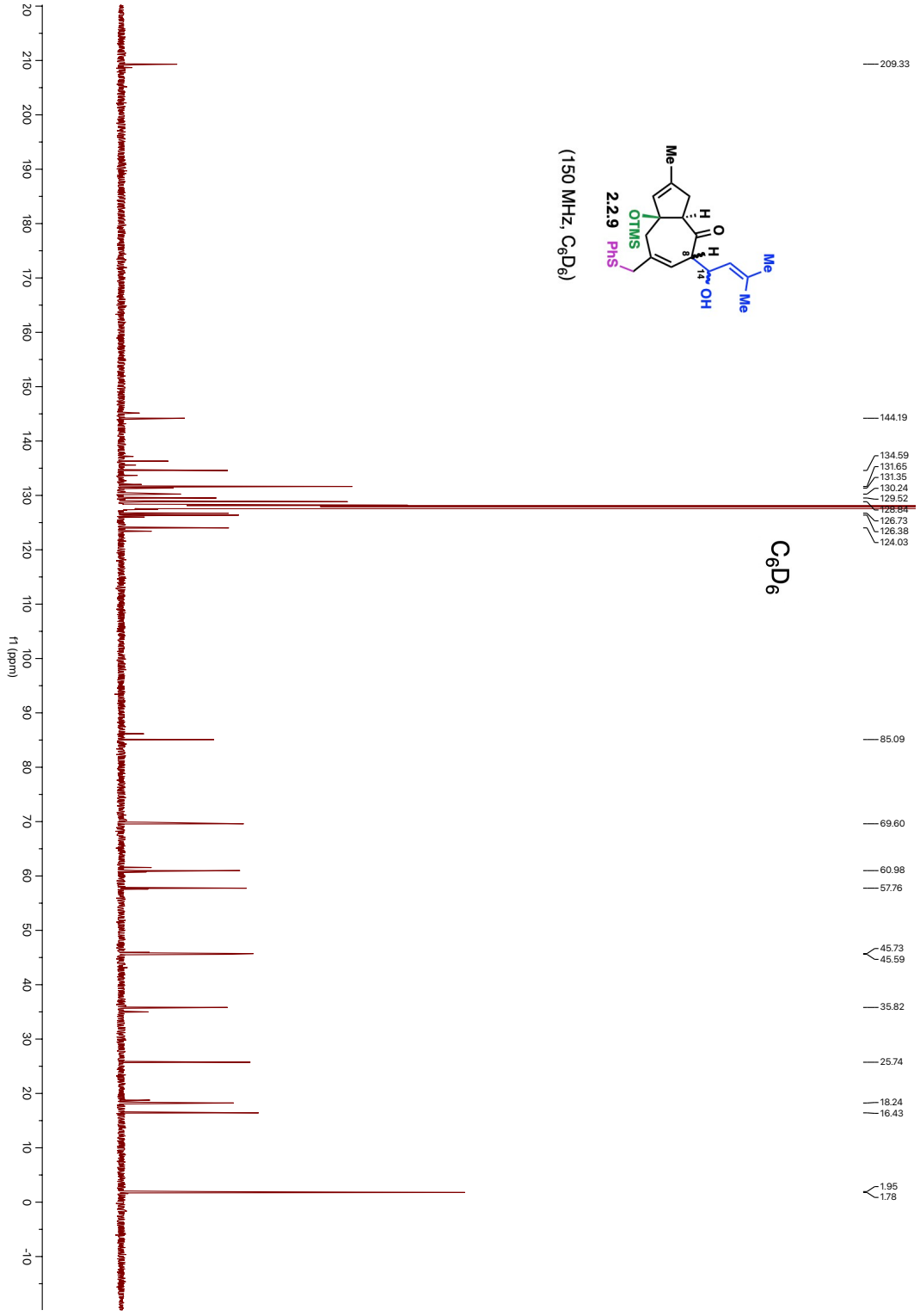

^{1}H, ^{13}C HSQC (600 MHz, C_6D_6)
f2 (ppm)
f1 (ppm)

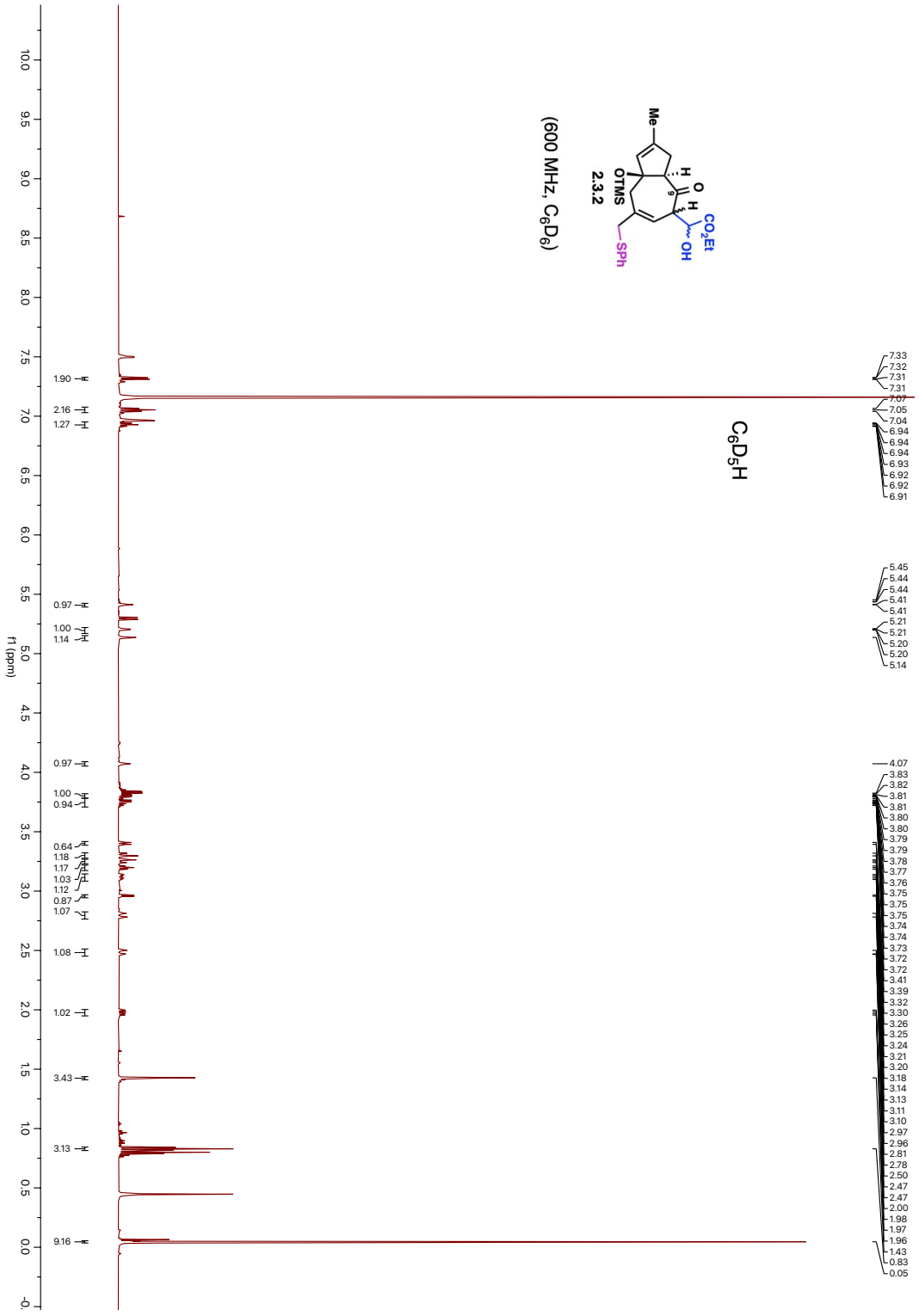

NOESY (700 MHz, C6D6)
(4.37,0.11)
(2.07,0.87)
Me
TMSO
0.08-0.11
2.07
H
O
H
4.37
0.88
f2 (ppm)
f1 (ppm)

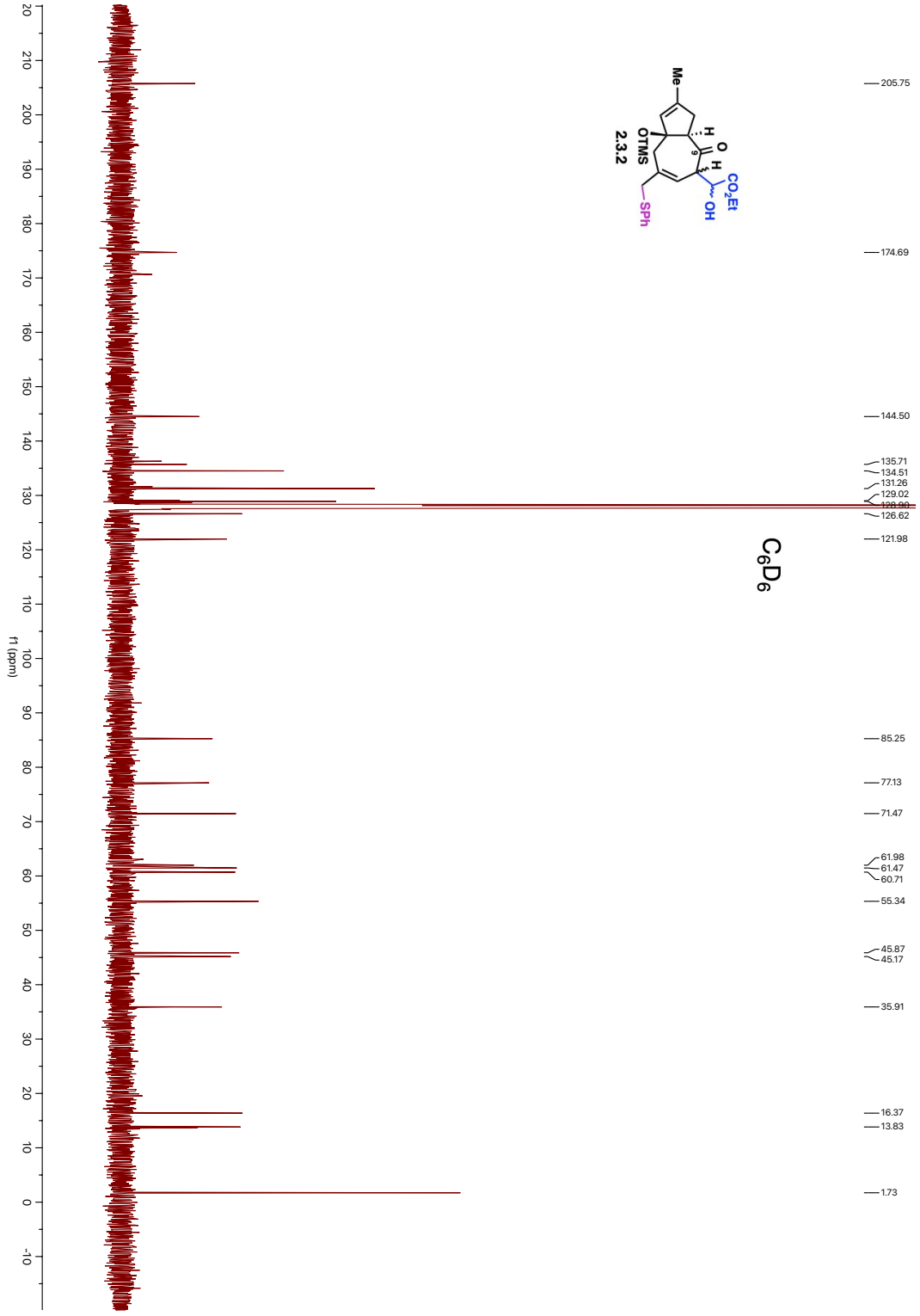

2.2.7
OTMS
Me
H
O
(600 MHz, C6D6)
C6D5H
f1 (ppm)
1.00
0.98
1.01
1.00
1.03
1.06
1.00
1.02
1.06
1.05
3.10
9.41
6.33
6.32
6.31
6.00
5.98
5.97
5.96
5.12
5.06
4.96
3.24
3.23
3.22
3.20
2.96
2.95
2.94
2.83
2.80
2.57
2.56
2.56
2.55
2.53
2.53
2.53
2.51
1.49
0.02

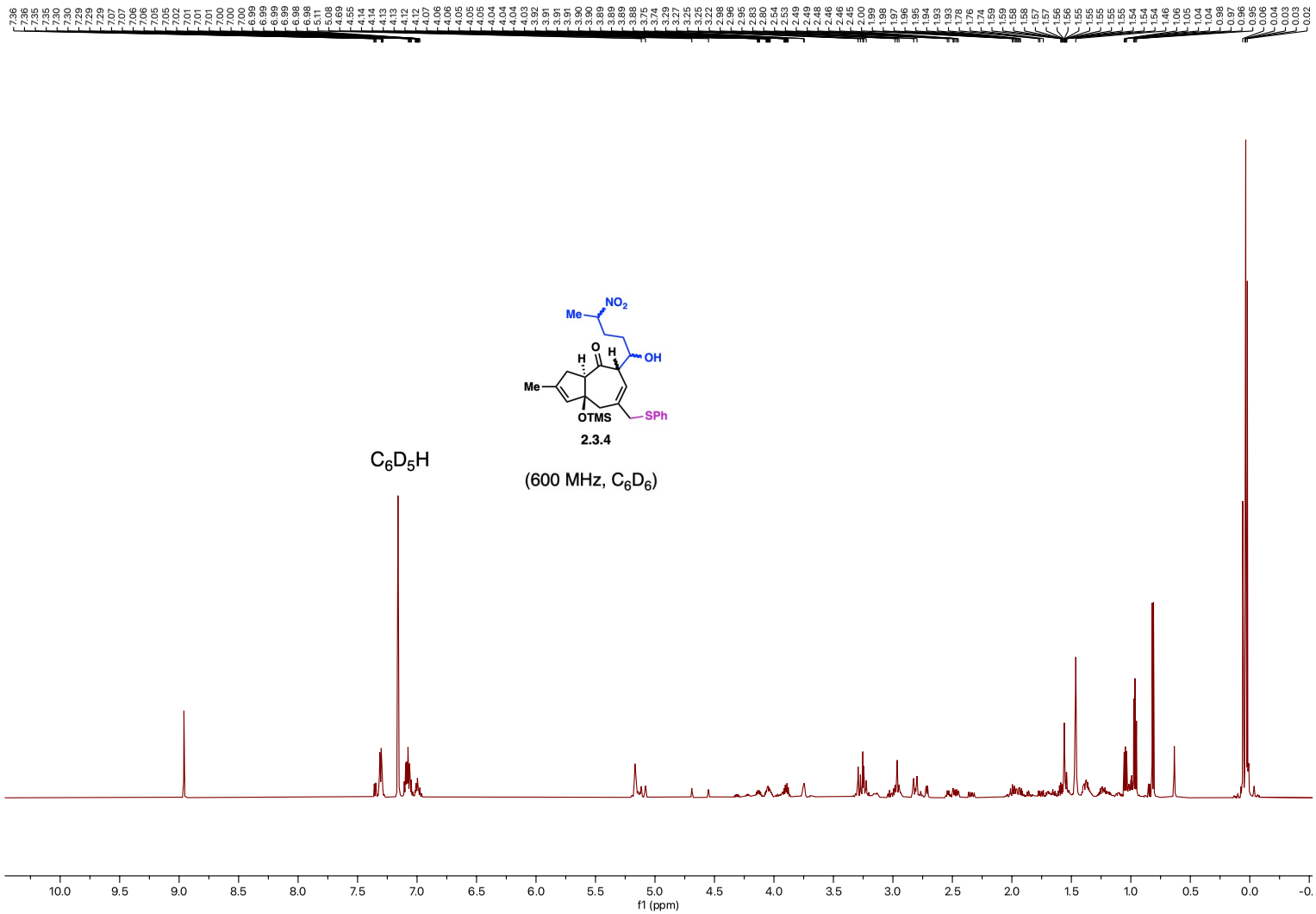

196.12
145.69
143.10
141.23
129.46
128.88
125.72
83.79
63.17
47.41
36.29
16.54
1.72
f1 (ppm)
(150 MHz, C6D6)
2.2.7
OTMS
Me
O
H
C6D6

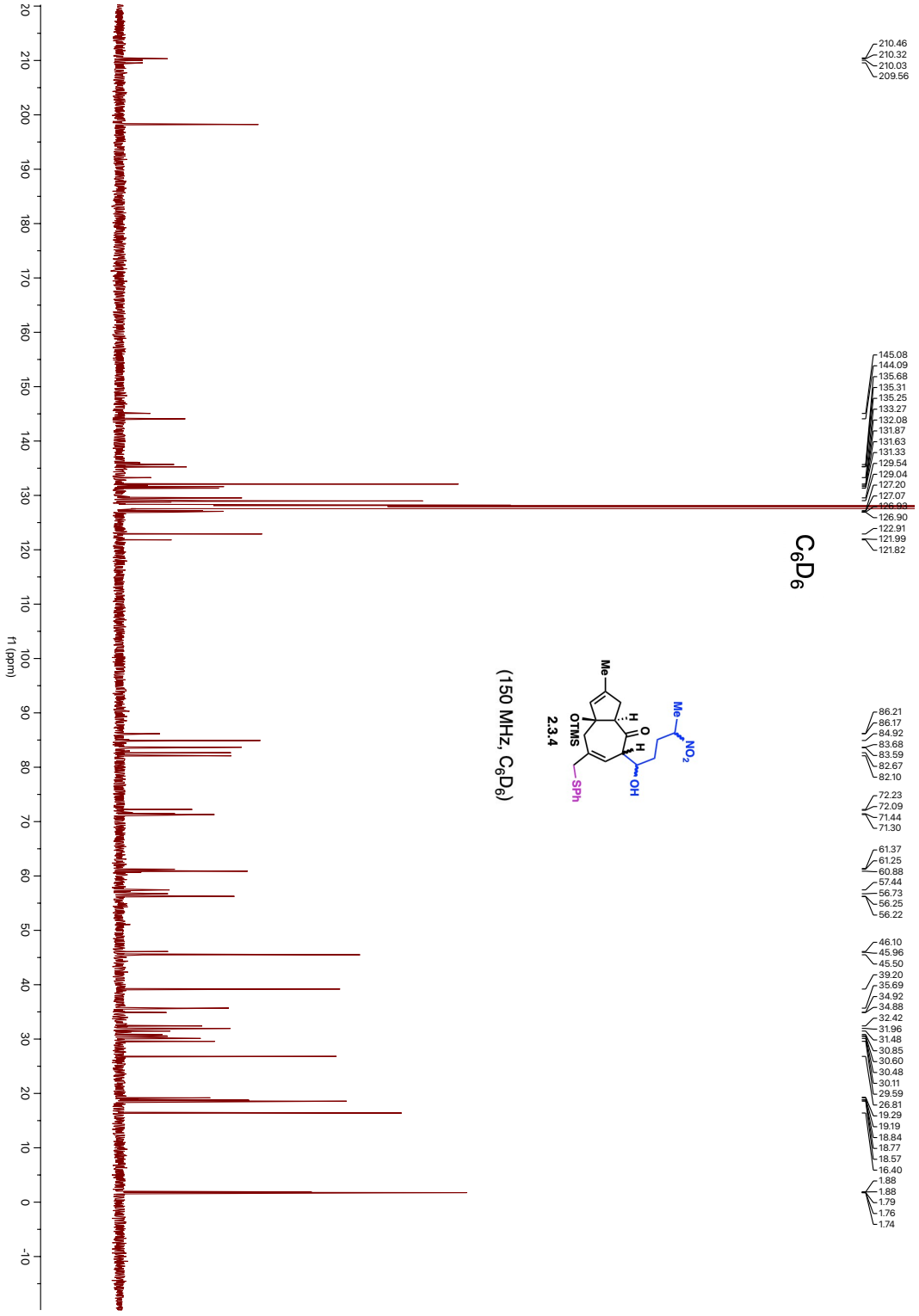

(600 MHz, C6D6)
C6D5H
2.2.9
OTMS
PhS
Me
OH
Me
f1 (ppm)

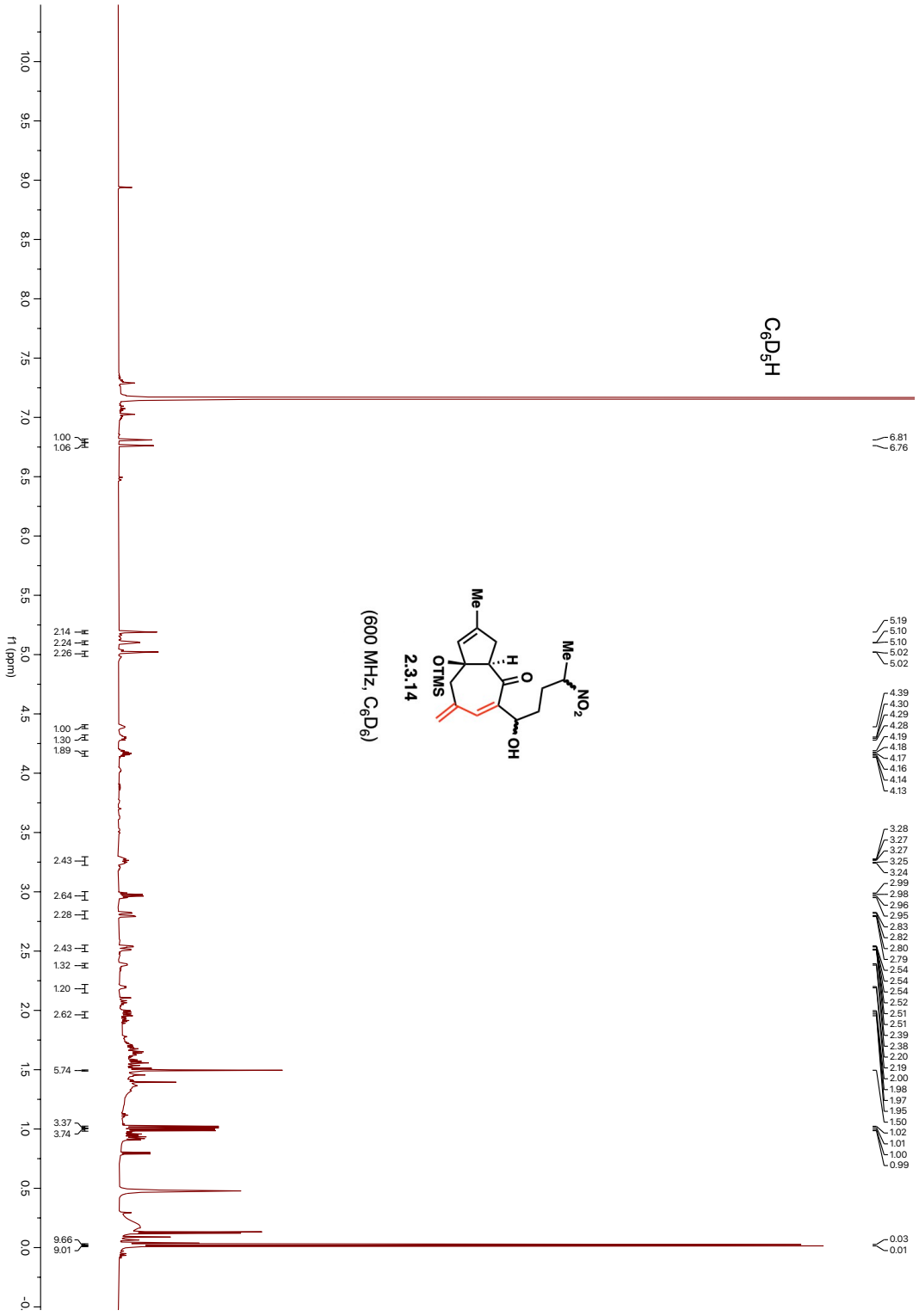

209.33
144.19
134.59
131.65
131.35
130.24
129.52
128.84
126.73
126.38
124.03
85.09
69.60
60.98
57.76
45.73
45.59
35.82
25.74
18.24
16.43
1.95
1.78
f1 (ppm)
C6D6
(150 MHz, C6D6)
2.2.9
OTMS
PhS
OH
Me
Me
Me
H
O
H

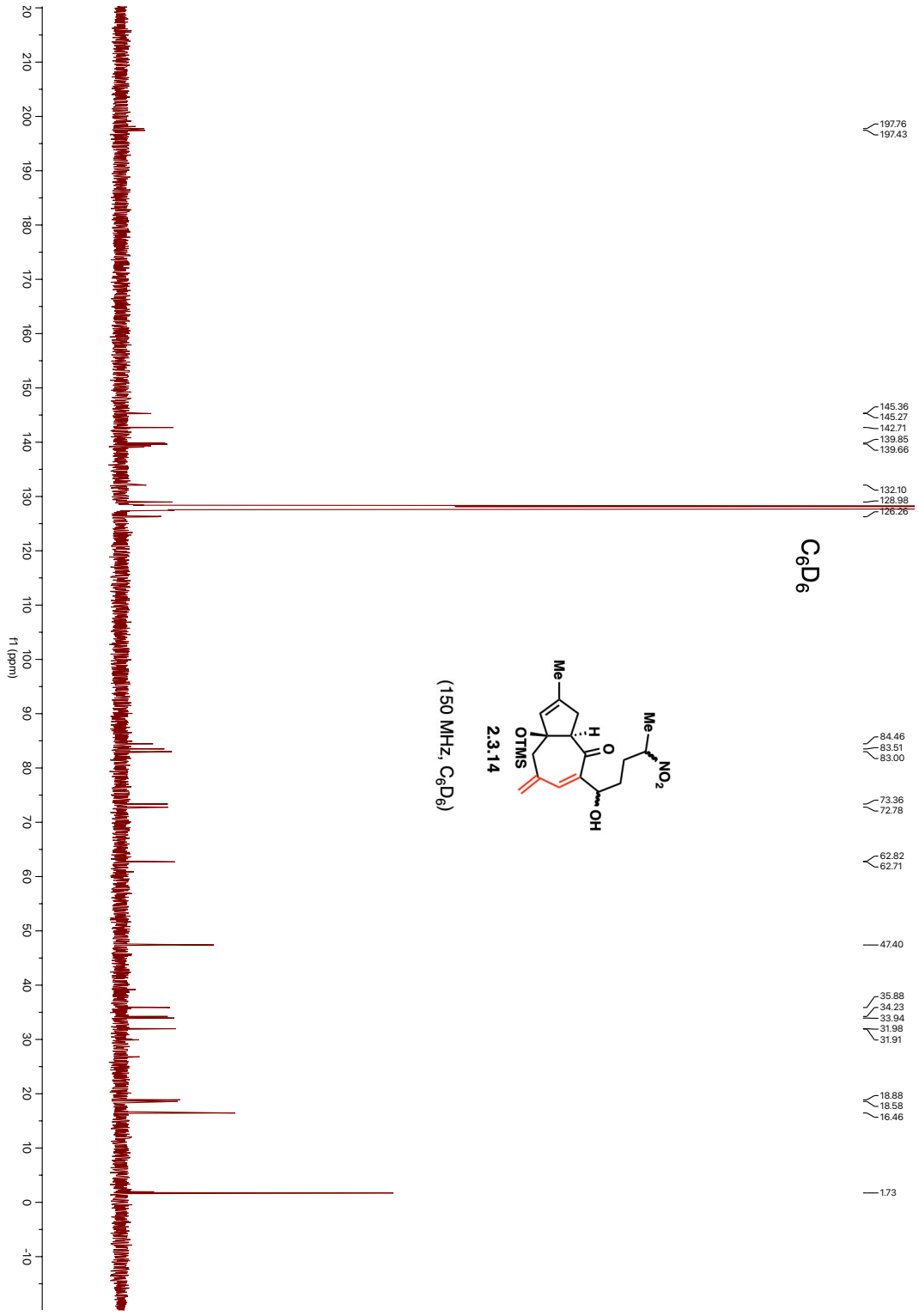

(600 MHz, C_6D_6)
2.3.2
OTMS
Me
SPh
CO_2Et
OH
C_6D_5H
f1 (ppm)

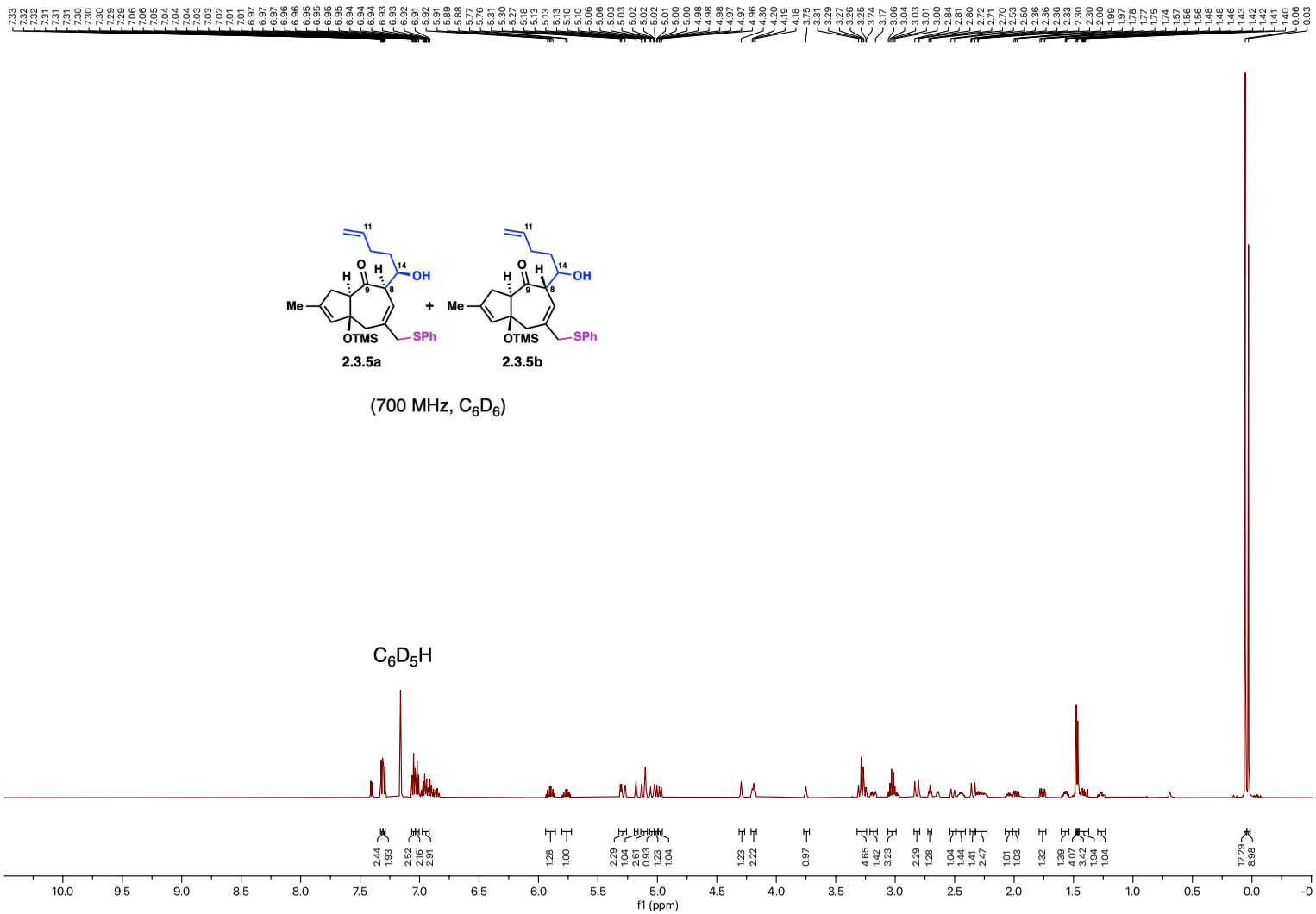

205.75
174.69
144.50
135.71
134.51
131.26
129.02
128.90
126.62
121.98
85.25
77.13
71.47
61.98
61.47
60.71
55.34
45.87
45.17
35.91
16.37
13.83
1.73
C6D6
Me
OTMS
2.3.2
H
O
H
9
CO2Et
OH
SPh
f1 (ppm)

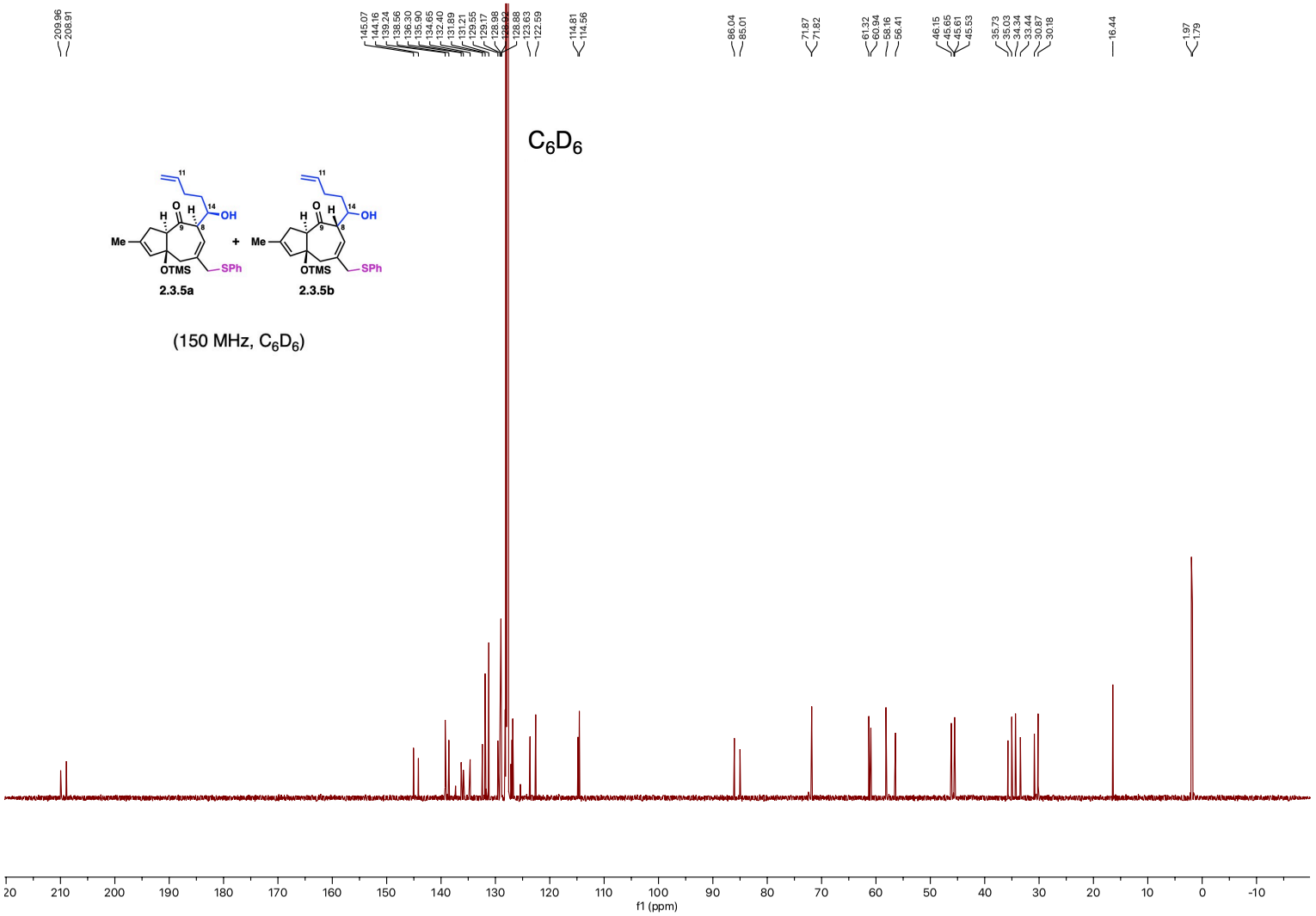

NO2
Me
O
H
H
OH
Me
OTMS
SPh
2.3.4
C6D5H
(600 MHz, C6D6)
f1 (ppm)

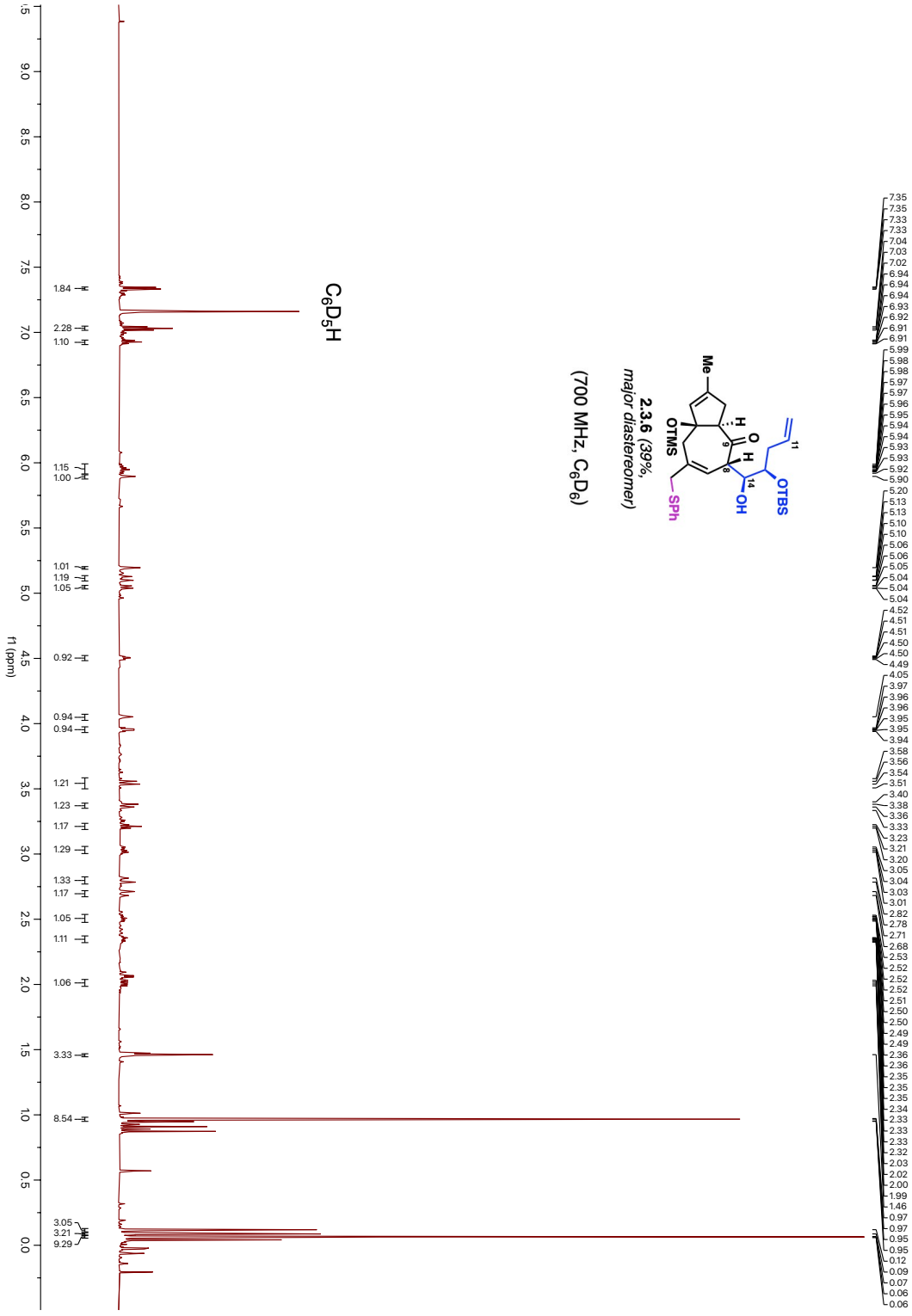

210.46
210.32
210.03
209.56
145.08
144.09
135.68
135.31
135.25
133.27
132.08
131.87
131.63
131.33
129.54
129.04
127.20
127.07
126.90
122.91
121.99
121.82
86.21
86.17
84.92
83.68
83.59
82.67
82.10
72.23
72.09
71.44
71.30
61.37
61.25
60.88
57.44
56.73
56.25
56.22
46.10
45.96
45.50
39.20
35.69
34.92
34.88
32.42
31.96
31.48
30.85
30.60
30.48
30.11
29.59
26.81
19.29
19.19
18.84
18.77
18.57
16.40
1.88
1.88
1.79
1.76
1.74
C6D6
(150 MHz, C6D6)
2.3.4
Me
OTMS
SPh
OH
NO2
f1 (ppm)

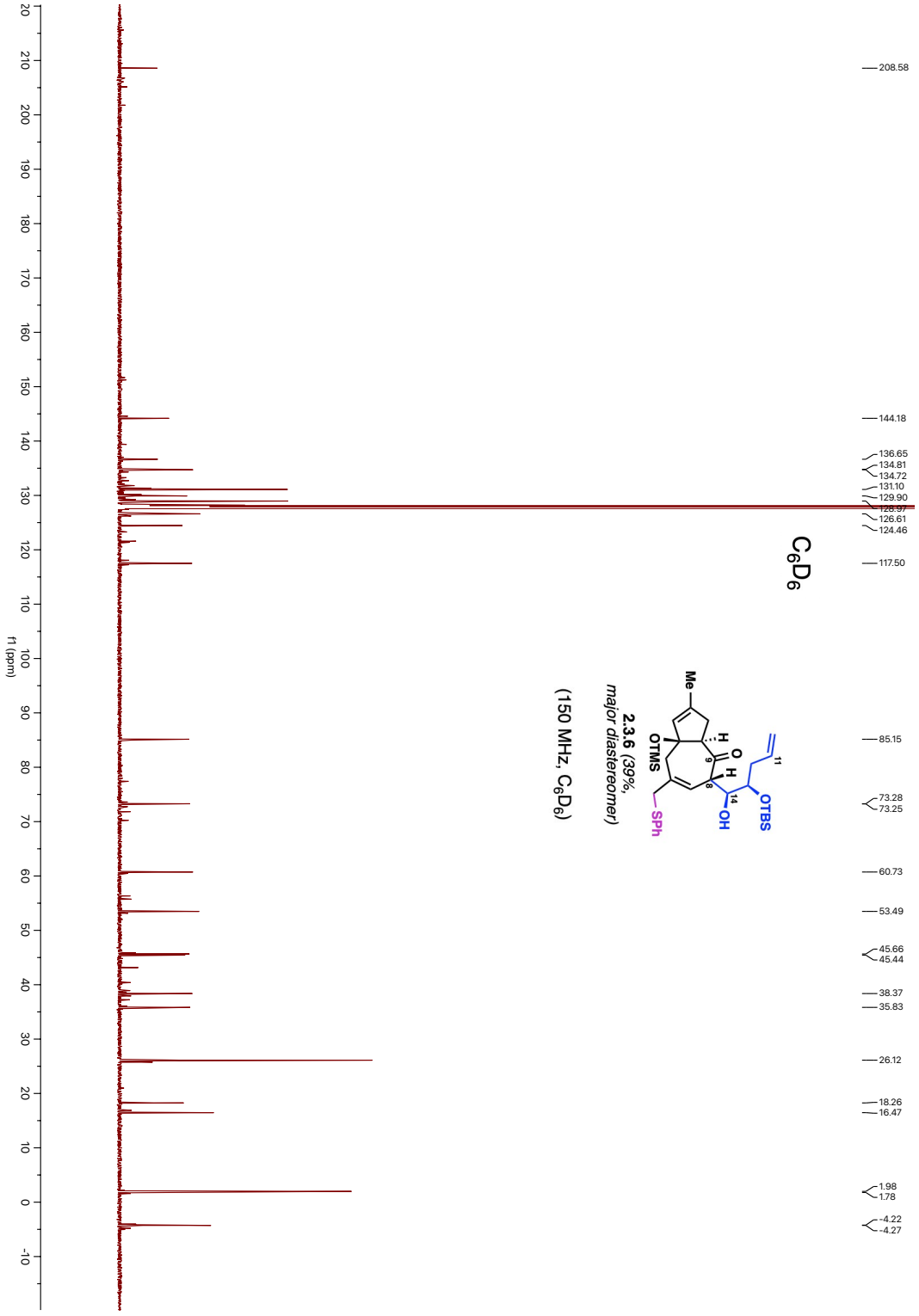

C6D5H
(600 MHz, C6D6)
2.3.14
OTMS
Me
H
O
Me
NO2
OH
f1 (ppm)
10.0
9.5
9.0
8.5
8.0
7.5
7.0
6.5
6.0
5.5
5.0
4.5
4.0
3.5
3.0
2.5
2.0
1.5
1.0
0.5
0.0
-0.
1.00
1.06
2.14
2.24
2.26
1.00
1.30
1.89
2.43
2.64
2.28
2.43
1.32
1.20
2.62
5.74
3.37
3.74
9.66
9.01
6.81
6.76
5.19
5.10
5.10
5.02
5.02
4.39
4.30
4.29
4.28
4.19
4.18
4.17
4.16
4.14
4.13
3.28
3.27
3.27
3.25
3.24
2.99
2.98
2.96
2.95
2.83
2.82
2.80
2.79
2.54
2.54
2.54
2.52
2.51
2.51
2.39
2.38
2.20
2.19
2.00
1.98
1.97
1.95
1.50
1.02
1.01
1.00
0.99
0.03
0.01

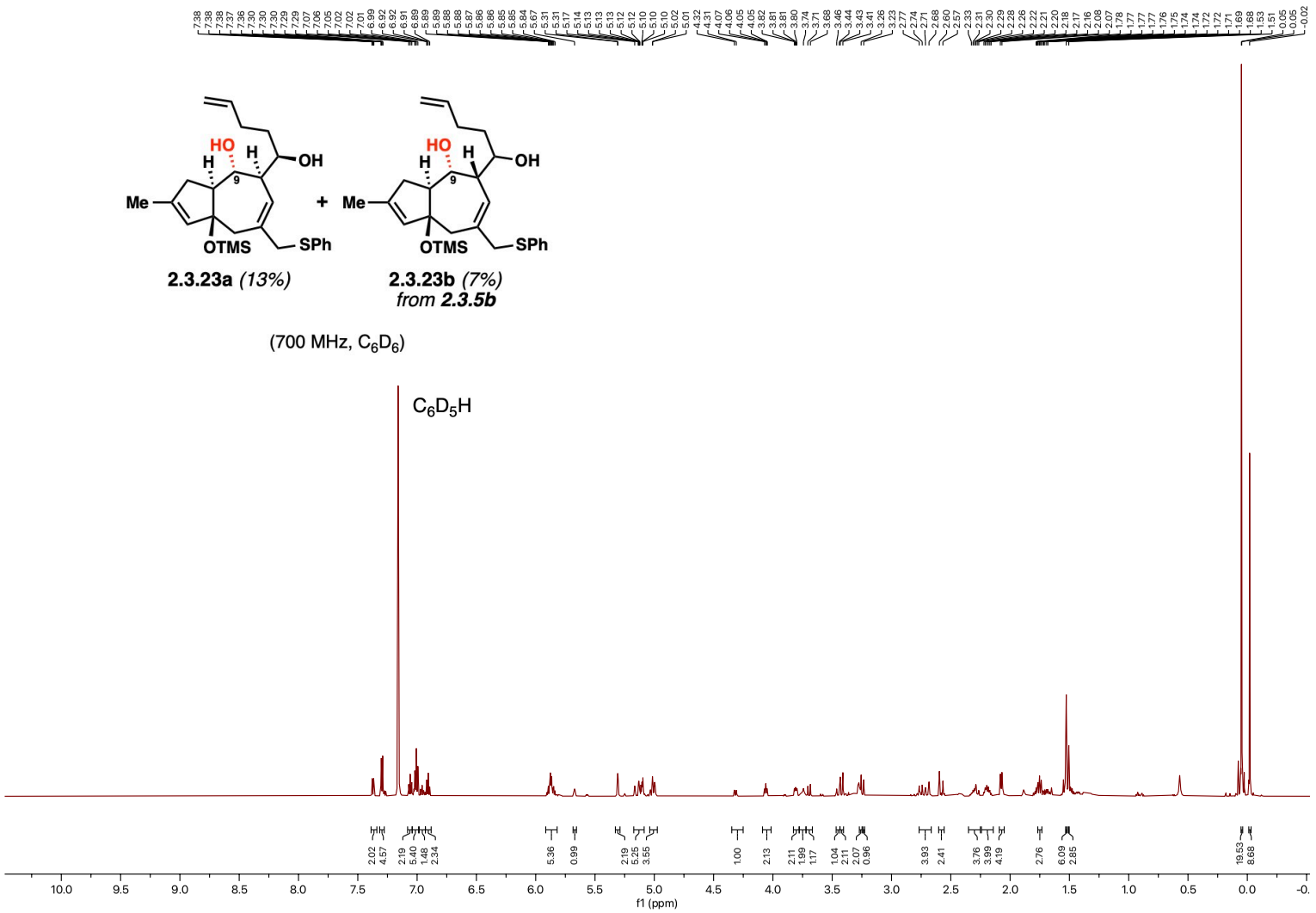

197.76
197.43
145.36
145.27
142.71
139.85
139.66
132.10
128.98
126.26
C6D6
84.46
83.51
83.00
73.36
72.78
62.82
62.71
47.40
35.88
34.23
33.94
31.98
31.91
18.88
18.58
16.46
1.73
Me
H
O
OTMS
Me
NO2
OH
2.3.14
(150 MHz, C6D6)
f1 (ppm)

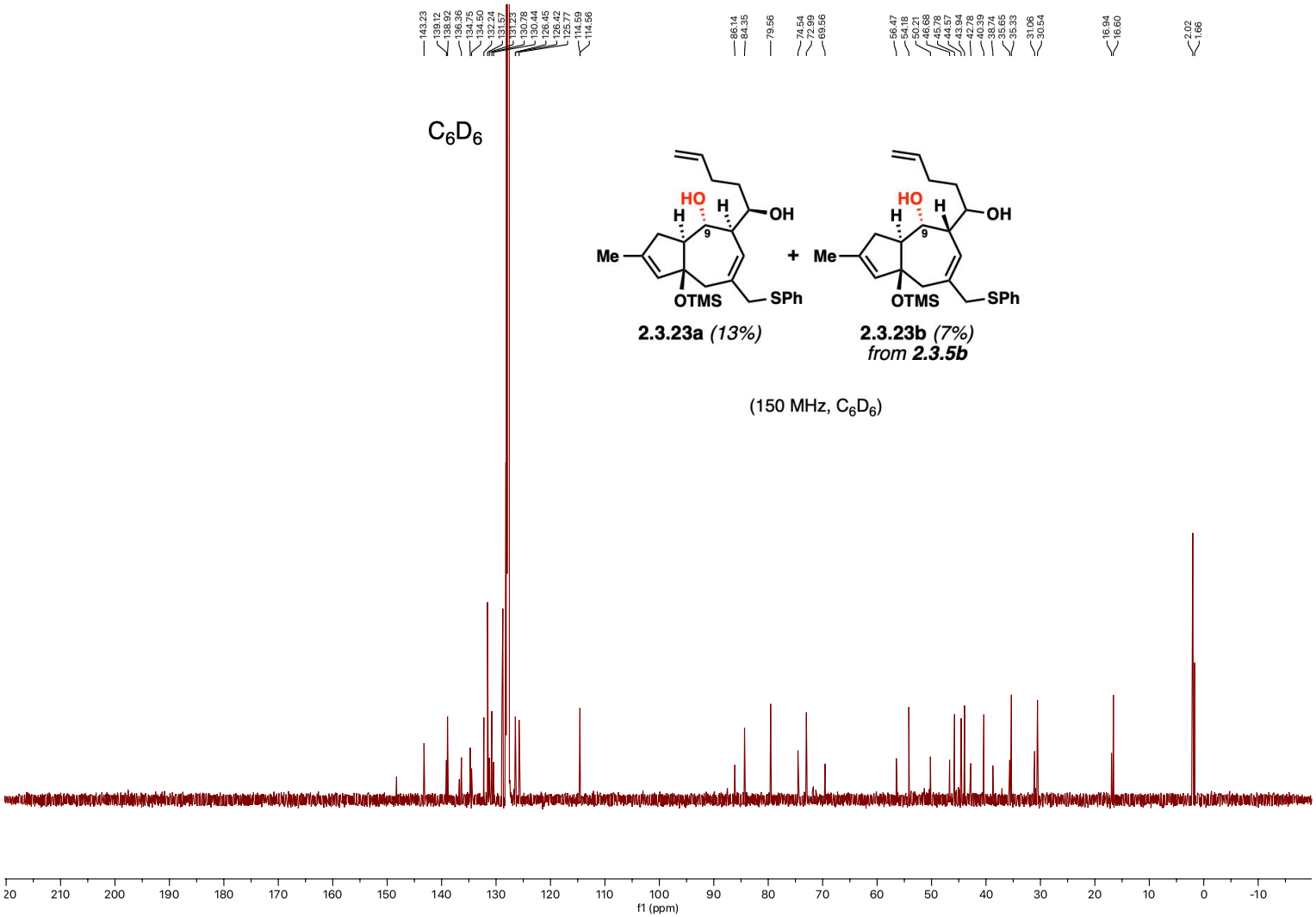

2.3.5a
2.3.5b
(700 MHz, C6D6)
C6D5H
f1 (ppm)

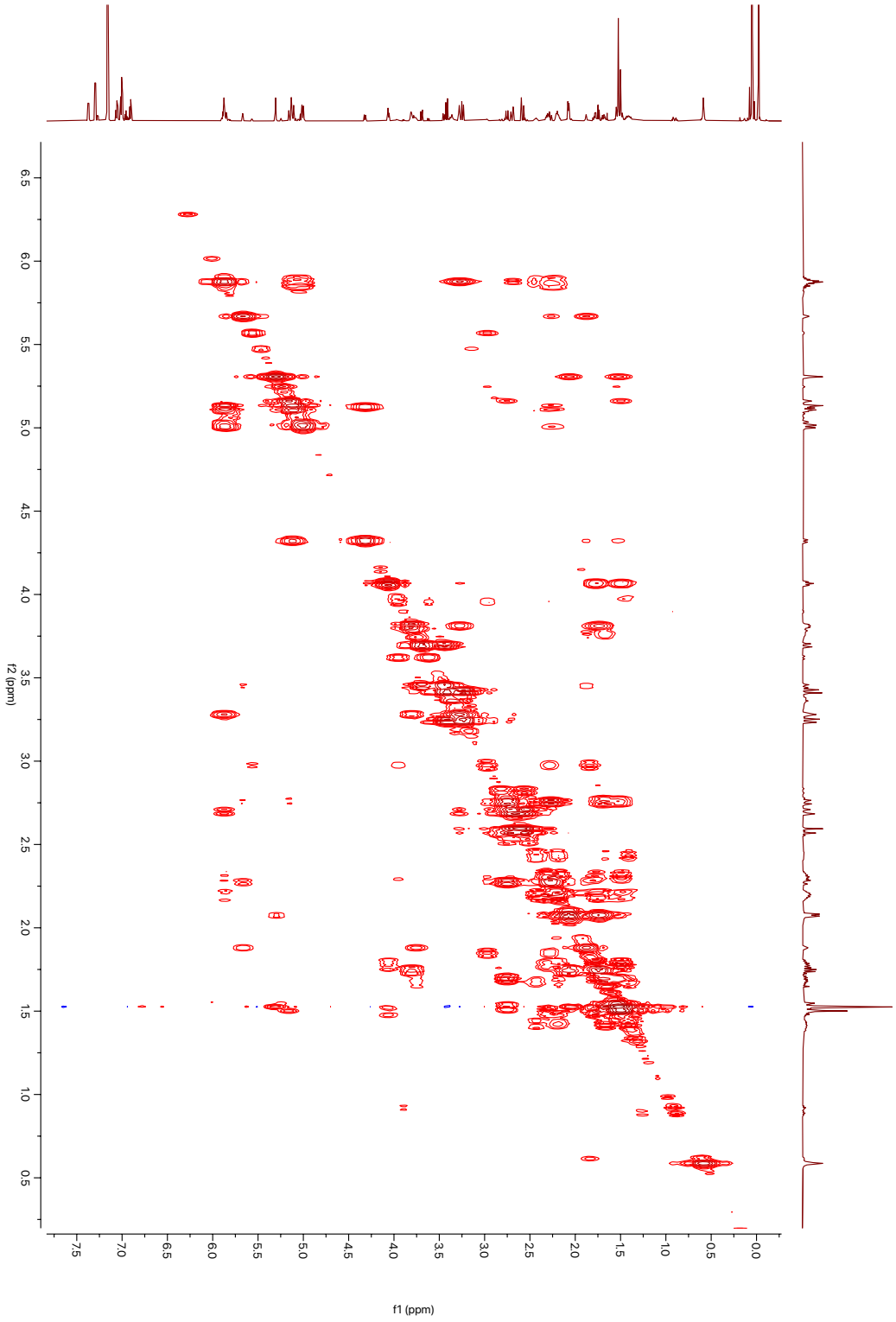

209.96
208.91
145.07
144.16
139.24
138.56
136.30
135.90
134.65
132.40
131.89
131.21
129.55
129.17
128.98
128.92
128.88
123.63
122.59
114.81
114.56
86.04
85.01
71.87
71.82
61.32
60.94
58.16
56.41
46.15
45.65
45.61
45.53
35.73
35.03
34.34
33.44
30.87
30.18
16.44
1.97
1.79
C6D6
Me
OTMS
SPh
OH
2.3.5a
2.3.5b
(150 MHz, C6D6)
f1 (ppm)

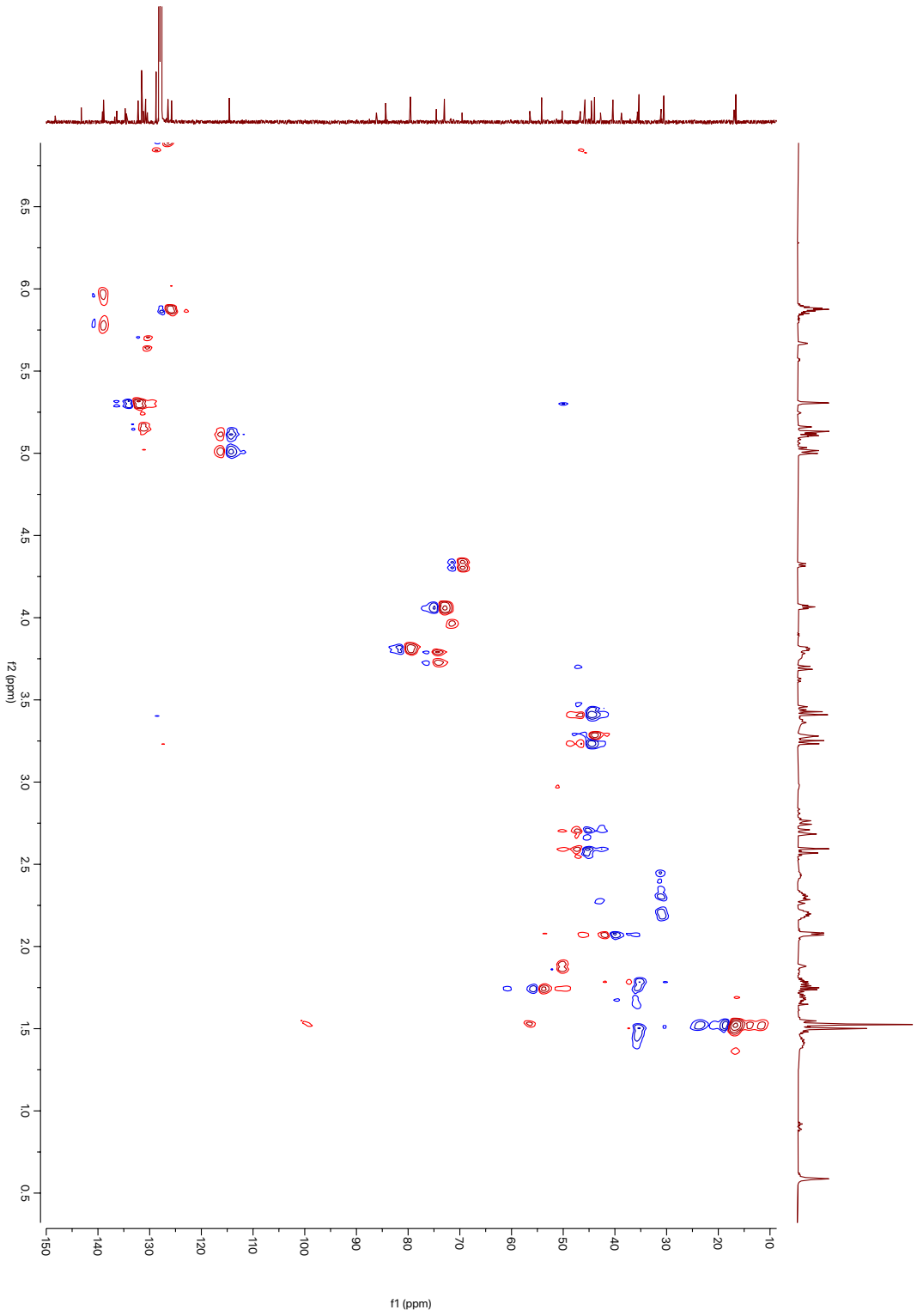

C6D5H
(700 MHz, C6D6)
2.3.6 (39%, major diastereomer)
Me
OTMS
SPh
OH
OTBS
f1 (ppm)

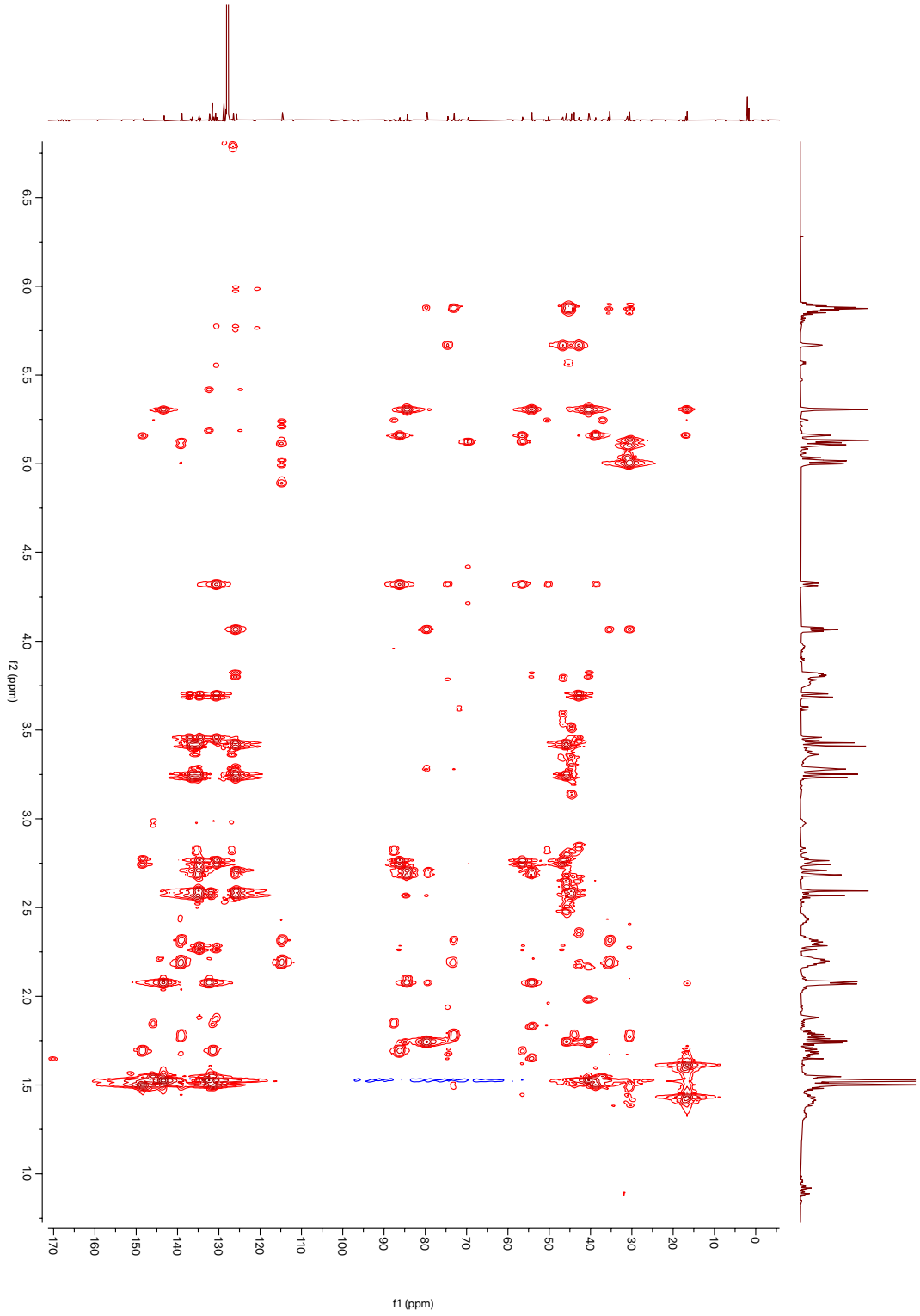

208.58
144.18
136.65
134.81
134.72
131.10
129.90
126.61
124.46
117.50
85.15
73.28
73.25
60.73
53.49
45.66
45.44
38.37
35.83
26.12
18.26
16.47
1.98
1.78
-4.22
-4.27
f1 (ppm)
C6D6
2.3.6 (39%, major diastereomer)
(150 MHz, C6D6)
Me
OTMS
SPh
OH
OTBS
H
O
H
9
8
14
11

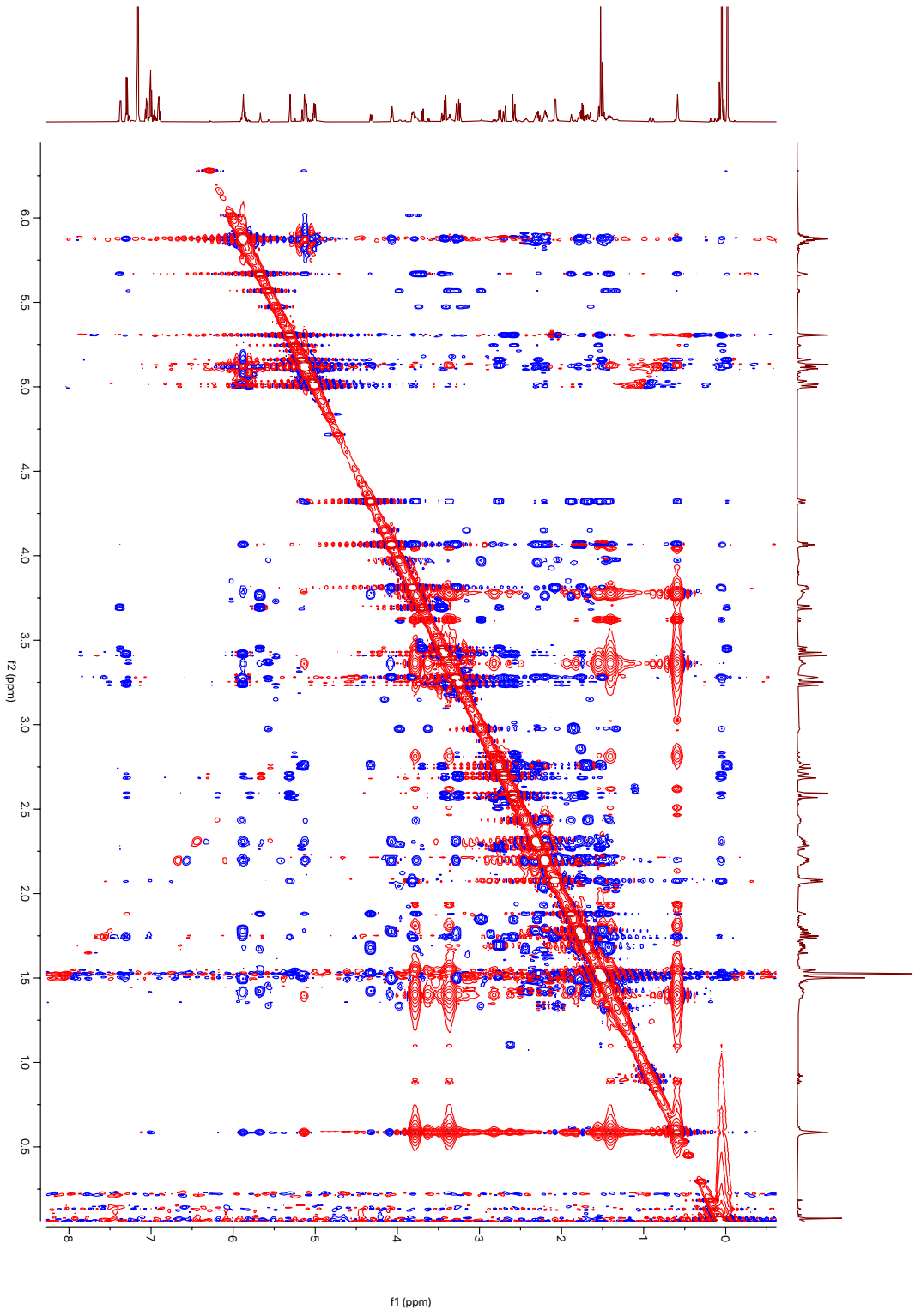

HO
H
H
OH
9
Me
OTMS
SPh
+
2.3.23a (13%)
2.3.23b (7%)
from 2.3.5b
(700 MHz, C6D6)
C6D5H
f1 (ppm)

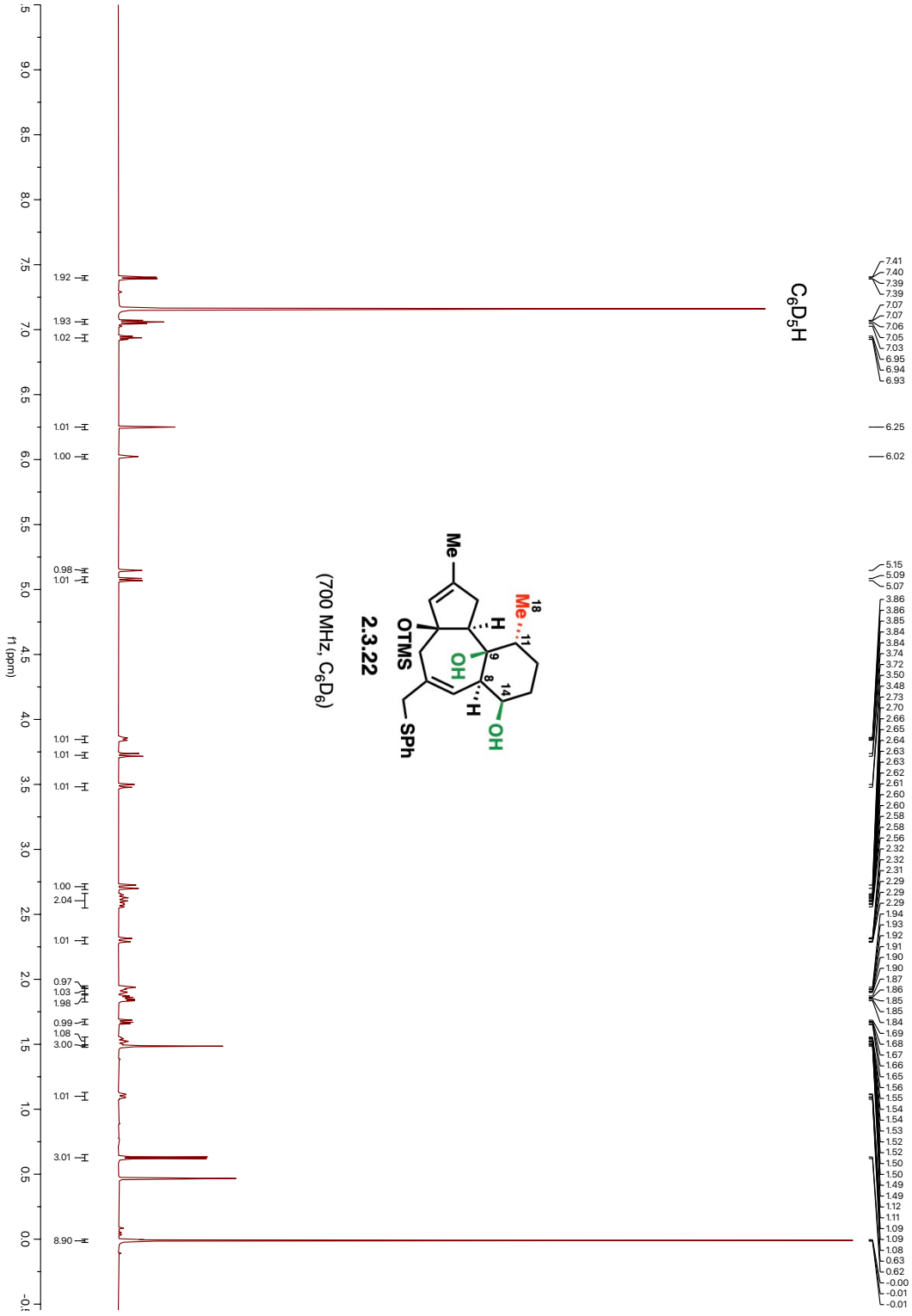

143.23
139.12
138.92
136.36
134.75
134.50
132.24
131.57
131.23
130.78
130.44
128.45
128.42
125.77
114.59
114.56
86.14
84.35
79.56
74.54
73.99
69.56
56.47
54.18
50.21
46.68
45.78
44.57
43.94
42.78
40.39
37.74
35.65
35.33
31.06
30.54
16.94
16.60
2.02
1.66
C6D6
HO
H
H
OH
9
Me
OTMS
SPh
+
2.3.23a (13%)
2.3.23b (7%)
from 2.3.5b
(150 MHz, C6D6)
f1 (ppm)

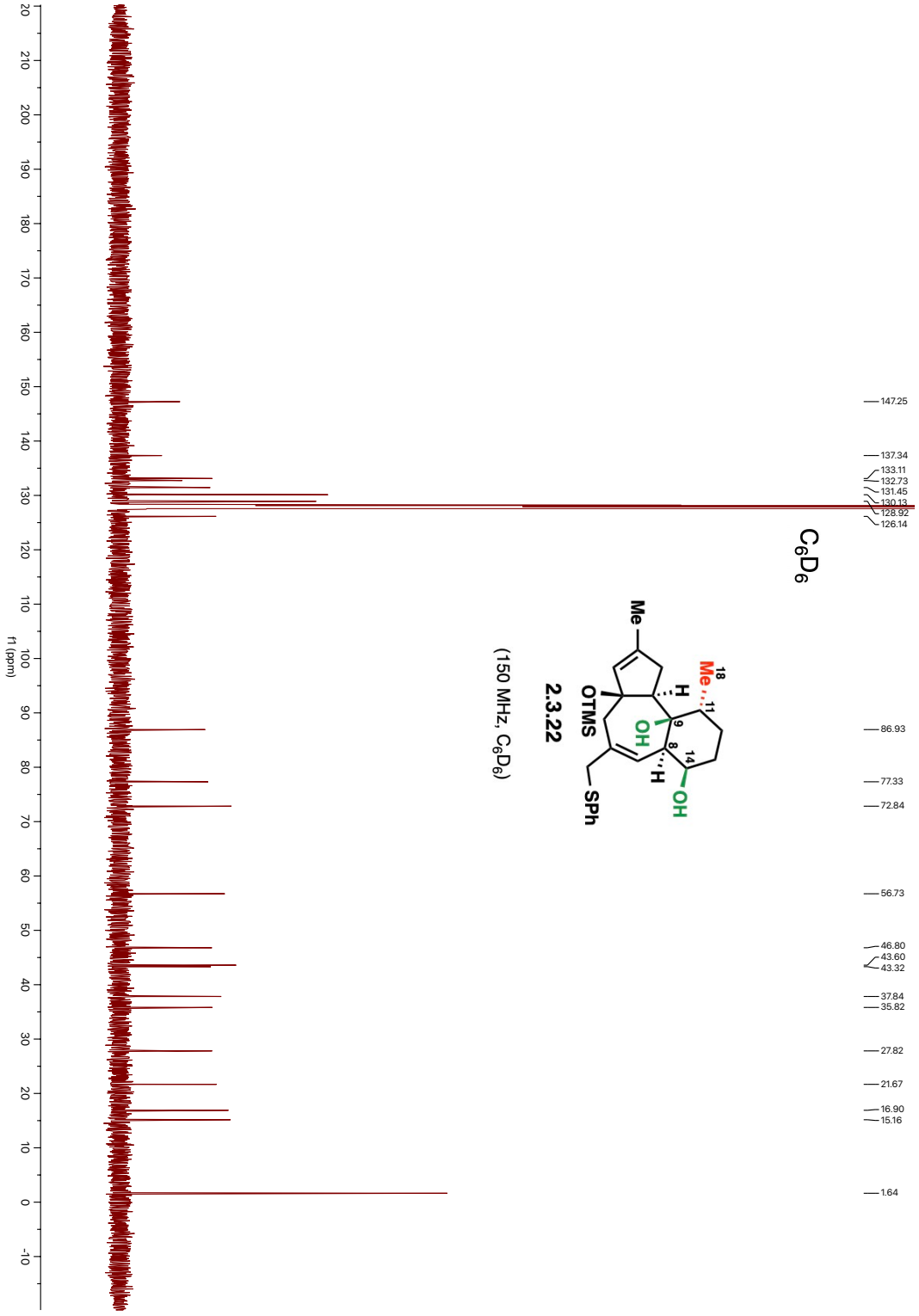

f2 (ppm)
f1 (ppm)

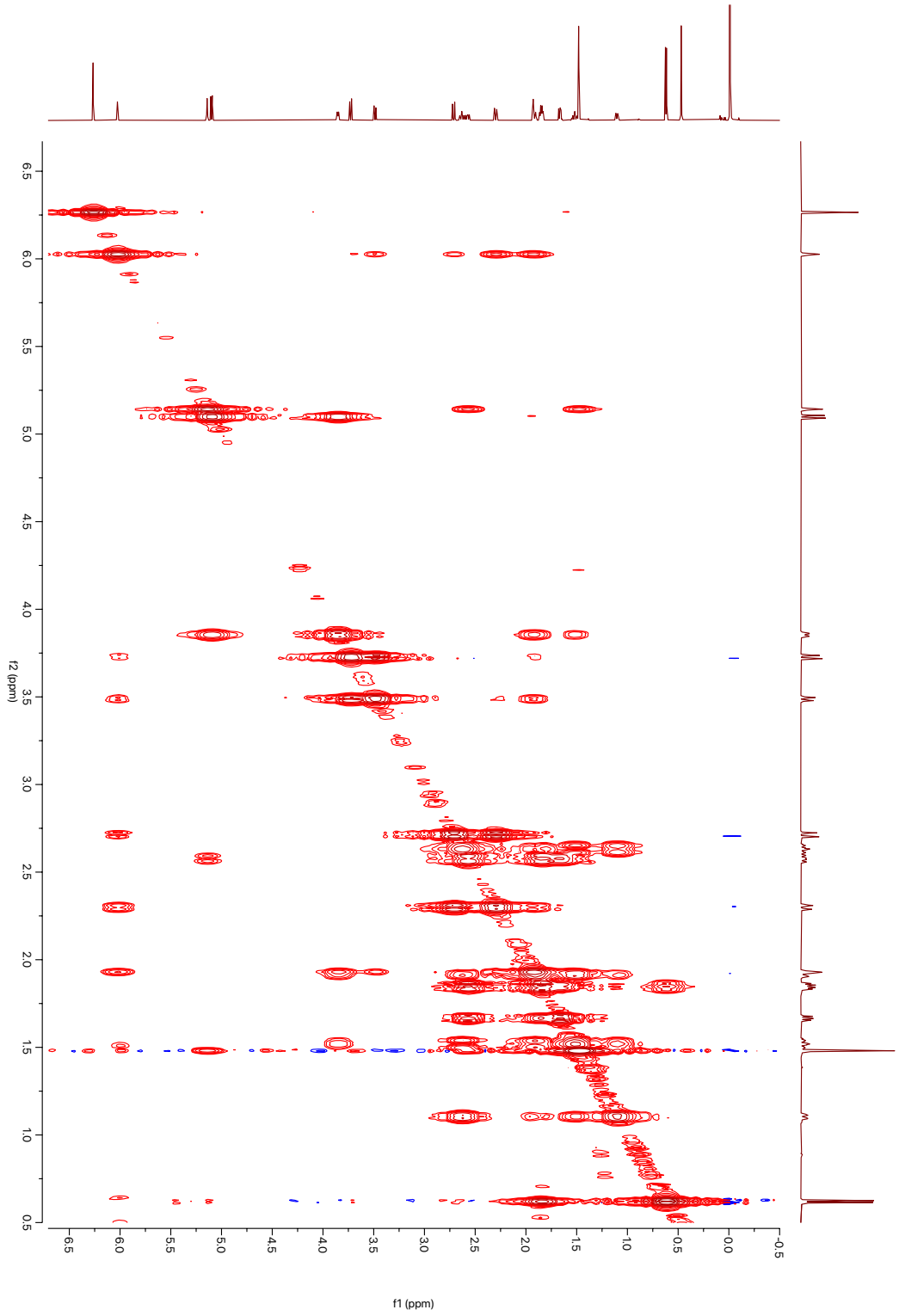

f2 (ppm)
f1 (ppm)

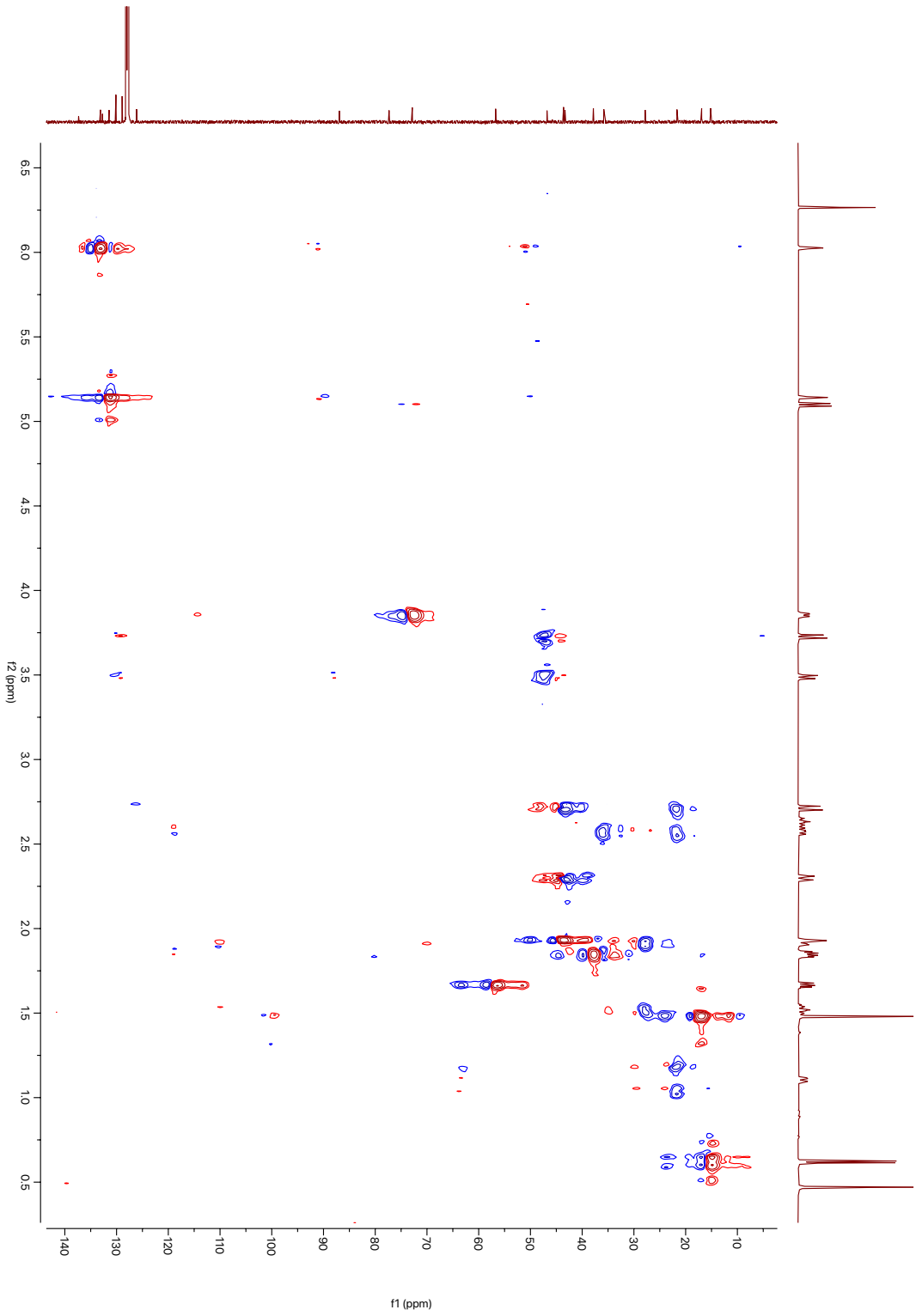

f2 (ppm)
f1 (ppm)

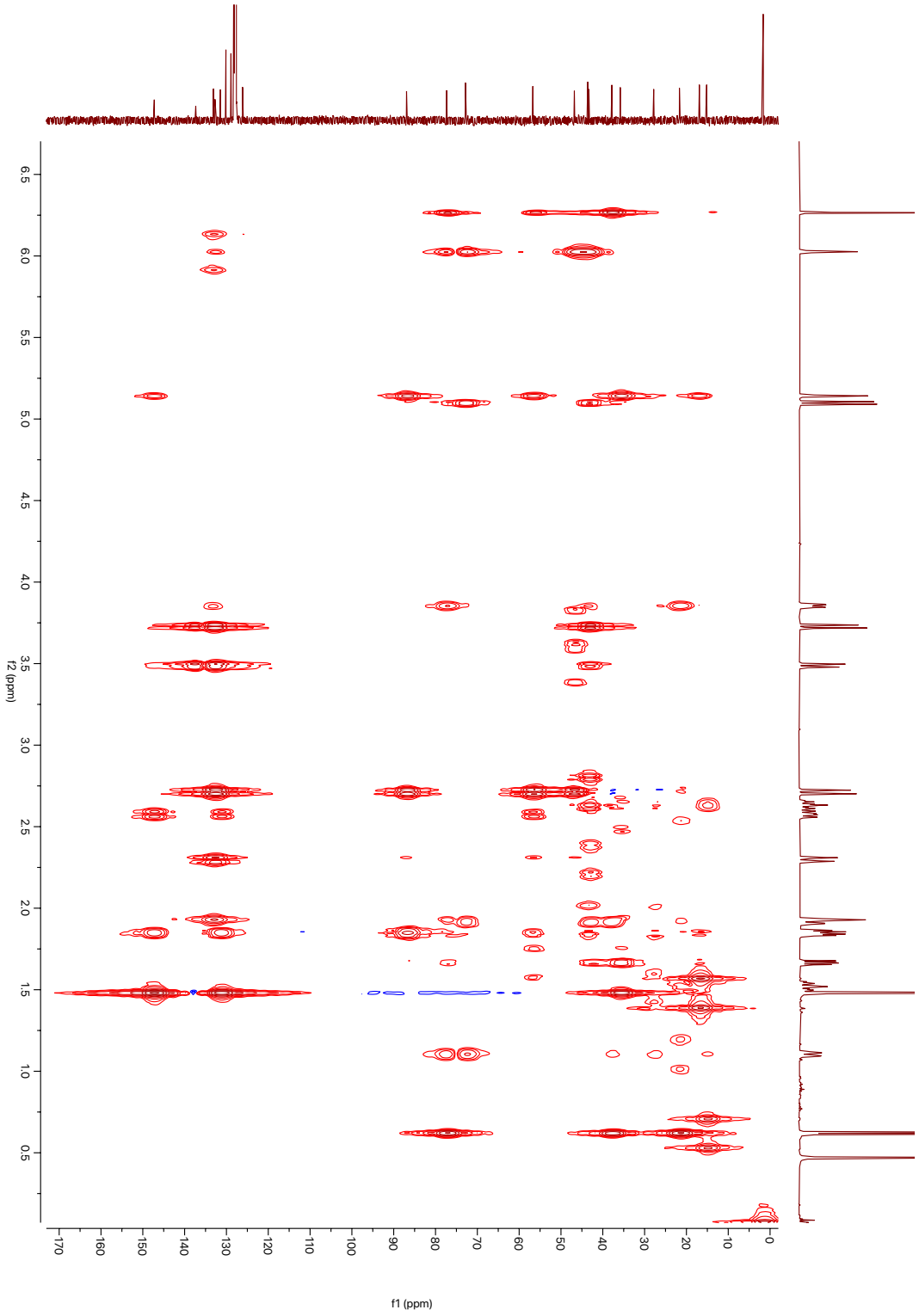

f2 (ppm)
f1 (ppm)

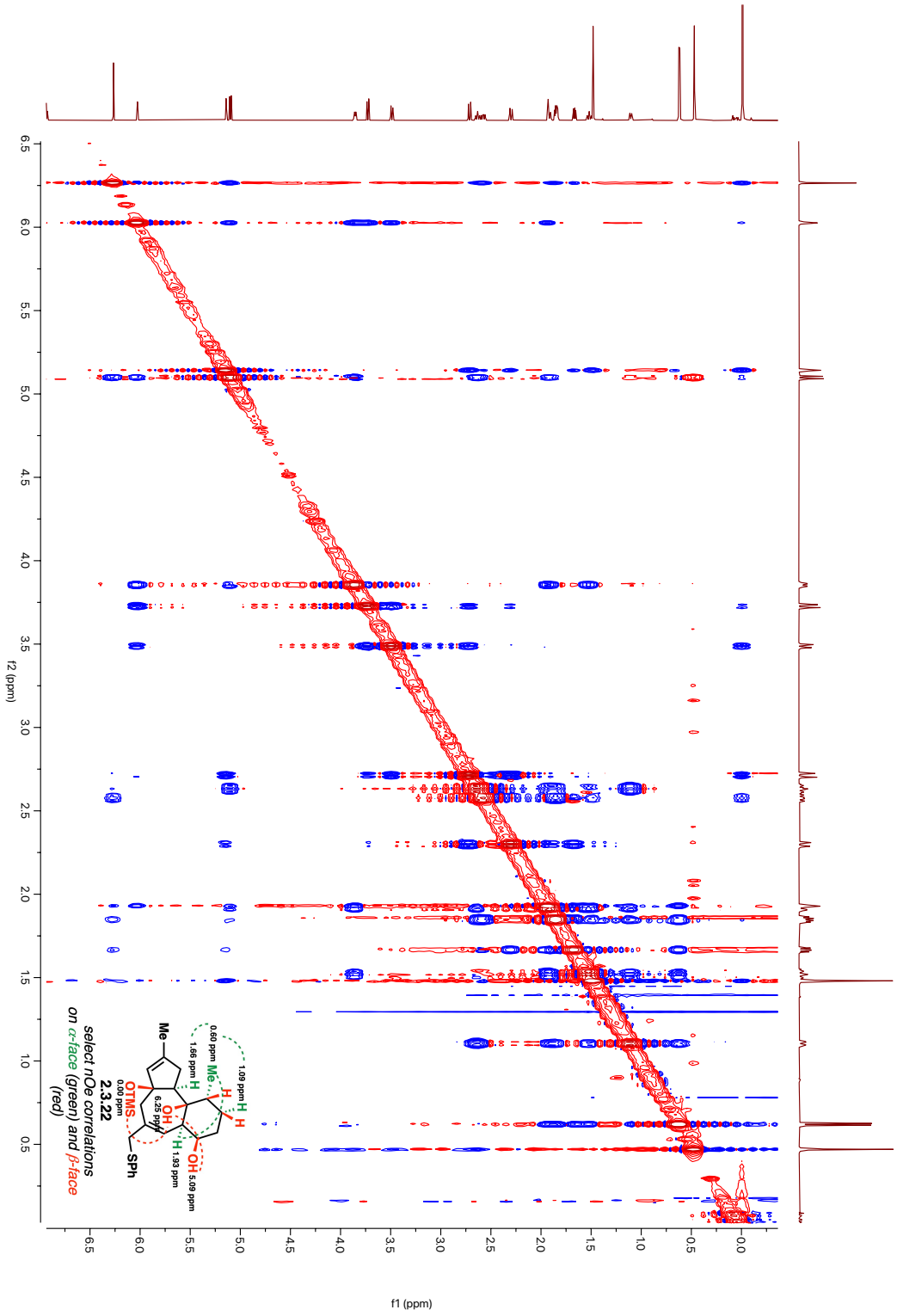

2.3.22
(700 MHz, C6D6)
C6D5H
Me
OTMS
SPh
OH
OH
H
H
Me
11
18
9
8
14
f1 (ppm)

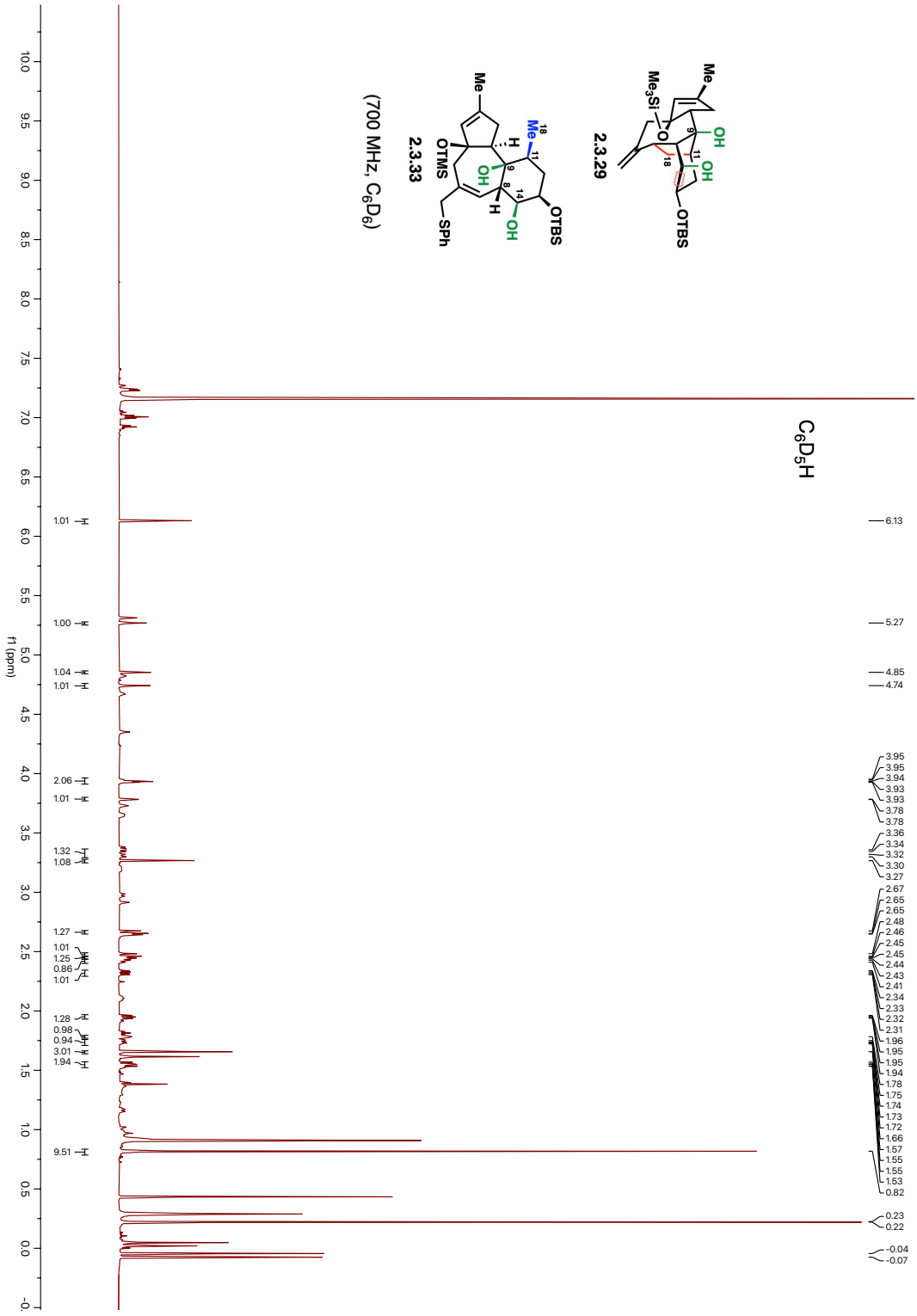

147.25
137.34
133.11
132.73
131.45
130.13
128.92
126.14
C6D6
Me
H
OH
OTMS
SPh
18
Me
11
9
8
14
OH
H
2.3.22
(150 MHz, C6D6)
86.93
77.33
72.84
56.73
46.80
43.60
43.32
37.84
35.82
27.82
21.67
16.90
15.16
1.64
f1 (ppm)

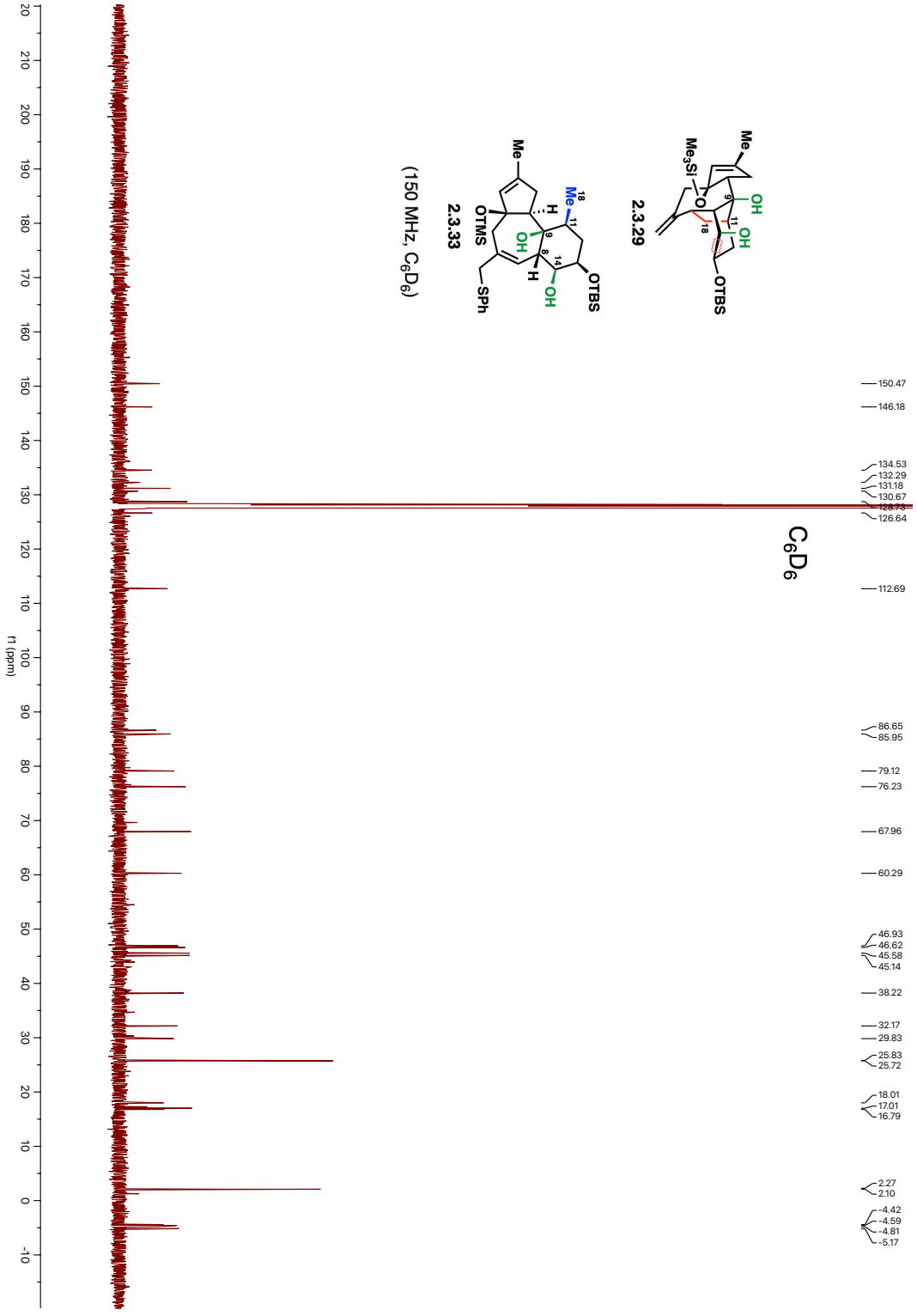

f2 (ppm)
f1 (ppm)

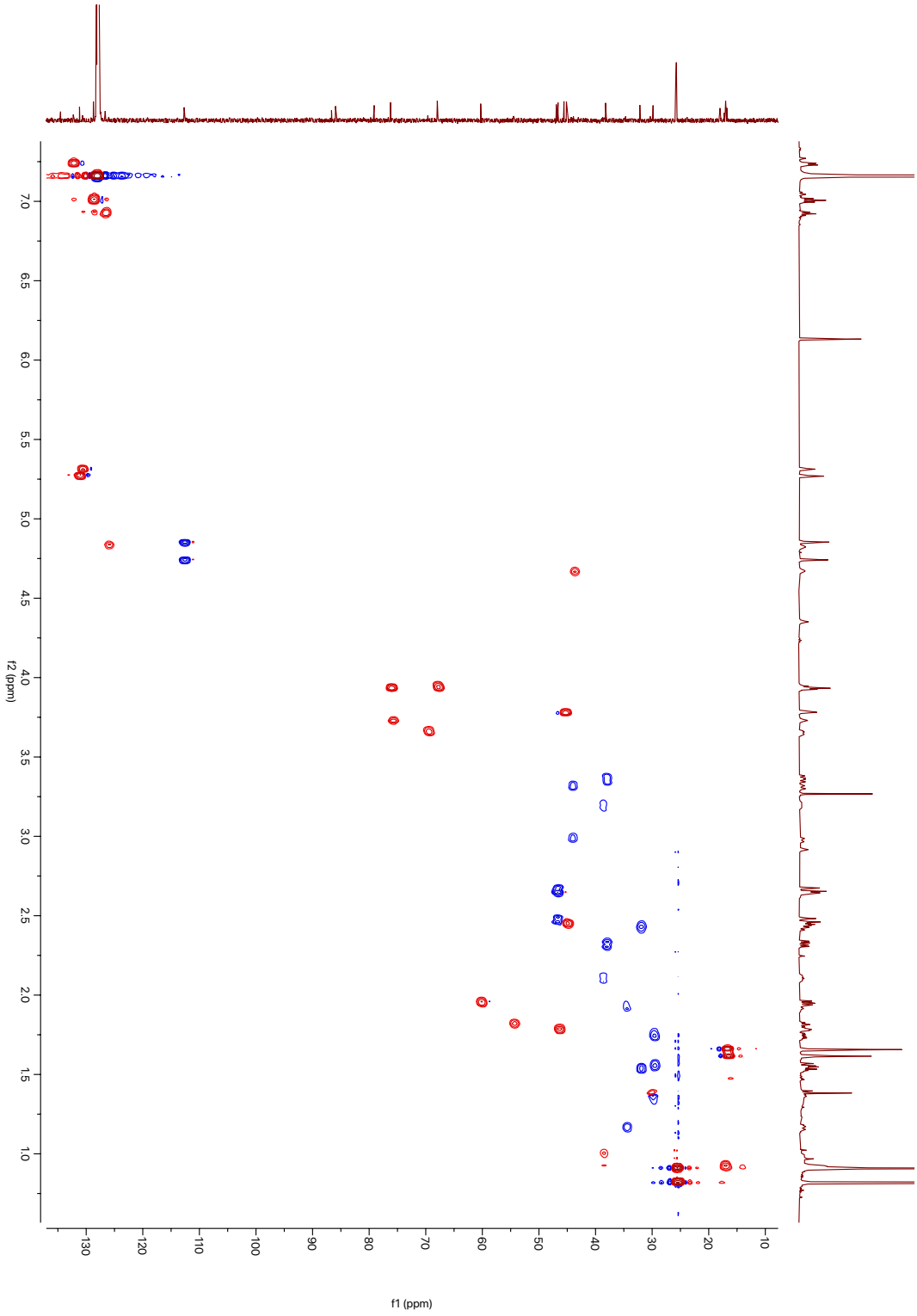

f2 (ppm)
f1 (ppm)

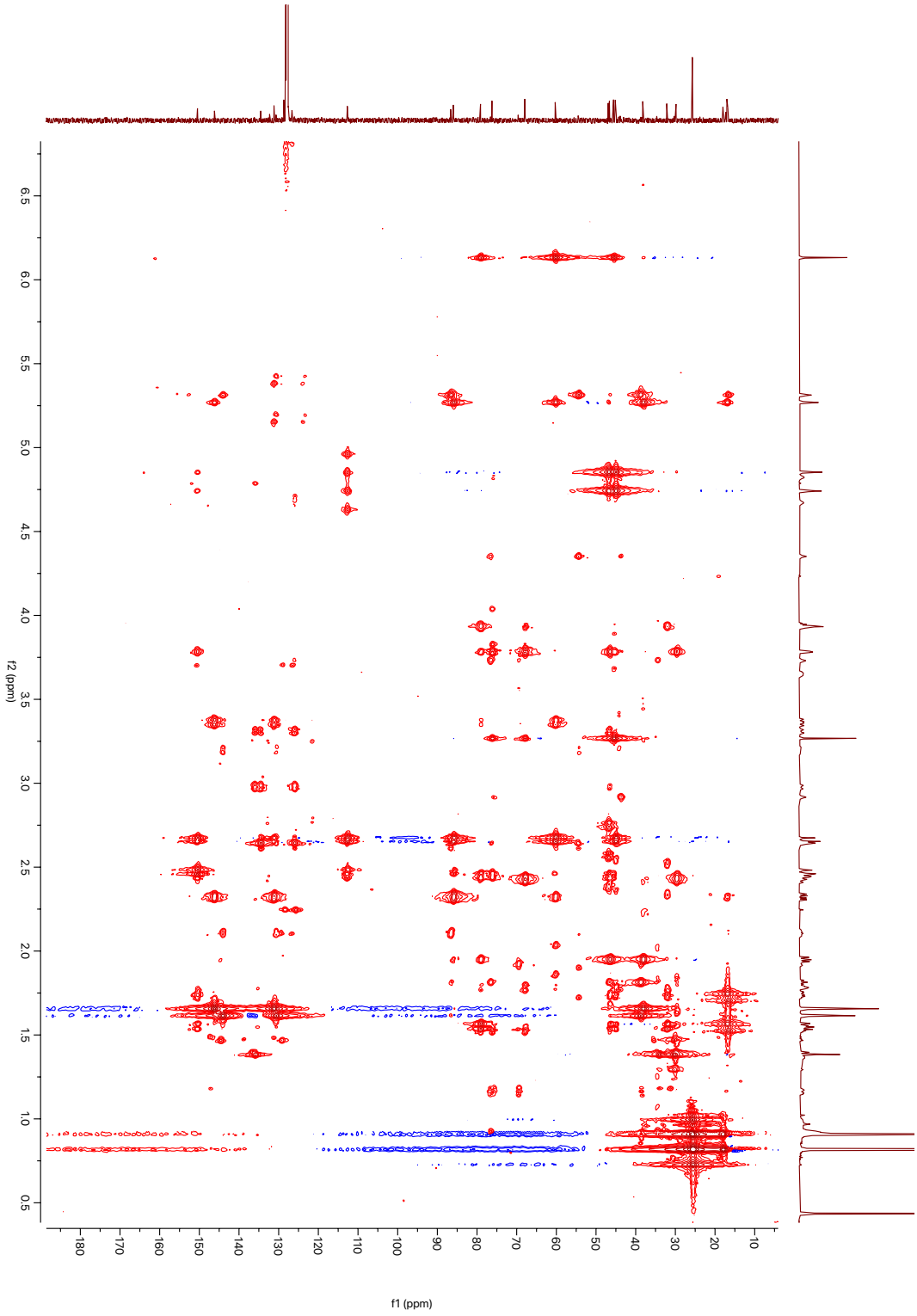

f2 (ppm)
f1 (ppm)

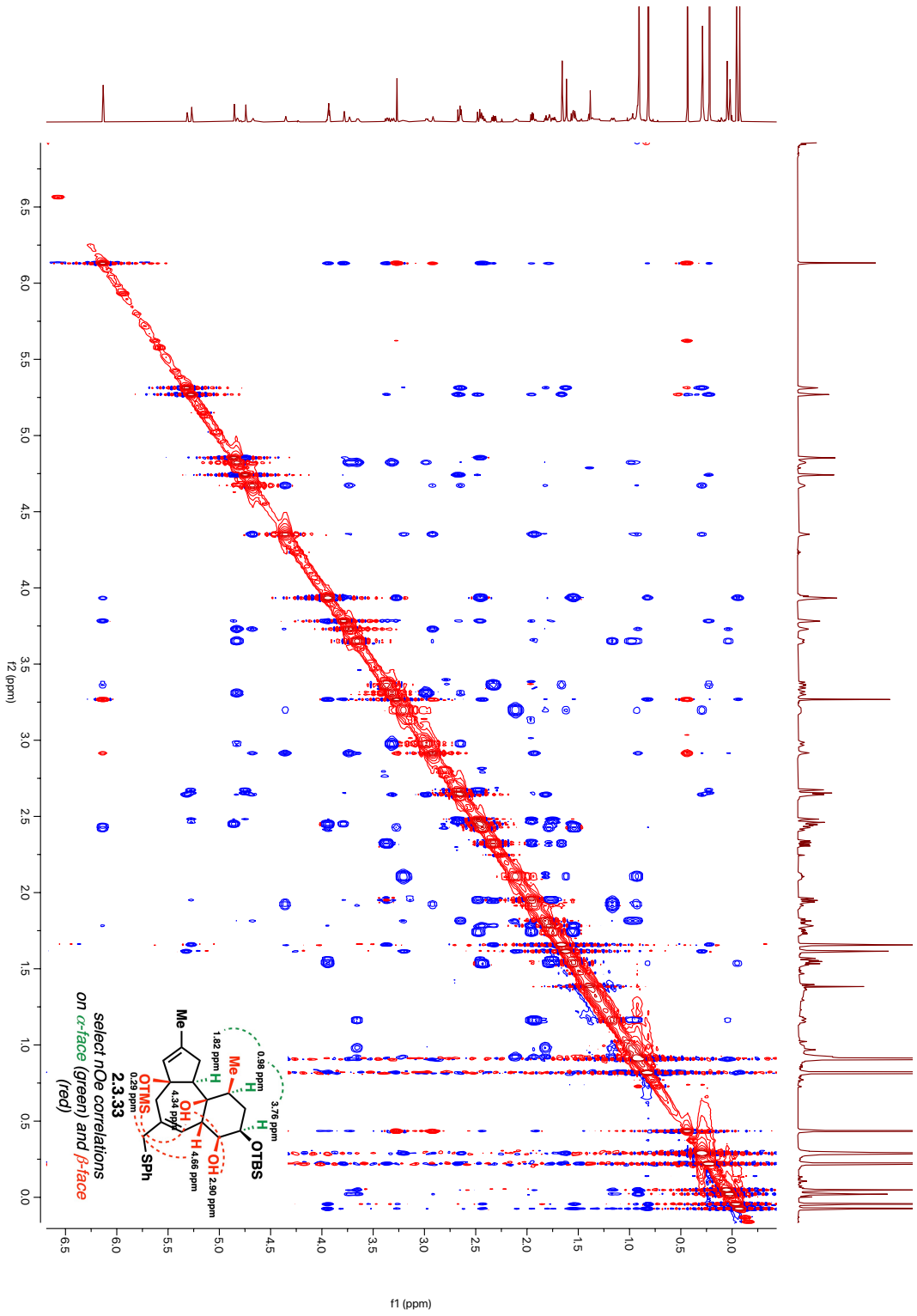

f2 (ppm)
f1 (ppm)
select nOe correlations
on α-face (green) and β-face
(red)
2.3.22
Me
OTMS
0.00 ppm
SPh
OH
6.25 ppm
OH 5.09 ppm
1.66 ppm
1.93 ppm
0.80 ppm
1.09 ppm

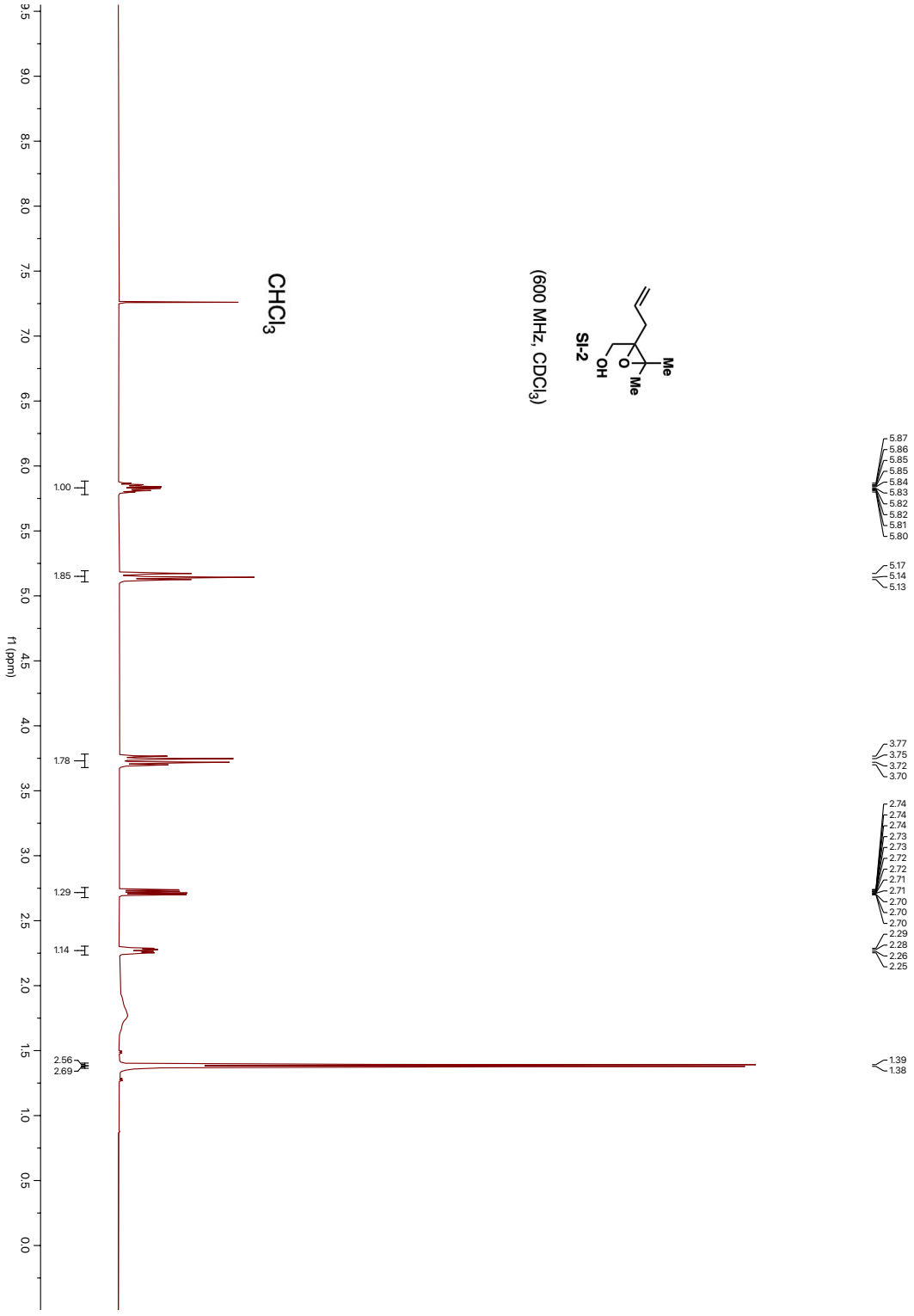

2.3.29
2.3.33
(700 MHz, C6D6)
C6D5H
f1 (ppm)

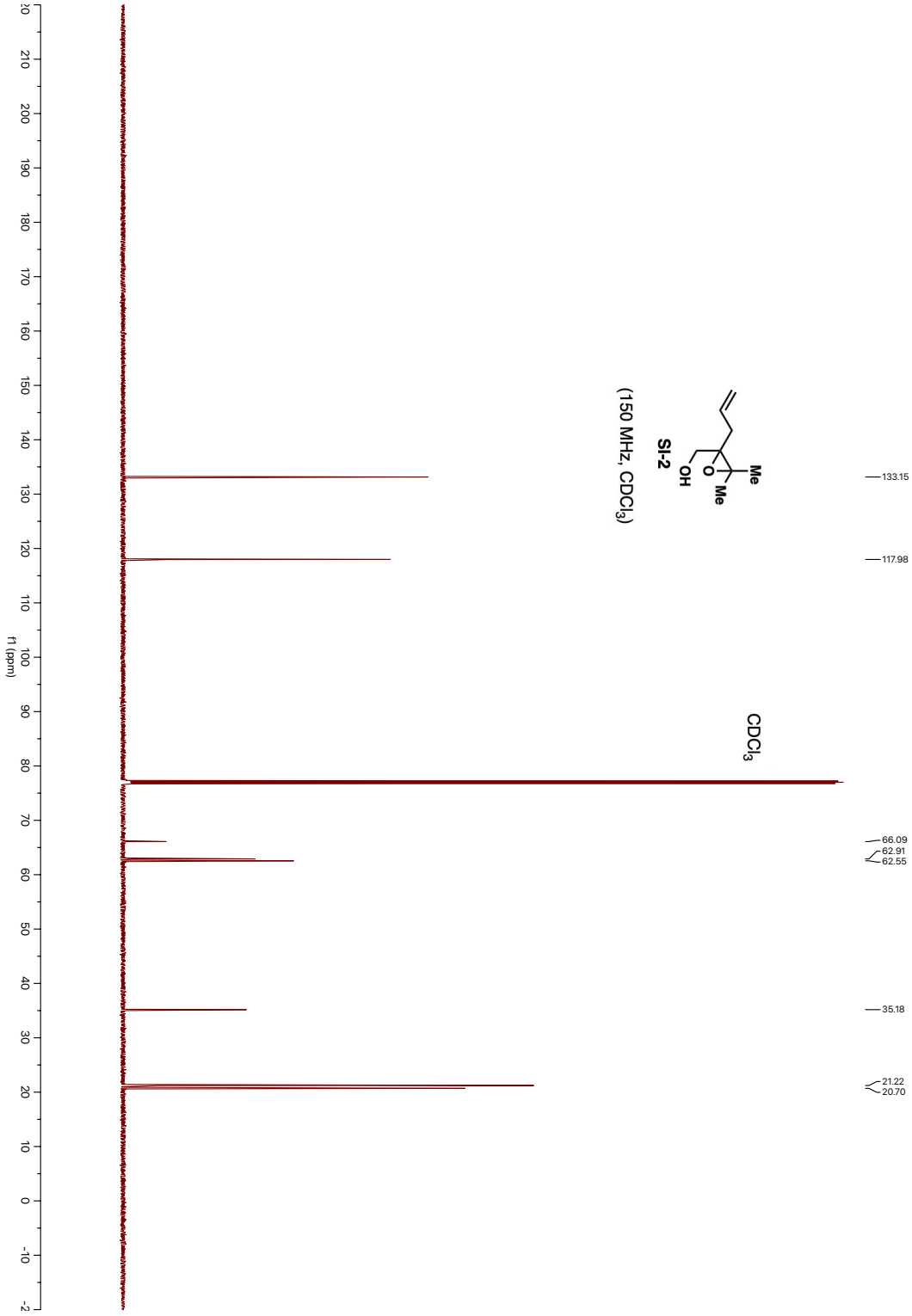

(150 MHz, C6D6)
2.3.33
2.3.29
C6D6
f1 (ppm)
150.47
146.18
134.53
132.29
131.18
130.67
128.73
126.64
112.69
86.65
85.95
79.12
76.23
67.96
60.29
46.93
46.62
45.58
45.14
38.22
32.17
29.83
25.83
25.72
18.01
17.01
16.79
2.27
2.10
-4.42
-4.59
-4.81
-5.17

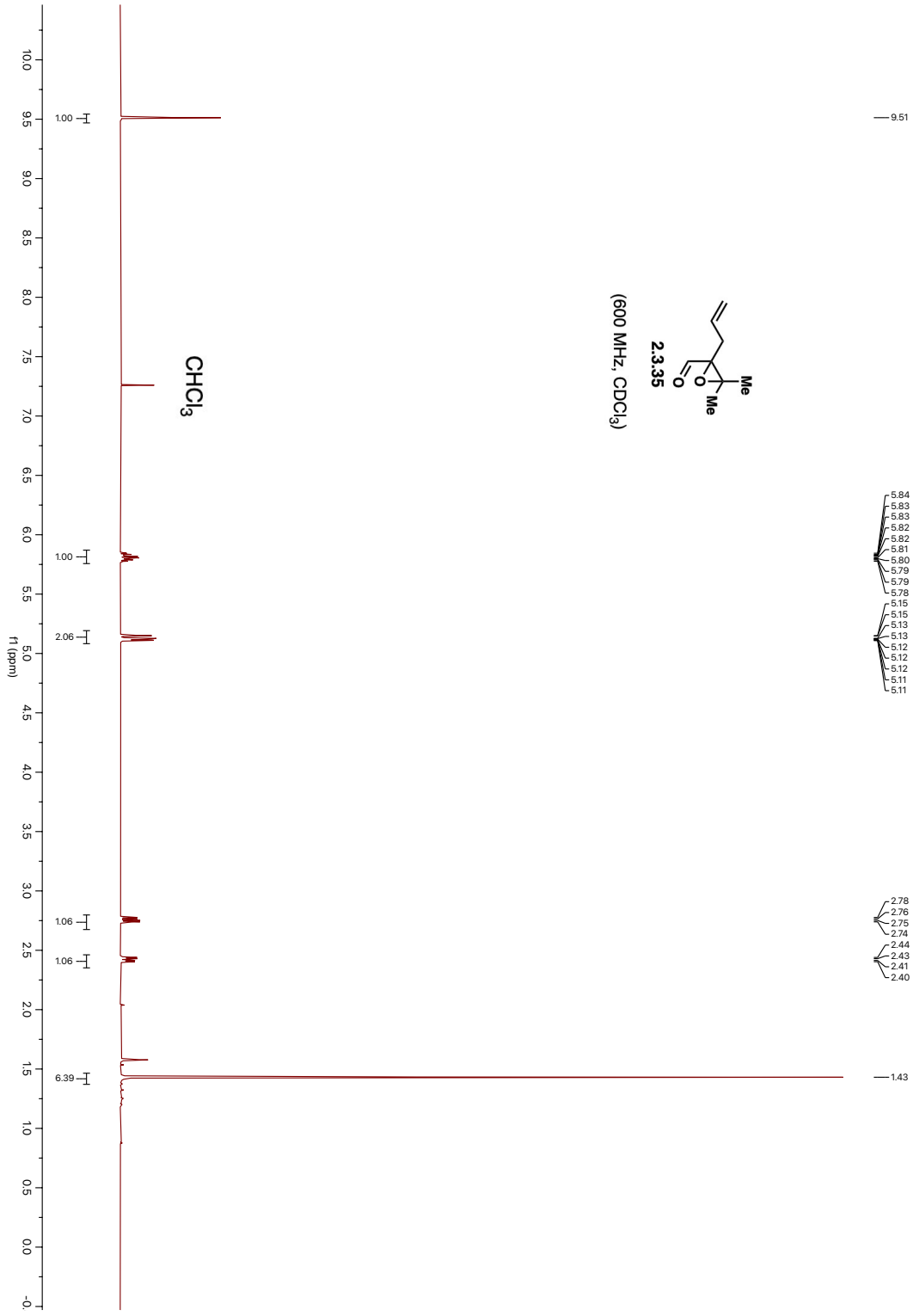

f2 (ppm)
f1 (ppm)

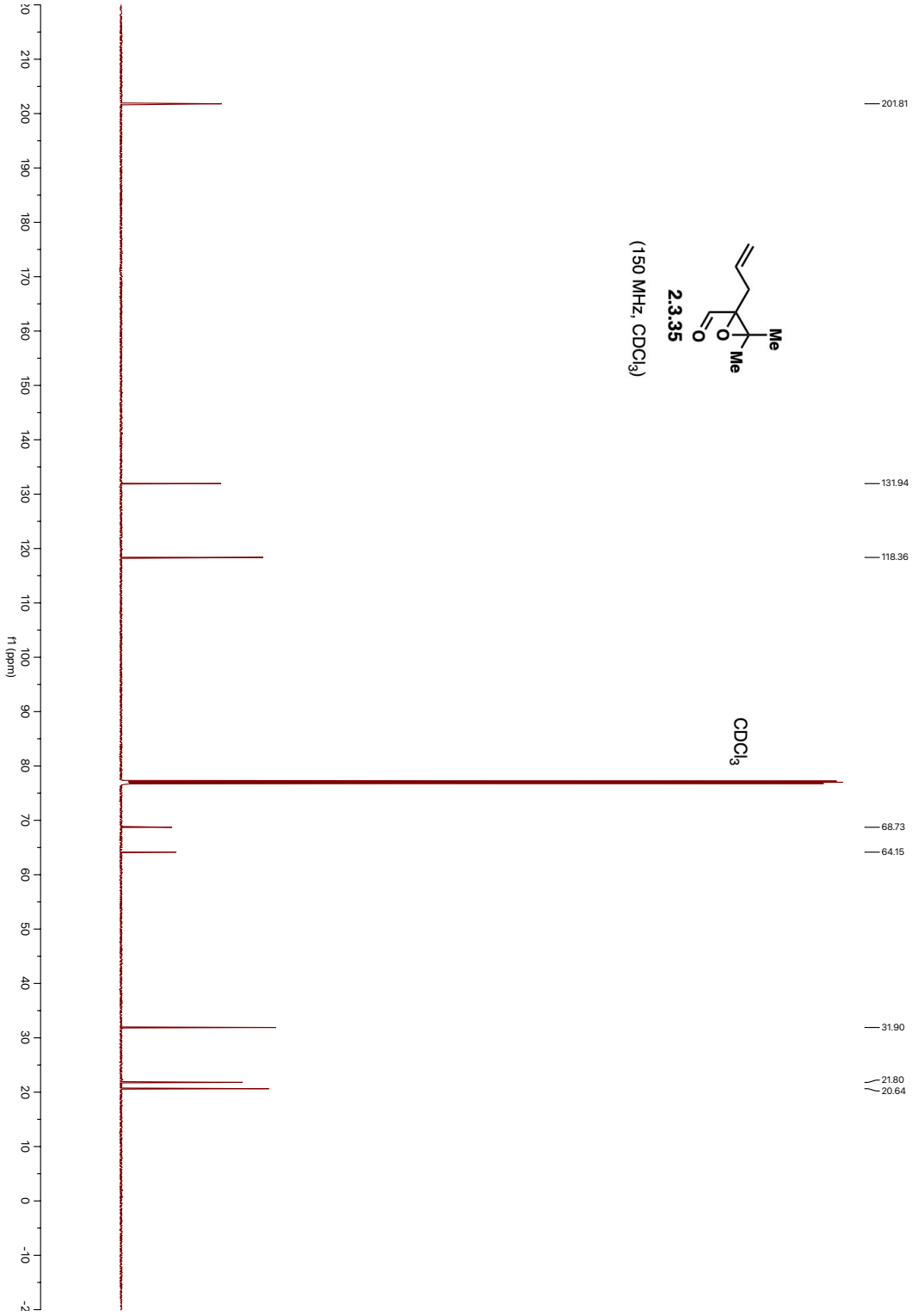

f2 (ppm)
f1 (ppm)

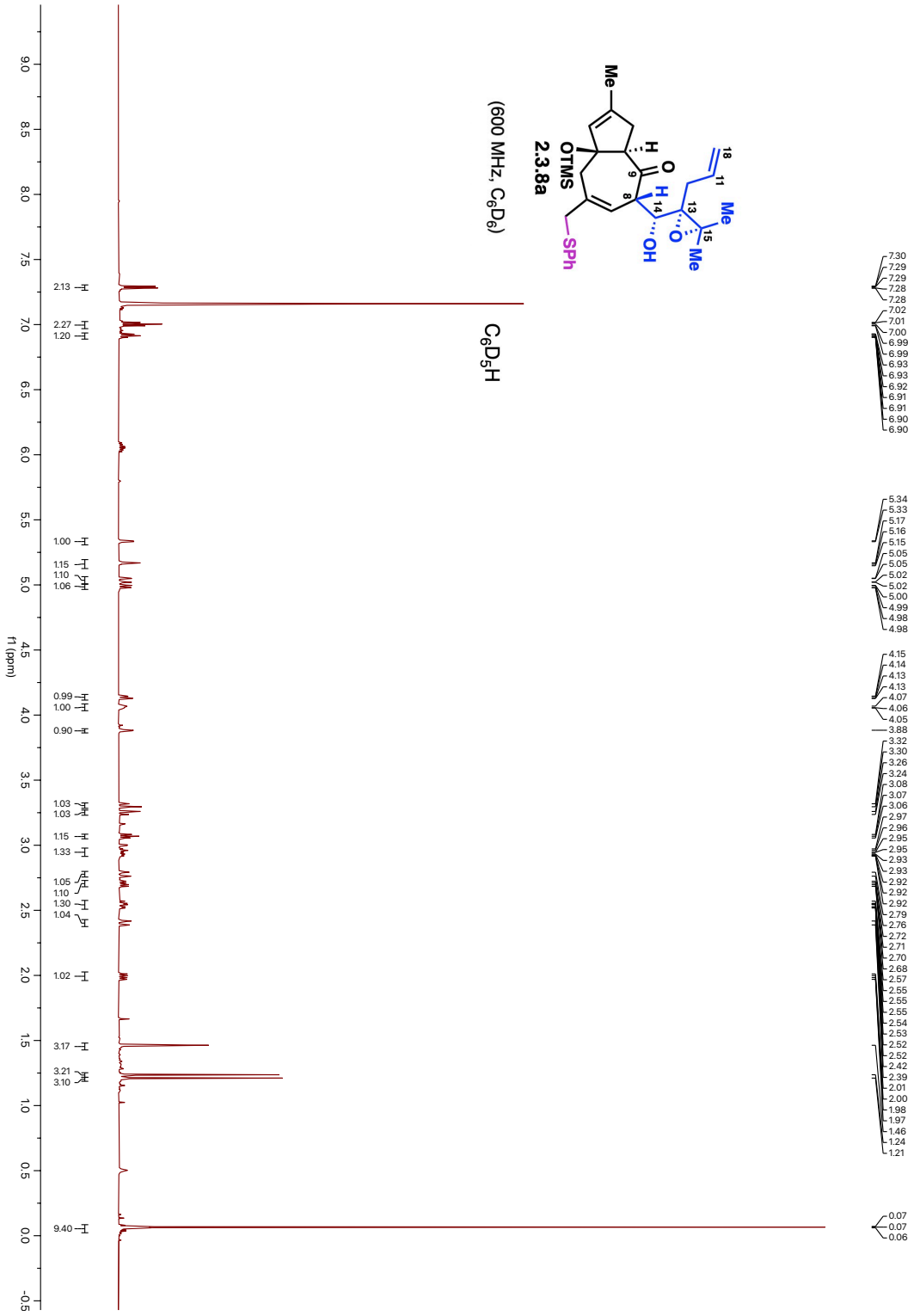

f2 (ppm)
f1 (ppm)
Me
1.82 ppm H
Me
H
0.98 ppm
3.76 ppm
H
OTBS
OTMS
0.29 ppm
OH
4.34 ppm
H
4.66 ppm
OH 2.90 ppm
SPh
2.3.33
select nOe correlations
on α-face (green) and β-face
(red)

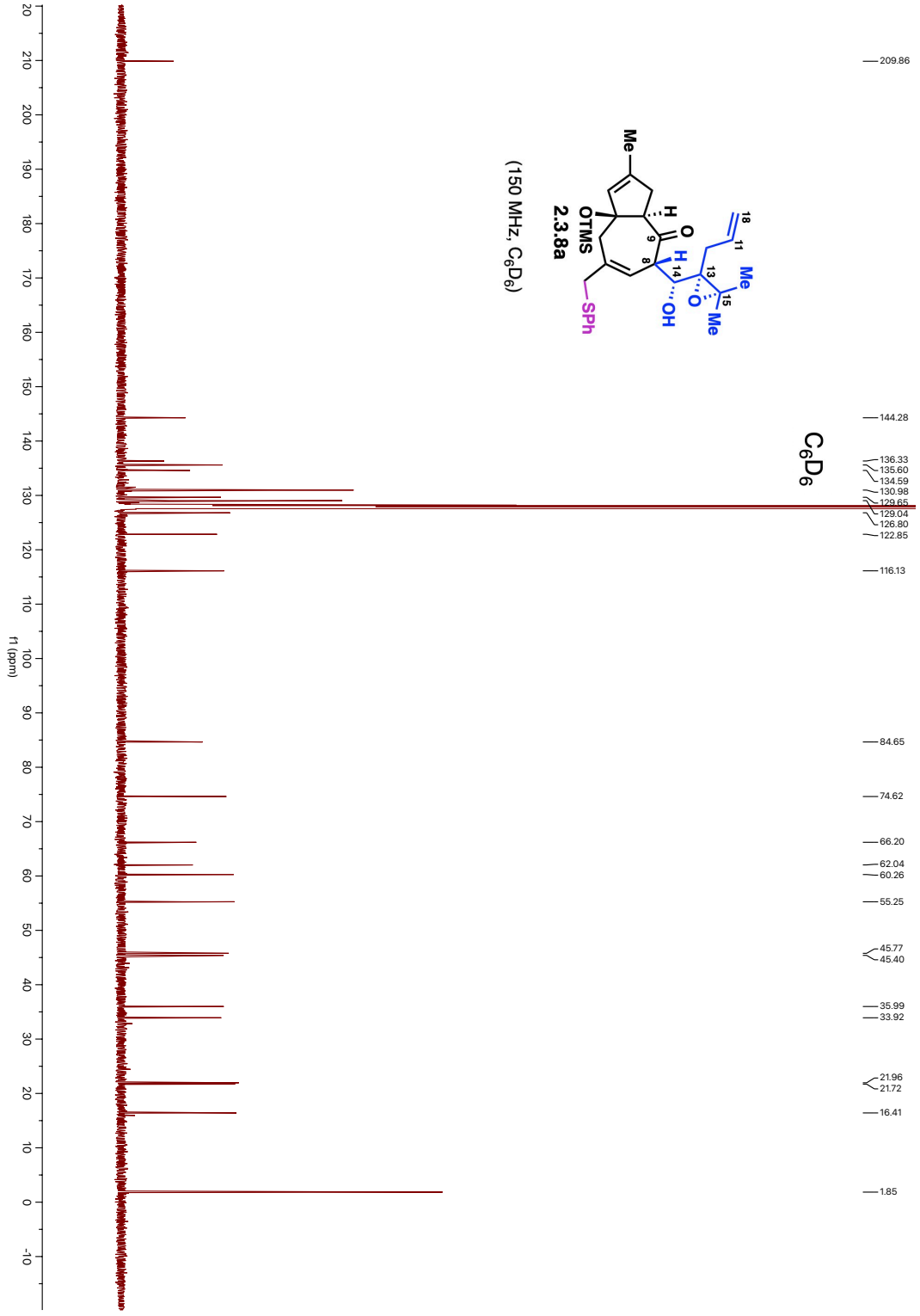

CHCl3
(600 MHz, CDCl3)
SI-2
OH
O
Me
Me
f1 (ppm)
1.00
1.85
1.78
1.29
1.14
2.56
2.69
5.87
5.86
5.85
5.85
5.84
5.83
5.82
5.82
5.81
5.80
5.17
5.14
5.13
3.77
3.75
3.72
3.70
2.74
2.74
2.74
2.73
2.73
2.72
2.72
2.71
2.71
2.70
2.70
2.70
2.29
2.28
2.26
2.25
1.39
1.38

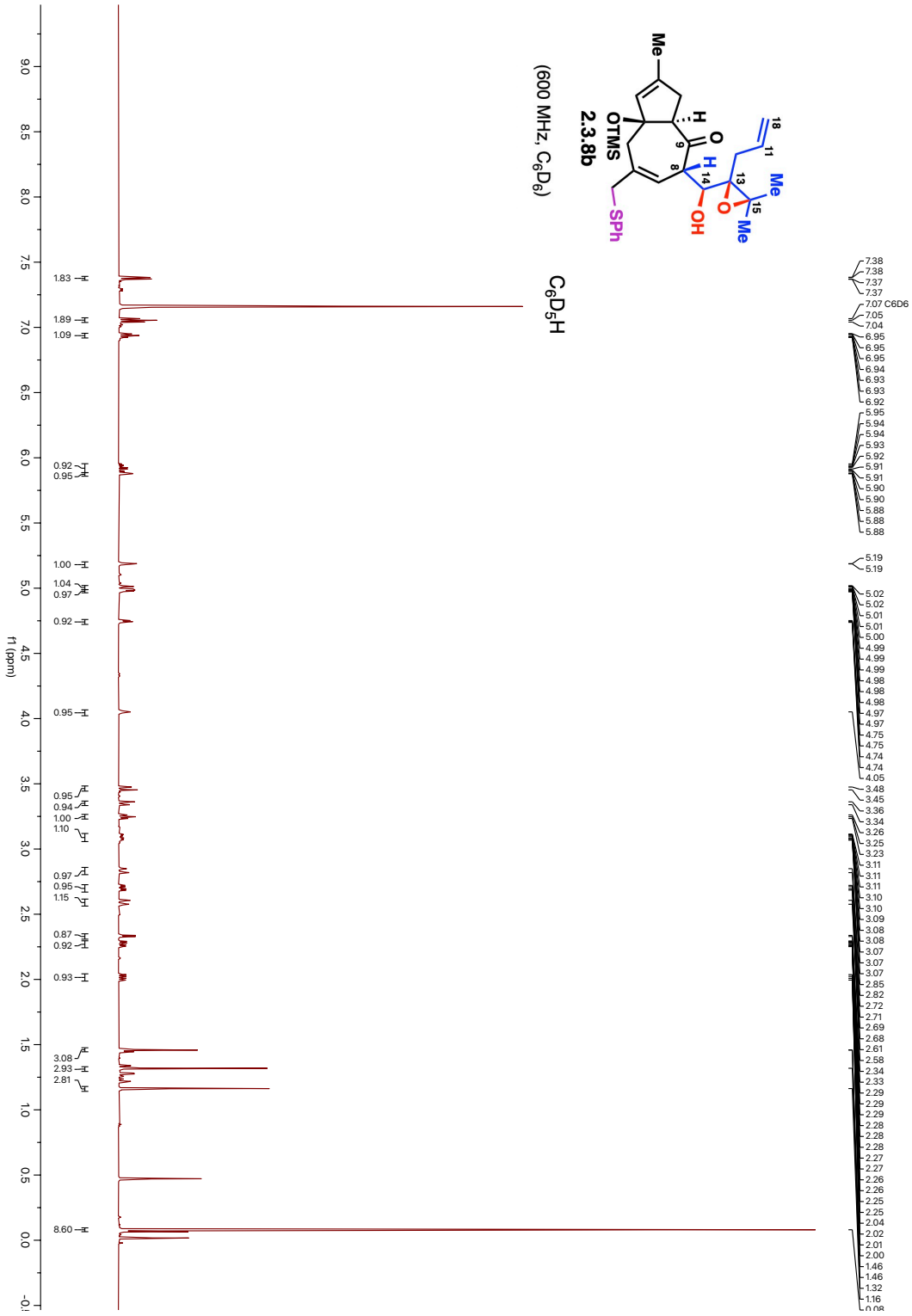

SI-2
(150 MHz, $CDCl_3$)
$CDCl_3$
133.15
117.98
66.09
62.91
62.55
35.18
21.22
20.70
f1 (ppm)

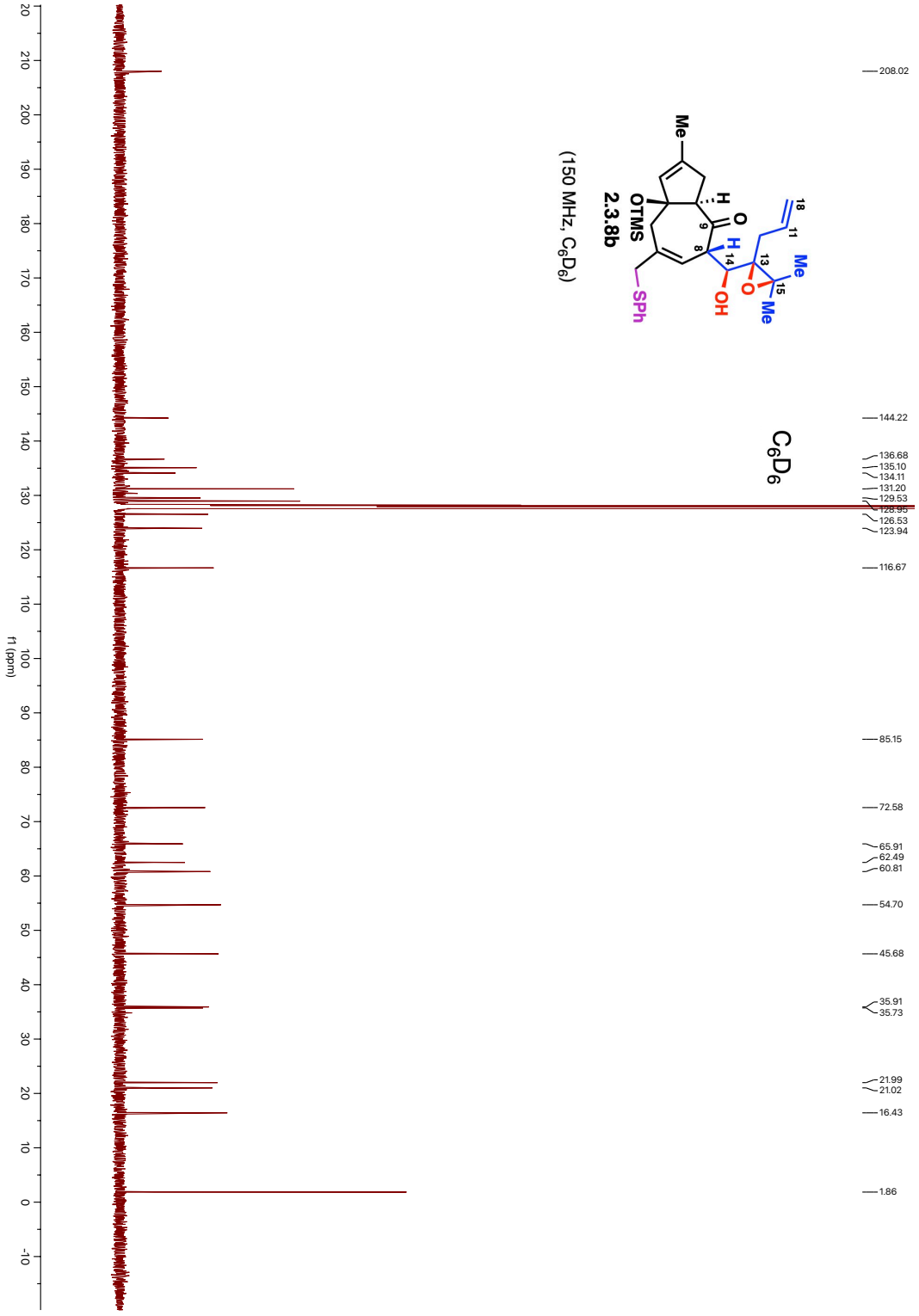

2.3.35
(600 MHz, CDCl3)
CHCl3
Me
Me
O
O
9.51
5.84
5.83
5.83
5.82
5.82
5.81
5.80
5.79
5.79
5.78
5.15
5.15
5.13
5.13
5.12
5.12
5.12
5.11
5.11
2.78
2.76
2.75
2.74
2.44
2.43
2.41
2.40
1.43
1.00
1.00
2.06
1.06
1.06
6.39
f1 (ppm)

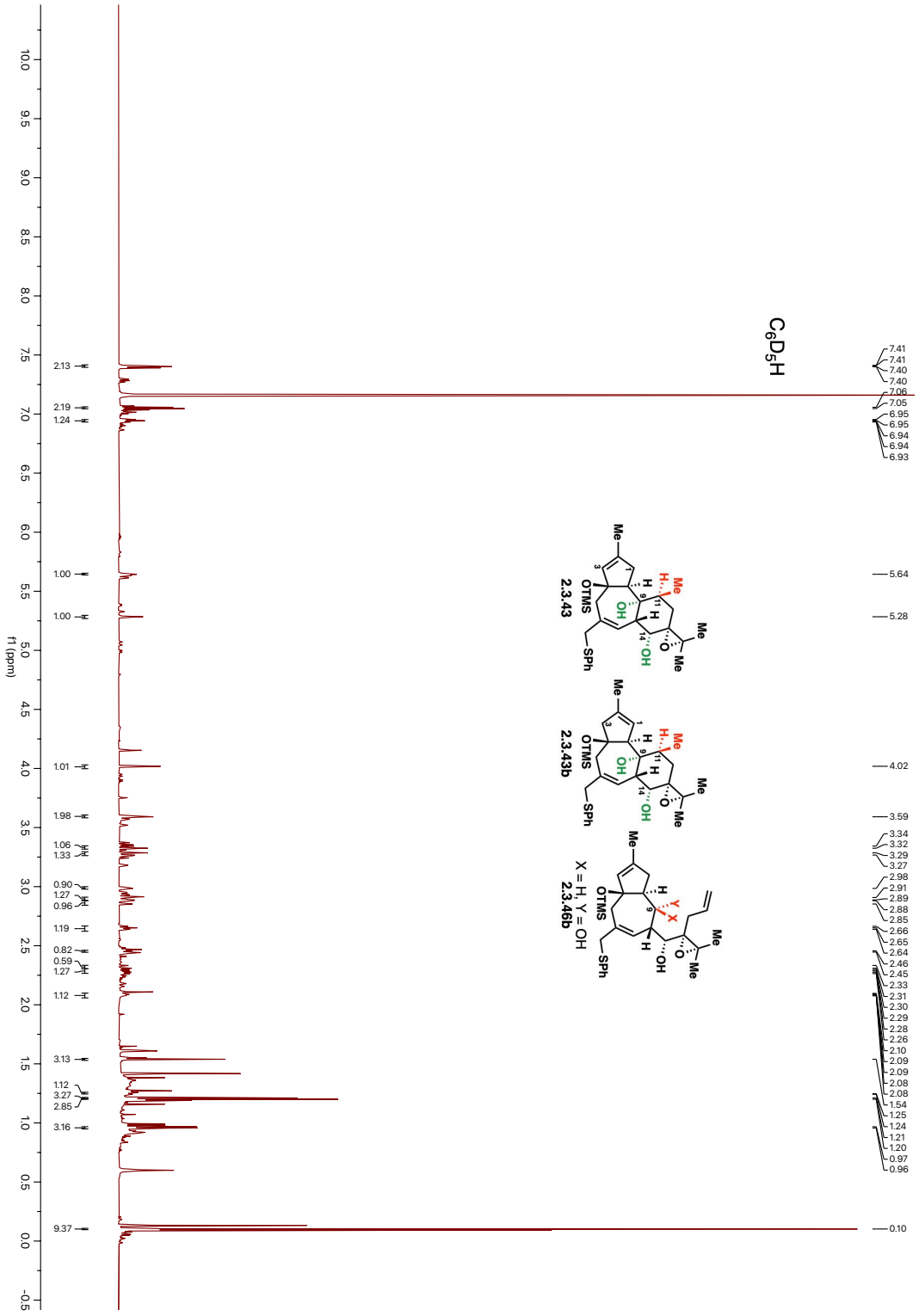

2.3.35
(150 MHz, CDCl3)
Me
O
O
Me
CDCl3
201.81
131.94
118.36
68.73
64.15
31.90
21.80
20.64
f1 (ppm)

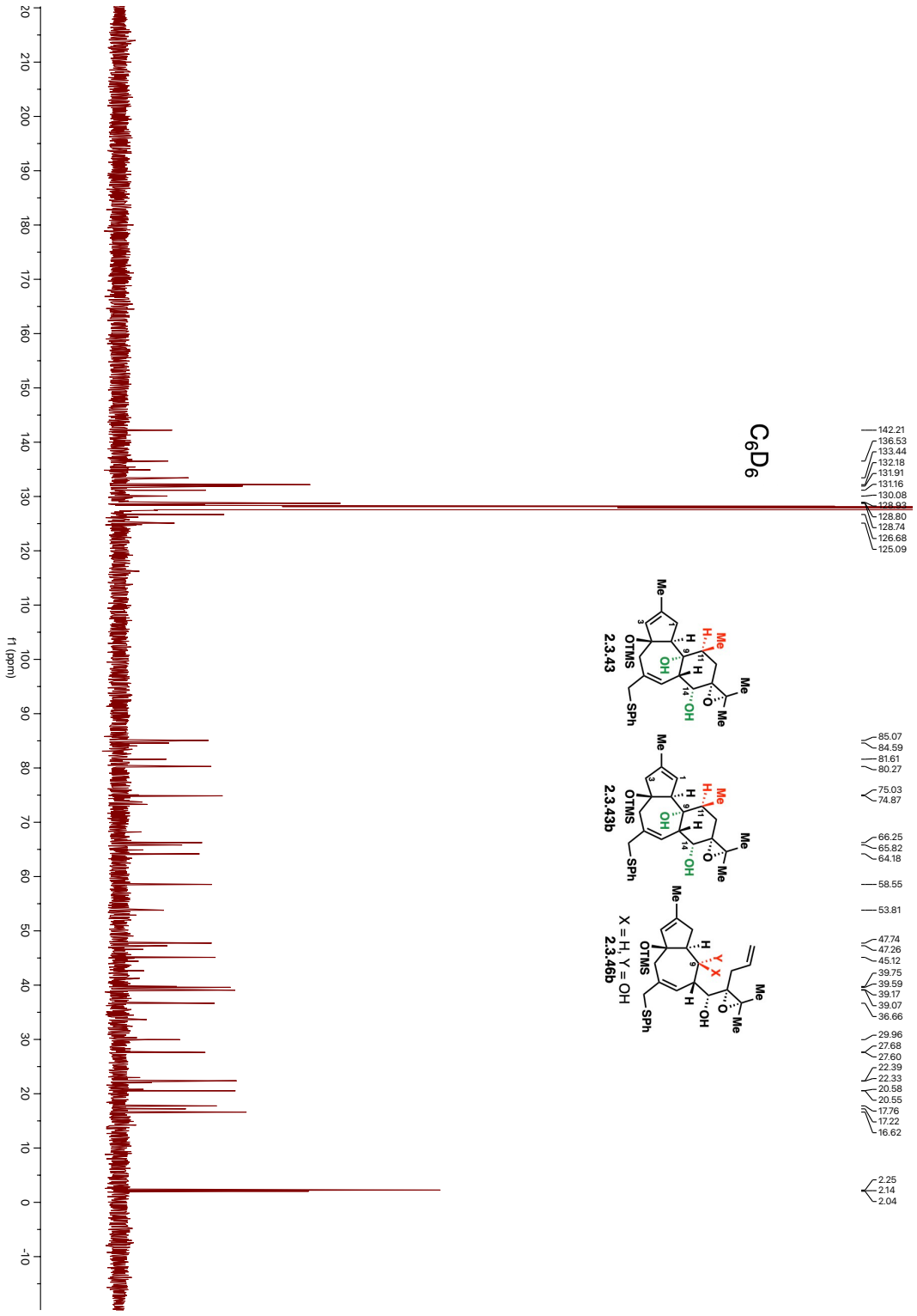

(600 MHz, C6D6)
C6D5H
2.3.8a
OTMS
SPh
OH
Me
Me
Me
f1 (ppm)

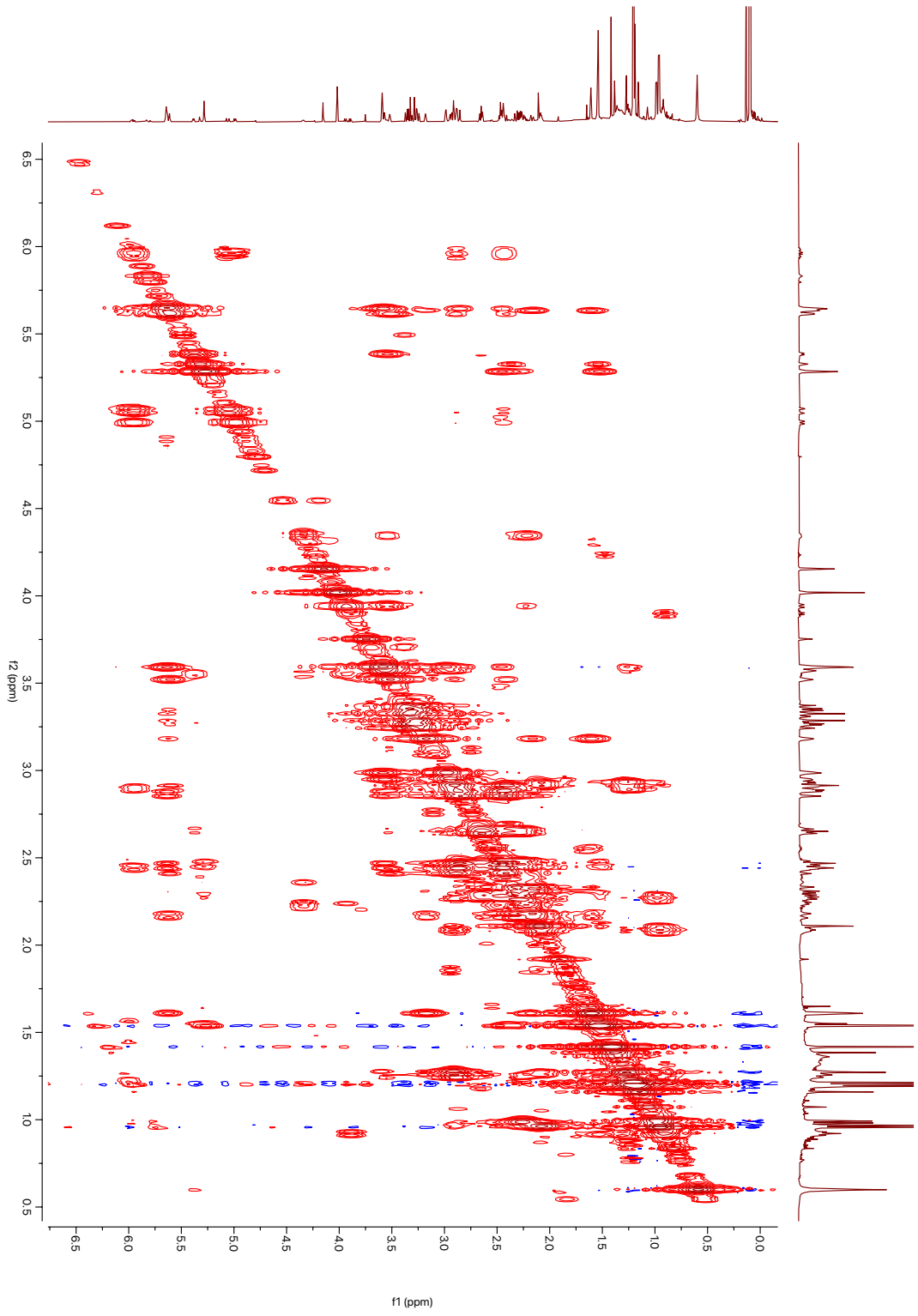

2.3.8a
(150 MHz, C6D6)
C6D6
f1 (ppm)
209.86
144.28
136.33
135.60
134.59
130.98
129.65
129.04
126.80
122.85
116.13
84.65
74.62
66.20
62.04
60.26
55.25
45.77
45.40
35.99
33.92
21.96
21.72
16.41
1.85

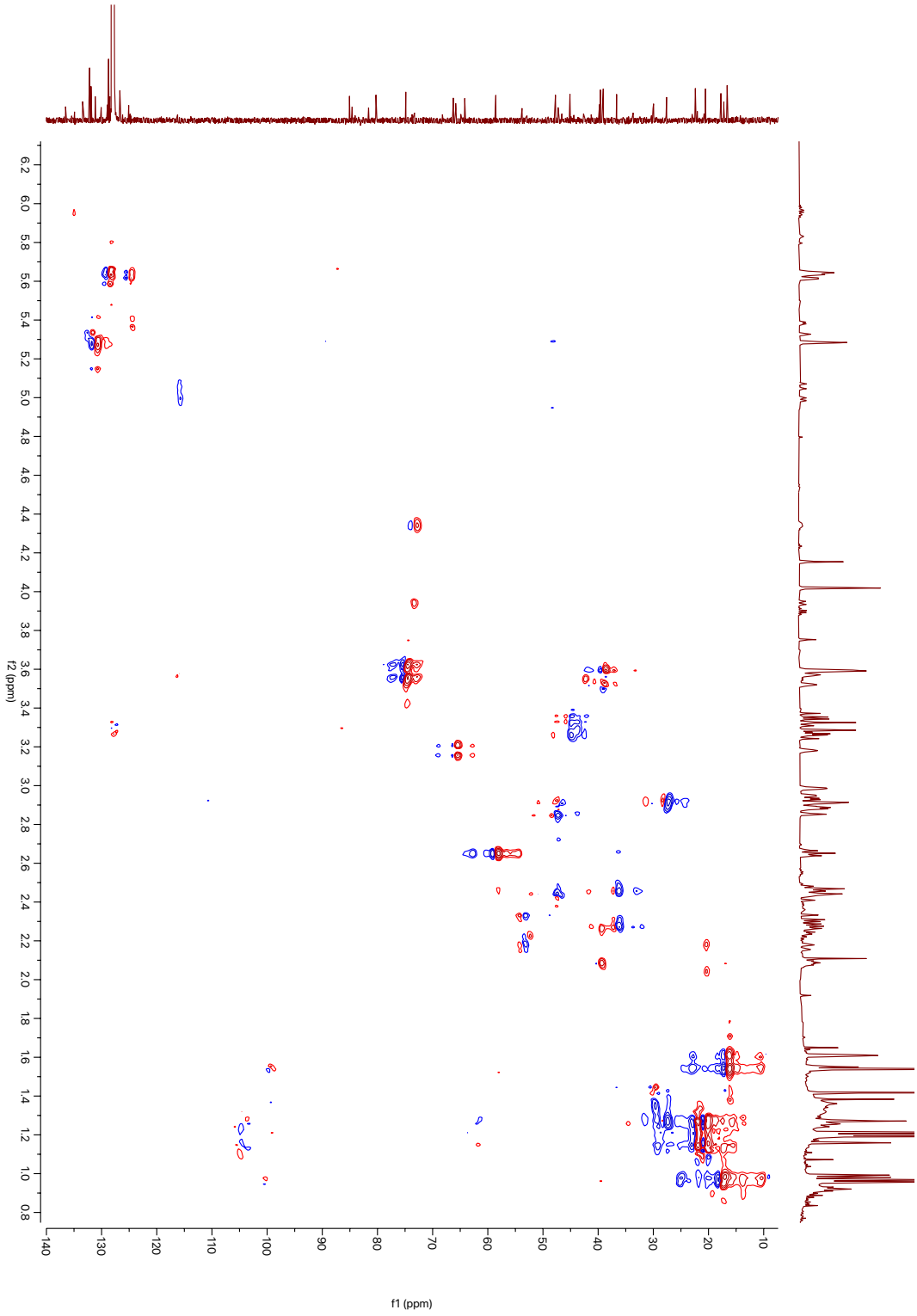

2.3.8b
OTMS
SPh
OH
Me
Me
Me
O
H
H
C6D5H
(600 MHz, C6D6)
f1 (ppm)

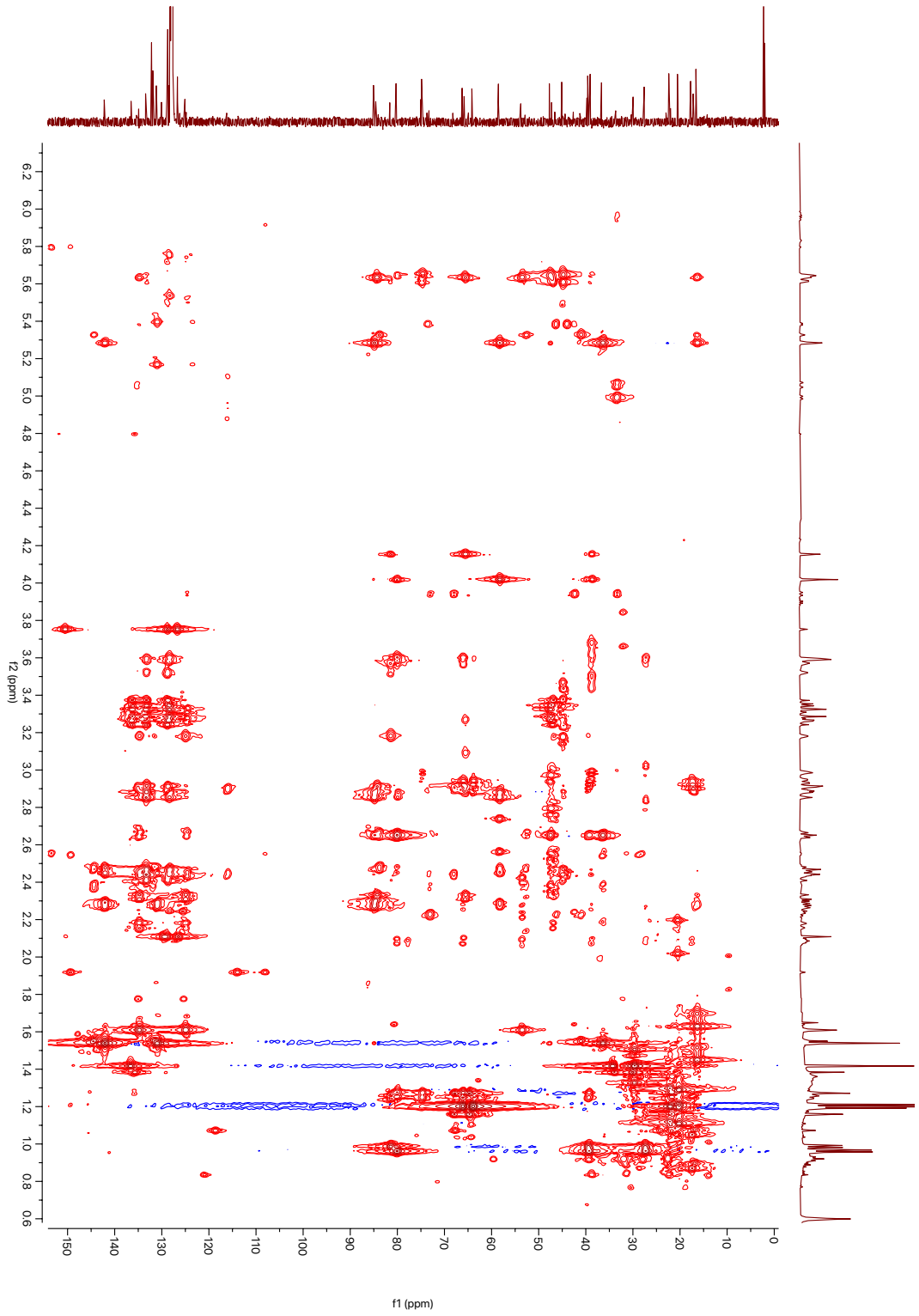

208.02
144.22
136.68
135.10
134.11
131.20
129.53
128.35
126.53
123.94
116.67
85.15
72.58
65.91
62.49
60.81
54.70
45.68
35.91
35.73
21.99
21.02
16.43
1.86
C6D6
(150 MHz, C6D6)
2.3.8b
OTMS
SPh
OH
Me
Me
Me
f1 (ppm)

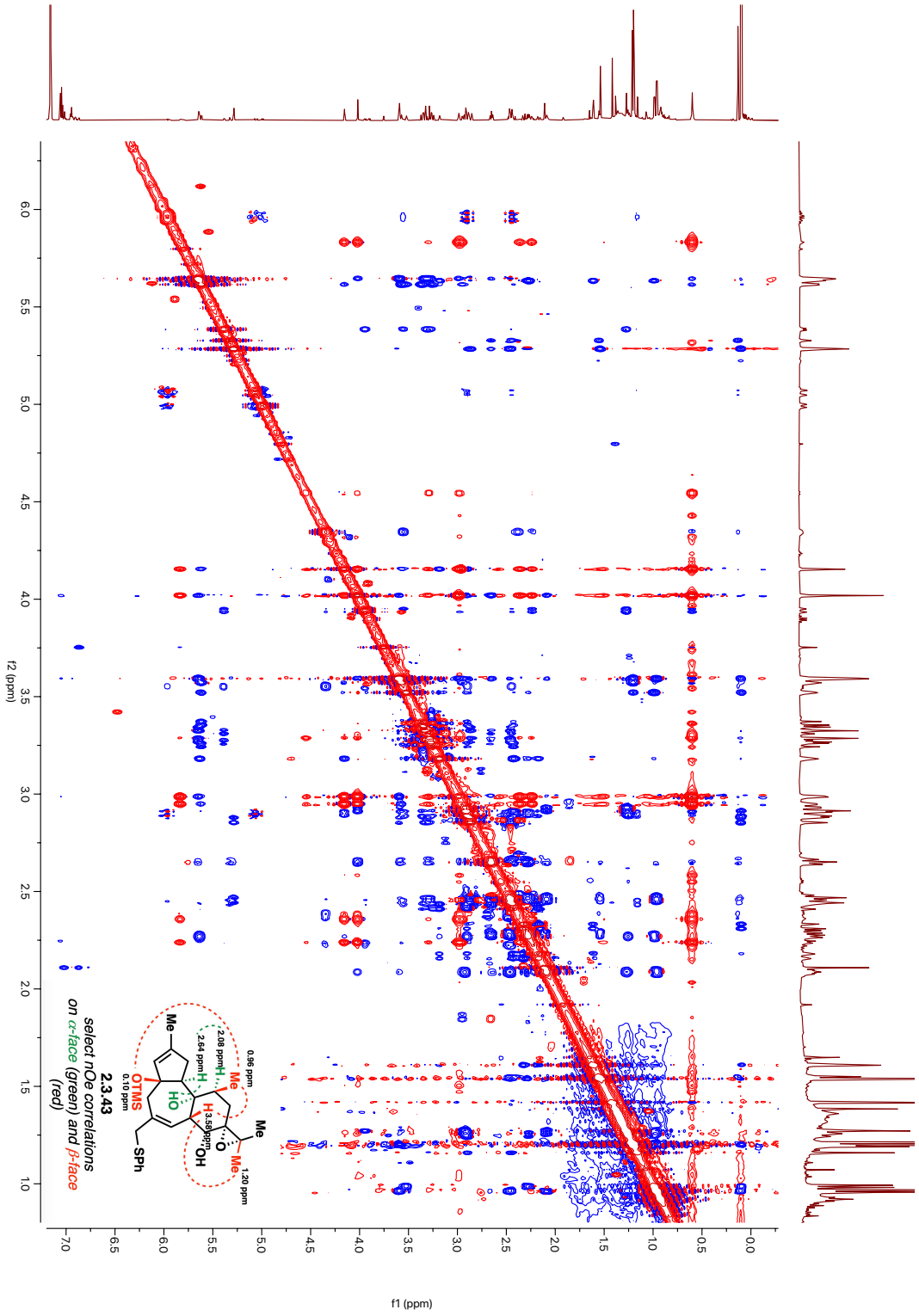

C6D5H
2.13
2.19
1.24
1.00
1.00
1.01
1.98
1.06
1.33
0.90
1.27
0.96
1.19
0.82
0.59
1.27
1.12
3.13
1.12
3.27
2.85
3.16
9.37
7.41
7.41
7.40
7.40
7.06
7.05
6.95
6.95
6.94
6.94
6.93
5.64
5.28
4.02
3.59
3.34
3.32
3.29
3.27
2.98
2.91
2.89
2.88
2.85
2.66
2.65
2.64
2.46
2.45
2.33
2.31
2.30
2.29
2.28
2.26
2.10
2.09
2.09
2.08
2.08
1.54
1.25
1.24
1.21
1.20
0.97
0.96
0.10
2.3.43
2.3.43b
X = H, Y = OH
2.3.46b
f1 (ppm)

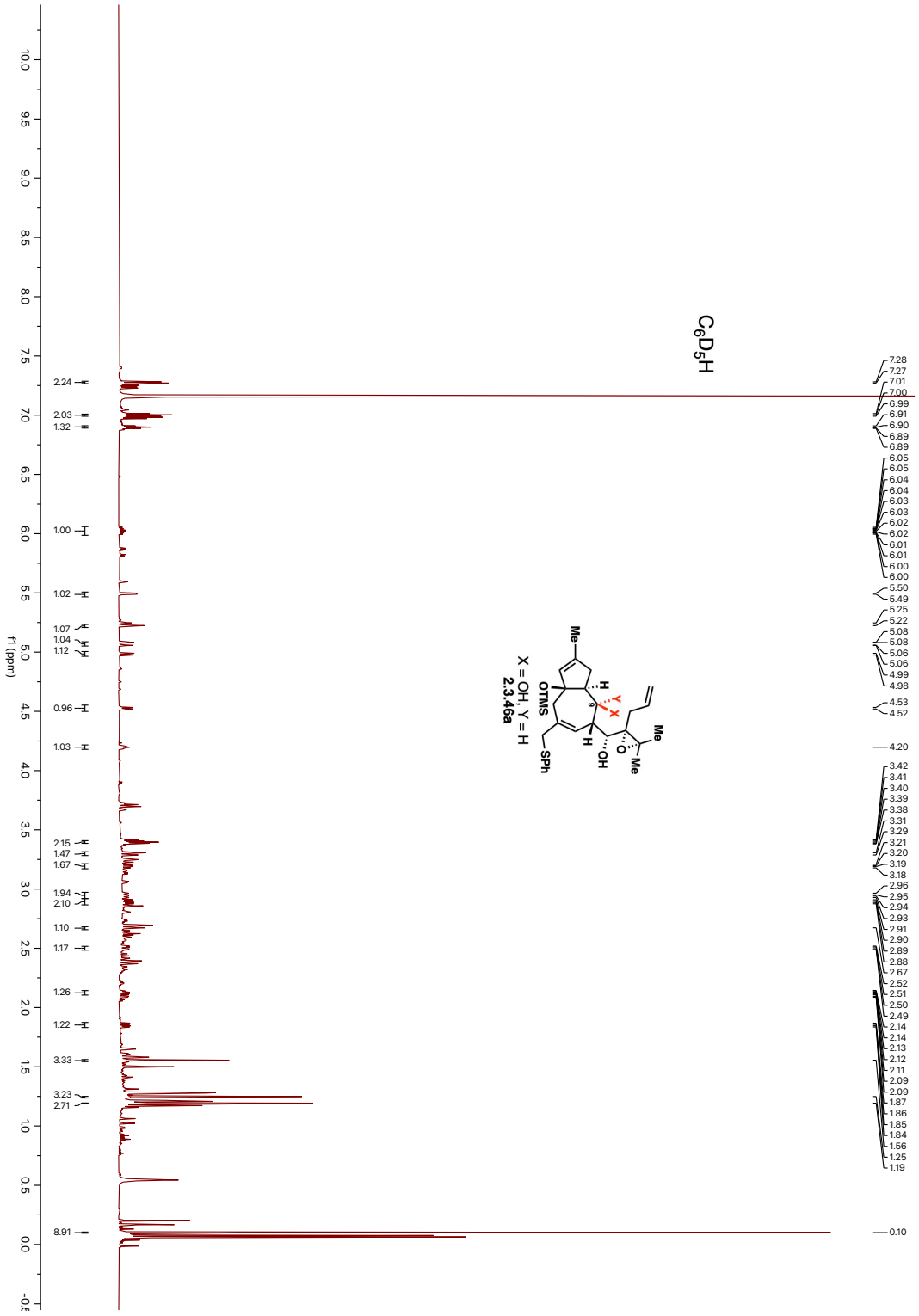

f1 (ppm)
20
210
200
190
180
170
160
150
140
130
120
110
100
90
80
70
60
50
40
30
20
10
0
-10
C6D6
142.21
136.53
133.44
132.18
131.91
131.16
130.08
128.80
128.74
126.68
125.09
85.07
84.59
81.61
80.27
75.03
74.87
66.25
65.82
64.18
58.55
53.81
47.74
47.26
45.12
39.75
39.59
39.17
39.07
36.66
29.96
27.68
27.60
22.39
22.33
20.58
20.55
17.76
17.22
16.62
2.25
2.14
2.04
2.3.43
2.3.43b
X = H, Y = OH
2.3.46b

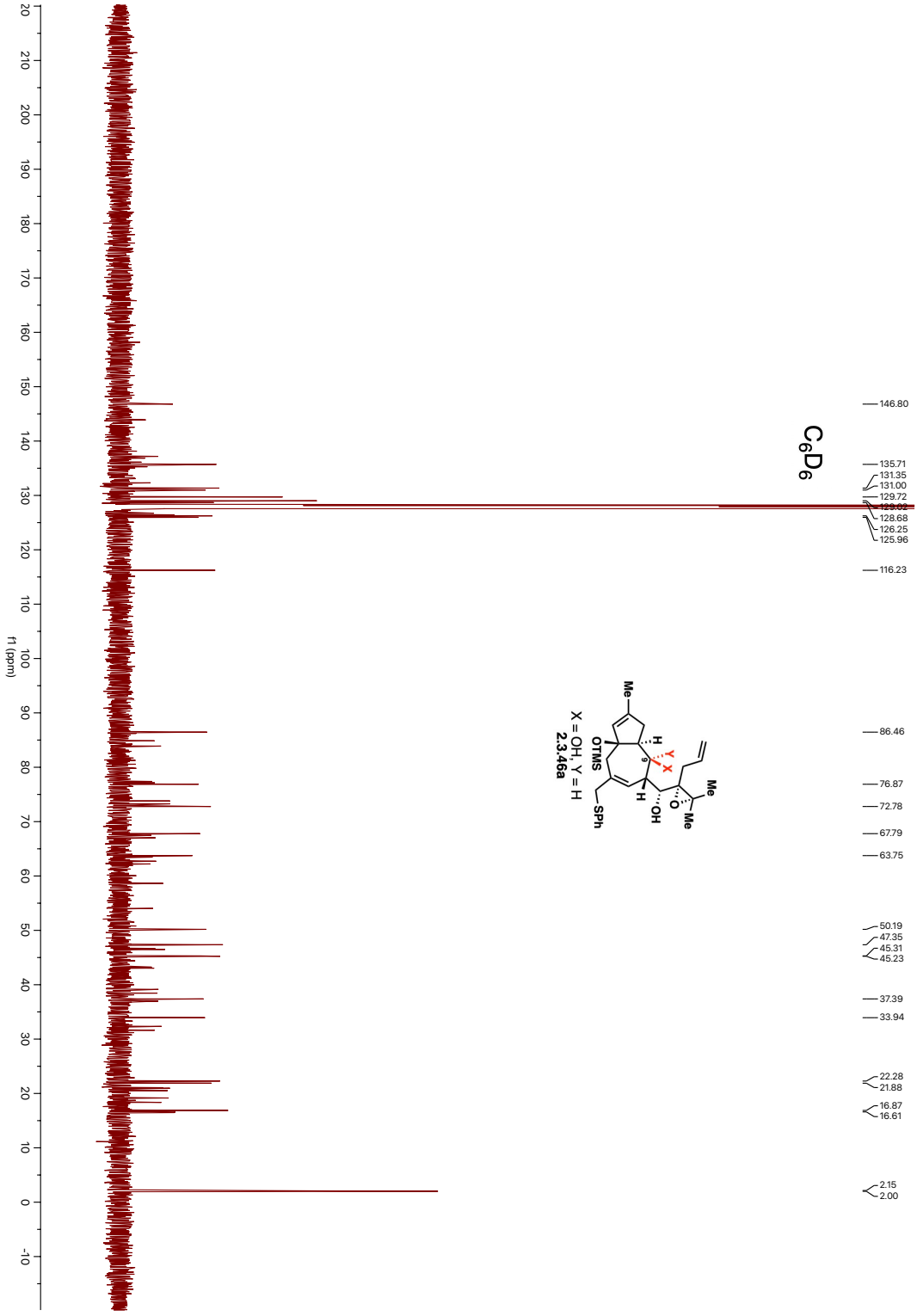

f2 (ppm)
f1 (ppm)

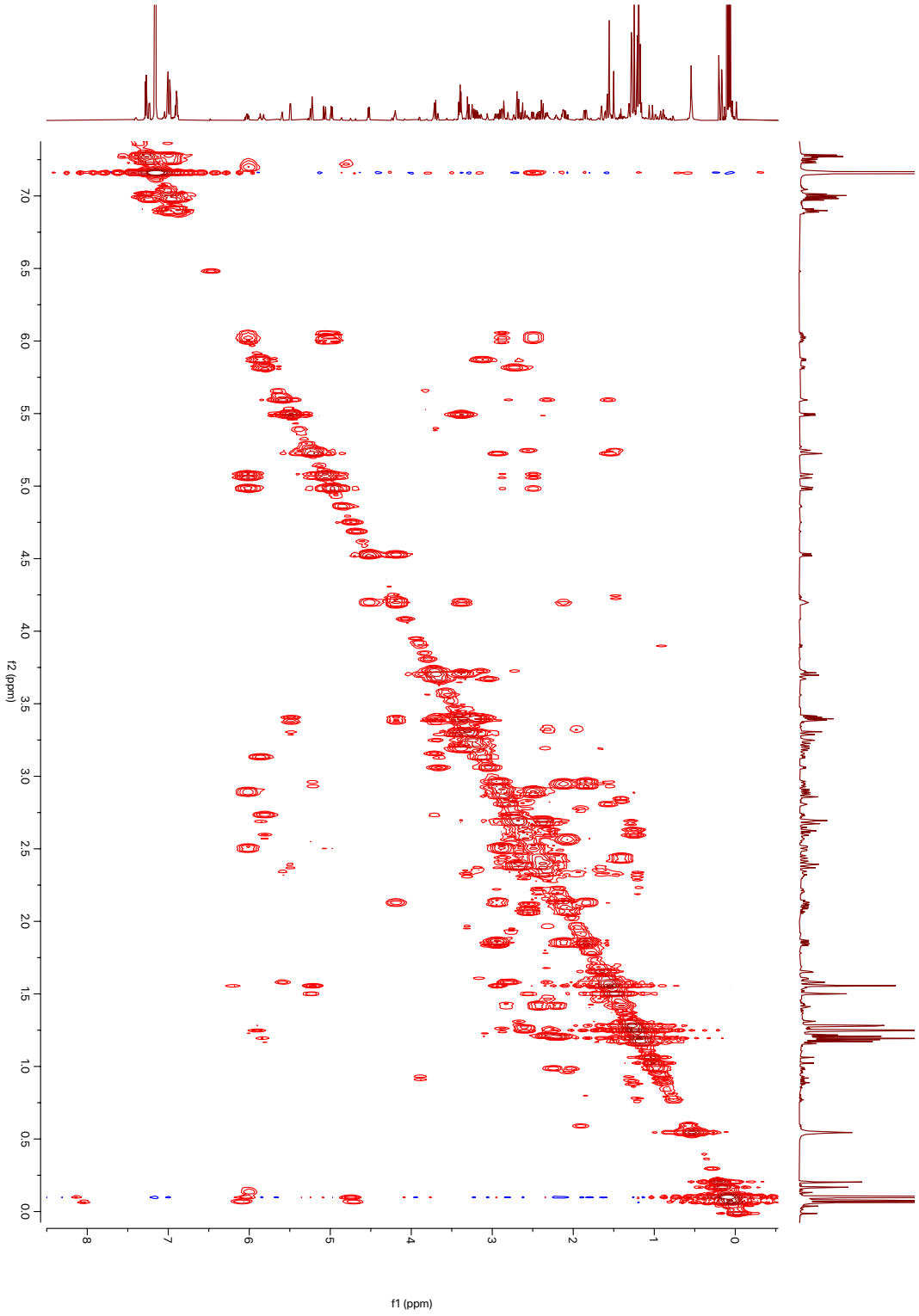

f2 (ppm)
f1 (ppm)

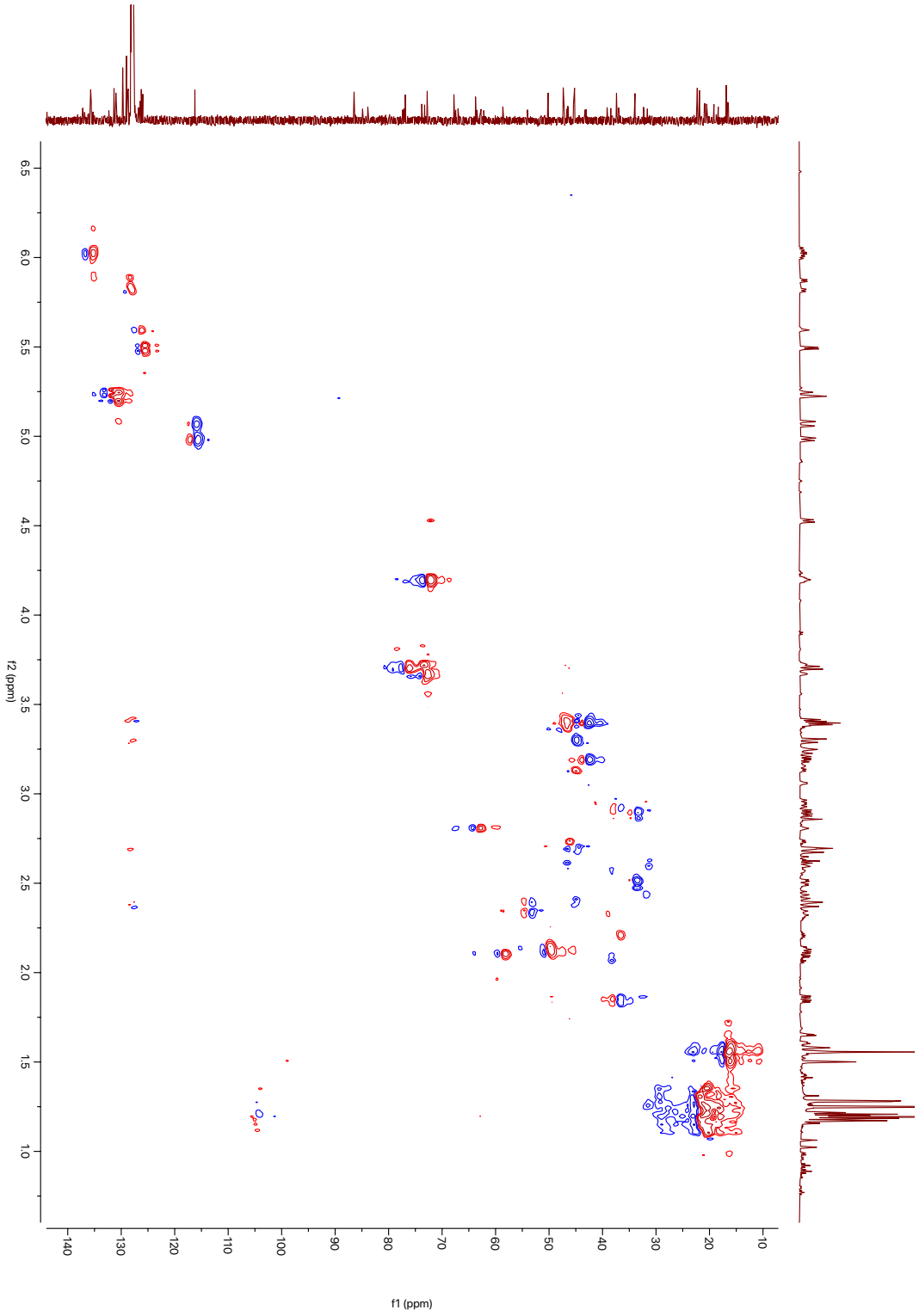

f2 (ppm)
f1 (ppm)

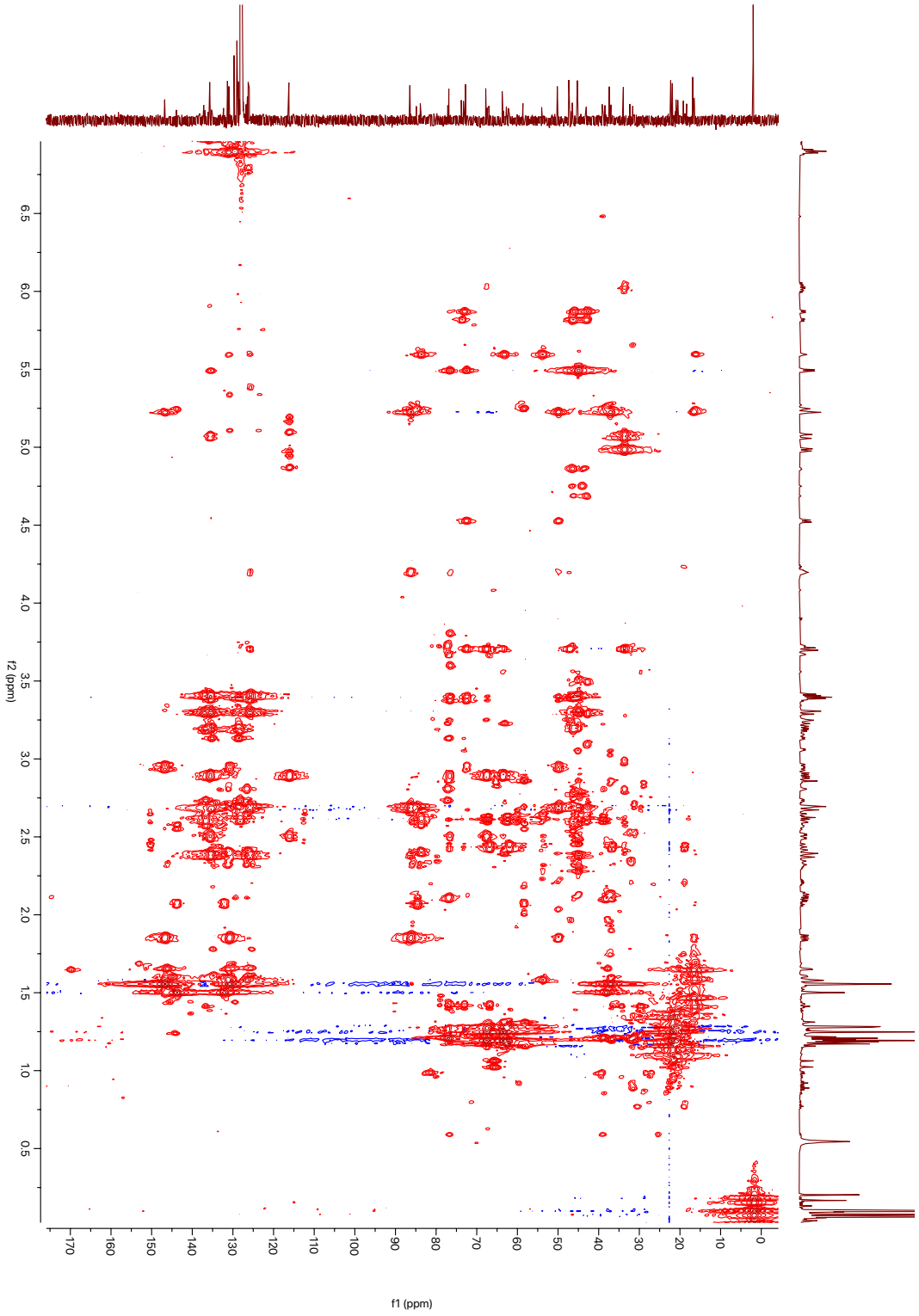

f2 (ppm)
f1 (ppm)
2.3.43
select nOe correlations
on α-face (green) and β-face
(red)
Me
OTMS
0.10 ppm
SPh
HO
H
2.64 ppm
H
2.08 ppm
Me
0.96 ppm
H
3.59 ppm
OH
O
Me
Me
1.20 ppm

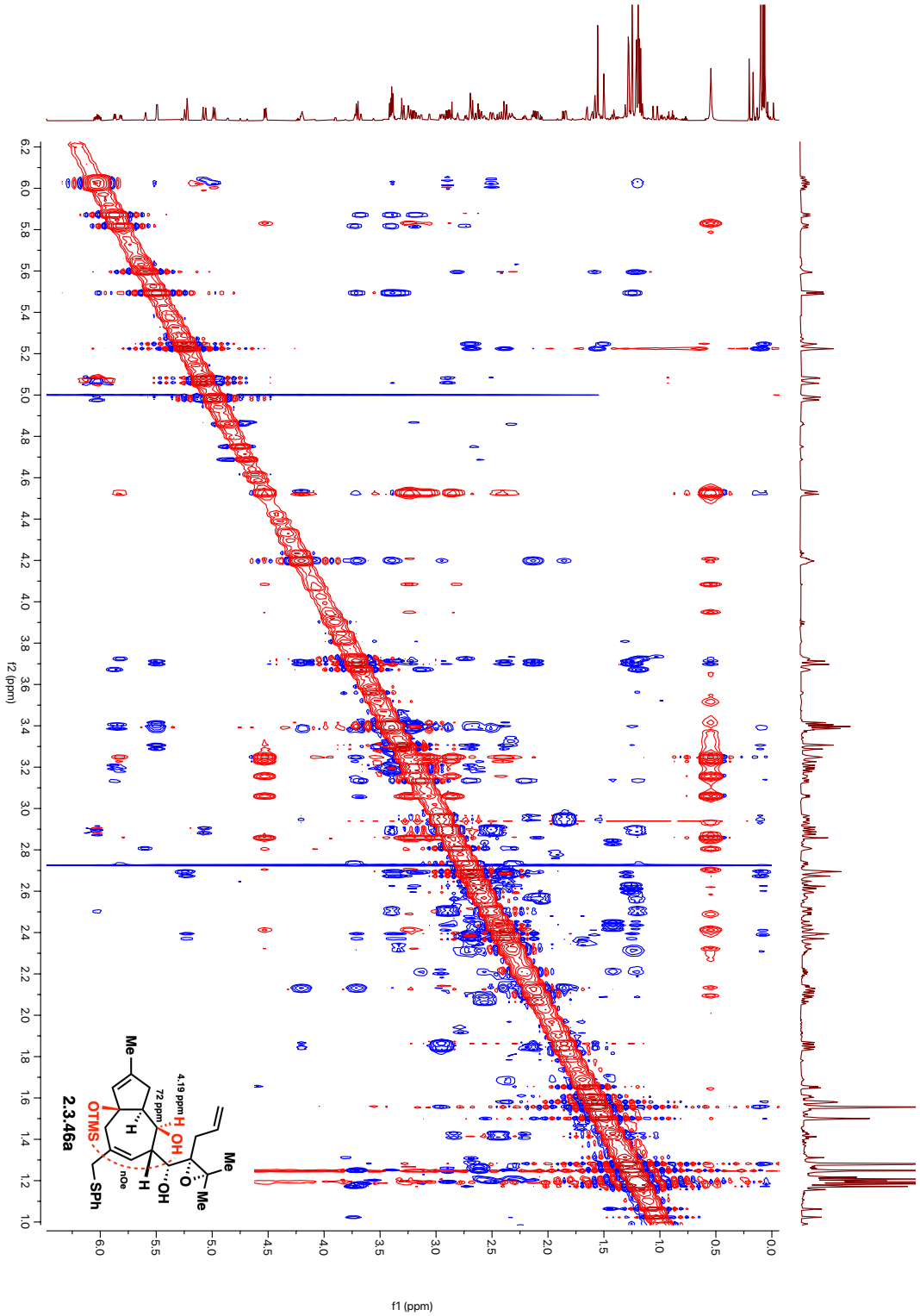

C6D5H
X = OH, Y = H
2.3.46a
OTMS
SPh
OH
Me
Me
Me
f1 (ppm)

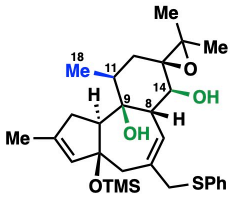

f1 (ppm)
C6D6
146.80
135.71
131.35
131.00
129.72
128.68
126.25
125.96
116.23
86.46
76.87
72.78
67.79
63.75
50.19
47.35
45.31
45.23
37.39
33.94
22.28
21.88
16.87
16.61
2.15
2.00
X = OH, Y = H
2.3.46a
Me
OTMS
SPh
OH
Me
Me


f2 (ppm)
f1 (ppm)


f2 (ppm)
6.5
6.0
5.5
5.0
4.5
4.0
3.5
3.0
2.5
2.0
1.5
1.0
140
130
120
110
100
90
80
70
60
50
40
30
20
10
f1 (ppm)

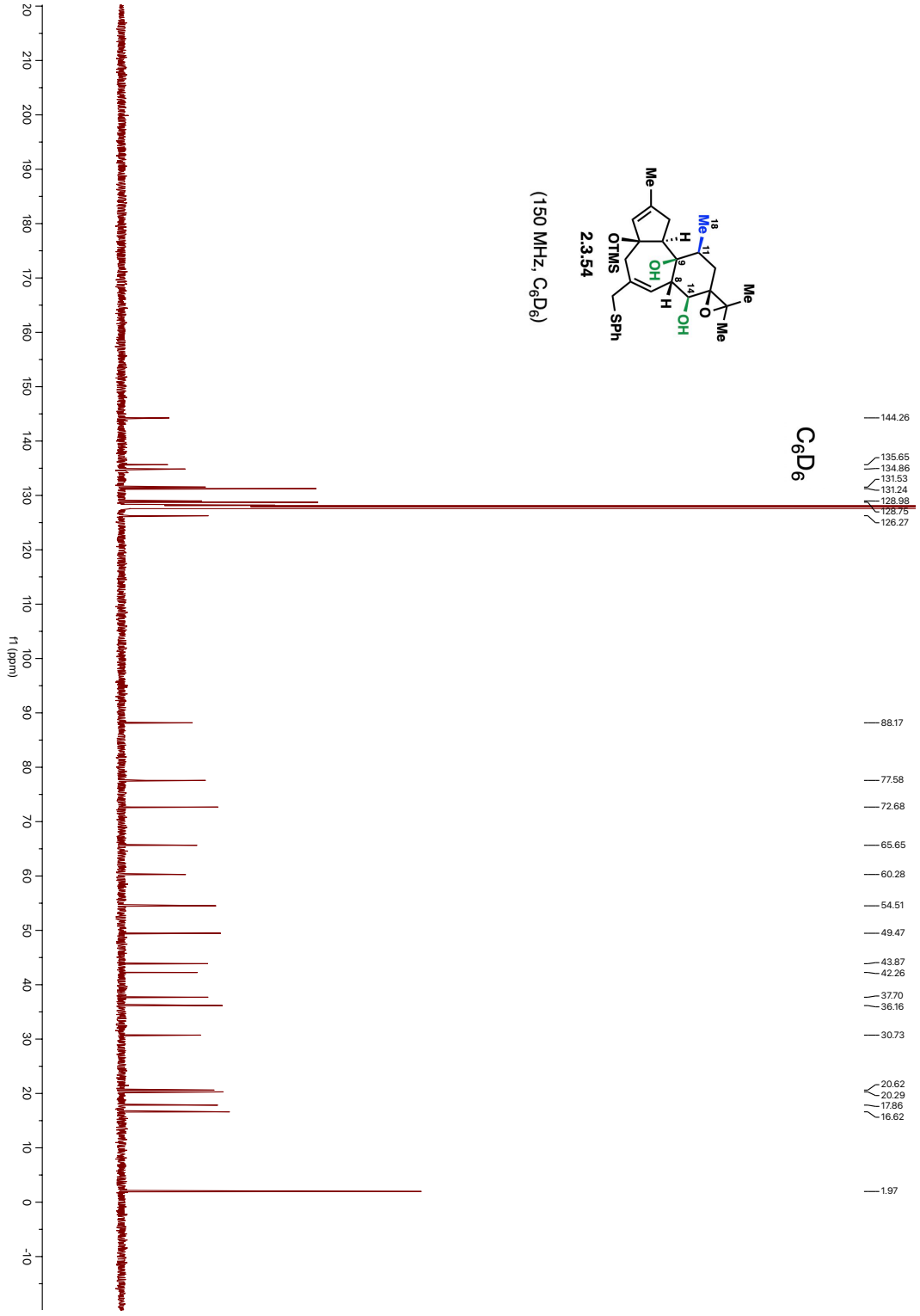

f2 (ppm)
f1 (ppm)

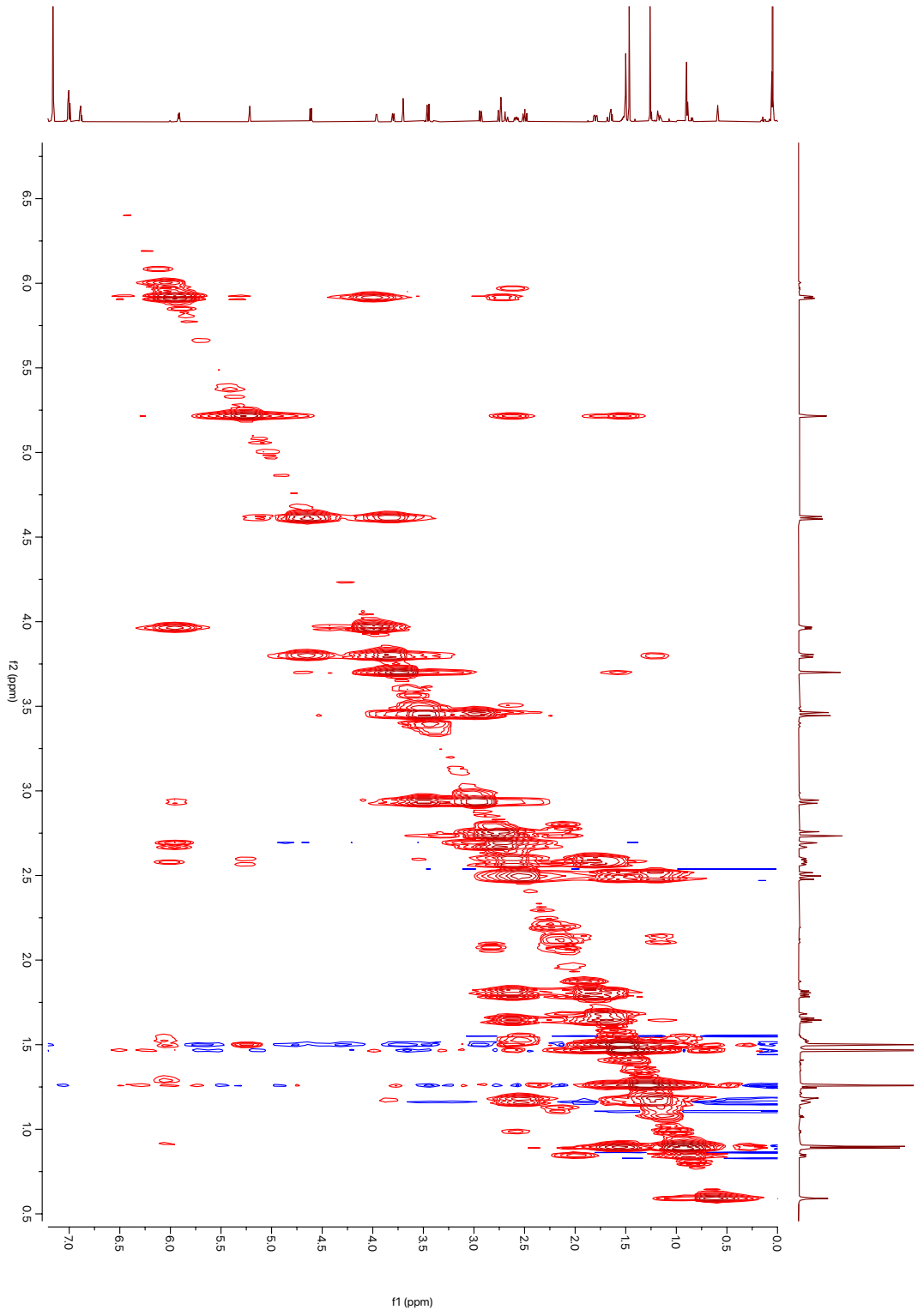

f2 (ppm)
f1 (ppm)
2.3.46a
Me
H
OTMS
SPh
nOe
H
OH
O
Me
4.19 ppm
72 ppm
H
OH
Me

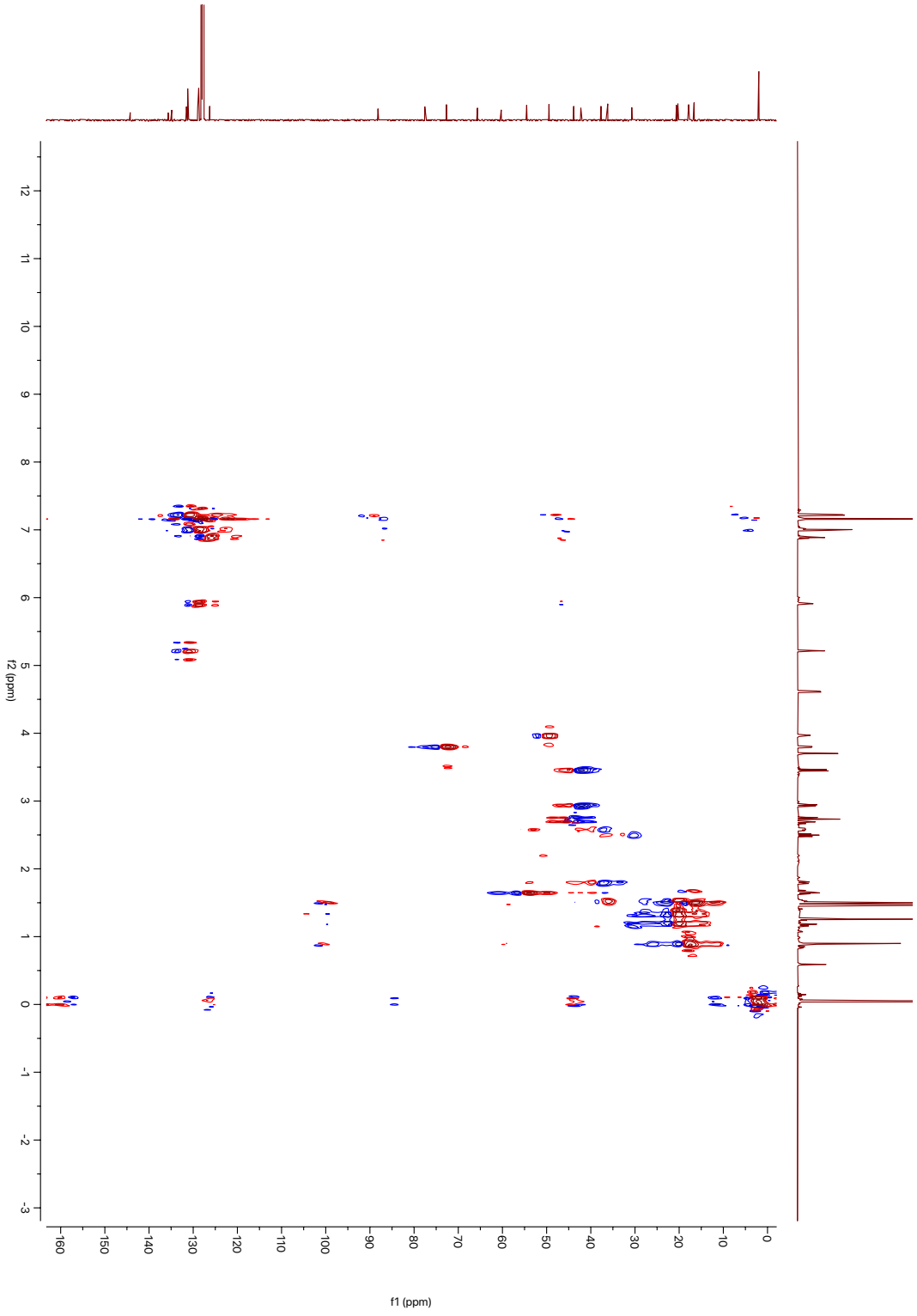


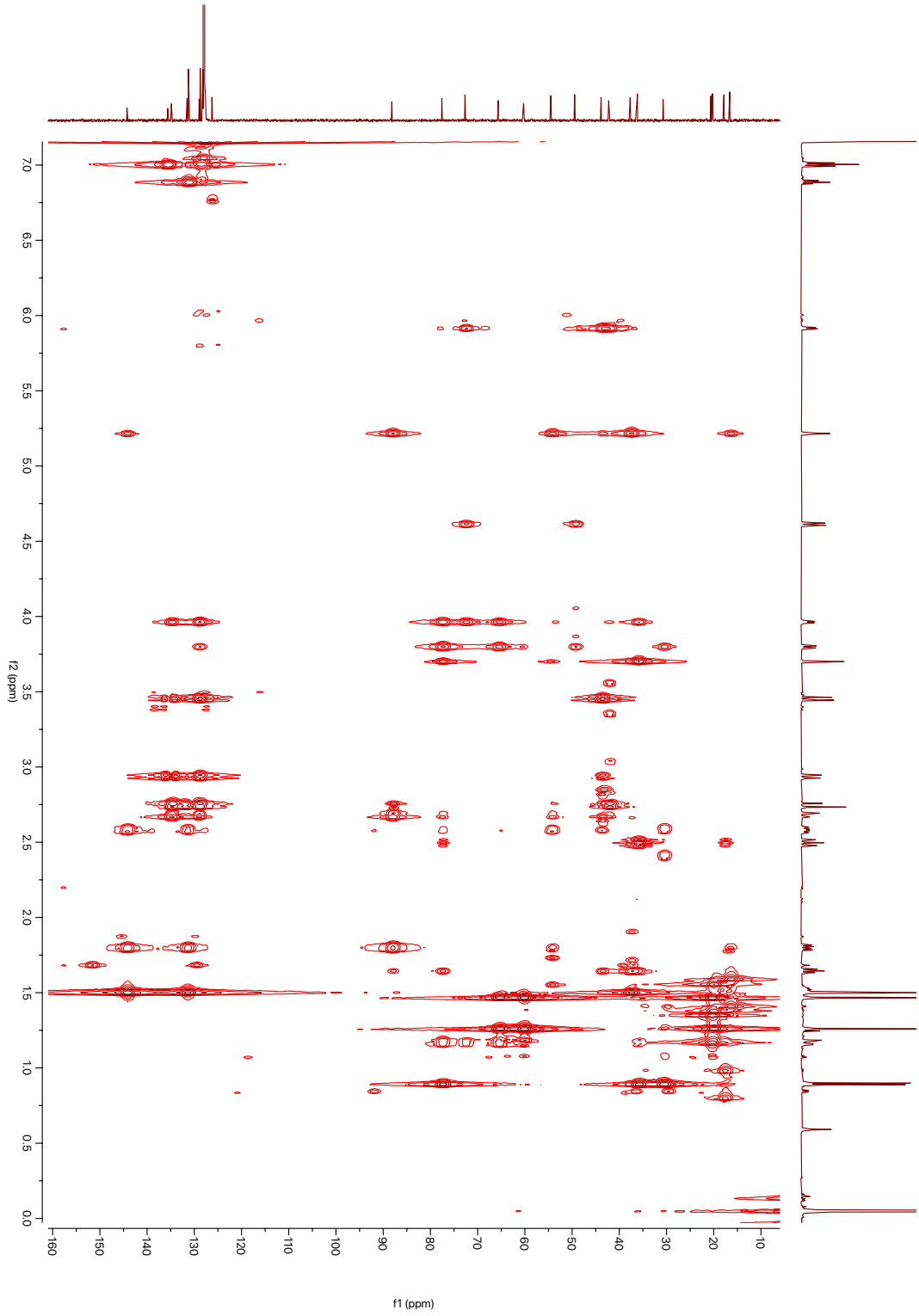
2.3.54

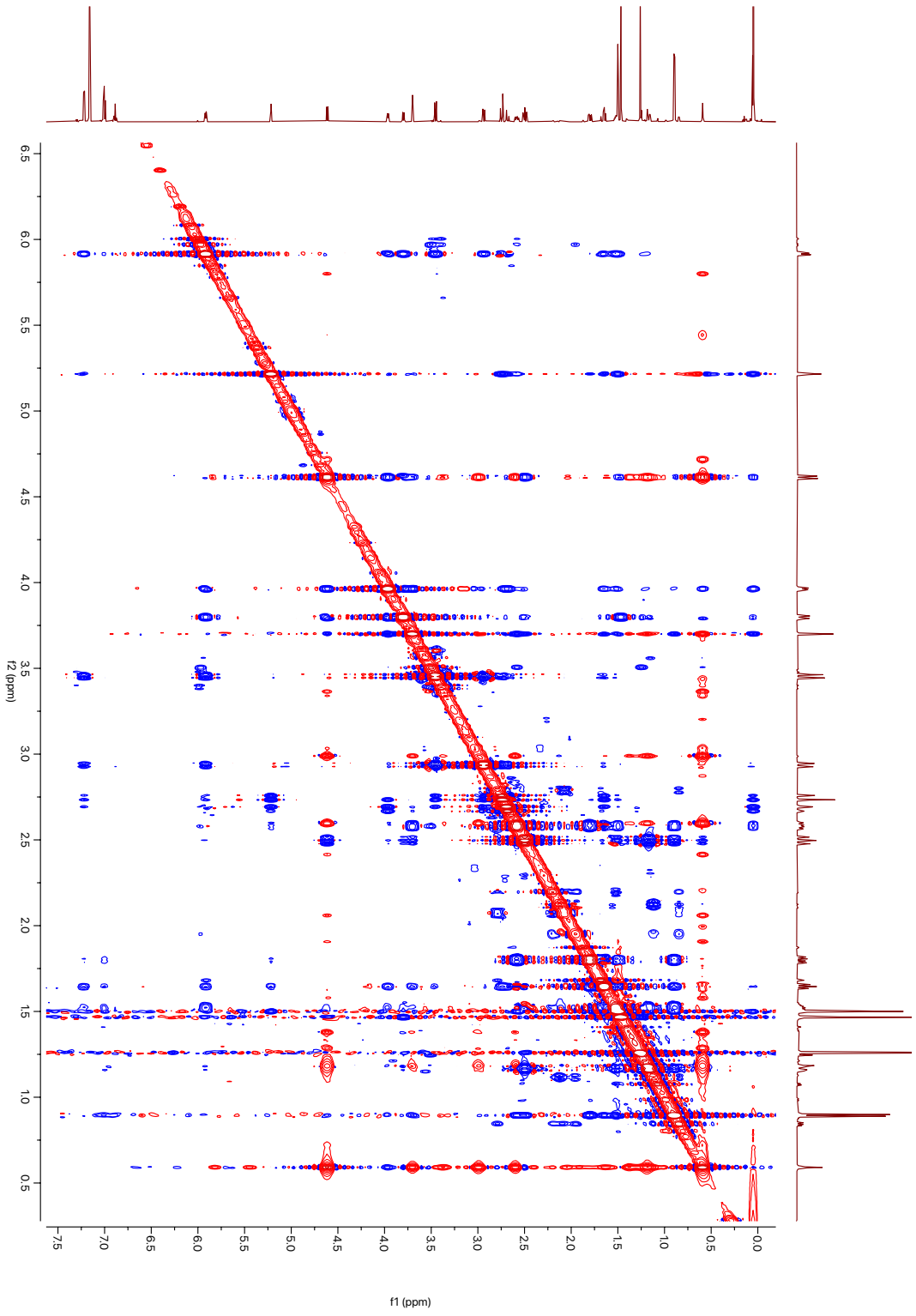
(700 MHz, C_6D_6)

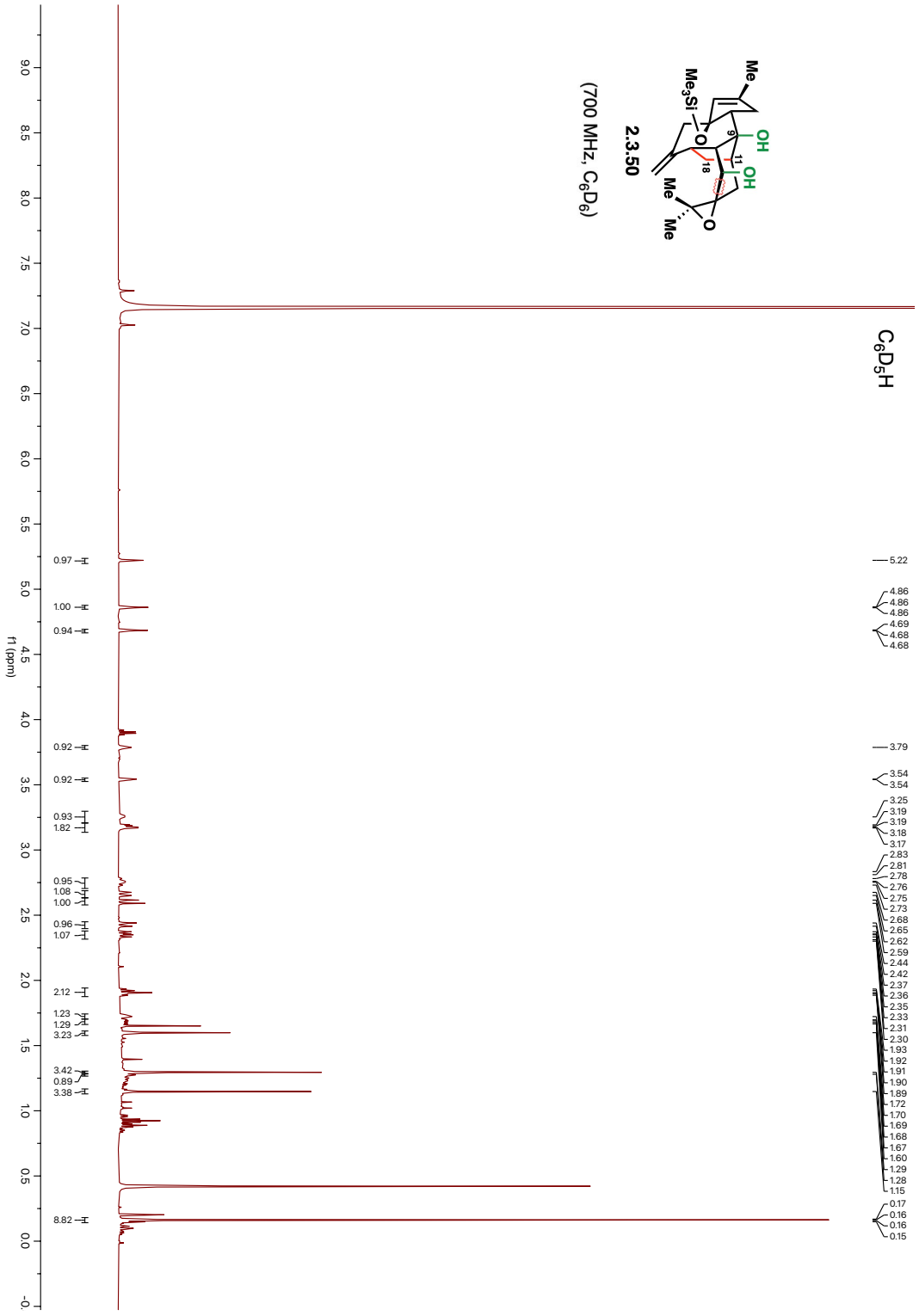

2.3.54
(150 MHz, C6D6)
C6D6
144.26
135.65
134.86
131.53
131.24
128.98
128.75
126.27
88.17
77.58
72.68
65.65
60.28
54.51
49.47
43.87
42.26
37.70
36.16
30.73
20.62
20.29
17.86
16.62
1.97
f1 (ppm)

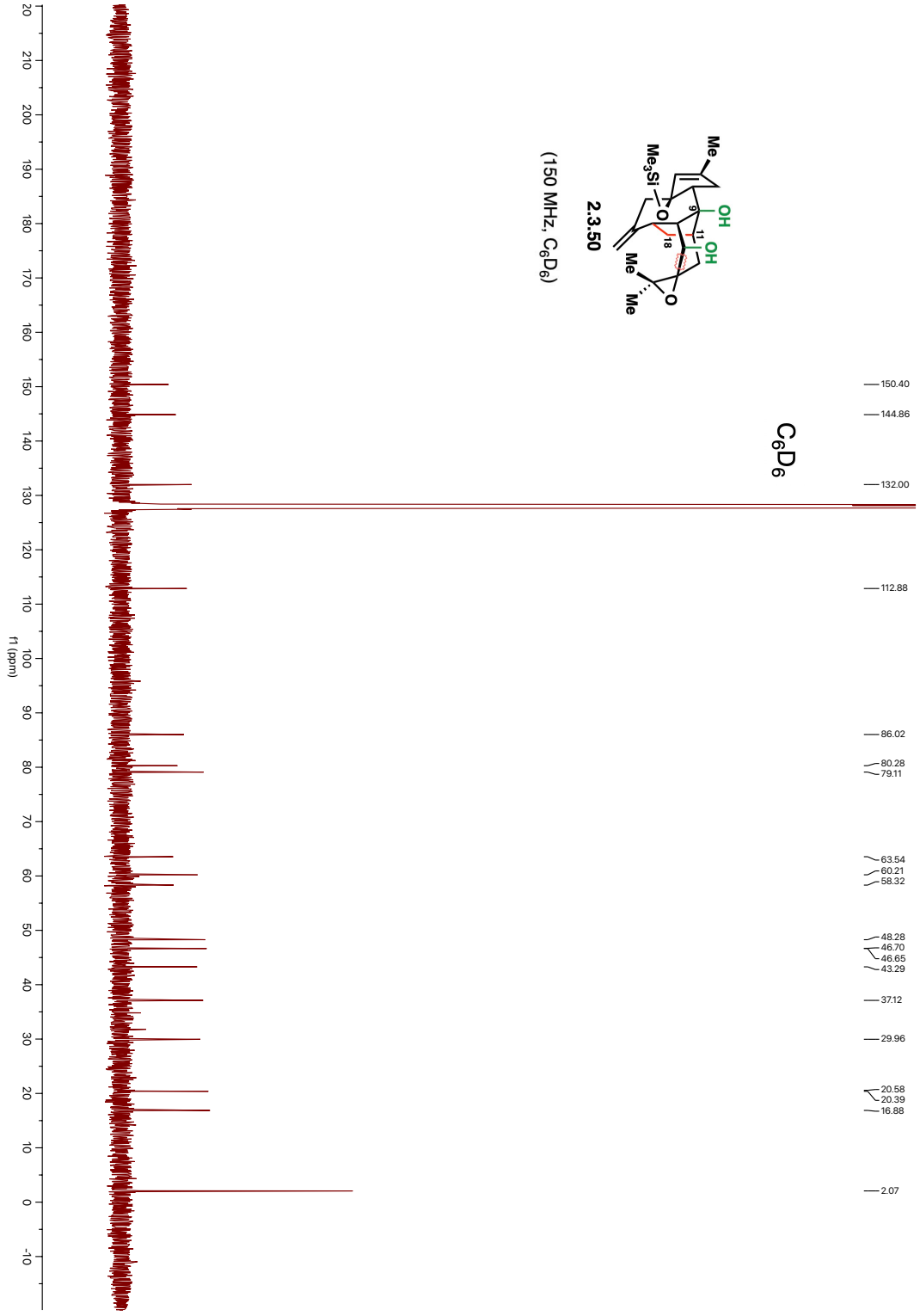

f2 (ppm)
f1 (ppm)

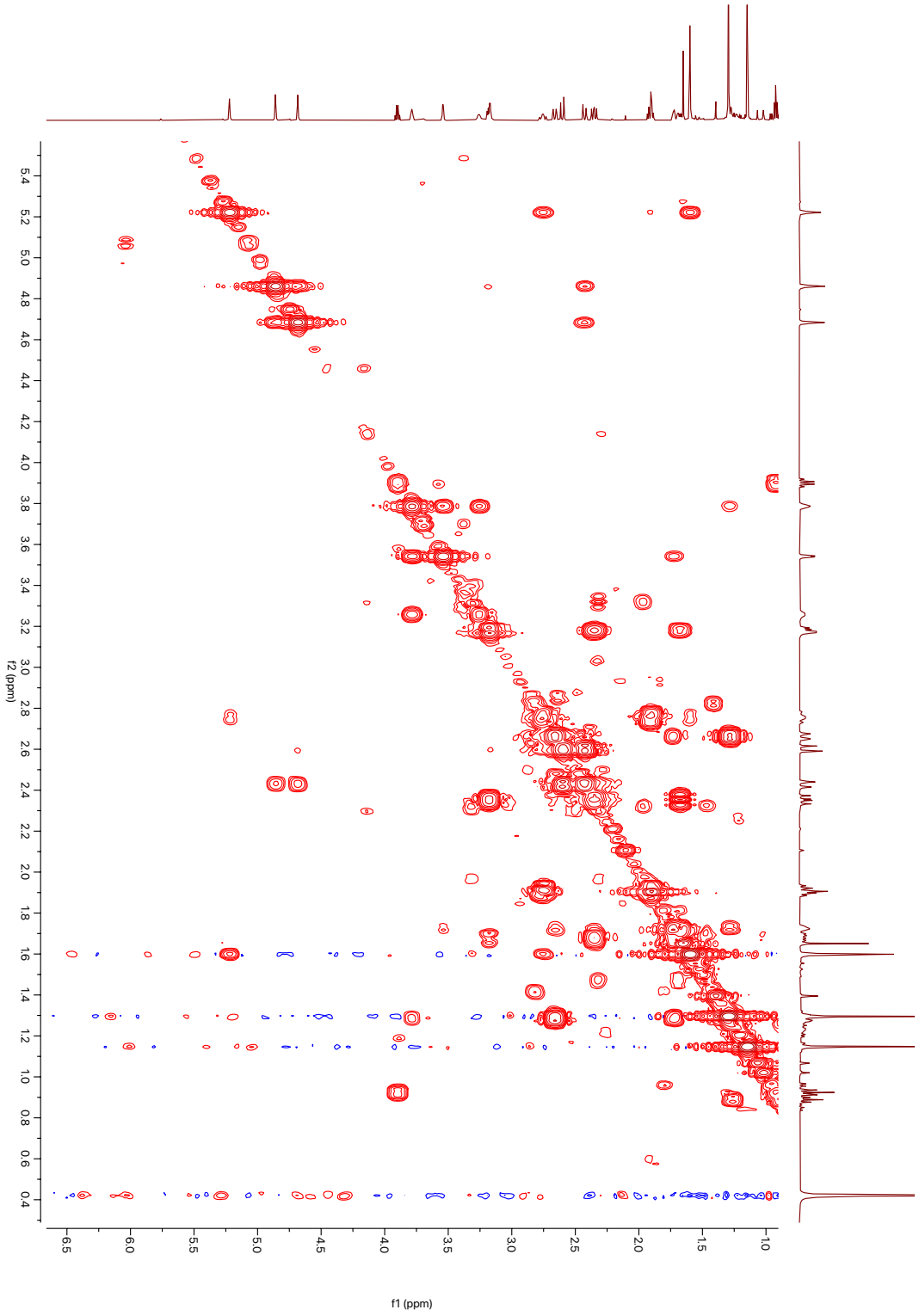

f2 (ppm)
f1 (ppm)

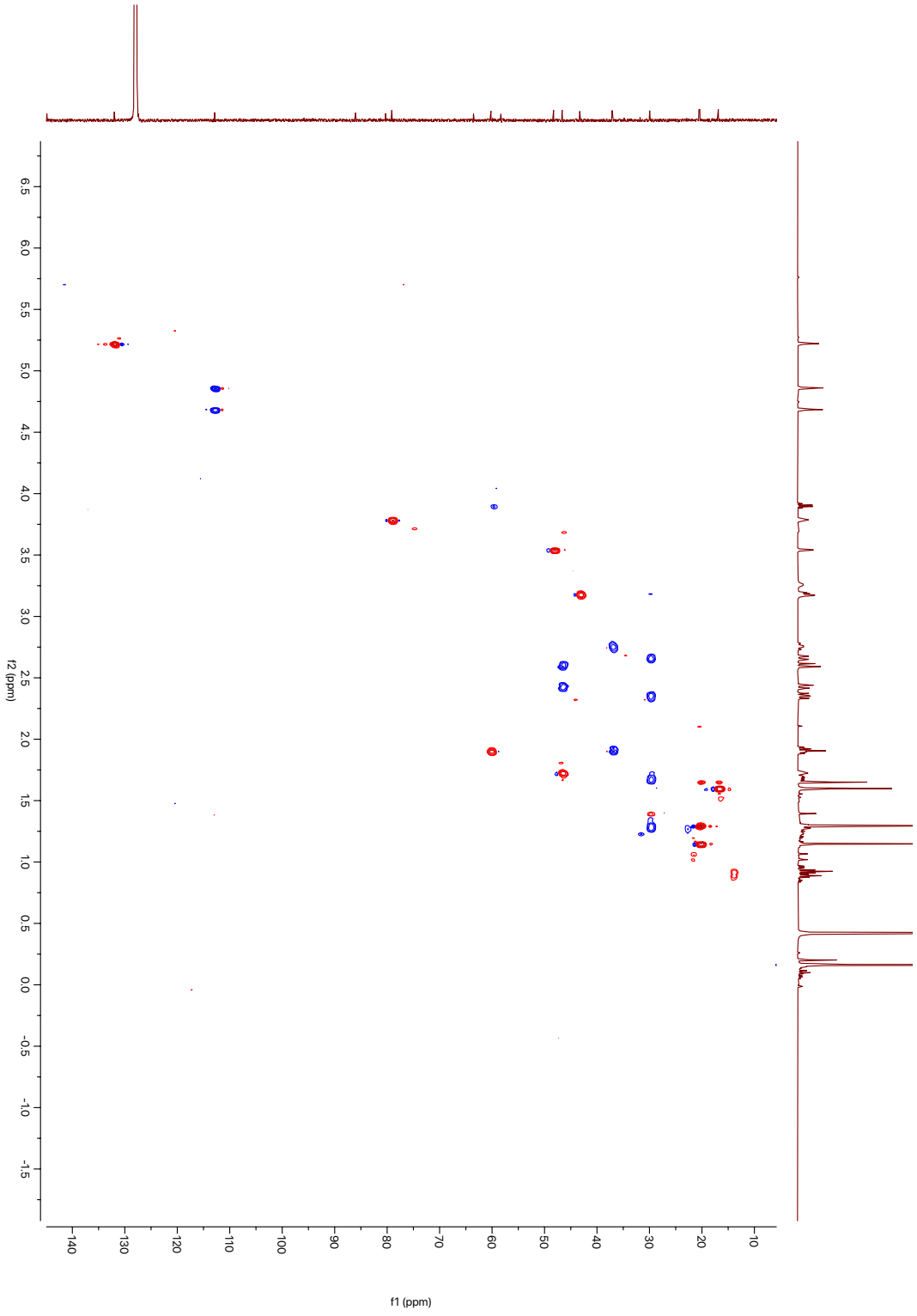

f2 (ppm)
f1 (ppm)

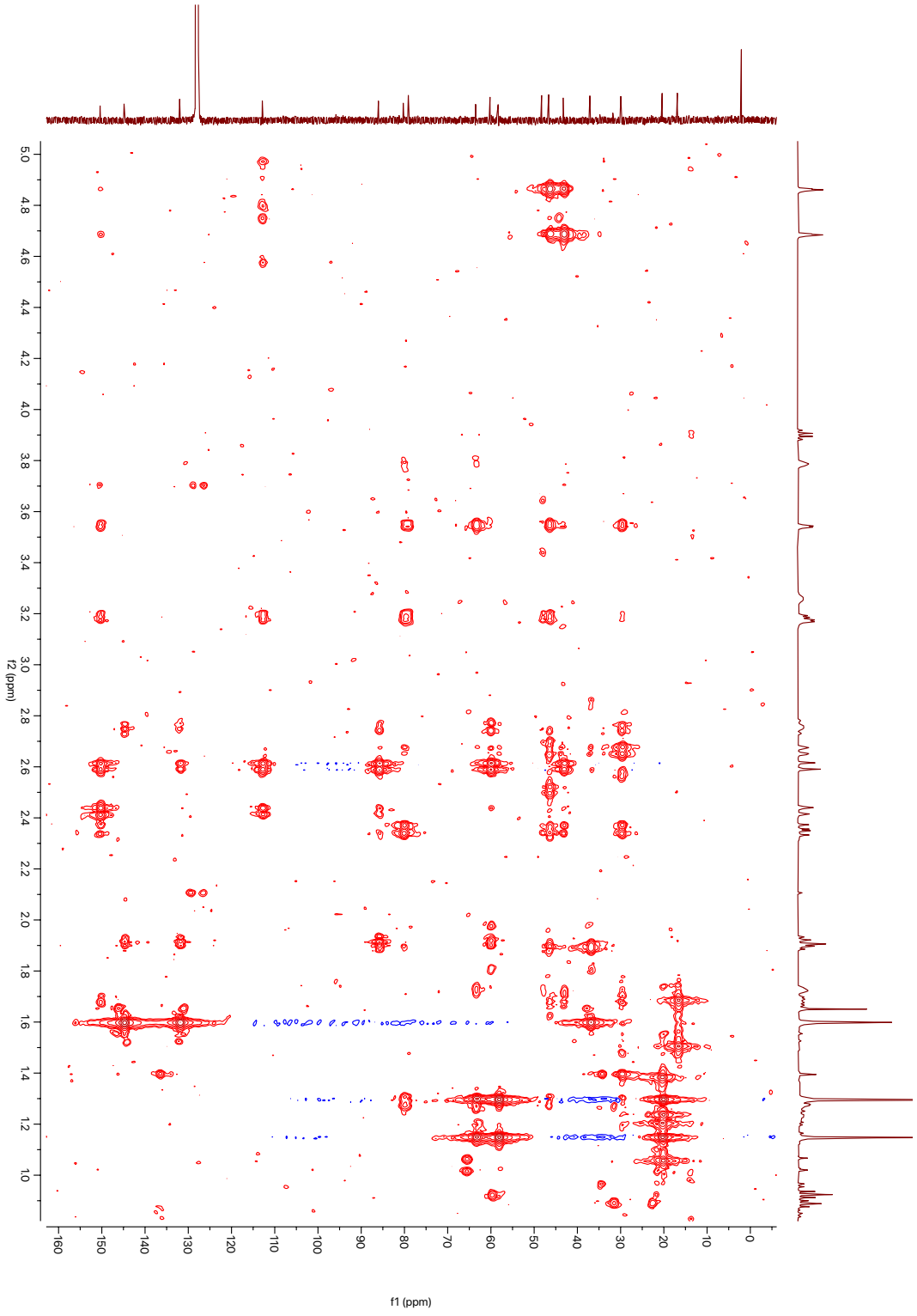

f2 (ppm)
f1 (ppm)

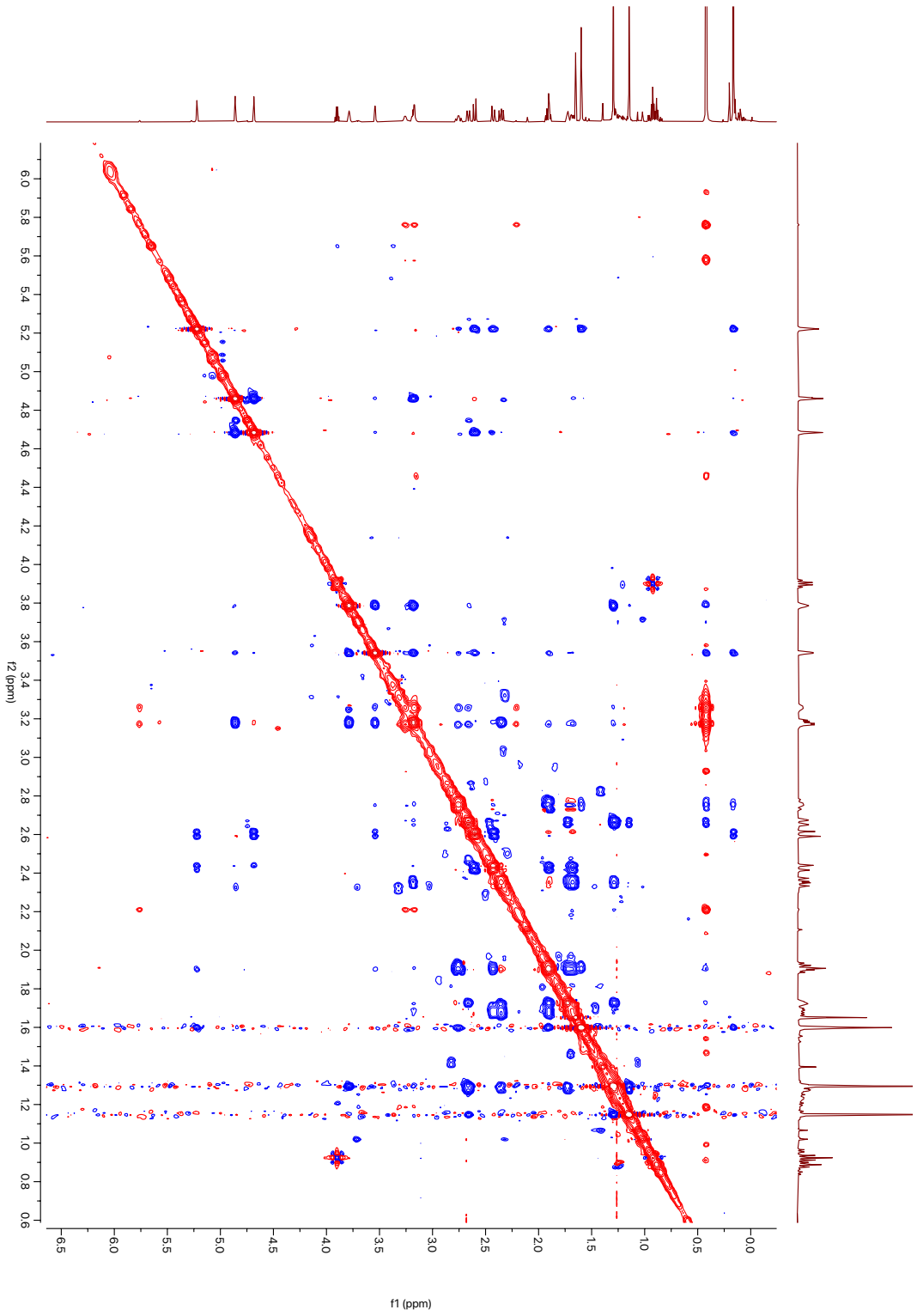

2.3.50
(700 MHz, C_6D_6)
C_6D_5H
f1 (ppm)

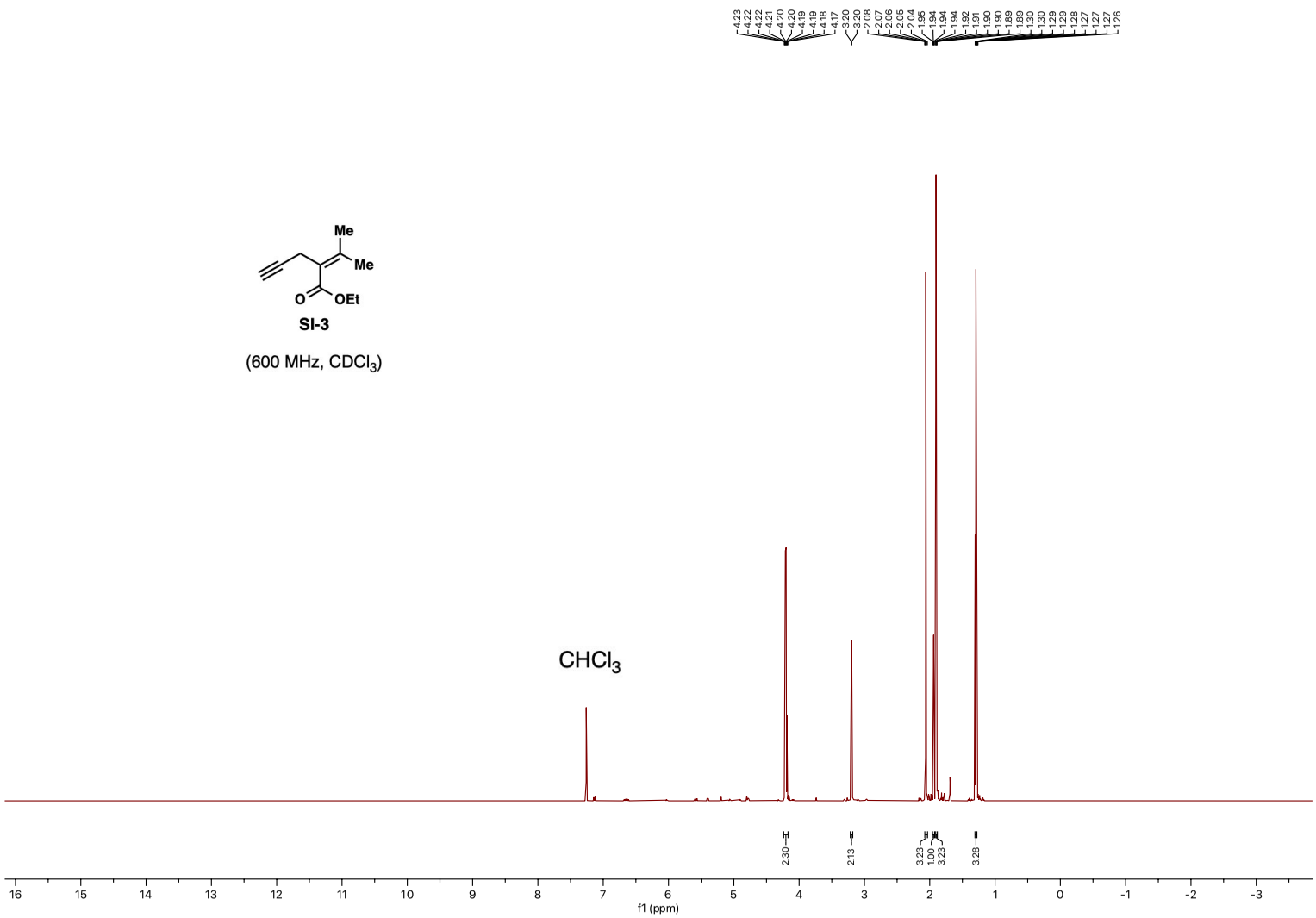

2.3.50
(150 MHz, C6D6)
C6D6
Me
Me3Si
O
OH
OH
Me
Me
O
9
11
18
150.40
144.86
132.00
112.88
86.02
80.28
79.11
63.54
60.21
58.32
48.28
46.70
46.65
43.29
37.12
29.96
20.58
20.39
16.88
2.07
f1 (ppm)

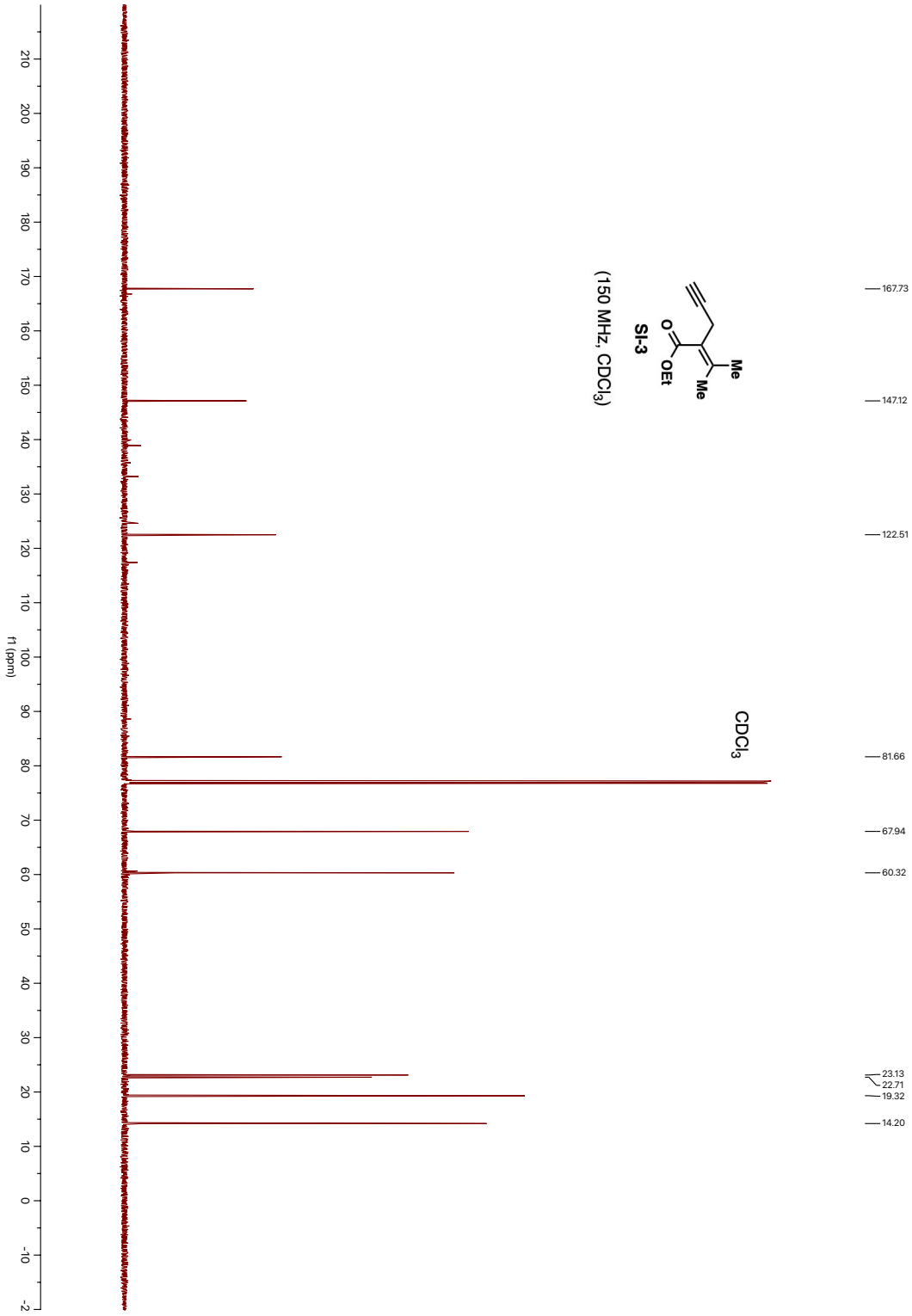

f2 (ppm)
f1 (ppm)

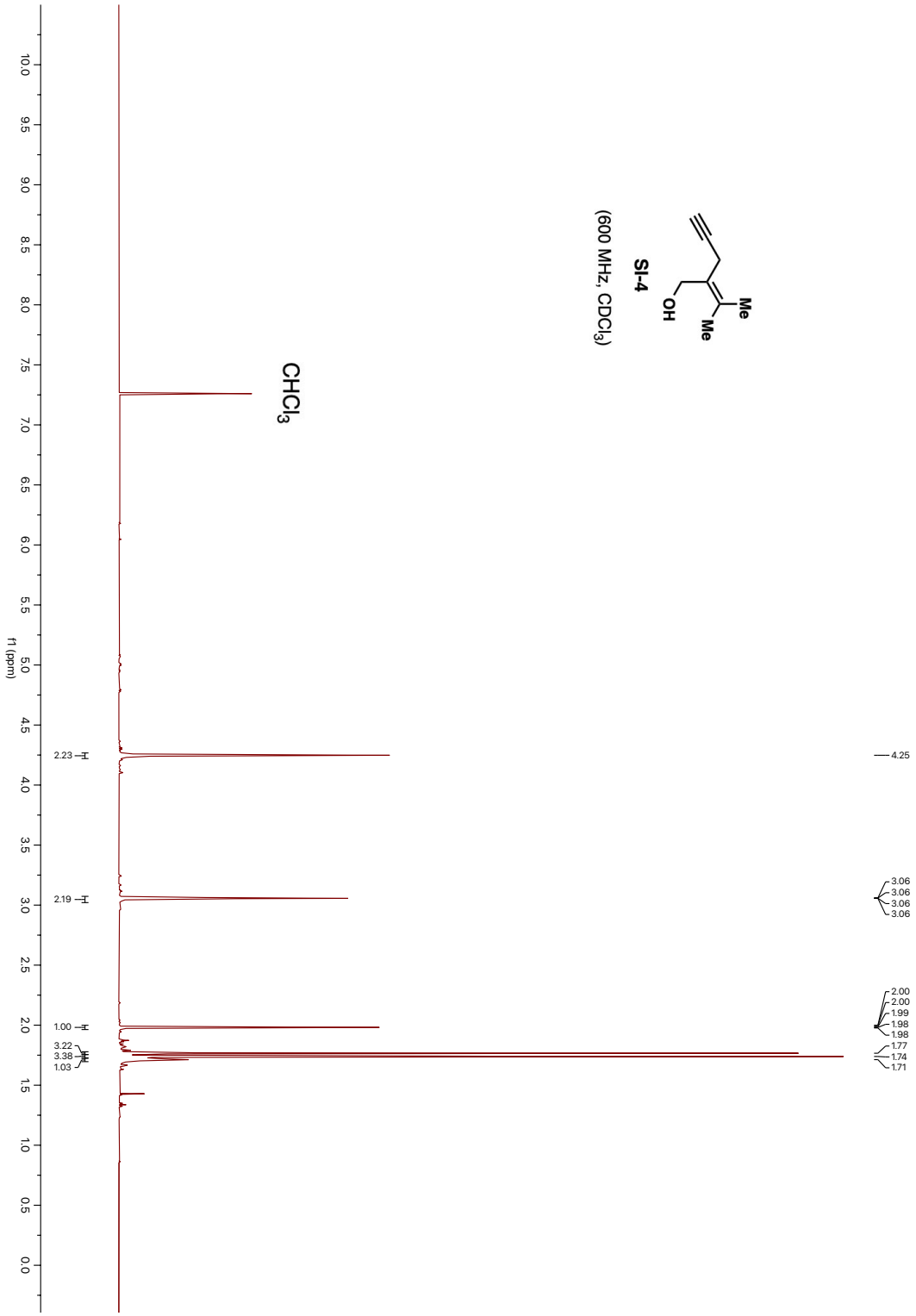

f2 (ppm)
f1 (ppm)

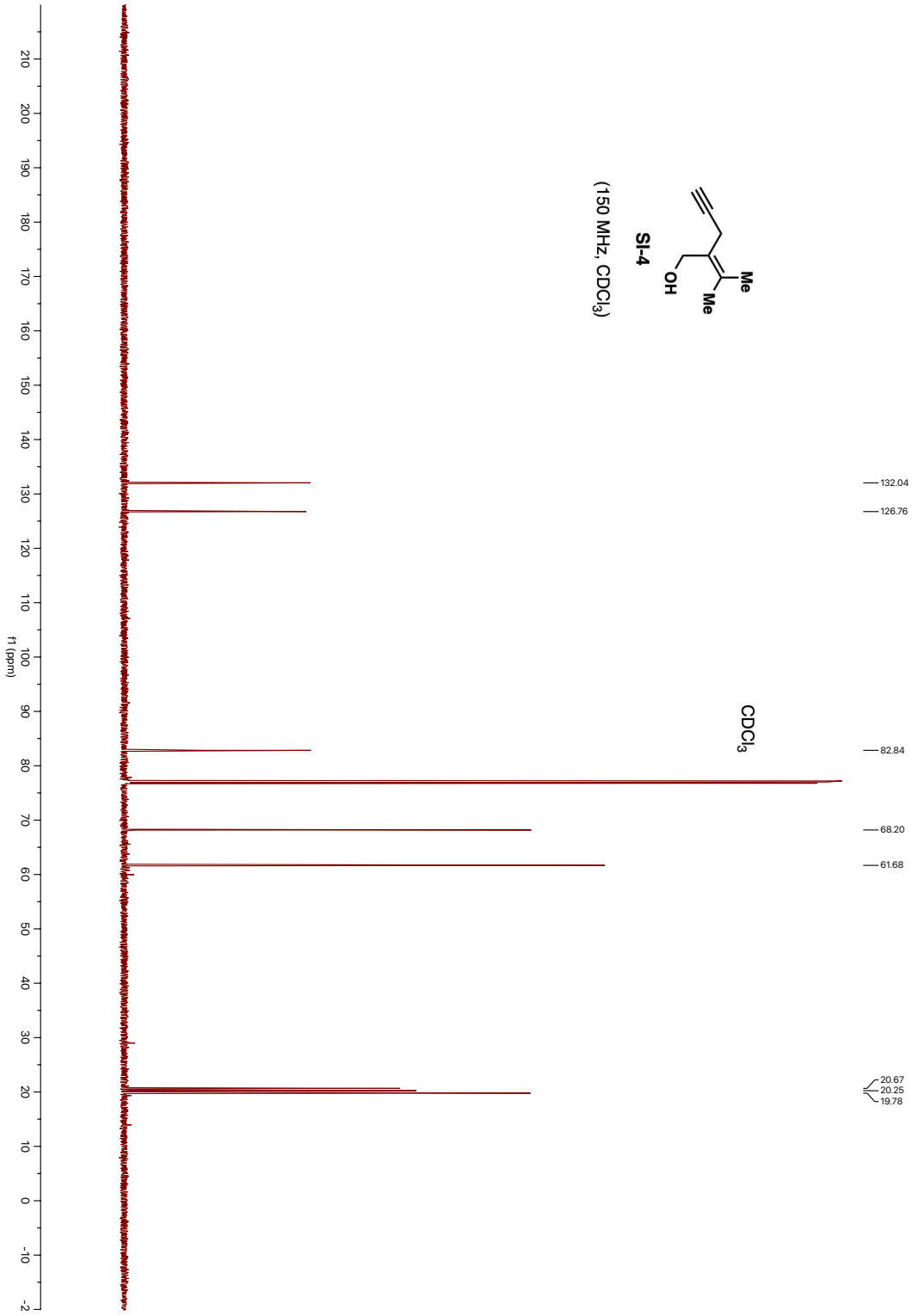

f2 (ppm)
f1 (ppm)

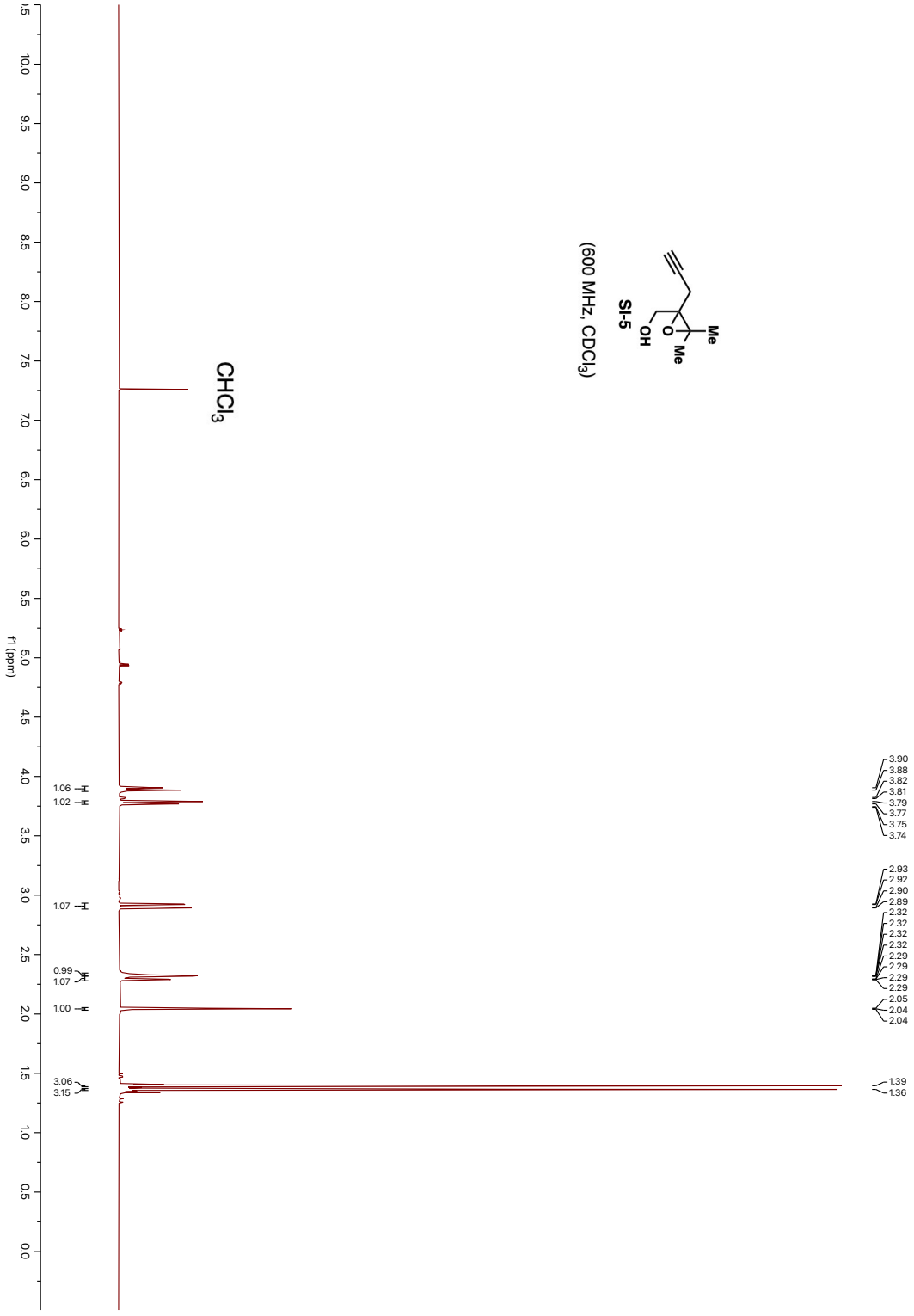

f2 (ppm)
f1 (ppm)

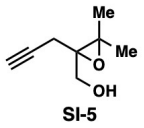

4.23
4.22
4.22
4.21
4.20
4.20
4.19
4.19
4.18
4.17
3.20
3.20
2.08
2.07
2.06
2.05
2.04
1.95
1.94
1.94
1.94
1.92
1.91
1.90
1.90
1.90
1.89
1.89
1.30
1.30
1.29
1.29
1.28
1.27
1.27
1.27
1.27
1.26
Me
Me
O
OEt
SI-3
(600 MHz, CDCl3)
CHCl3
2.30
2.13
3.23
1.03
3.23
3.28
16
15
14
13
12
11
10
9
8
7
6
5
4
3
2
1
0
-1
-2
-3
f1 (ppm)


SI-3
(150 MHz, CDCl3)
CDCl3
Me
Me
OEt
O
167.73
147.12
122.51
81.66
67.94
60.32
23.13
22.71
19.32
14.20
f1 (ppm)
210
200
190
180
170
160
150
140
130
120
110
100
90
80
70
60
50
40
30
20
10
0
-10
-2


SI-4
(600 MHz, $CDCl_3$)
Me
Me
OH
$CHCl_3$
f1 (ppm)
10.0
9.5
9.0
8.5
8.0
7.5
7.0
6.5
6.0
5.5
5.0
4.5
4.0
3.5
3.0
2.5
2.0
1.5
1.0
0.5
0.0
2.23
2.19
1.00
3.22
3.38
1.03
4.25
3.06
3.06
3.06
3.06
2.00
2.00
1.99
1.98
1.98
1.77
1.74
1.71

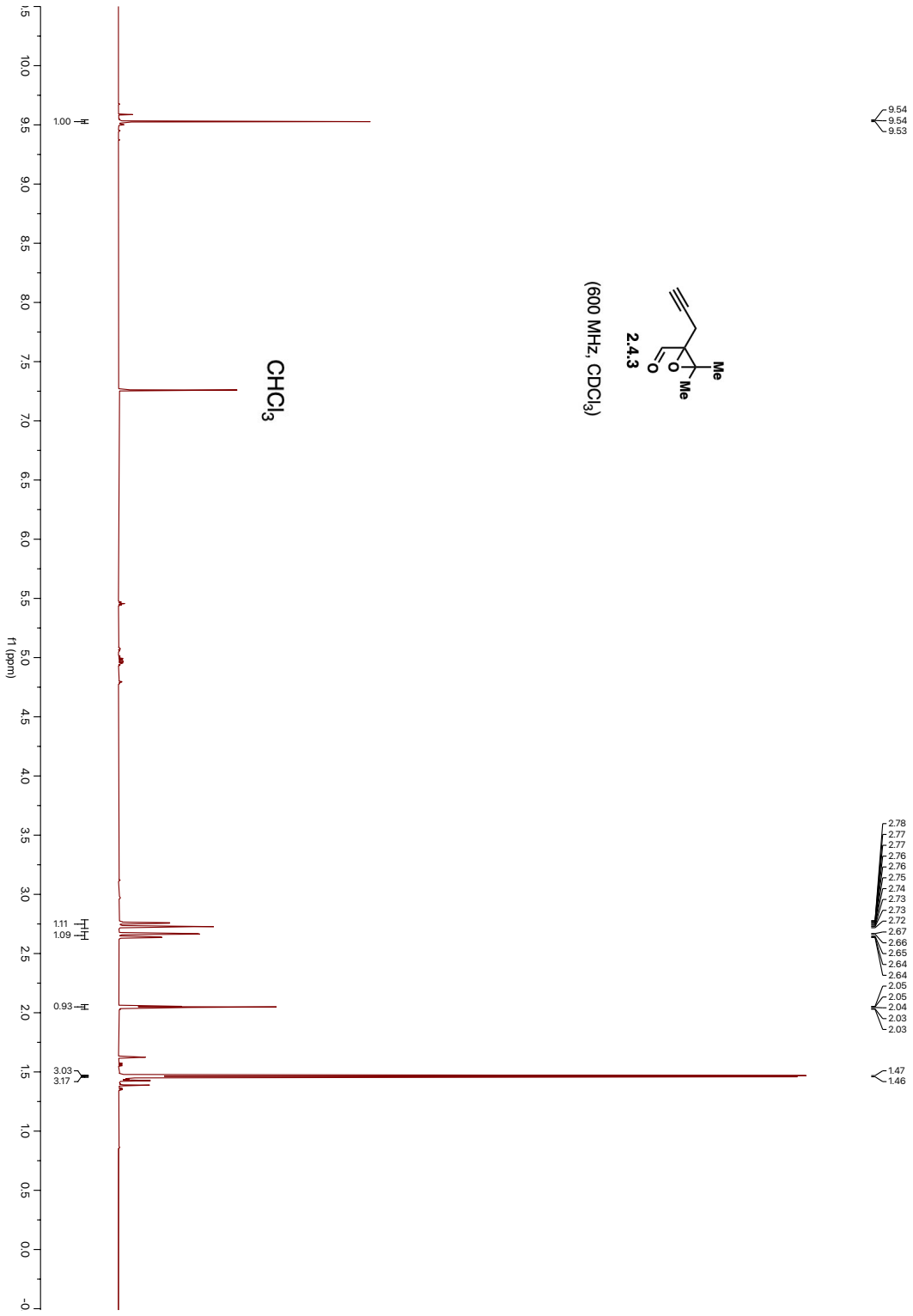

SI-4
(150 MHz, CDCl3)
Me
Me
OH
CDCl3
132.04
126.76
82.84
68.20
61.68
20.67
20.25
19.78
f1 (ppm)

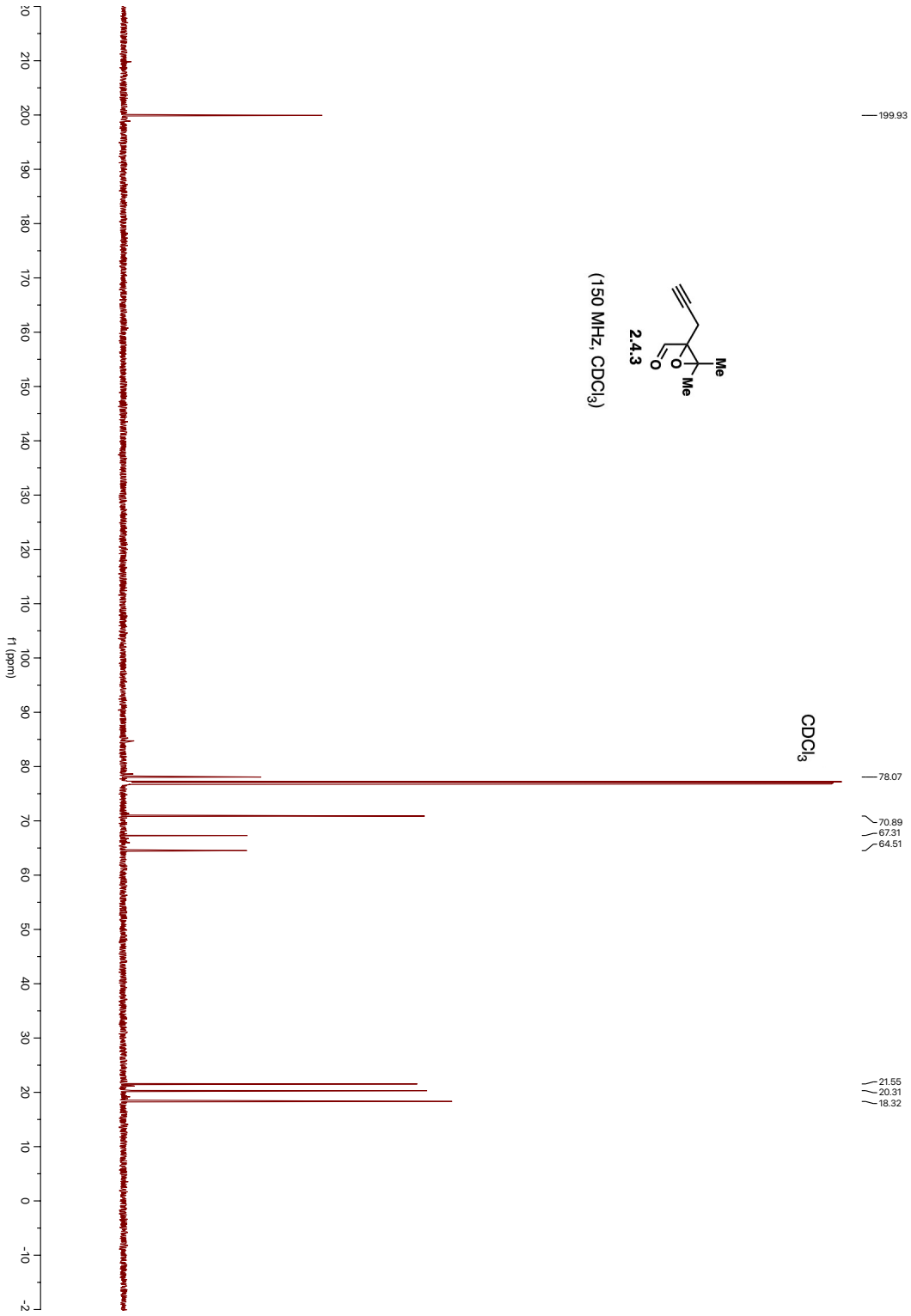

SI-5
(600 MHz, CDCl3)
CHCl3
Me
O
Me
OH
f1 (ppm)
1.06
1.02
1.07
0.99
1.07
1.00
3.06
3.15
3.90
3.88
3.82
3.81
3.79
3.77
3.75
3.74
2.93
2.92
2.90
2.89
2.32
2.32
2.32
2.32
2.29
2.29
2.29
2.29
2.05
2.04
2.04
1.39
1.36

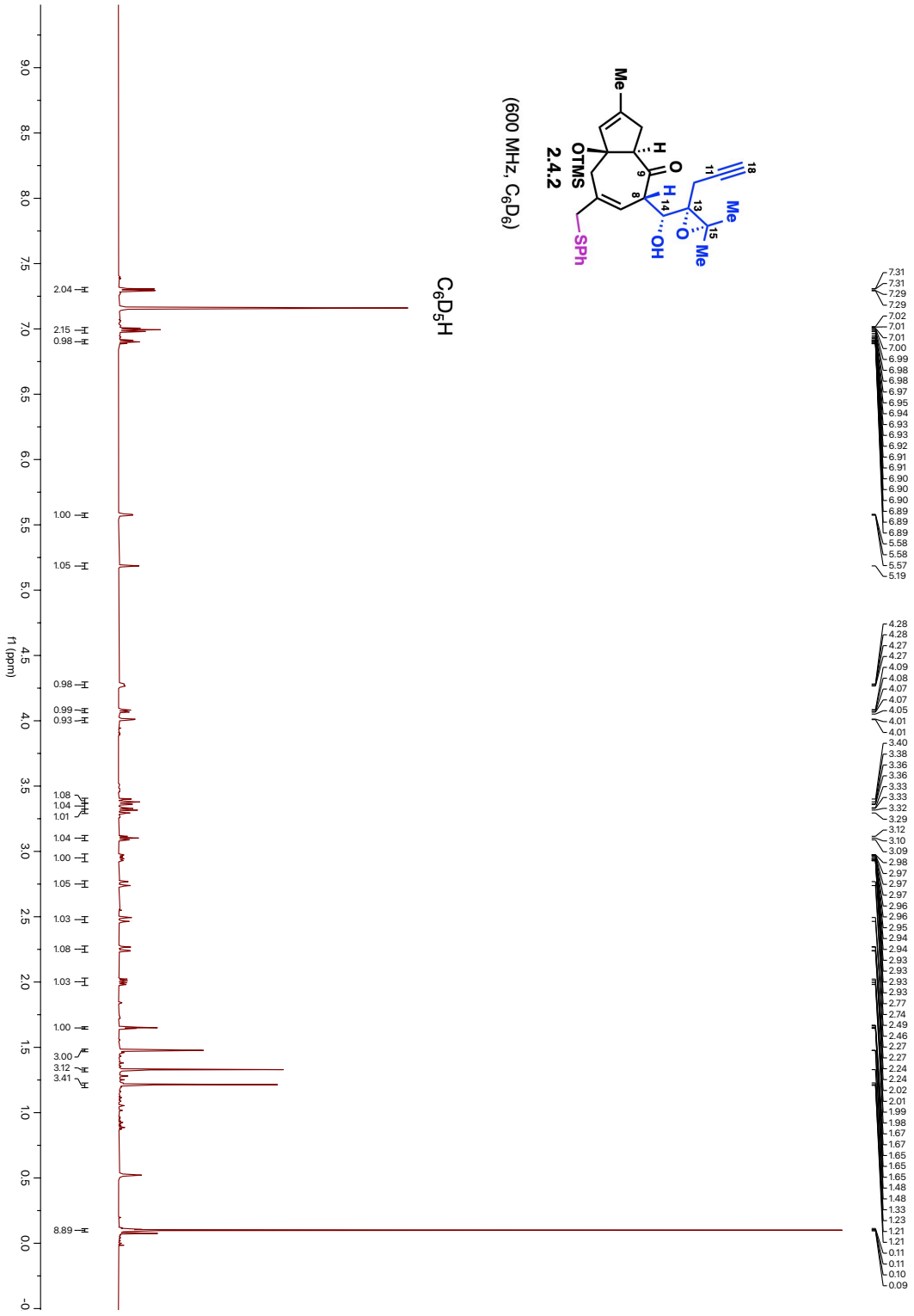


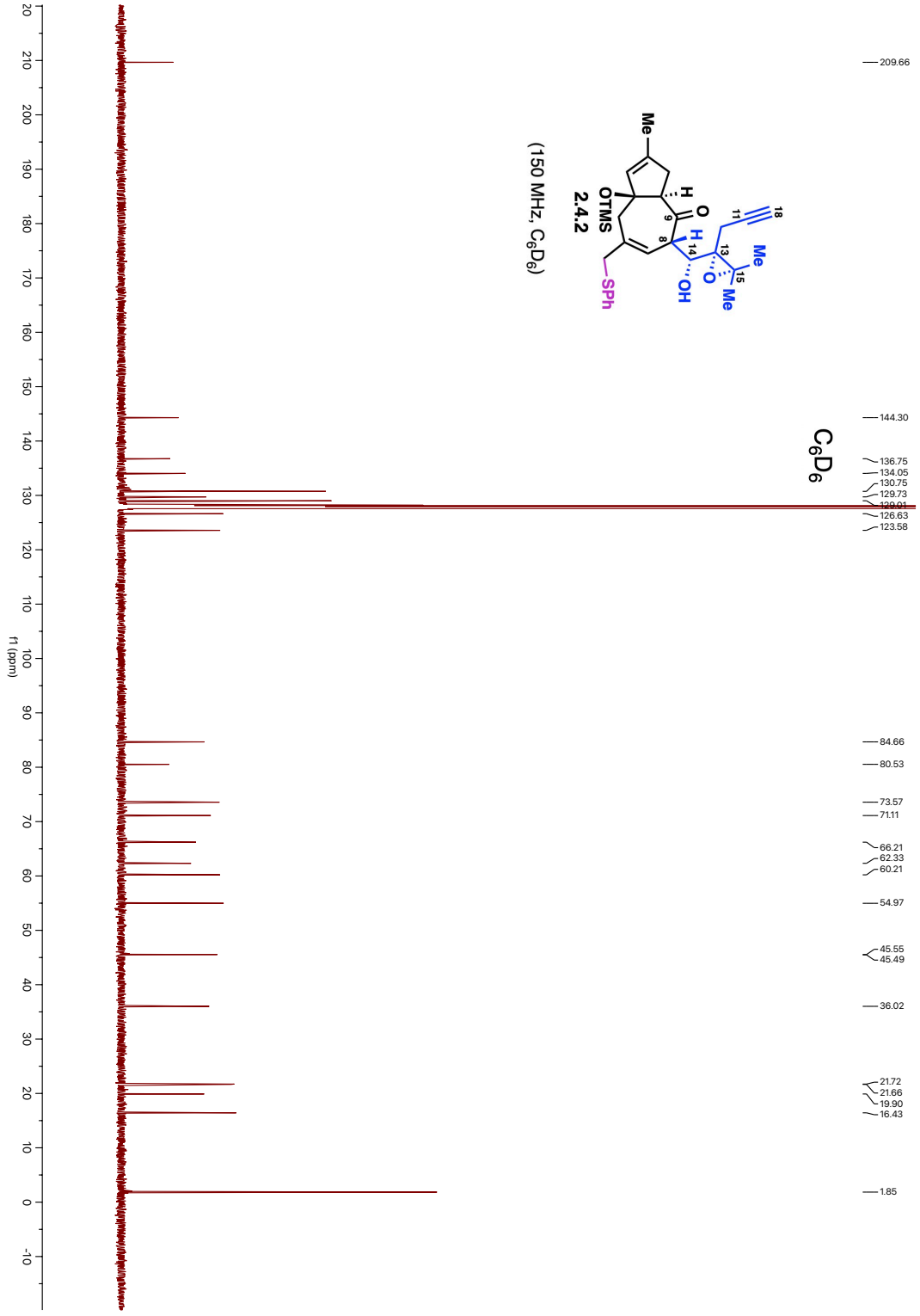
SI-5

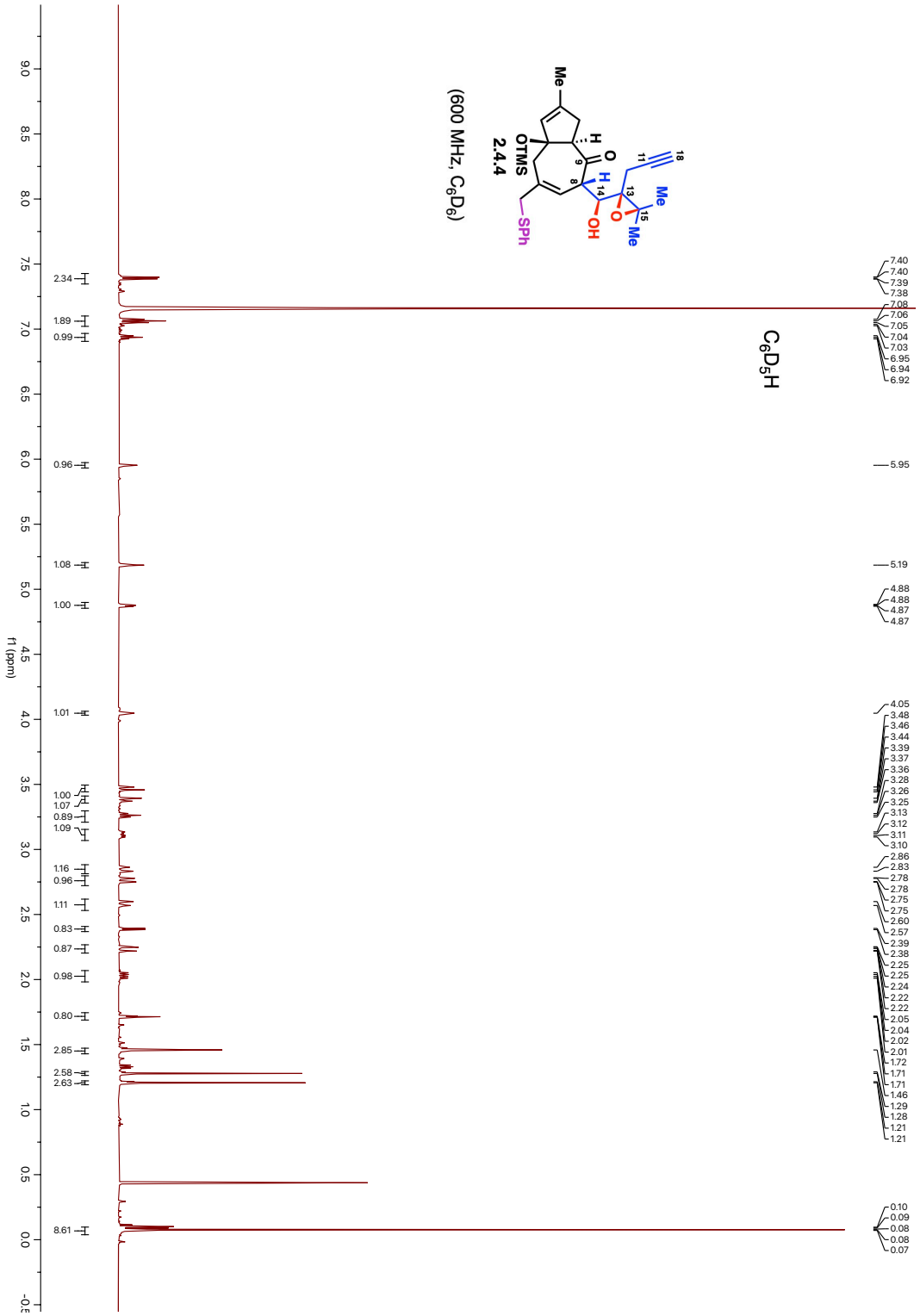
(150 MHz, $CDCl_3$)

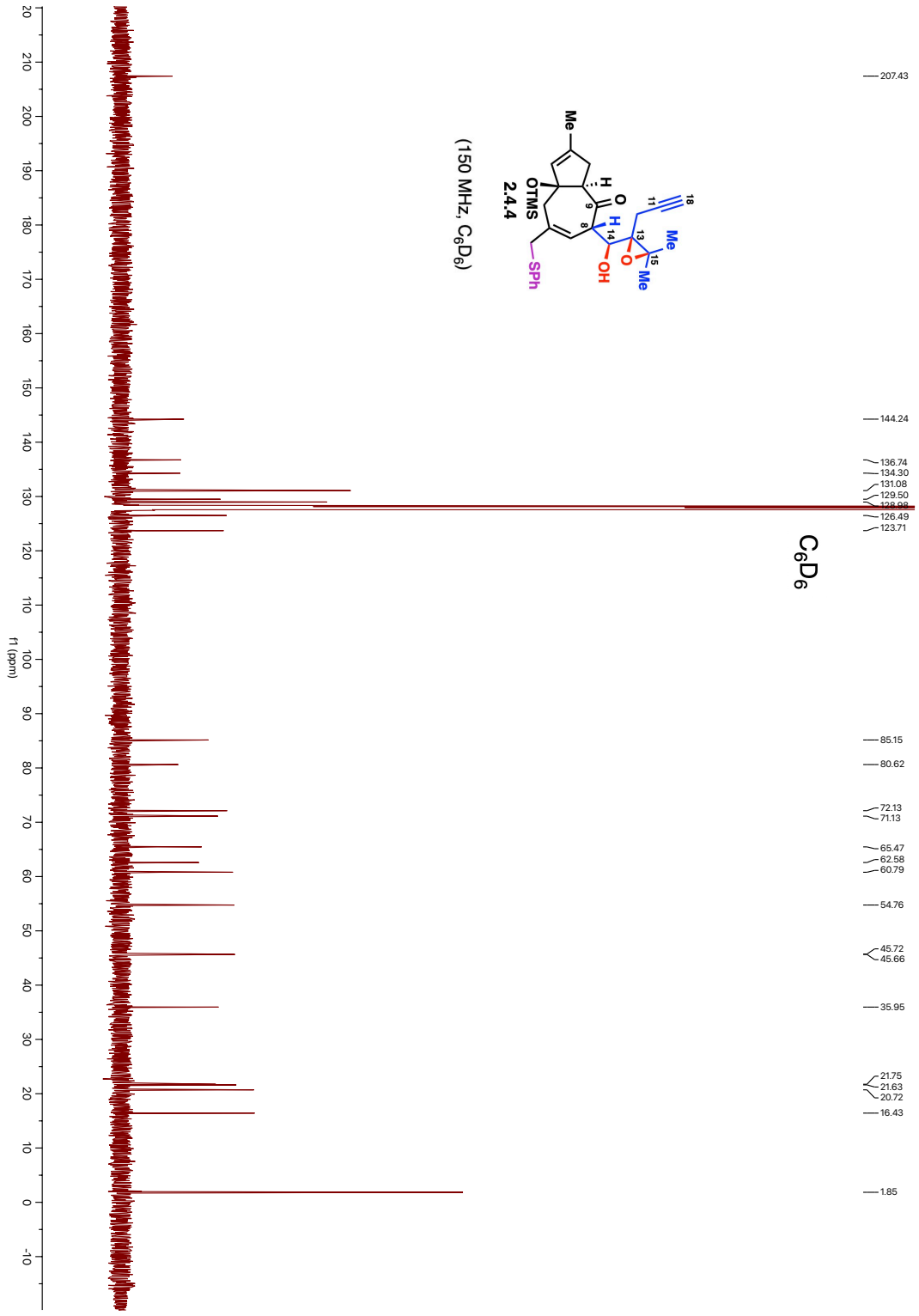

2.4.3
(600 MHz, CDCl3)
CHCl3
Me
Me
O
O
O
f1 (ppm)
1.00
1.11
1.09
0.93
3.03
3.17
9.54
9.54
9.53
2.78
2.77
2.77
2.76
2.76
2.75
2.74
2.73
2.73
2.72
2.67
2.66
2.65
2.64
2.64
2.05
2.05
2.04
2.03
2.03
1.47
1.46

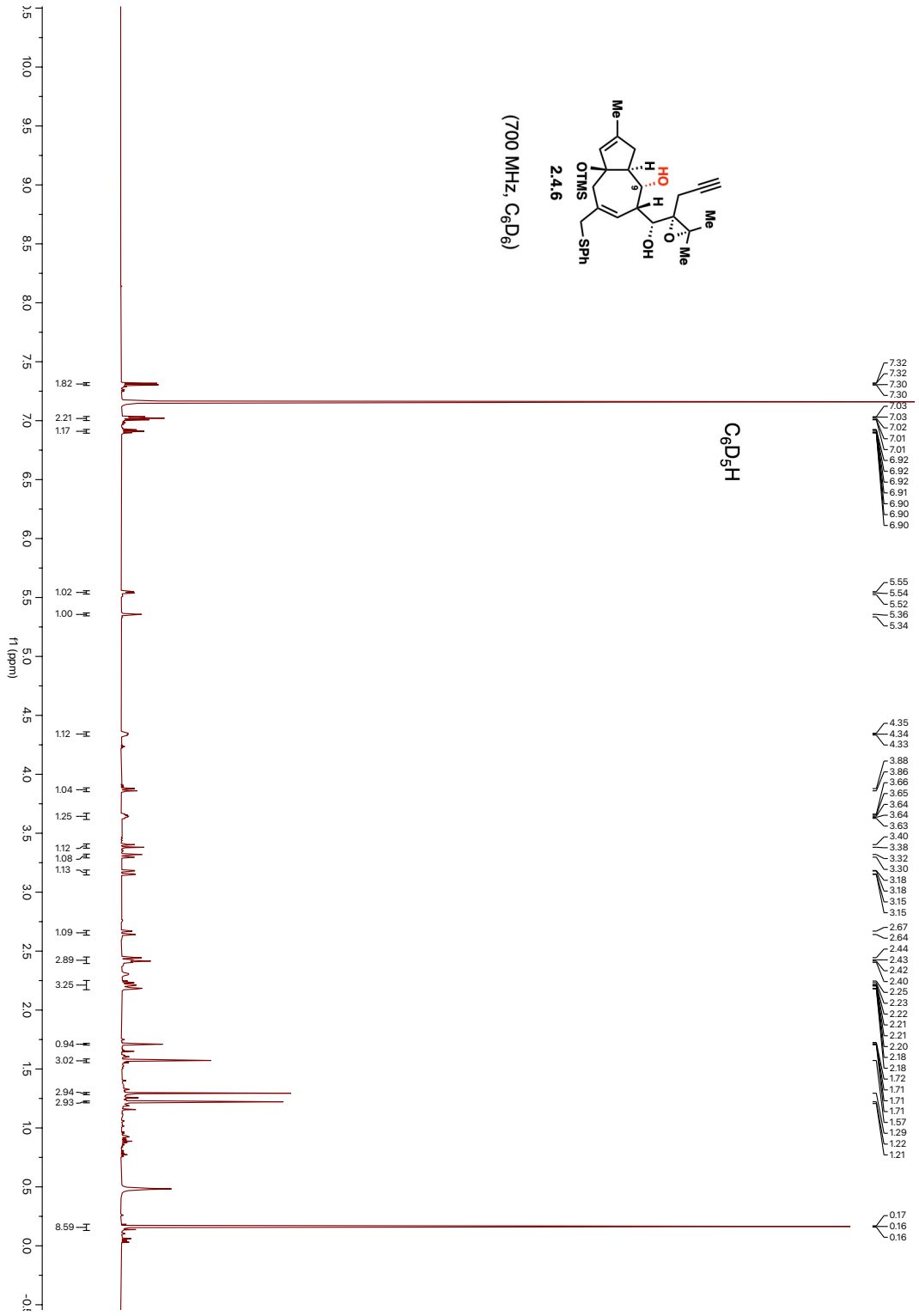

2.4.3
(150 MHz, CDCl3)
Me
O
O
Me
CDCl3
199.93
78.07
70.89
67.31
64.51
21.55
20.31
18.32
f1 (ppm)

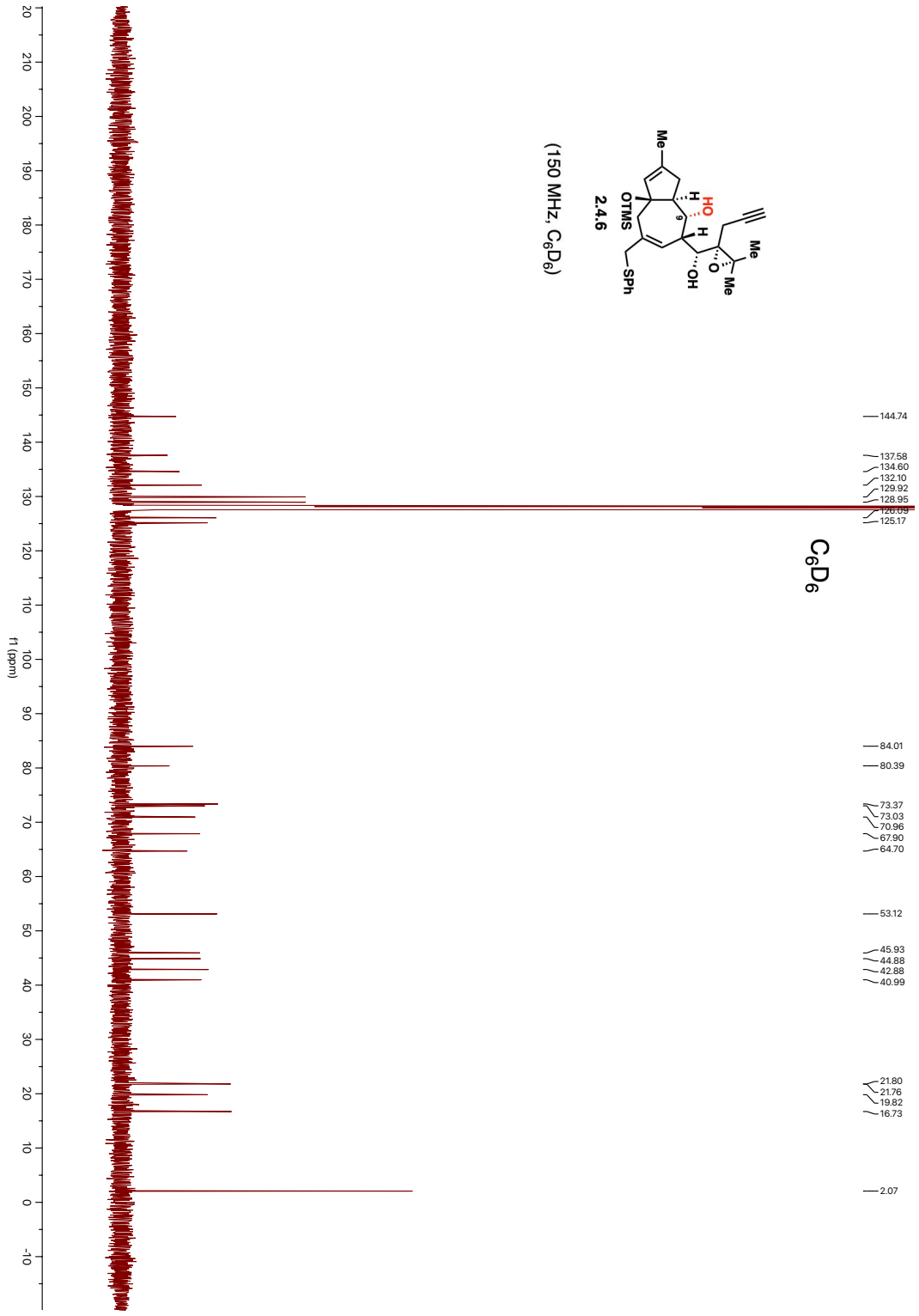

(600 MHz, C6D6)
C6D5H
OTMS
2.4.2
SPh
OH
Me
f1 (ppm)

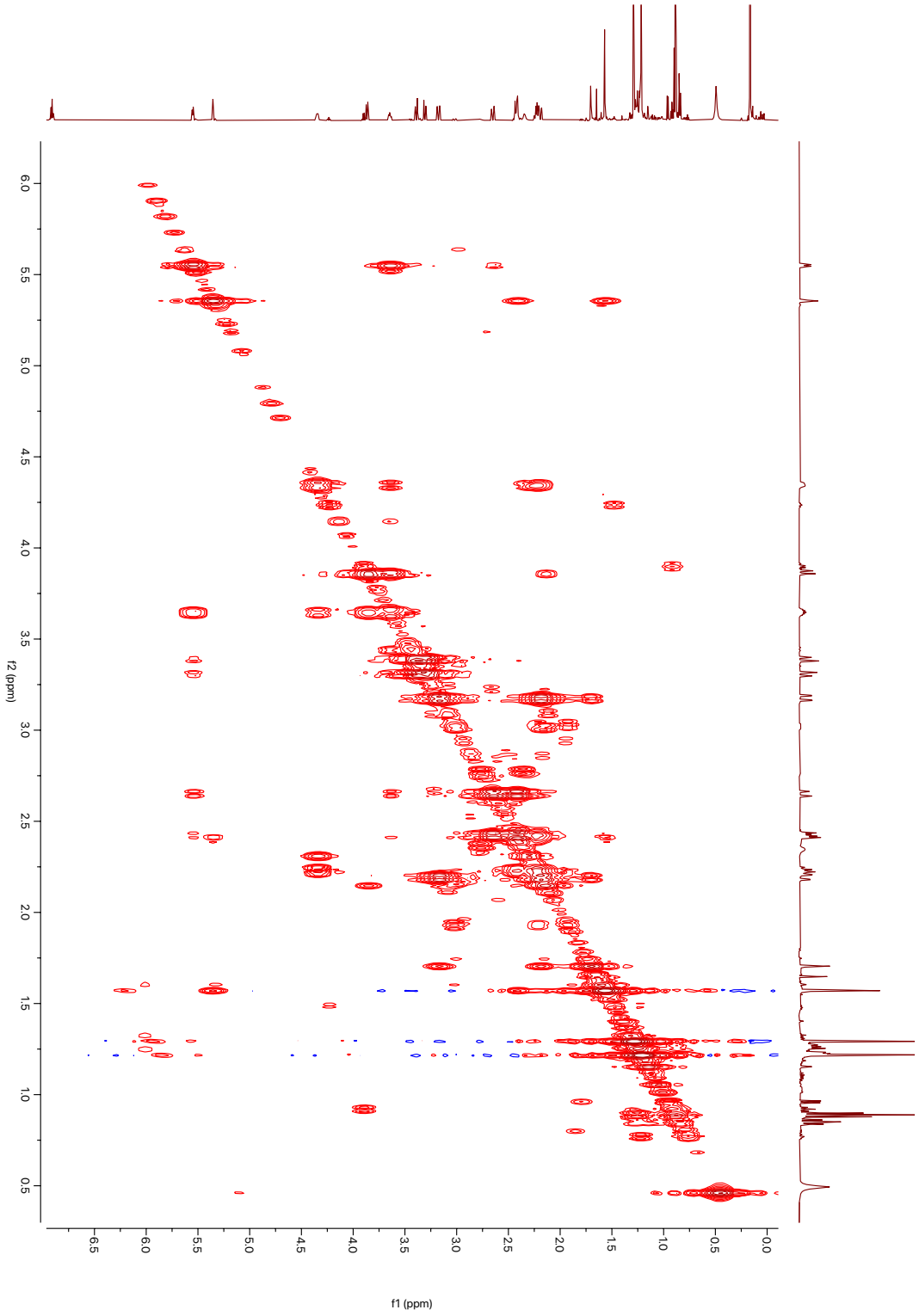

2.4.2
(150 MHz, C6D6)
C6D6
f1 (ppm)
209.66
144.30
136.75
134.05
130.75
129.73
129.01
126.63
123.58
84.66
80.53
73.57
71.11
66.21
62.33
60.21
54.97
45.55
45.49
36.02
21.72
21.66
19.90
16.43
1.85

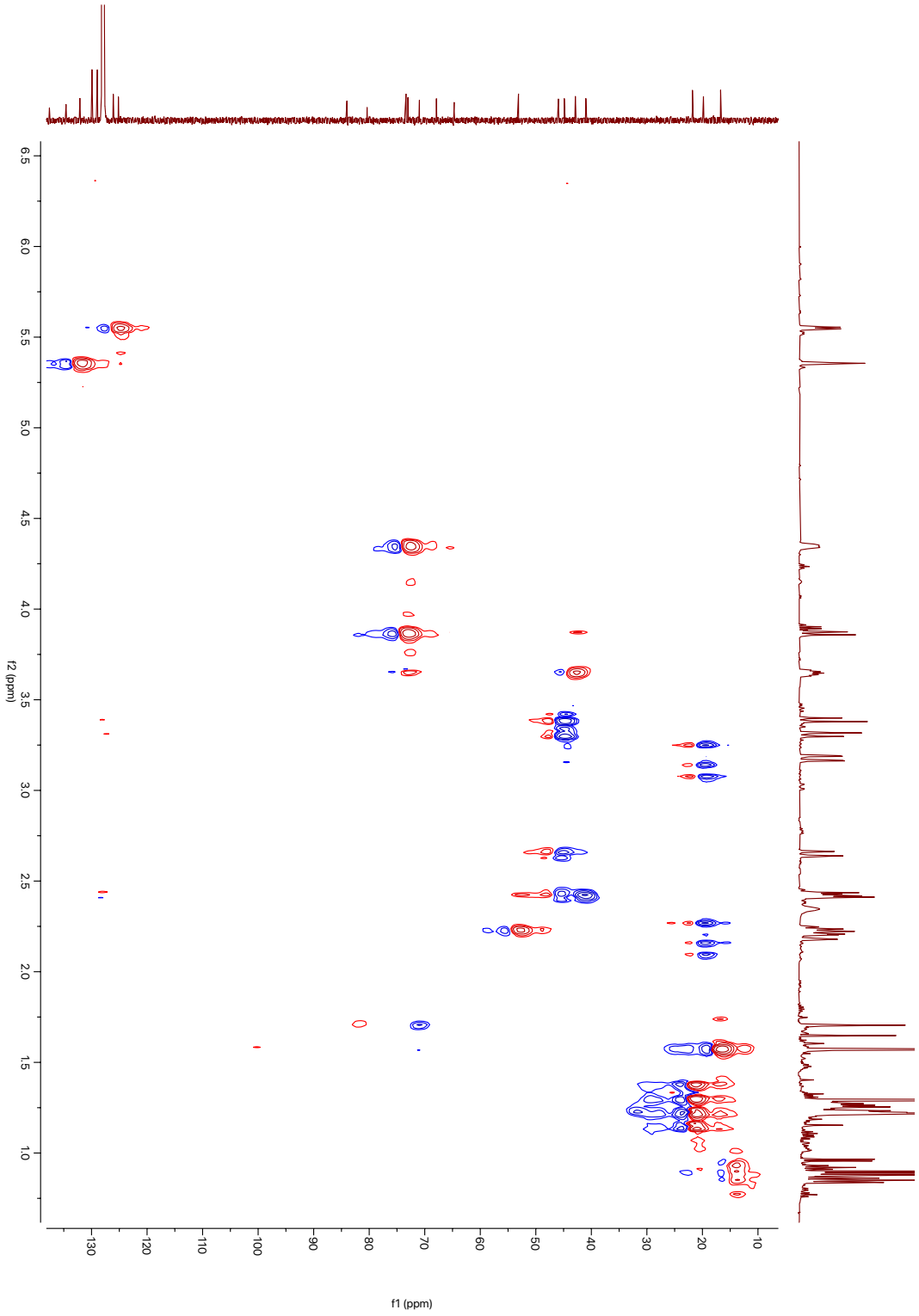

2.4.4
OTMS
SPh
OH
Me
Me
Me
(600 MHz, C6D6)
C6D5H
f1 (ppm)

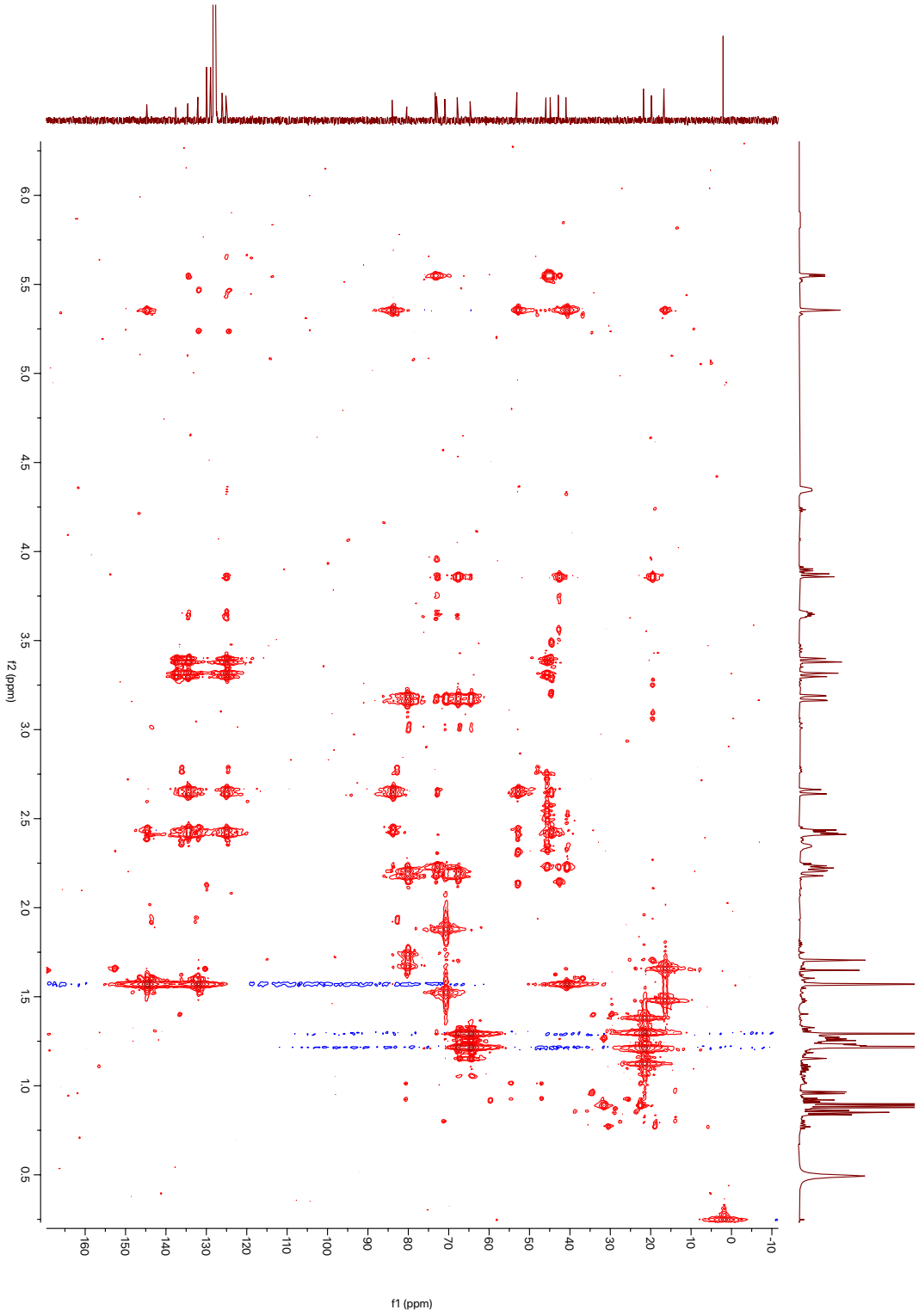

(150 MHz, C6D6)
2.4.4
OTMS
SPh
OH
Me
Me
Me
C6D6
207.43
144.24
136.74
134.30
131.08
129.50
128.98
126.49
123.71
85.15
80.62
72.13
71.13
65.47
62.58
60.79
54.76
45.72
45.66
35.95
21.75
21.63
20.72
16.43
1.85
f1 (ppm)

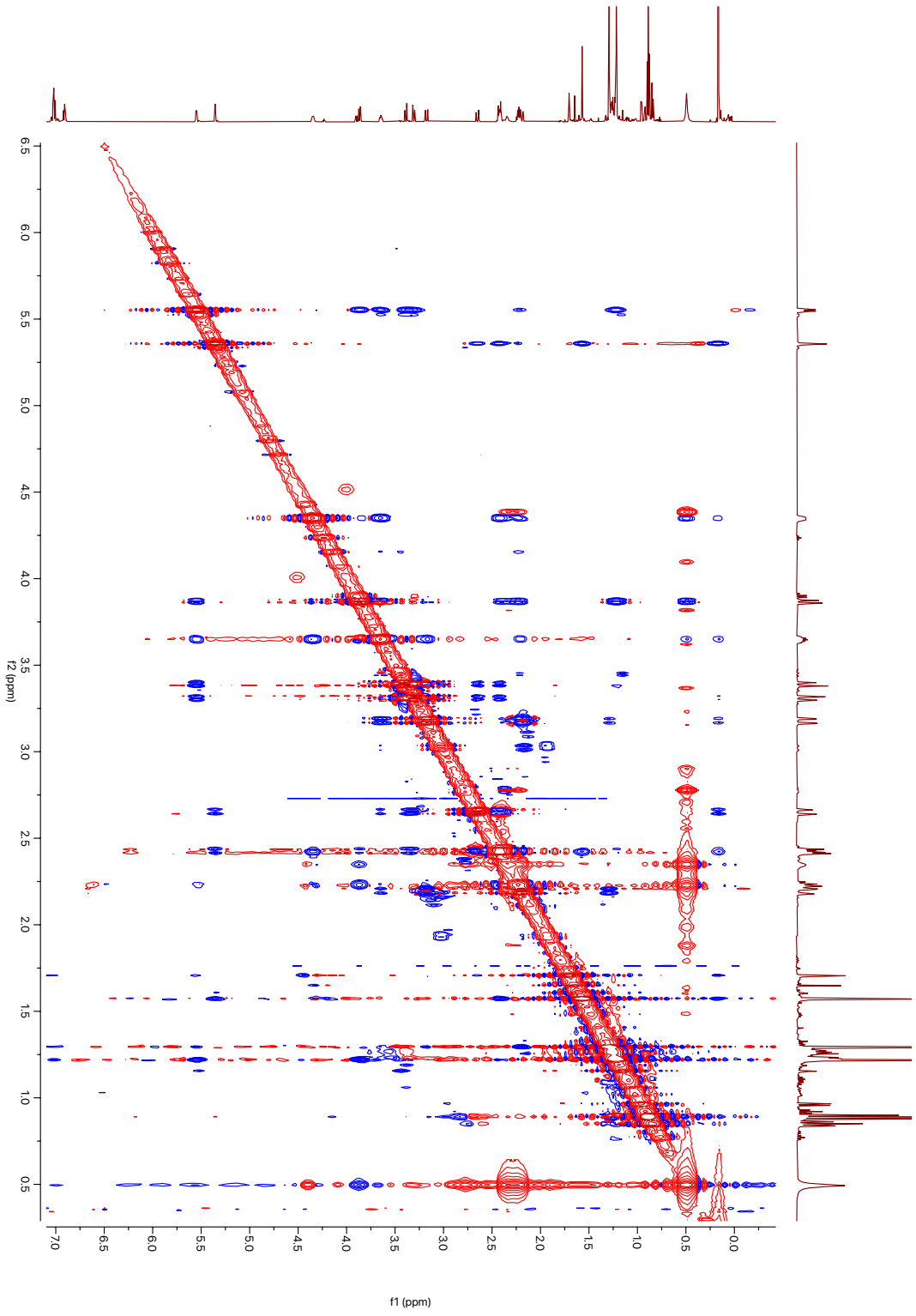

(700 MHz, C6D6)
2.4.6
OTMS
SPh
OH
HO
Me
Me
Me
C6D5H
f1 (ppm)

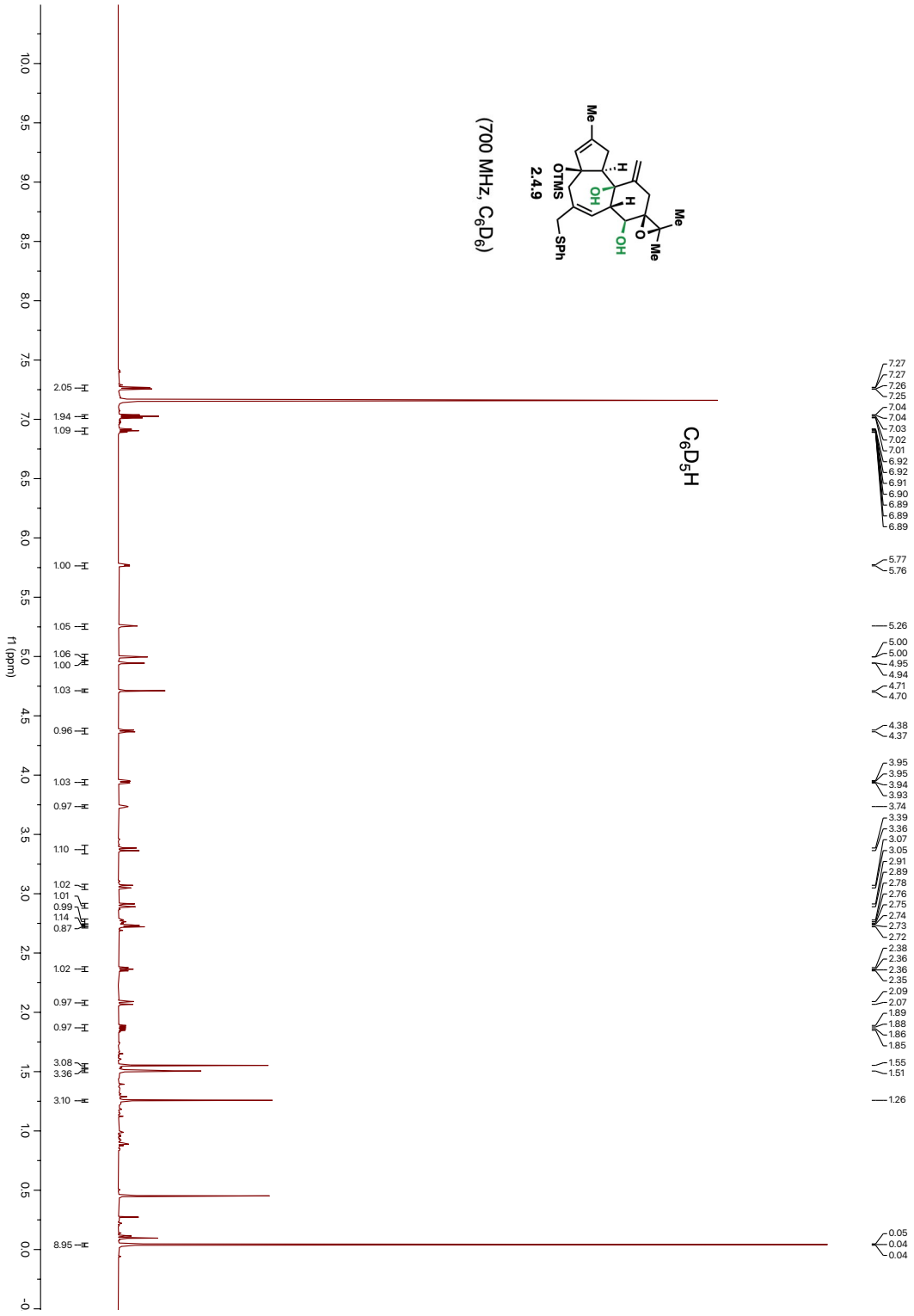

(150 MHz, C6D6)
2.4.6
OTMS
SPh
OH
HO
Me
Me
Me
C6D6
144.74
137.58
134.60
132.10
129.92
128.95
126.09
125.17
84.01
80.39
73.37
73.03
70.96
67.90
64.70
53.12
45.93
44.88
42.88
40.99
21.80
21.76
19.82
16.73
2.07
f1 (ppm)

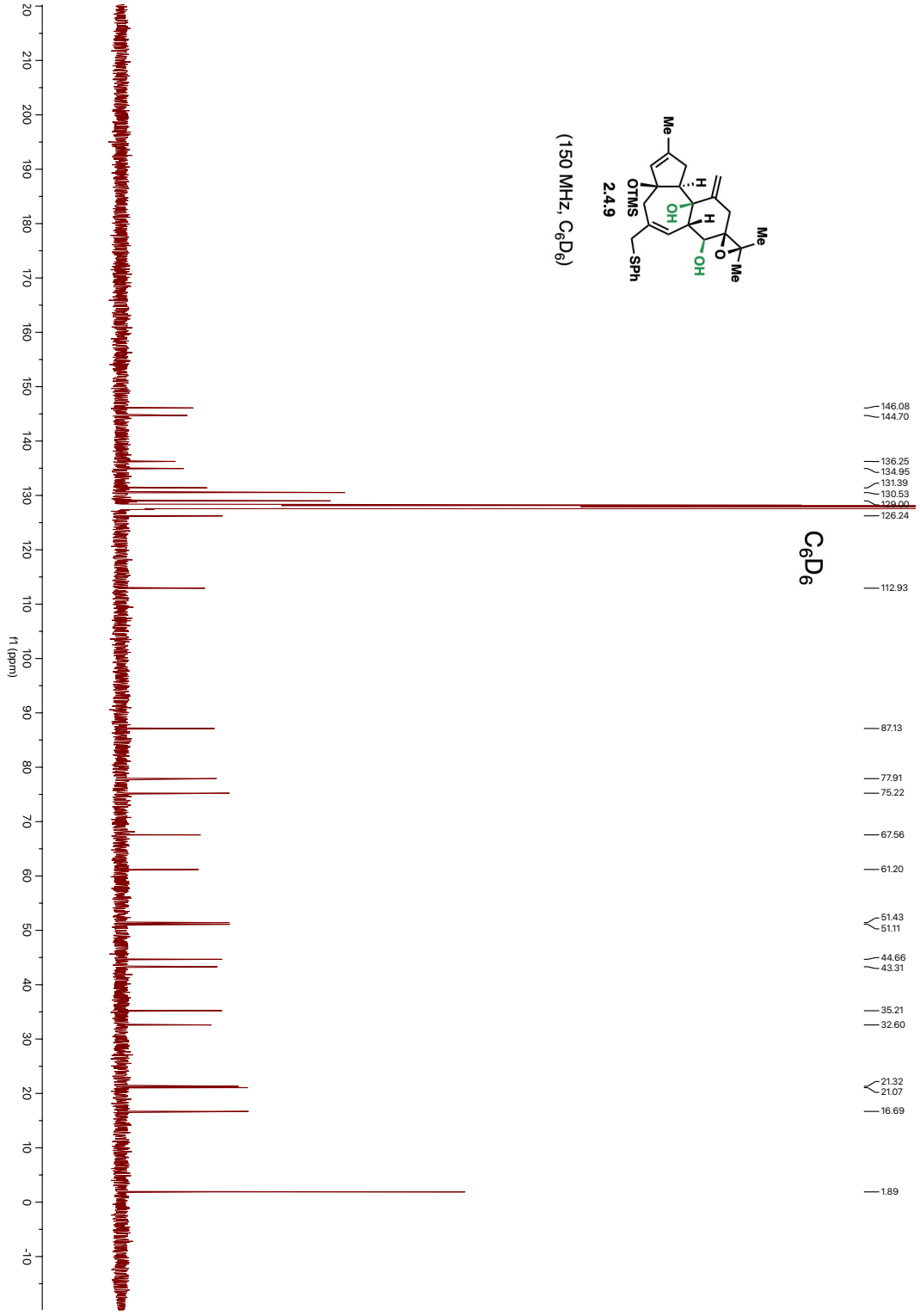

f2 (ppm)
f1 (ppm)

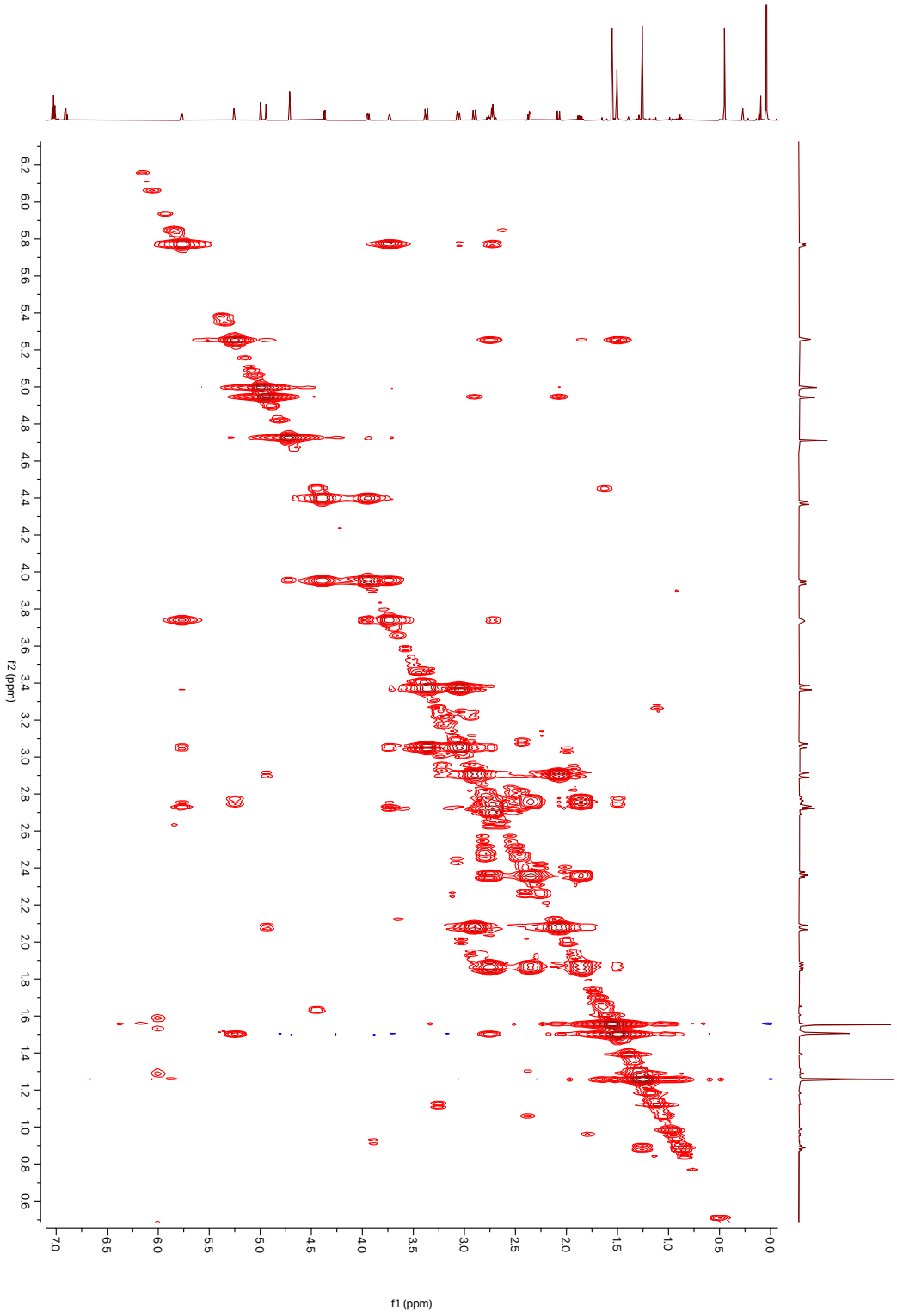

f2 (ppm)
f1 (ppm)

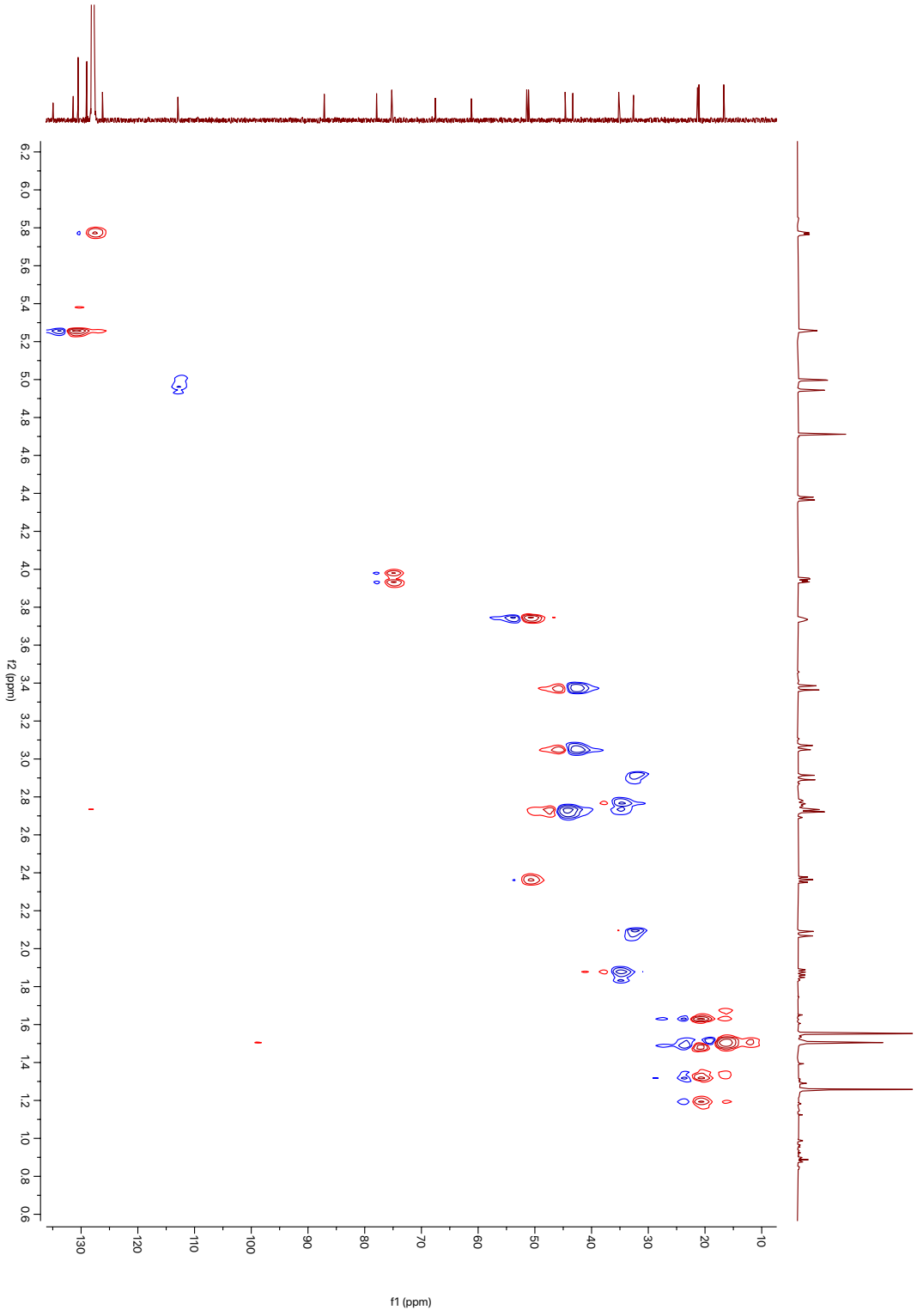

f2 (ppm)
f1 (ppm)

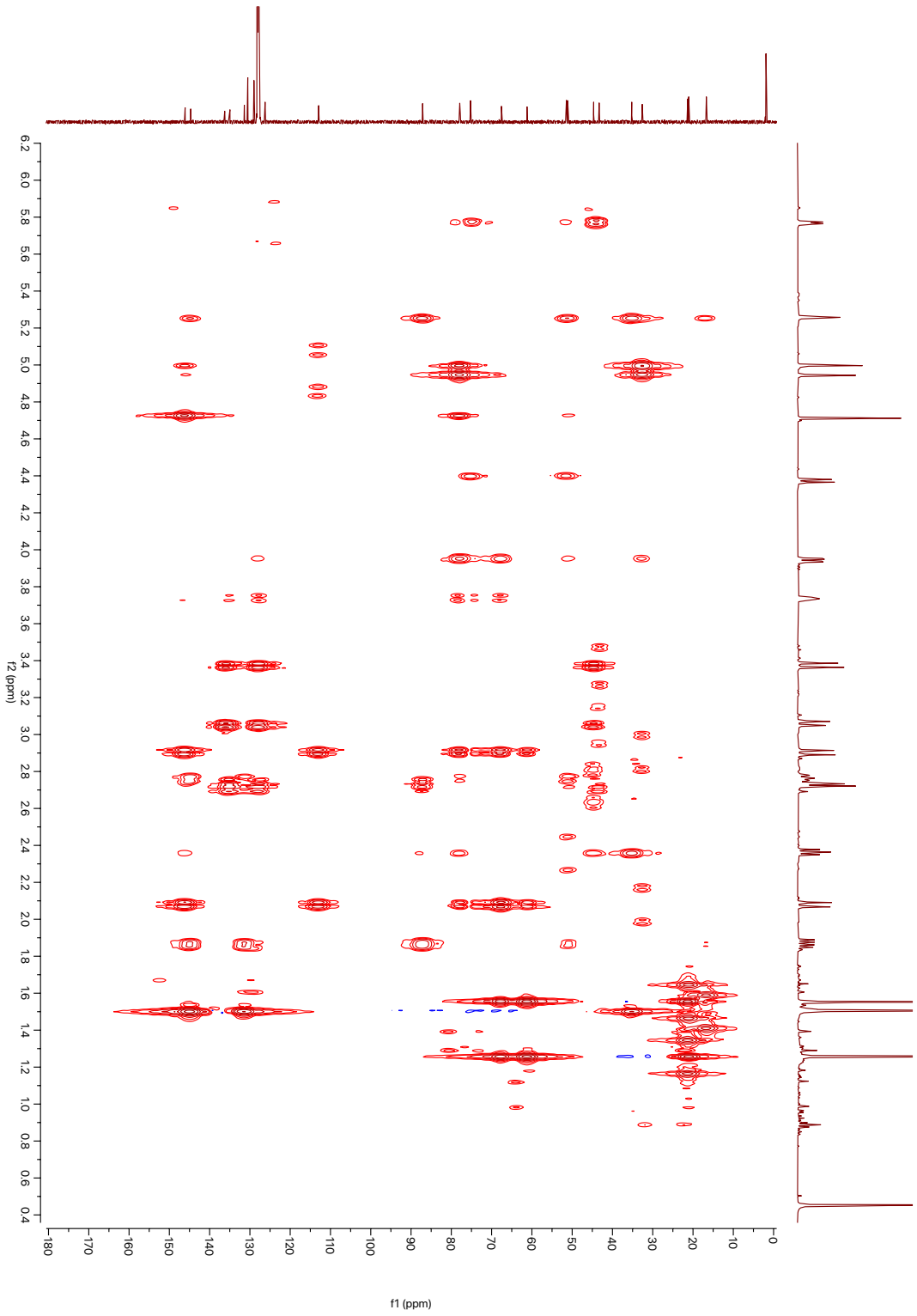

f2 (ppm)
f1 (ppm)

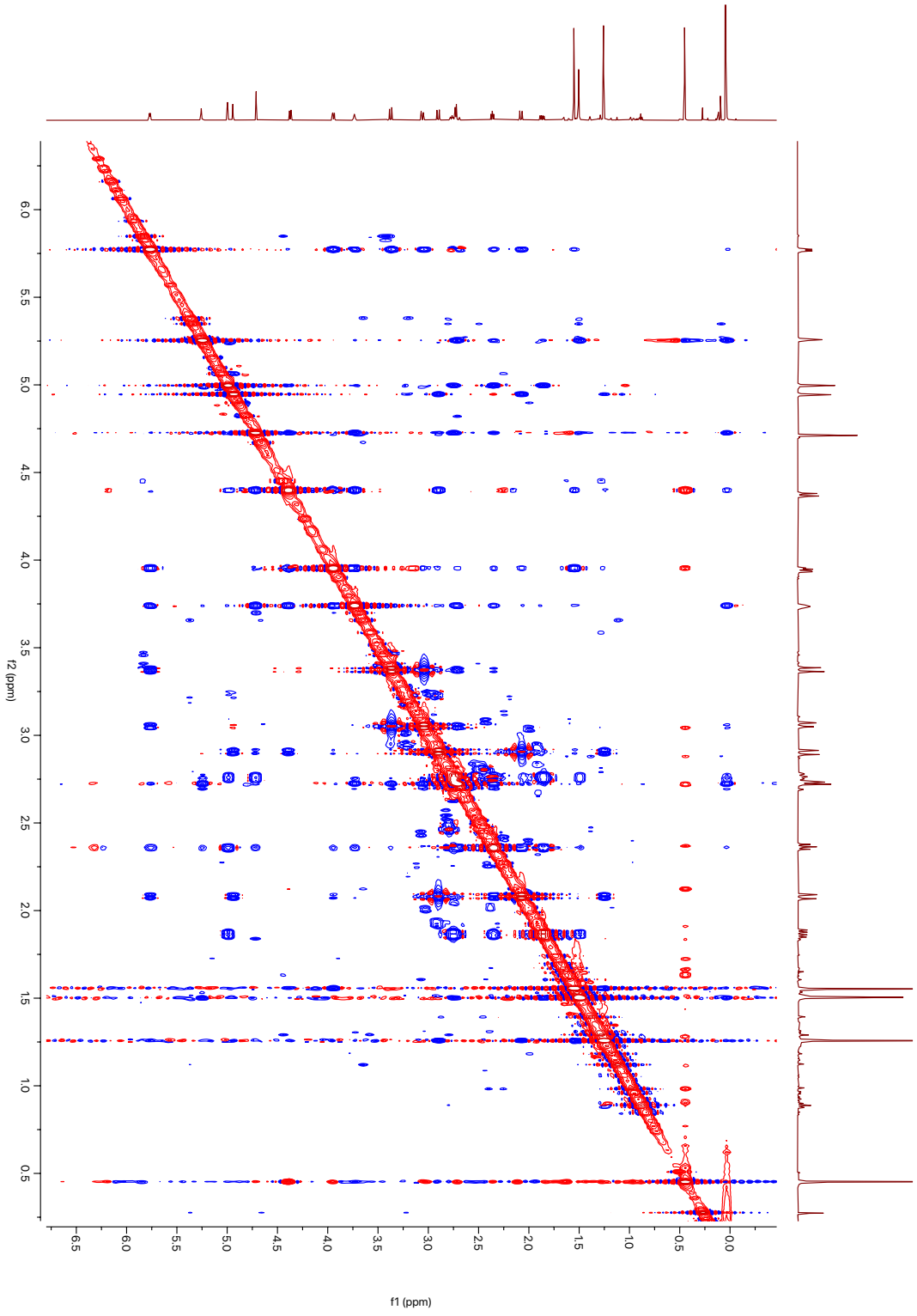

(700 MHz, C6D6)
2.4.9
OTMS
SPh
OH
OH
Me
Me
Me
O
H
H
C6D5H
f1 (ppm)
2.05
1.94
1.09
1.00
1.05
1.06
1.00
1.03
0.96
1.03
0.97
1.10
1.02
1.01
0.99
1.14
0.87
1.02
0.97
0.97
3.08
3.36
3.10
8.95
7.27
7.27
7.26
7.25
7.04
7.04
7.03
7.02
7.01
6.92
6.92
6.91
6.90
6.89
6.89
6.89
5.77
5.76
5.26
5.00
5.00
4.95
4.94
4.71
4.70
4.38
4.37
3.95
3.95
3.94
3.93
3.74
3.39
3.36
3.07
3.05
2.91
2.89
2.78
2.76
2.75
2.74
2.73
2.72
2.38
2.36
2.36
2.35
2.09
2.07
1.89
1.88
1.86
1.85
1.55
1.51
1.26
0.05
0.04
0.04

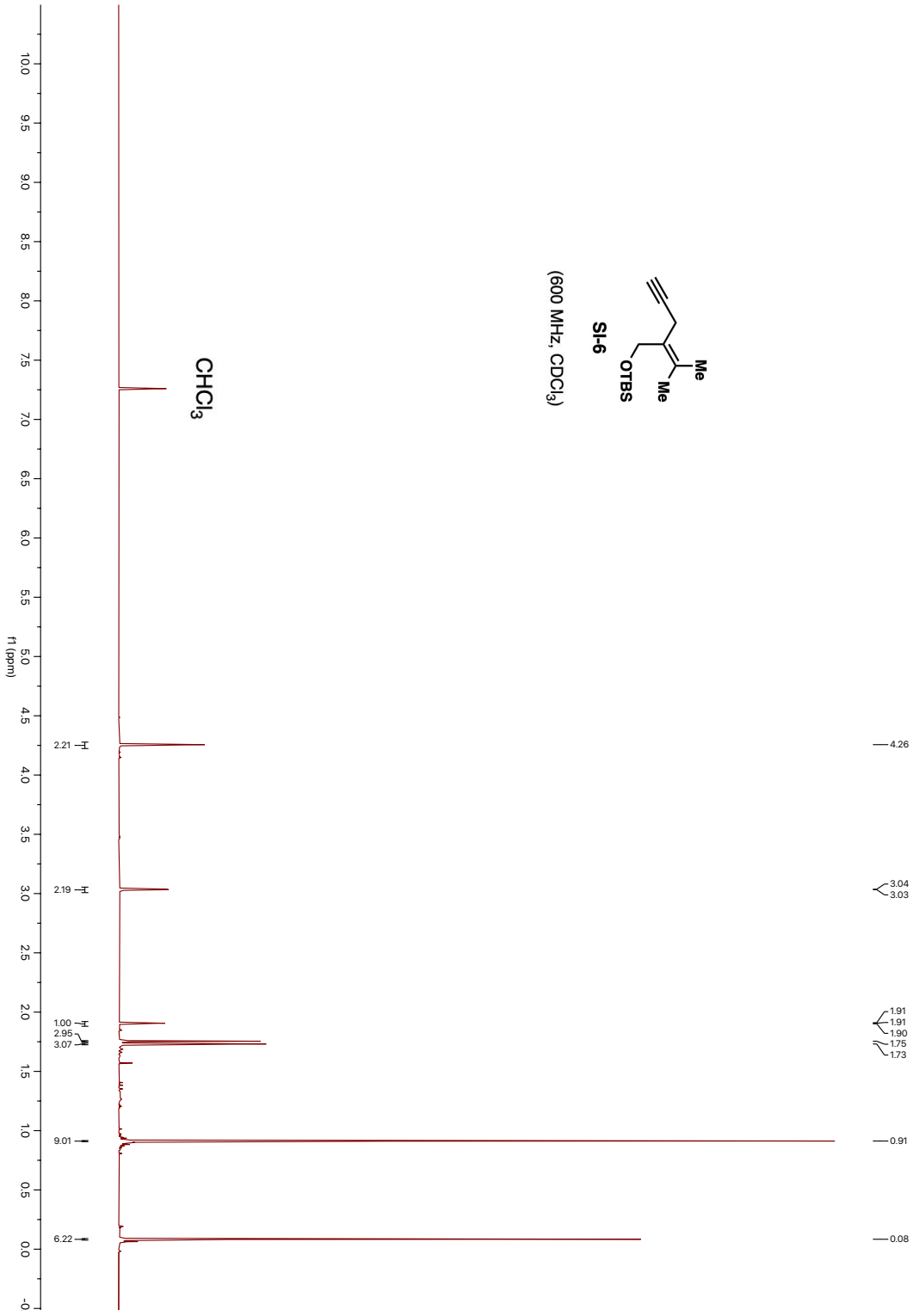

2.4.9
(150 MHz, C6D6)
C6D6
f1 (ppm)
146.08
144.70
136.25
134.95
131.39
130.53
129.00
126.24
112.93
87.13
77.91
75.22
67.56
61.20
51.43
51.11
44.66
43.31
35.21
32.60
21.32
21.07
16.69
1.89

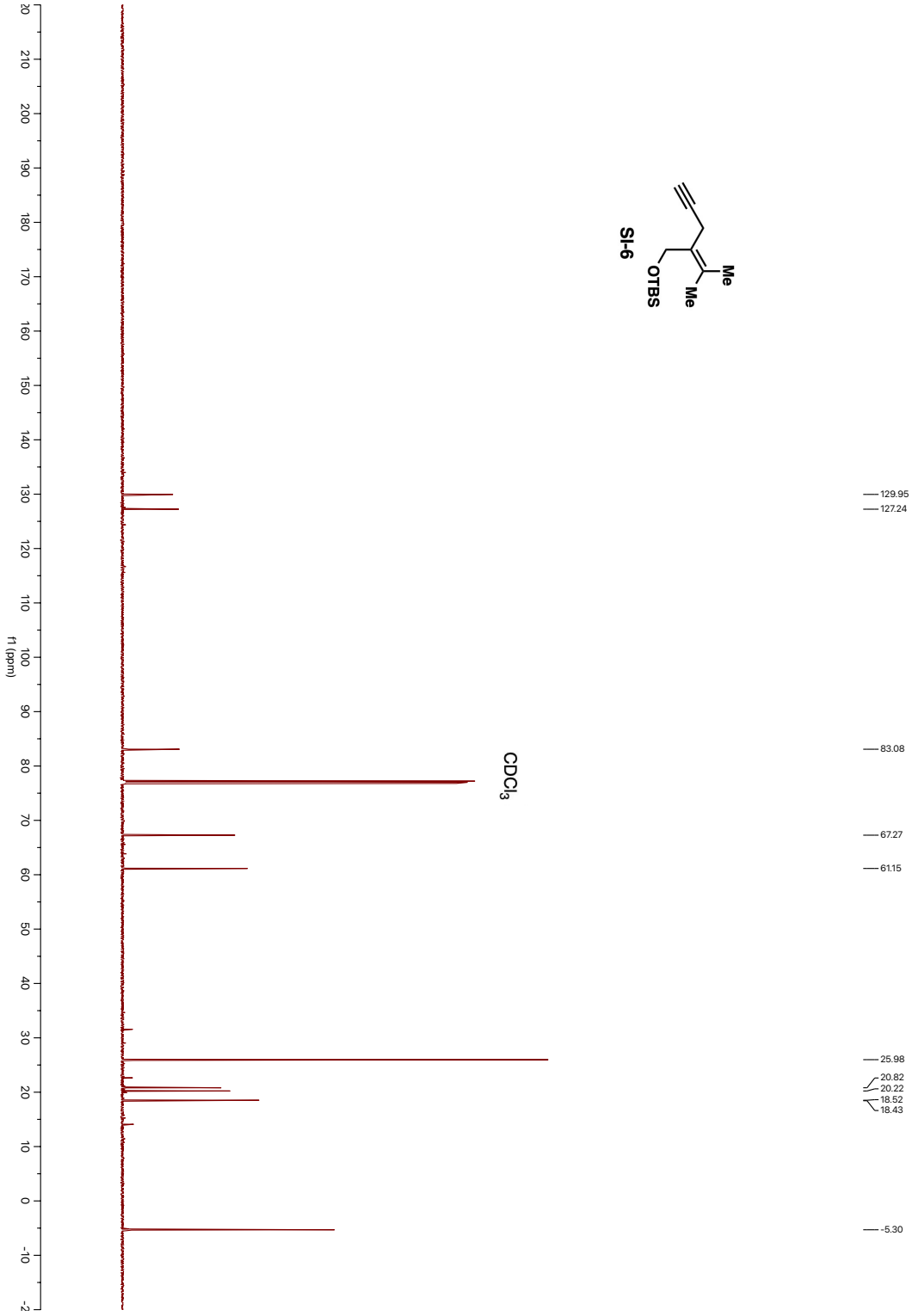

f2 (ppm)
f1 (ppm)

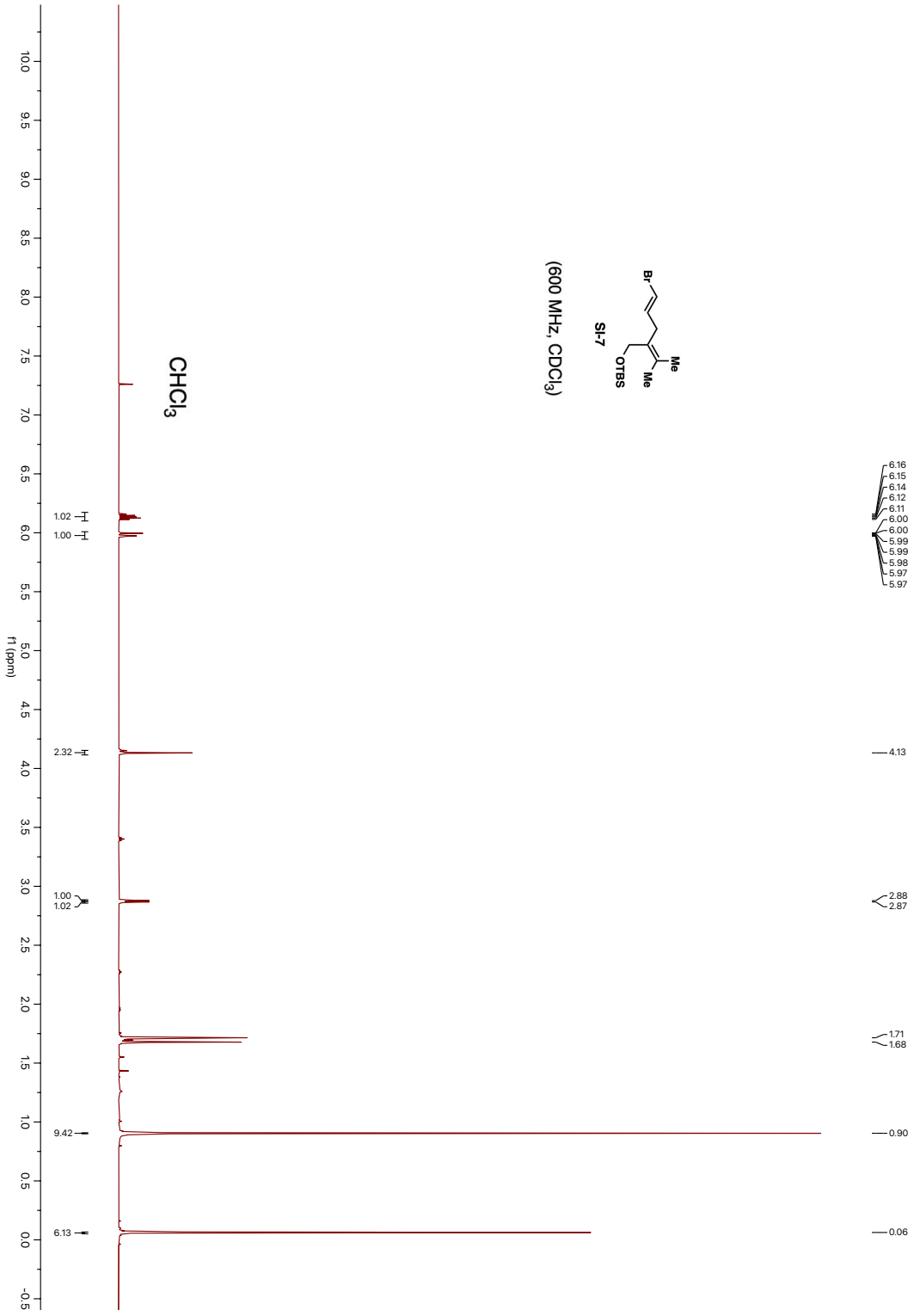

f2 (ppm)
f1 (ppm)

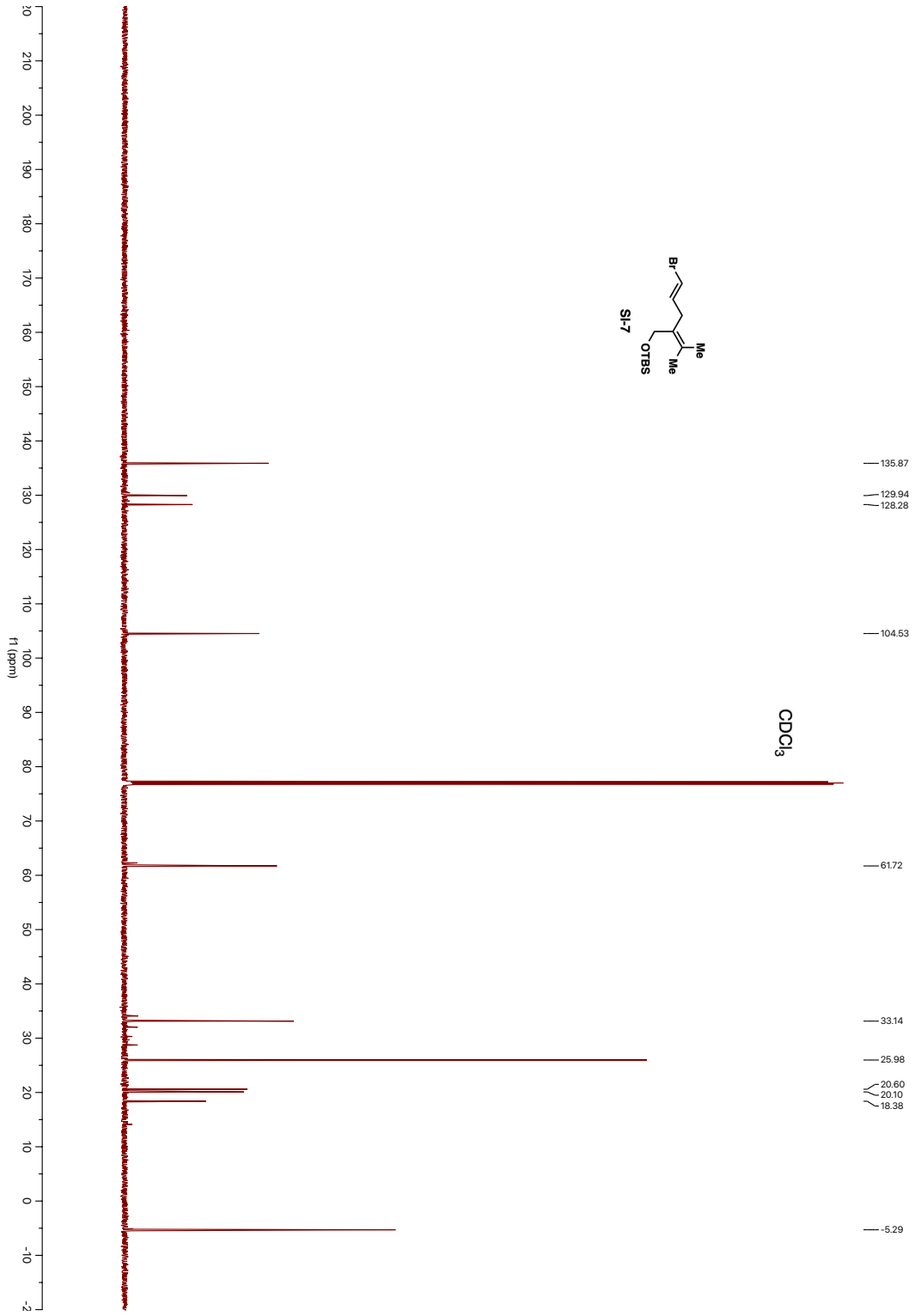

f2 (ppm)
f1 (ppm)

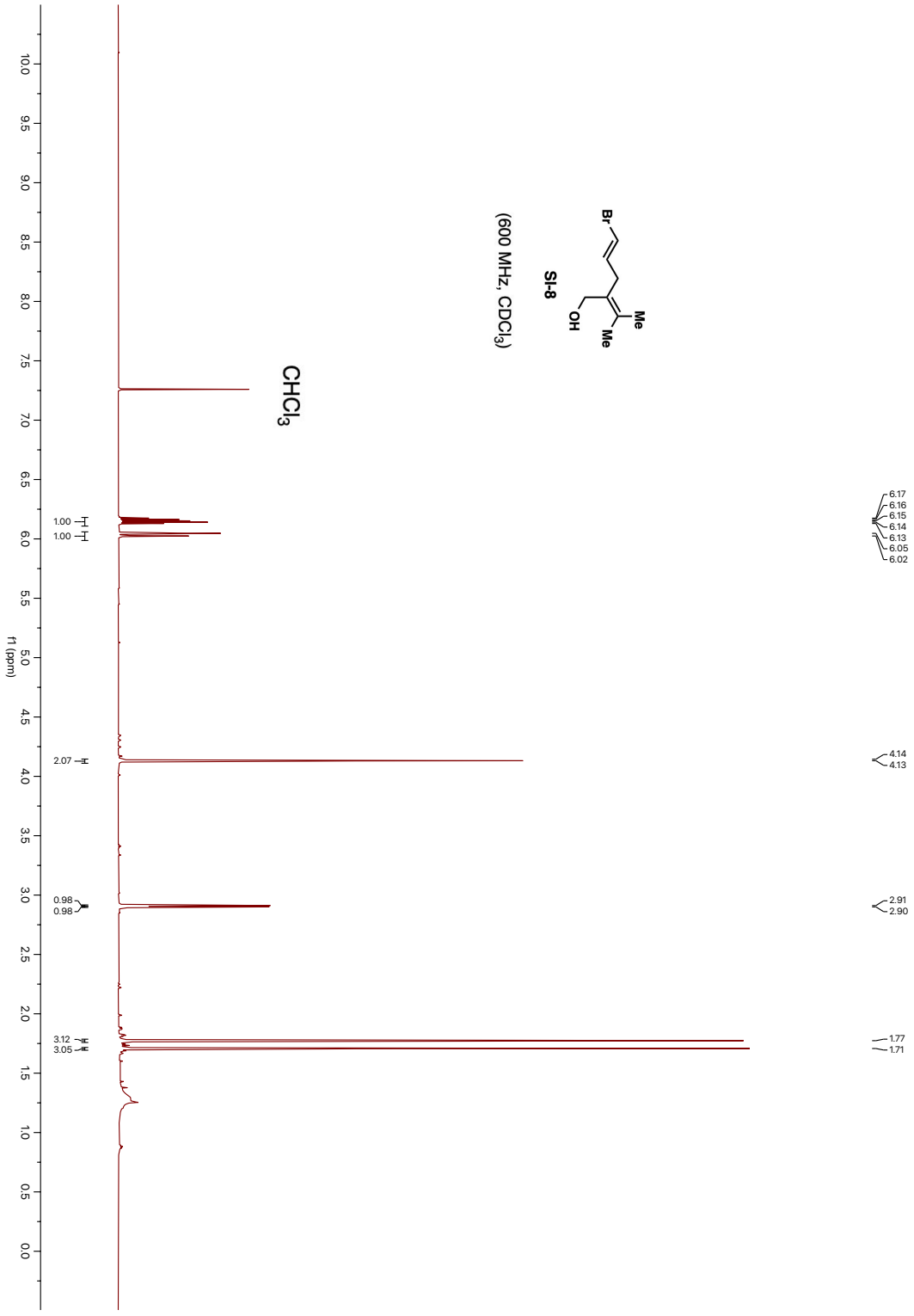

f2 (ppm)
f1 (ppm)

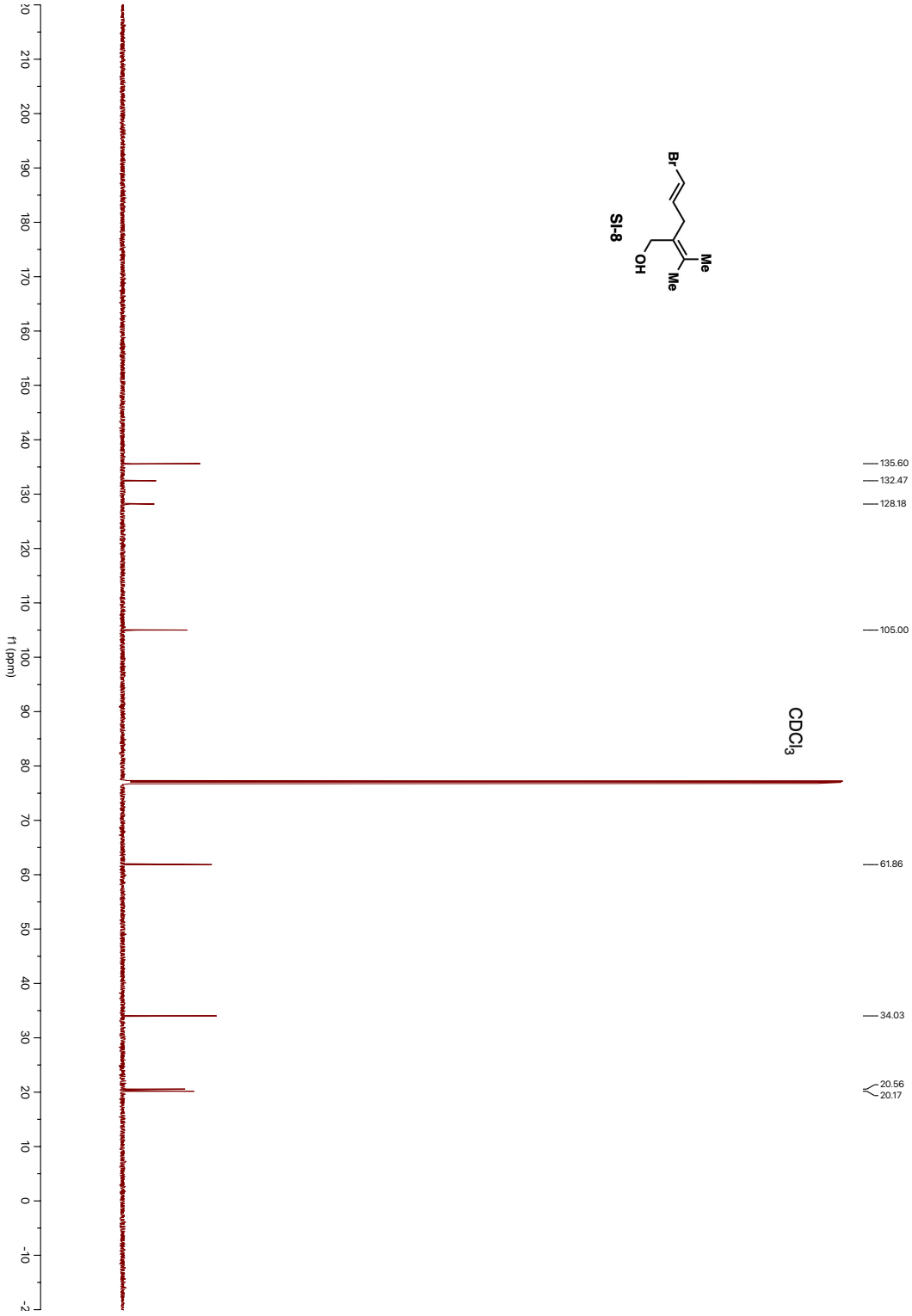

SI-6
(600 MHz, $CDCl_3$)
$CHCl_3$
Me
Me
OTBS
f1 (ppm)
2.21
2.19
1.00
2.95
3.07
9.01
6.22
4.26
3.04
3.03
1.91
1.91
1.90
1.75
1.73
0.91
0.08

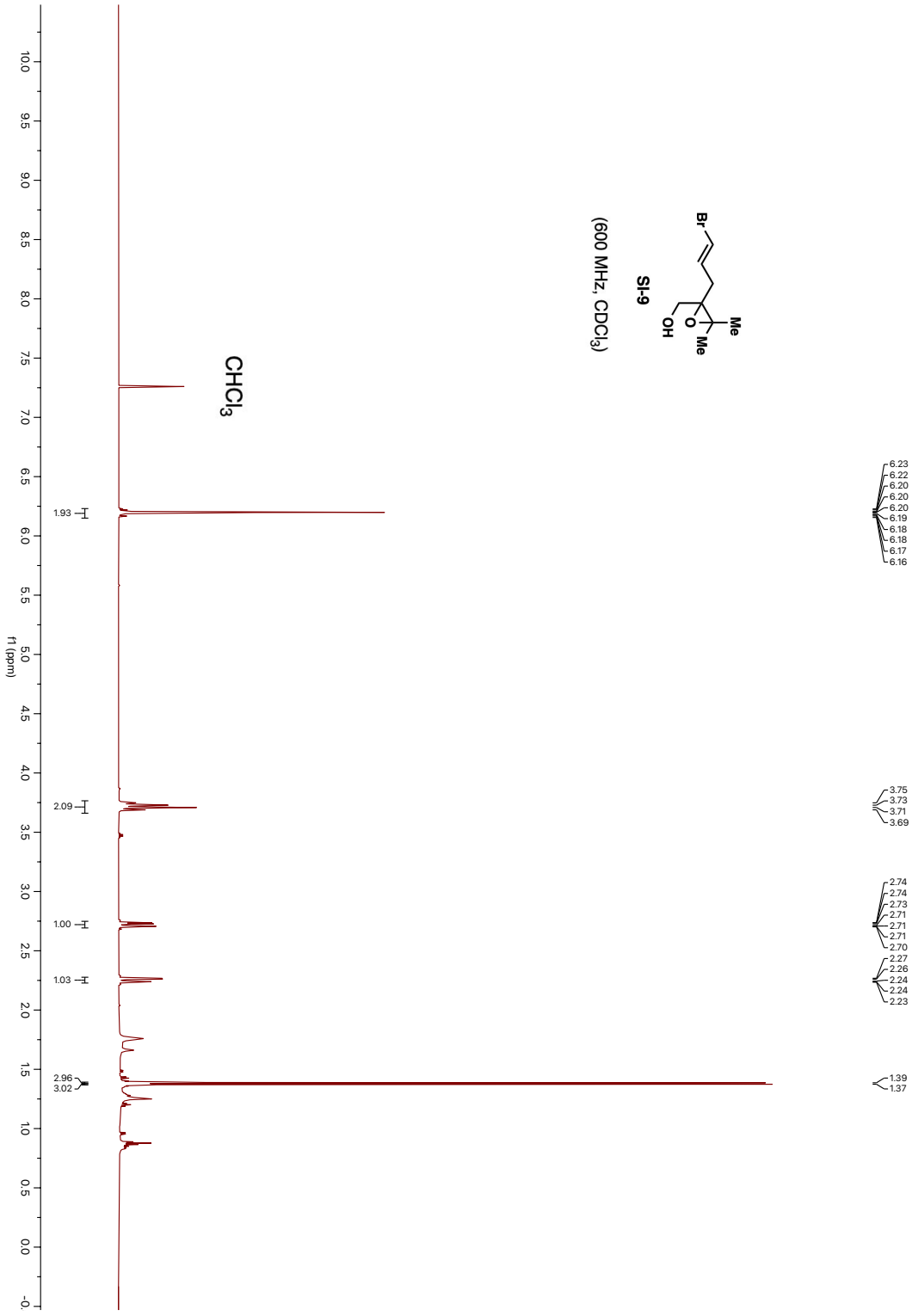

SI-6
OTBS
Me
Me
CDCl3
129.95
127.24
83.08
67.27
61.15
25.98
20.82
20.22
18.52
18.43
-5.30
f1 (ppm)

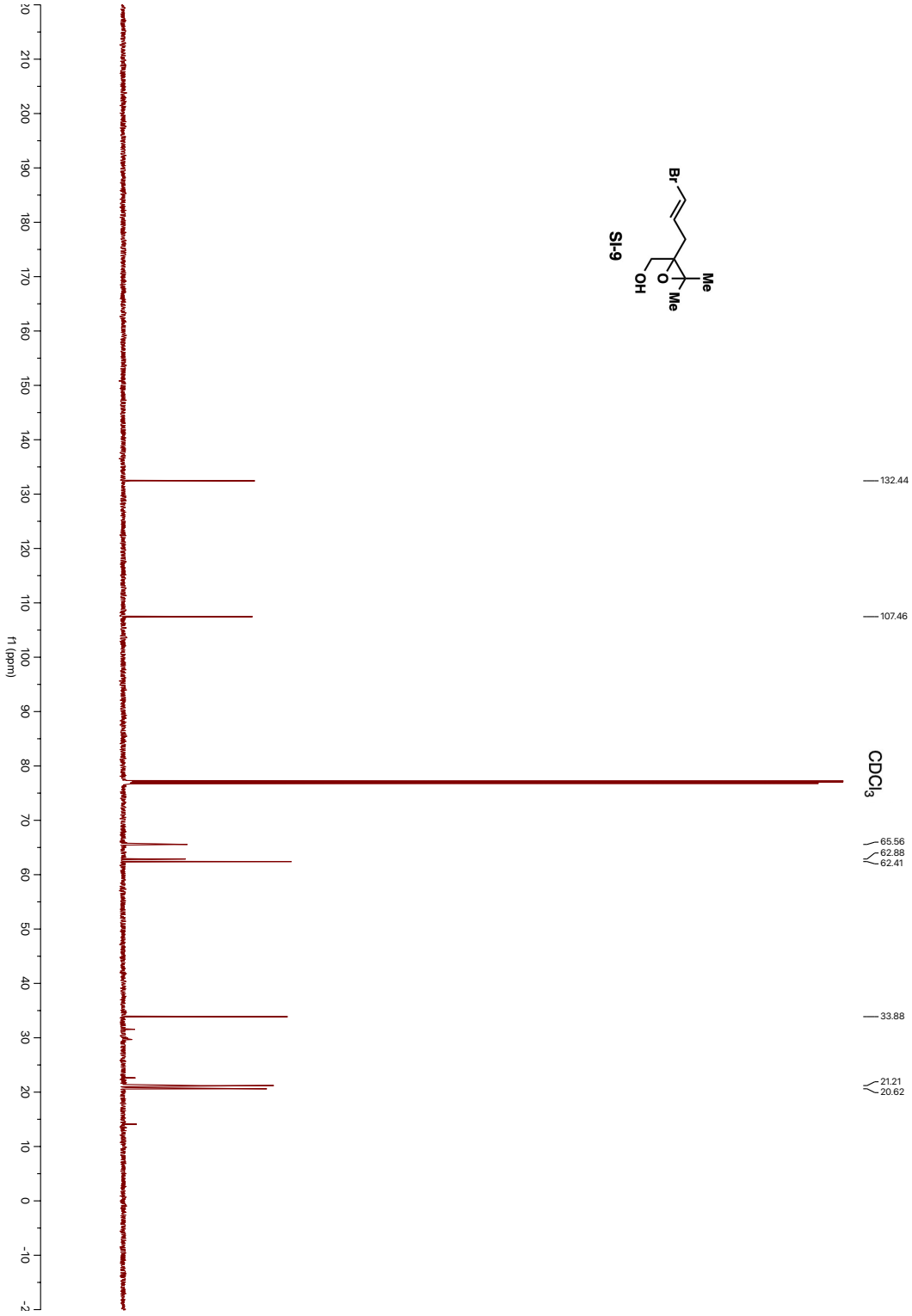

Si-7
(600 MHz, CDCl3)
CHCl3
Br
Me
Me
OTBS
f1 (ppm)
10.0
9.5
9.0
8.5
8.0
7.5
7.0
6.5
6.0
5.5
5.0
4.5
4.0
3.5
3.0
2.5
2.0
1.5
1.0
0.5
0.0
-0.5
1.02
1.00
2.32
1.00
1.02
9.42
6.13
6.16
6.15
6.14
6.12
6.11
6.00
6.00
5.99
5.99
5.98
5.97
5.97
4.13
2.88
2.87
1.71
1.68
0.90
0.06

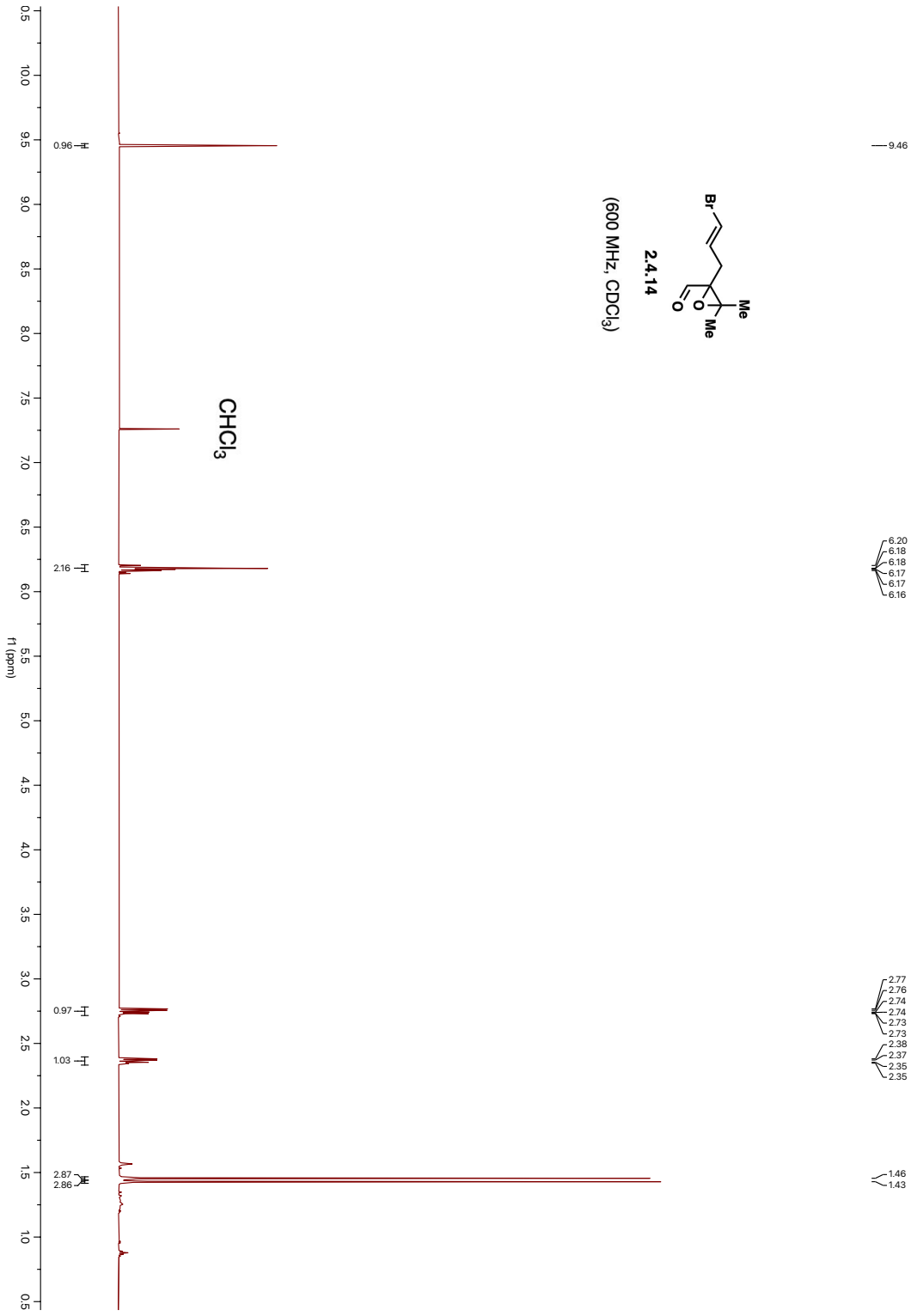

Si-7
OTBS
Me
Me
Br
CDCl3
135.87
129.94
128.28
104.53
61.72
33.14
25.98
20.60
20.10
18.38
-5.29
f1 (ppm)

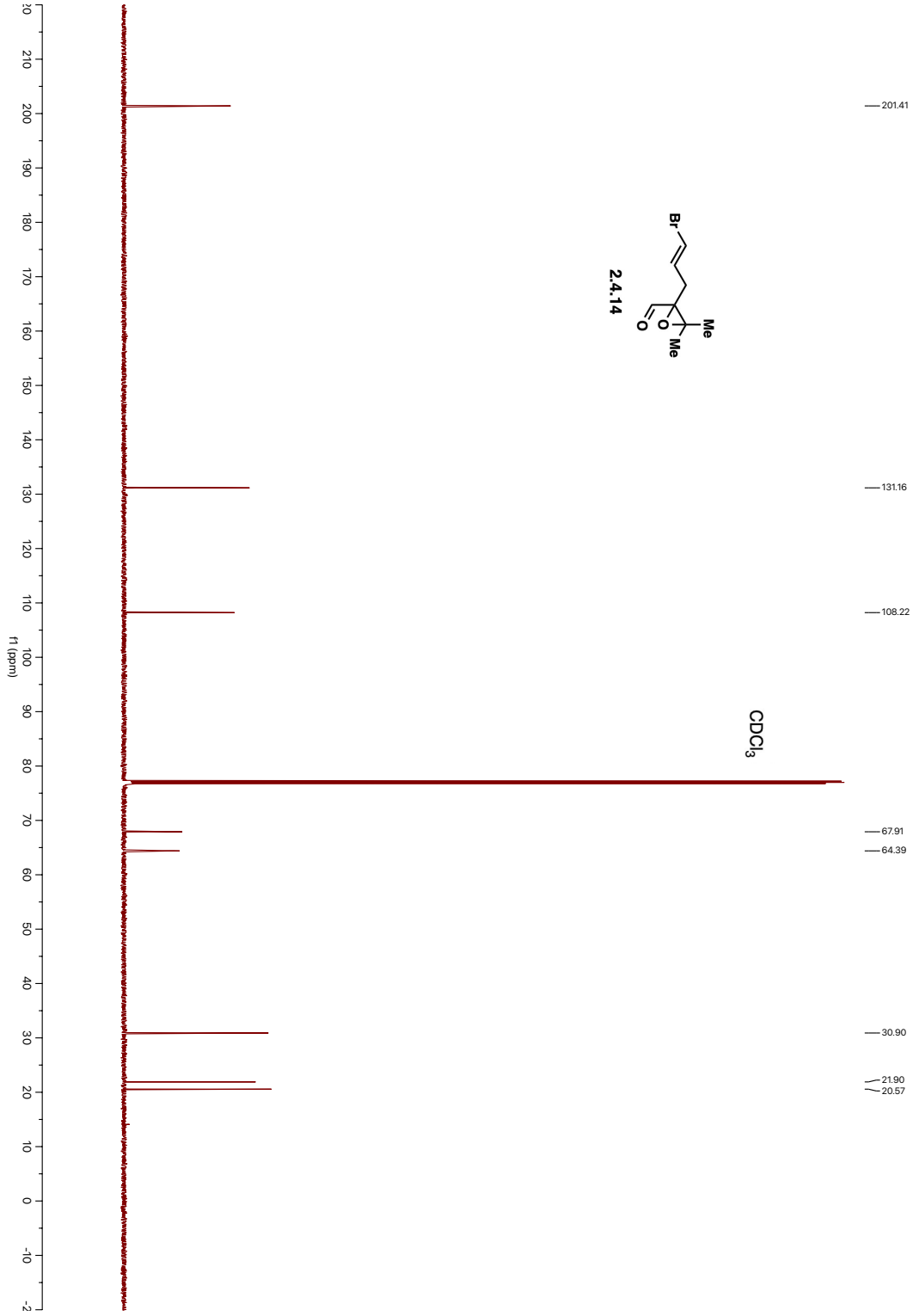

Si-8
(600 MHz, CDCl3)
CHCl3
Br
Me
Me
OH
f1 (ppm)
10.0
9.5
9.0
8.5
8.0
7.5
7.0
6.5
6.0
5.5
5.0
4.5
4.0
3.5
3.0
2.5
2.0
1.5
1.0
0.5
0.0
1.00
1.00
2.07
0.98
0.98
3.12
3.05
6.17
6.16
6.15
6.14
6.13
6.05
6.02
4.14
4.13
2.91
2.90
1.77
1.71

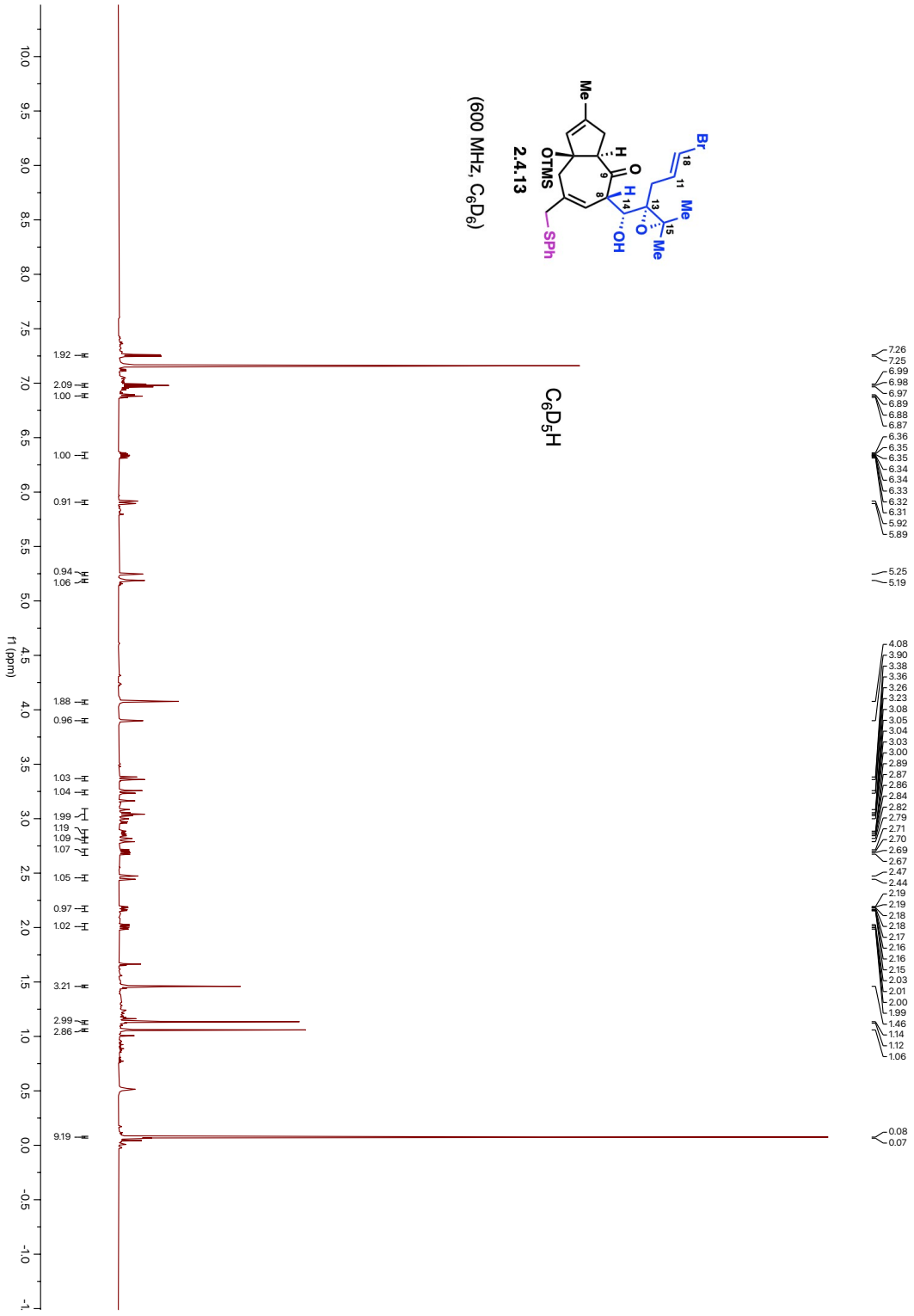

SI-8
Br
Me
Me
OH
CDCl3
135.60
132.47
128.18
105.00
61.86
34.03
20.56
20.17
f1 (ppm)

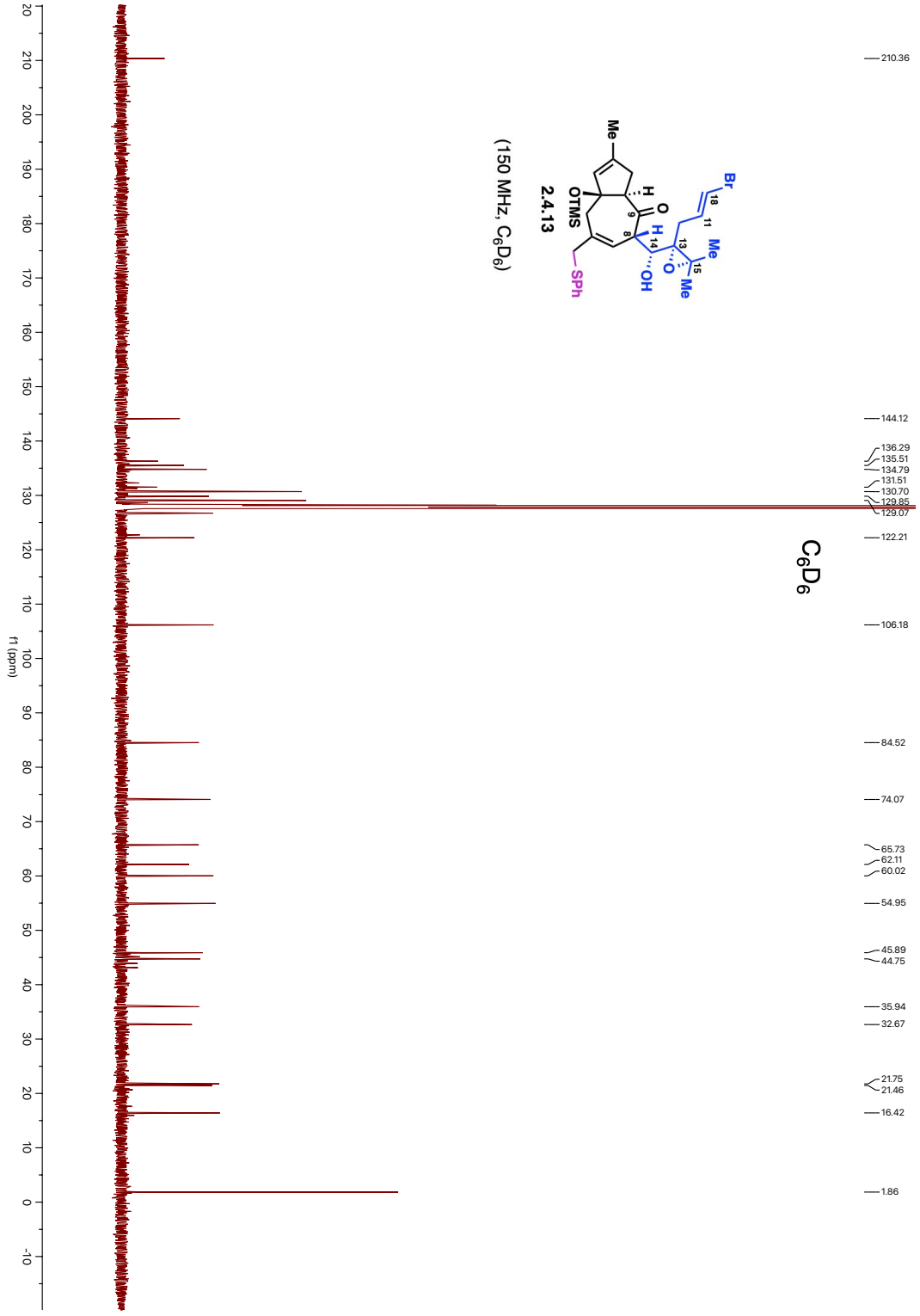

SI-9
(600 MHz, CDCl3)
CHCl3
Br
Me
O
Me
OH
f1 (ppm)
1.93
2.09
1.00
1.03
2.96
3.02
6.23
6.22
6.20
6.20
6.20
6.19
6.18
6.18
6.17
6.16
3.75
3.73
3.71
3.69
2.74
2.74
2.73
2.71
2.71
2.71
2.70
2.27
2.26
2.24
2.24
2.23
1.39
1.37

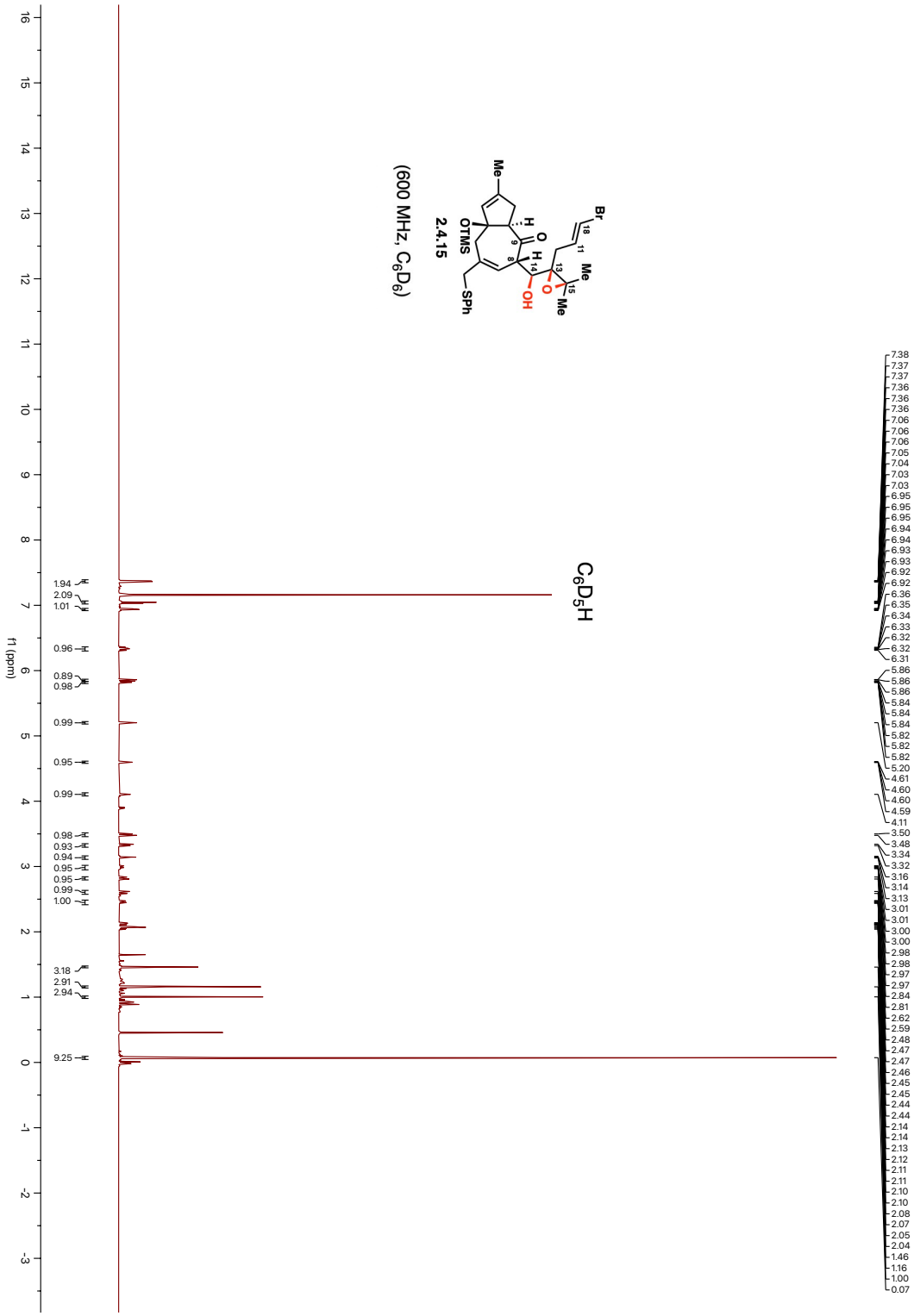

Si-9
Br
Me
Me
OH
O
132.44
107.46
CDCl3
65.56
62.88
62.41
33.88
21.21
20.62
f1 (ppm)

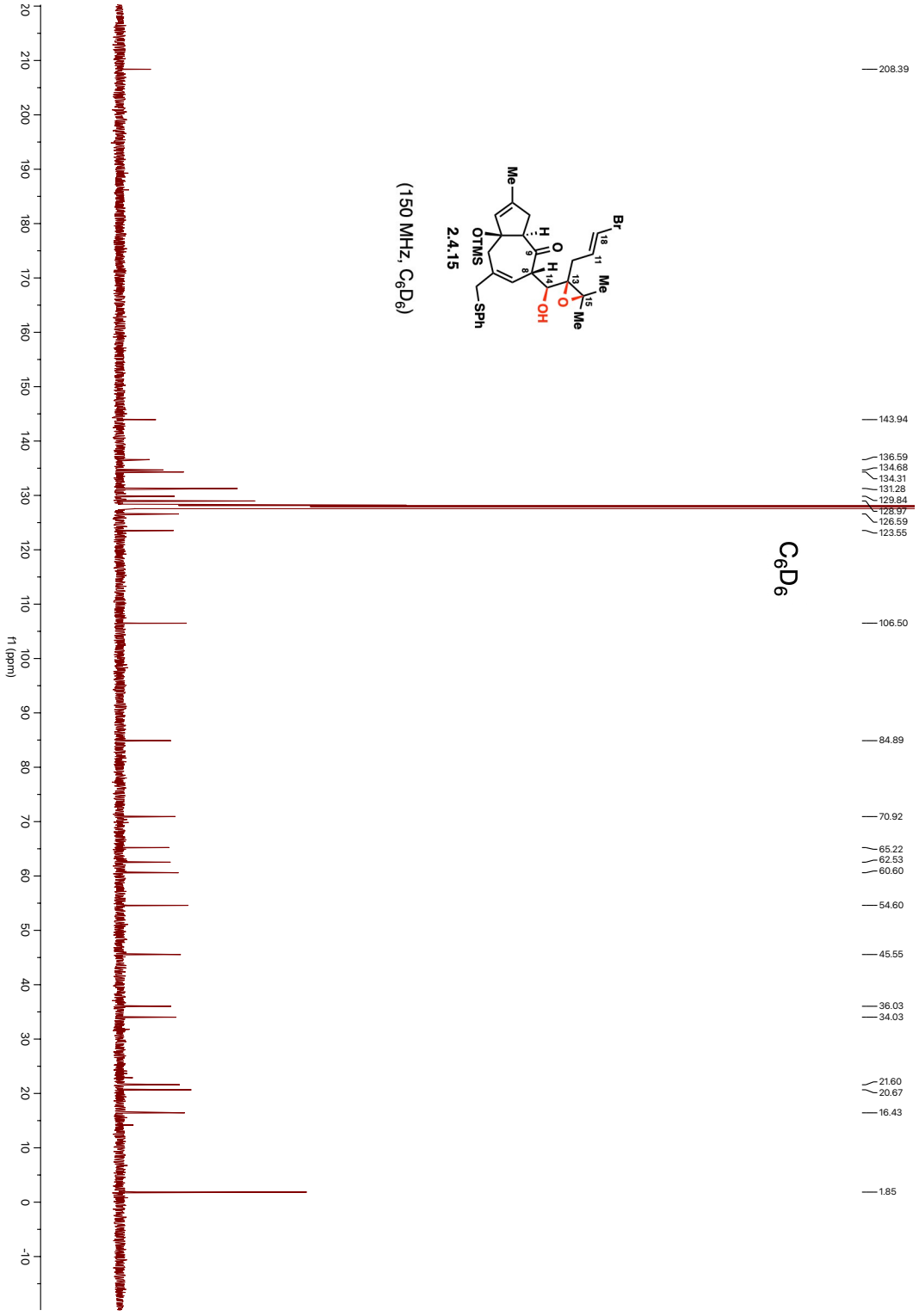

2.4.14
(600 MHz, $CDCl_3$)
Br
Me
O
O
Me
$CHCl_3$
f1 (ppm)
0.96
2.16
0.97
1.03
2.87
2.86
9.46
6.20
6.18
6.18
6.17
6.17
6.16
2.77
2.76
2.74
2.74
2.73
2.73
2.38
2.37
2.35
2.35
1.46
1.43

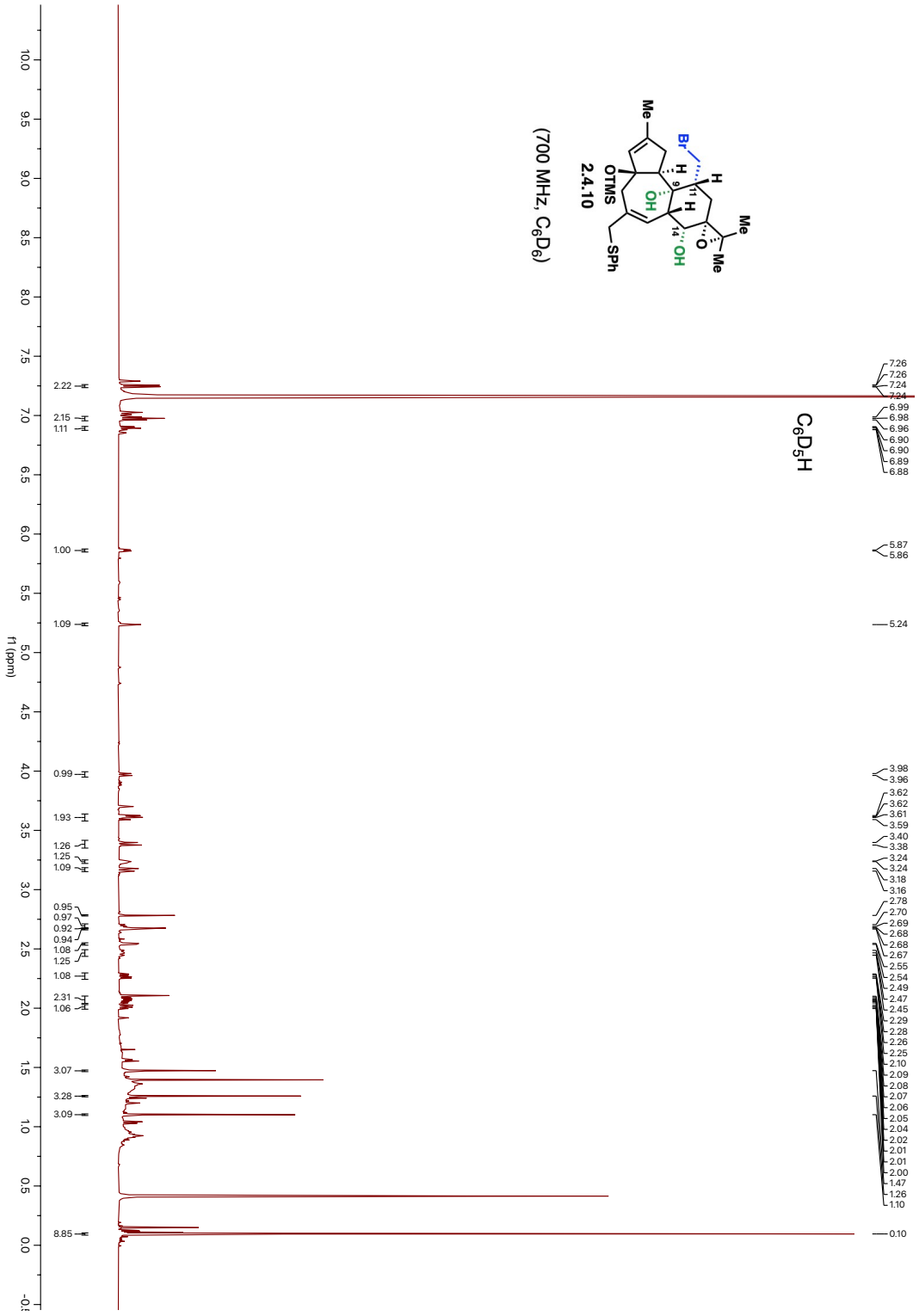

Br
Me
O
O
Me
2.4.14
CDCl3
201.41
131.16
108.22
67.91
64.39
30.90
21.90
20.57
f1 (ppm)

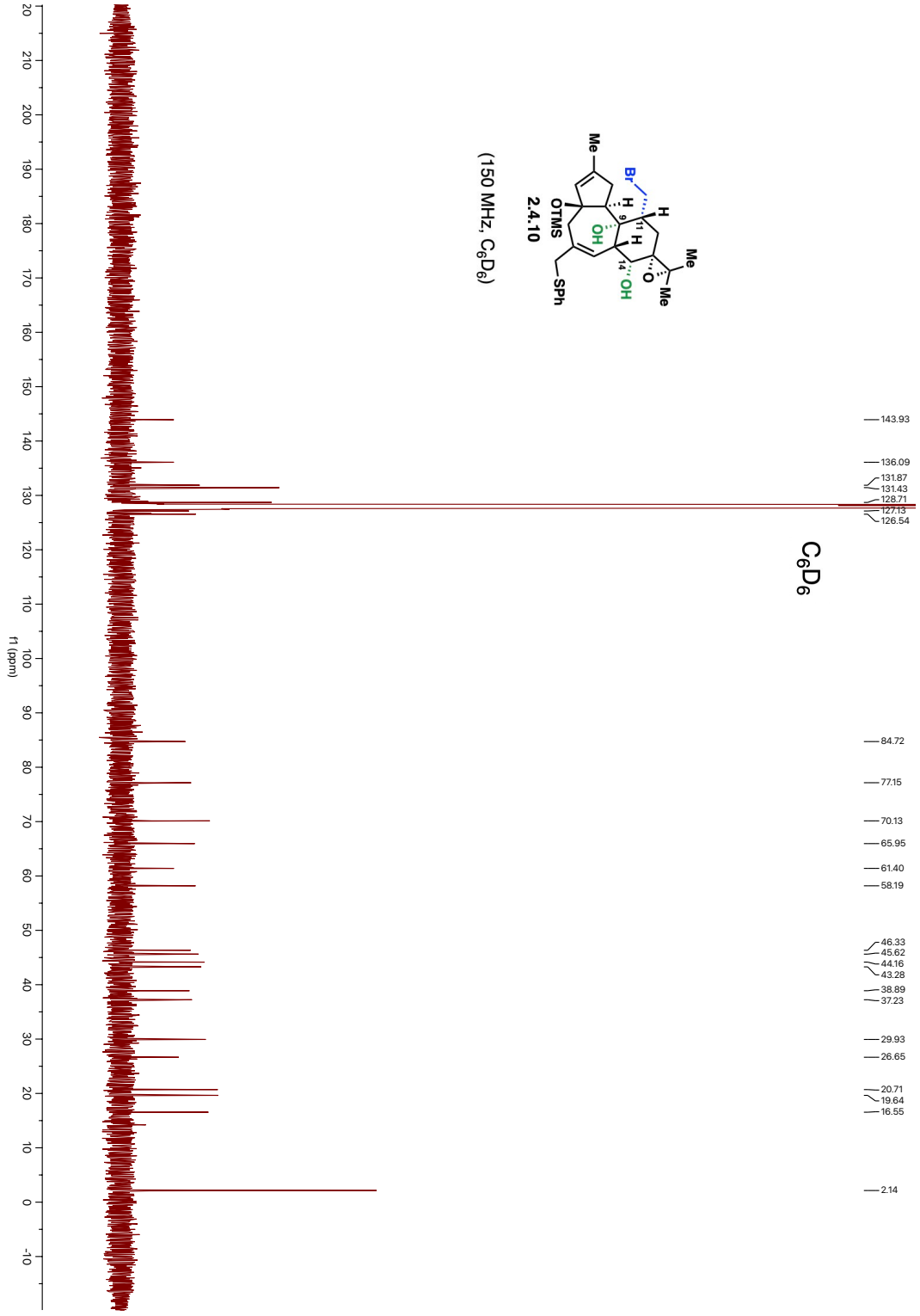

2.4.13
(600 MHz, C_6D_6)
C_6D_5H
f1 (ppm)

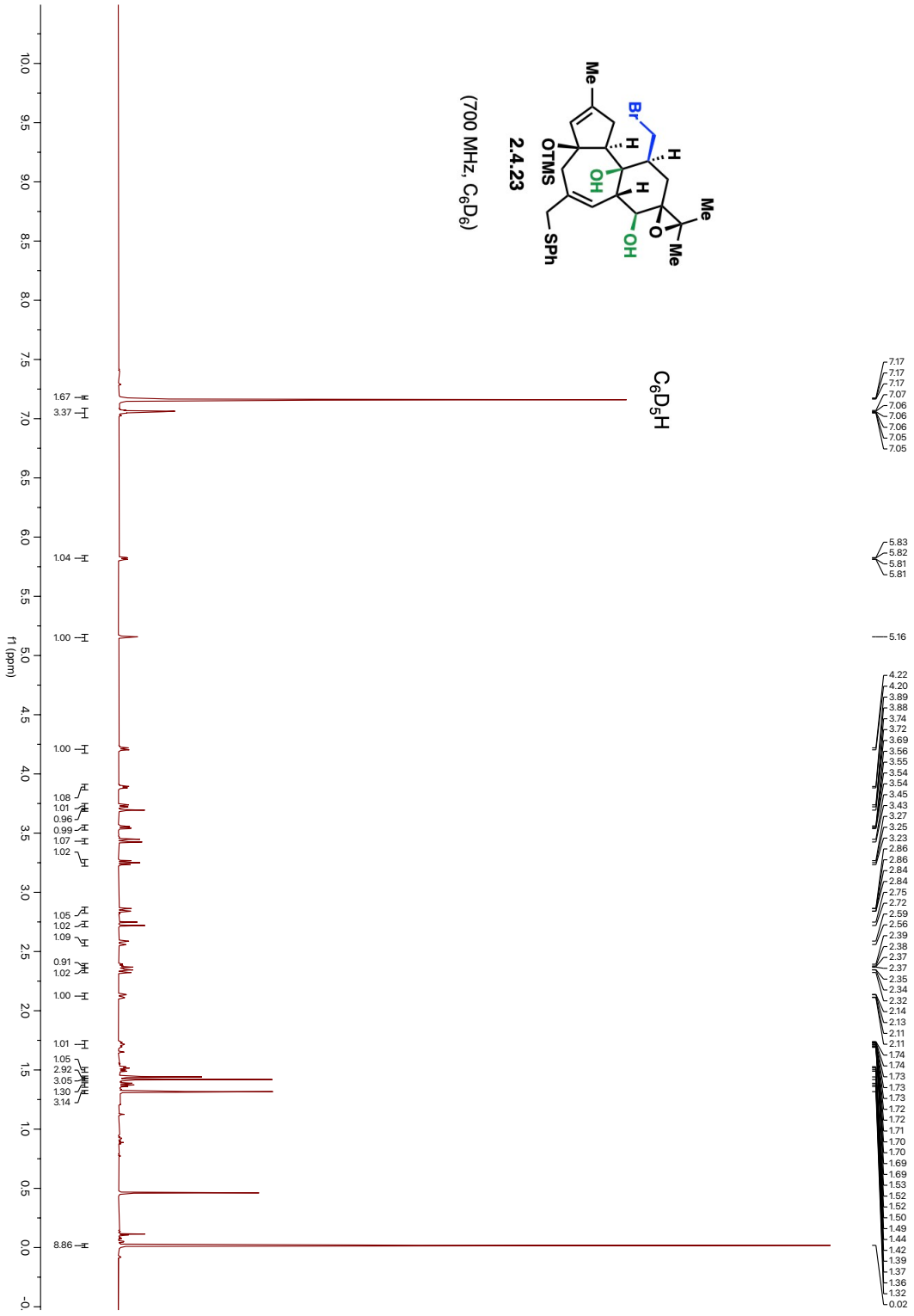

2.4.13
(150 MHz, C6D6)
C6D6
f1 (ppm)
210.36
144.12
136.29
135.51
134.79
131.51
130.70
129.85
129.07
122.21
106.18
84.52
74.07
65.73
62.11
60.02
54.95
45.89
44.75
35.94
32.67
21.75
21.46
16.42
1.86

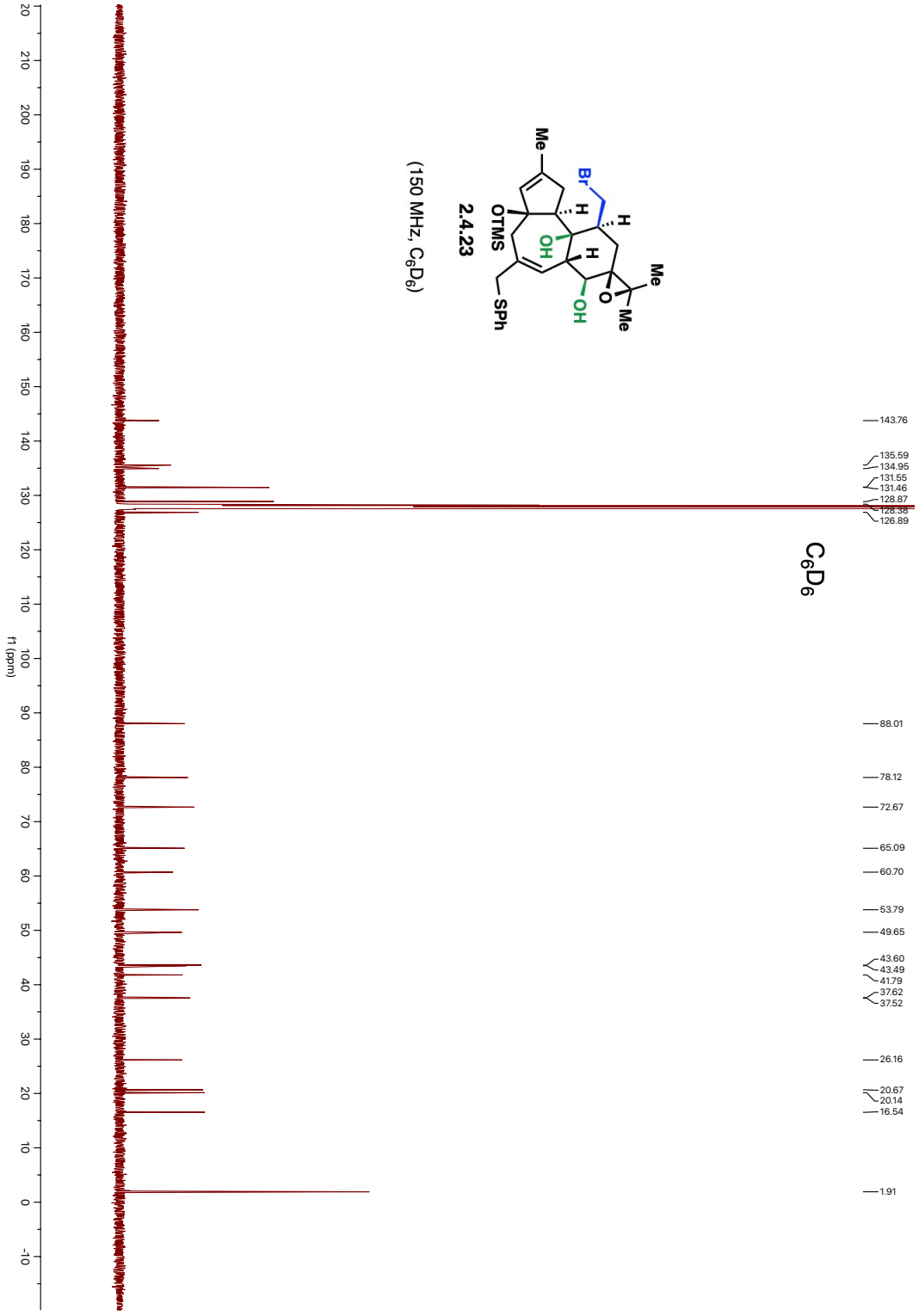

2.4.15
(600 MHz, C_6D_6)
C_6D_5H
f1 (ppm)

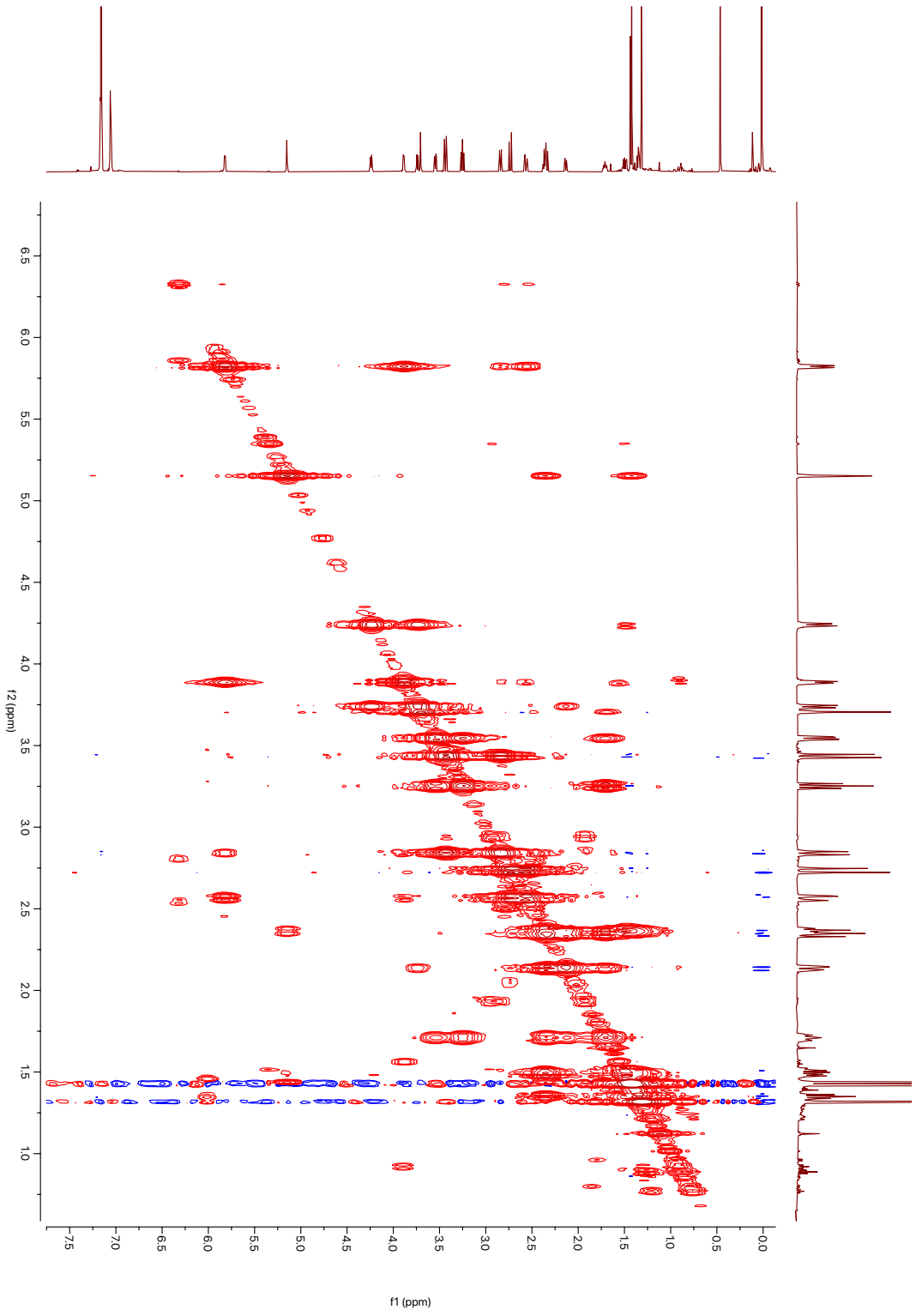

2.4.15
(150 MHz, C6D6)
C6D6
208.39
143.94
136.59
134.68
134.31
131.28
129.84
128.97
126.59
123.55
106.50
84.89
70.92
65.22
62.53
60.60
54.60
45.55
36.03
34.03
21.60
20.67
16.43
1.85
f1 (ppm)

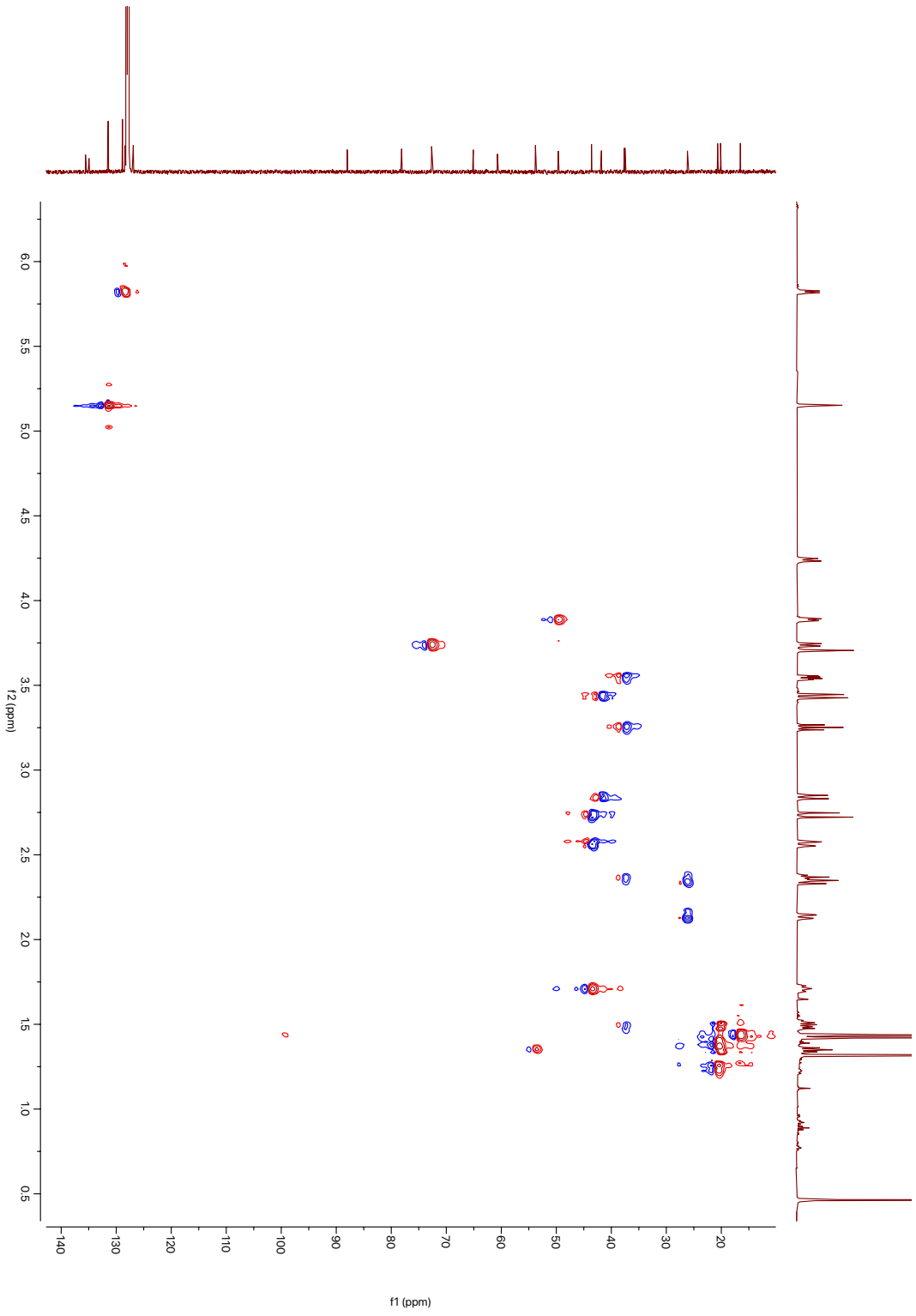

2.4.10
(700 MHz, C_6D_6)
C_6D_5H
f1 (ppm)

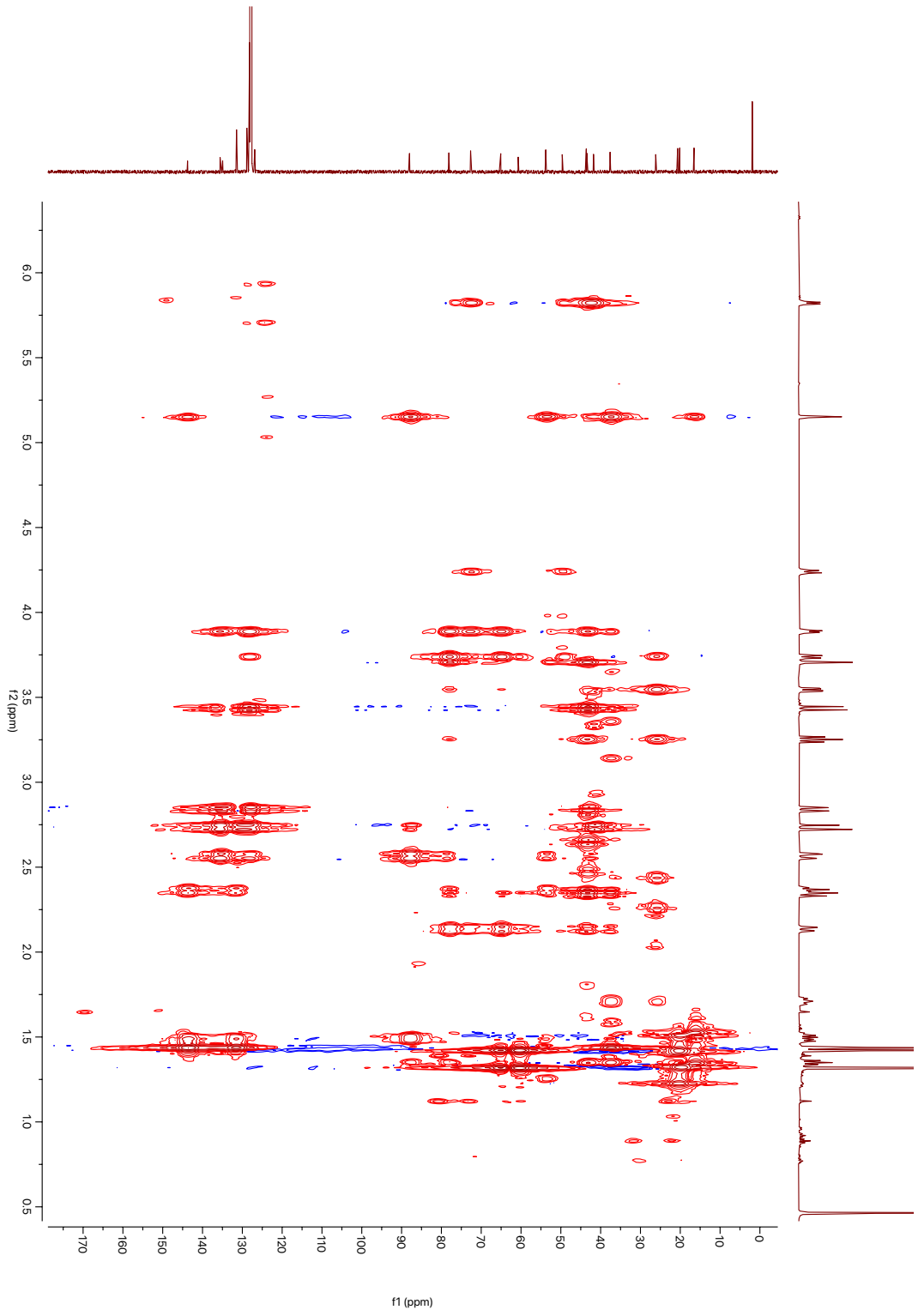

2.4.10
(150 MHz, C6D6)
C6D6
f1 (ppm)
143.93
136.09
131.87
131.43
128.71
127.13
126.54
84.72
77.15
70.13
65.95
61.40
58.19
46.33
45.62
44.16
43.28
38.89
37.23
29.93
26.65
20.71
19.64
16.55
2.14

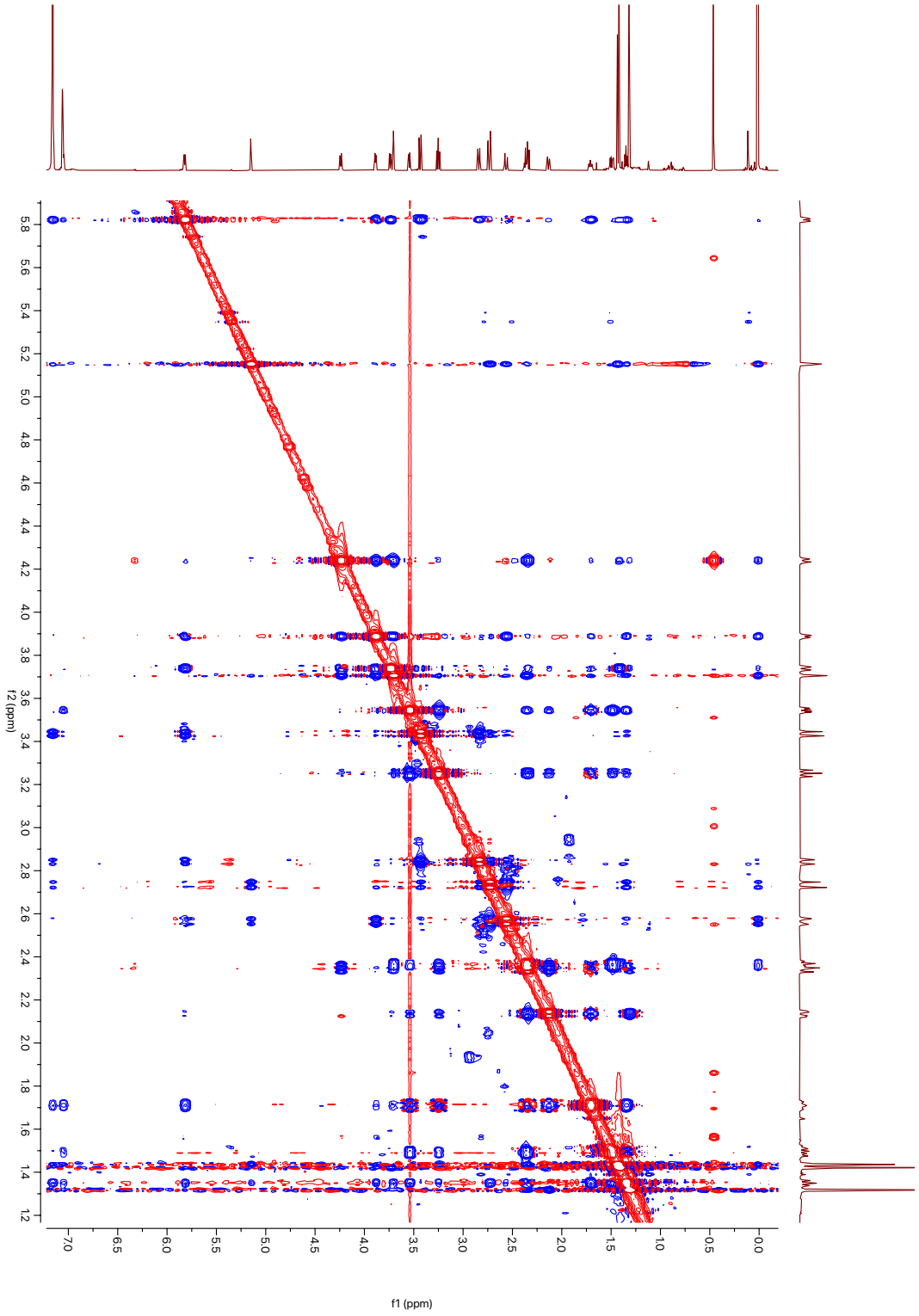

(700 MHz, C_6D_6)
2.4.23
C_6D_5H
f1 (ppm)

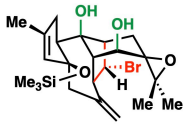

(150 MHz, C6D6)
2.4.23
C6D6
f1 (ppm)
143.76
135.59
134.95
131.55
131.46
128.87
128.38
126.89
88.01
78.12
72.67
65.09
60.70
53.79
49.65
43.60
43.49
41.79
37.62
37.52
26.16
20.67
20.14
16.54
1.91


f2 (ppm)
f1 (ppm)


f2 (ppm)
f1 (ppm)

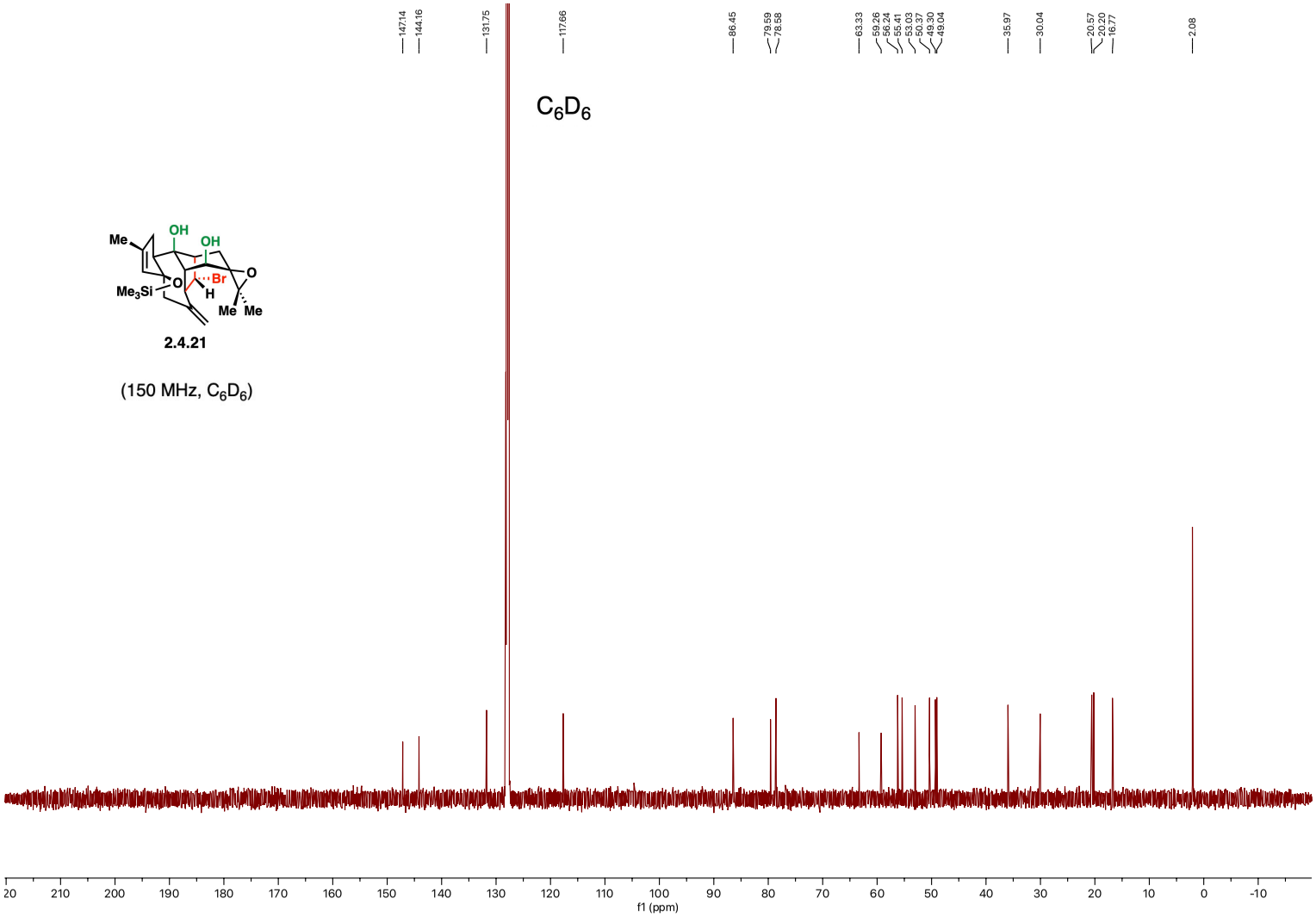

f2 (ppm)
6.0
5.5
5.0
4.5
4.0
3.5
3.0
2.5
2.0
1.5
1.0
0.5
f1 (ppm)
170
160
150
140
130
120
110
100
90
80
70
60
50
40
30
20
10
0

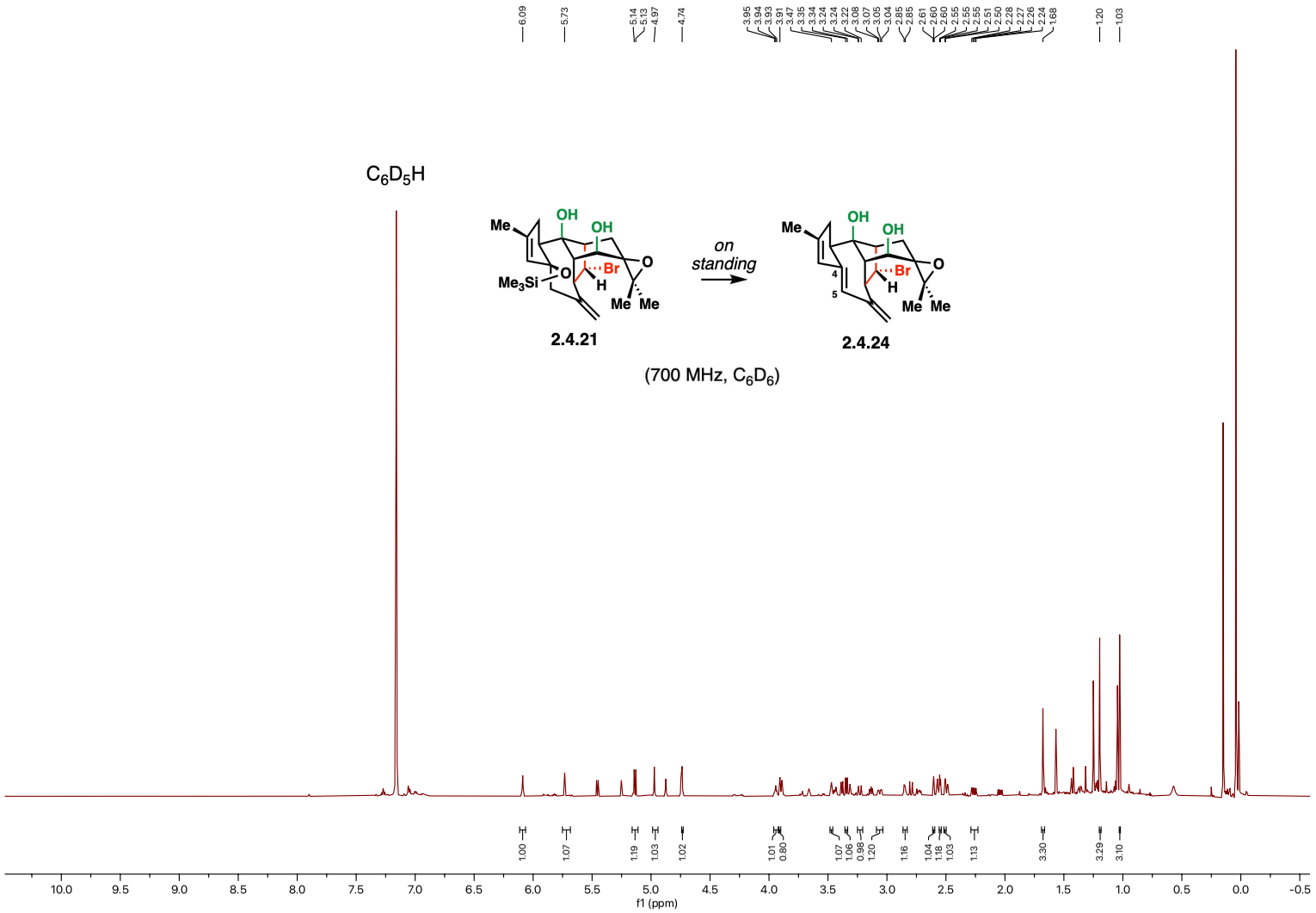

f2 (ppm)
f1 (ppm)

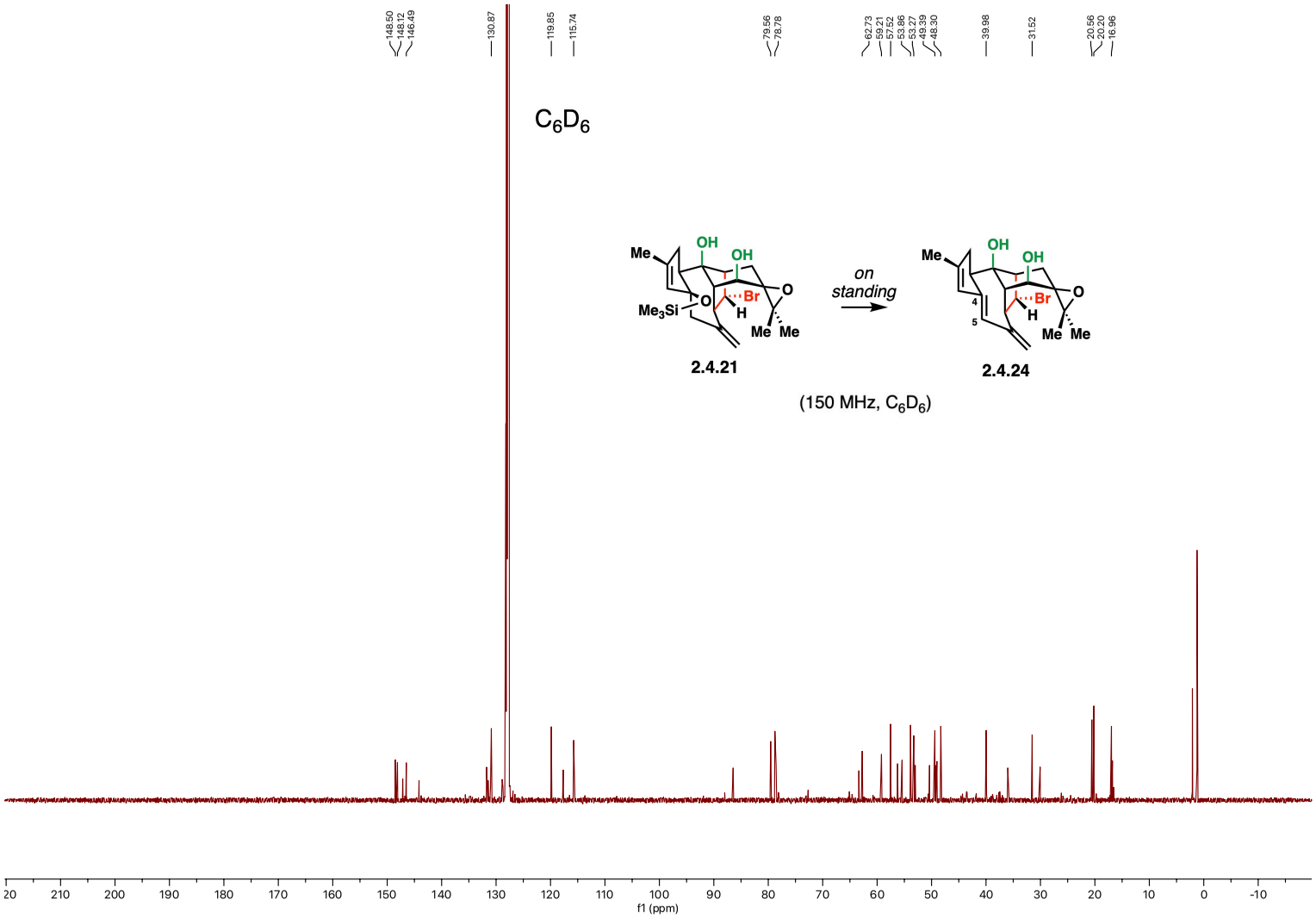


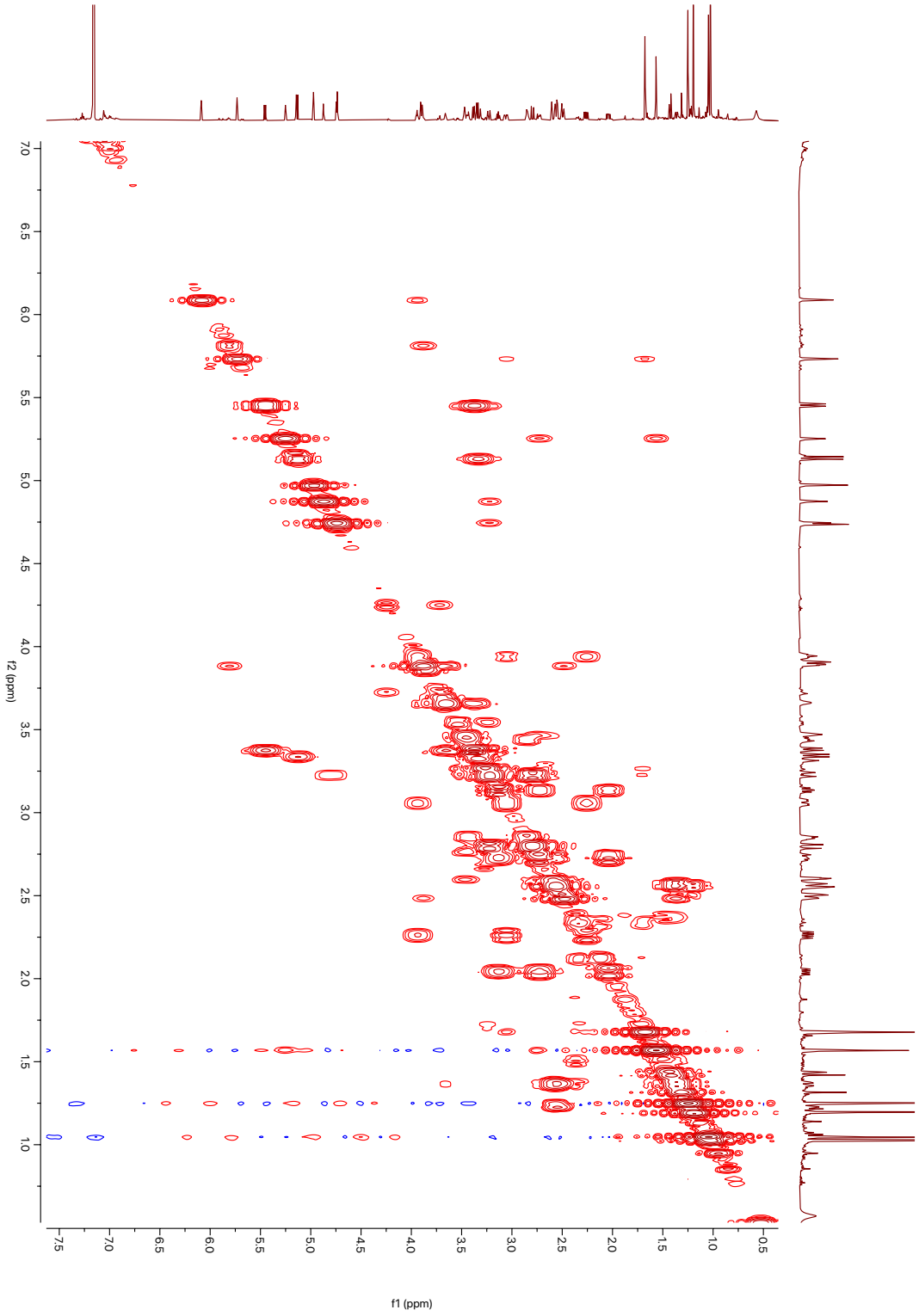
2.4.21

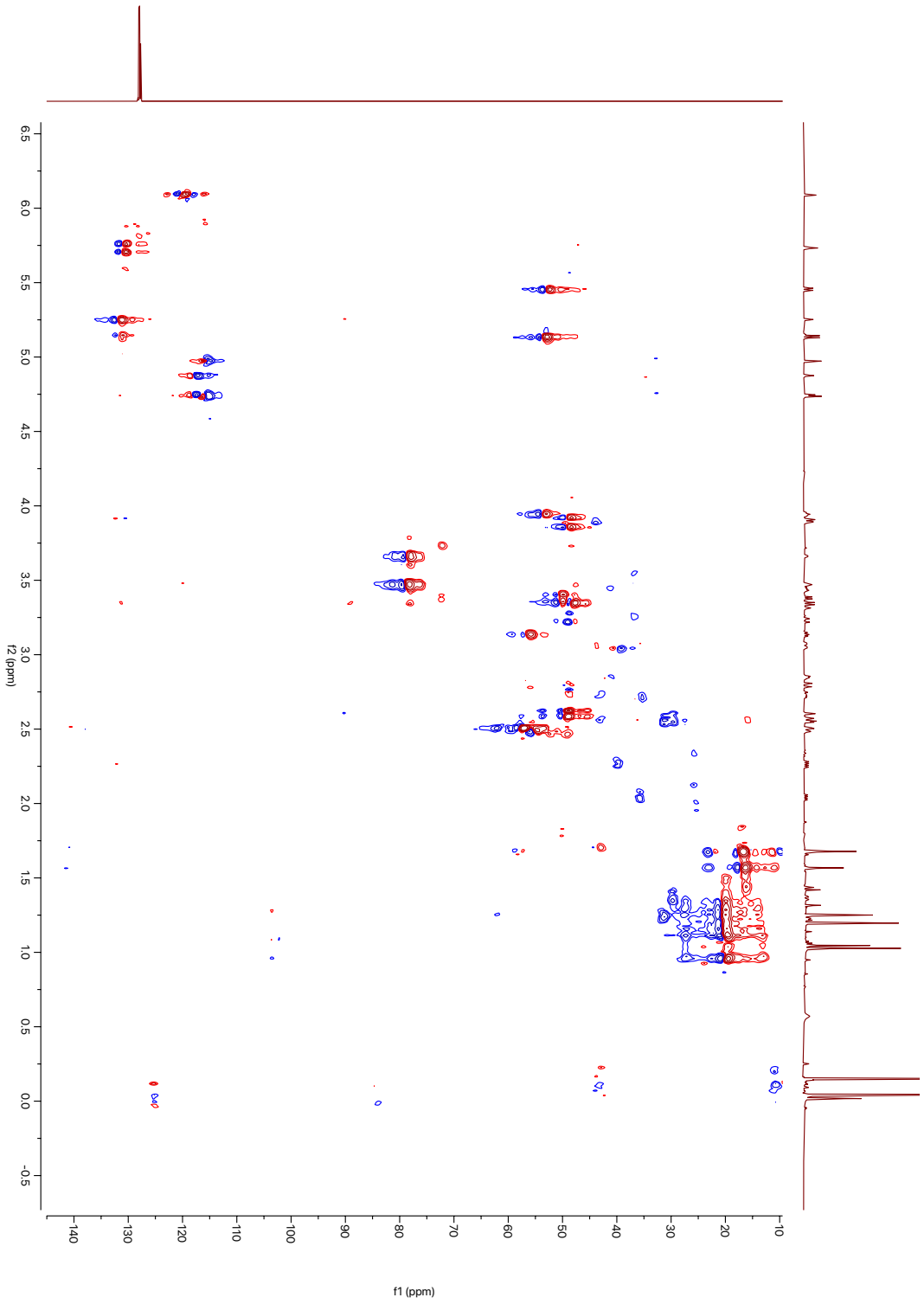
(700 MHz, C_6D_6)

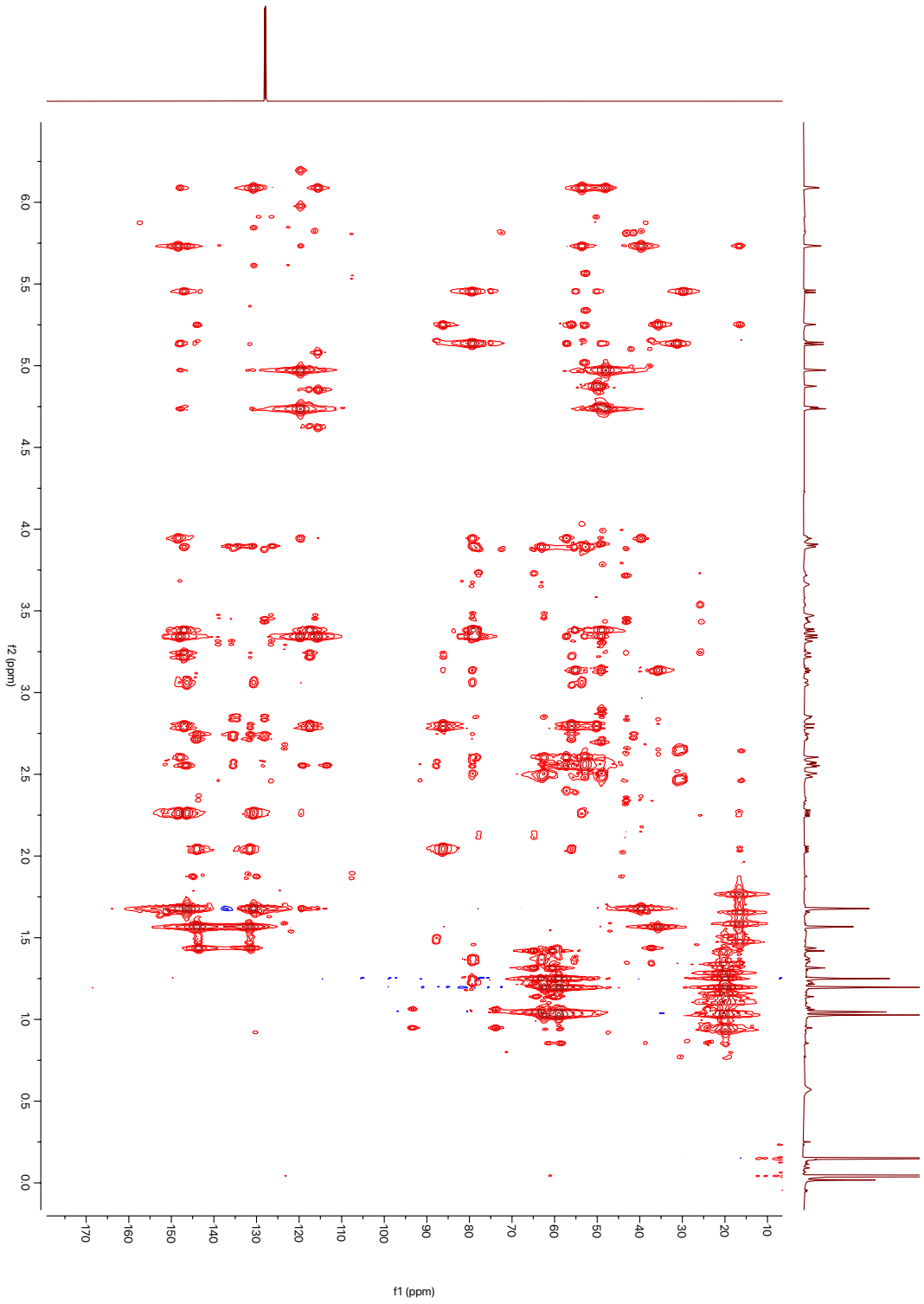

147.14
144.16
131.75
117.66
86.45
79.59
78.58
63.33
59.26
56.24
55.41
53.03
50.37
49.30
49.04
35.97
30.04
20.57
20.20
16.77
2.08
C6D6
OH
OH
Me
Me3Si
O
Br
H
O
Me
Me
2.4.21
(150 MHz, C6D6)
f1 (ppm)

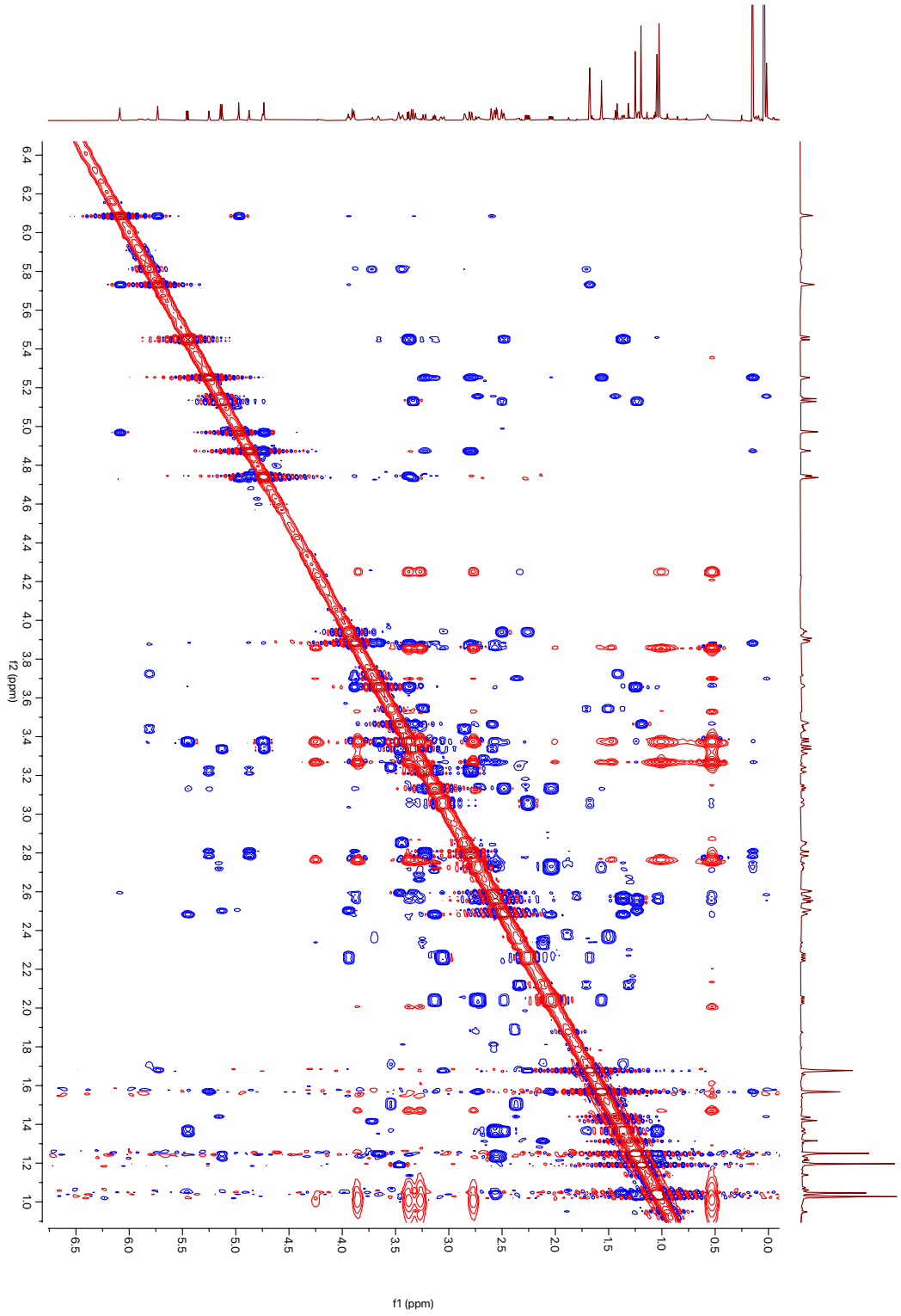

6.09
5.73
5.14
5.13
4.97
4.74
3.95
3.94
3.93
3.91
3.47
3.35
3.34
3.24
3.24
3.22
3.08
3.07
3.05
3.04
2.85
2.85
2.61
2.60
2.60
2.55
2.55
2.55
2.51
2.50
2.28
2.27
2.26
2.24
1.68
1.20
1.03
C6D5H
Me
OH
OH
O
Br
H
Me3Si
O
Me
Me
2.4.21
on
standing
Me
OH
OH
4
5
Br
H
O
Me
Me
2.4.24
(700 MHz, C6D6)
1.00
1.07
1.19
1.03
1.02
1.01
0.80
1.07
1.06
0.98
1.20
1.16
1.04
1.18
1.03
1.13
3.30
3.29
3.10
10.0
9.5
9.0
8.5
8.0
7.5
7.0
6.5
6.0
5.5
5.0
4.5
4.0
3.5
3.0
2.5
2.0
1.5
1.0
0.5
0.0
-0.5
f1 (ppm)

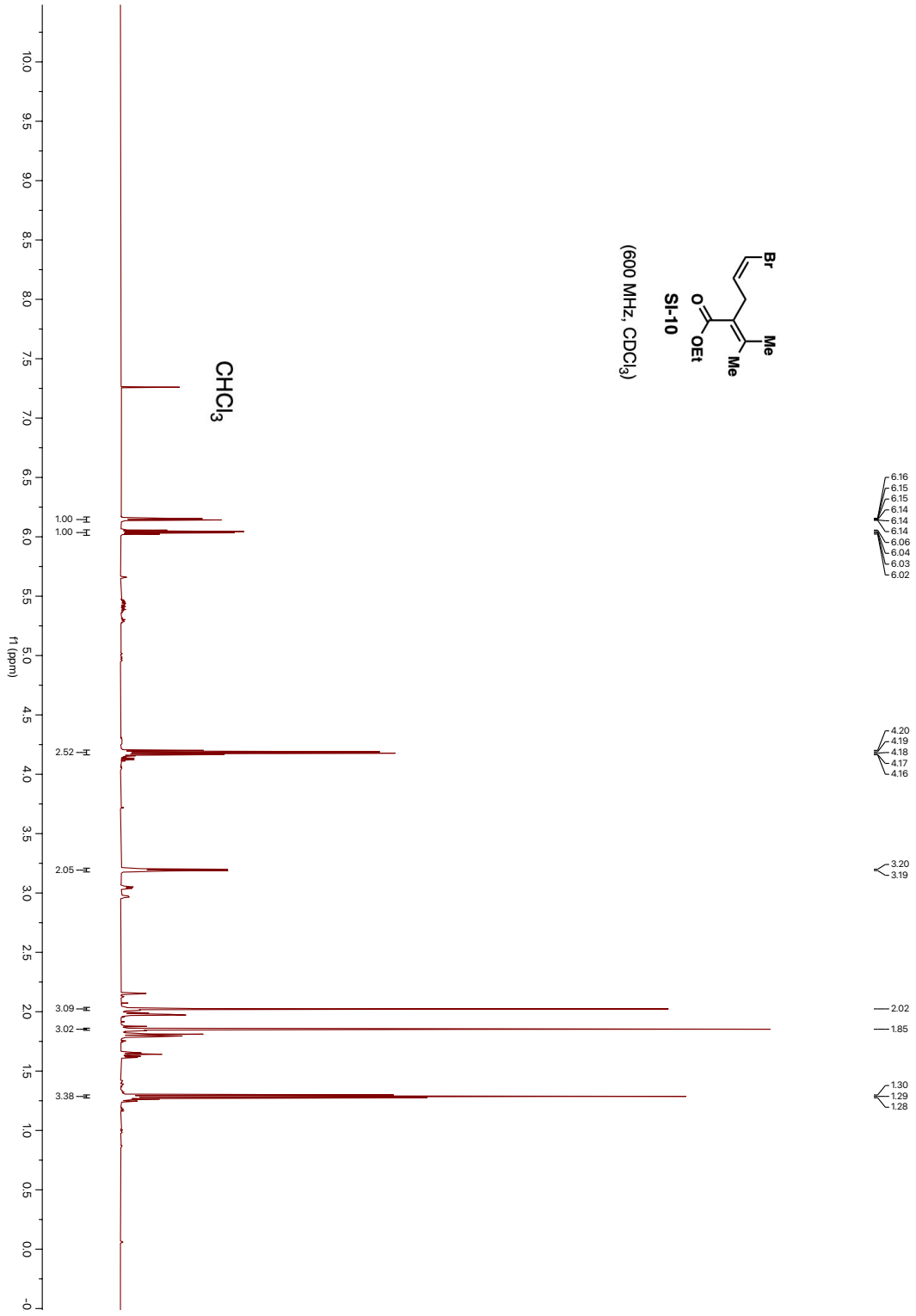

148.50
147.72
146.49
130.87
119.85
115.74
79.56
78.78
62.73
59.21
57.52
53.86
53.27
49.39
48.30
39.98
31.52
20.56
20.20
16.96
C6D6
Me
OH
OH
O
Br
H
Me3Si
Me Me
2.4.21
on
standing
4
5
2.4.24
(150 MHz, C6D6)
f1 (ppm)

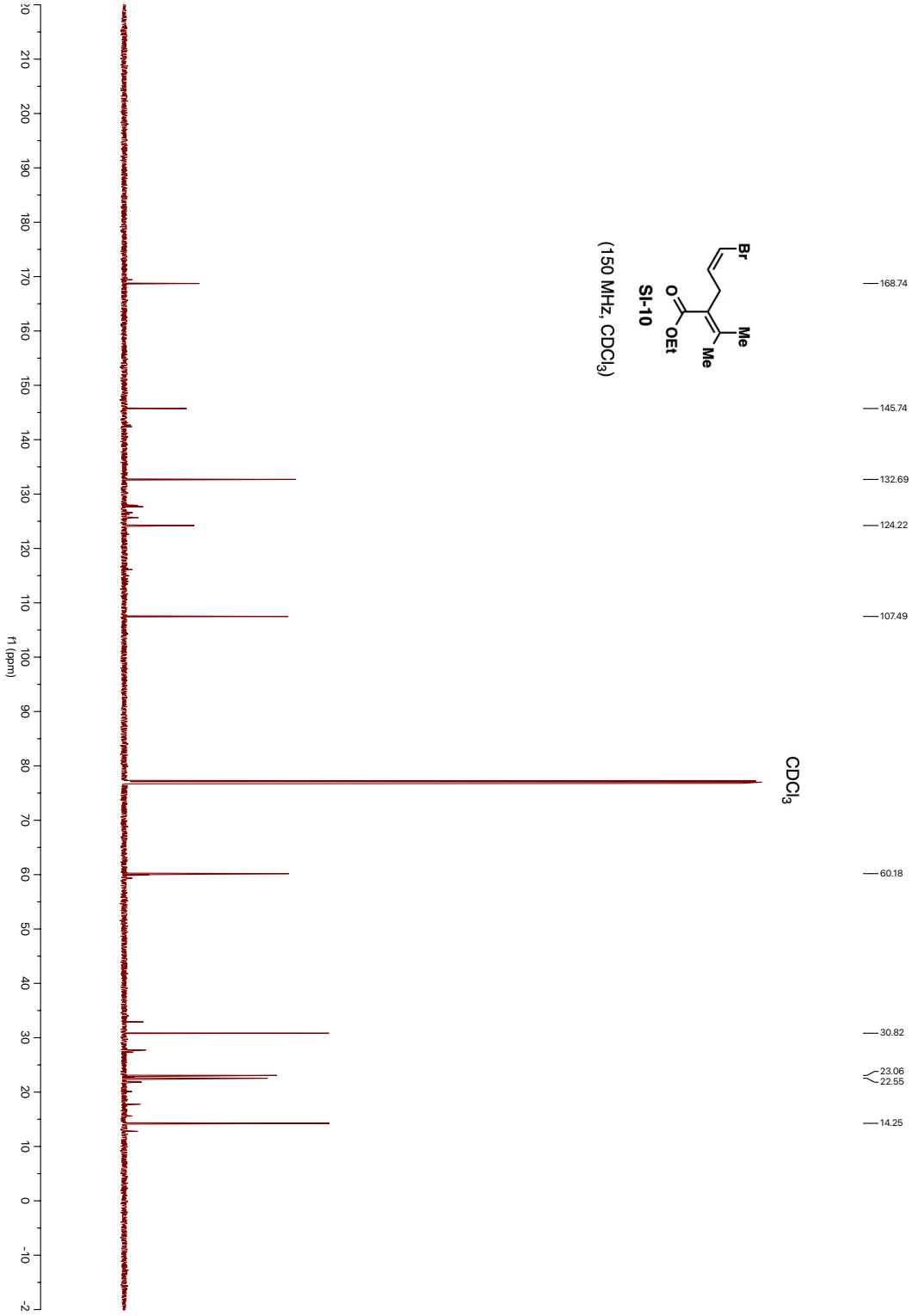

f2 (ppm)
f1 (ppm)

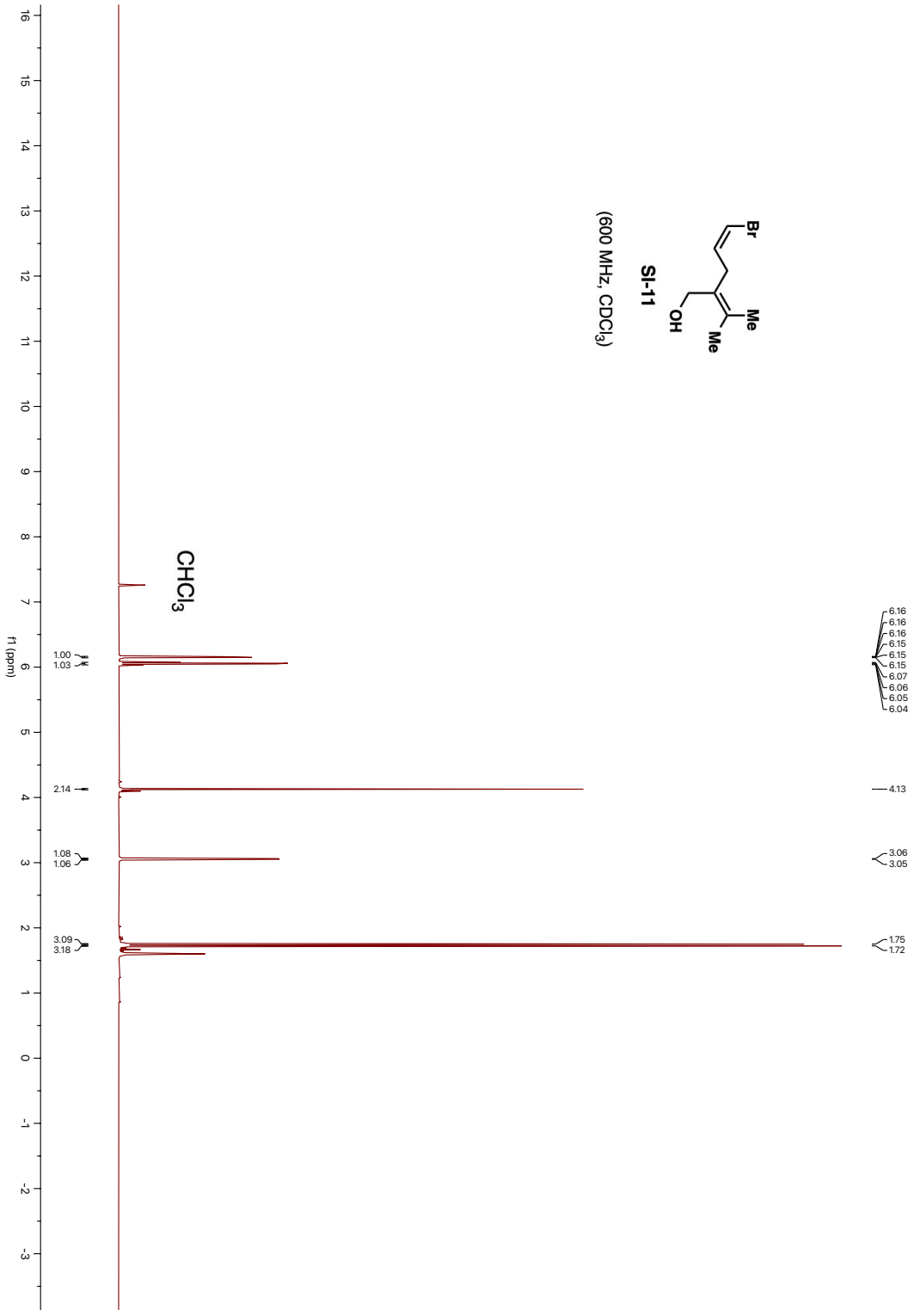

f2 (ppm)
f1 (ppm)

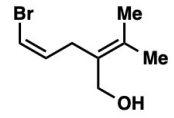

f2 (ppm)
f1 (ppm)


f2 (ppm)
f1 (ppm)


SI-10
(600 MHz, $CDCl_3$)
$CHCl_3$
f1 (ppm)
1.00
1.00
2.52
2.05
3.09
3.02
3.38
6.16
6.15
6.15
6.14
6.14
6.14
6.06
6.04
6.03
6.02
4.20
4.19
4.18
4.17
4.16
3.20
3.19
2.02
1.85
1.30
1.29
1.28

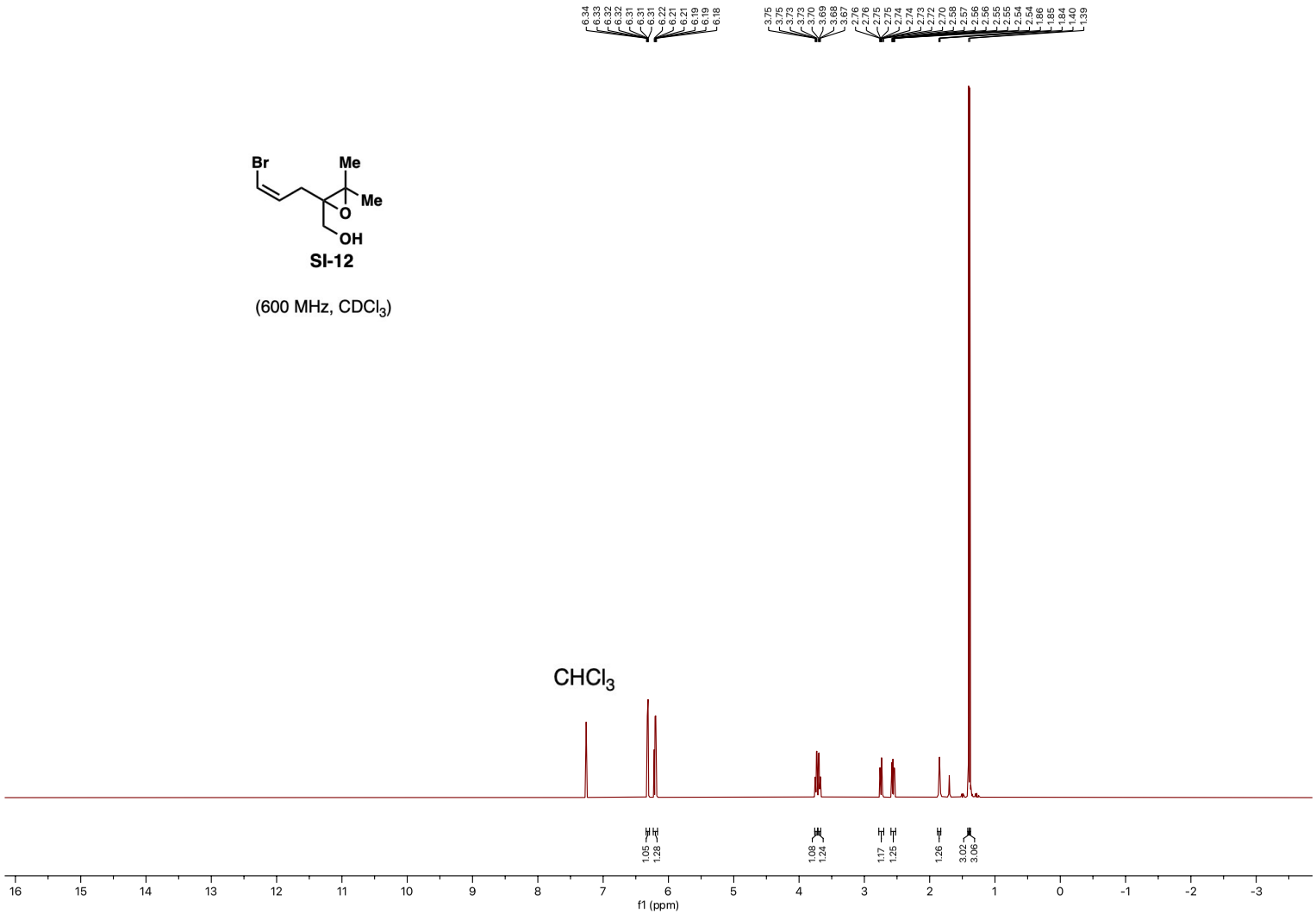

Br
Me
Me
O
OEt
SI-10
(150 MHz, CDCl3)
168.74
145.74
132.69
124.22
107.49
CDCl3
60.18
30.82
23.06
22.55
14.25
f1 (ppm)

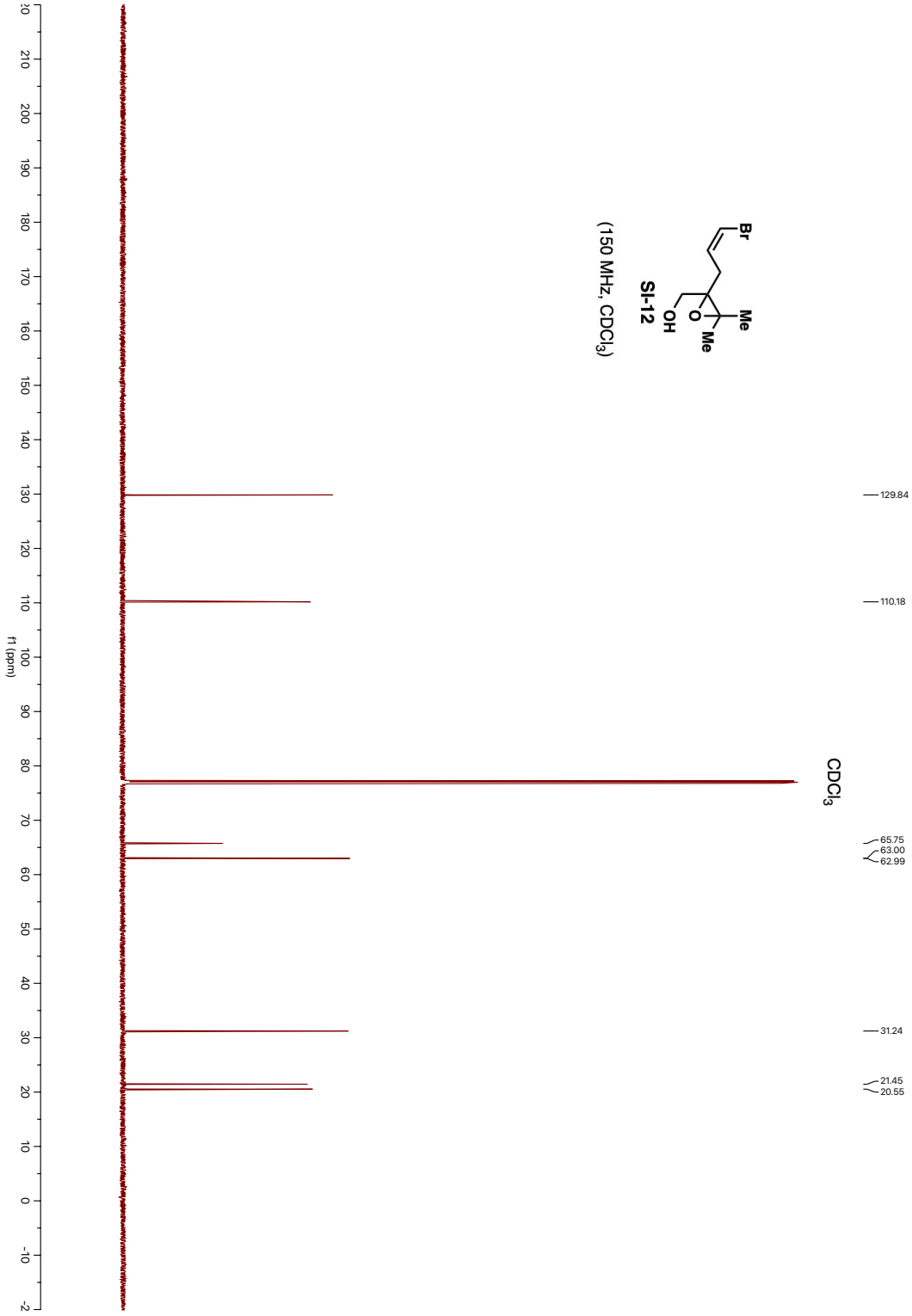

Br
Me
Me
OH
SI-11
(600 MHz, CDCl3)
CHCl3
f1 (ppm)
16
15
14
13
12
11
10
9
8
7
6
5
4
3
2
1
0
-1
-2
-3
1.00
1.03
2.14
1.08
1.06
3.09
3.18
6.16
6.16
6.16
6.15
6.15
6.15
6.07
6.06
6.05
6.04
4.13
3.06
3.05
1.75
1.72

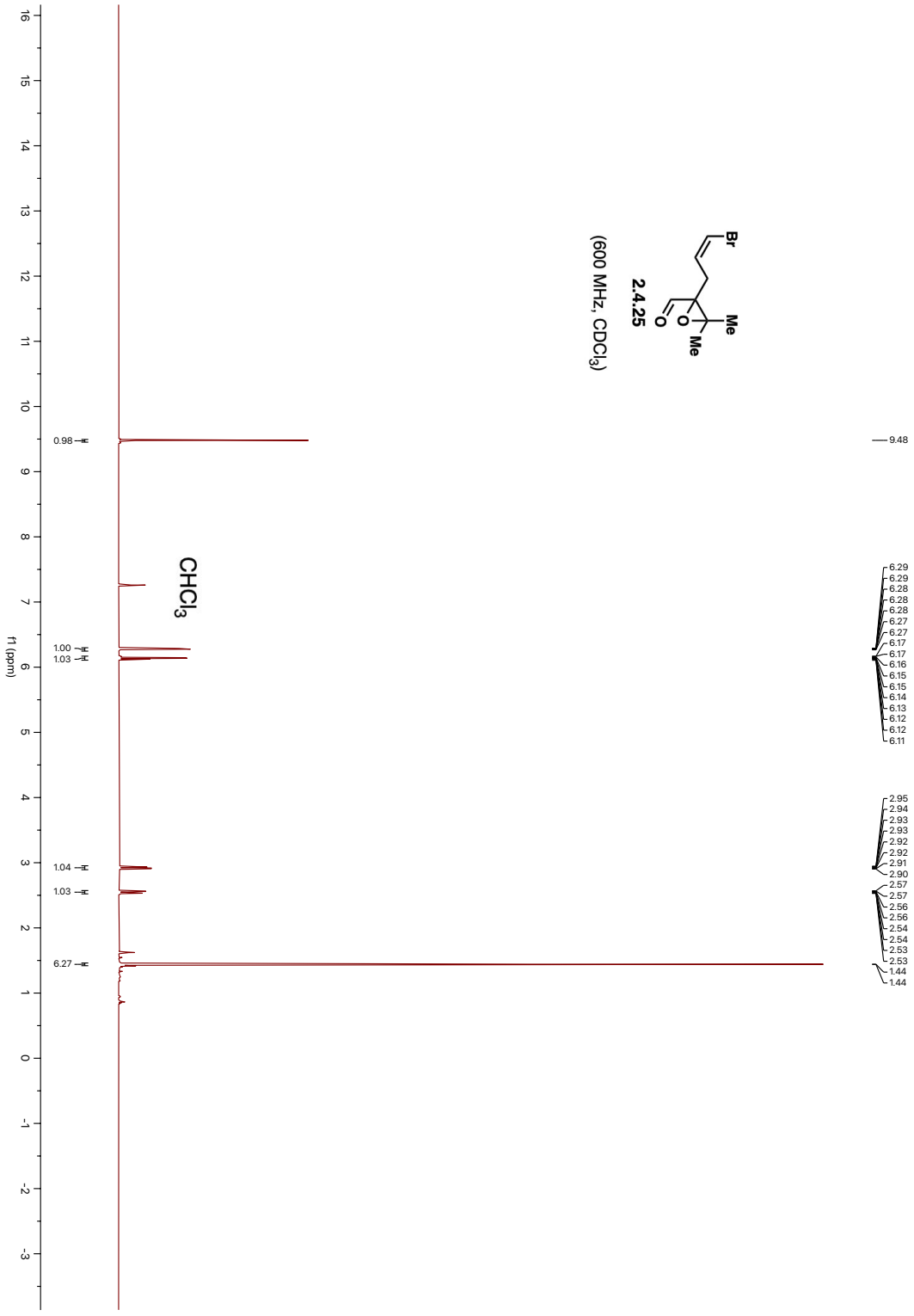


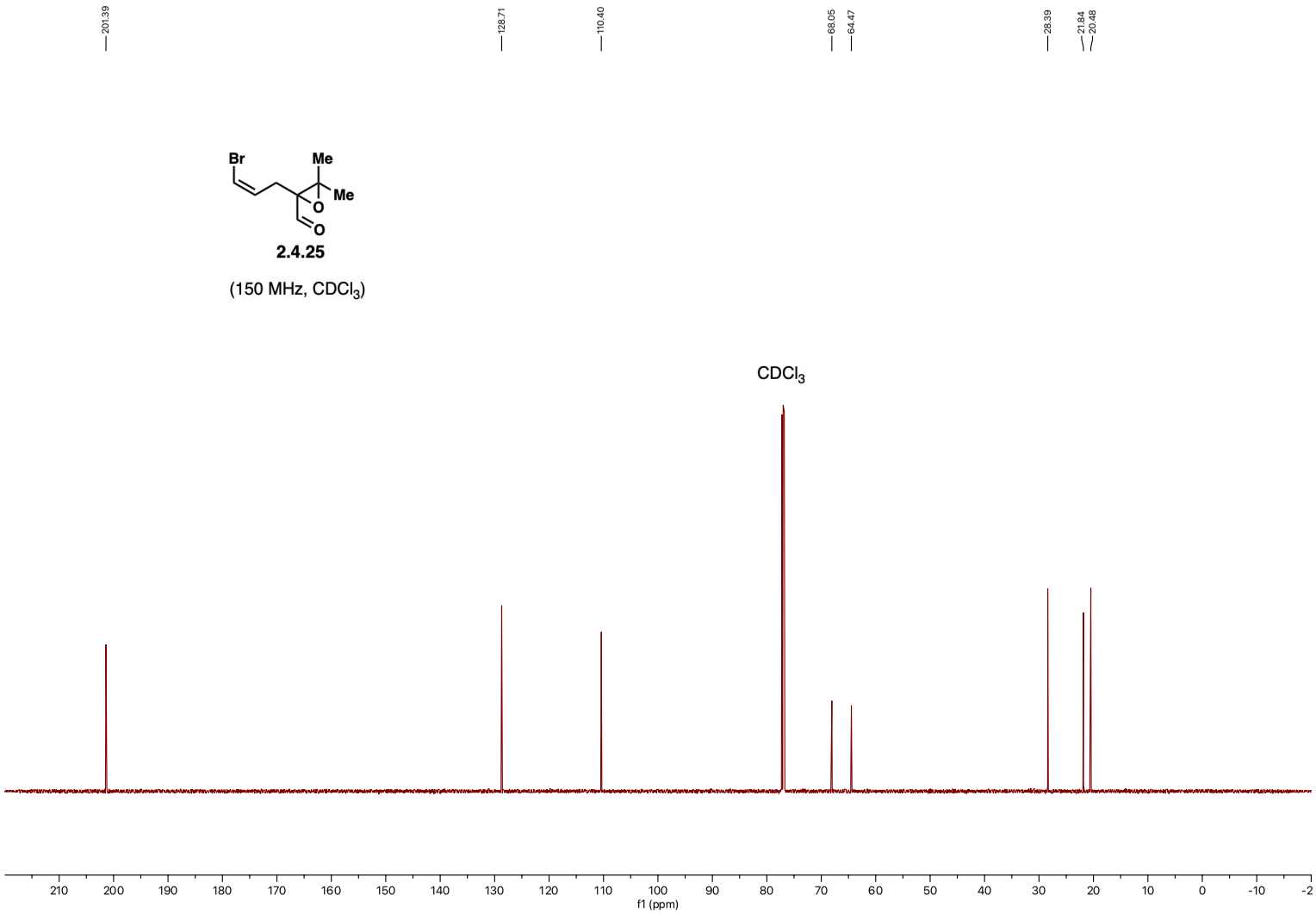
SI-11

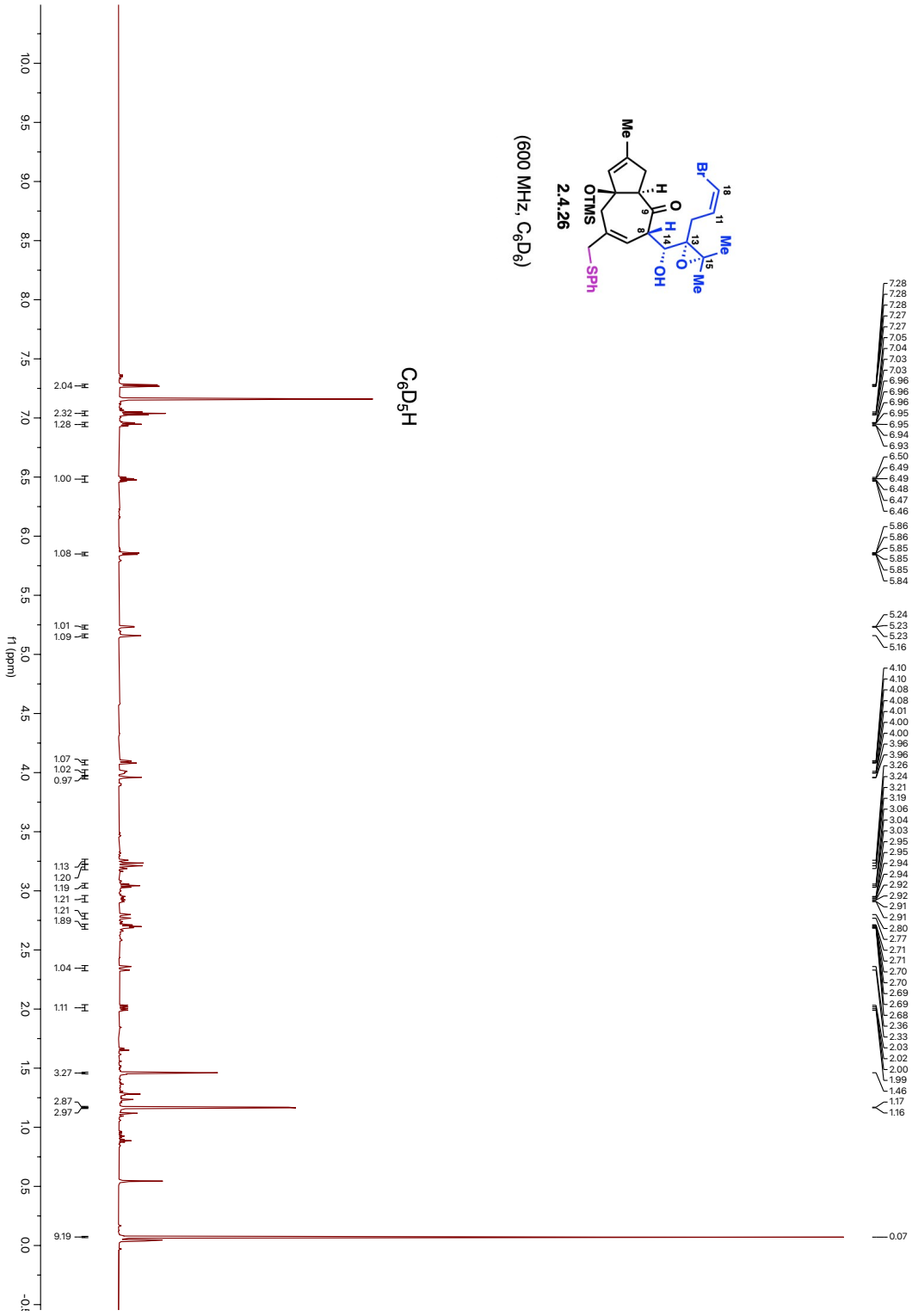
(150 MHz, $CDCl_3$)

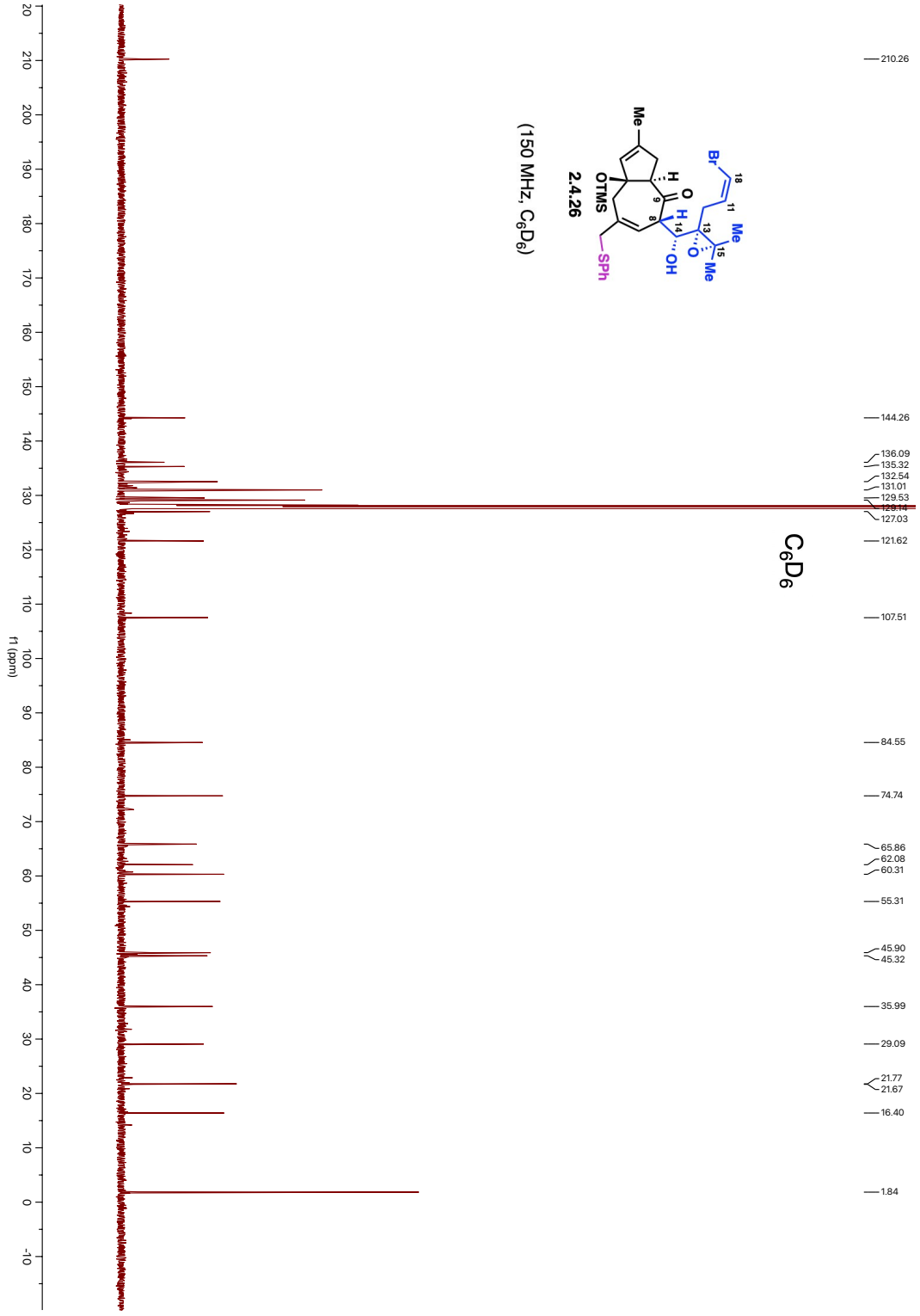

Br
Me
Me
O
OH
SI-12
(600 MHz, CDCl3)
CHCl3
f1 (ppm)

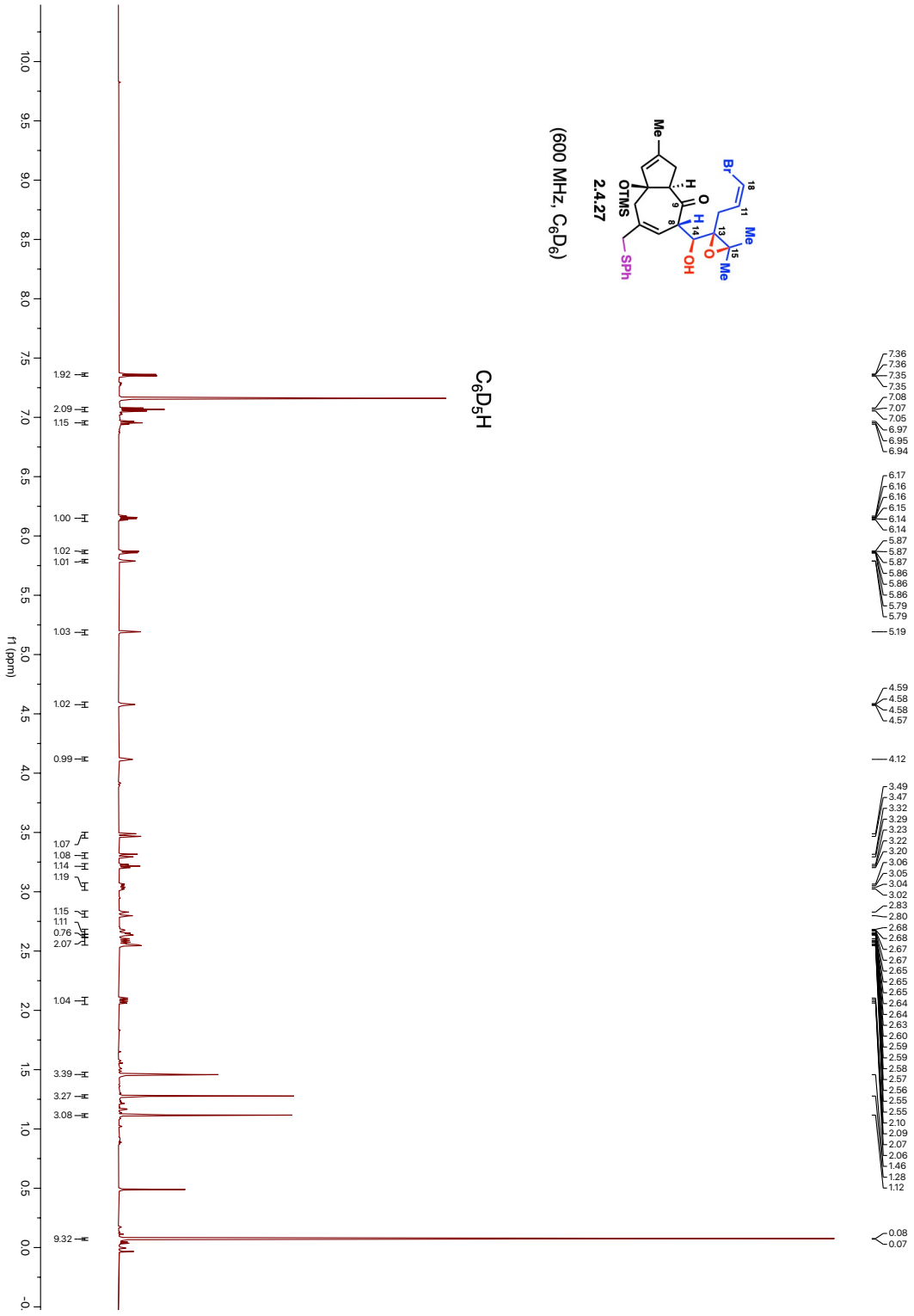

SI-12
(150 MHz, CDCl3)
Br
Me
O
Me
OH
CDCl3
129.84
110.18
65.75
63.00
62.99
31.24
21.45
20.55
f1 (ppm)

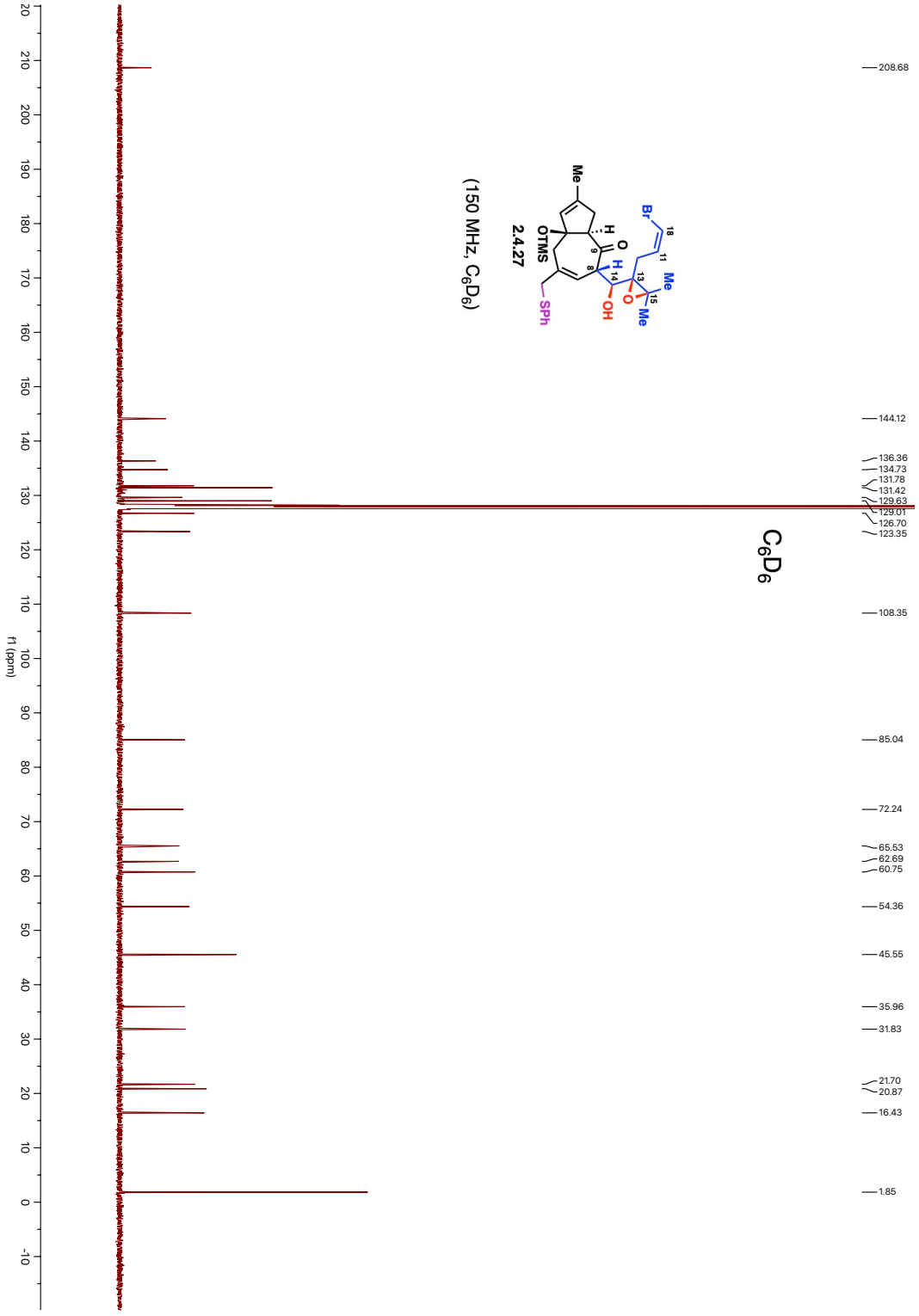

2.4.25
(600 MHz, $CDCl_3$)
Br
Me
Me
O
O
$CHCl_3$
0.98 H
1.00 H
1.03 H
1.04 H
1.03 H
6.27 H
f1 (ppm)
9.48
6.29
6.29
6.28
6.28
6.28
6.27
6.27
6.17
6.17
6.16
6.15
6.15
6.14
6.13
6.12
6.12
6.11
2.95
2.94
2.93
2.93
2.92
2.92
2.91
2.90
2.57
2.57
2.56
2.56
2.54
2.54
2.53
2.53
1.44
1.44

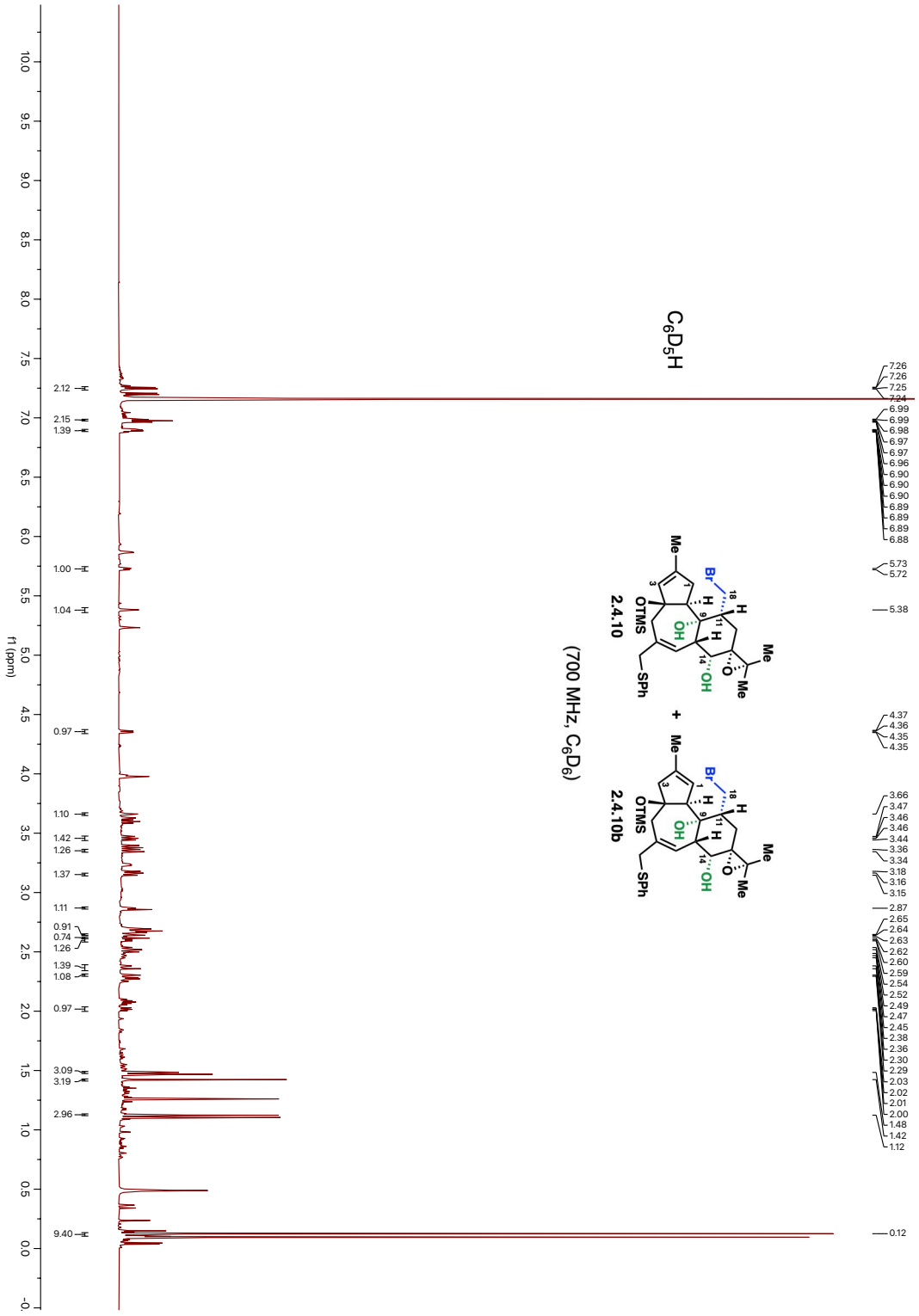

201.39
128.71
110.40
68.05
64.47
28.39
21.84
20.48
Br
Me
Me
O
O
2.4.25
(150 MHz, CDCl3)
CDCl3
210
200
190
180
170
160
150
140
130
120
110
100
90
80
70
60
50
40
30
20
10
0
-10
-2
f1 (ppm)

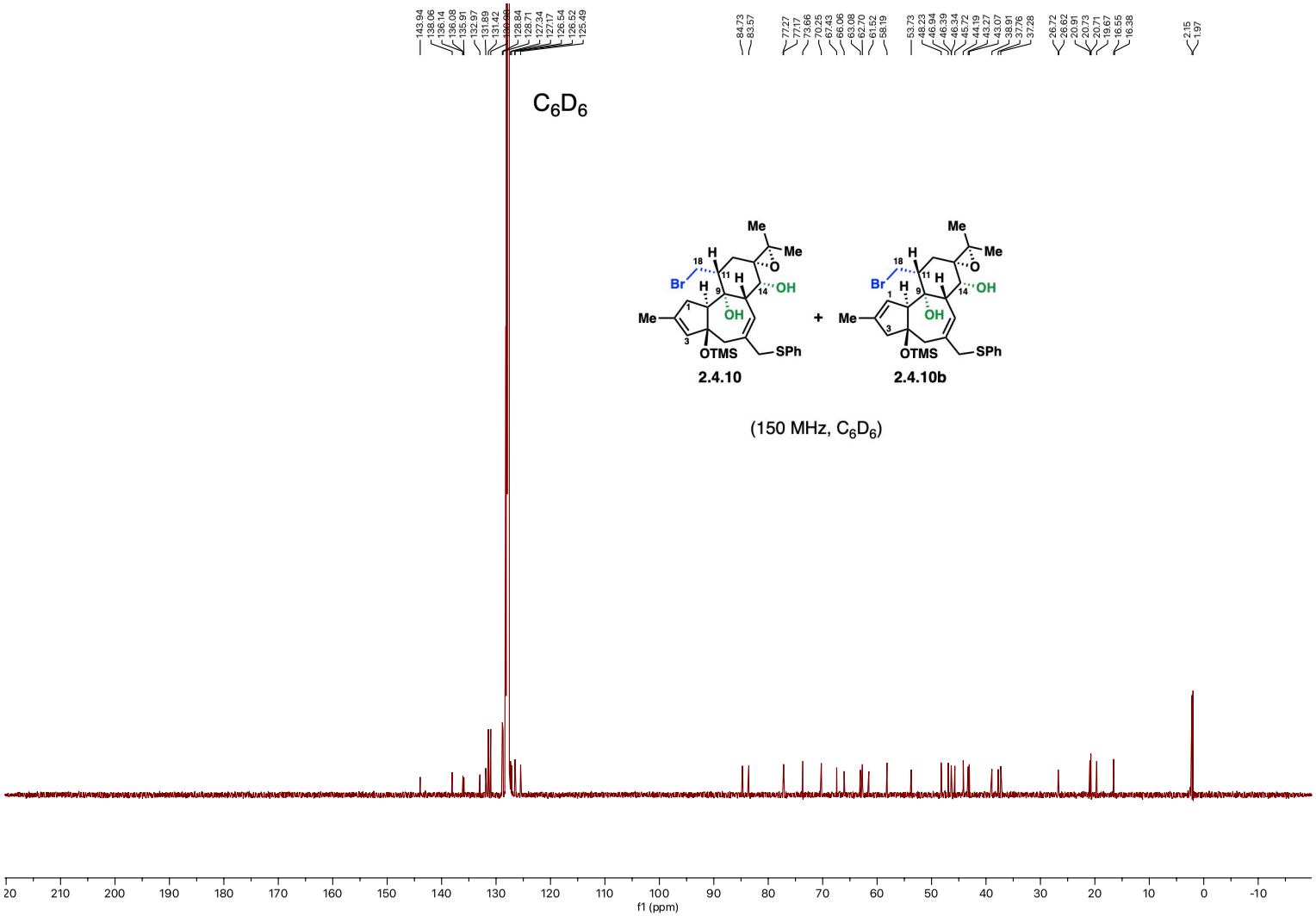

(600 MHz, C_6D_6)
2.4.26
C_6D_5H
f1 (ppm)

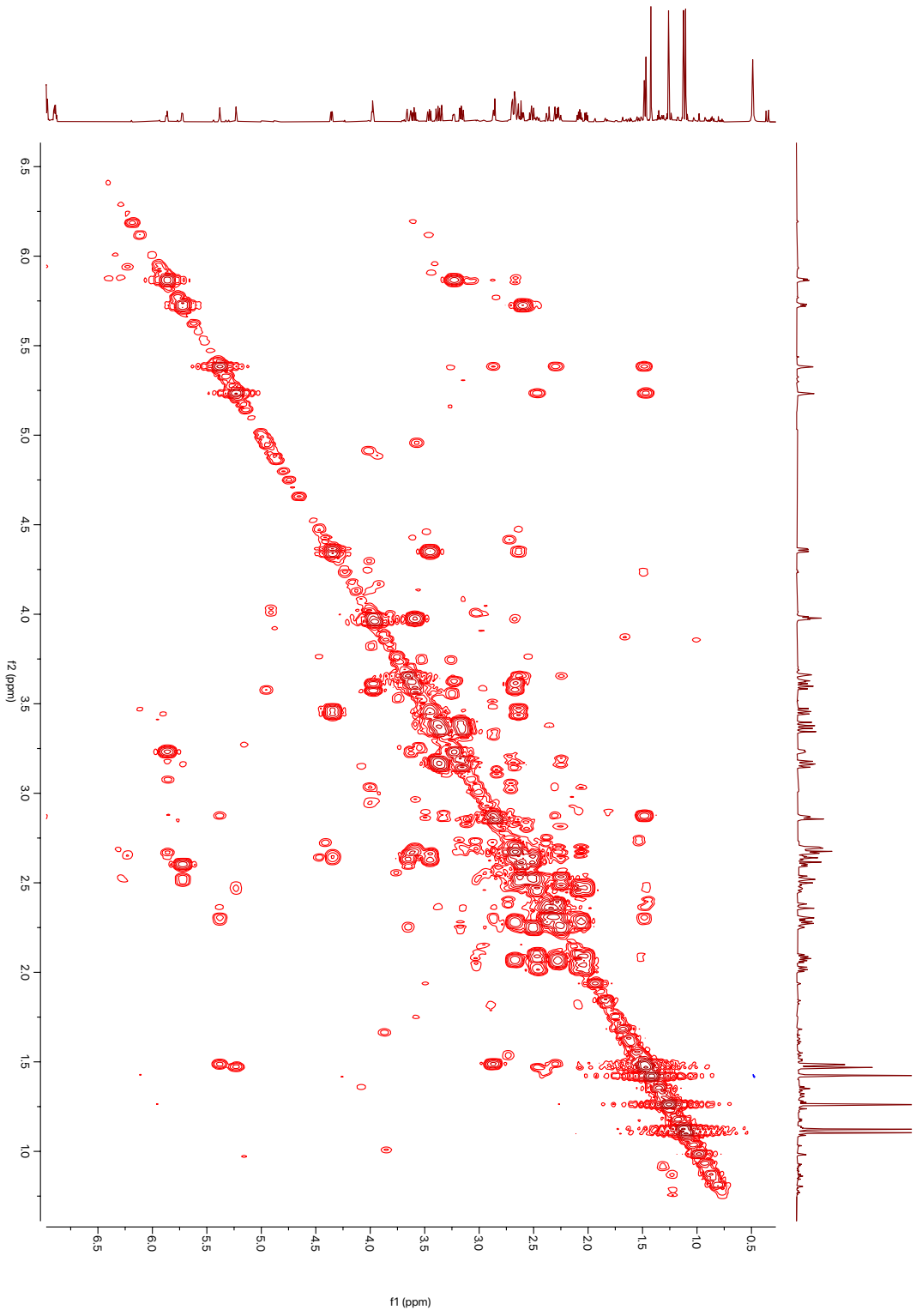

(150 MHz, C6D6)
2.4.26
C6D6
f1 (ppm)
210.26
144.26
136.09
135.32
132.54
131.01
129.53
128.14
127.03
121.62
107.51
84.55
74.74
65.86
62.08
60.31
55.31
45.90
45.32
35.99
29.09
21.77
21.67
16.40
1.84

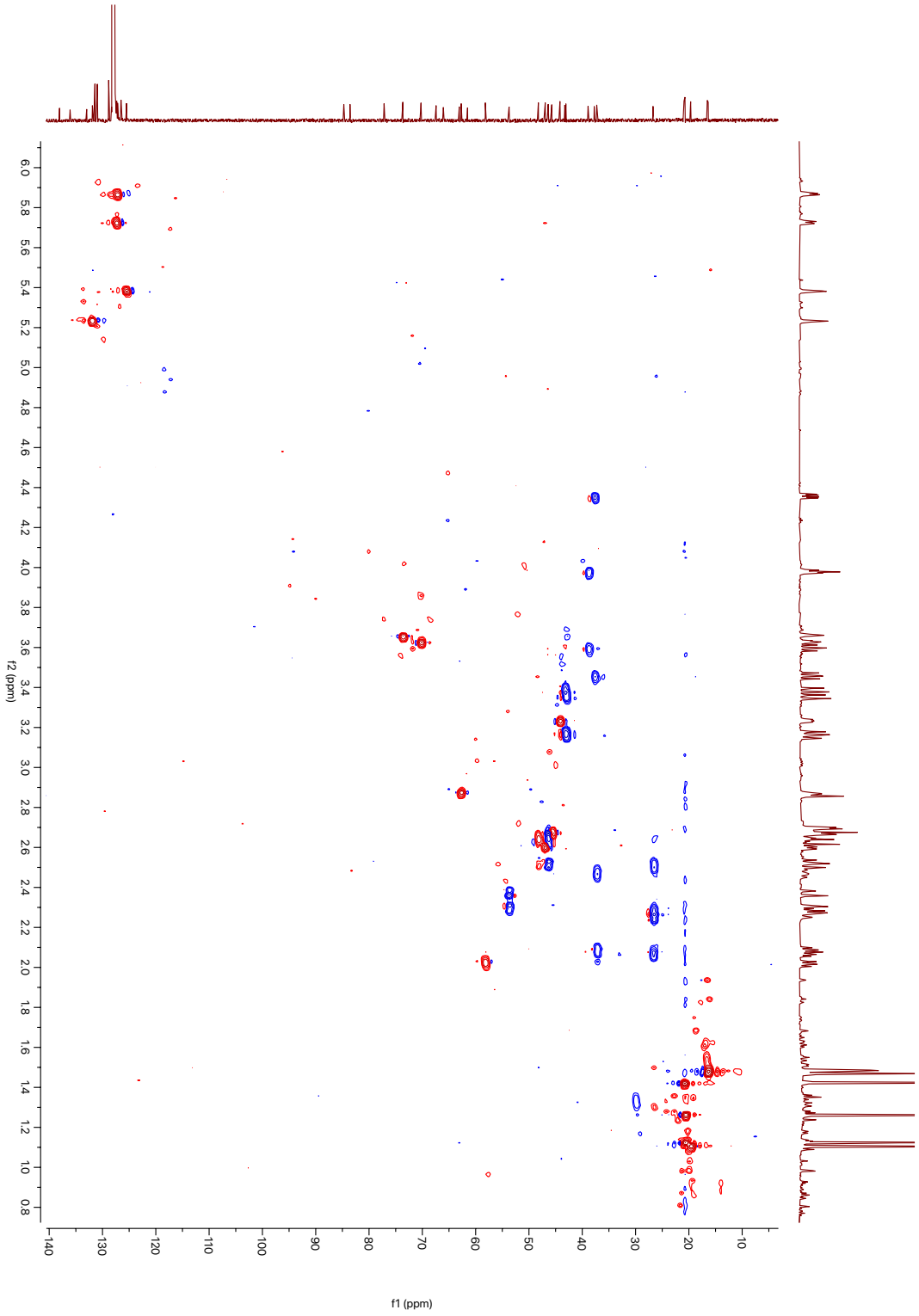

(600 MHz, C_6D_6)
2.4.27
OTMS
SPh
OH
Me
Br
Me
Me
C_6D_5H
f1 (ppm)

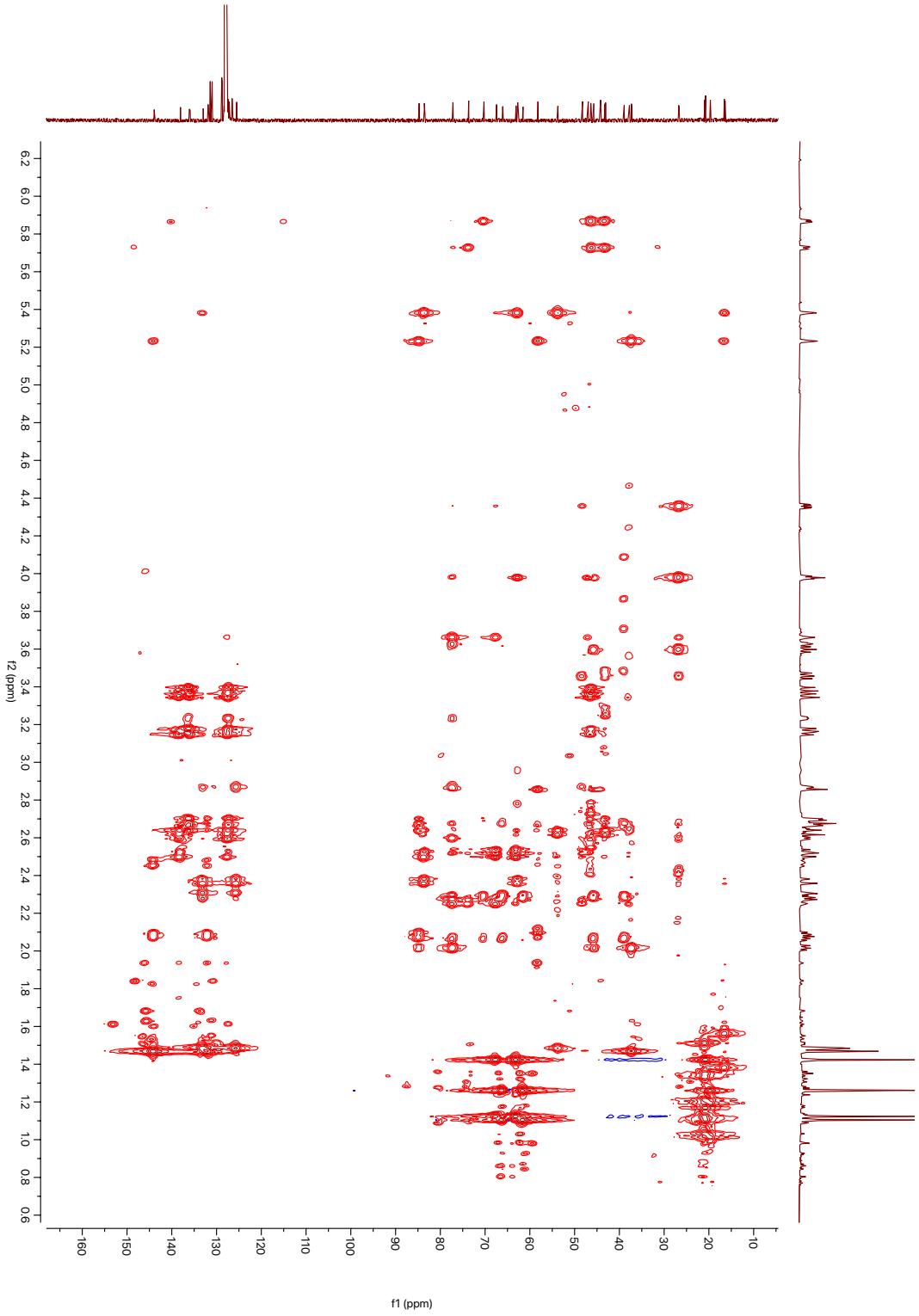

208.68
144.12
136.36
134.73
131.78
131.42
129.63
129.01
126.70
123.35
108.35
85.04
72.24
65.53
62.69
60.75
54.36
45.55
35.96
31.83
21.70
20.87
16.43
1.85
C6D6
(150 MHz, C6D6)
2.4.27
OTMS
SPh
OH
Me
Br
Me
Me
O
H
O
H
f1 (ppm)

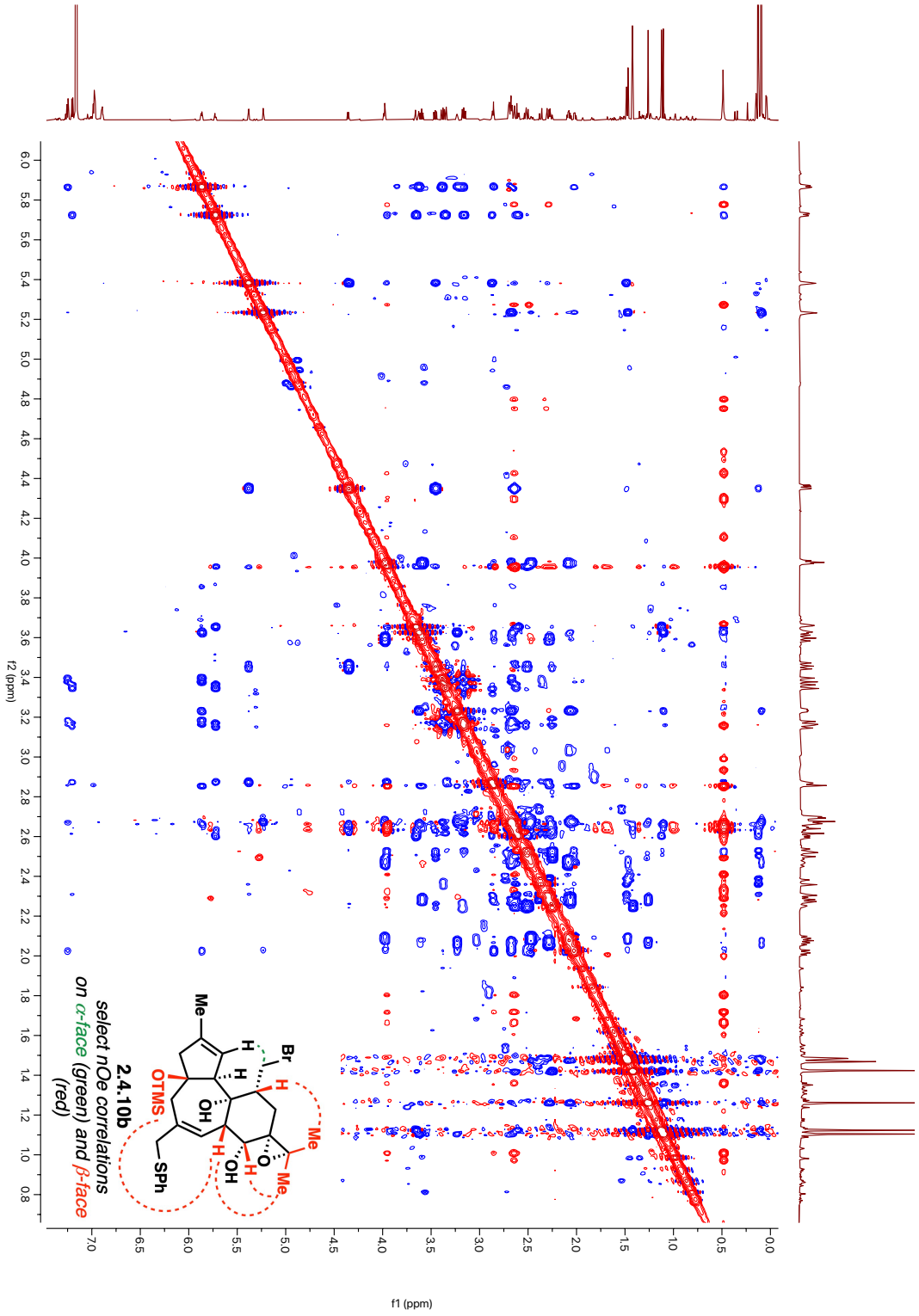

C6D5H
(700 MHz, C6D6)
2.4.10
2.4.10b
OTMS
SPh
Br
OH
Me
O
f1 (ppm)

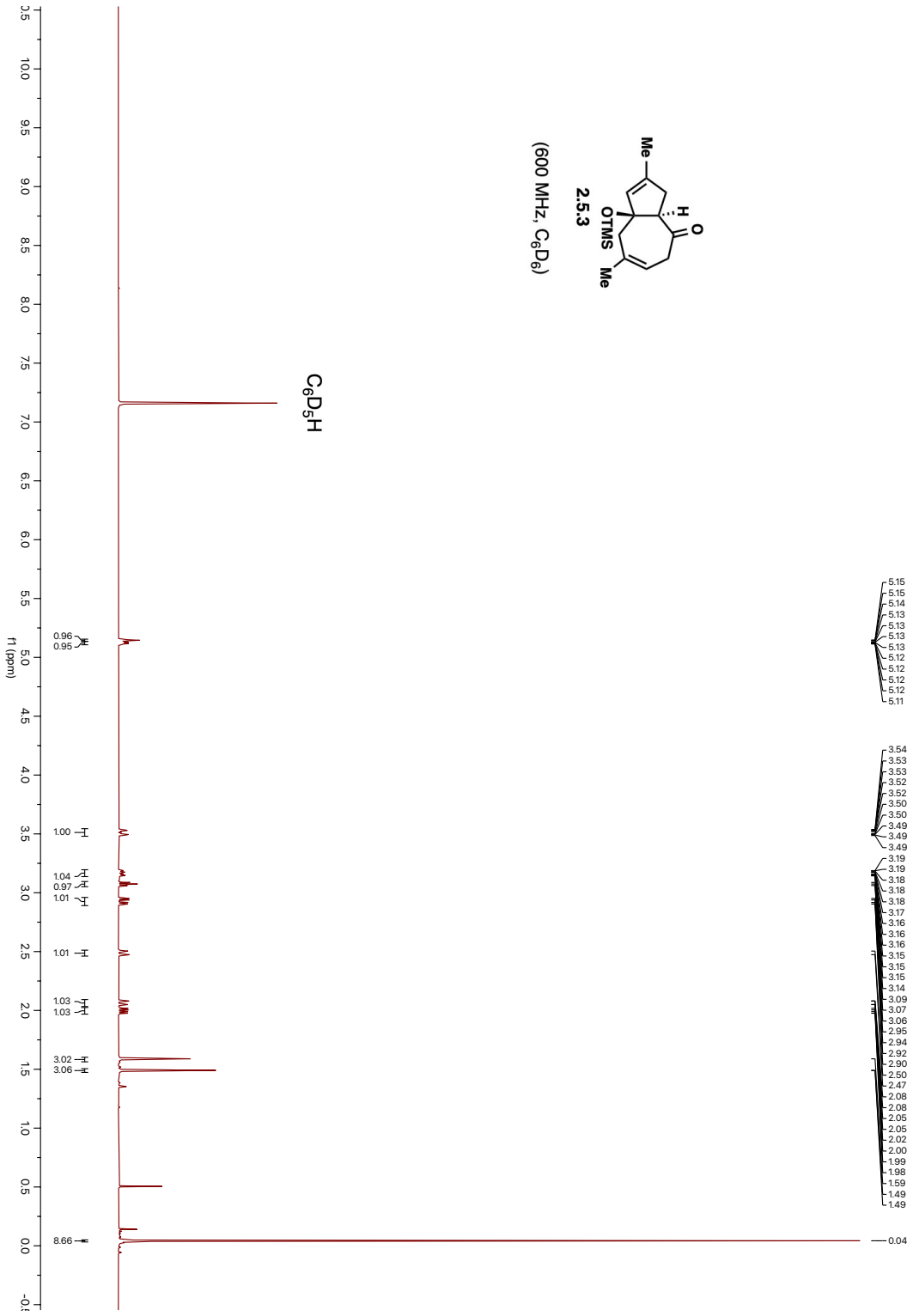

143.94
138.06
136.14
136.08
135.91
132.97
131.89
131.42
130.66
128.84
128.71
127.34
127.17
126.54
126.52
125.49
84.73
83.57
77.27
77.17
73.66
70.25
67.43
66.06
63.08
62.70
61.52
58.19
53.73
48.23
46.94
46.39
46.14
45.72
44.19
43.27
43.07
38.91
37.76
37.28
26.72
26.62
26.05
20.73
20.71
19.67
16.55
16.38
2.15
1.97
C6D6
Me
Me
H
18
O
Br
H
11
H
9
14
OH
1
OH
Me
3
OTMS
SPh
2.4.10
+
2.4.10b
(150 MHz, C6D6)
f1 (ppm)

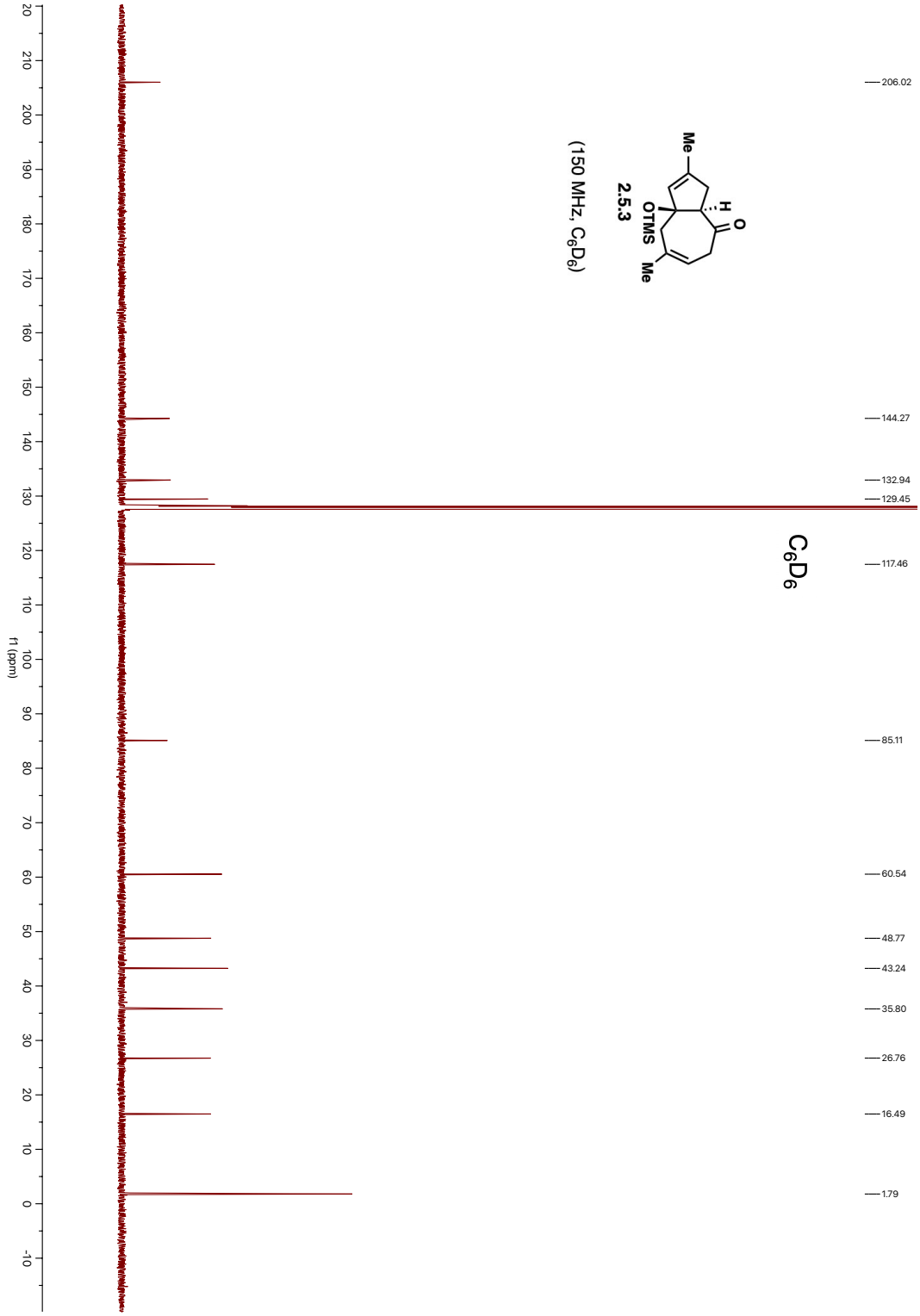

f2 (ppm)
f1 (ppm)
6.5
6.0
5.5
5.0
4.5
4.0
3.5
3.0
2.5
2.0
1.5
1.0
0.5

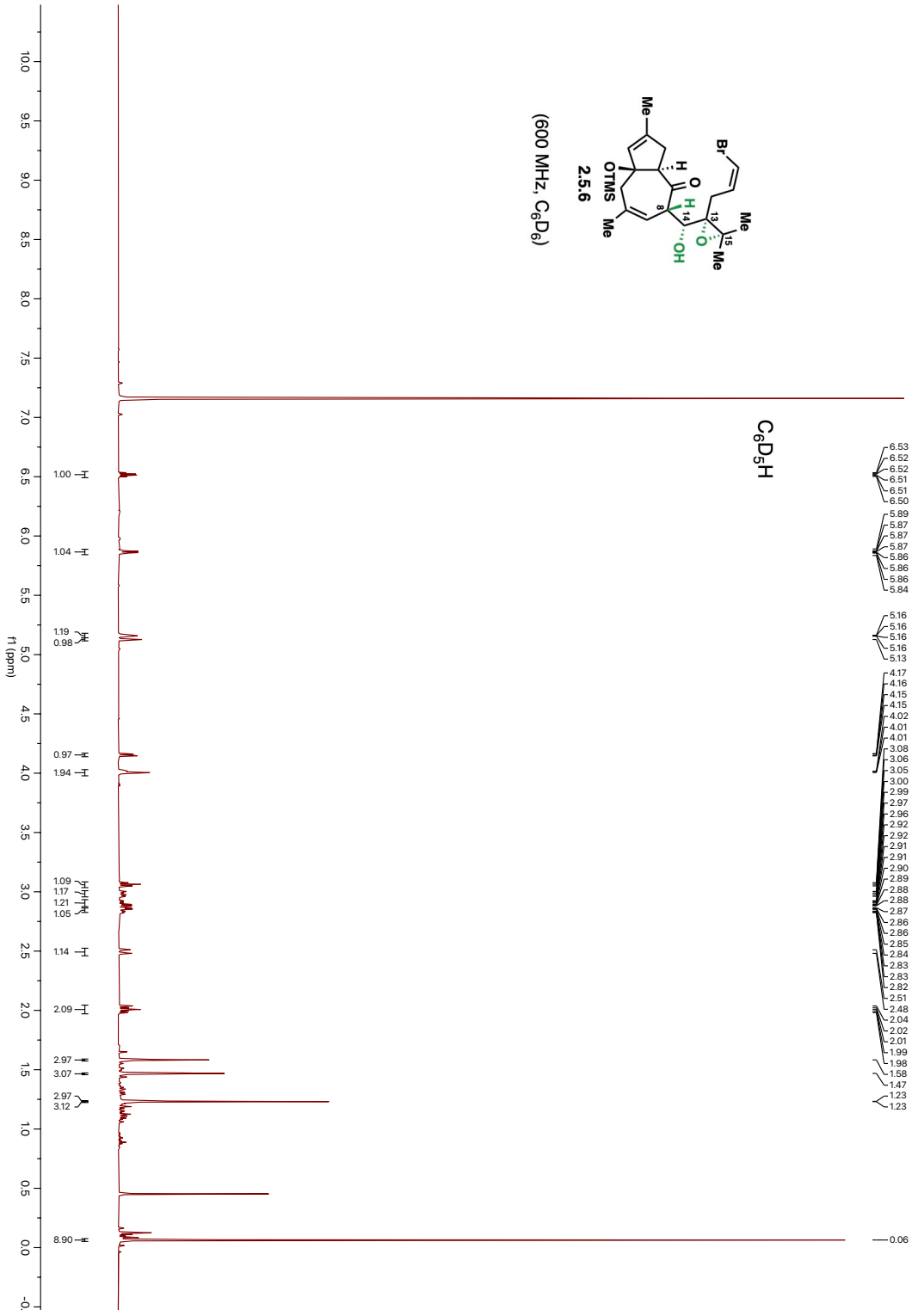

f2 (ppm)
f1 (ppm)

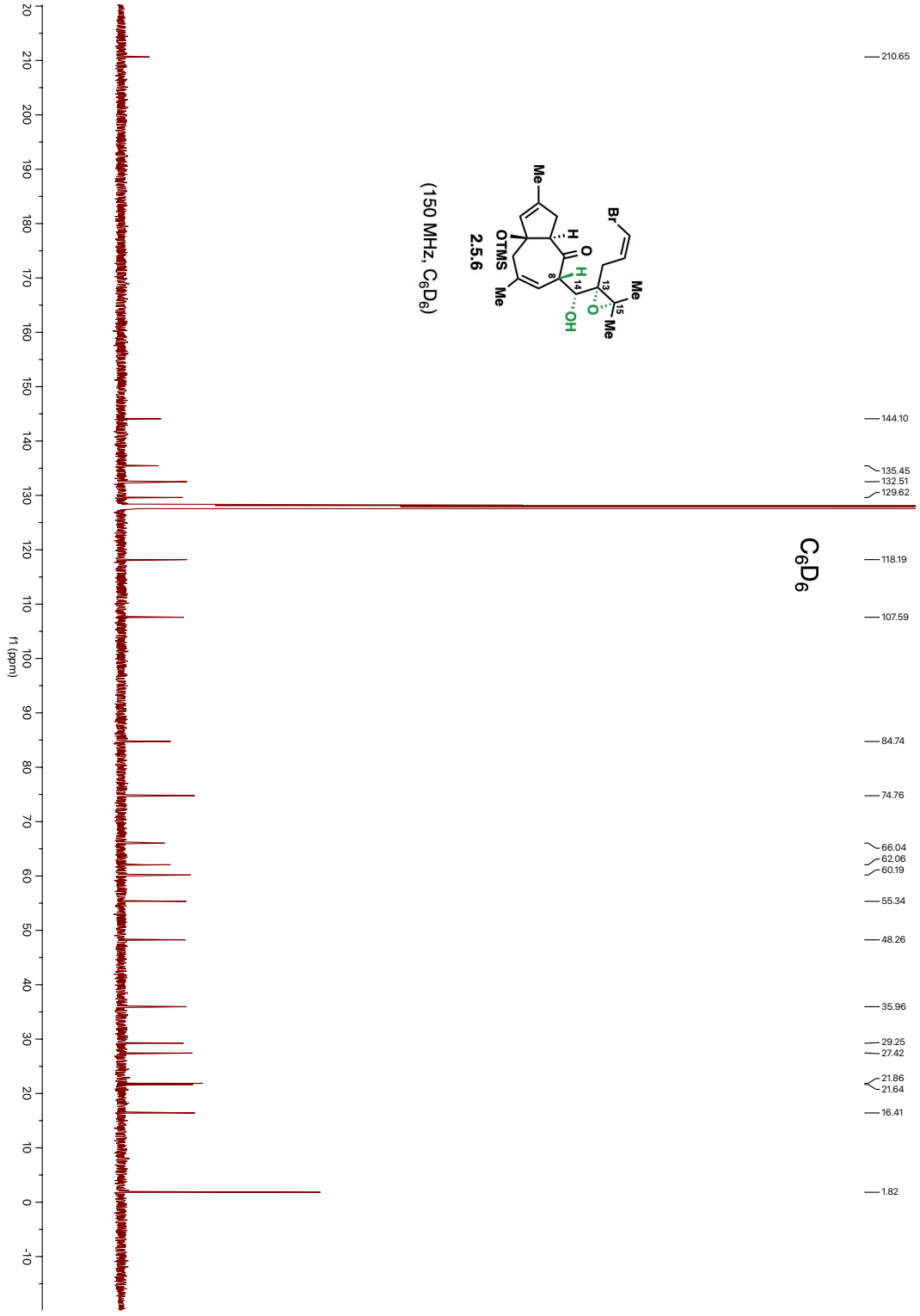

f2 (ppm)
f1 (ppm)

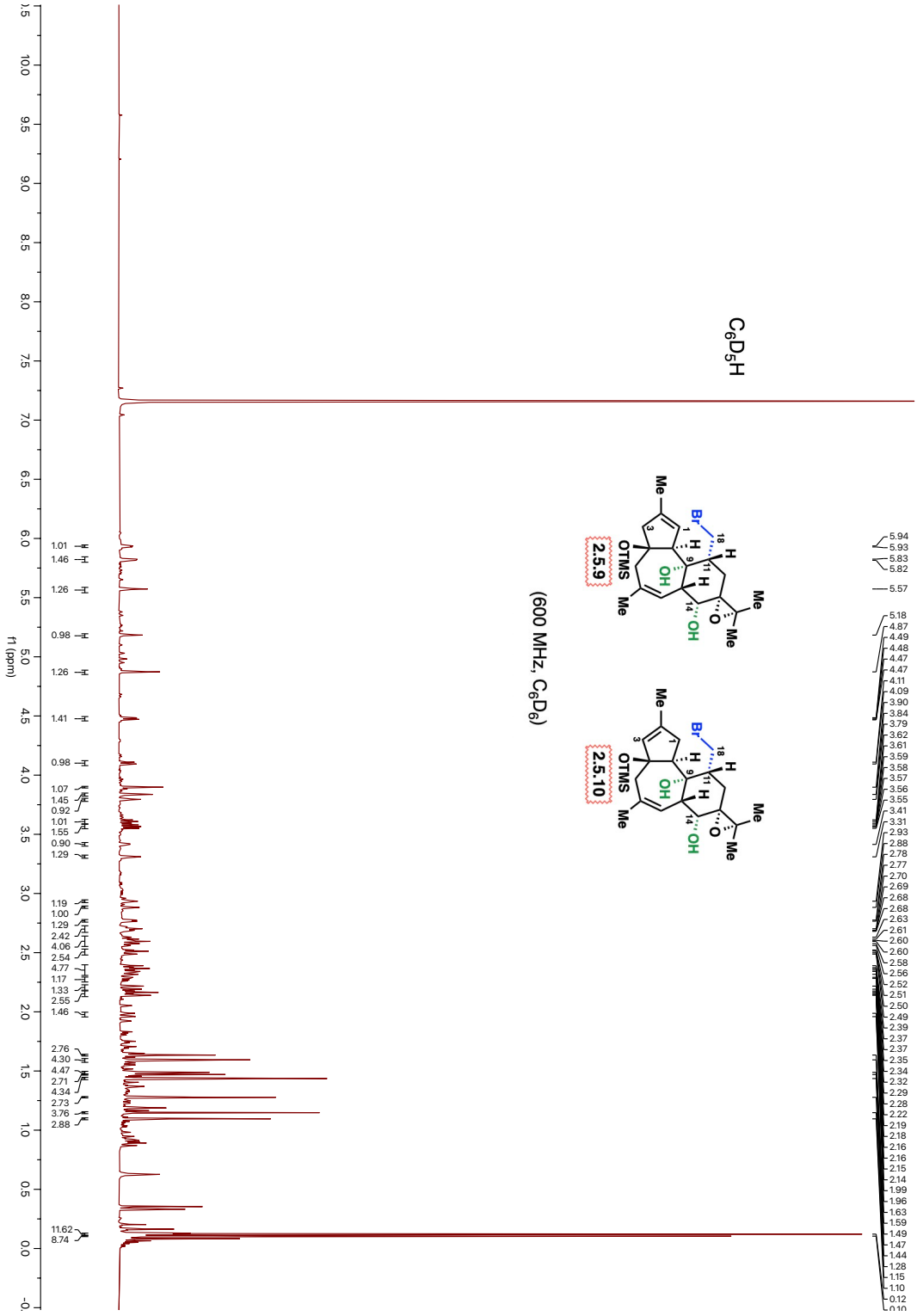

f2 (ppm)
f1 (ppm)
2.4.10b
select nOe correlations
on α-face (green) and β-face
(red)
Me
H
H
OTMS
OH
H
OH
H
O
Me
Me
Br
H
SPh

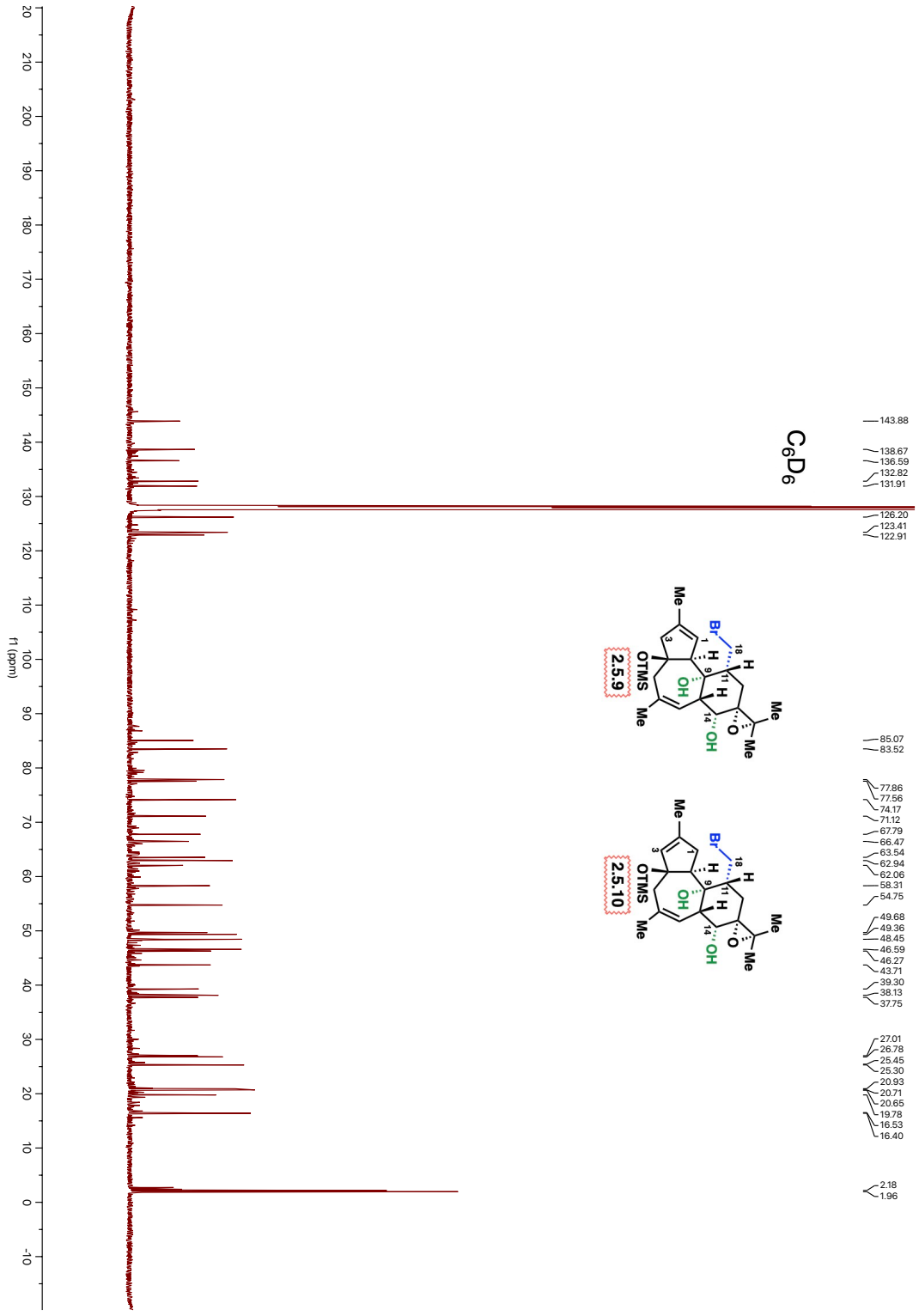

2.5.3
OTMS
Me
Me
H
O
(600 MHz, C_6D_6)
C_6D_5H
f1 (ppm)
0.96
0.95
1.00
1.04
0.97
1.01
1.01
1.03
1.03
3.02
3.06
8.66
5.15
5.15
5.14
5.13
5.13
5.13
5.13
5.12
5.12
5.12
5.12
5.11
3.54
3.53
3.53
3.52
3.52
3.50
3.50
3.49
3.49
3.49
3.19
3.19
3.18
3.18
3.18
3.17
3.16
3.16
3.16
3.15
3.15
3.15
3.14
3.09
3.07
3.06
2.95
2.94
2.92
2.90
2.50
2.47
2.08
2.08
2.05
2.05
2.02
2.00
1.99
1.98
1.59
1.49
1.49
0.04

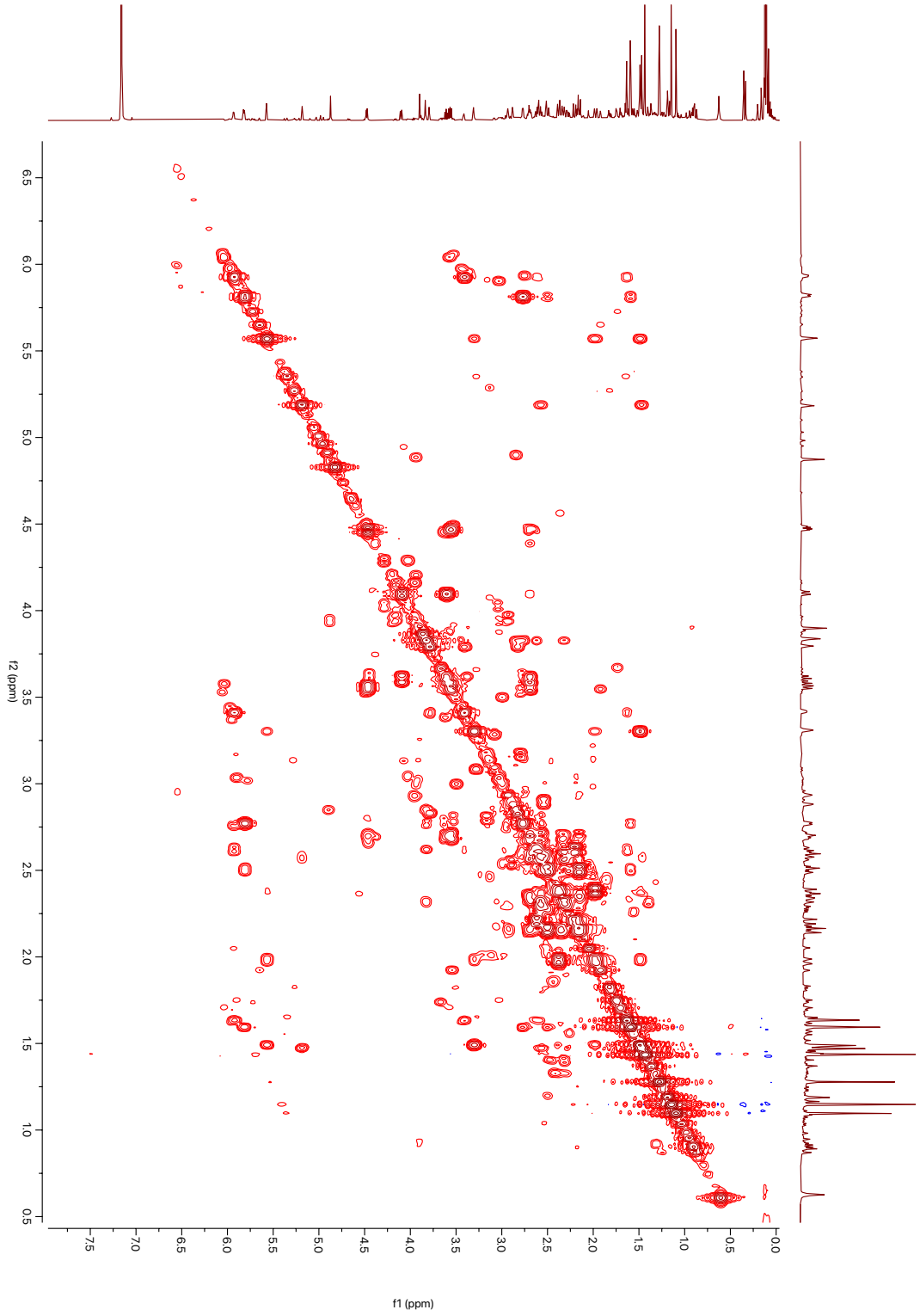

Me
H
O
OTMS
Me
2.5.3
(150 MHz, C6D6)
206.02
144.27
132.94
129.45
C6D6
117.46
85.11
60.54
48.77
43.24
35.80
26.76
16.49
1.79
f1 (ppm)

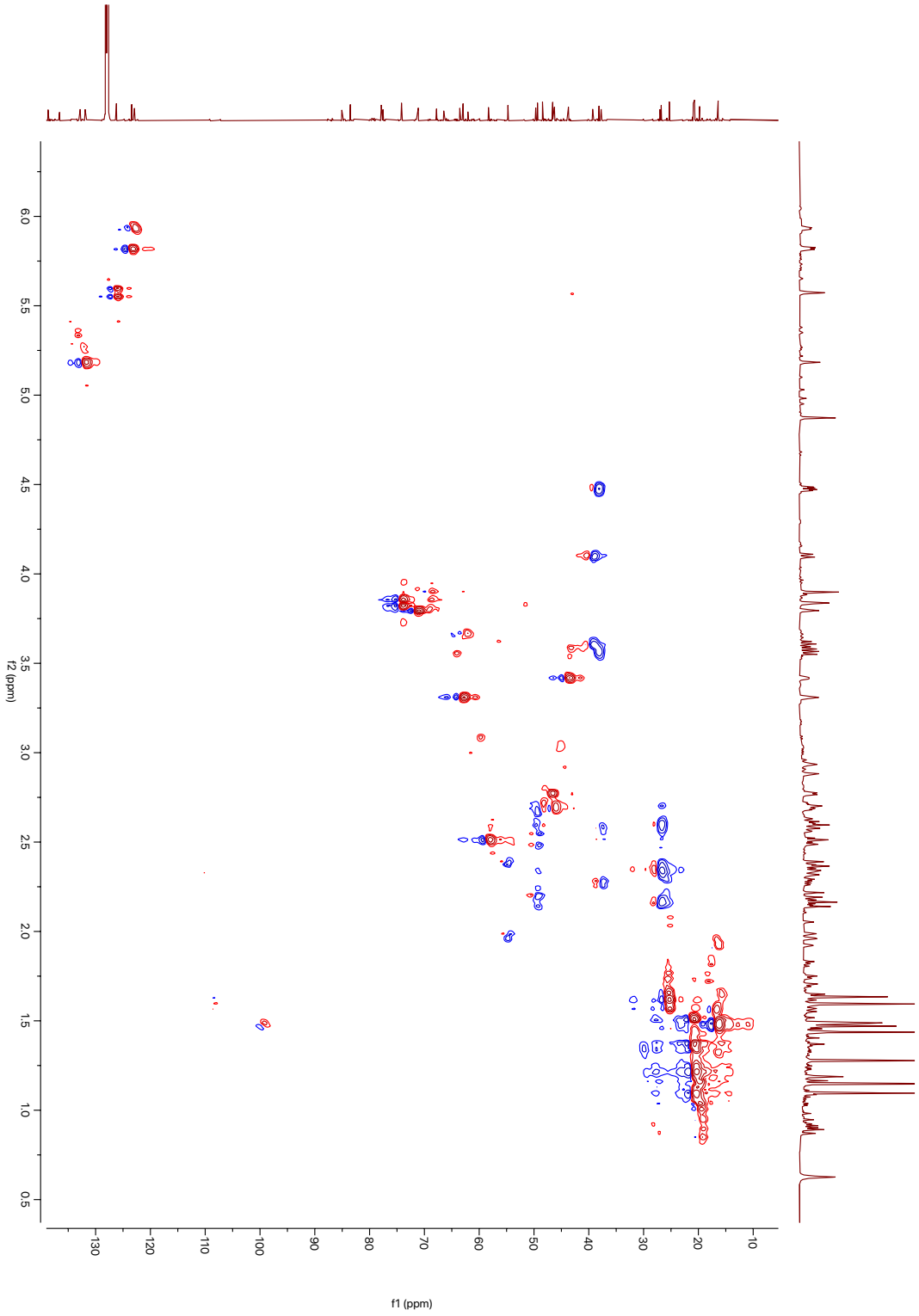

(600 MHz, C6D6)
2.5.6
C6D5H
f1 (ppm)

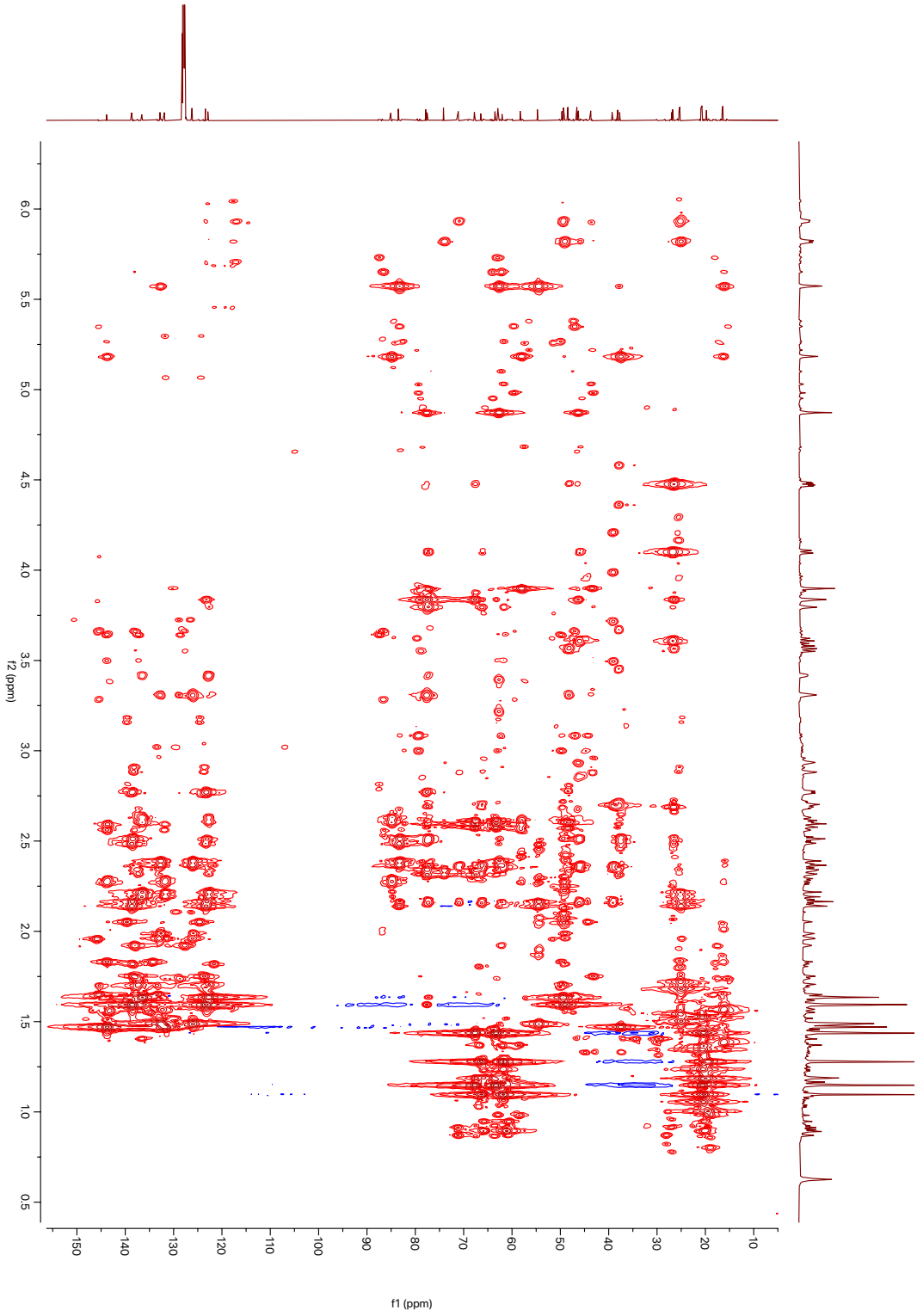

(150 MHz, C6D6)
2.5.6
C6D6
f1 (ppm)
210.65
144.10
135.45
132.51
129.62
118.19
107.59
84.74
74.76
66.04
62.06
60.19
55.34
48.26
35.96
29.25
27.42
21.86
21.64
16.41
1.82

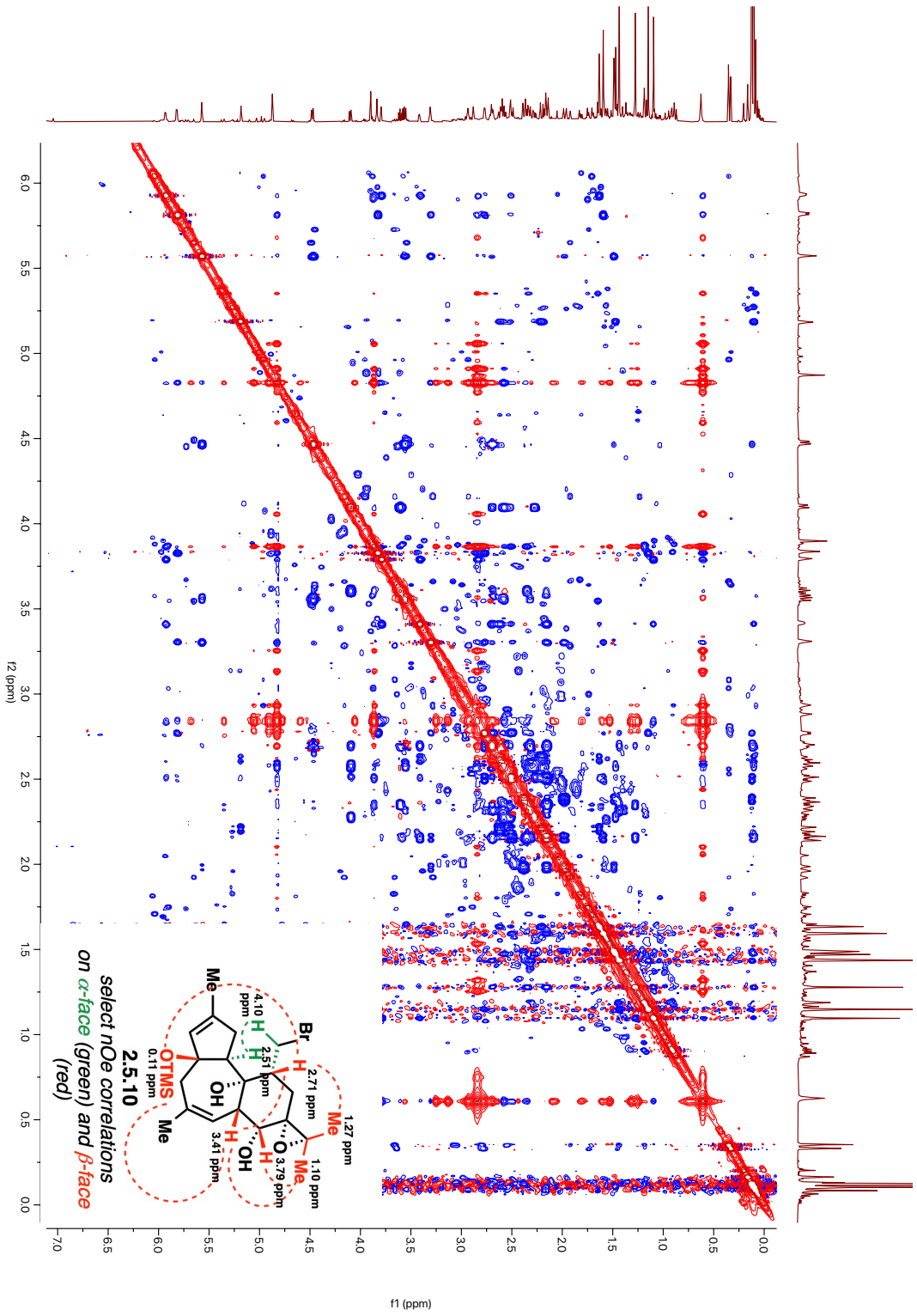

C6D5H
(600 MHz, C6D6)
2.5.9
2.5.10
OTMS
Me
OH
Br
H
O
f1 (ppm)

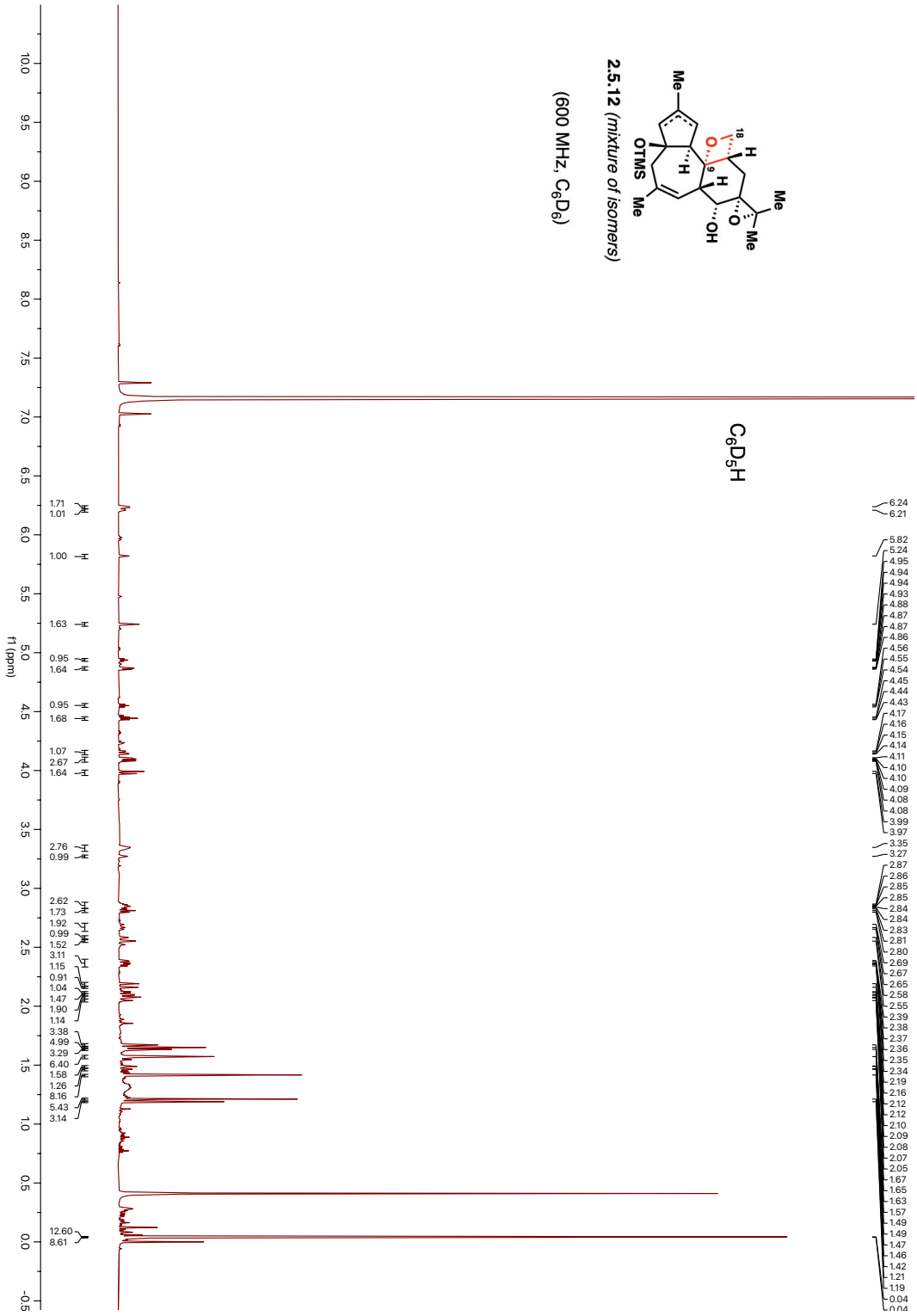

C6D6
2.5.9
2.5.10
143.88
138.67
136.59
132.82
131.91
126.20
123.41
122.91
85.07
83.52
77.86
77.56
74.17
71.12
67.79
66.47
63.54
62.94
62.06
58.31
54.75
49.68
49.36
48.45
46.59
46.27
43.71
39.30
38.13
37.75
27.01
26.78
25.45
25.30
20.93
20.71
20.65
19.78
16.53
16.40
2.18
1.96
f1 (ppm)

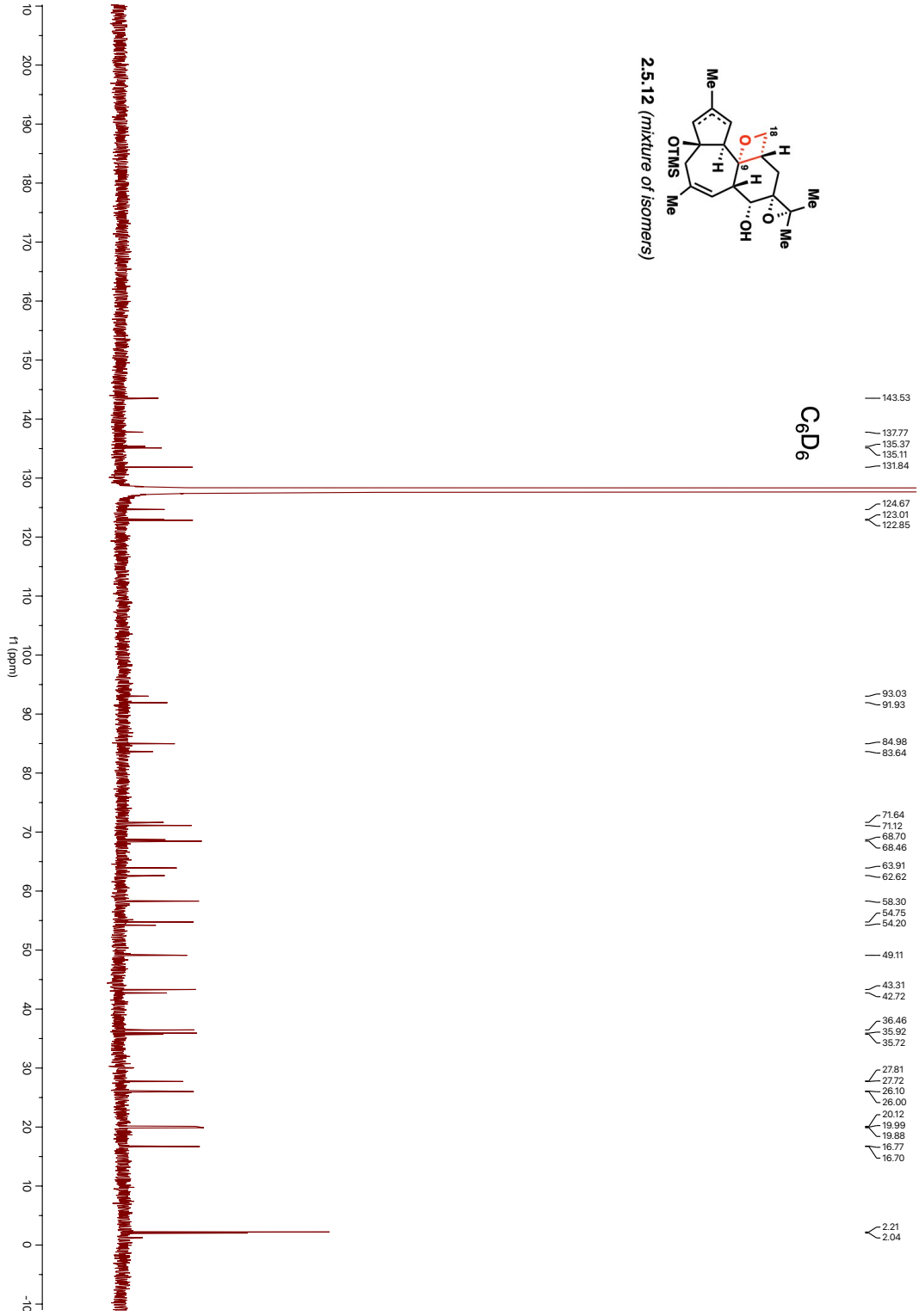

f2 (ppm)
f1 (ppm)

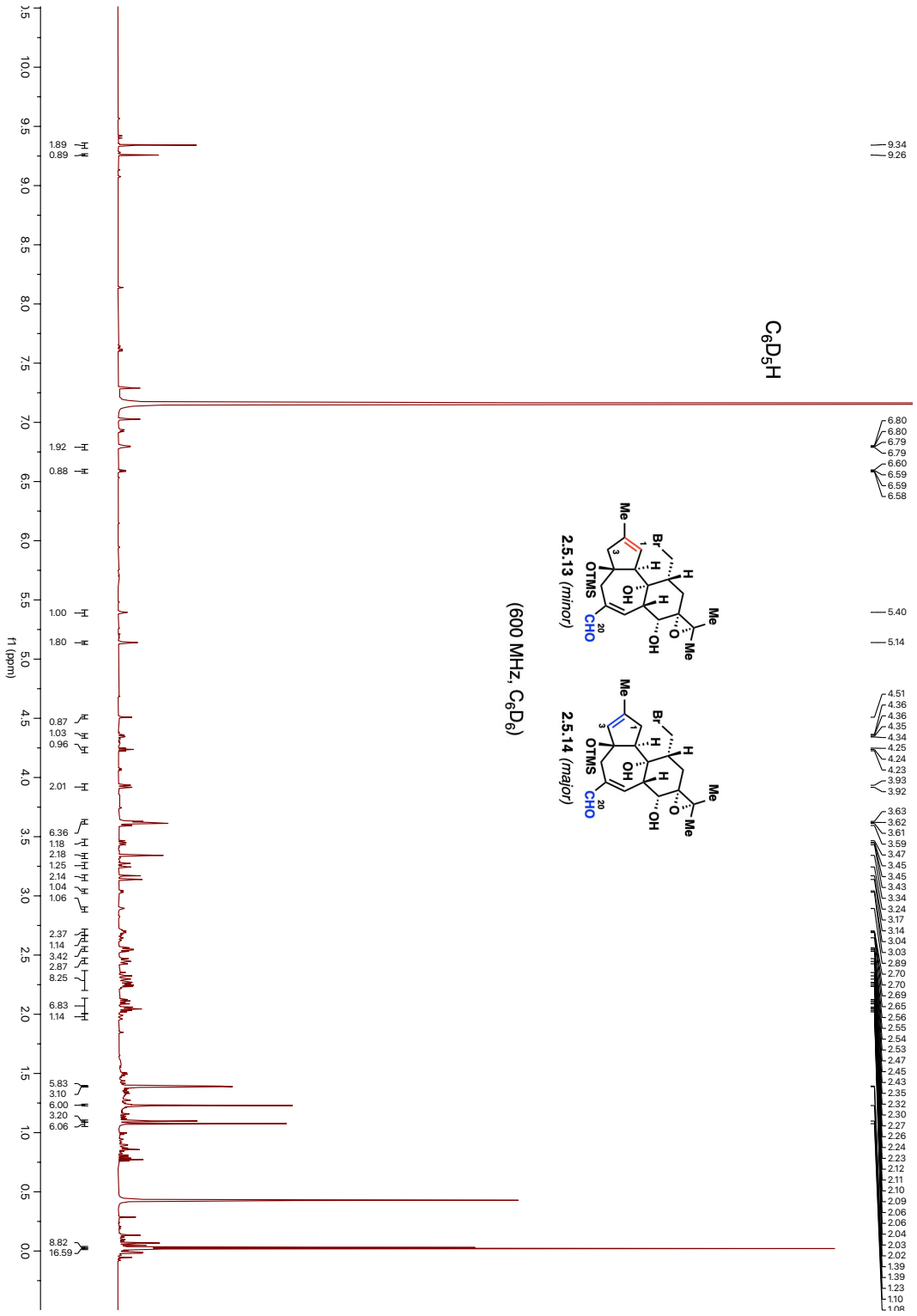

f2 (ppm)
f1 (ppm)

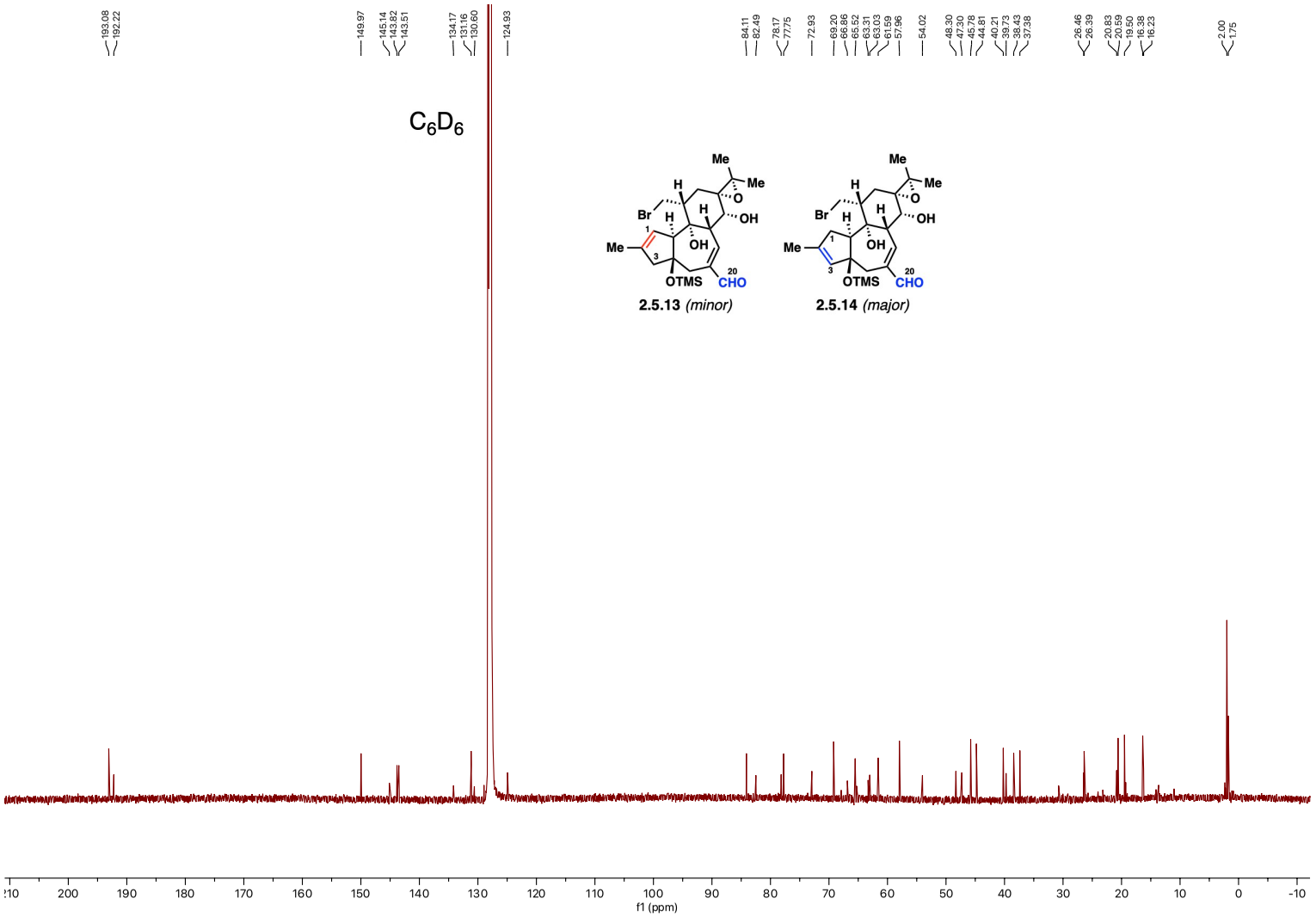

f2 (ppm)
f1 (ppm)

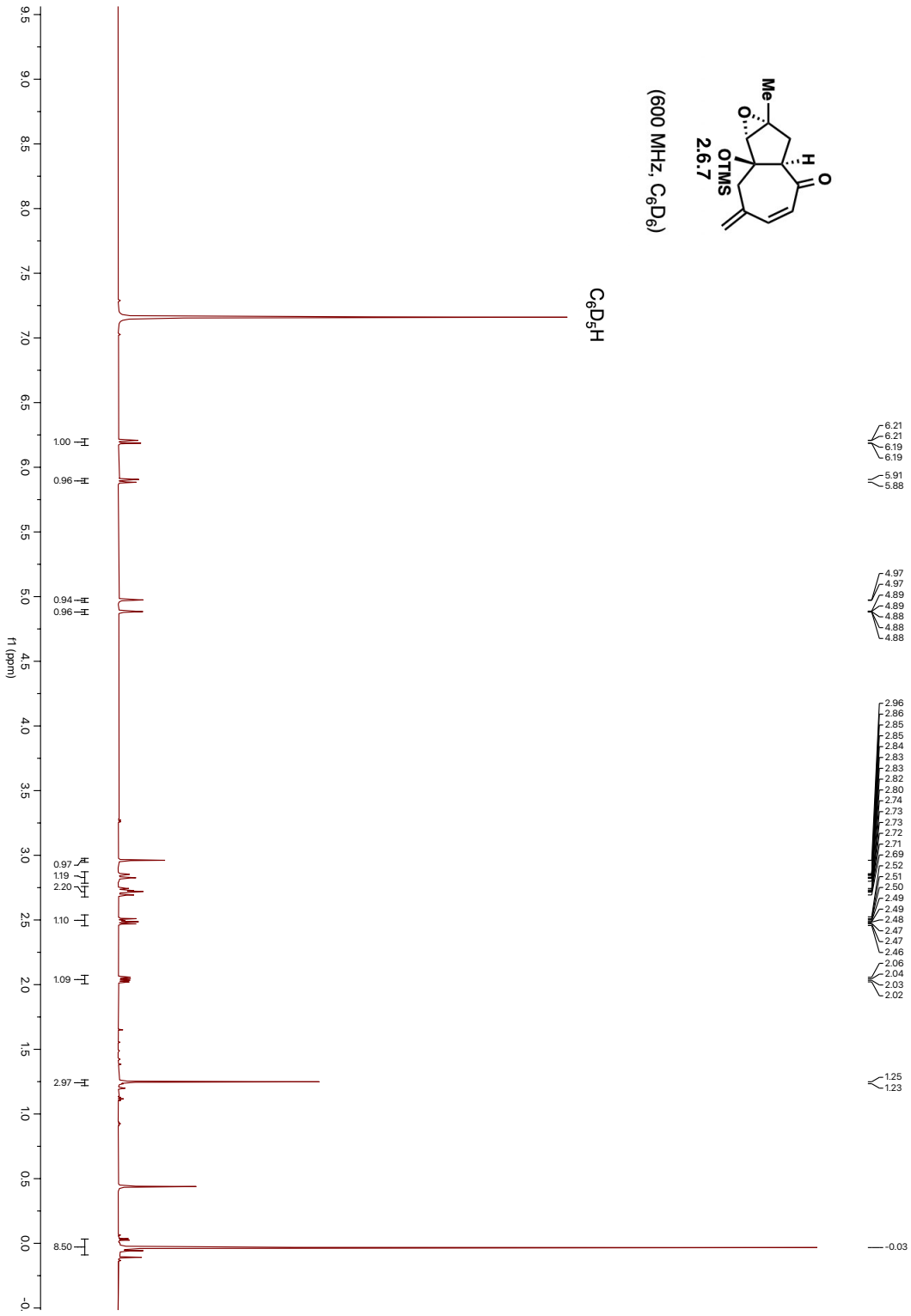

f2 (ppm)
f1 (ppm)
2.5.10
select nOe correlations
on α-face (green) and β-face
(red)
Me
OTMS
0.11 ppm
Me
OH
H
3.41 ppm
OH
H
4.10 ppm
H
2.51 ppm
Br
H
2.71 ppm
O
3.79 ppm
Me
1.27 ppm
Me
1.10 ppm

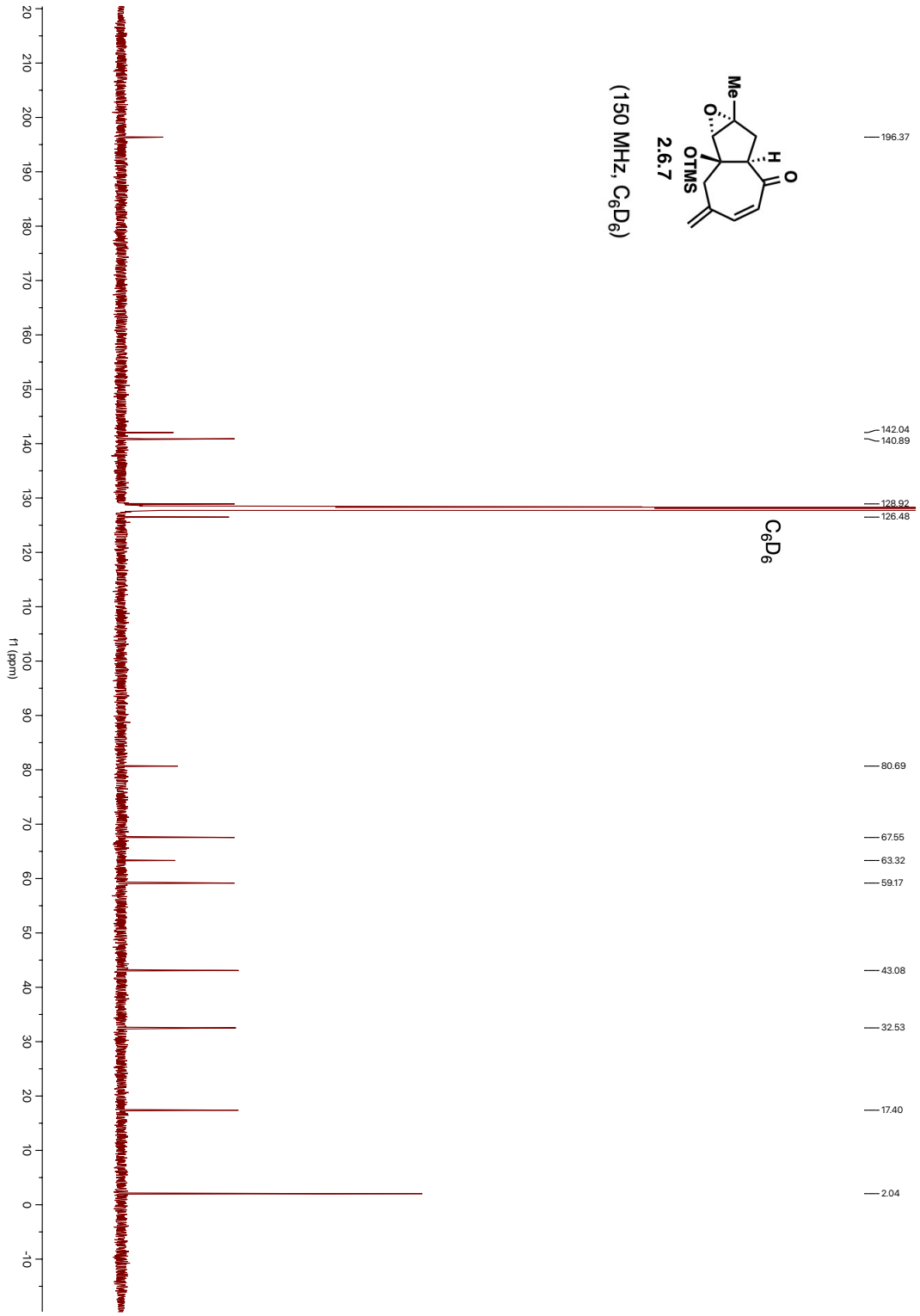

2.5.12 (mixture of isomers)
(600 MHz, C_6D_6)
C_6D_5H
f1 (ppm)

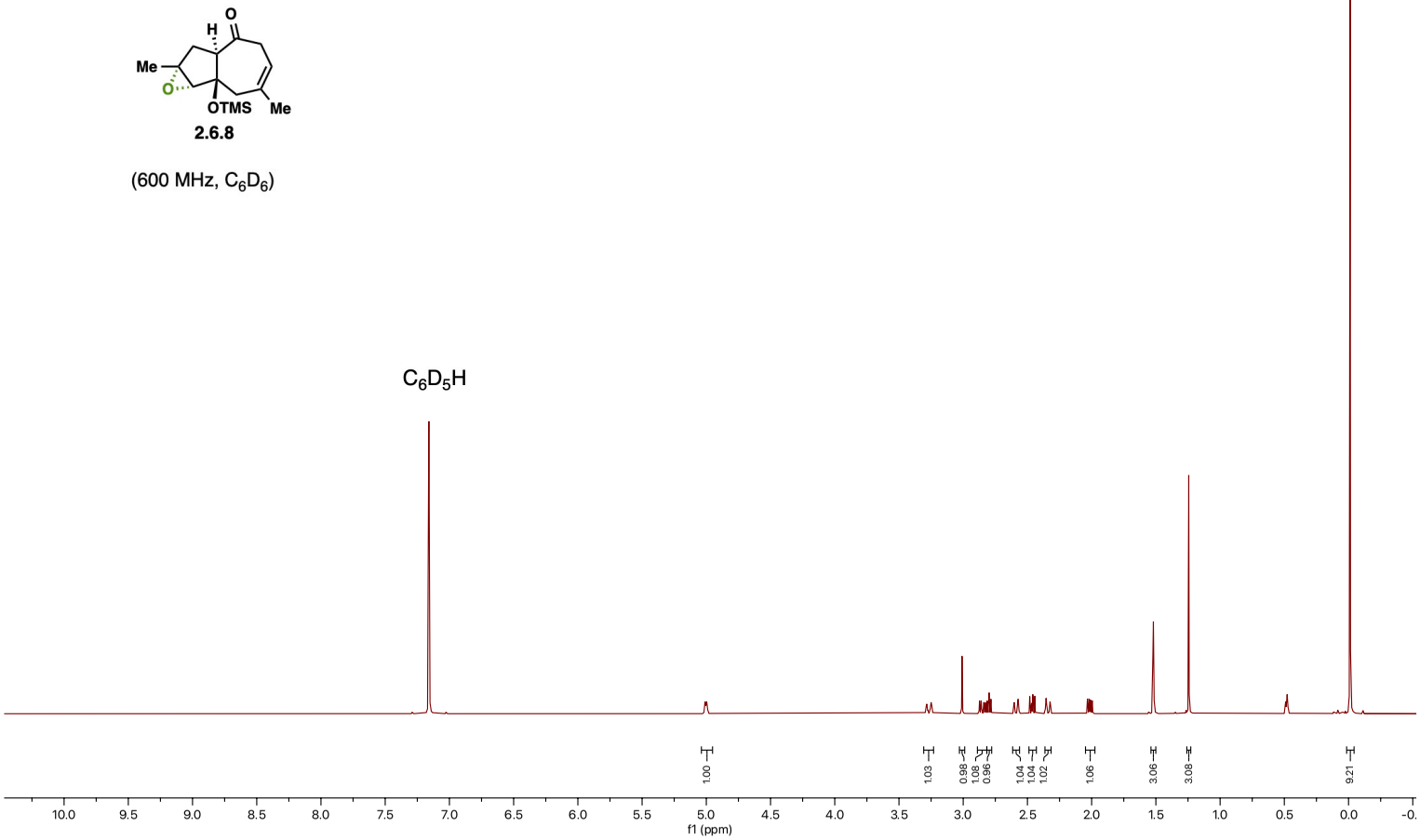

2.5.12 (mixture of isomers)
C6D6
143.53
137.77
135.37
135.11
131.84
124.67
123.01
122.85
93.03
91.93
84.98
83.64
71.64
71.12
68.70
68.46
63.91
62.62
58.30
54.75
54.20
49.11
43.31
42.72
36.46
35.92
35.72
27.81
27.72
26.10
26.00
20.12
19.99
19.88
16.77
16.70
2.21
2.04
f1 (ppm)

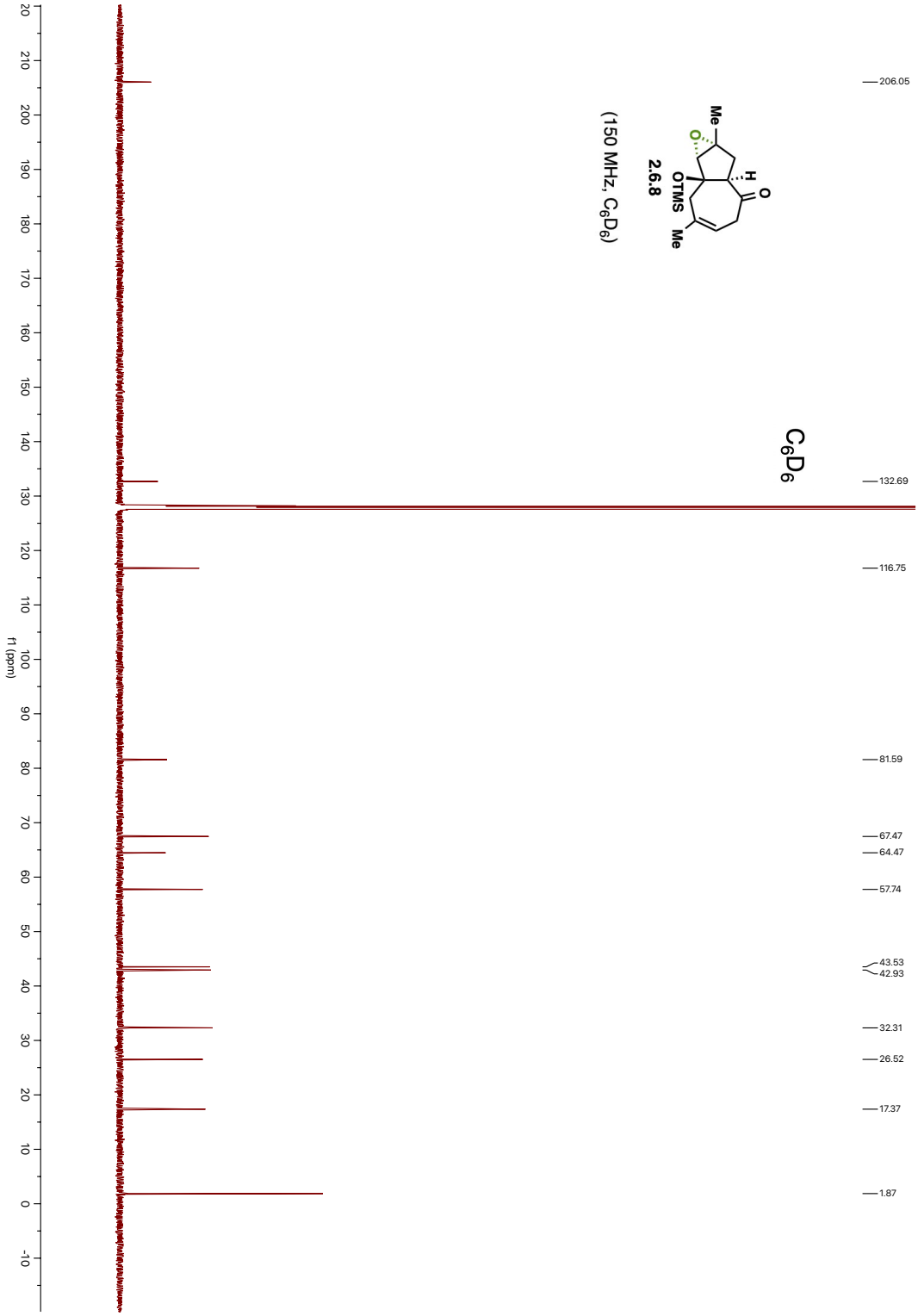

C6D5H
(600 MHz, C6D6)
2.5.13 (minor)
2.5.14 (major)
f1 (ppm)

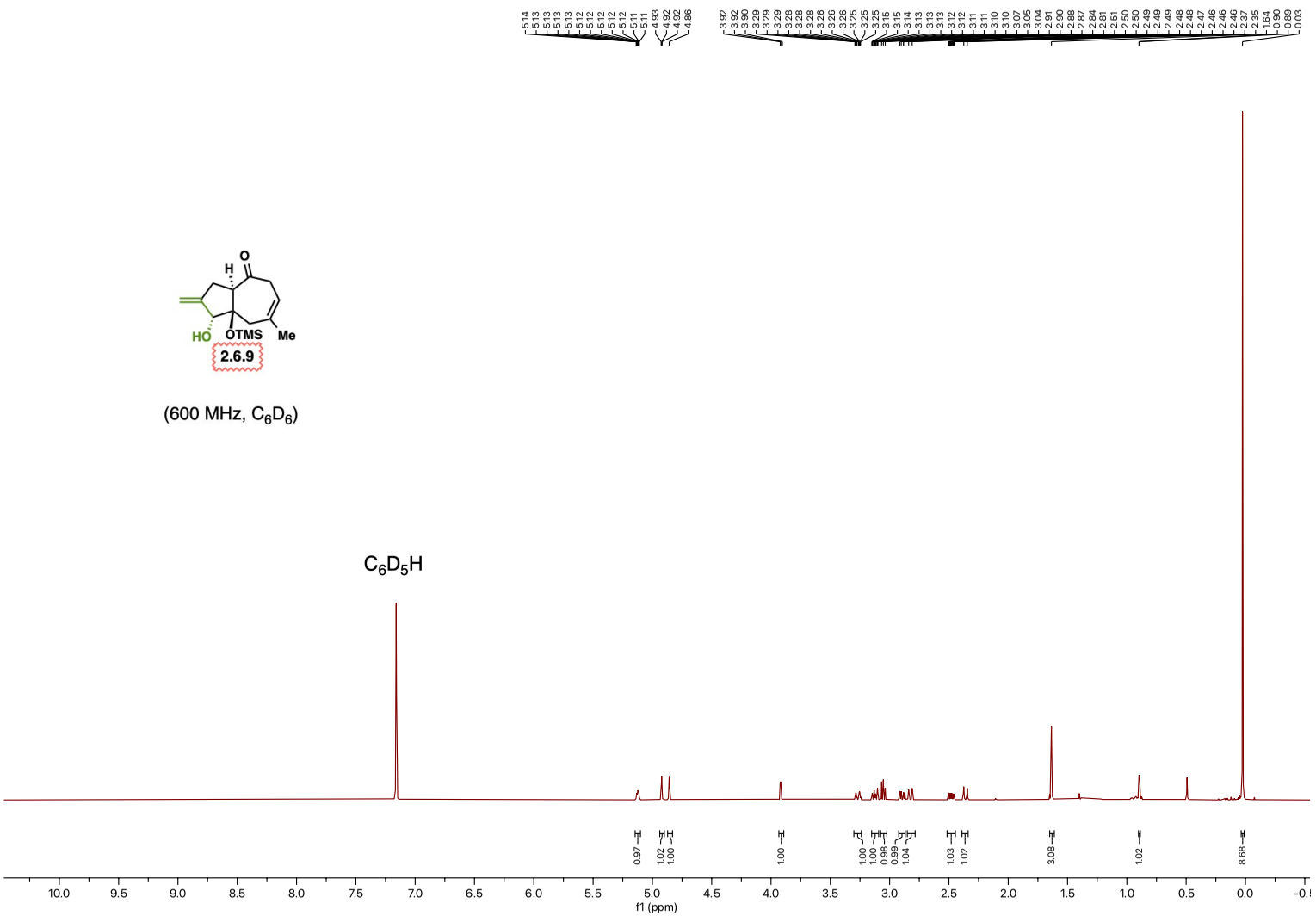

193.08
192.22
149.97
145.14
143.82
143.51
134.17
131.16
130.60
124.93
84.11
82.49
78.17
77.75
72.93
69.20
66.86
65.52
63.31
63.03
61.59
57.96
54.02
48.30
47.30
45.78
44.81
40.21
39.73
38.43
37.38
26.46
26.39
20.83
20.59
19.50
16.38
16.23
2.00
1.75
C6D6
Me
Me
H
O
Br
H
H
OH
1
Me
3
OH
OTMS
20
CHO
2.5.13 (minor)
2.5.14 (major)
f1 (ppm)

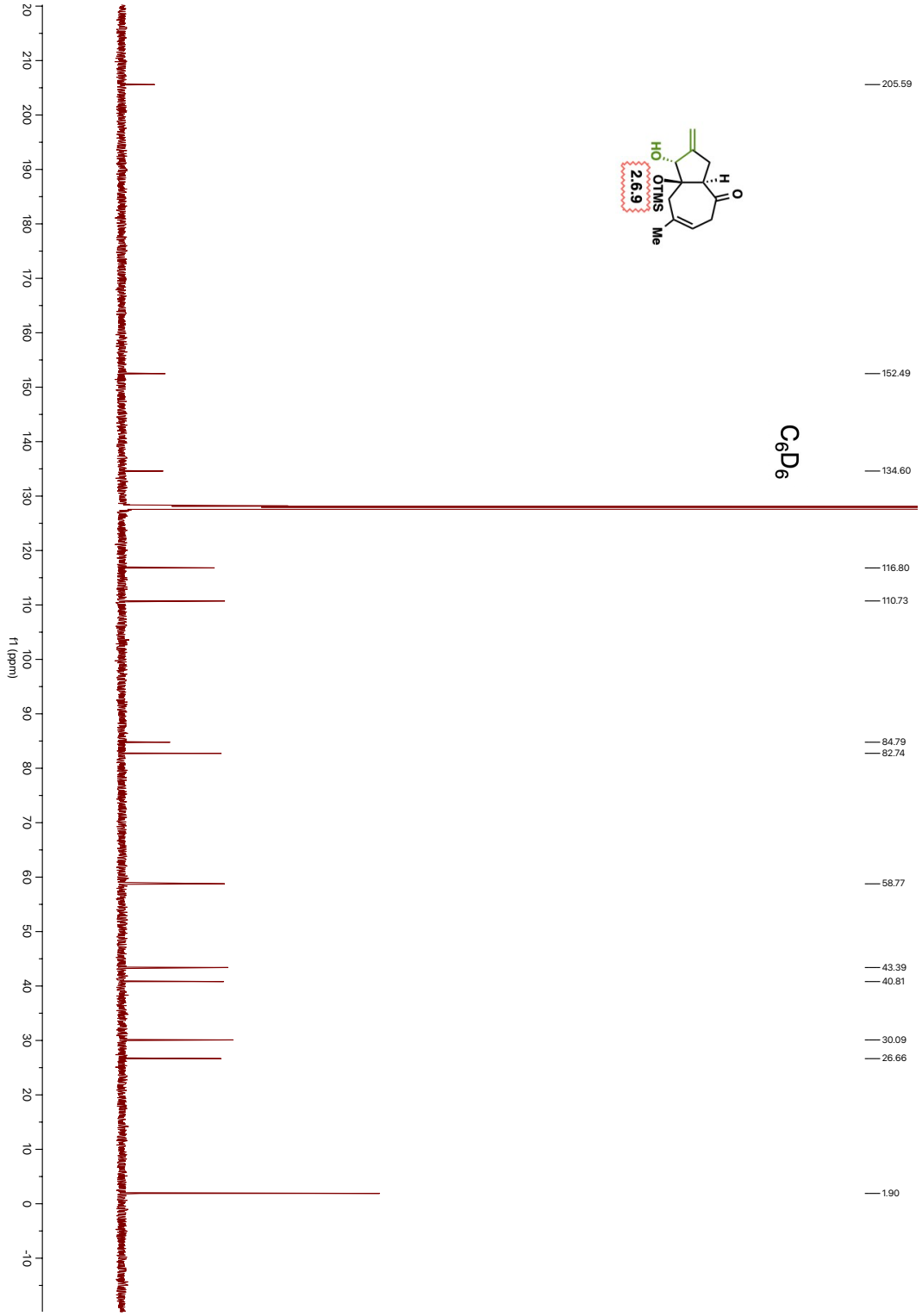

2.6.7
(600 MHz, C_6D_6)
C_6D_5H
f1 (ppm)

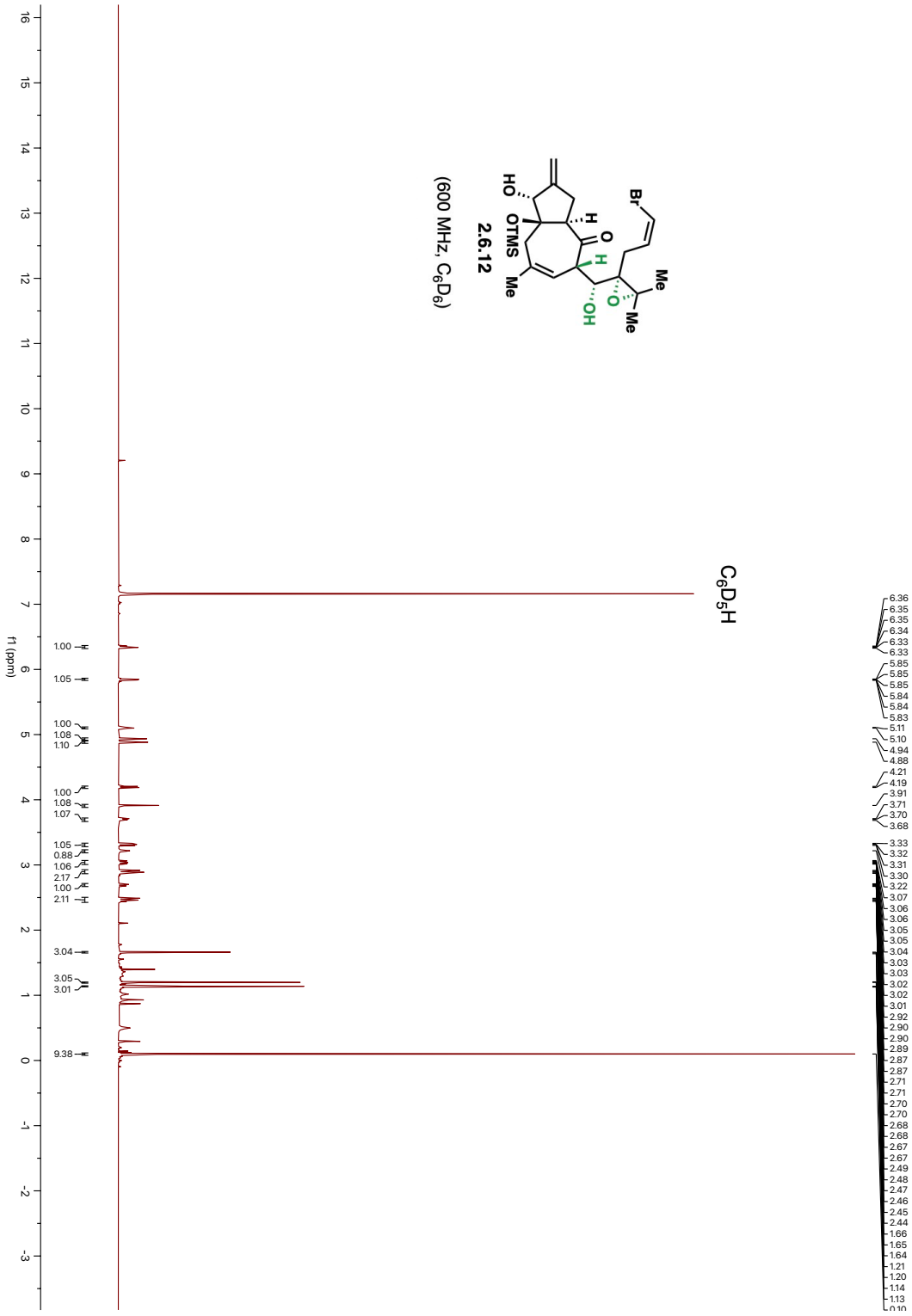

2.6.7
(150 MHz, C6D6)
Me
O
H
O
OTMS
196.37
142.04
140.89
128.92
126.48
C6D6
80.69
67.55
63.32
59.17
43.08
32.53
17.40
2.04
f1 (ppm)

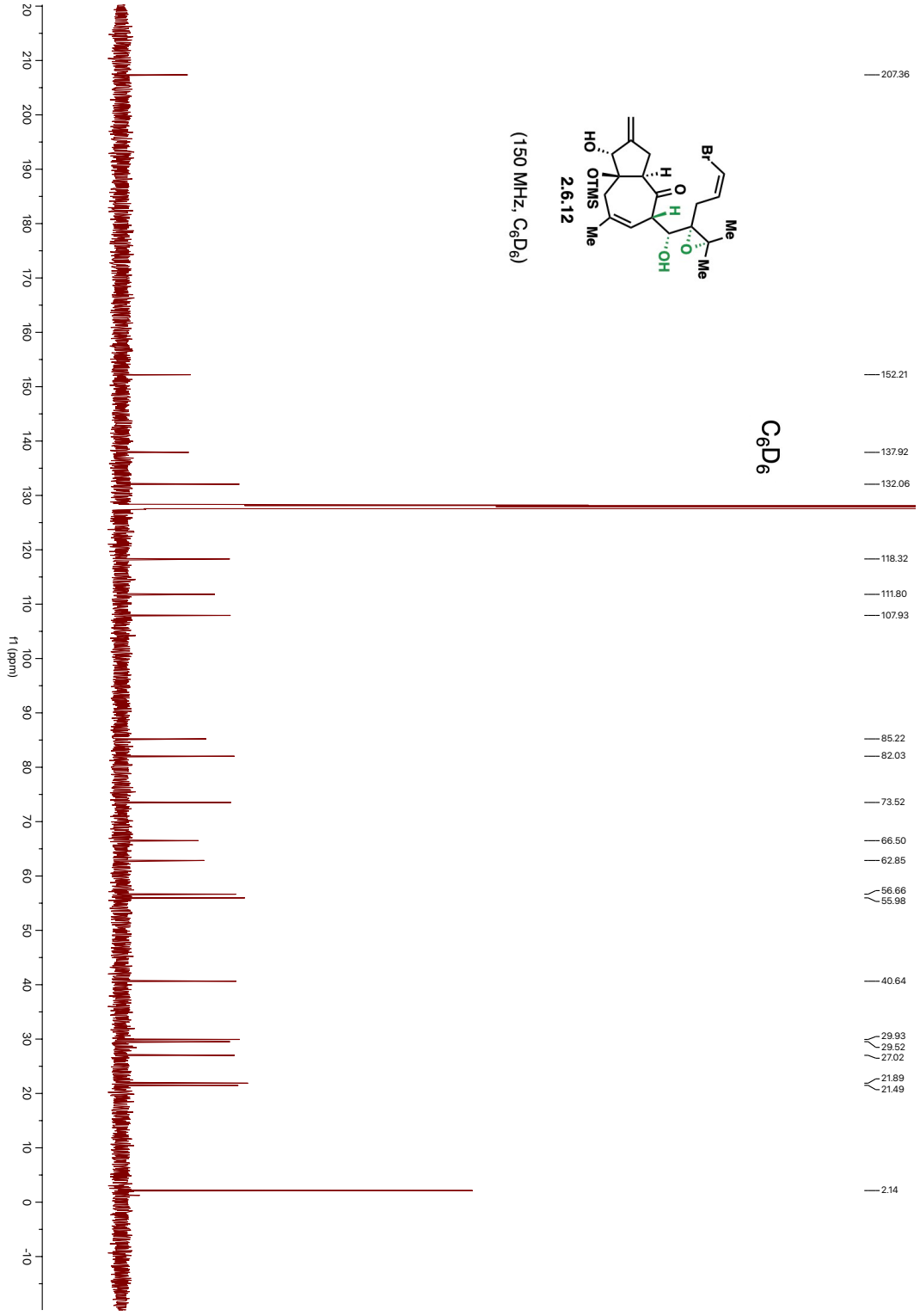

O
H
Me
O
OTMS
Me
2.6.8
(600 MHz, C6D6)
C6D5H
f1 (ppm)

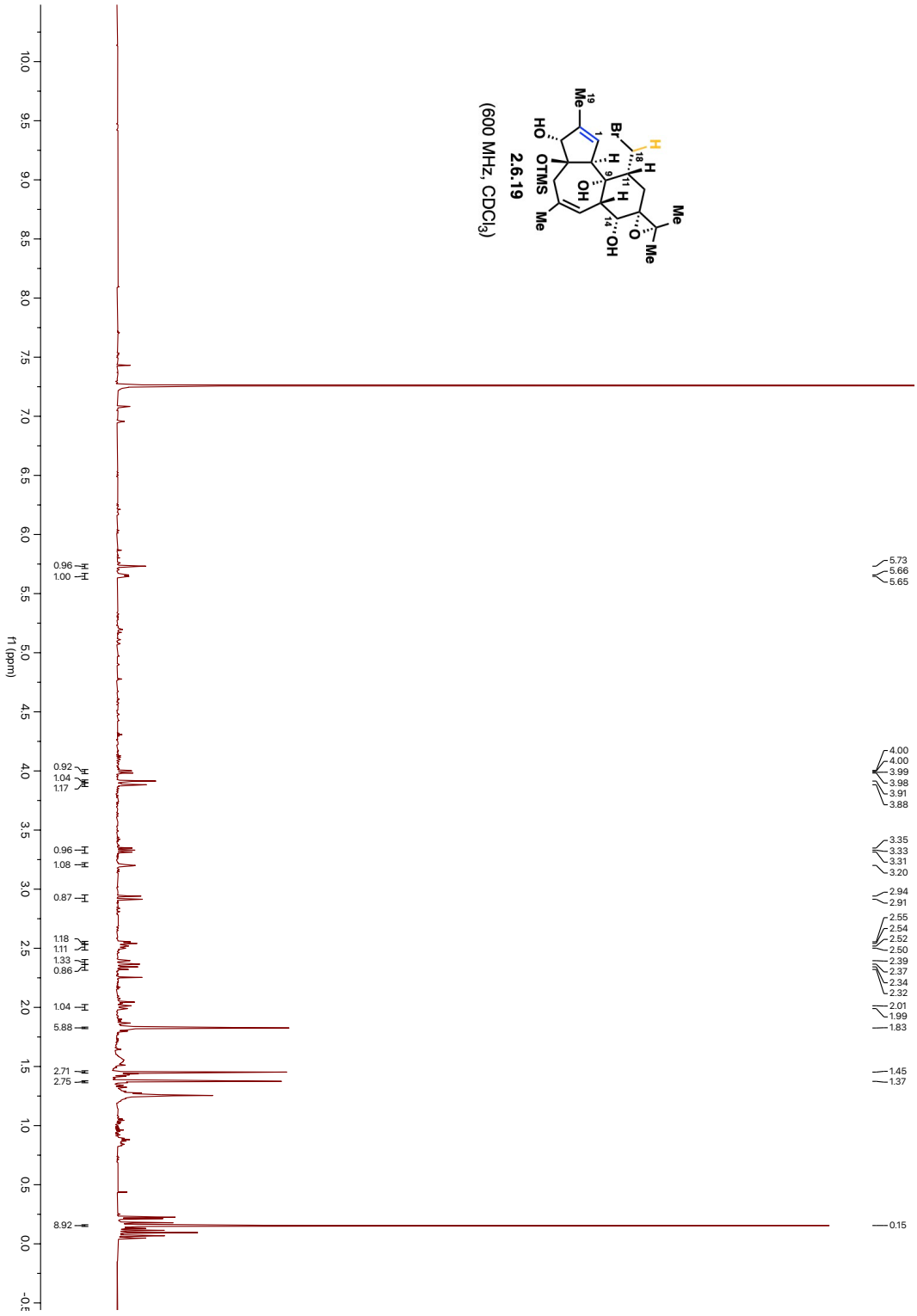

206.05
132.69
116.75
81.59
67.47
64.47
57.74
43.53
42.93
32.31
26.52
17.37
1.87
C6D6
(150 MHz, C6D6)
2.6.8
Me
O
H
O
OTMS
Me
f1 (ppm)

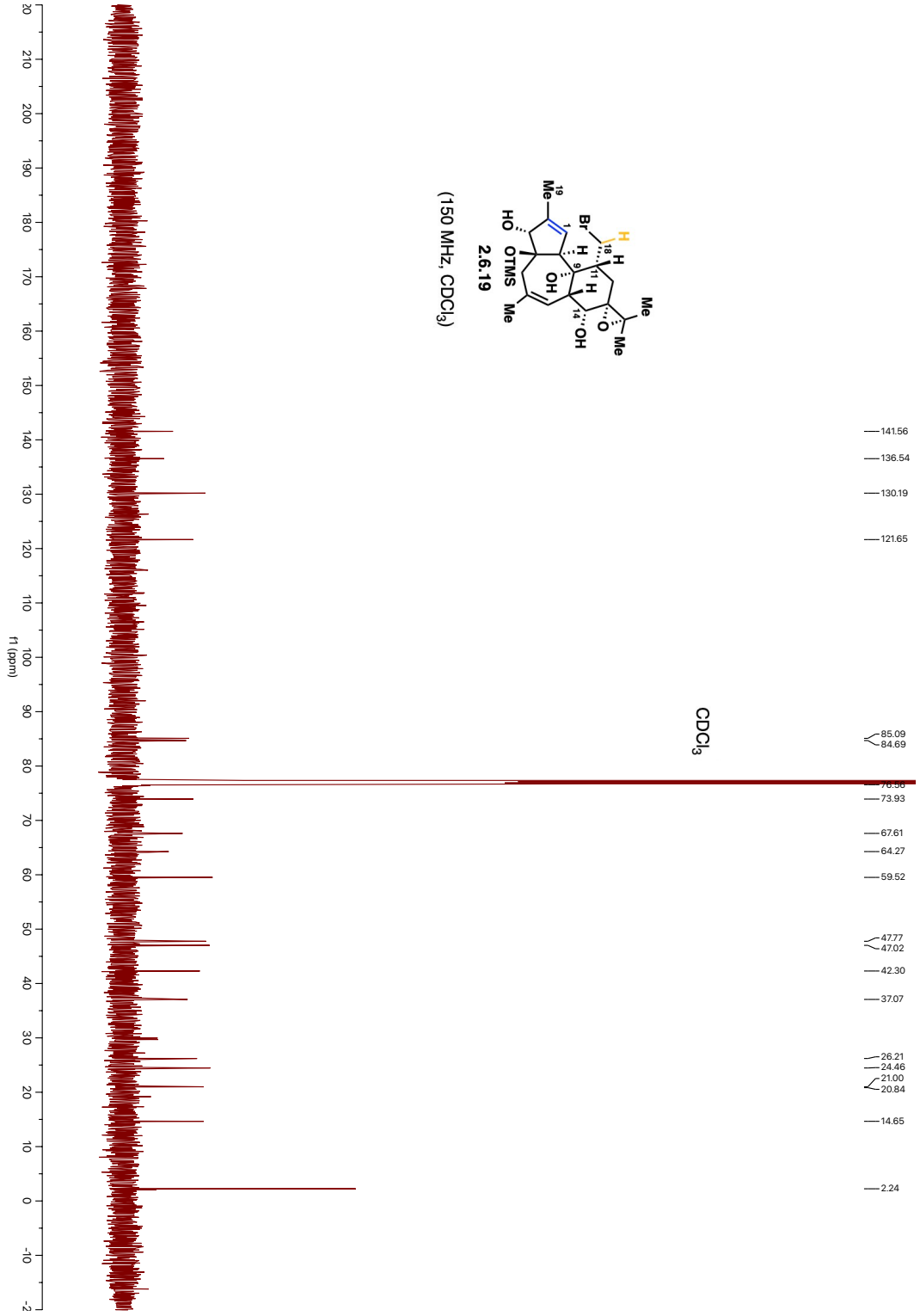

5.14
5.13
5.13
5.13
5.13
5.12
5.12
5.12
5.12
5.12
5.11
5.11
4.93
4.92
4.92
4.92
4.86
3.92
3.92
3.90
3.29
3.29
3.28
3.28
3.28
3.26
3.26
3.25
3.25
3.25
3.15
3.15
3.14
3.13
3.13
3.13
3.12
3.12
3.11
3.11
3.10
3.10
3.07
3.05
3.04
3.01
2.90
2.88
2.87
2.84
2.81
2.51
2.50
2.50
2.49
2.49
2.49
2.48
2.48
2.47
2.46
2.46
2.46
2.37
2.35
1.64
0.90
0.89
0.03
O
H
HO
OTMS
Me
2.6.9
(600 MHz, C6D6)
C6D5H
0.97
1.02
1.00
1.00
1.00
1.00
0.98
0.99
1.04
1.03
1.02
3.08
1.02
8.68
10.0
9.5
9.0
8.5
8.0
7.5
7.0
6.5
6.0
5.5
5.0
4.5
4.0
3.5
3.0
2.5
2.0
1.5
1.0
0.5
0.0
f1 (ppm)

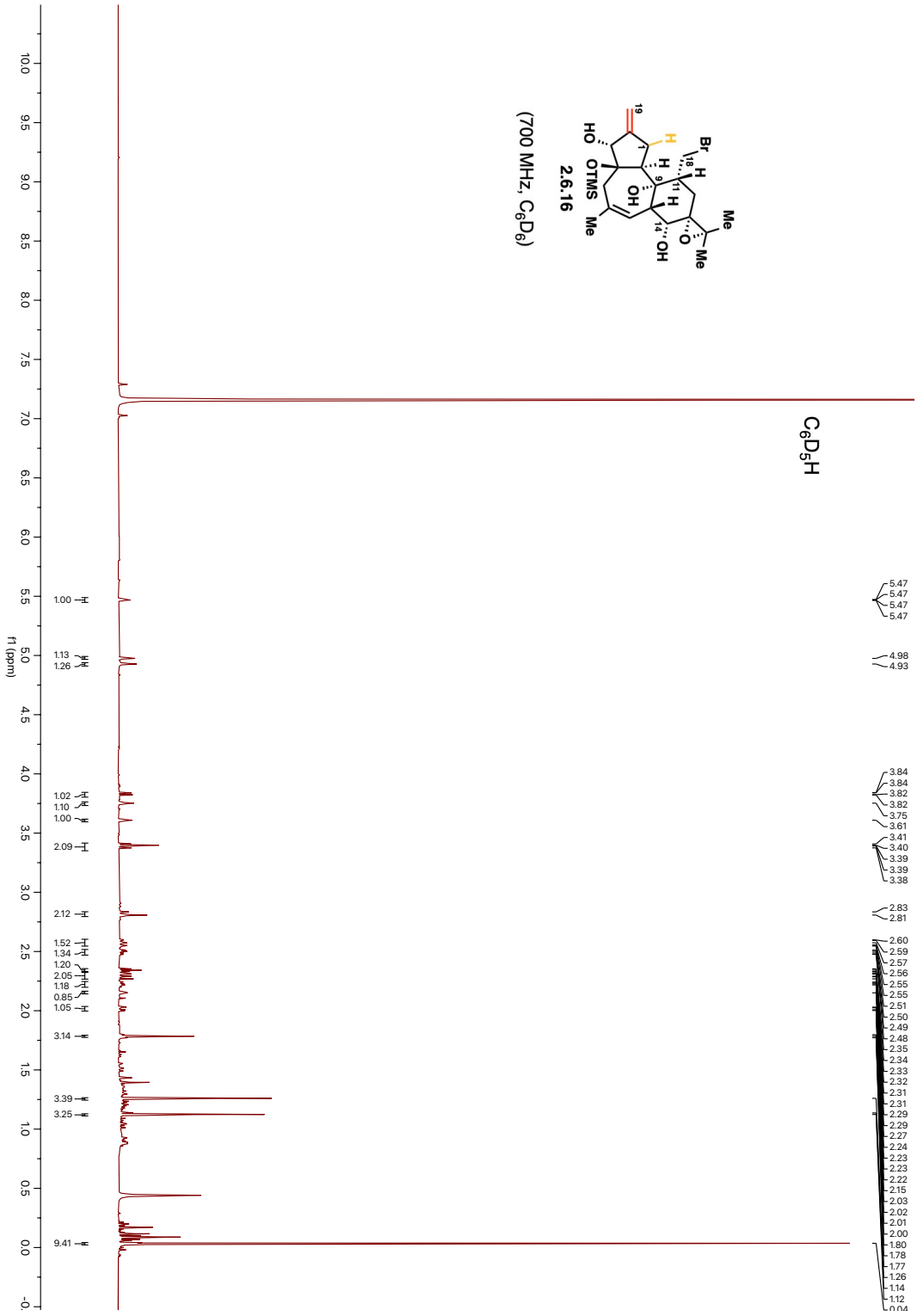

205.59
152.49
134.60
116.80
110.73
84.79
82.74
58.77
43.39
40.81
30.09
26.66
1.90
C6D6
HO
OTMS
Me
H
O
2.6.9
f1 (ppm)

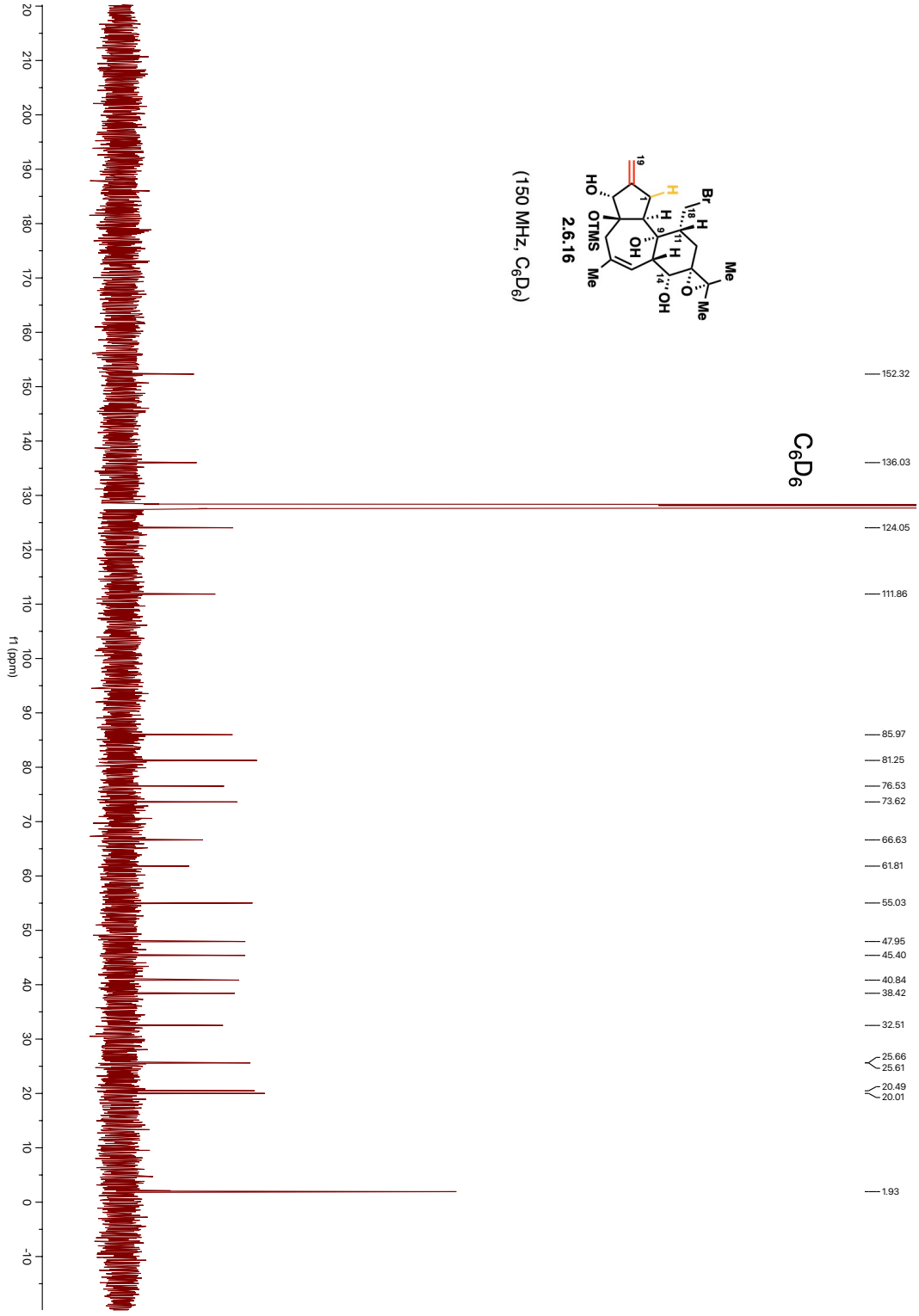

2.6.12
(600 MHz, C6D6)
C6D5H
f1 (ppm)

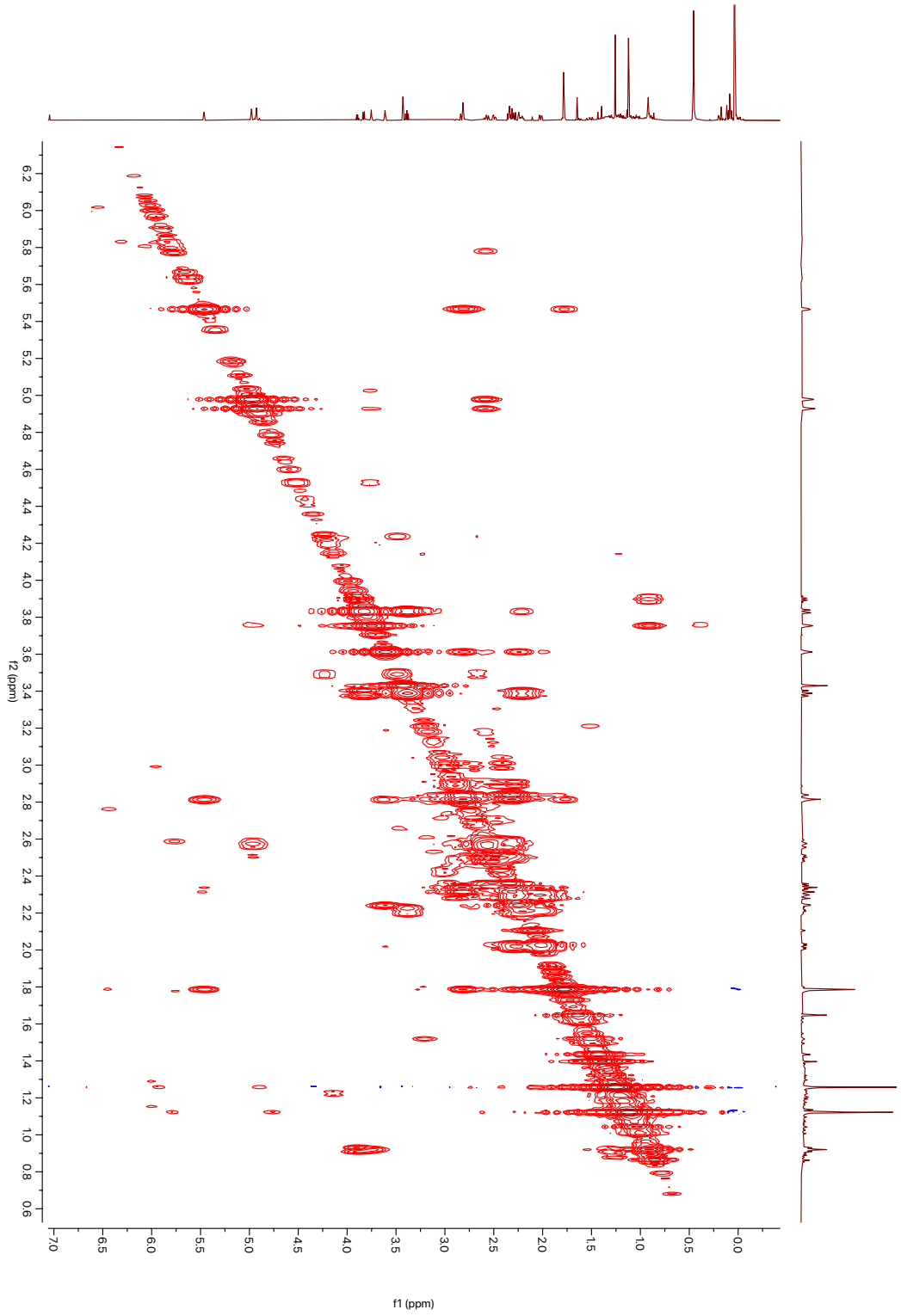

207.36
152.21
137.92
132.06
118.32
111.80
107.93
85.22
82.03
73.52
66.50
62.85
56.66
55.98
40.64
29.93
29.52
27.02
21.89
21.49
2.14
f1 (ppm)
C6D6
(150 MHz, C6D6)
2.6.12
HO
OTMS
Me
Br
Me
Me
OH
O
H
O
H

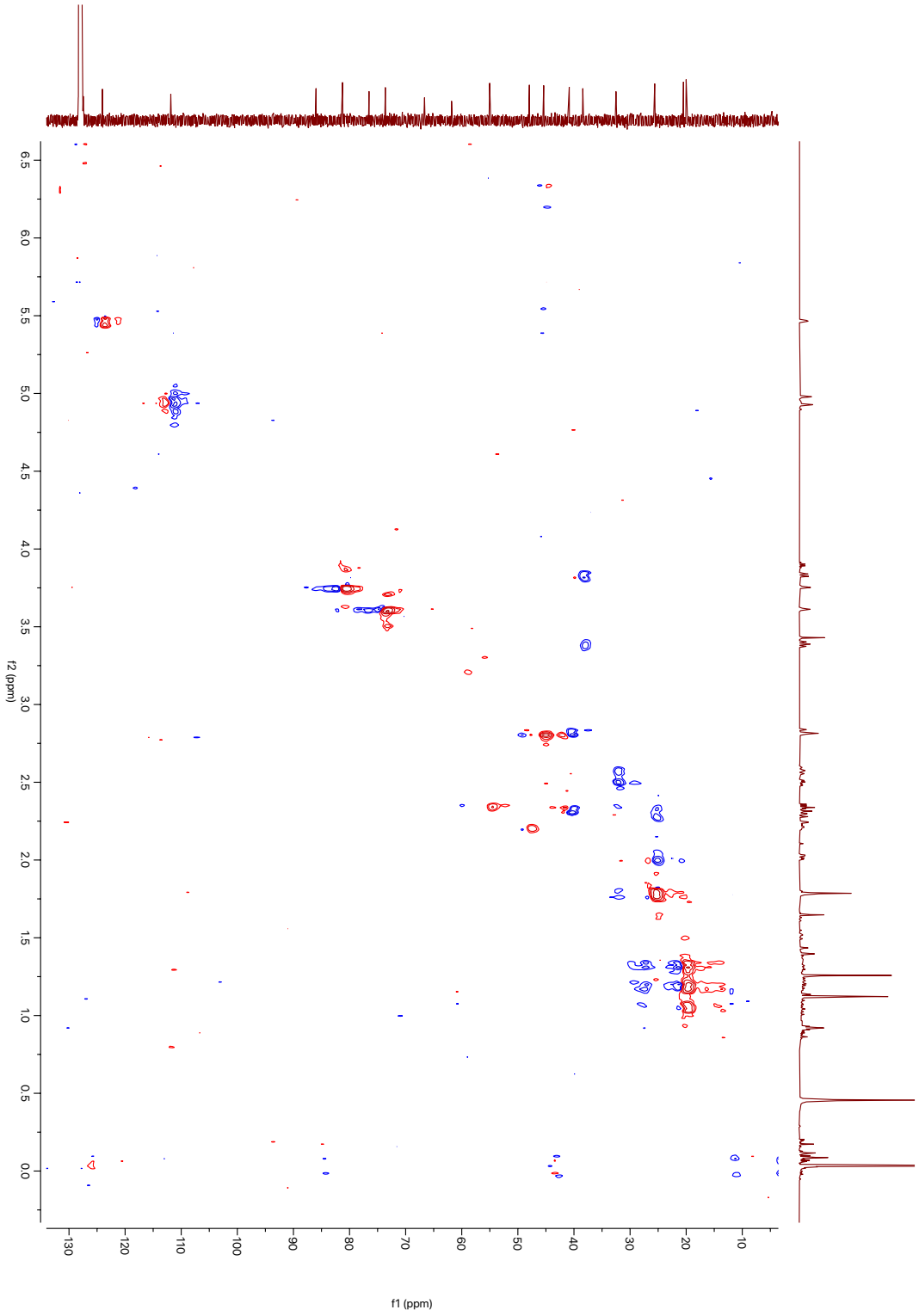

2.6.19
(600 MHz, CDCl3)
f1 (ppm)
0.96
1.00
0.92
1.04
1.17
0.96
1.08
0.87
1.18
1.11
1.33
0.86
1.04
5.88
2.71
2.75
8.92
5.73
5.66
5.65
4.00
4.00
3.99
3.98
3.91
3.88
3.35
3.33
3.31
3.20
2.94
2.91
2.55
2.54
2.52
2.50
2.39
2.37
2.34
2.32
2.01
1.99
1.83
1.45
1.37
0.15

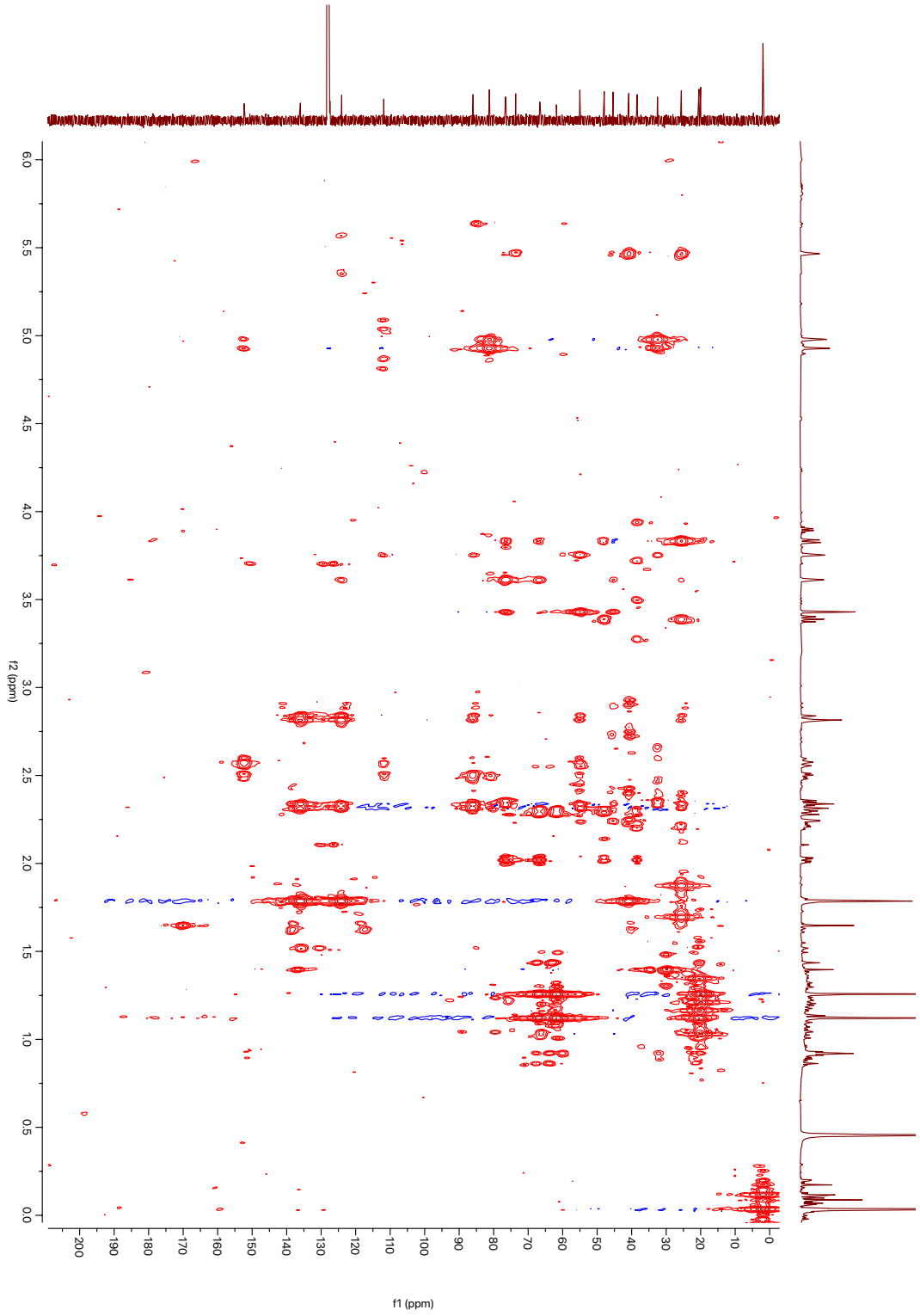

2.6.19
(150 MHz, CDCl3)
CDCl3
141.56
136.54
130.19
121.65
85.09
84.69
73.93
67.61
64.27
59.52
47.77
47.02
42.30
37.07
26.21
24.46
21.00
20.84
14.65
2.24
f1 (ppm)

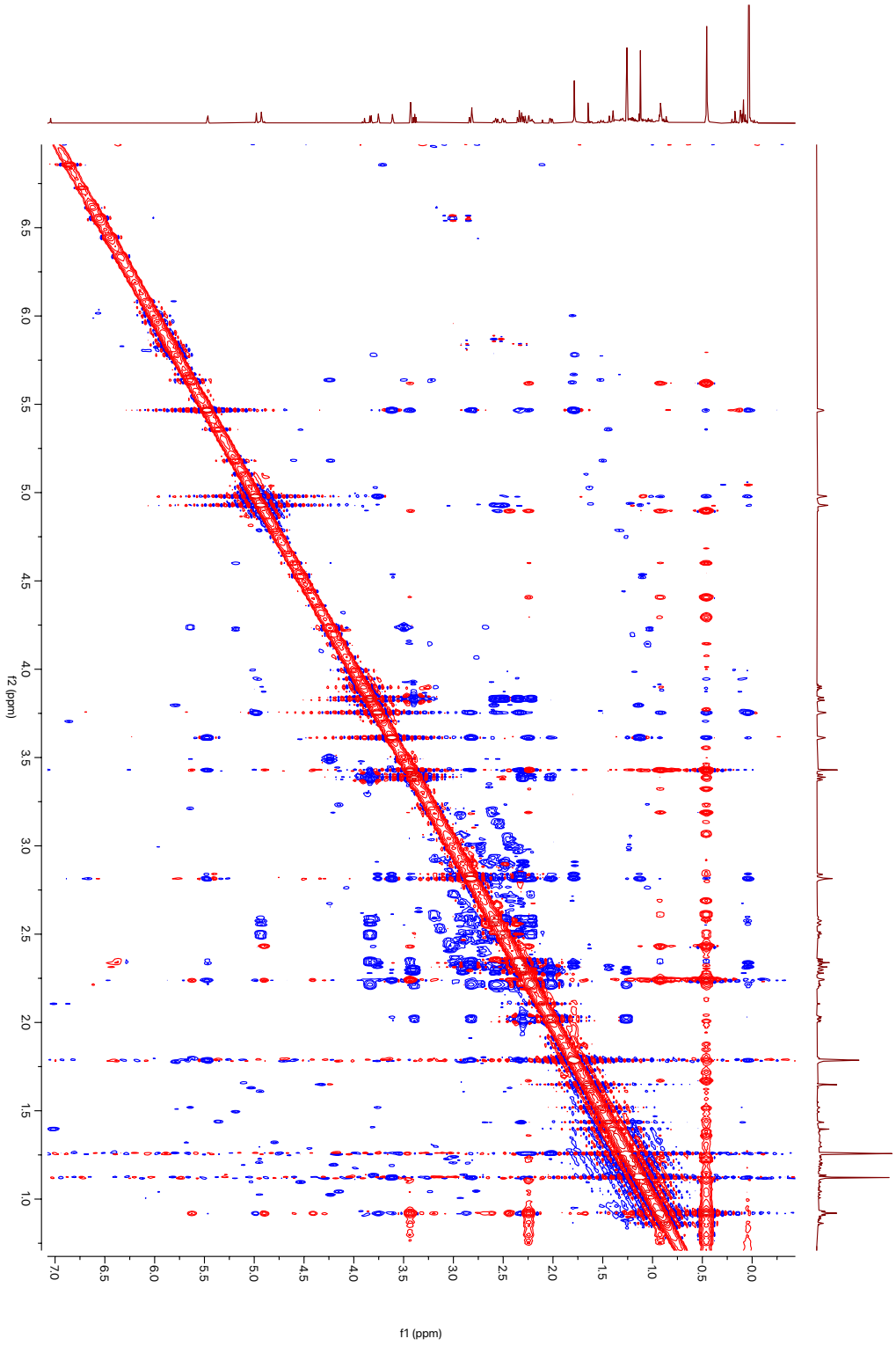

2.6.16
(700 MHz, C6D6)
C6D5H
f1 (ppm)

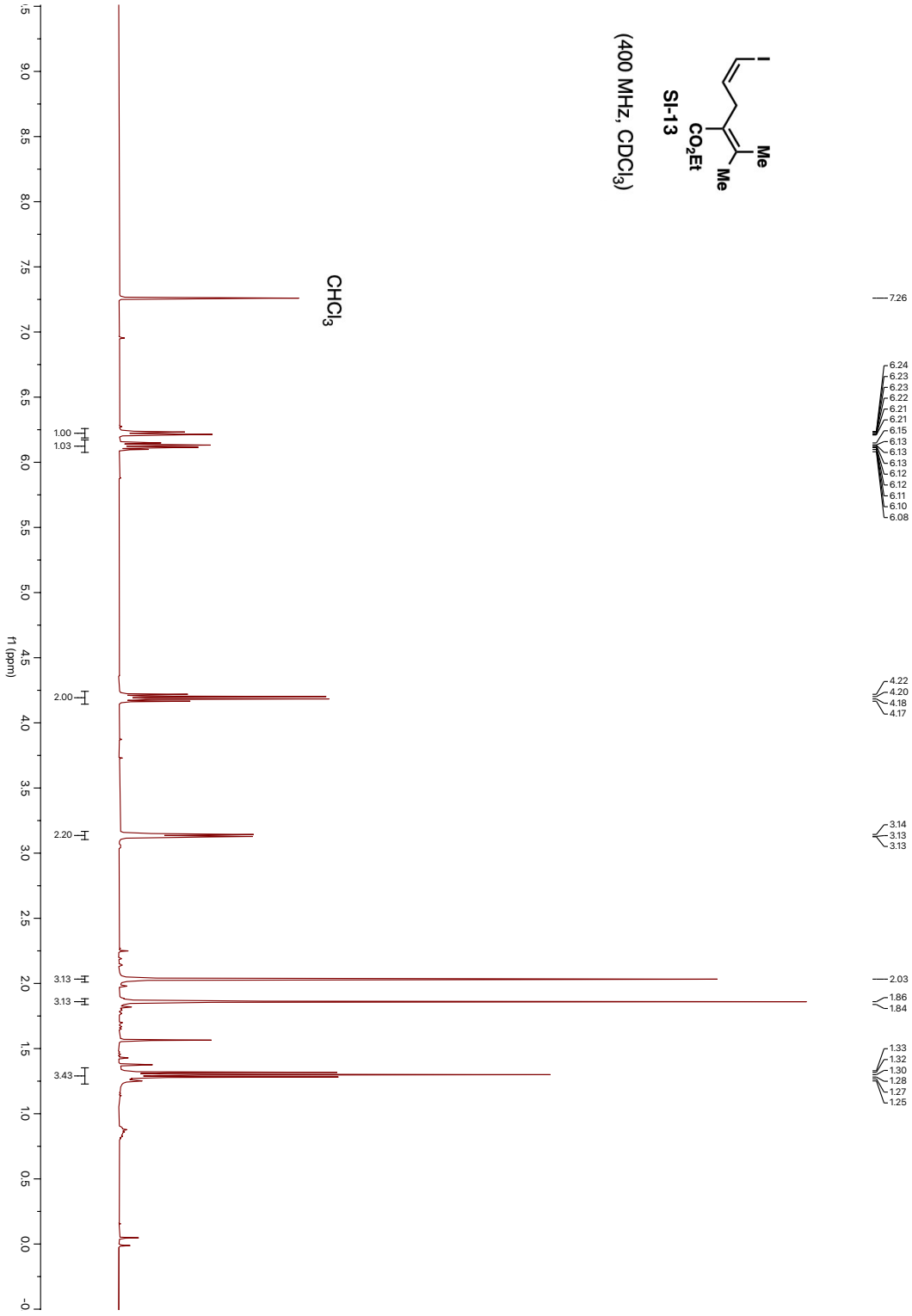

2.6.16
(150 MHz, C6D6)
C6D6
f1 (ppm)
152.32
136.03
124.05
111.86
85.97
81.25
76.53
73.62
66.63
61.81
55.03
47.95
45.40
40.84
38.42
32.51
25.66
25.61
20.49
20.01
1.93

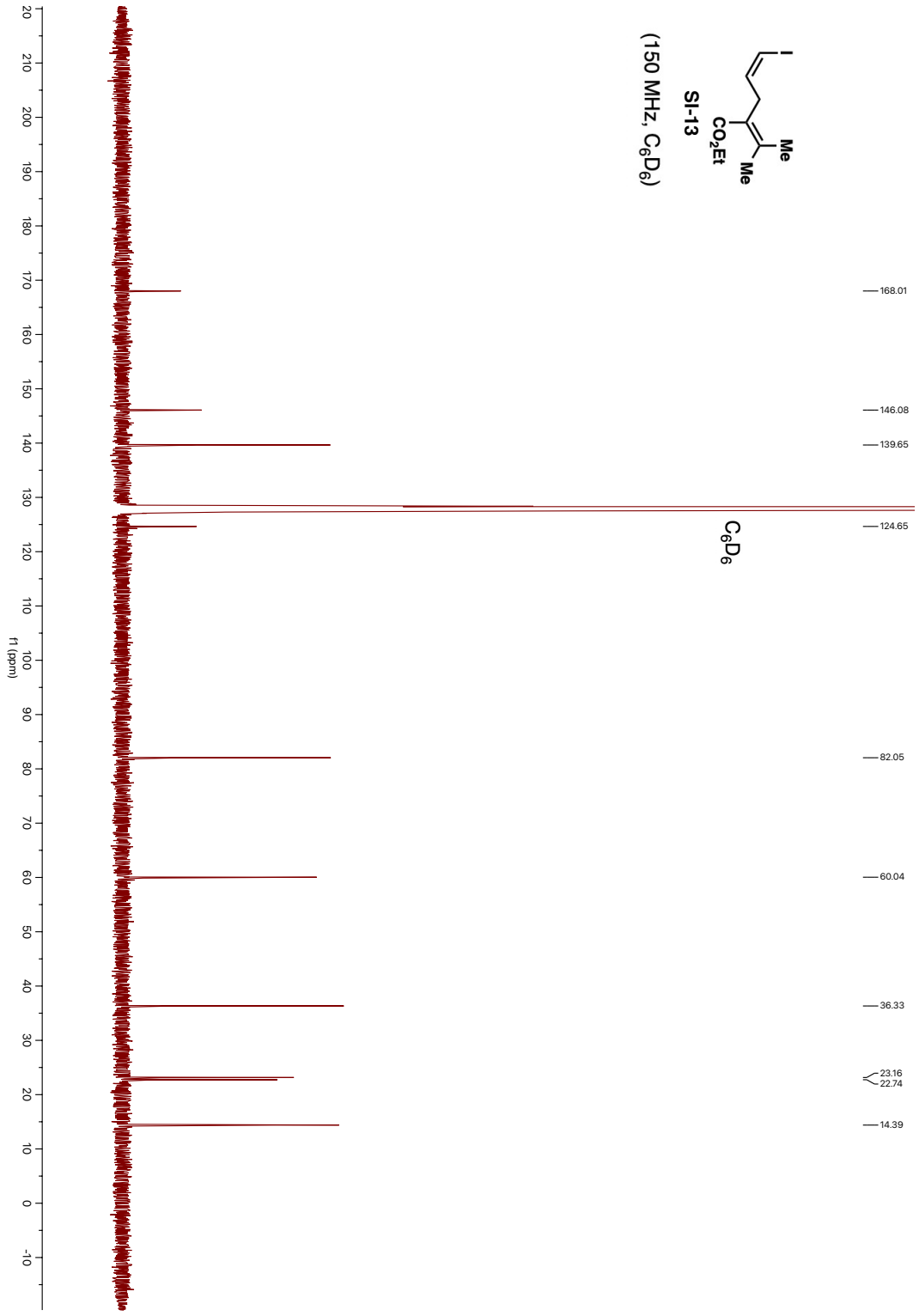

f2 (ppm)
f1 (ppm)

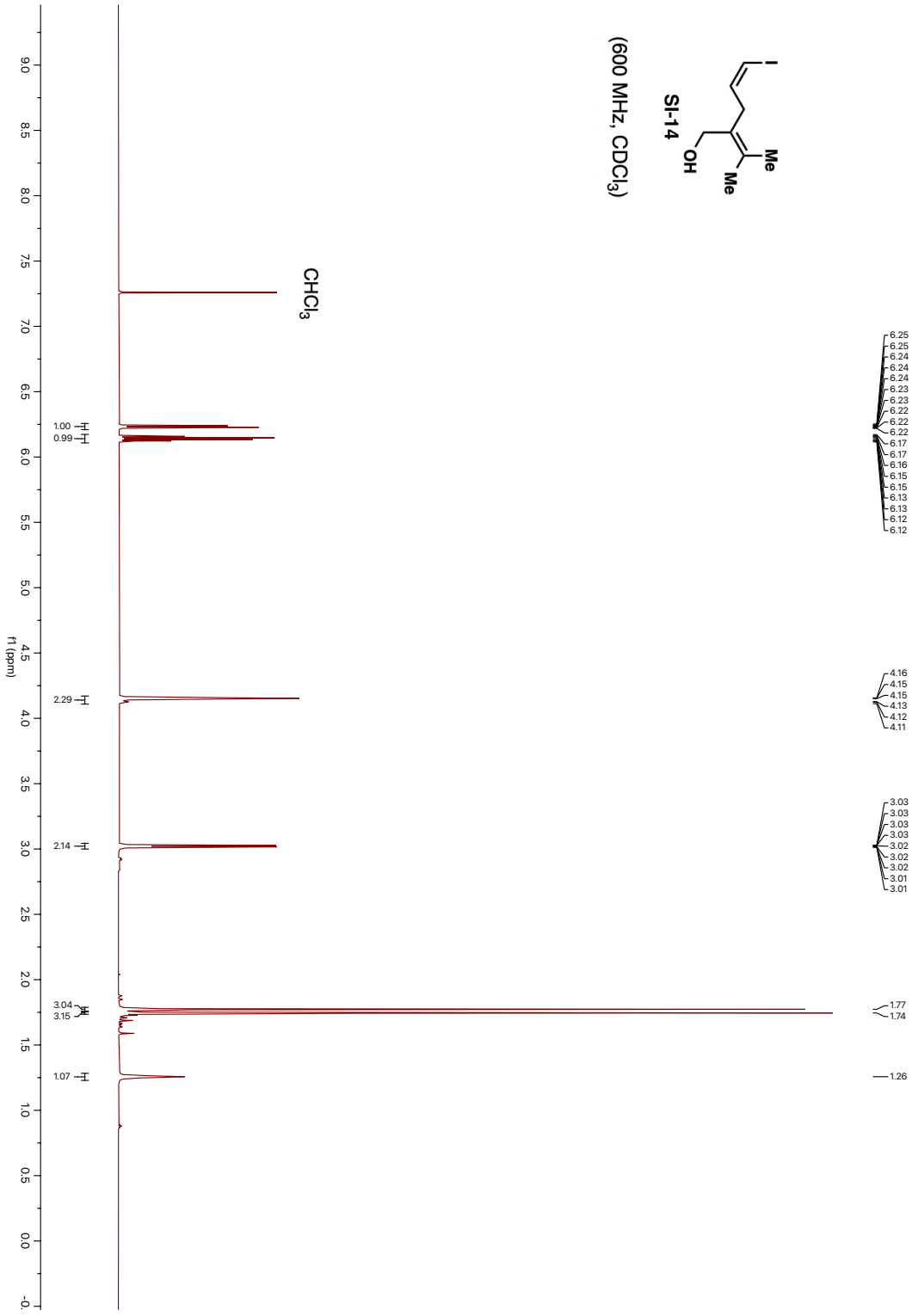

f2 (ppm)
f1 (ppm)

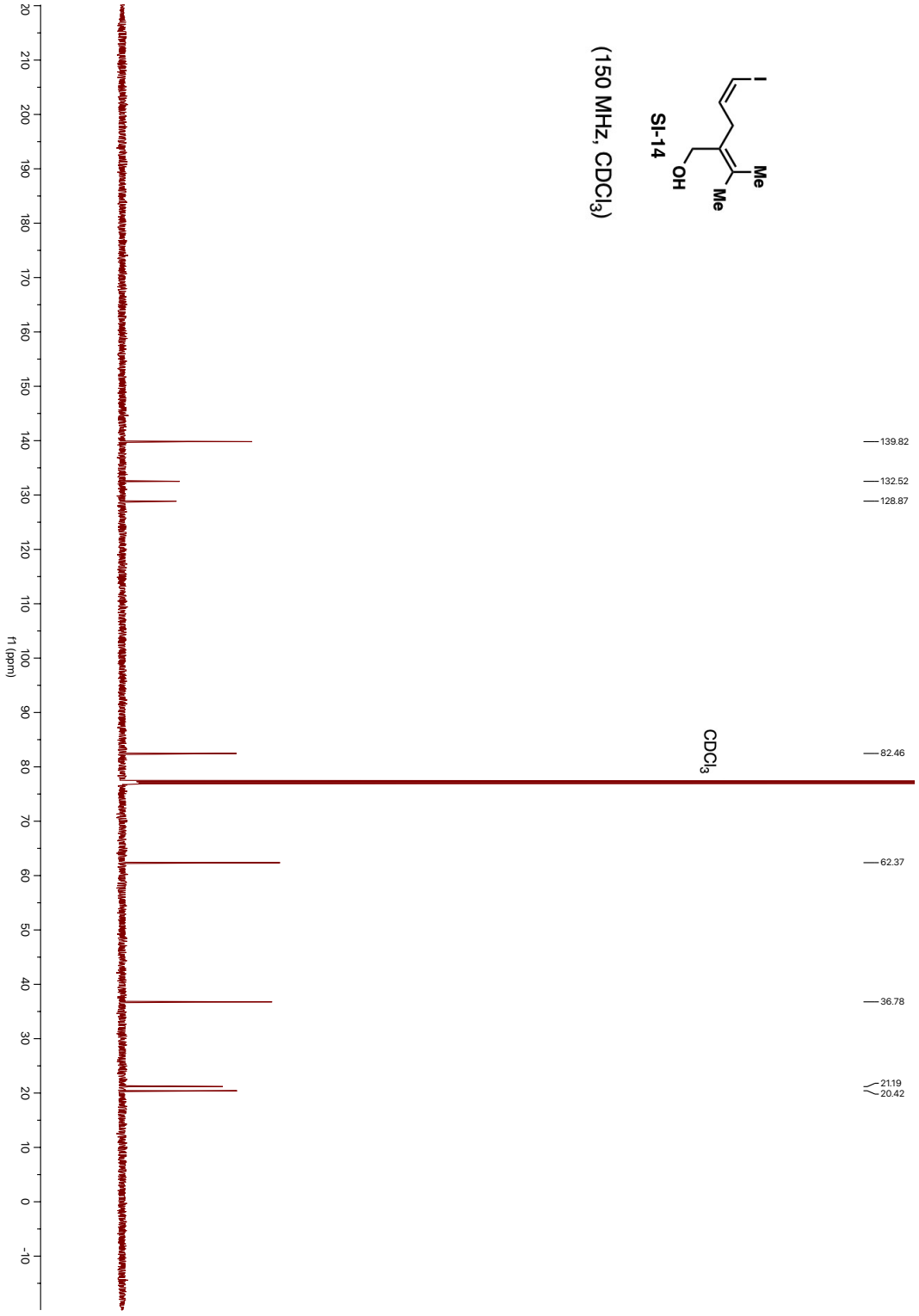

f2 (ppm)
f1 (ppm)

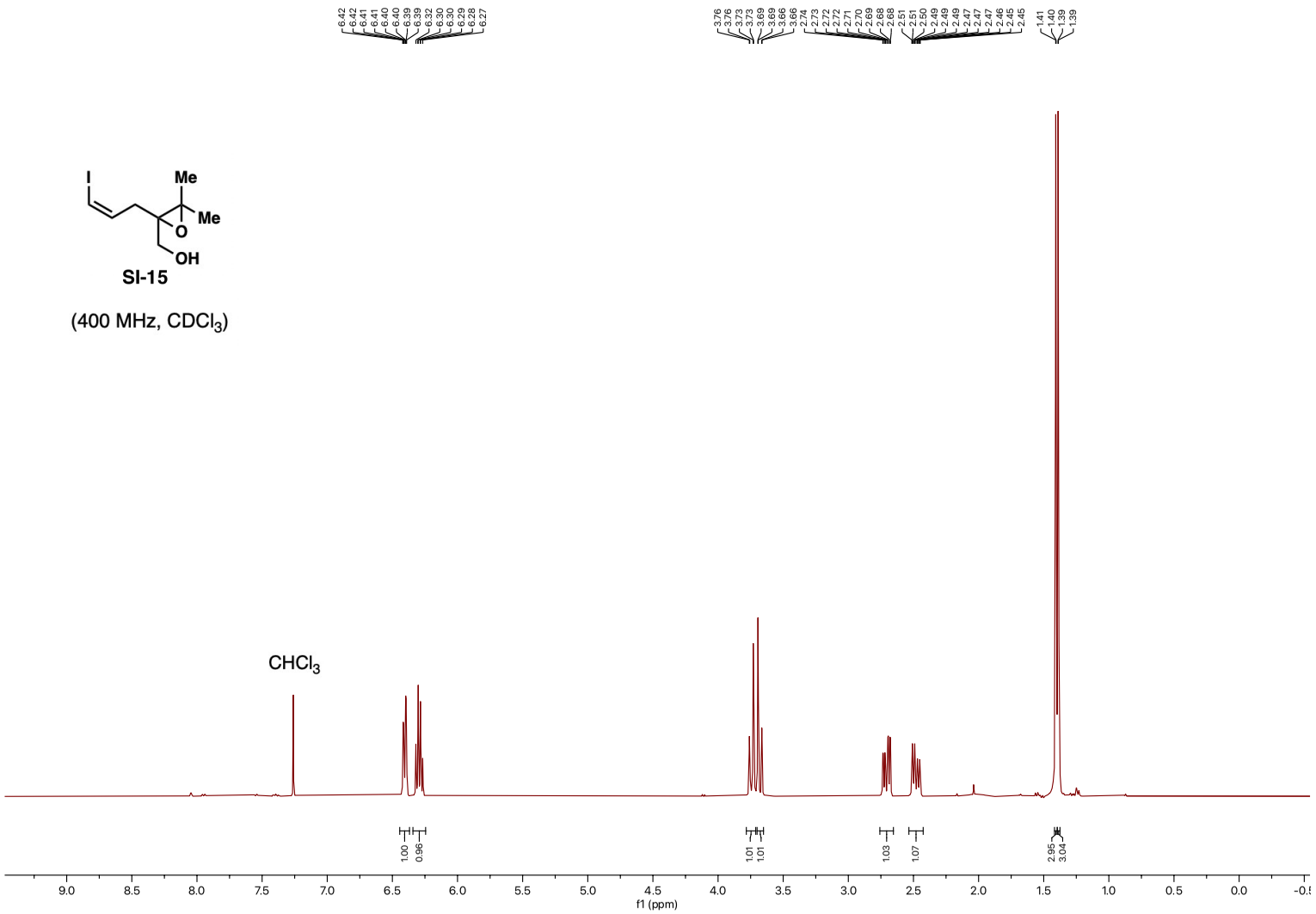

f2 (ppm)
f1 (ppm)

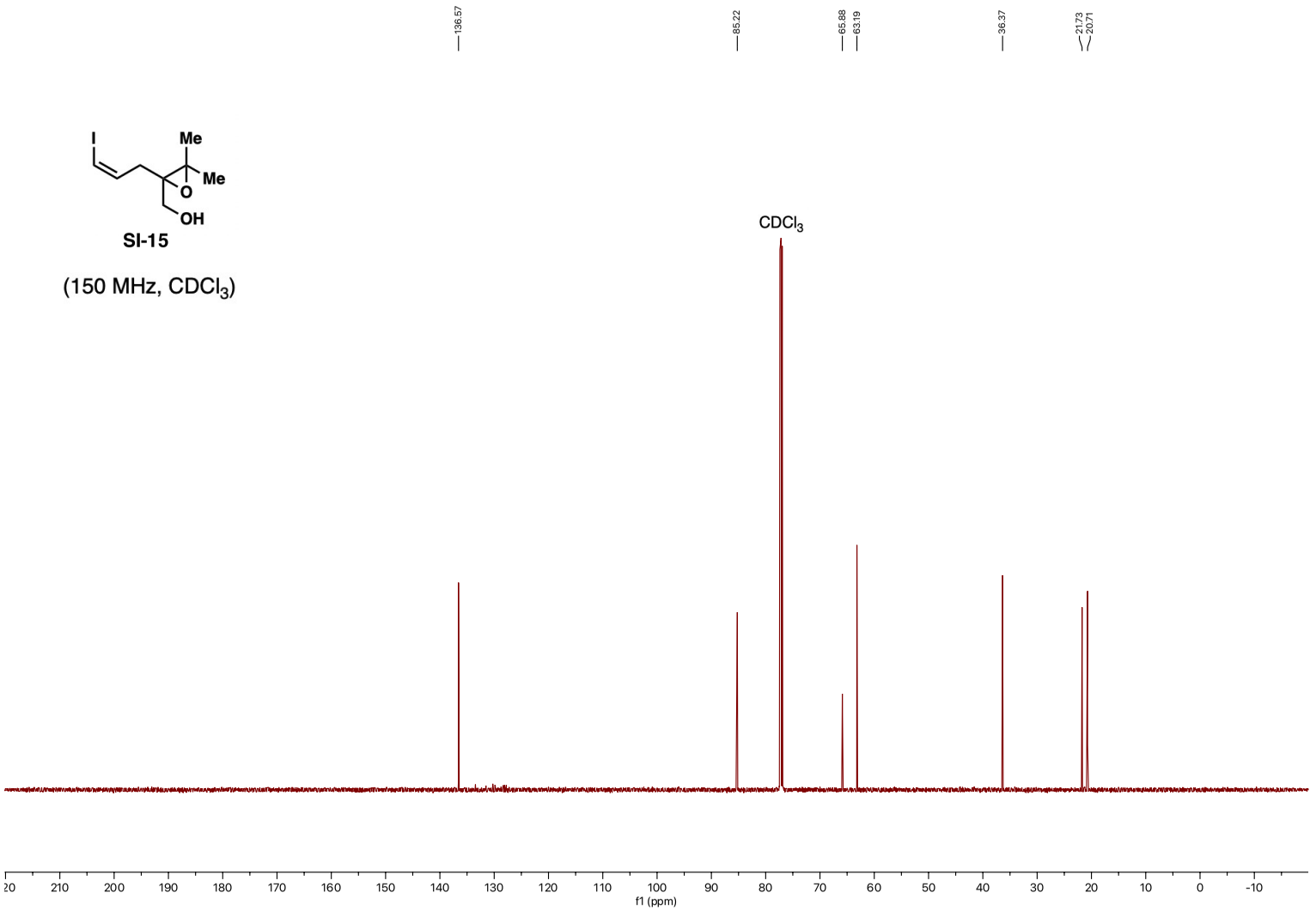

SI-13
(400 MHz, $CDCl_3$)
$CHCl_3$
f1 (ppm)
7.26
6.24
6.23
6.23
6.22
6.21
6.21
6.15
6.13
6.13
6.13
6.13
6.12
6.12
6.11
6.10
6.08
4.22
4.20
4.18
4.17
3.14
3.13
3.13
2.03
1.86
1.84
1.33
1.32
1.30
1.28
1.27
1.25
1.00
1.03
2.00
2.20
3.13
3.13
3.43


SI-13
(150 MHz, C6D6)
Me
Me
CO2Et
C6D6
168.01
146.08
139.65
124.65
82.05
60.04
36.33
23.16
22.74
14.39
f1 (ppm)


SI-14
(600 MHz, CDCl3)
CHCl3
f1 (ppm)
1.00
0.99
2.29
2.14
3.04
3.15
1.07
6.25
6.25
6.24
6.24
6.24
6.23
6.23
6.22
6.22
6.22
6.17
6.17
6.16
6.15
6.15
6.13
6.13
6.12
6.12
4.16
4.15
4.15
4.13
4.12
4.11
3.03
3.03
3.03
3.03
3.02
3.02
3.02
3.01
3.01
1.77
1.74
1.26

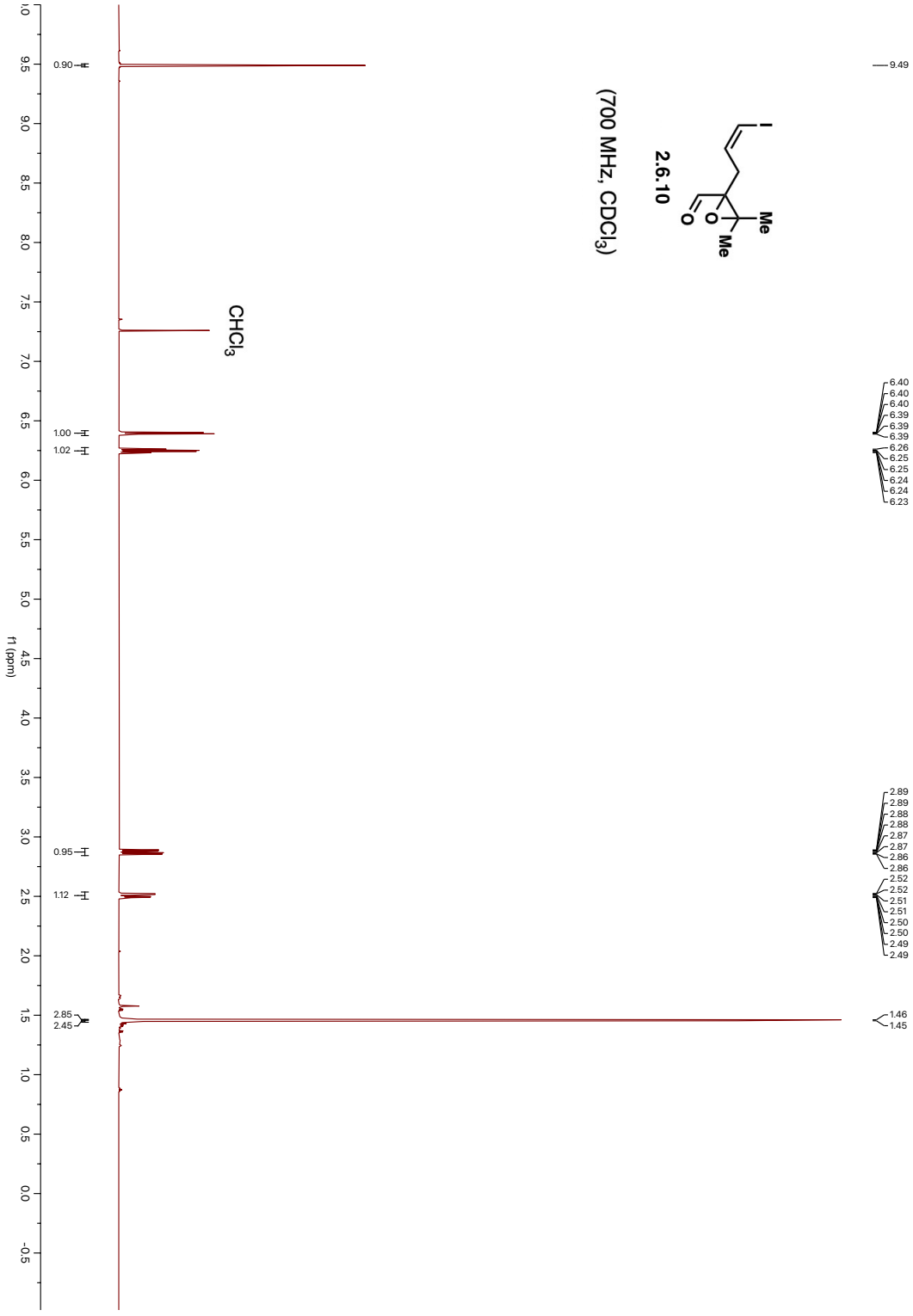

SI-14
(150 MHz, CDCl3)
Me
Me
OH
I
CDCl3
139.82
132.52
128.87
82.46
62.37
36.78
21.19
20.42
f1 (ppm)

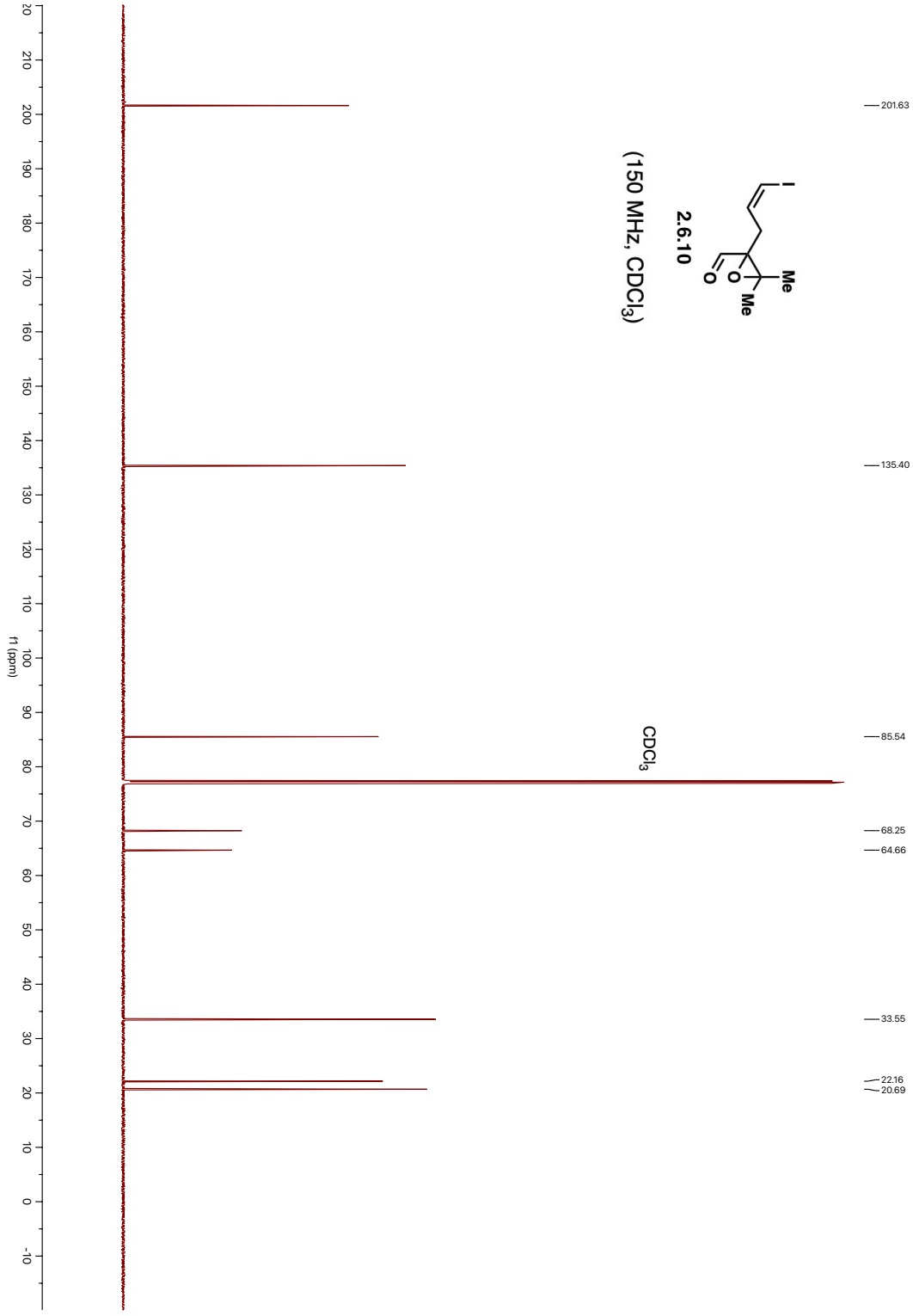

6.42
6.42
6.41
6.41
6.40
6.40
6.39
6.39
6.32
6.30
6.30
6.29
6.28
6.27
3.76
3.76
3.73
3.73
3.69
3.69
3.66
3.66
2.74
2.73
2.72
2.72
2.71
2.70
2.69
2.68
2.68
2.51
2.51
2.50
2.49
2.49
2.49
2.47
2.47
2.47
2.46
2.45
2.45
1.41
1.40
1.39
1.39
I
Me
Me
O
OH
SI-15
(400 MHz, CDCl3)
CHCl3
1.00
0.96
1.01
1.01
1.03
1.07
2.95
3.04
9.0
8.5
8.0
7.5
7.0
6.5
6.0
5.5
5.0
4.5
4.0
3.5
3.0
2.5
2.0
1.5
1.0
0.5
0.0
f1 (ppm)

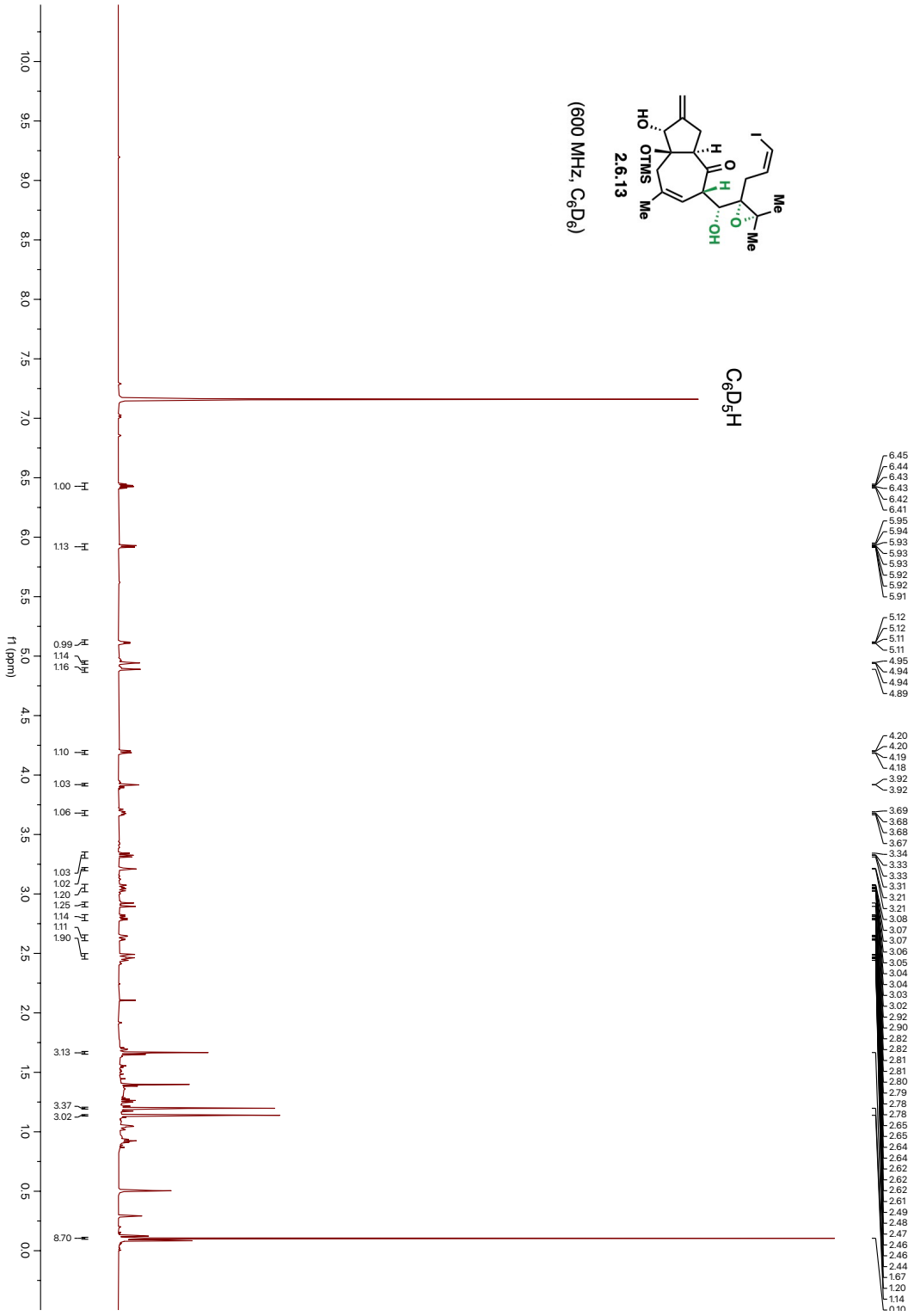


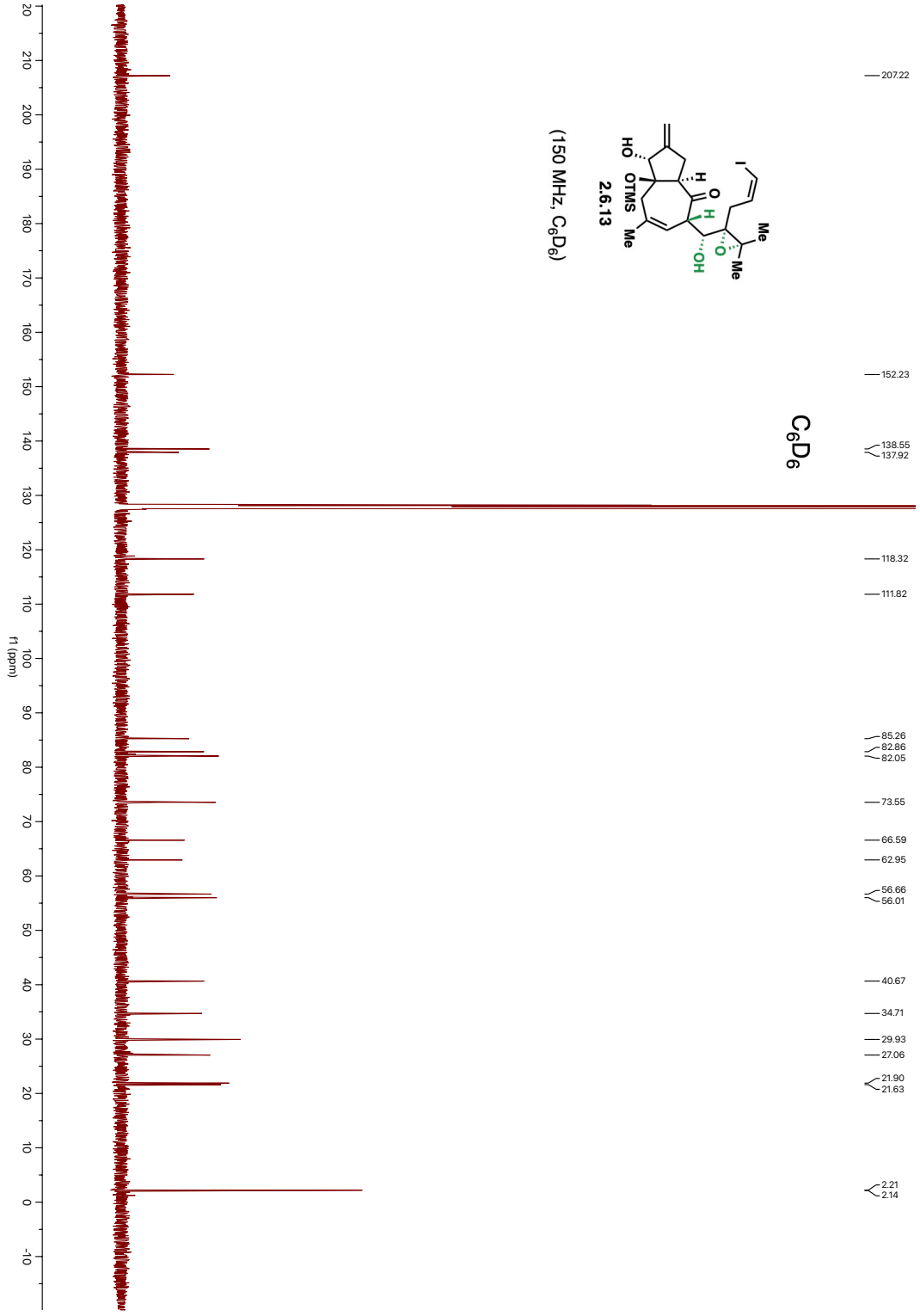
SI-15

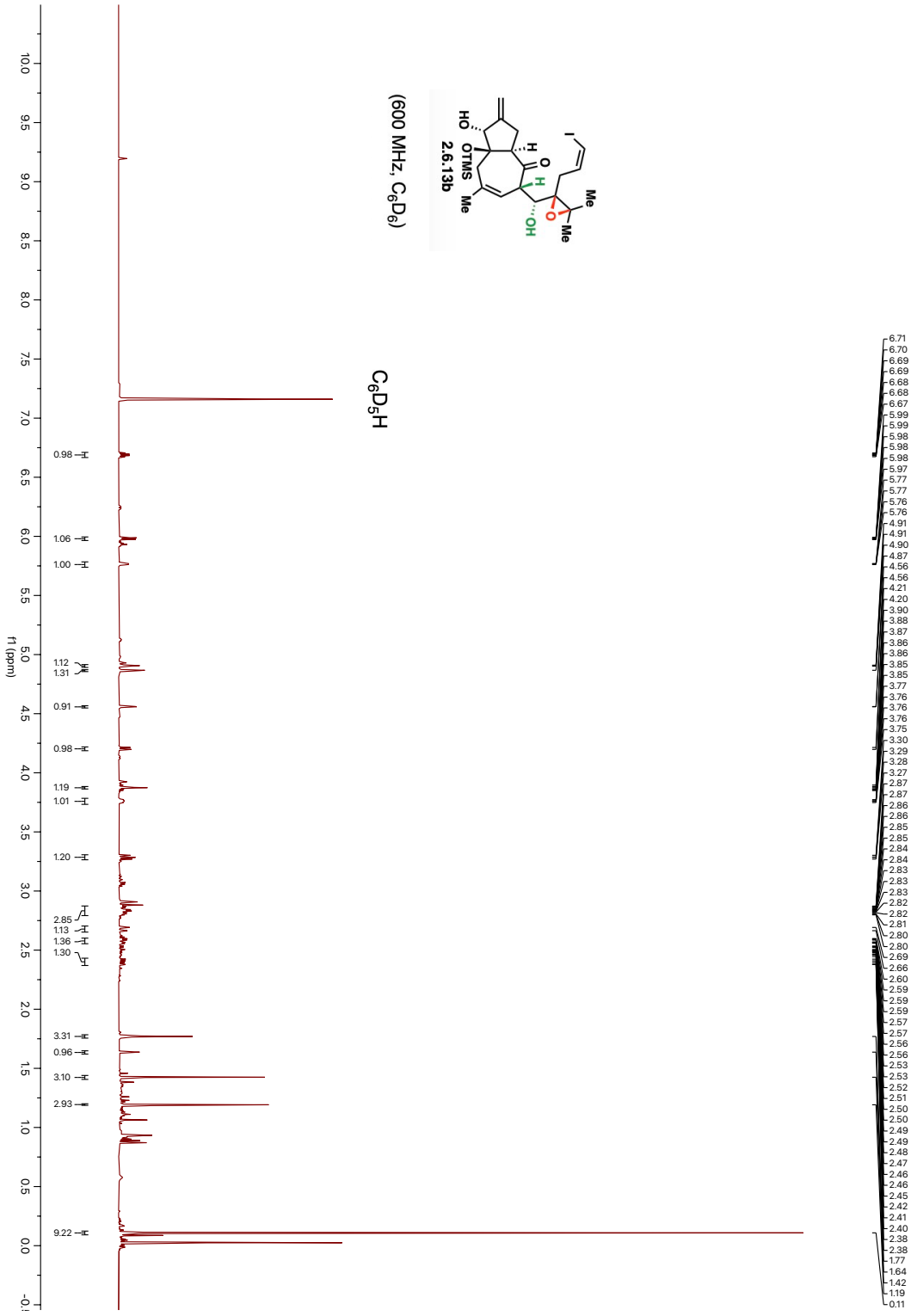
(150 MHz, $CDCl_3$)

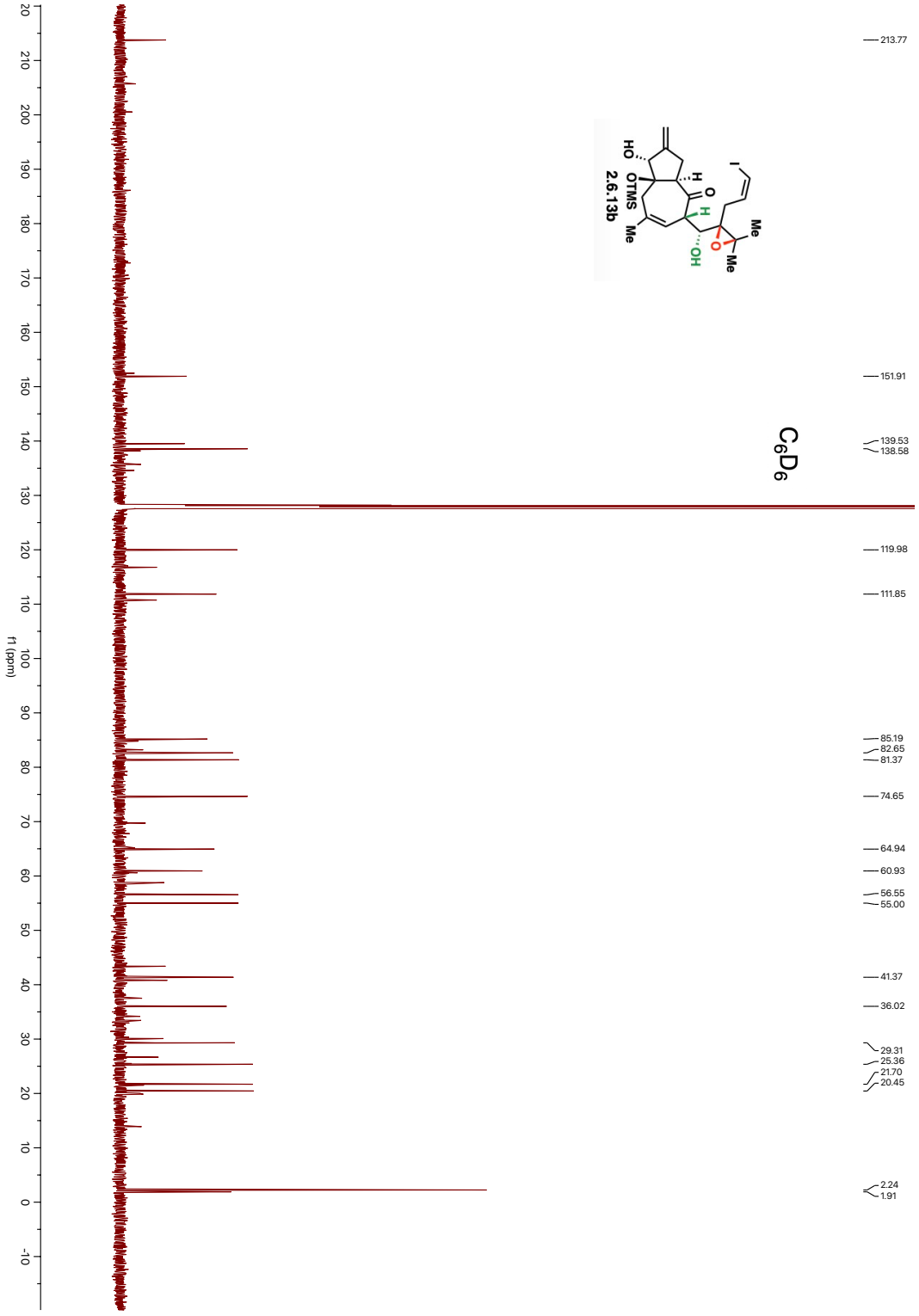

2.6.10
(700 MHz, CDCl3)
CHCl3
f1 (ppm)
9.49
6.40
6.40
6.40
6.39
6.39
6.39
6.26
6.25
6.25
6.24
6.24
6.23
2.89
2.89
2.88
2.88
2.87
2.87
2.86
2.86
2.52
2.52
2.51
2.51
2.50
2.50
2.49
2.49
1.46
1.45
0.90
1.00
1.02
0.95
1.12
2.85
2.45

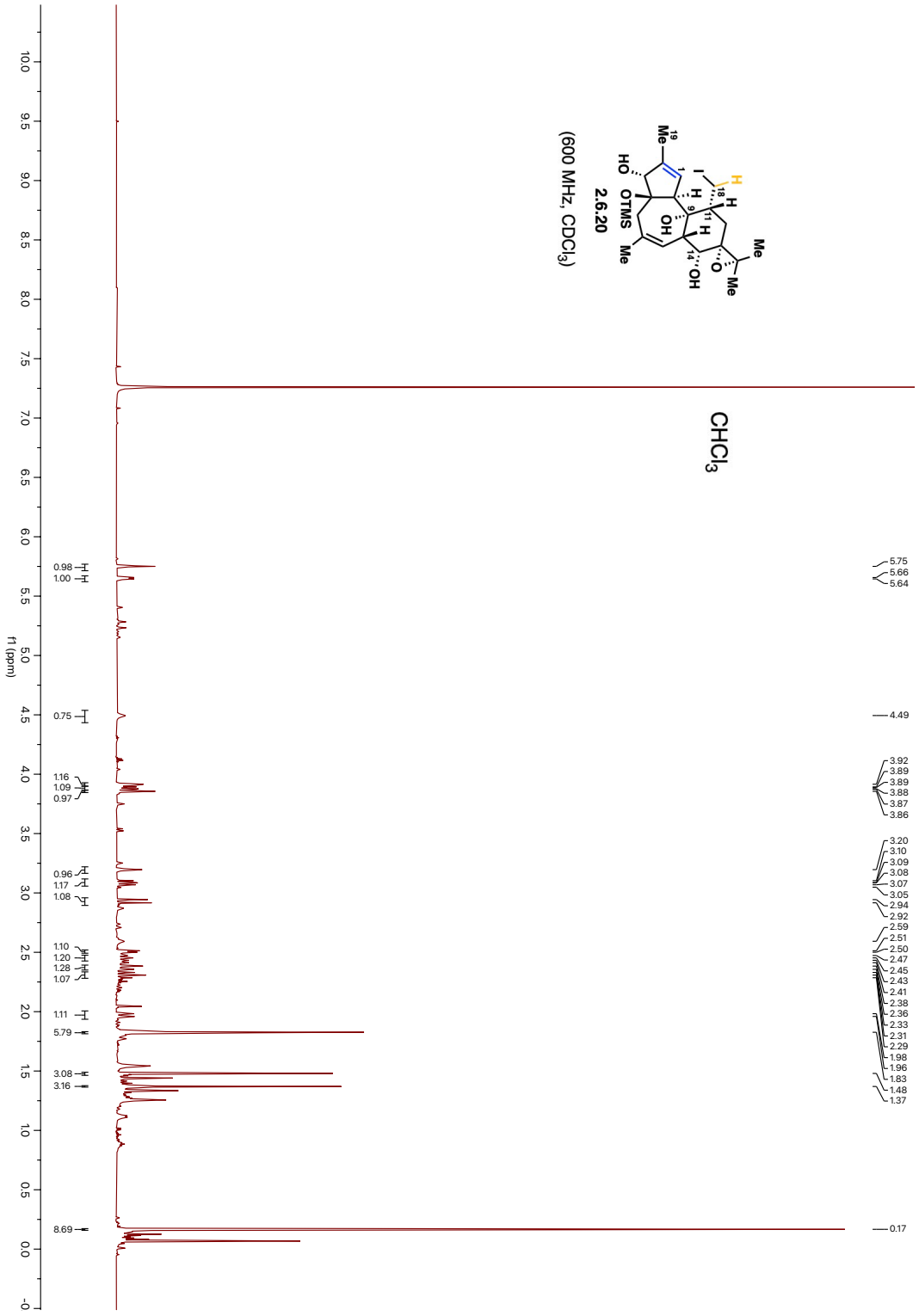

2.6.10
(150 MHz, CDCl3)
Me
Me
O
O
I
CDCl3
201.63
135.40
85.54
68.25
64.66
33.55
22.16
20.69
f1 (ppm)

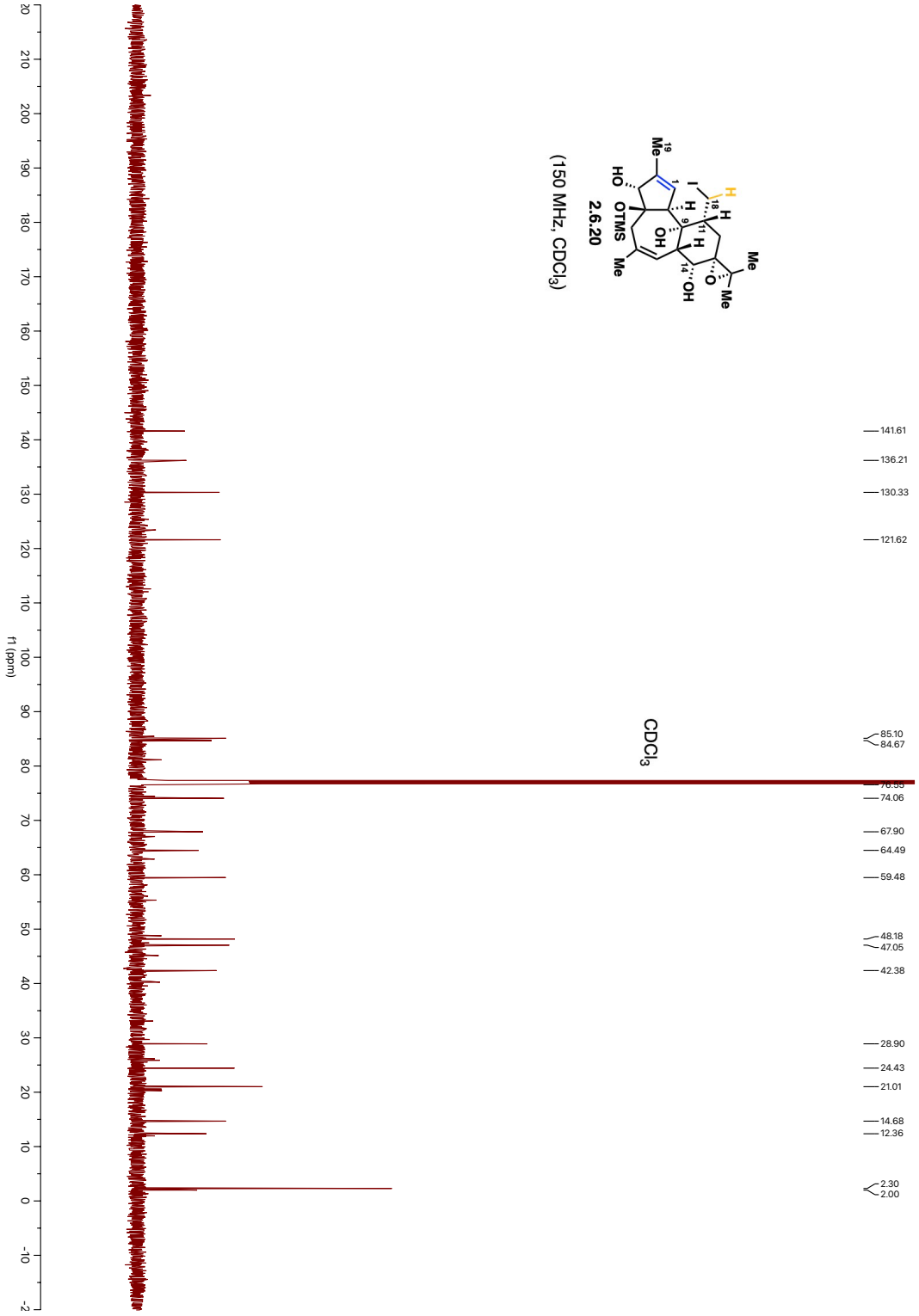

(600 MHz, C6D6)
2.6.13
HO
OTMS
Me
O
H
O
H
OH
O
Me
Me
I
C6D5H
f1 (ppm)
10.0
9.5
9.0
8.5
8.0
7.5
7.0
6.5
6.0
5.5
5.0
4.5
4.0
3.5
3.0
2.5
2.0
1.5
1.0
0.5
0.0
1.00
1.13
0.99
1.14
1.16
1.10
1.03
1.06
1.03
1.02
1.20
1.25
1.14
1.11
1.90
3.13
3.37
3.02
8.70
6.45
6.44
6.43
6.43
6.42
6.41
5.95
5.94
5.93
5.93
5.93
5.92
5.92
5.91
5.12
5.12
5.11
5.11
4.95
4.94
4.94
4.89
4.20
4.20
4.19
4.18
3.92
3.92
3.69
3.68
3.68
3.67
3.34
3.33
3.33
3.31
3.21
3.21
3.08
3.07
3.07
3.06
3.05
3.04
3.04
3.03
3.02
2.92
2.90
2.82
2.82
2.81
2.81
2.80
2.79
2.78
2.78
2.65
2.65
2.64
2.64
2.62
2.62
2.62
2.61
2.49
2.48
2.47
2.46
2.46
2.44
1.67
1.20
1.14

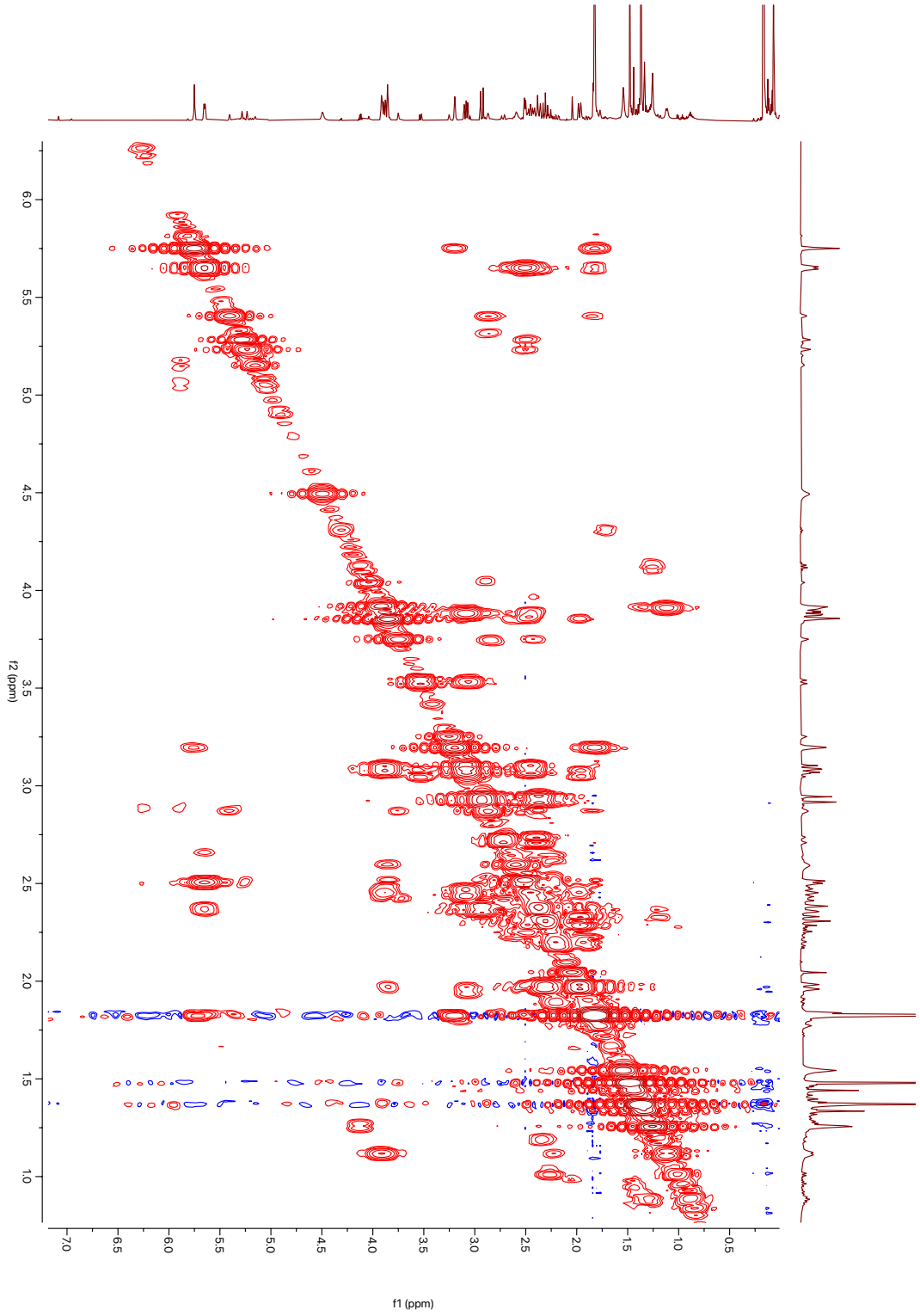

207.22
152.23
138.55
137.92
118.32
111.82
85.26
82.86
82.05
73.55
66.59
62.95
56.66
56.01
40.67
34.71
29.93
27.06
21.90
21.63
2.21
2.14
f1 (ppm)
C6D6
(150 MHz, C6D6)
2.6.13
HO
OTMS
Me
Me
Me
OH
O
H
O
H

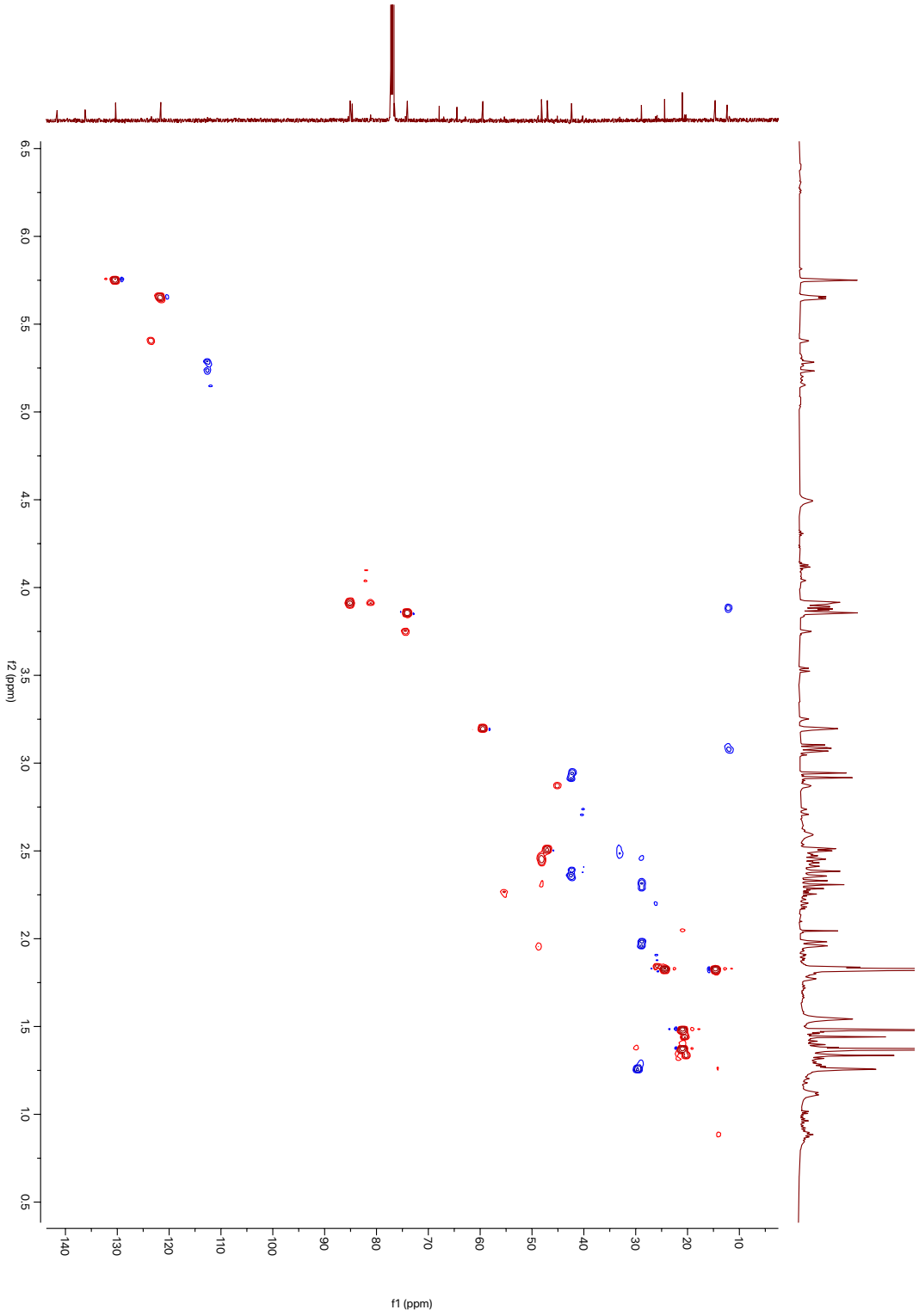

(600 MHz, C_6D_6)
C_6D_5H
HO
OTMS
Me
2.6.13b
OH
Me
Me
f1 (ppm)
0.98
1.06
1.00
1.12
1.31
0.91
0.98
1.19
1.01
1.20
2.85
1.13
1.36
1.30
3.31
0.96
3.10
2.93
9.22

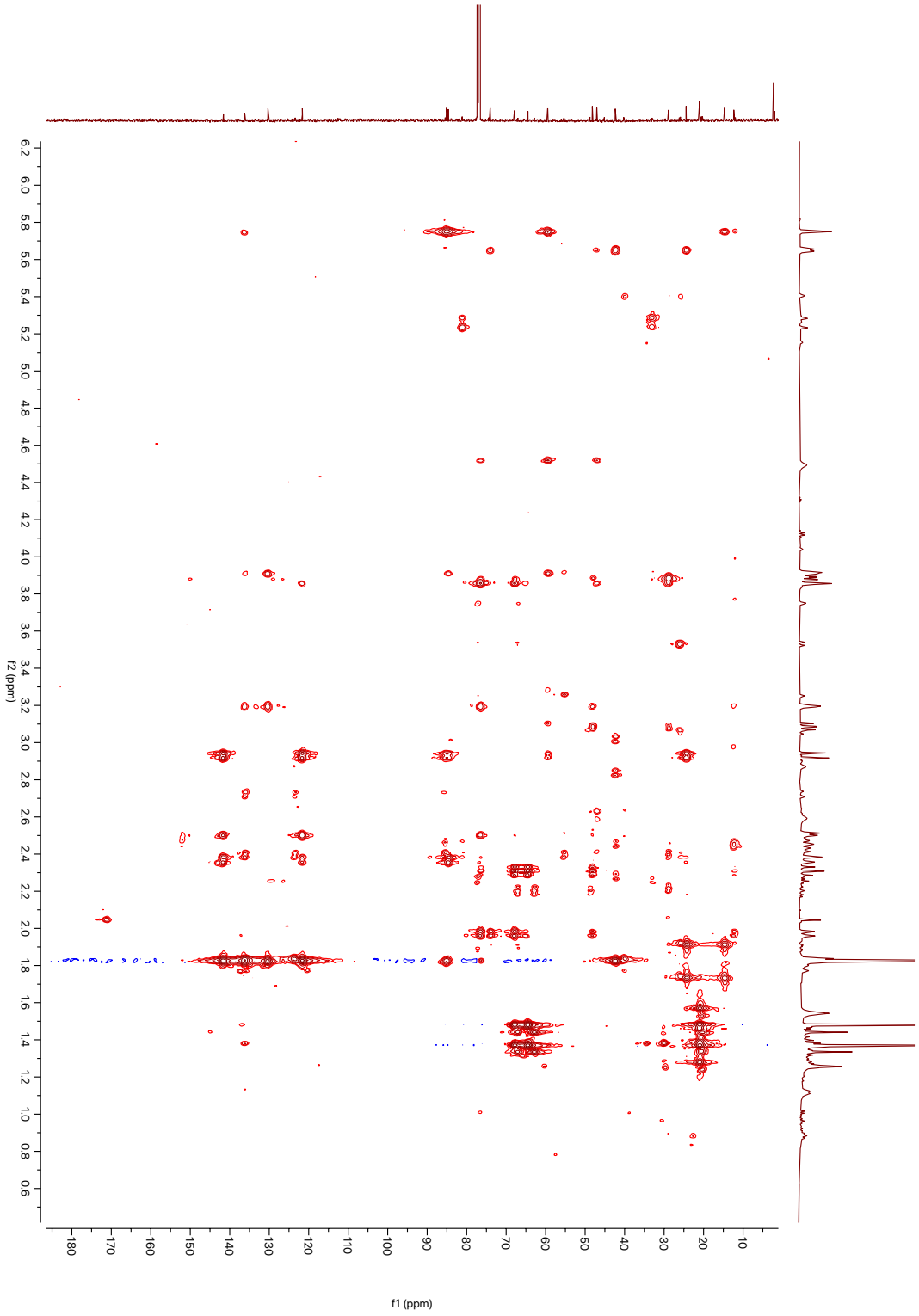

213.77
151.91
139.53
138.58
119.98
111.85
85.19
82.65
81.37
74.65
64.94
60.93
56.55
55.00
41.37
36.02
29.31
25.36
21.70
20.45
2.24
1.91
C6D6
2.6.13b
HO
OTMS
Me
H
O
H
OH
O
Me
Me
I
f1 (ppm)

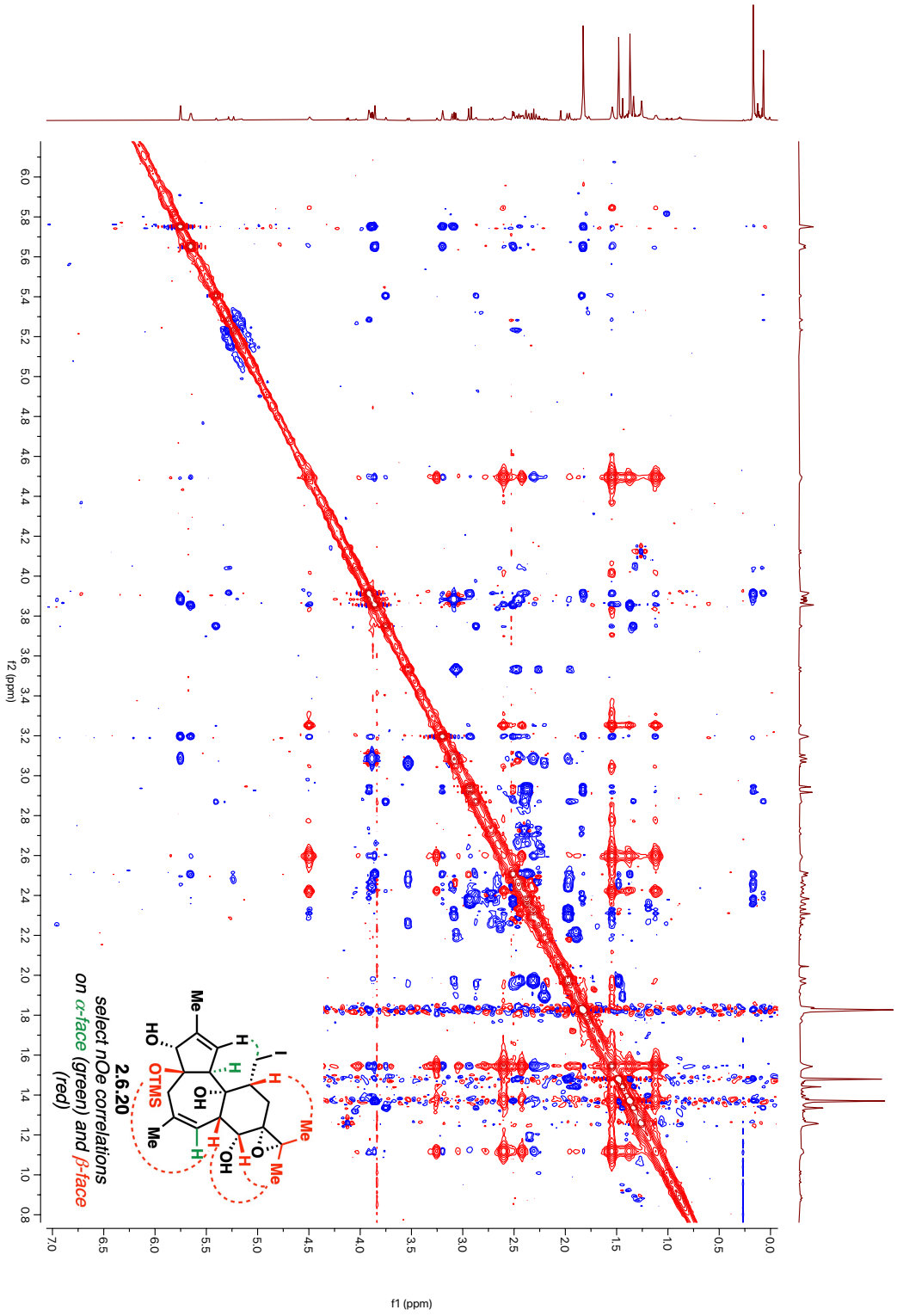

2.6.20
(600 MHz, CDCl3)
CHCl3
f1 (ppm)
0.98
1.00
0.75
1.16
1.09
0.97
0.96
1.17
1.08
1.10
1.20
1.28
1.07
1.11
5.79
3.08
3.16
8.69
5.75
5.66
5.64
4.49
3.92
3.89
3.89
3.88
3.87
3.86
3.20
3.10
3.09
3.08
3.07
3.05
2.94
2.92
2.59
2.51
2.50
2.47
2.45
2.43
2.41
2.38
2.36
2.33
2.31
2.29
1.98
1.96
1.83
1.48
1.37
0.17

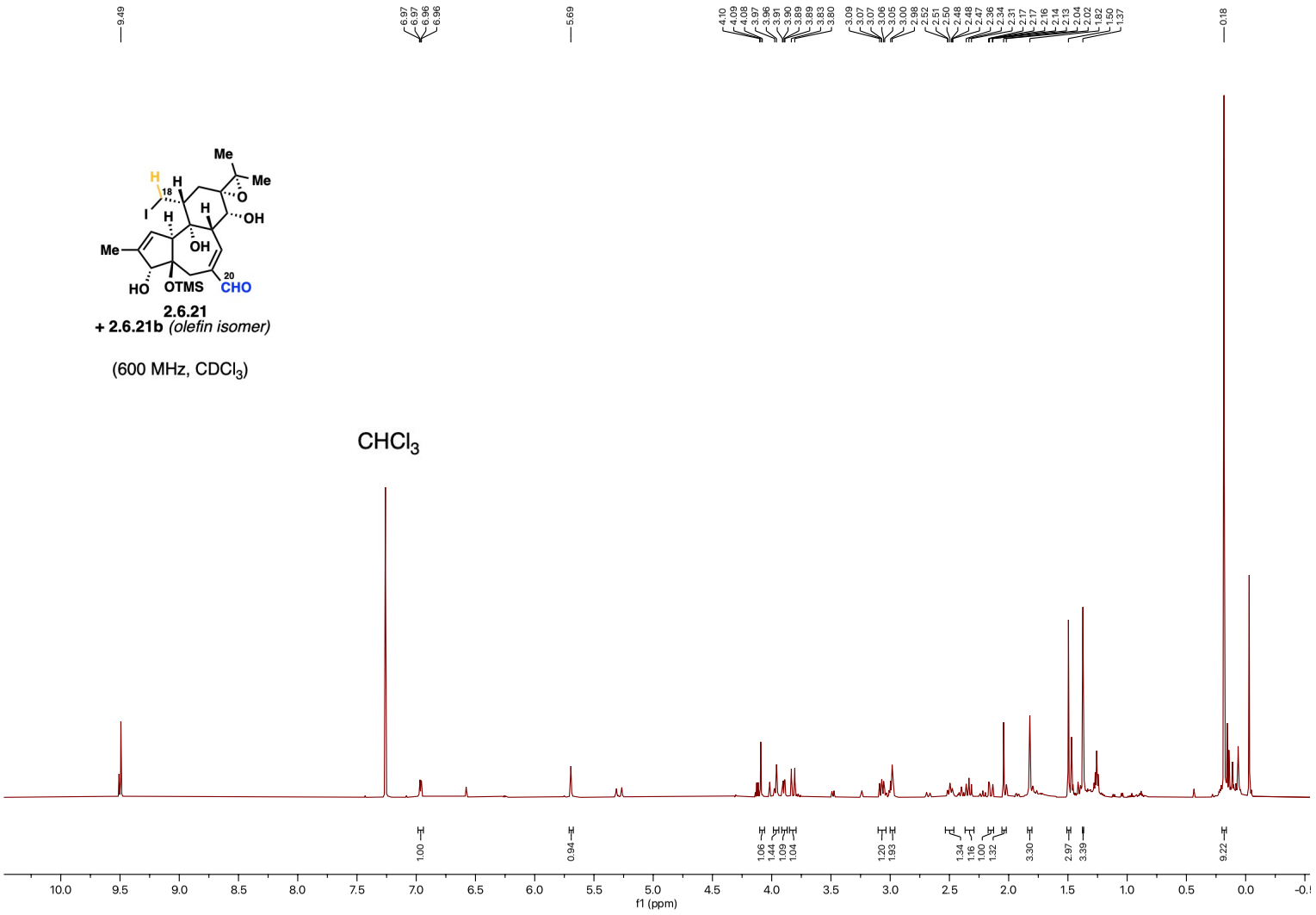

2.6.20
(150 MHz, CDCl3)
CDCl3
141.61
136.21
130.33
121.62
85.10
84.67
74.06
67.90
64.49
59.48
48.18
47.05
42.38
28.90
24.43
21.01
14.68
12.36
2.30
2.00
f1 (ppm)

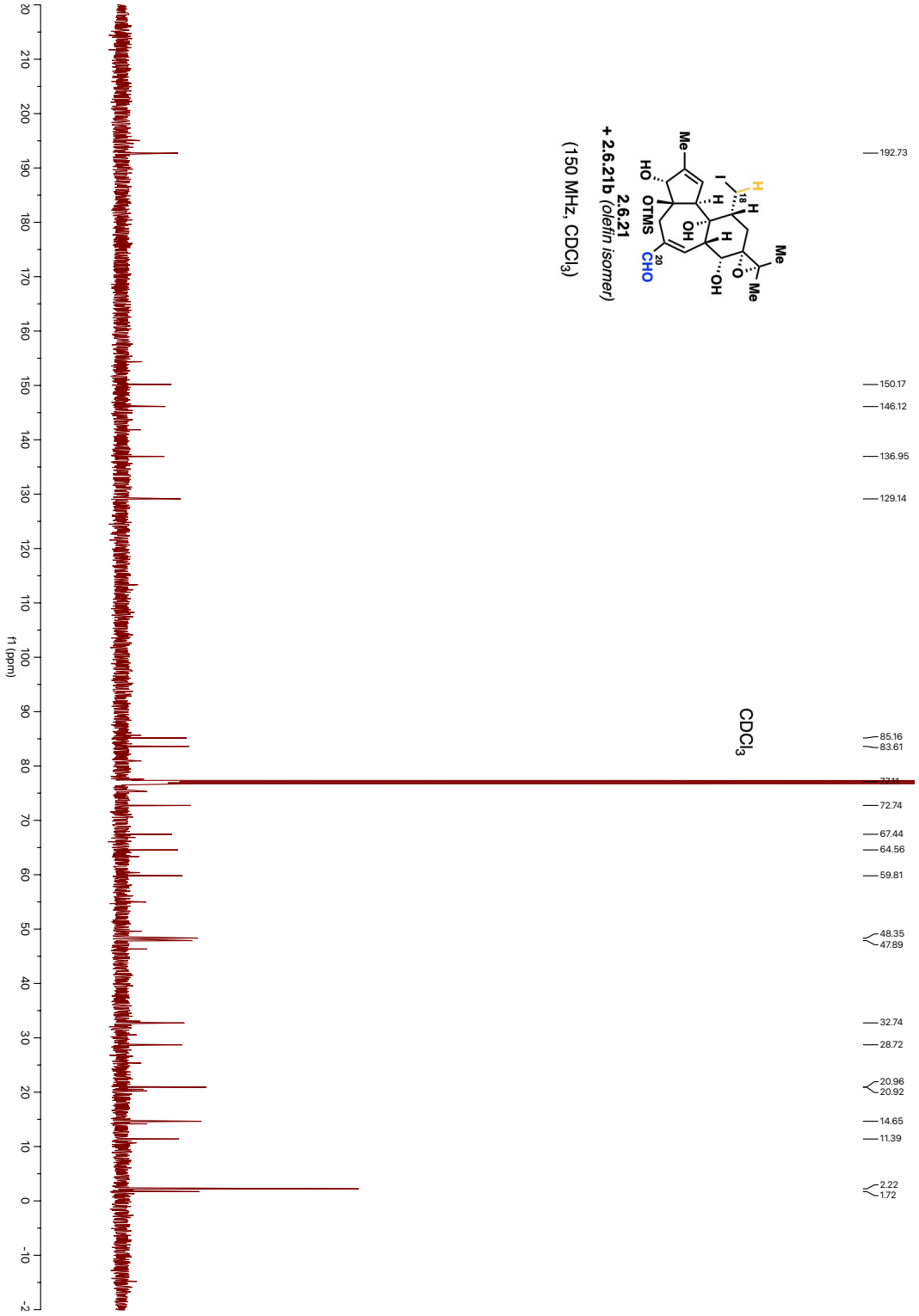

f2 (ppm)
f1 (ppm)

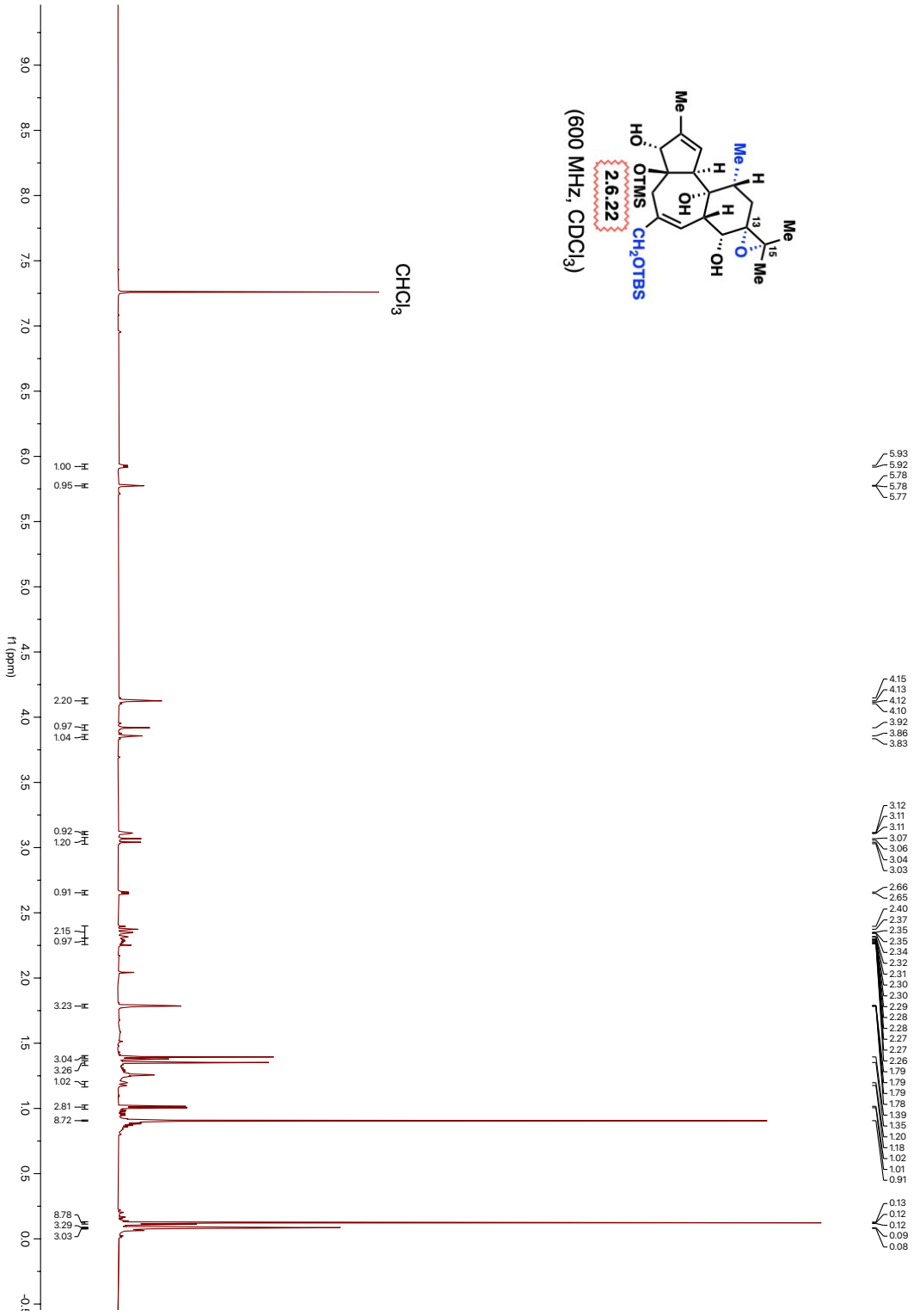

f2 (ppm)
f1 (ppm)

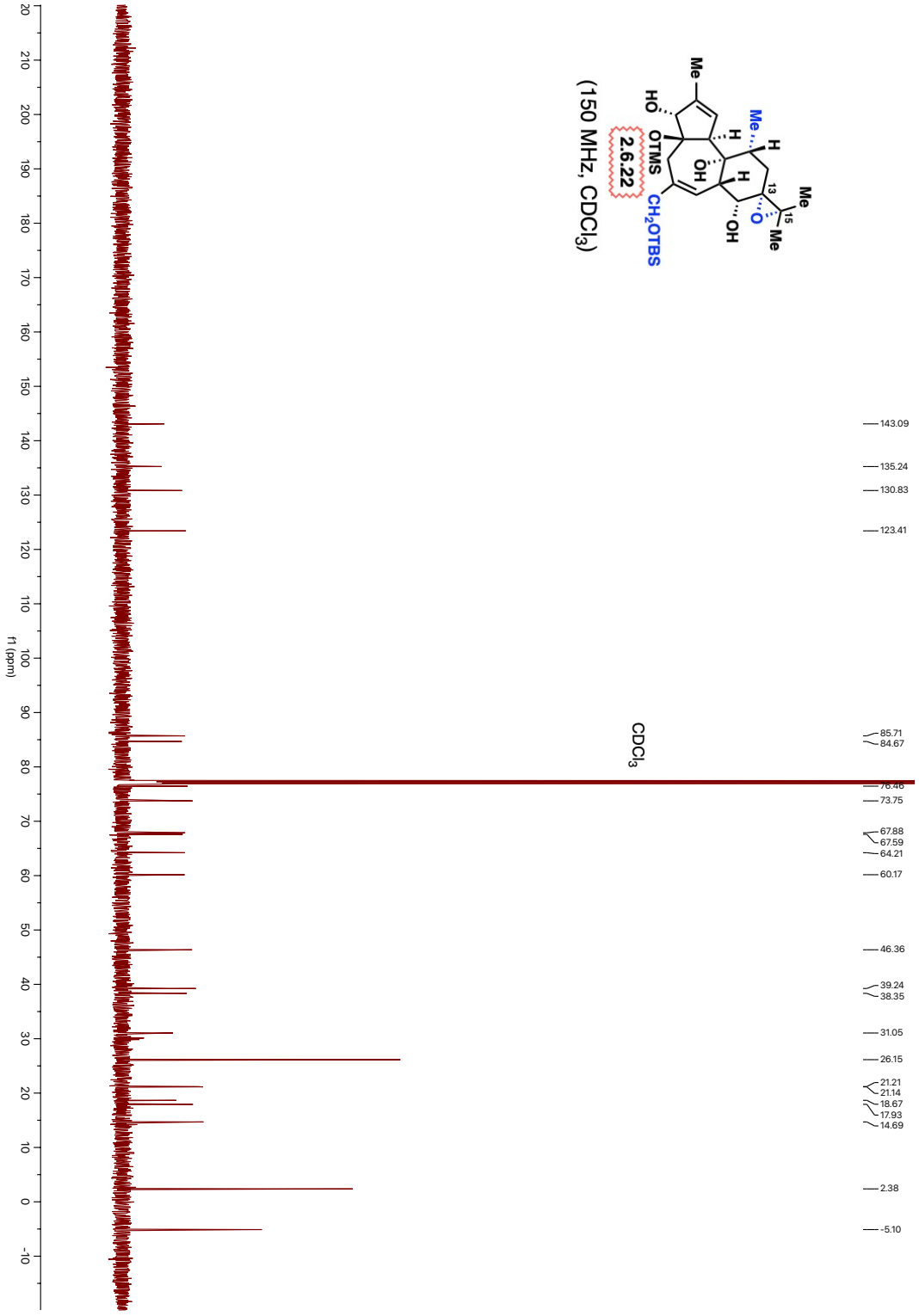

f2 (ppm)
f1 (ppm)

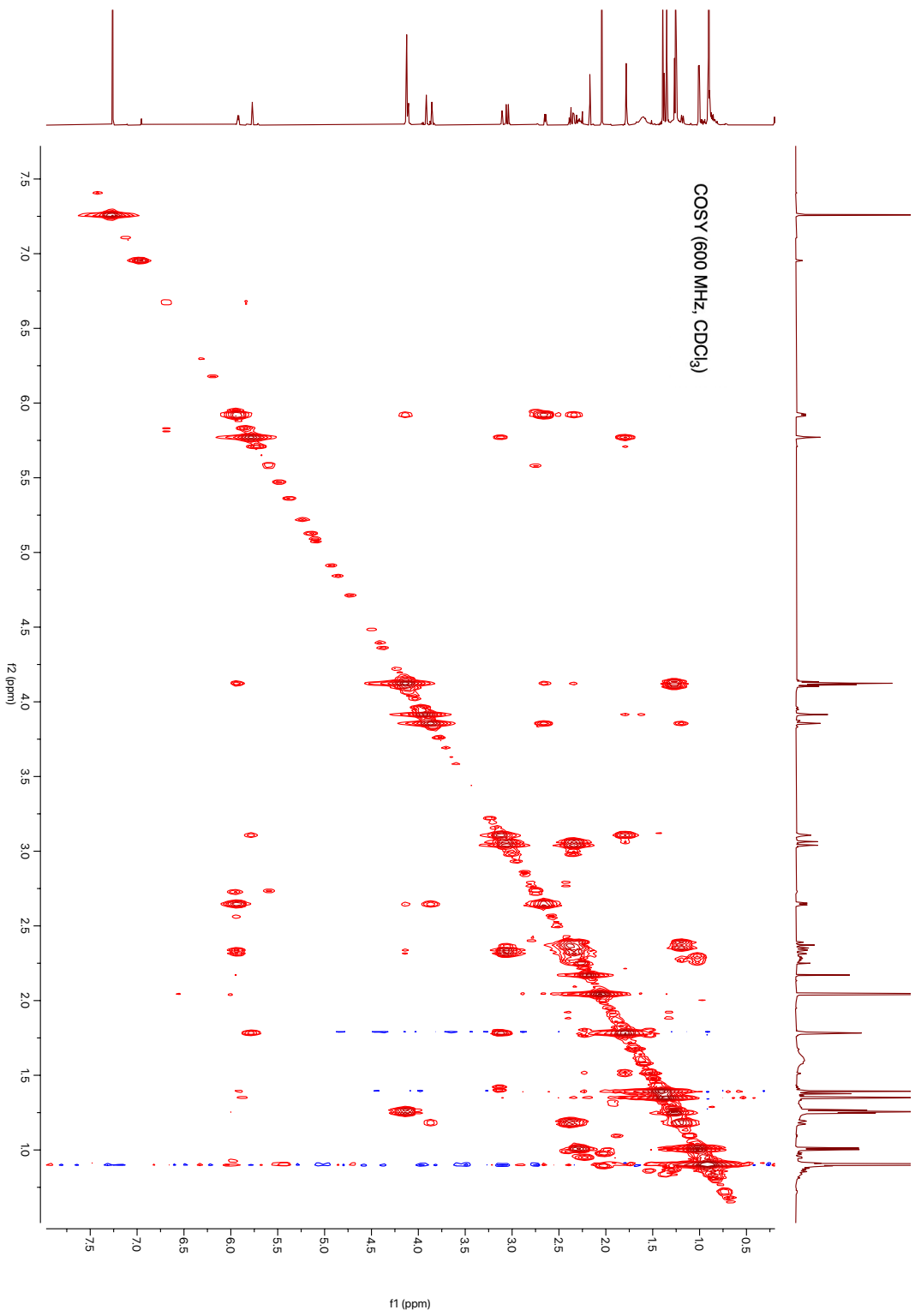

f2 (ppm)
f1 (ppm)
2.6.20
select nOe correlations
on α-face (green) and β-face
(red)
HO
OTMS
Me
Me
OH
OH
O
Me
Me
H
H
H
H
H
H
H
I

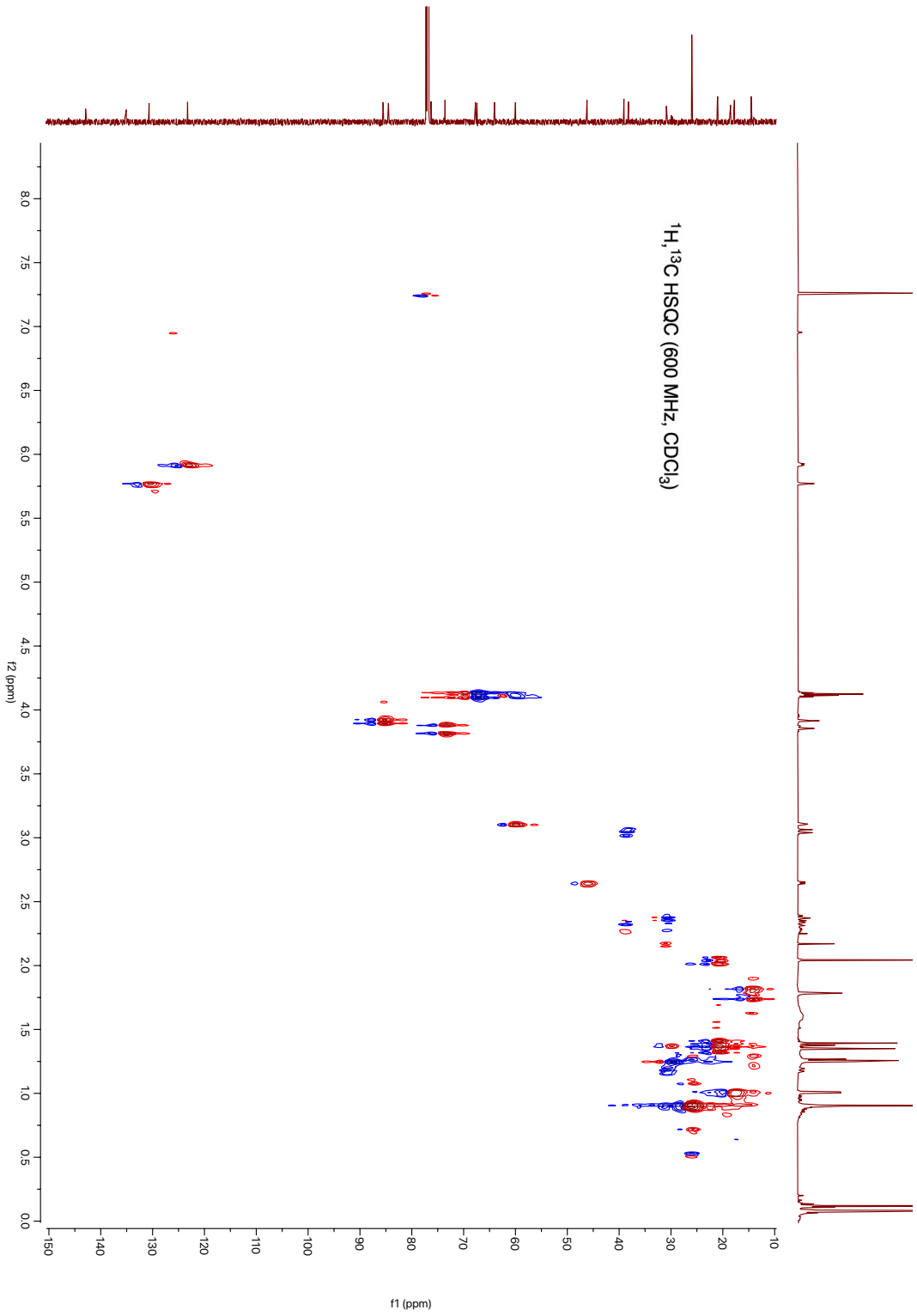

9.49
6.97
6.97
6.96
6.96
5.69
4.10
4.09
4.08
3.97
3.96
3.91
3.90
3.89
3.89
3.83
3.80
3.09
3.07
3.07
3.06
3.05
3.00
2.98
2.52
2.51
2.50
2.48
2.48
2.47
2.36
2.34
2.31
2.17
2.17
2.16
2.14
2.13
2.04
2.02
1.82
1.59
1.37
0.18
Me
Me
H
H
18
O
I
H
H
OH
Me
OH
HO
OTMS
20
CHO
2.6.21
+ 2.6.21b (olefin isomer)
(600 MHz, CDCl3)
CHCl3
1.00
0.94
1.06
1.44
1.09
1.04
1.20
1.93
1.34
1.16
1.00
1.32
3.30
2.97
3.39
9.22
10.0
9.5
9.0
8.5
8.0
7.5
7.0
6.5
6.0
5.5
5.0
4.5
4.0
3.5
3.0
2.5
2.0
1.5
1.0
0.5
0.0
f1 (ppm)

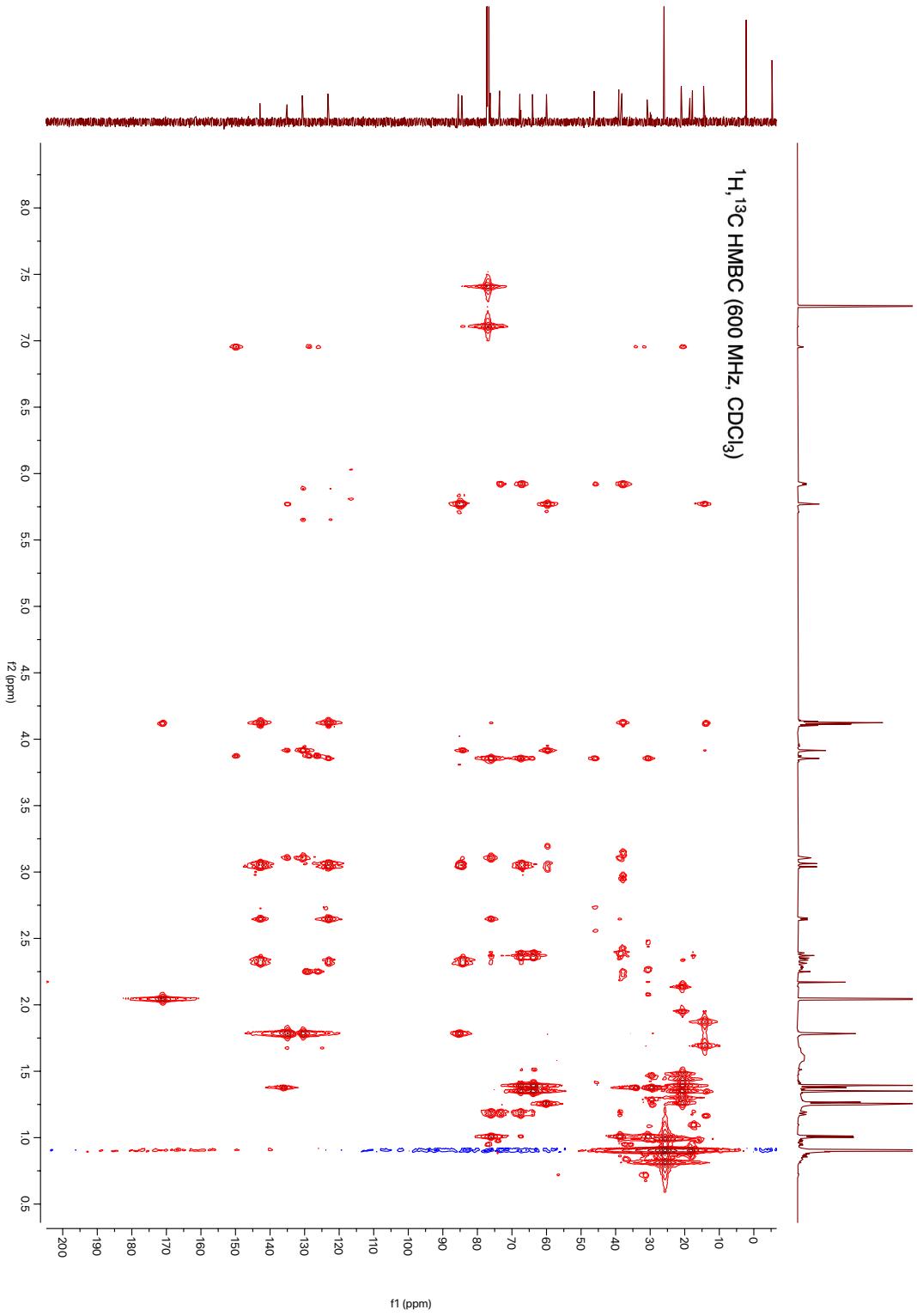

2.6.21
+ 2.6.21b (olefin isomer)
(150 MHz, CDCl3)
CDCl3
192.73
150.17
146.12
136.95
129.14
85.16
83.61
72.74
67.44
64.56
59.81
48.35
47.89
32.74
28.72
20.96
20.92
14.65
11.39
2.22
1.72
f1 (ppm)

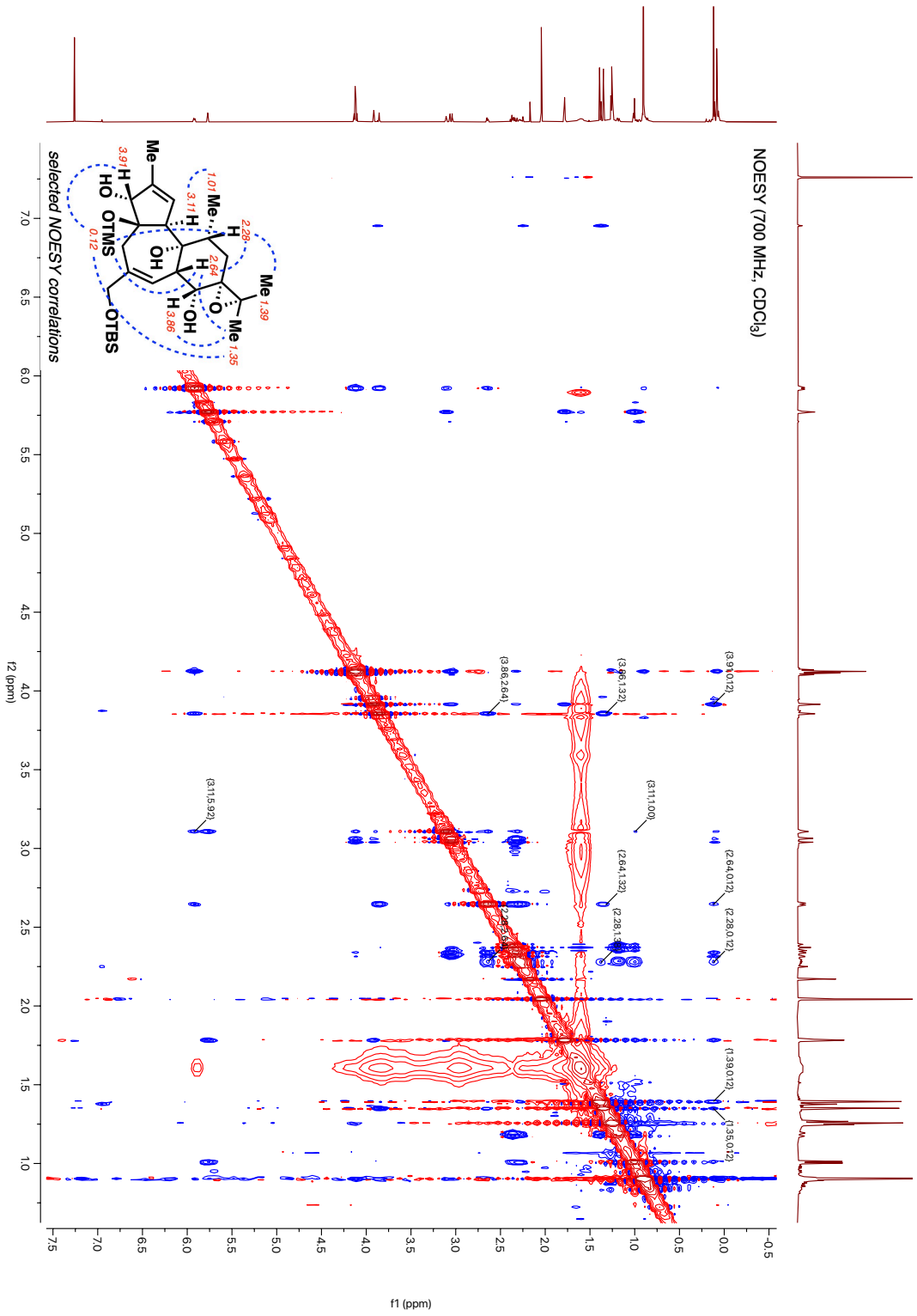

2.6.22
(600 MHz, CDCl3)
CHCl3
f1 (ppm)

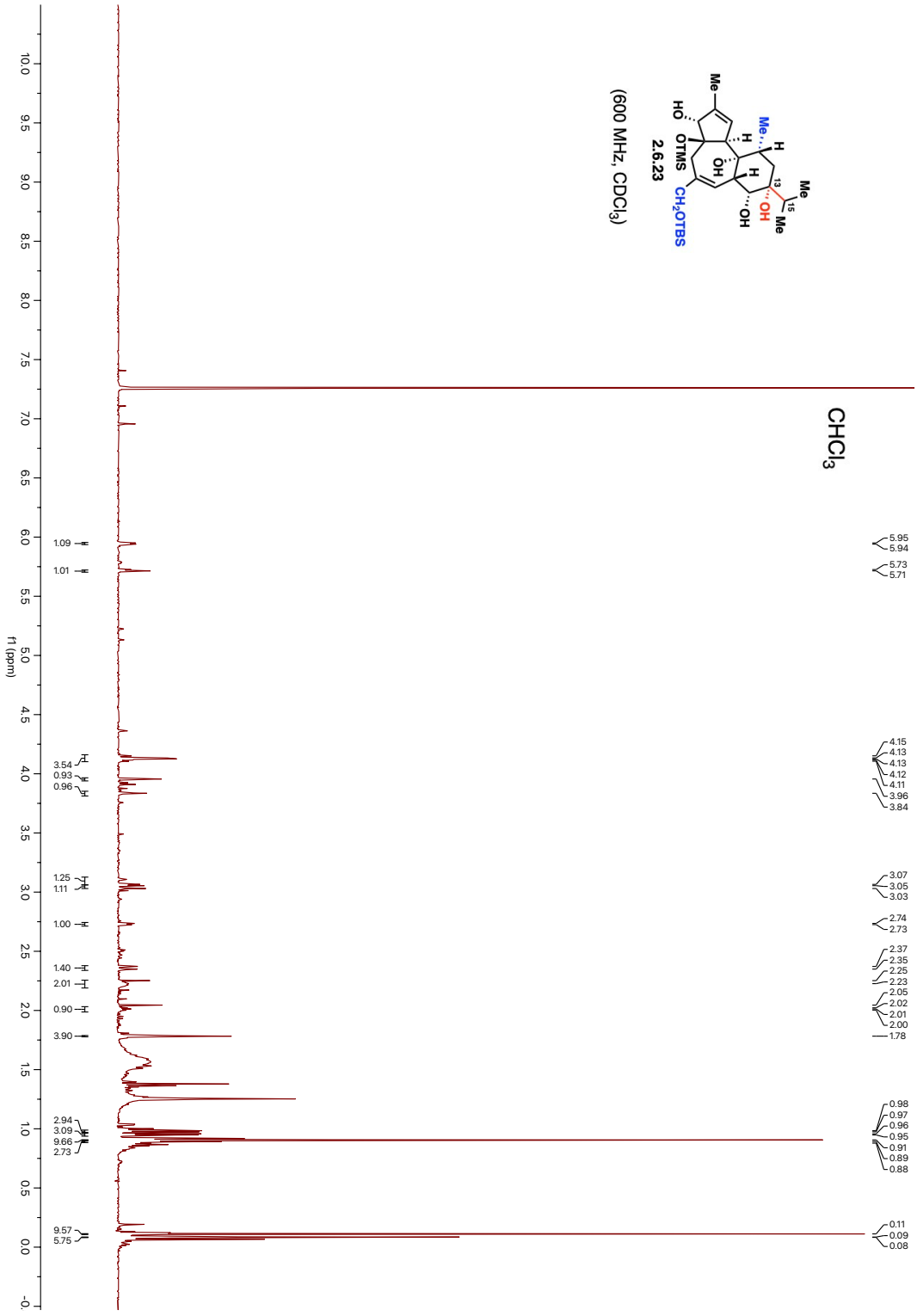

2.6.22
(150 MHz, CDCl3)
CDCl3
f1 (ppm)
143.09
135.24
130.83
123.41
85.71
84.67
76.46
73.75
67.88
67.59
64.21
60.17
46.36
39.24
38.35
31.05
26.15
21.21
21.14
18.67
17.93
14.69
2.38
-5.10

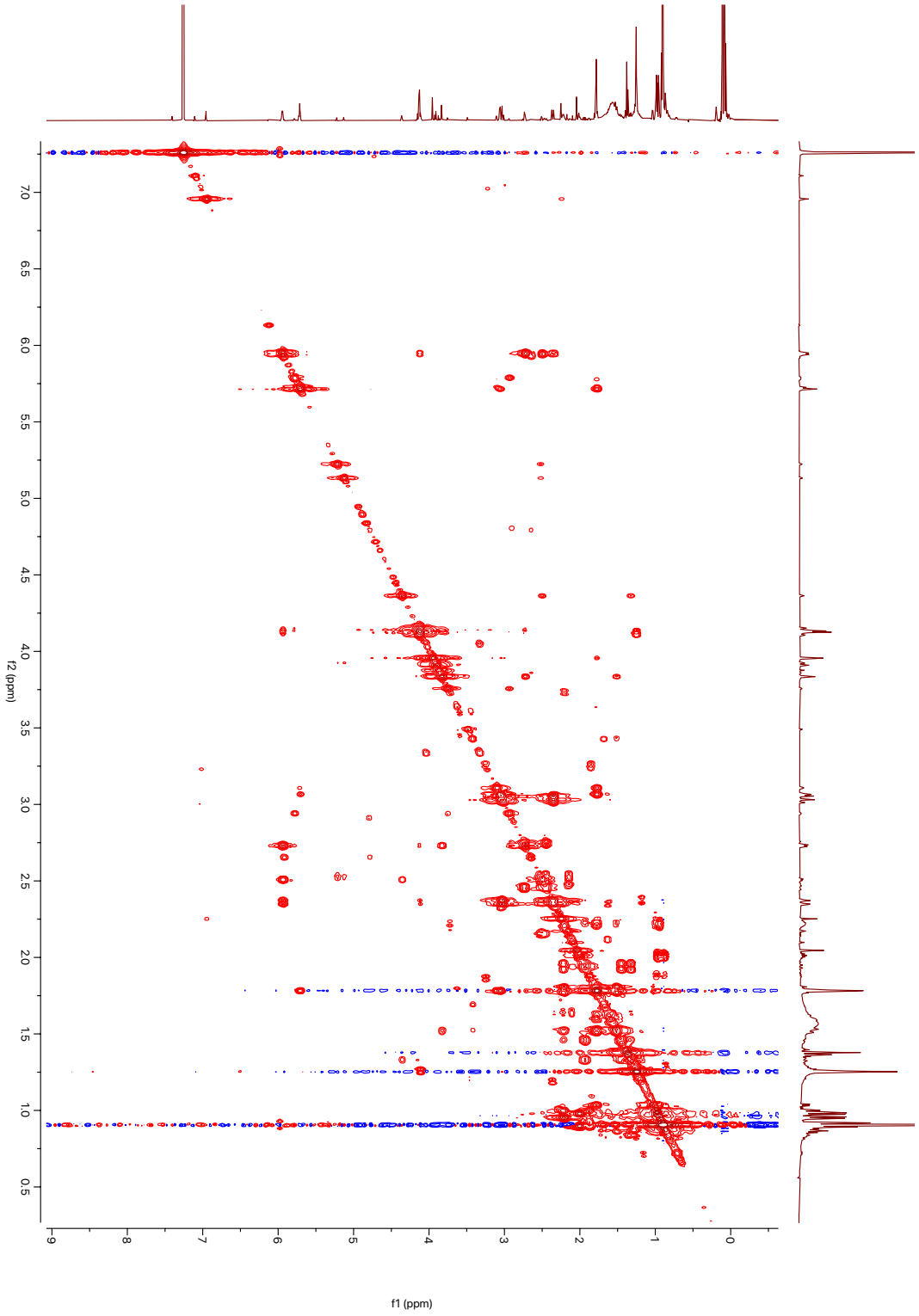

COSY (600 MHz, CDCl3)
f2 (ppm)
f1 (ppm)

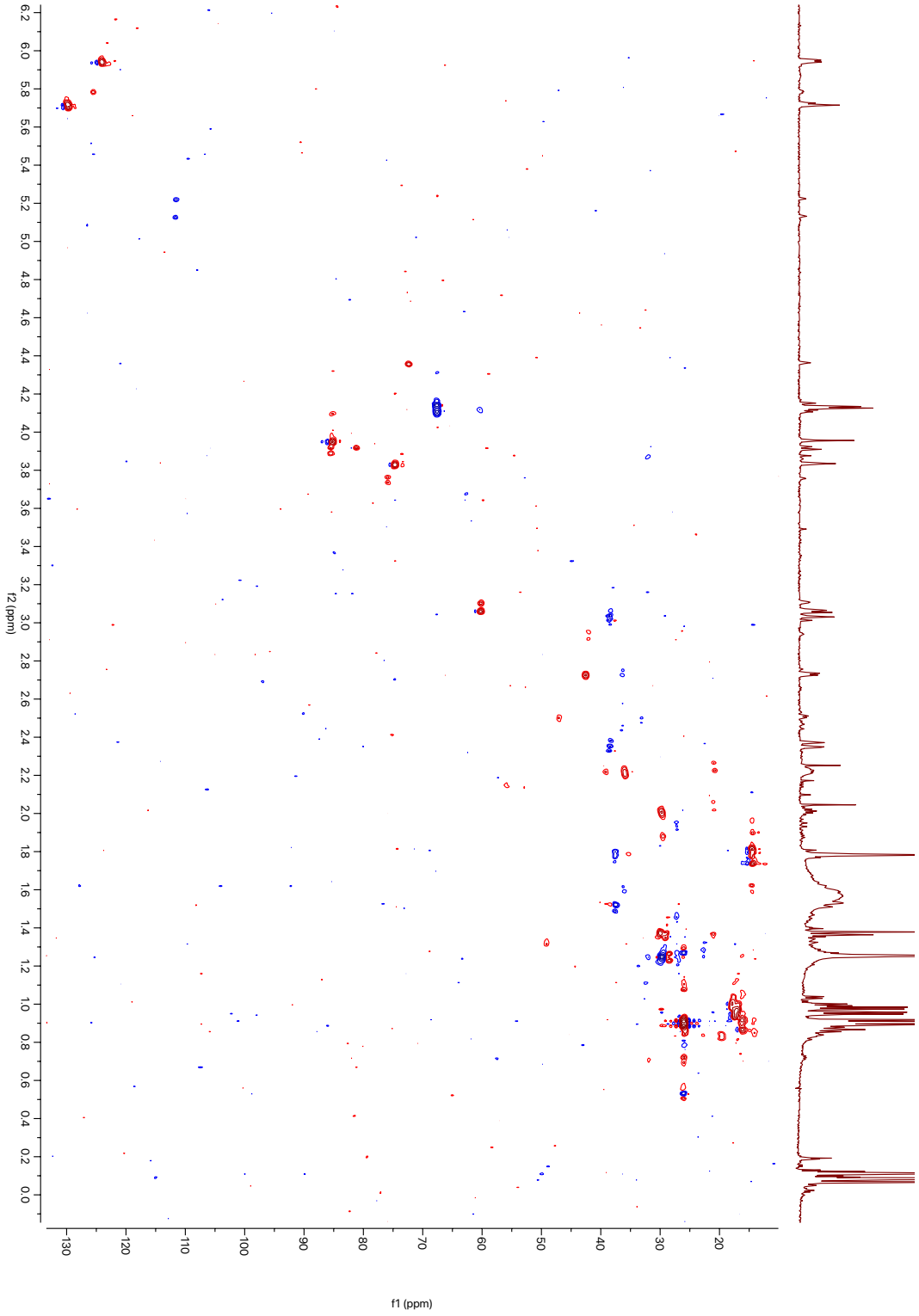

$^{1}H, ^{13}C$ HSQC (600 MHz, $CDCl_3$)
f2 (ppm)
f1 (ppm)

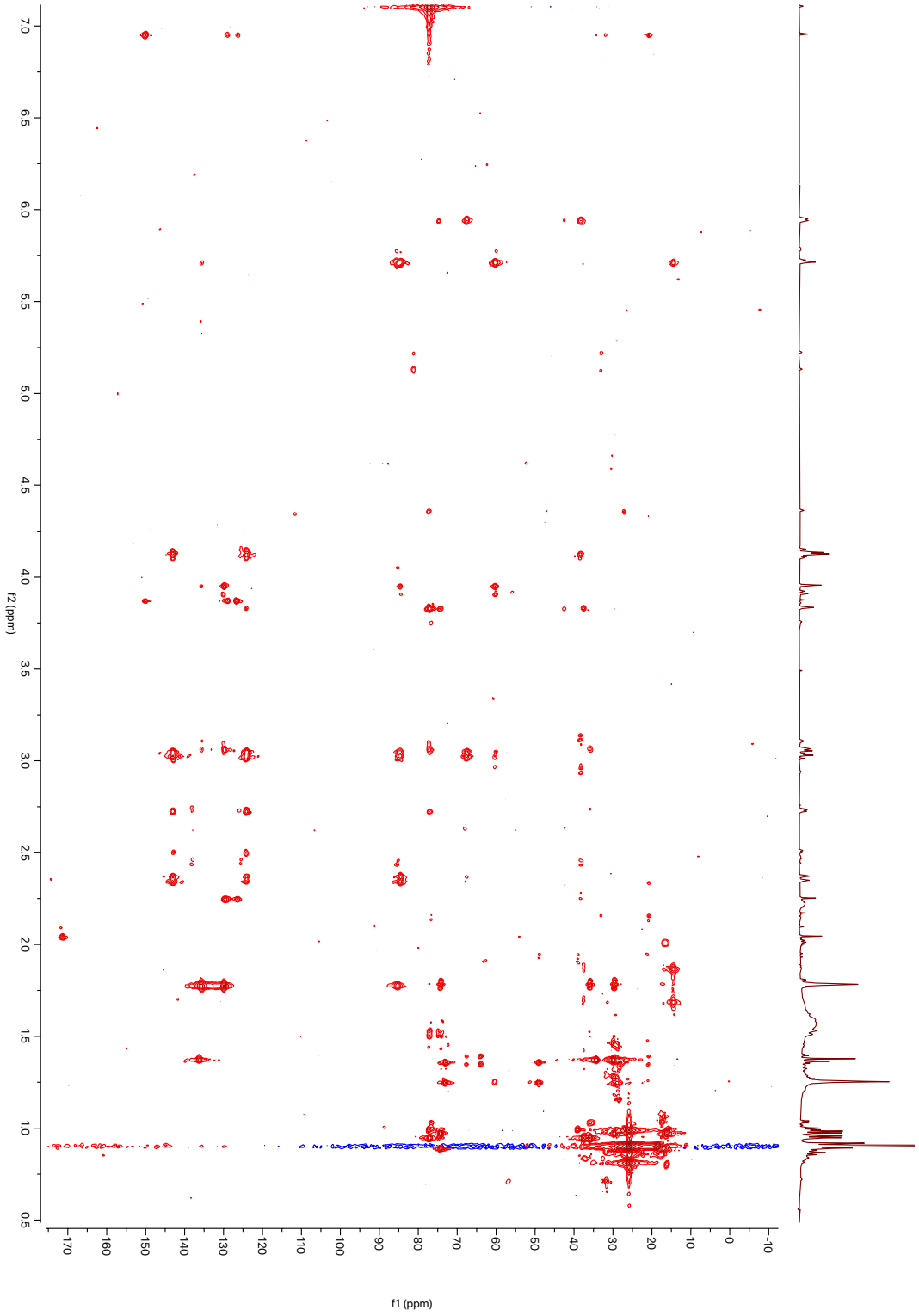

$^{1}H, ^{13}C$ HMBC (600 MHz, $CDCl_3$)
f2 (ppm)
f1 (ppm)

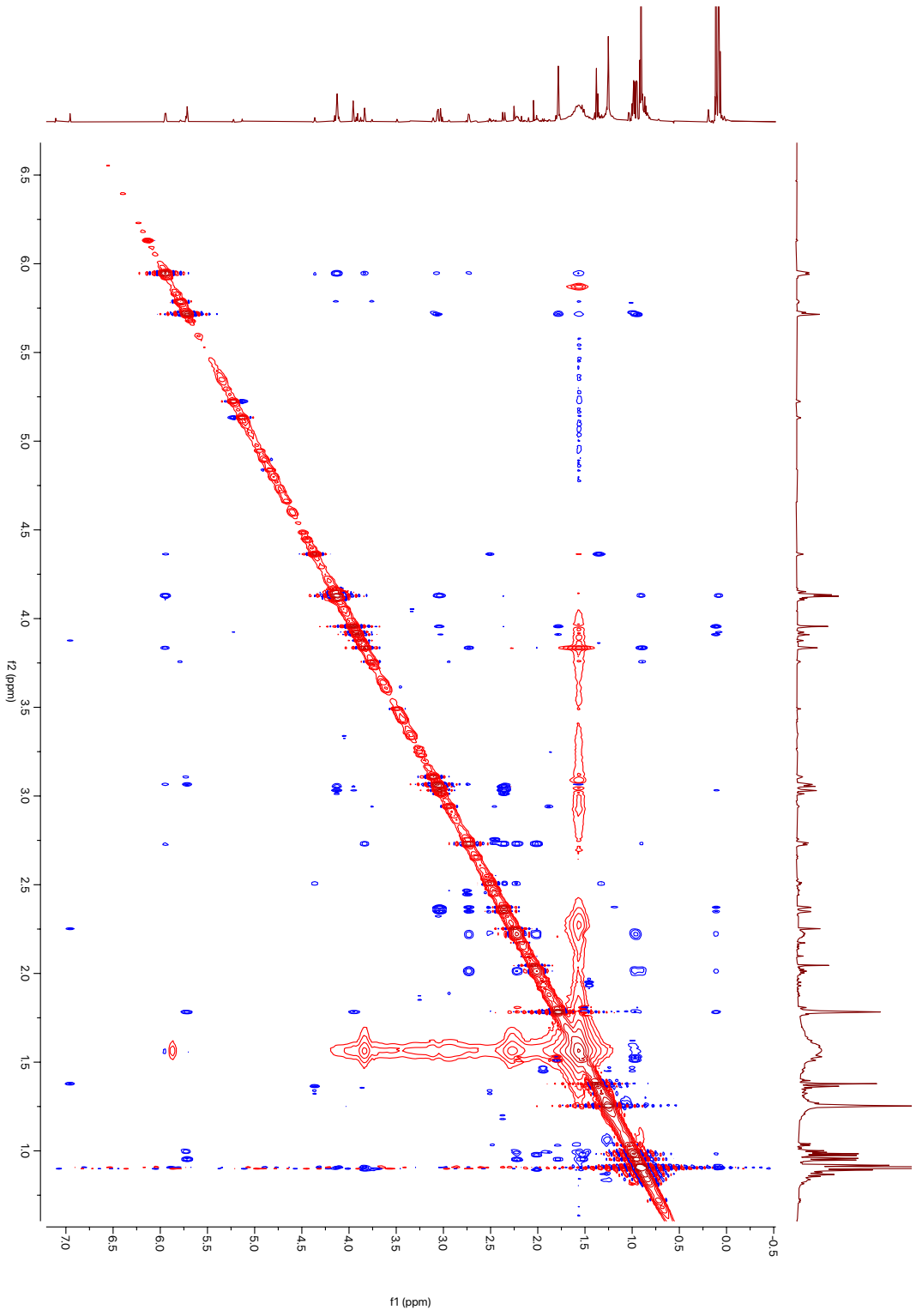

NOESY (700 MHz, CDCl3)
selected NOESY correlations
Me
3.91
H
HO
OTMS
0.12
OTBS
1.01
Me
3.11
H
OH
2.64
H
2.28
Me
1.39
H
3.86
O
OH
Me
1.35
(3.86,2.64)
(3.86,1.32)
(3.91,0.12)
(3.11,5.92)
(3.11,1.00)
(2.64,1.32)
(2.64,0.12)
(2.28,1.32)
(2.28,0.12)
(1.39,0.12)
(1.35,0.12)
f2 (ppm)
f1 (ppm)

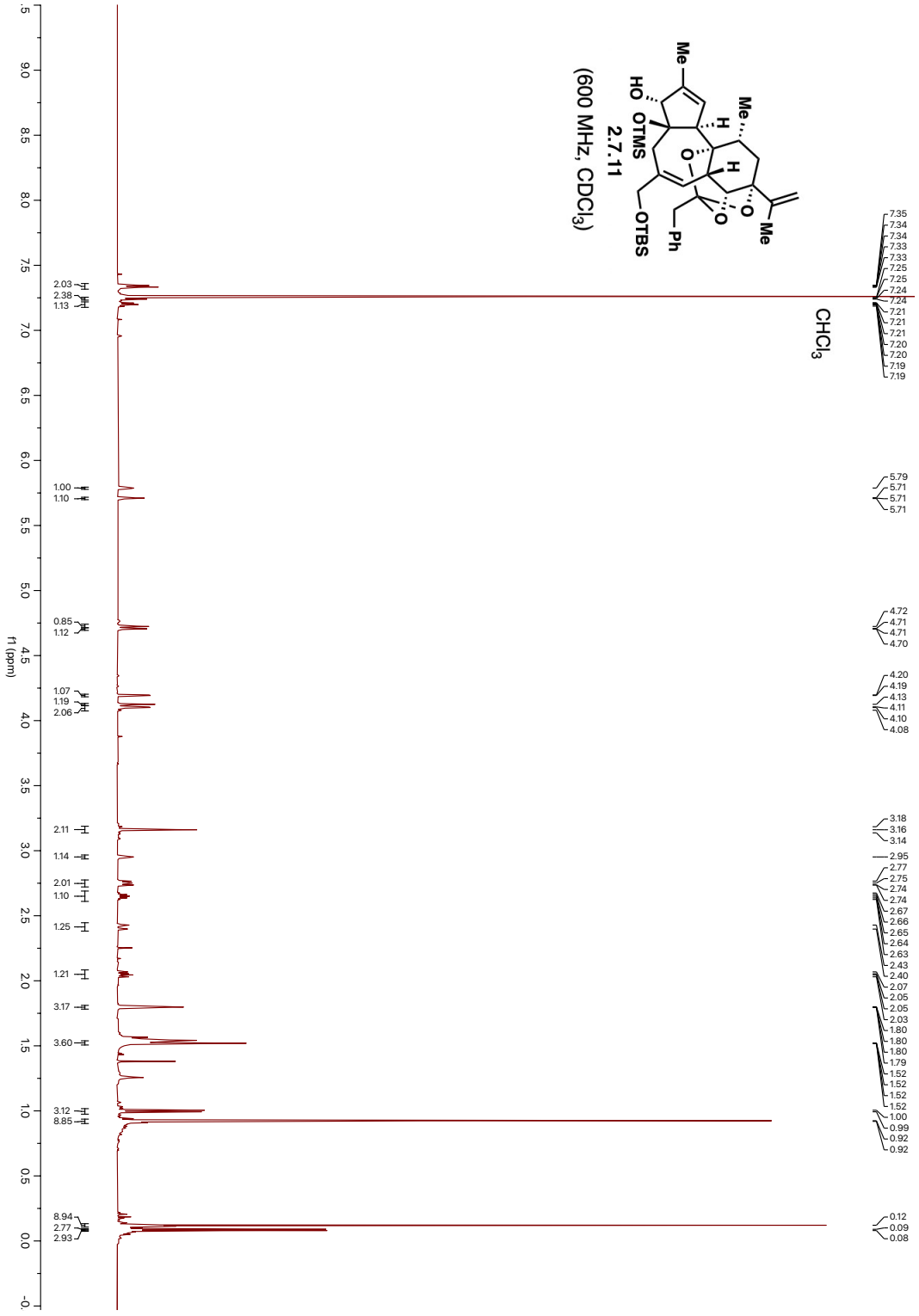

2.6.23
(600 MHz, CDCl3)
CHCl3
f1 (ppm)

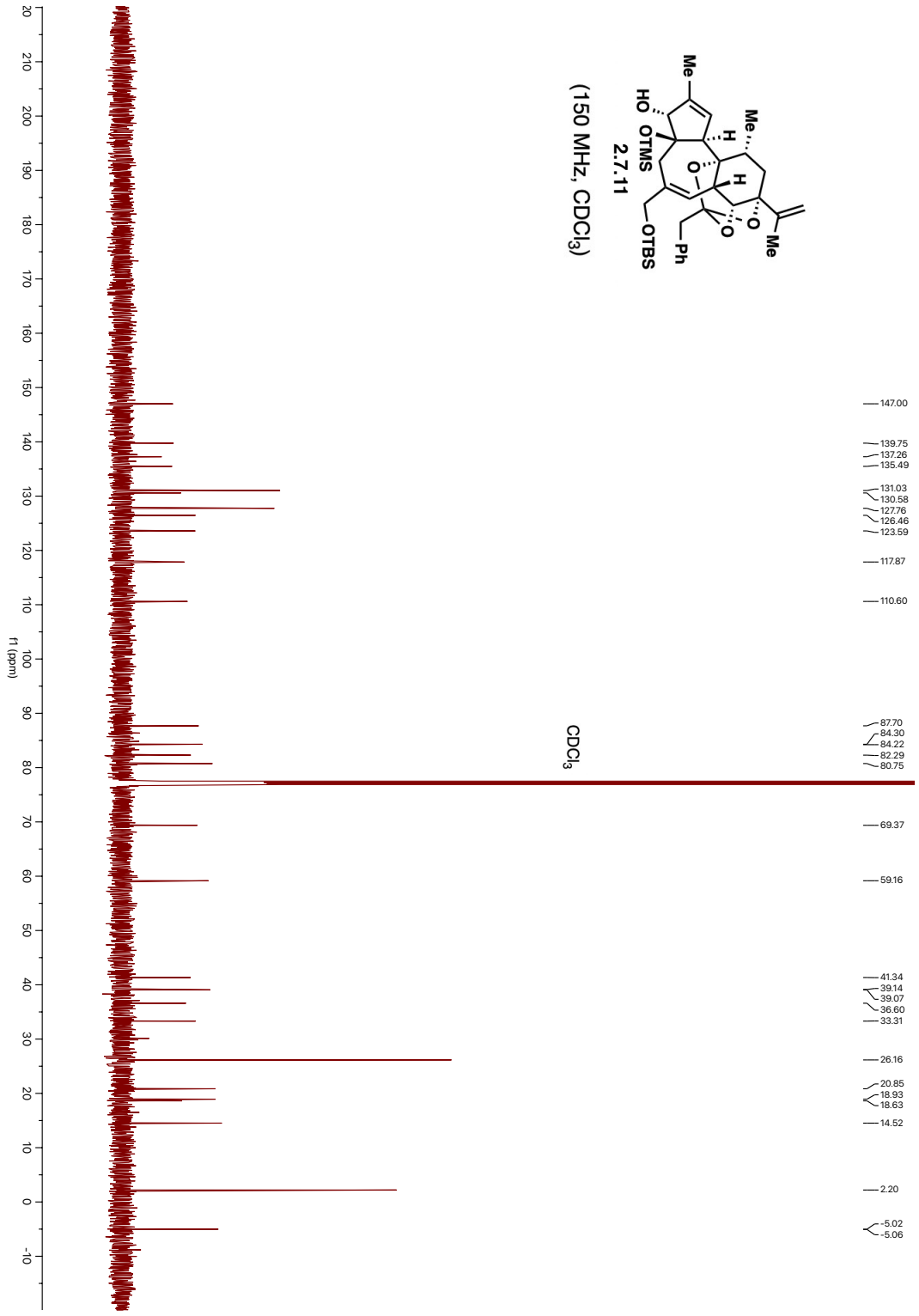

f2 (ppm)
f1 (ppm)

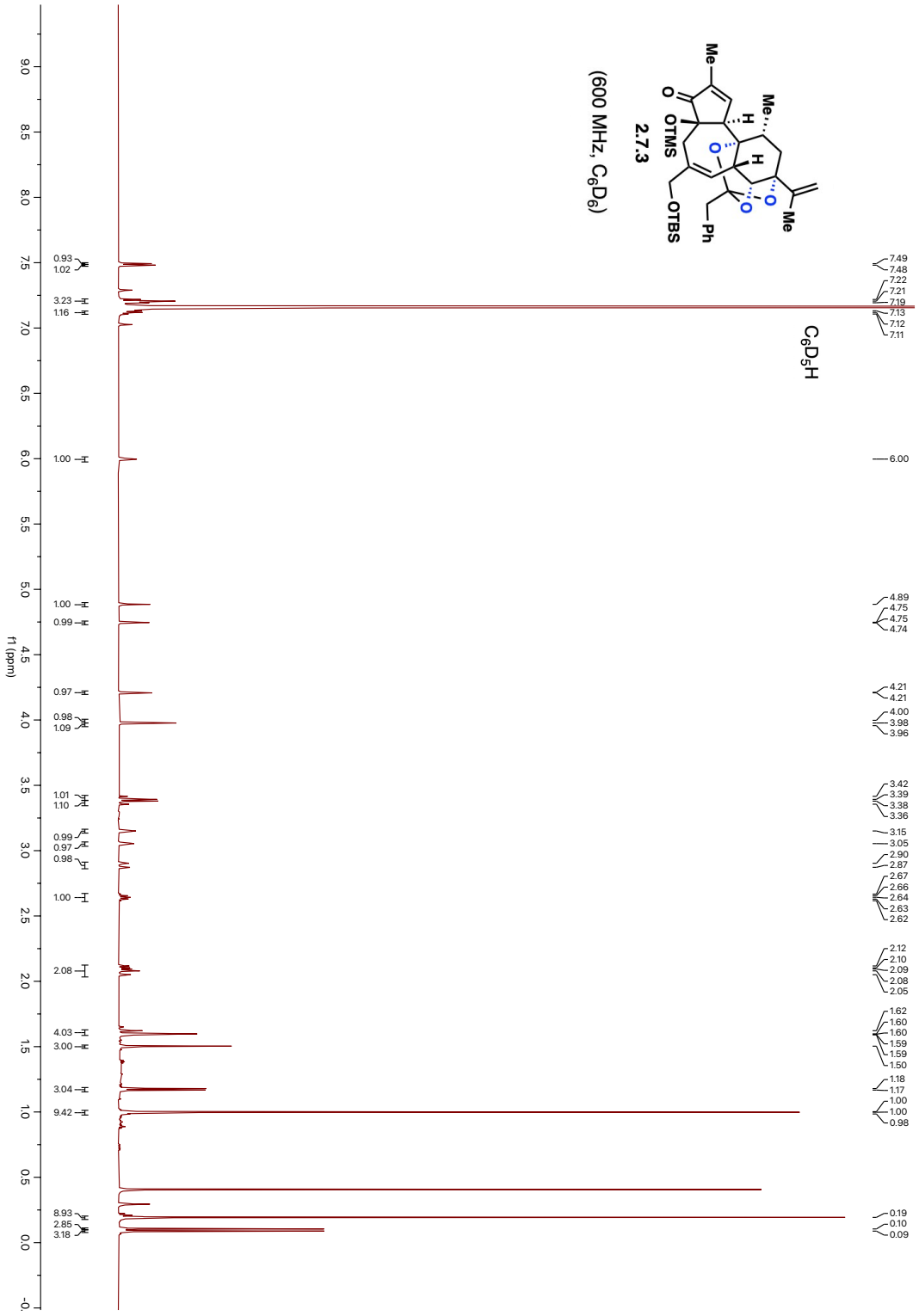

f2 (ppm)
f1 (ppm)

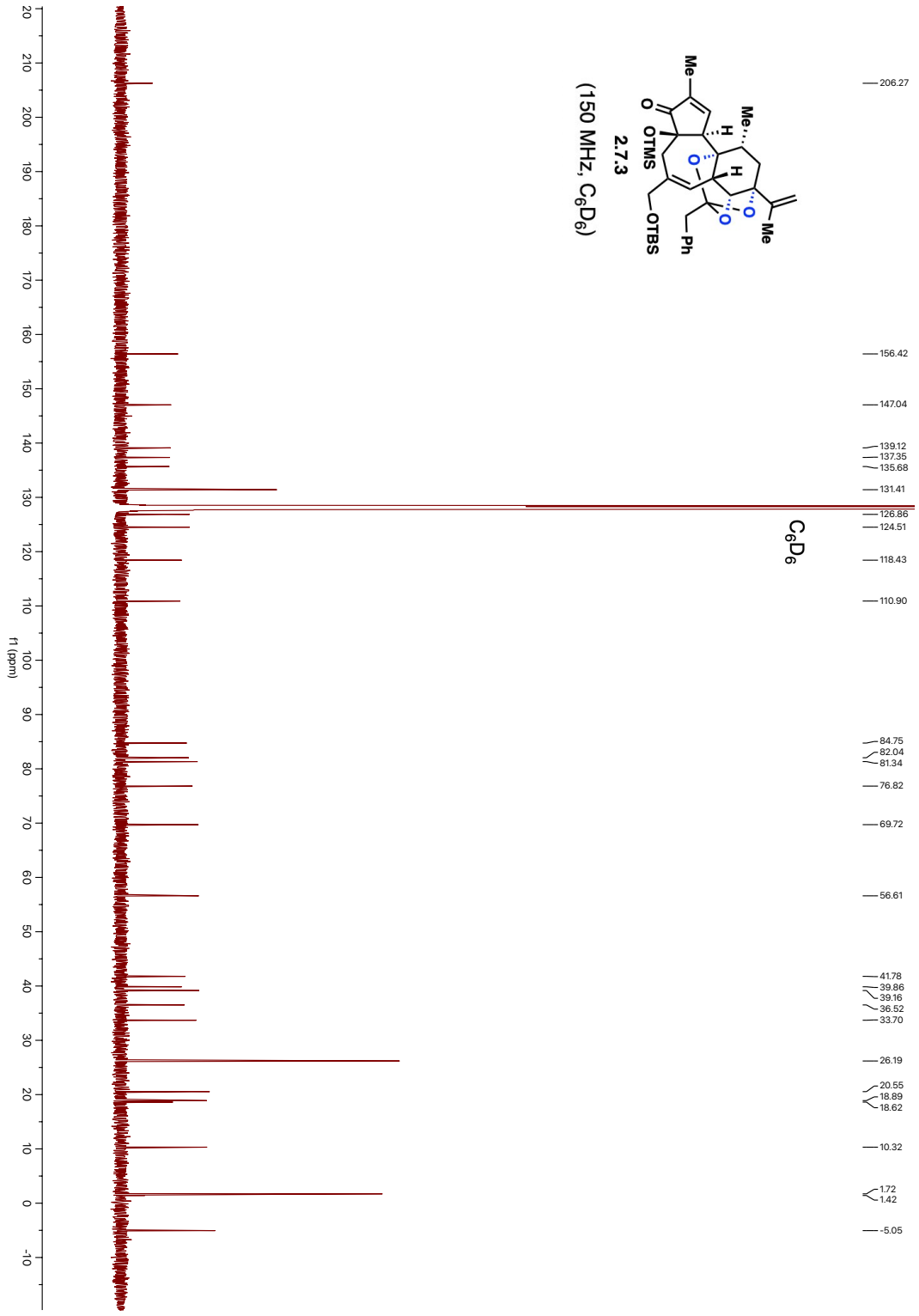

f2 (ppm)
f1 (ppm)

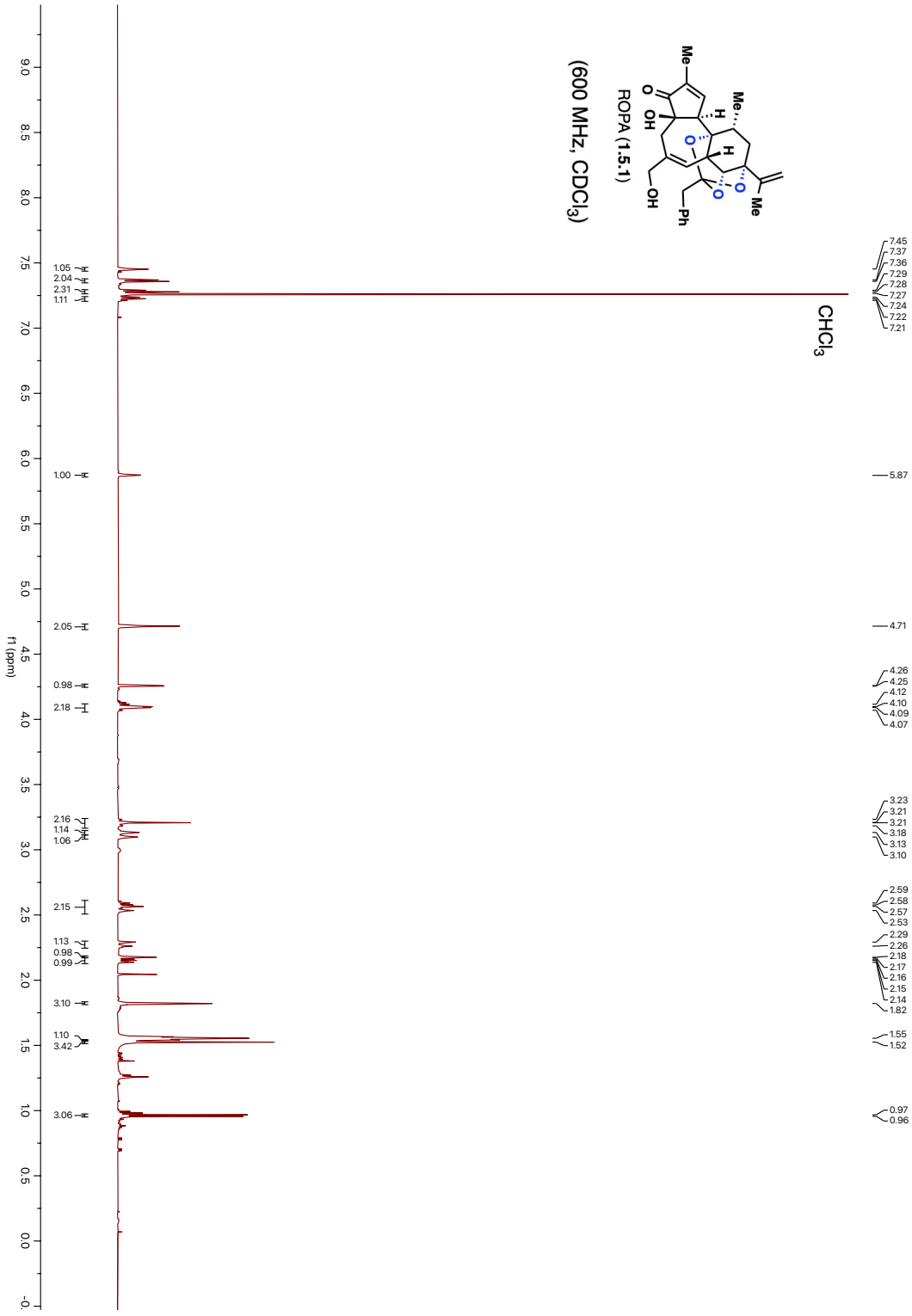

f2 (ppm)
f1 (ppm)

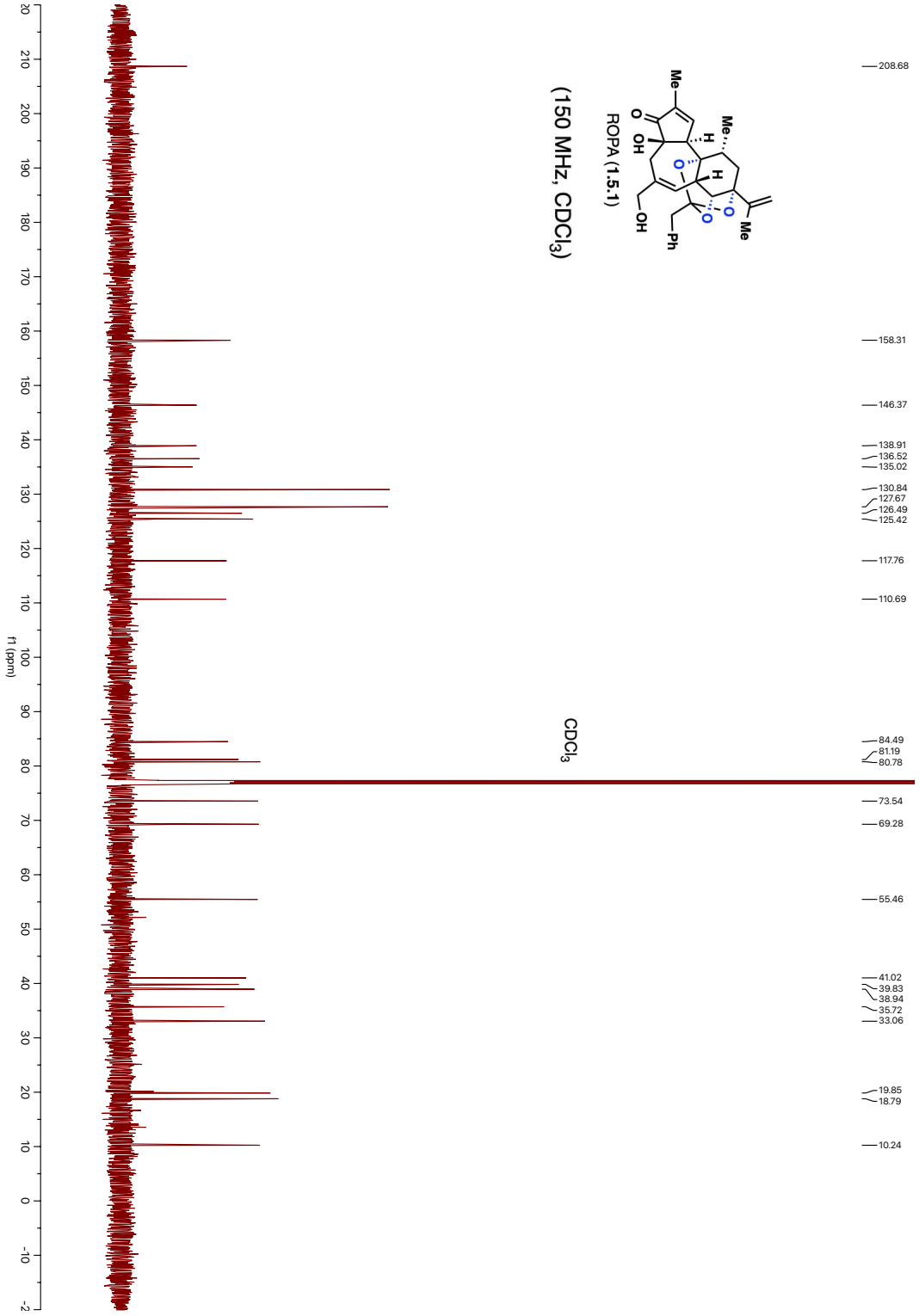

2.7.11
(600 MHz, CDCl3)
CHCl3
f1 (ppm)

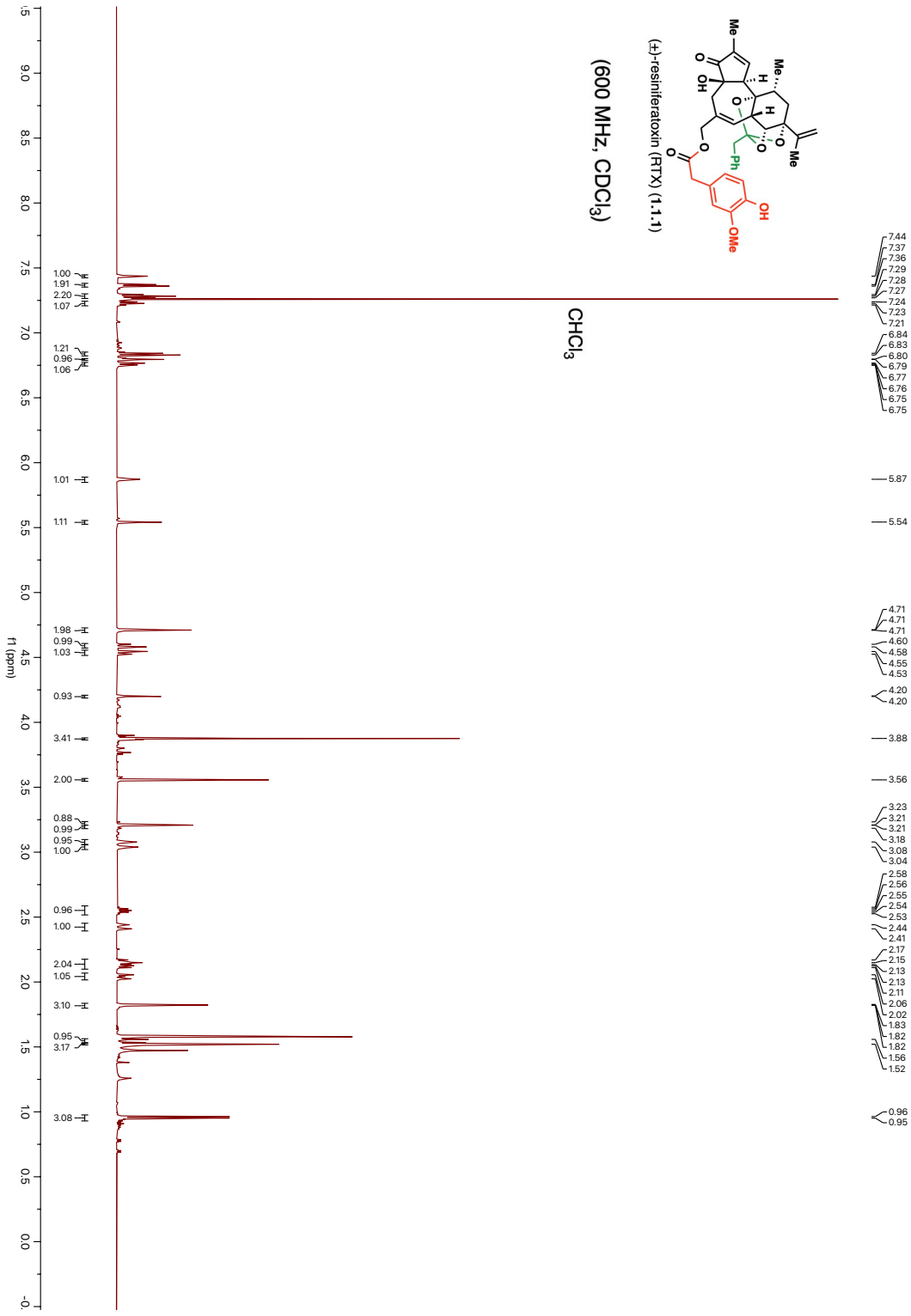

2.7.11
(150 MHz, CDCl3)
CDCl3
147.00
139.75
137.26
135.49
131.03
130.58
127.76
126.46
123.59
117.87
110.60
87.70
84.30
84.22
82.29
80.75
69.37
59.16
41.34
39.14
39.07
36.60
33.31
26.16
20.85
18.93
18.63
14.52
2.20
-5.02
-5.06
f1 (ppm)

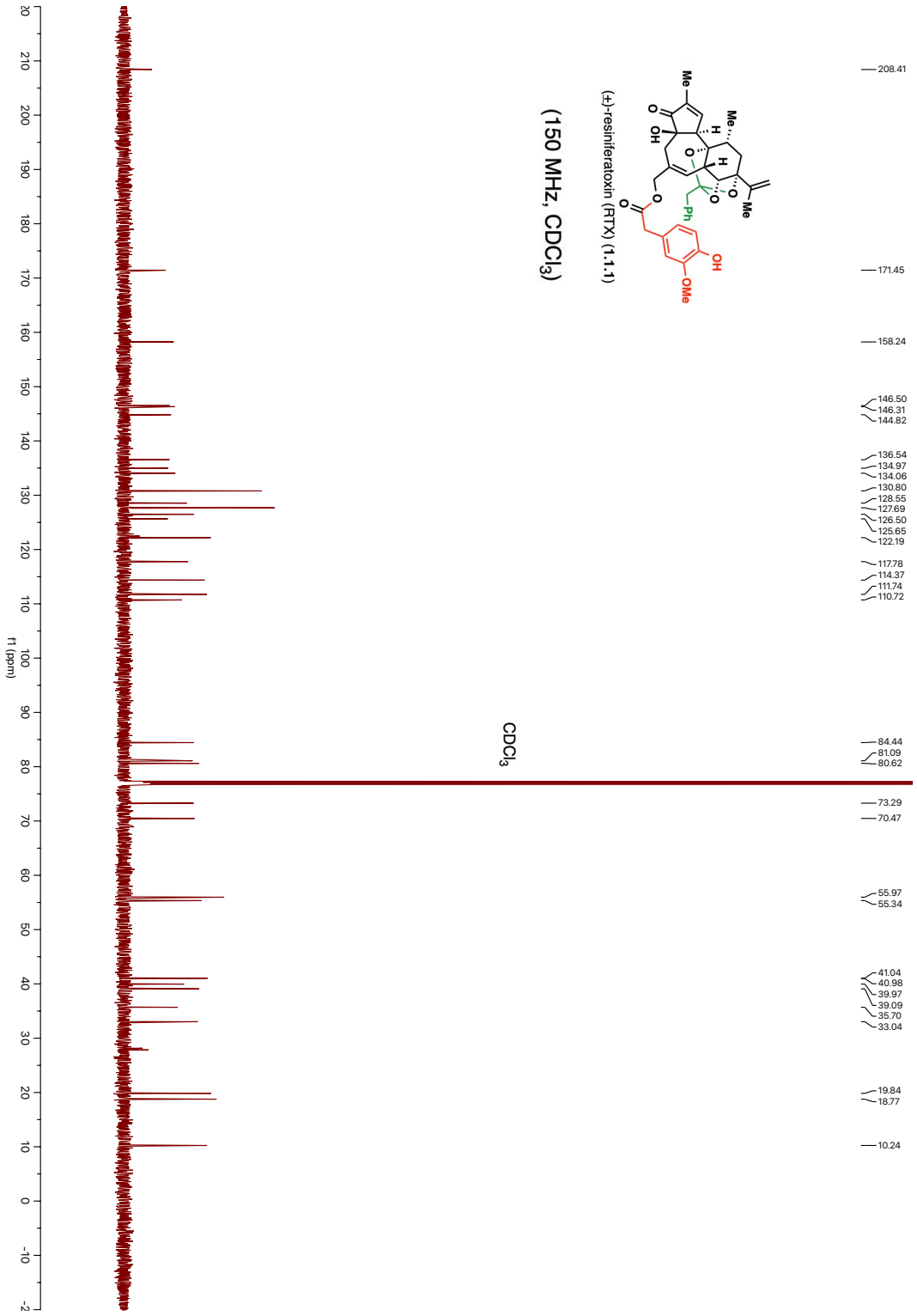

(600 MHz, C6D6)
2.7.3
C6D5H
f1 (ppm)

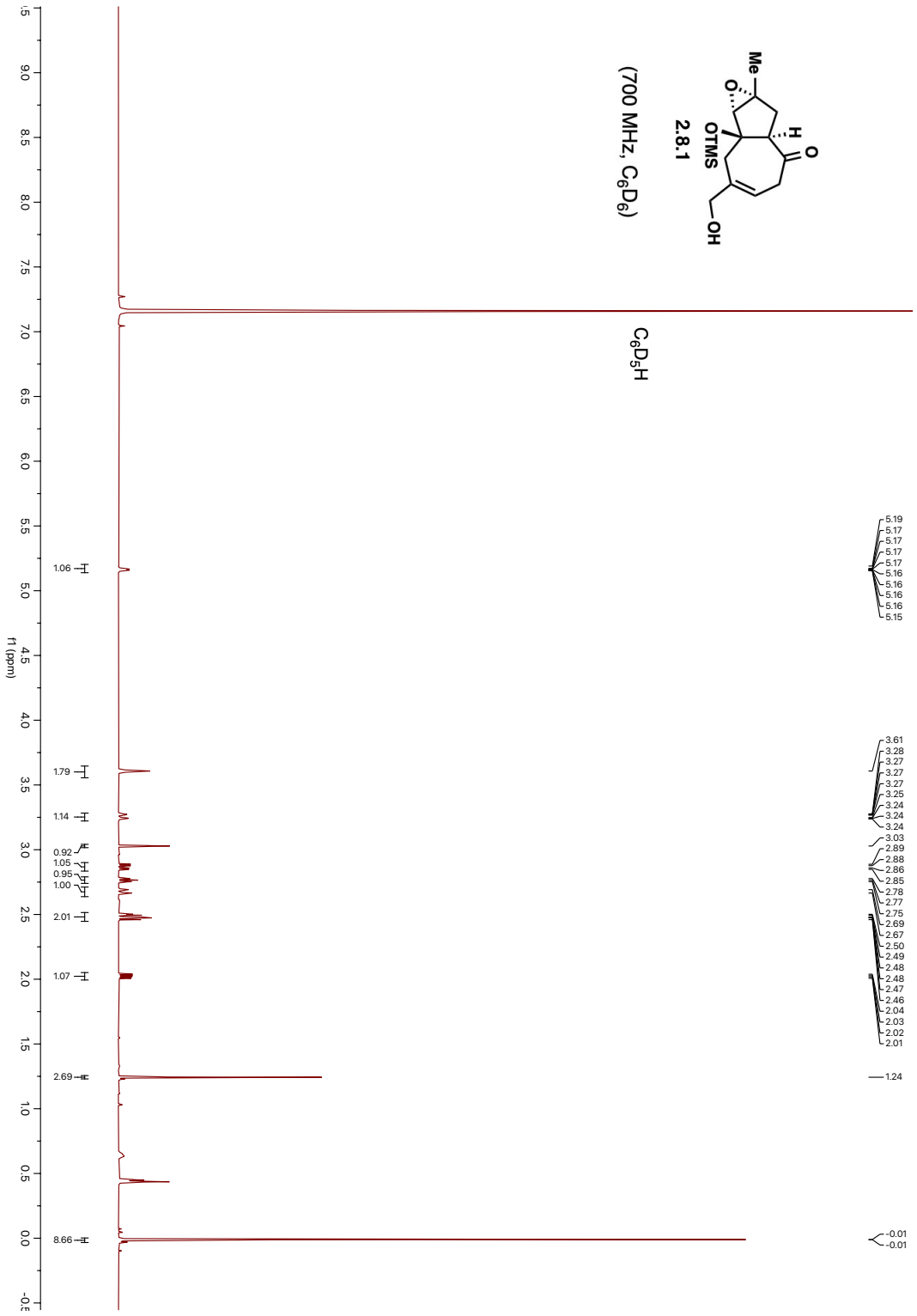

2.7.3
(150 MHz, C_6D_6)
OTMS
OTBS
Ph
Me
Me
Me
O
H
H
O
O
O
C_6D_6
206.27
156.42
147.04
139.12
137.35
135.68
131.41
126.86
124.51
118.43
110.90
84.75
82.04
81.34
76.82
69.72
56.61
41.78
39.86
39.16
36.52
33.70
26.19
20.55
18.89
18.62
10.32
1.72
1.42
-5.05
f1 (ppm)

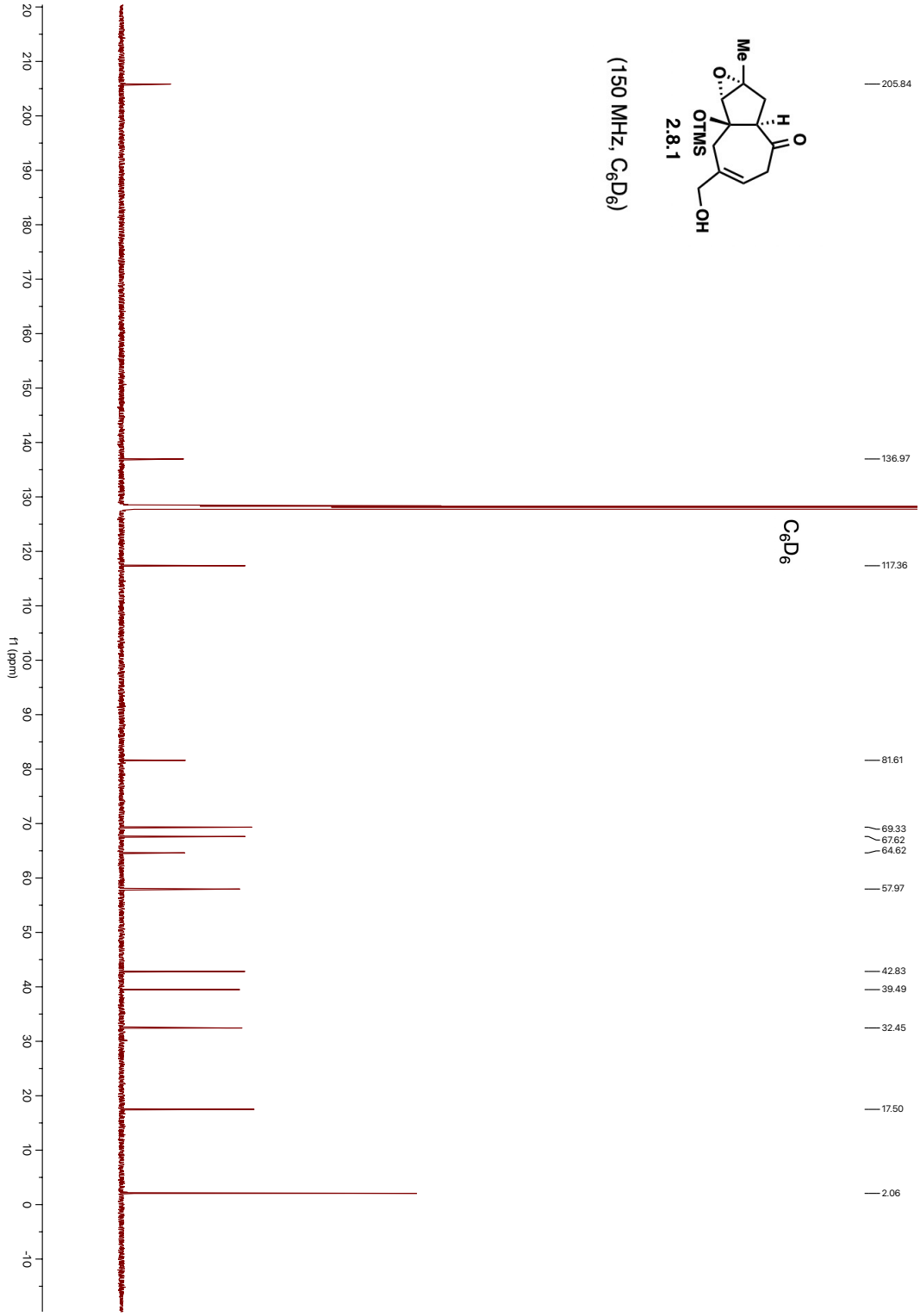

ROPA (1.5.1)
(600 MHz, CDCl3)
CHCl3
f1 (ppm)

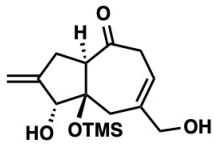

ROPA (1.5.1)
(150 MHz, CDCl3)
CDCl3
f1 (ppm)
208.68
158.31
146.37
138.91
136.52
135.02
130.84
127.67
126.49
125.42
117.76
110.69
84.49
81.19
80.78
73.54
69.28
55.46
41.02
39.83
38.94
35.72
33.06
19.85
18.79
10.24


(600 MHz, CDCl3)
CHCl3
(±)-resiniferatoxin (RTX) (1.1.1)
Me
Me
Me
OH
O
O
O
O
O
O
Ph
OH
OMe
f1 (ppm)
1.00
1.91
2.20
1.07
1.21
0.96
1.06
1.01
1.11
1.98
0.99
1.03
0.93
3.41
2.00
0.88
0.99
0.95
1.00
0.96
1.00
2.04
1.05
3.10
0.95
3.17
3.08
7.44
7.37
7.36
7.29
7.28
7.27
7.24
7.23
7.21
6.84
6.83
6.80
6.79
6.77
6.76
6.75
6.75
5.87
5.54
4.71
4.71
4.71
4.60
4.58
4.55
4.53
4.20
4.20
3.88
3.56
3.23
3.21
3.21
3.18
3.08
3.04
2.58
2.56
2.55
2.54
2.53
2.44
2.41
2.17
2.15
2.13
2.13
2.11
2.06
2.02
1.83
1.82
1.82
1.56
1.52
0.96
0.95


(150 MHz, CDCl3)
(±)-resiniferatoxin (RTX) (1.1.1)
CDCl3
208.41
171.45
158.24
146.50
146.31
144.82
136.54
134.97
134.06
130.80
128.55
127.69
126.50
125.65
122.19
117.78
114.37
111.74
110.72
84.44
81.09
80.62
73.29
70.47
55.97
55.34
41.04
40.98
39.97
39.09
35.70
33.04
19.84
18.77
10.24
f1 (ppm)

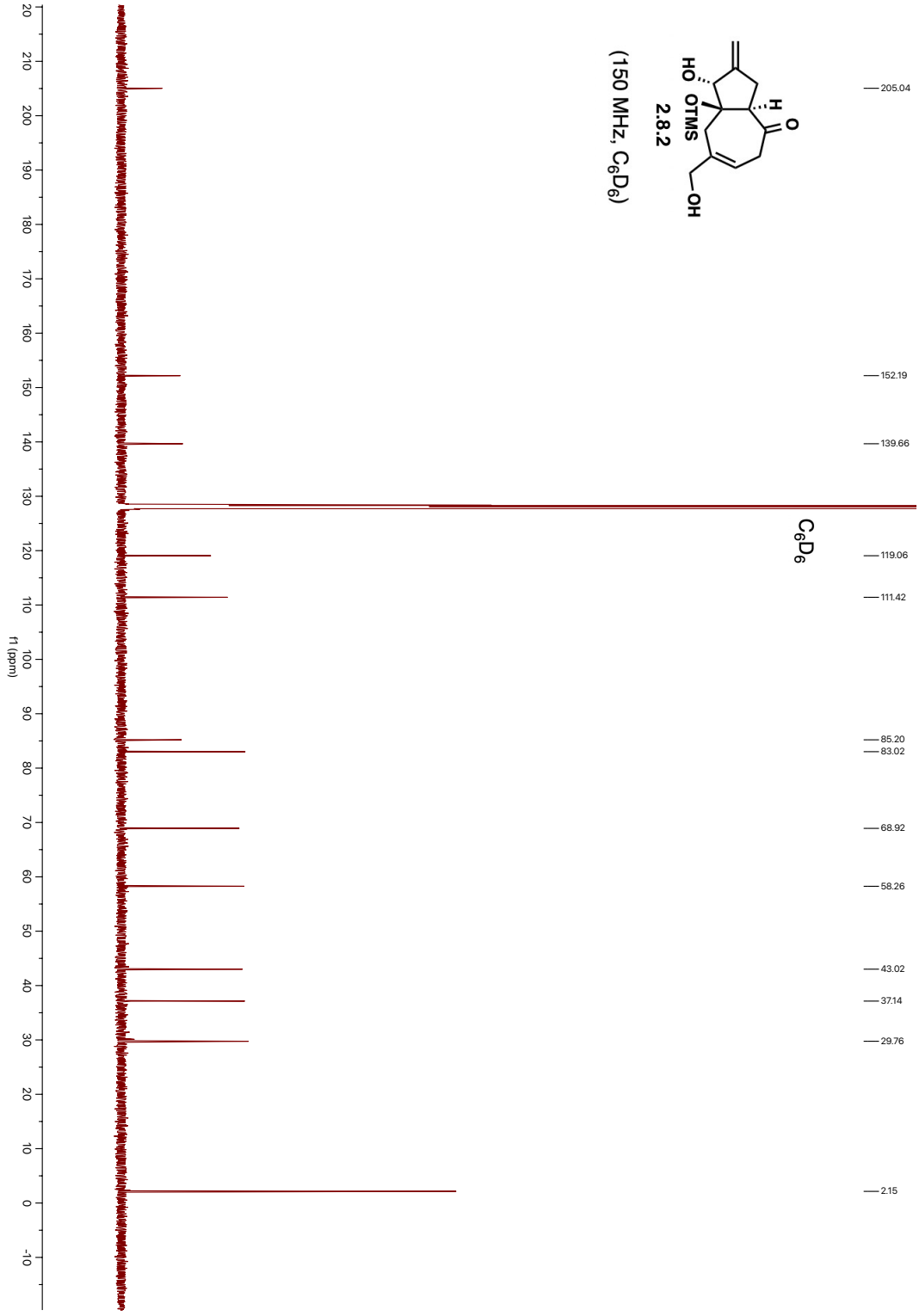

(700 MHz, C6D6)
2.8.1
Me
O
OTMS
H
O
OH
C6D5H
f1 (ppm)
1.06
1.79
1.14
0.92
1.05
0.95
1.00
2.01
1.07
2.69
8.66
5.19
5.17
5.17
5.17
5.17
5.16
5.16
5.16
5.16
5.15
3.61
3.28
3.27
3.27
3.27
3.25
3.24
3.24
3.24
3.03
2.89
2.88
2.86
2.85
2.78
2.77
2.75
2.69
2.67
2.50
2.49
2.48
2.48
2.47
2.46
2.04
2.03
2.02
2.01
1.24
-0.01
-0.01

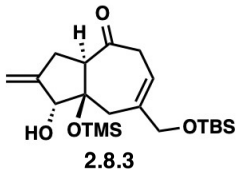

(150 MHz, C6D6)
2.8.1
Me
O
OTMS
H
O
OH
C6D6
205.84
136.97
117.36
81.61
69.33
67.62
64.62
57.97
42.83
39.49
32.45
17.50
2.06
f1 (ppm)



2.8.2

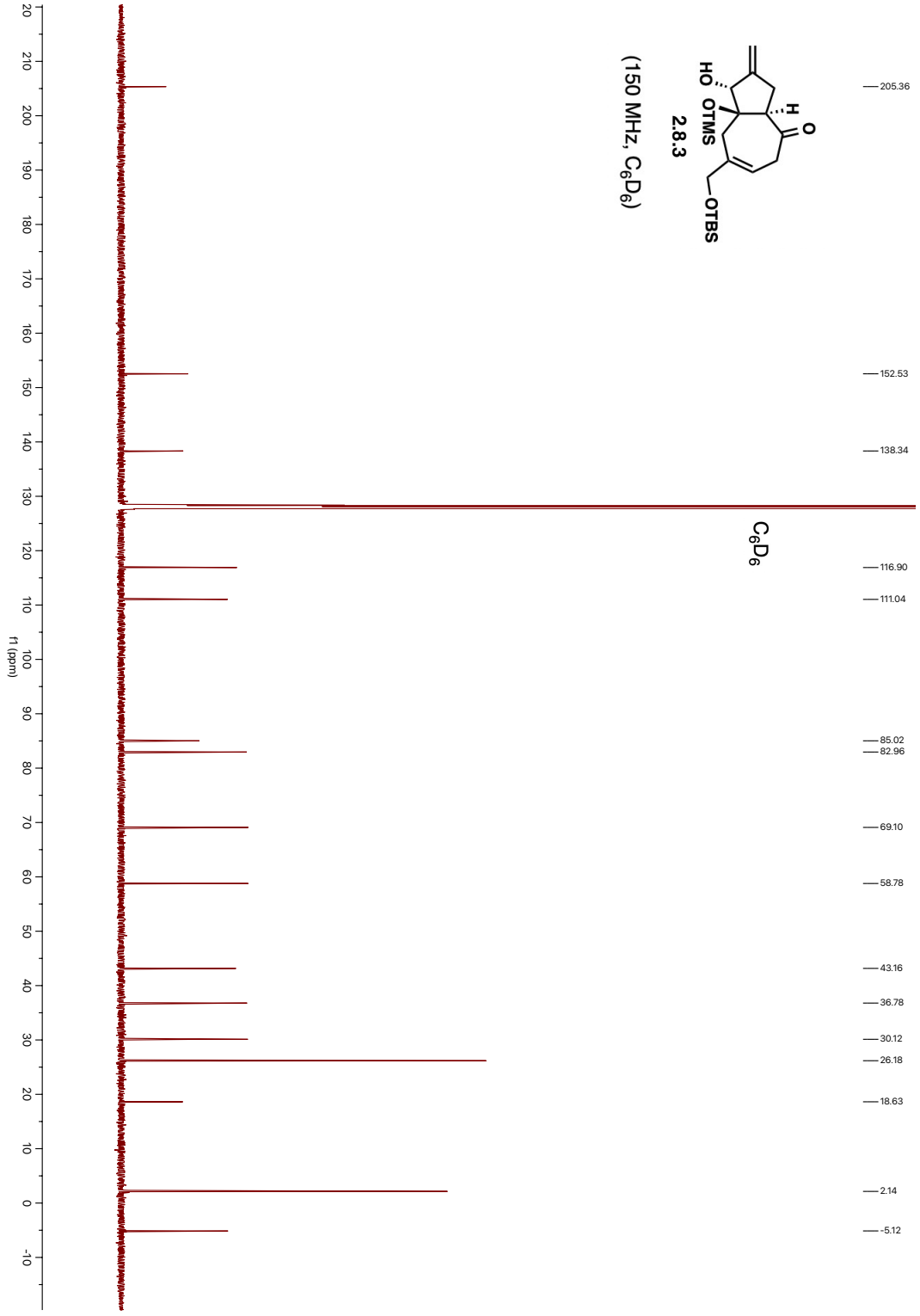
(400 MHz, C_6D_6)

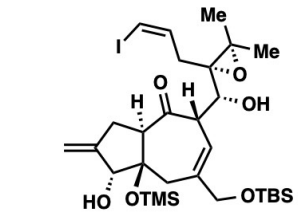

2.8.2
(150 MHz, C_6D_6)
HO
OTMS
H
O
OH
C_6D_6
205.04
152.19
139.66
119.06
111.42
85.20
83.02
68.92
58.26
43.02
37.14
29.76
2.15
f1 (ppm)



2.8.3

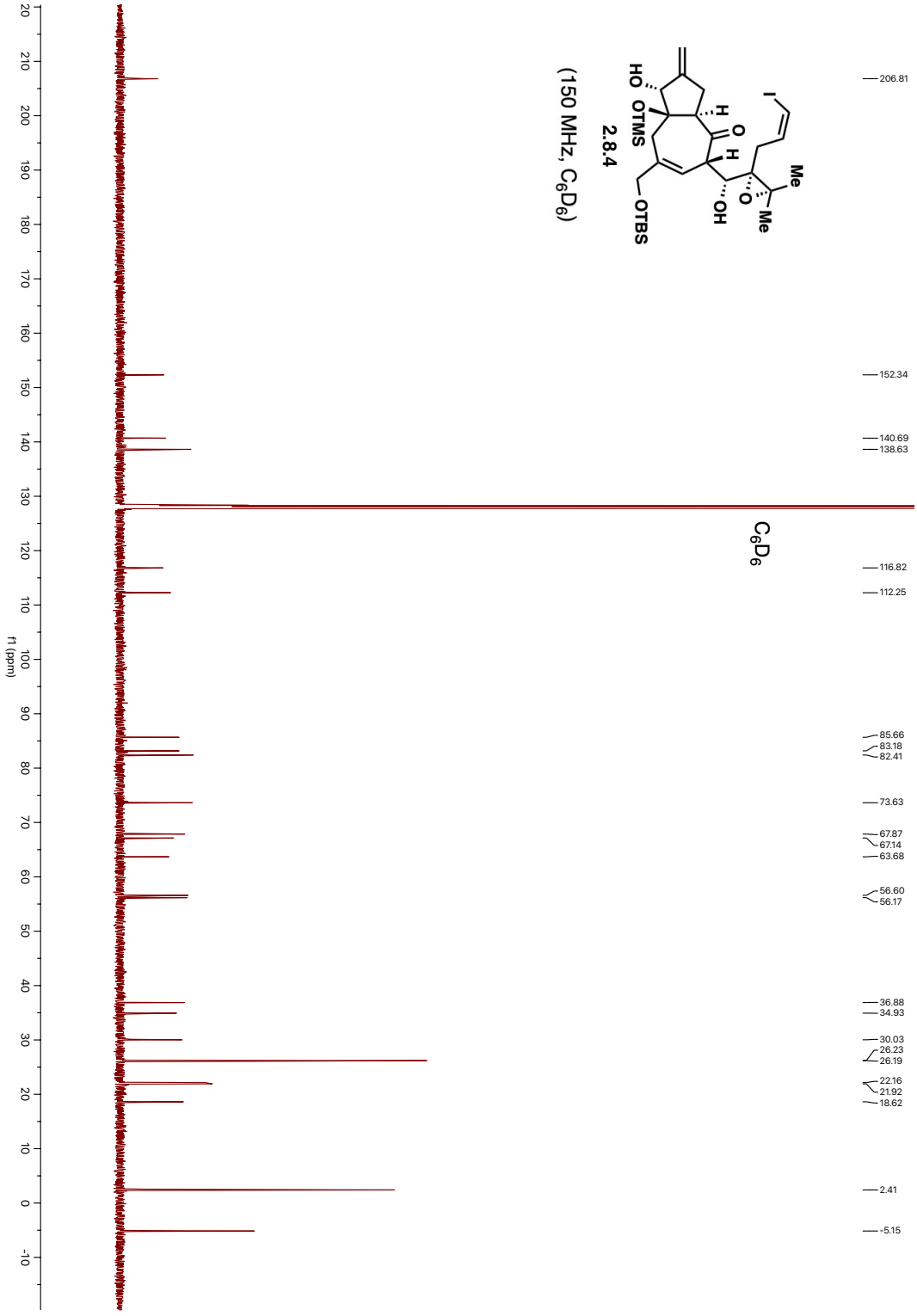
(400 MHz, C_6D_6)

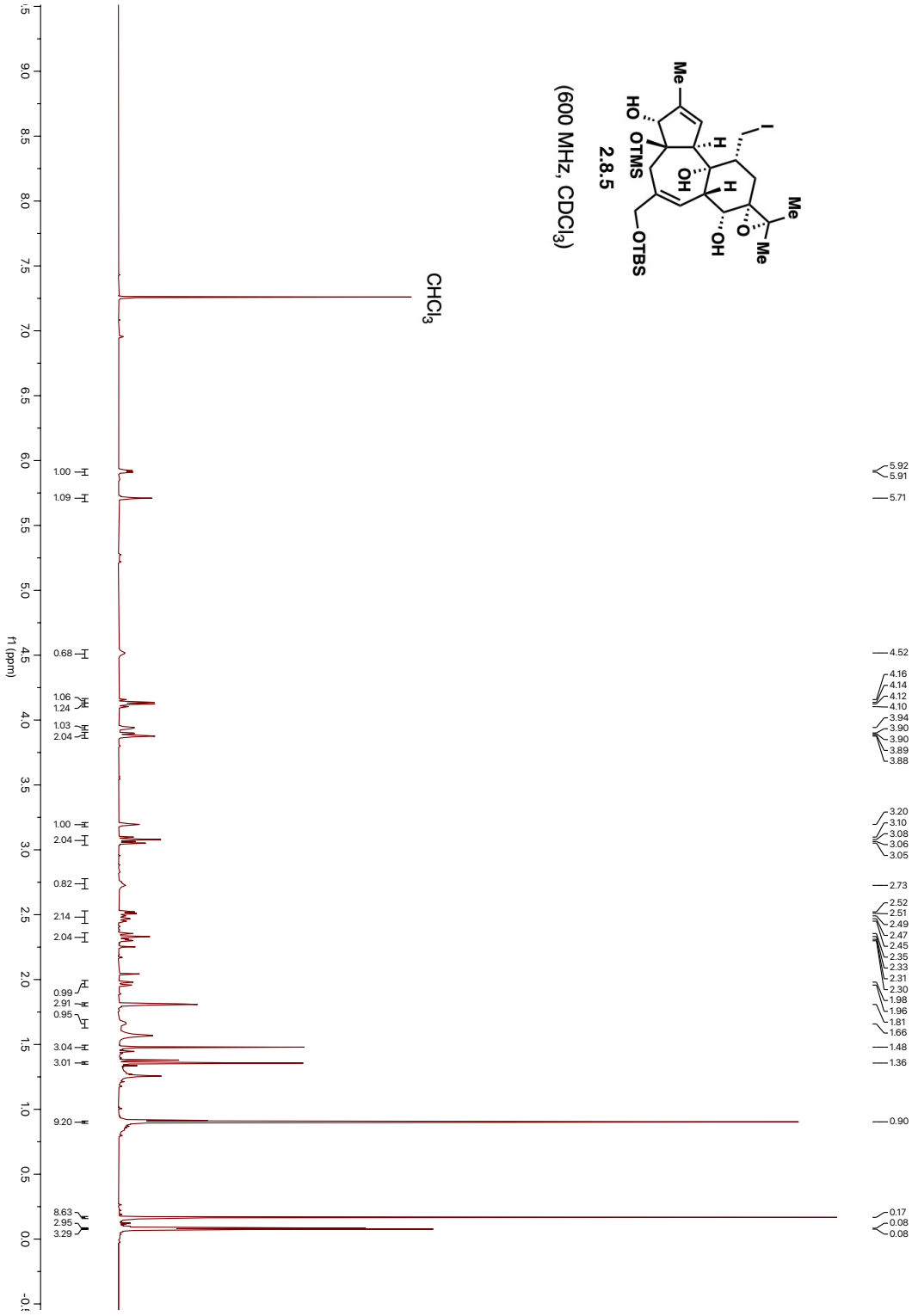

2.8.3
(150 MHz, C_6D_6)
HO OTMS
OTBS
O
H
C_6D_6
205.36
152.53
138.34
116.90
111.04
85.02
82.96
69.10
58.78
43.16
36.78
30.12
26.18
18.63
2.14
-5.12
f1 (ppm)

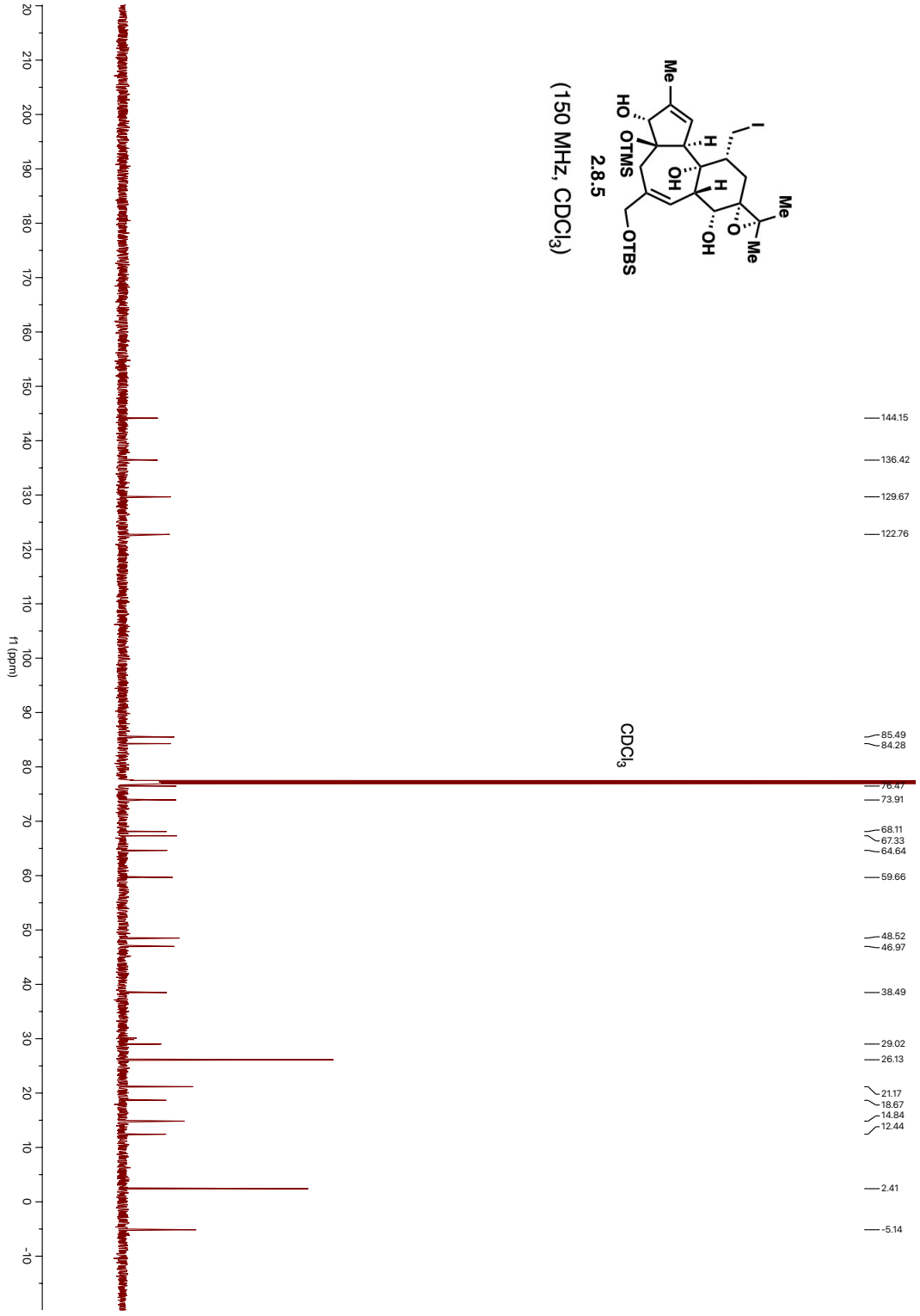


2.8.4

(600 MHz, C_6D_6)


2.8.4
(150 MHz, C_6D_6)
HO OTMS
OTBS
OH
Me
Me
I
C_6D_6
206.81
152.34
140.69
138.63
116.82
112.25
85.66
83.18
82.41
73.63
67.87
67.14
63.68
56.60
56.17
36.88
34.93
30.03
26.23
26.19
22.16
21.92
18.62
2.41
-5.15
f1 (ppm)


2.8.5
(600 MHz, $CDCl_3$)
$CHCl_3$
f1 (ppm)


Me
HO
OTMS
H
OH
H
I
Me
O
OH
Me
OTBS
2.8.5
(150 MHz, CDCl3)
CDCl3
144.15
136.42
129.67
122.76
85.49
84.28
76.47
73.91
68.11
67.33
64.64
59.66
48.52
46.97
38.49
29.02
26.13
21.17
18.67
14.84
12.44
2.41
-5.14
f1 (ppm)